Investigation of adenoviral immune neutralization and tropism for improved targeted gene delivery

Estrella López Gordo

MSc, BSc. (Hons)

Submitted in fulfilment of the requirements for the Degree of Doctor of Philosophy

Institute of Cardiovascular and Medical Sciences

College of Medicine, Veterinary & Life Sciences

University of Glasgow

September 2016

University of Glasgow

"We used to think that our fate was in our stars, but now we know that, in large measure, our fate is in our genes"

"Science moves with the spirit of an adventure characterized both by youthful arrogance and by the belief that the truth, once found, would be simple as well as pretty"

James Watson,

Author's Declaration

I declare that this thesis has been written entirely by myself and it is the result of my own work except when explicit reference is made to the contribution of others. This thesis has not been submitted previously for any other degree at any institution. The research was carried out in the Institute of Cardiovascular and Medical Sciences, University of Glasgow, under the supervision of Prof. Andrew Baker, Dr. Stuart A. Nicklin and Dr. Laura Denby.

Estrella López Gordo

September 2016

Acknowledgements

First, I would like to express my gratitude to my supervisors Professor Andrew H. Baker, Dr. Stuart A. Nicklin and Dr. Laura Denby for their advice and guidance through the PhD journey, for showing me how to approach scientific questions, pushing me to improve as a scientist and always challenging me. Specially, I would like to thank Dr. Stuart A. Nicklin for giving me such incredibly fast and valuable feedback during my writing phase, which I deeply appreciate, and for always being so approachable to discuss science and such a brilliant mentor, Dr. Laura Denby for cheering me up and encourage me in stressful and long days in the lab, and Professor Andrew H. Baker for showing me his trust on my work.

Special thanks to the European Commission for funding this research and to all the members of the ADVance Marie Curie initial training network for making all this experience possible and giving me the opportunity to interact with and learn from excellent scientists and meet great people like Iva, Nick or Anandi that have now become good friends. My sincere appreciation to Professor Urs Greber and Dr. Maarit Suomalainen for training me on new laboratory techniques and for their valuable advice, Dr. Angela C. Bradshaw for the academic support and for always being so nice and patient to answer my million questions, Nicola Britton, Gregor Aitchison, Elaine Butler and all the members of the Central Research Facility for the kindness and technical support, and colleagues in the BHF Glasgow Cardiovascular Research Centre (Institute of Cardiovascular and Medical Sciences) for sharing their skills and knowledge. Also, I would like to thank my office mates Chris Lavery, Valters, Josie and Izah as well as Chris Breen, the BHF girls, Raquel, Margaret and other friends I made in this building for sharing laughs, interesting stories and lots of tea and for being there for my ups and downs during my PhD.

Many thanks to my capoeira Senzala family: Contramestre Bom Menino, Michael, Paulo, Blair, Rob, Jason, John, Joe, Sussy, Neus, … which has made me feel so welcome and has given me so much energy and love during these now four years in Glasgow, and to Andrea for always keeping me so active and for the good long chats. Also, thanks to all the climbing crew: Alvaro, Sergio, James, Dora, Pete, … that has reminded me how passionate I am about climbing and how to never give up and always pursue your dreams. Also, thanks to my crazy girls Mariana and Lanette for always being ready for new adventures, for making me laugh and be there on the tough times, a Gemma, quien a pesar de la distancia ha estado tan cerca y me ha apoyado en los momentos más difíciles, i al Sergi i la Marta per compartir tants bons moments i tantes aventures.

Finalmente, me gustaría agradecer a Albert por estar a mi lado durante todo este tiempo, apoyándome y haciéndome reír cuando más lo he necesitado y, en definitiva, por formar parte de mi vida. Y sin duda alguna, a mi familia y a Juanma, a quienes les dedico este trabajo, por su apoyo incondicional, su confianza en mí y su comprensión, por transmitirme toda su fuerza y amor y por animarme a siempre seguir adelante.

Table of Contents

List of Tables

List of Figures

List of publications

Publications

Lopez-Gordo E, Doszpoly A, Duffy MR, Coughlan L, Bradshaw AC, White KM, Denby L, Nicklin SA, Baker AH. Defining a novel role for the coxsackie and adenovirus receptor in human adenovirus serotype 5 transduction *in vitro* in the presence of mouse serum. Journal of Virology. 2016 [under revision].

Lopez-Gordo E, Denby L, Nicklin SA, Baker AH. The importance of coagulation factors binding to adenovirus: historical perspectives and implications for gene delivery. Expert Opin Drug Deliv. 2014 Nov;11(11):1795-813.

Lopez-Gordo E, Podgorski II, Downes N, Alemany R. Circumventing antivector immunity: potential use of nonhuman adenoviral vectors. Hum Gene Ther. 2014 Apr;25(4):285-300.

Abstracts and posters

Lopez-Gordo E, Coughlan L, White KM, Bradshaw AC, Denby L, Nicklin SA, Baker AH. Dissecting immune responses to HAdV-5 in wild type and immunocompromised mouse serum reveals a new mechanism of transduction via the coxsackie and adenovirus receptor. Abstract presentation for the Fairbairn Award at the BSGCT Annual Conference 2016.

Lopez-Gordo E, Denby L, Nicklin SA, Baker AH. Assessing HAdV-5 immune neutralization and tropism *in vitro* and *in vivo* in immunocompetent and immunocompromised mice. Poster presentation at the ESGCT Annual Conference 2015.

Lopez-Gordo E, Denby L, Nicklin SA, Baker AH. Assessing HAdV-5 immune neutralization and tropism *in vitro* and *in vivo* in immunocompetent and immunocompromised mice. Poster presentation at the BSGCT Annual Conference 2015.

Lopez-Gordo E, Denby L, Nicklin SA, Baker AH. Tropism-modification of adenoviral vectors for targeted-gene delivery. Poster presentation at the 11th International Adenovirus meeting 2014.

Abbreviations, acronyms and symbols

AAV	Adeno-associated viruses
ABTS	2,2'-azino-bis(3-ethylbenzothiazoline-6-sulphonic acid)
ACEIs	Angiotensin-converting enzyme inhibitors
ADA	Adenosine deaminase deficiency
ADP	Adenovirus death protein
AGO2	Argonaute 2
AIM2	Absent in melanoma 2
AP	Antarctic phosphatase
APC	Antigen presenting cell
APS	Ammonium persulphate
ARBs	Angiotensin II receptor blockers
ASC	Apoptosis-associated speck-like protein containing a caspase-recruitment domain
ATRX	ATP-dependent helicase
AU	Arbitrary units
AVP	Adenoviral protease
Amp^R	Ampicillin resistance gene
BAP	Biotin acceptor peptide
BCA	Bicinchoninic acid
BSA	Bovine serum albumin
C3	Complement component 3
C4	Complement component 4
C4BP	C4b-binding protein
C5	Complement protein 5
CAR	Coxsackie and adenovirus receptor
CAV-2	Adenovirus canine serotype 2
CBP	CREB-binding protein
CBs	Cajal bodies
CCL5	C-C motif chemokine ligand 5
CDC25A	Cell division cycle 25A
CDK2	Cyclin dependent kinase 2
CF	Cystic fibrosis
CKD	Chronic kidney disease
CMV-IEP	Cytomegalovirus immediate-early promoter
CNSF	Congenital nephrotic syndrome of the Finnish type
CPE	Cytopathic effect
CR	Conserved region
CR1	Complement receptor 1
CT	Cycle threshold
CTL	Cytotoxic T lymphocyte
CUL	Cullin
cDC	Conventional dendritic cells
cDNA	Complementary DNA
cGAS	Cyclic GMP-AMP synthase

DAI	DNA-dependent activator of IRFs
DAPI	4’,6-diamidino-2-penylindole
DAXX	Death domain-associated protein
DBP	ssDNA-binding protein
DC	Dendritic cell
DDR	DNA damage response
DDX41	DEAD-box helicase 41
DM	Diabetes mellitus
DMD	Duchenne muscular dystrophy
DMEM	Dulbecco’s Modified Eagle Medium
DMS	Diffuse mesangial sclerosis
DMSO	Dimethyl sulphoxide
DN	Diabetic nephropathy
DNA-PK	DNA-dependent protein kinase
DPBS	Dulbecco’s calcium and magnesium free PBS
DPPC	Dipalmitoyl phosphatidylcholine
DSB	Double strand breaks
DSG2	Desmoglein 2
DTT	Dithiothreitol
dNTP	Deoxyribonucleotide triphosphates
ddNTP	Dideoxyribonucleotide triphosphates
E. coli	*Escherichia coli*
EDTA	Ethylenediamine tetra-acetic acid
EGF	Epidermal growth factor
EGFR	Epidermal growth factor receptor
EIF2AK2	Eukaryotic translation initiation factor 2 α kinase 2
ELISA	Enzyme-linked immunosorbent assay
ER	Endoplasmic reticulum
ESRF	End-stage renal failure
EphA2R	Ephrin A2 receptor
FAS	Fas cell surface death receptor
FCM	Flow cytometry
FCS	Fetal calf serum
FGF	Fibroblast growth factor
FIX	Coagulation factor IX
FK	Fiber knob
FRT	Flippase recognition target
FSGS	Focal segmental glomerulosclerosis
FVII	Coagulation factor VII
FX	Coagulation factor X
FXI	Coagulation factor XI
FXII	Coagulation factor XII
Fab	Fragment antigen-binding
FcR	Antibody constant fraction receptors
g	Gravitational force
GFR	Glomerular filtration rate

GLA	Glutamic acid
GMP	Good Manufacturing Practice
GN	Glomerulonephritis
GON	Group of Nine
GOS	Group of Six
GRO	Growth-related oncogene
GSK3	S6K and inhibition of glycogen synthase kinase 3
GlcA	D-glucuronic acid
GlcN	N-acetylglucosamine
Gln	Glutamine
H2B	Histone 2B
H4	Histone 4
HAdV	Human adenovirus
HD	Helper-dependent
HER	Human embryonic retina
HMGB1	High mobility group box 1
HRP	Horseradish peroxidase
HS	Heparan sulphate
HS-GAG	Heparan sulphate glycosaminoglycans
HSPG	Heparan sulphate proteoglycan
HVR	Hypervariable region
hCAR	Human coxsackie and adenovirus receptor
hFX	Human FX
hTfR	Human transferrin receptor
ICC	Immunocytochemistry
IFN	Interferon
IHC	Immunohistochemistry
IL	Interleukin
IP-10	IFN-inducible protein 10
IRF	Interferon regulatory factor
ISG	IFN-stimulated gene
ISGF3	IFN-stimulated gene factor 3
ISRE	Interferon-stimulated response element
ITR	Inverted terminal repeats
IU	Infectious unit
IdoA	L-iduronic acid
JNK	c-Jun N-terminal kinase
KC	Kupffer cell
KD	Equilibrium dissociation constant
KLC	Kinesin-1 light-chain
KLRC1	Killer cell lectin like receptor C1
KR	Kringle
Kan^R	Kanamycin resistance gene
ka	Association rate constant
kd	Dissociation rate constant
K_D	Equilibrium dissociation constant

L4P	L4 specific promoter
LB	Luria Broth
LITR	Left inverted terminal repeat
LPL	Lipoprotein lipase
LRP	Low-density lipoprotein receptor-related protein
loxP	Locus of X-over P1
MAD2L2	MAD2 mitotic arrest deficient-like 2
MAPK	p38 mitogen-activated protein kinase
MAPK3	Mitogen-activated protein kinase 3
MCD	Minimal change disease
MCKD1	Medullary cystic kidney disease type 1
MDA5	Melanoma differentiation-associated protein 5
MDFF	Molecular dynamic flexible fitting
MEM	Minimum Essential Medium
MHC	Major histocompatibility complex
MHC-I-α2	α2 domain of the major histocompatibility complex-I
MICA	MHC-I chain-related protein A
MICB	MHC-I chain-related protein B
MK2	MAPKAP kinase 2
MLP	Major late promoter
MLTU	Major late transcriptional unit
MOI	Multiplicity of infection
MTOC	Microtubule organising centre
MWCO	Molecular weight cut-off
MYD88	Myeloid differentiation primary response 88
MZ	Marginal zone
mFX	Mouse FX
N/A	Not applicable
NAbs	Neutralizing IgG antibodies
ND	Not determined
NF	Nuclear factor
NF-κB	Nuclear factor-kappa B
NHAdV	Non-human adenovirus
NHEJ	Non-homologous end joining
NK	Natural killer
NLRP3	NOD-like receptor family pyrin domain containing 3
NLS	Nuclear localization signal
NPC	Nuclear pore complex
NPM1	Nucleophosmin
NTA	Nanoparticle Tracking Analysis
NXF1	Nuclear RNA export factor 1
Neo^R	Neomycin resistance gene
O.C.T	Optimal cutting temperature compound
OOR	Out of range
ORF/Orf	Open reading frame
PAD	Peripheral arterial disease

PAF1	Paf1/RNA polymerase II complex component
PC	Protein C
PCN	Penicillin
PCR	Polymerase chain reaction
PD	Parkinson's disease
PEG	Polyethylene glycol
PFA	Paraformaldehyde
Pfu	Plaque forming units
PI3K	Phosphoinositide-3-OH kinase
PIV	Pathogen-free environment in microisolator individually ventilated
PKA	Protein kinase A
PKC	Protein kinase C
PKR	Protein kinase RNA-activated
PML-NB	Promyelocytic leukemia-nuclear body
PP2A	Protein phosphatase IIA
PPH	Peripentonal hexon
PRR	Pattern recognition receptors
PSGL-1	P-selectin glycoprotein ligand-1
PSMB	Immunoproteasome subunit beta
PTPRC	Protein tyrosine phosphatase receptor type C
$PURO^R$	Puromycin resistance gene
PVDF	Polyvinylidene difluoride
pDC	Plasmacytoid dendritic cell
pDNA	Plasmid DNA
pHPMA	Poly[N-(2-hydroxypropyl)methacrylamide]
pRb	Retinoblastoma tumor suppressor
pTP	Pre-terminal protein
pVI	Pre-protein VI
pVIn	Pre-protein VI cleaved N-terminal
pVII	Pre-protein VII
qPCR	Quantitative real-time polymerase chain reaction
RAAS	Renin-angiotensin-aldosterone system
RCA	Replication-competent adenoviruses
REC	Renal epithelium-derived cells
RFP	Red fluorescent protein
RFU	Relative fluorescence units
RGD	Arginine-glycine-aspartic acid
RGE	Arginine-glycine-glutamic acid
RID	Receptor internalization and degradation
RIG-I	Retinoic acid-inducible gene I
RISC	RNA-induced silencing complex
RLU	Relative light units
RNF20	Ring finger protein 20
RPE	R-phycoerythrin
rpm	Revolutions per minute
RPMI	Roswell Park Memorial Institute

S.O.C	Super optimal broth with catabolite repression
SA	Sialic acid-containing glycoproteins
SCID	Severe combined immunodeficiency
SDS	Sodium dodecyl sulphate
SEM	Standard error of the mean
SF	Serum-free
SLO	Streptolysin O
SP	Serine protease
NaP	Sodium pyruvate
SPR	Surface plasmon resonance
SPRI	Solid phase reversible immobilization
SR	Scavenger receptor
SR-A	Scavenger receptor A
STAT	Signal transducer and activator of transcription
Sm	Streptomycin
Sm^R	Streptomycin
Sp100	Speckled protein 100kDa
sCAR	Soluble ectodomain of CAR
scFv	Single-chain antibody
svaRNA	Small viral RNAs
TAP	Tandem affinity purification
TBK1	TRAF family member-associated NF-κB activator-binding kinase 1
TBST	TBS-Tween
TEMED	N,N,N',N'-tetramethylethylenediamine
TIMP-3	Tissue inhibitor of metalloproteinases-3
TLR	Toll-like Receptor
TNF	Tumor necrosis factor
TP	Terminal protein
TRAIL	TNF-related apoptosis-inducing ligand
TRIM21	Tripartite motif-containing protein 21
Th	T helper
VA-I	Virus-associated RNA I
VA-II	Virus-associated RNA II
VCAM-1	Vascular cell adhesion molecule-1
VCP	Valosin-containing protein
VEGF	Vascular endothelial growth factor
VWF	Von Willebrand factor
Vp	Viral particle
WB	Western blotting
X-Gal	5-bromo-4-chloro-3-indolyl-β-D-galactoside
XPO1	Exportin 1
Ψ	Adenoviral DNA packaging signal

Abstract

Human adenovirus serotype 5 (HAdV-5)-based gene delivery vectors are an attractive option for gene therapy applications because they can deliver large transgenes to a broad range of tissues, allow high level transgene expression, have negligible risk of insertional mutagenesis and are easily produced at high titers. Unfortunately, their high immunogenicity and liver and spleen-associated toxicity when intravascularly administered and high prevalence of neutralizing antibodies in patients remain challenges to be overcome for the generation of safe HAdV-5-based vectors for systemic gene therapy. The discovery that coagulation factor X (FX), a zymogen of a vitamin K-dependent serine protease that circulates in the bloodstream, simultaneously binds HAdV-5 hexon and heparan sulphate proteoglycans (HSPGs) to mediate hepatic transduction enabled the generation of HAdV-5 vectors with substantially reduced liver transduction via the manipulation of key amino acid residues in the adenoviral hexon protein. However, FX was also recently shown to protect HAdV-5 from neutralization by preventing binding of natural IgM antibodies to HAdV-5 capsids and it was reported that, in the absence of FX-binding and neutralization, HAdV-5 vectors can use alternative FX-independent transduction pathways for hepatocyte transduction. These findings highlight the complex interactions between adenoviruses and host blood factors and cells as well as the need for further research on these processes. Here, the interactions that mediate hepatic and splenic tropism of HAdV-5-based vectors and activation of the anti-viral immune response following intravascular delivery were investigated and targeted HAdV-5 delivery to the kidney was assessed.

Liver and spleen transduction was assessed in immunocompetent C57BL/6 and immunocompromised Rag $2^{-/-}$ or NSG mice lacking different components of the immune response, following intravascular administration of wild type or FX-binding deficient HAdV-5 vectors. HAdV-5 virions were neutralized in C57BL/6 mice in the absence of FX-binding, confirming a role for FX in protecting HAdV-5 from *in vivo* neutralization. However, NSG mice, which lack both innate and adaptive immunity, failed to neutralize FX-binding deficient HAdV-5 virions. Interestingly, administration of FX-binding deficient HAdV-5 vectors to IgM antibody-deficient Rag $2^{-/-}$ mice revealed that IgM antibodies might not be required for *in vivo* neutralization of HAdV-5, indicating that innate immunity alone might be sufficient. In agreement with previous reports, exposure of FX-binding deficient HAdV-5 vectors to C57BL/6 serum or wild type HAdV-5 vectors to C57BL/6 serum pre-incubated with the FX inhibitor X-bp led to HAdV-5 neutralization *in*

vitro. In contrast, Rag $2^{-/-}$ and NSG serum failed to neutralize HAdV-5 *in vitro* in the absence of FX-binding, indicating that IgM antibodies are essential for *in vitro* HAdV-5 neutralization. This suggests *in vitro* and *in vivo* adenovirus neutralization is mediated by different mechanisms.

Importantly, administration of FX-binding deficient HAdV-5 vectors to NSG mice, which were unable to neutralize HAdV-5, confirmed the existence of alternative FX-independent pathways for liver and spleen transduction in the absence of neutralization. CAR and $\alpha_v\beta_{3,5}$ integrins were assessed as possible host cell receptors for HAdV-5 transduction of these tissues in immunocompetent and immunocompromised mice. The use of CAR or $\alpha_v\beta_{3,5}$ integrin-binding ablated HAdV-5 vectors revealed that CAR and $\alpha_v\beta_{3,5}$ integrins might serve as receptors for HAdV-5 liver transduction in immunocompetent C57BL/6 mice in contrast to immunocompromised Rag $2^{-/-}$ mice. Neither CAR nor $\alpha_v\beta_{3,5}$ integrins mediated HAdV-5 spleen transduction in either mouse strain. Furthermore, administration of HAdV-5 vectors simultaneously ablated for FX and $\alpha_v\beta_{3,5}$ integrin-binding to NSG mice showed that $\alpha_v\beta_{3,5}$ integrins play no role in liver or spleen transduction in the absence of neutralization. With the aim to define novel FX-independent pathways of HAdV-5 transduction *in vitro* that might be relevant *in vivo,* cell transduction was assessed for wild type or FX-binding deficient HAdV-5 vectors in the presence of immunocompromised Rag $2^{-/-}$ serum or serum that had been pre-incubated with X-bp. These studies confirmed the existence of FX-independent mechanisms able to enhance HAdV-5 cell transduction *in vitro* in the presence of mouse serum and absence of neutralization. To identify the receptor(s) involved in *in vitro* HAdV-5 transduction in the presence of mouse serum, soluble recombinant HAdV-5 fiber knob was used to block access of virions to CAR and wild type or FX-binding deficient HAdV-5 cell transduction was assessed in high and low CAR-expressing cell lines in the presence of C57BL/6 or Rag $2^{-/-}$ serum with or without X-bp. HAdV-5 predominantly used a FX-independent pathway for cell transduction of high CAR-expressing cell lines in the presence of Rag $2^{-/-}$ serum and soluble fiber knob substantially reduced both C57BL/6 and Rag $2^{-/-}$ serum-enhanced transduction in such cell lines, suggesting a role for CAR, Conversely, HAdV-5 used the FX-mediated pathway or other FX and CAR-independent pathways for low CAR-expressing cell line transduction. Importantly, the use of CAR-binding deficient HAdV-5 vectors demonstrated that CAR usage in this setting does not rely on direct interactions of HAdV-5 with CAR, thus implicating a role for a mouse serum protein(s) in this process. To investigate these different pathways further, virions were fluorescently labelled with Alexa Fluor 488 dye and HAdV-5 cell binding, uptake and endosomal membrane penetration were

characterized in the presence of FX by microscopic assessment of individual virions at the single cell level. FX substantially enhanced virion cell binding but had minimal effect on virion uptake and it was suggested to decrease efficiency of endosomal membrane penetration, limiting escape of virions from endosomes into the cytosol.

Finally, FX and CAR-binding deficient HAdV-5 vectors were engineered to incorporate renal-targeting peptides found by *in vitro* phage display into the HI loop of the fiber knob domain for kidney-specific gene therapy. The resultant mutant HAdV-5 vectors were tested for their specificity in mediating gene delivery to ligand-expressing cells *in vitro* but failed to achieve specific targeting.

Together, these findings contribute to a deeper understanding of the interactions between HAdV-5 vectors and host blood components and cell receptors, and their implications for liver and spleen transduction and neutralization of virions. The studies presented in this thesis highlight the limitations of current re-targeting strategies and the need for further research to successfully develop efficient HAdV-5-based vectors for systemic gene therapy.

Chapter 1 Introduction

1.1 Gene therapy and gene therapy vectors

Currently, one of the most promising fields in biomedicine is gene therapy, a set of techniques that allows the treatment of diseases with no effective current medication, through the manipulation of the genome of the affected individual (Miller, 1992). The concept originated with a focus on inherited and acquired diseases where a particular gene encodes a mutation/s that results in a loss of function and thus needs to be replaced with a functional copy of the gene (replacement gene therapy) (e.g: replacement of coagulation factor IX gene in hemophilia). The concept soon broadened to include suicide gene therapy, which is aimed at inducing death in mutated cells (e.g: oncolytic adenoviruses to kill cancer cells), suppressive gene therapy to inhibit the expression of deleterious gene products (e.g: shRNA to silence huntingtin mRNA in Huntington), and immune gene therapy to modulate the immune response to infections or mutated self-cells (e.g: chimeric antigen receptor (CAR) T cell technology to stimulate an immune response against cancer). However, it was not until the emergence of new technologies such as sequencing platforms and advances in the field of recombinant DNA along with a deeper knowledge in cell biology driven by the sequencing of the human genome (Lander et al., 2001), which widened the scope of genetic targets, that gene therapy became a feasible option. Importantly, thanks to the remarkable progress made in the last three decades in the development of gene transfer vehicles able to deliver therapeutic transgenes to target cells with relatively high efficiency, viral vectors became the key players and gene therapy finally reached the clinic in 1990 for the treatment of the rare autosomal recessive severe combined immunodeficiency (SCID) disorder (Blaese et al., 1995). Subsequently, the number of clinical trials increased exponentially, mainly focused on cancer (64.4%) but also to treat monogenic diseases (10%), infectious diseases (7.6%), cardiovascular diseases (7.5%), neurological diseases (1.8%), ocular diseases (1.8%), inflammatory diseases (0.6%), etc. (The Journal of Gene Medicine: Clinical Trial, 2016) (Figure 1-1). Despite the large number of clinical trials starting each year, only a few progress through phases towards reaching the market. For instance, of all clinical trials to date, 57.6% reached phase I, 20.3% phase I/II, 17.1% phase II, 1% phase II/III, 3.7% phase III and only 0.1% reached phase IV (The Journal of Gene Medicine: Clinical Trial, 2016). Indeed, it is a significant challenge to successfully pass pharmacodynamics, pharmacokinetics and safety tests and, in fact, only a few gene therapy products have been approved so far in China, Philippines, Russia and the EU (e.g: Gendicine employing an adenoviral vector encoding p53 for the treatment of head and neck squamous cell carcinoma [reviewed by (Peng, 2005, Chen et al., 2014)], alipogene tiparvovec (Glybera) employing an adeno-associated

vector (AAV) encoding the human lipoprotein lipase (LPL) complementary DNA (cDNA) for the treatment of lipoprotein lipase deficiency (Gaudet et al., 2010), Neovasculgen employing a plasmid DNA encoding the vascular endothelial growth factor (VEGF) for the treatment of peripheral arterial disease (PAD) (Burleva and Babushkina, 2016), or Strimvelis employing a retroviral vector encoding the human adenosine deaminase (ADA) cDNA sequence for the treatment of ADA-SCID (Hoggatt, 2016)) (see below and section 1.3.2).

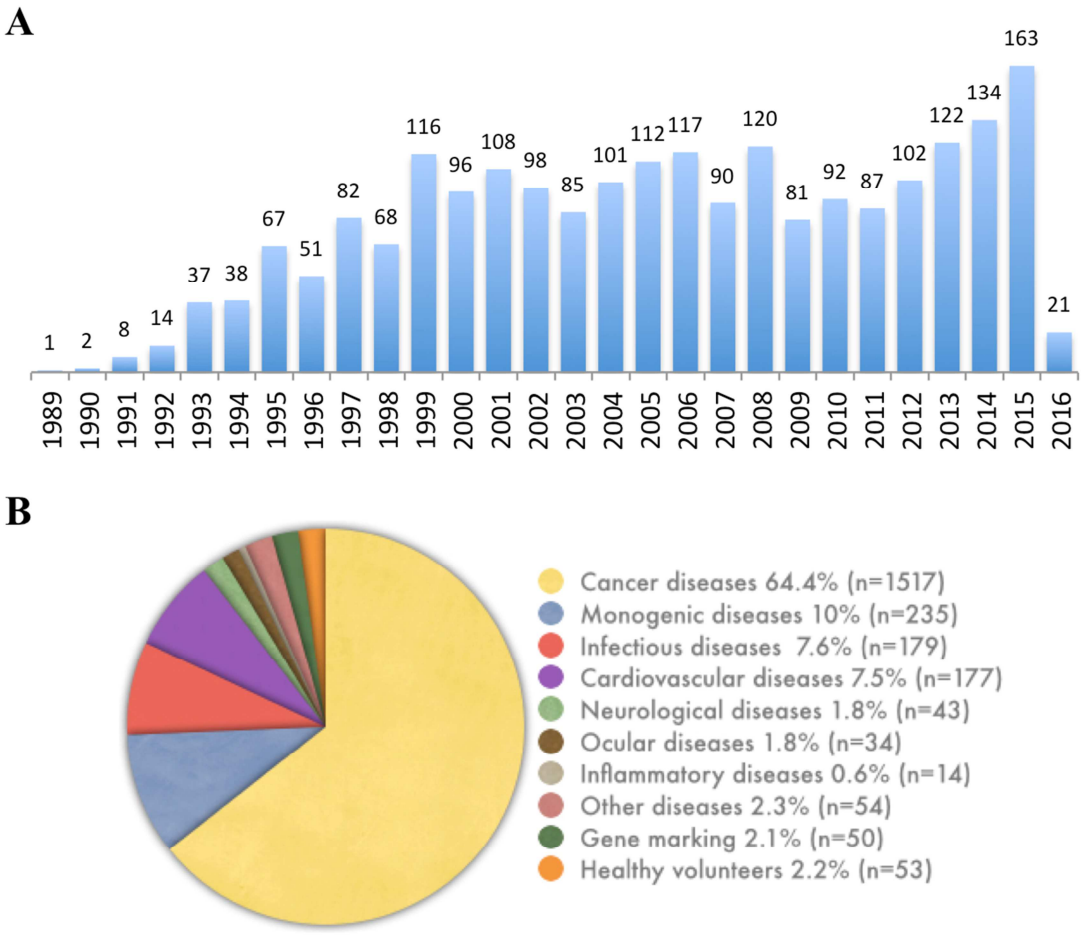

Figure 1-1. Gene therapy clinical trials. A) Number of gene therapy clinical trials approved by years to date. A total of 142 gene therapy clinical trials have not been assigned to any particular year and thus have been omitted from display on the chart. Numbers are indicated in the figure. B) Gene therapy clinical trials by indication to date. Numbers and percentages are indicated in the figure. Figure in (B) reproduced with permission from (The Journal of Gene Medicine: Clinical Trial, 2016). Copyright® 2016 by John Wiley and Sons Ltd.

Viral vectors are based on the virus' capacity to deliver the viral genome to the cytoplasm or nucleus of eukaryotic cells. There is a short list of viral vectors that can be safely used in *in vivo* protocols, which includes retroviral, lentiviral, adeno-associated and adenoviral vectors (Lukashev and Zamyatnin, 2016, Kotterman et al., 2015) (Figure 1-2). Alternative viral vectors such as those based on herpes simplex virus, poxvirus and vaccinia virus as

well as non-viral vectors, are also currently being developed (Figure 1-2). Retroviral vectors are able to transduce dividing cells with high efficiency and integrate their genome into the host cell, are easy to manipulate for cloning and have a broad cell tropism and low immunogenicity. Despite the retroviral vectors' capability to integrate their genome into the host cell was commonly thought to be a desirable feature for gene therapy viral vectors because it allows long-term therapeutic gene expression, integration events were shown to occur more frequently into actively transcribed genome loci, thus increasing the risk of insertional mutagenesis (Cattoglio et al., 2010, Wu et al., 2003, Hacein-Bey-Abina et al., 2008). Also, the fact that retroviral vectors cannot transduce non-dividing cells is yet another limitation. To overcome these problems, lentiviral vectors emerged as a safer alternative to γ-retrovirus-based retroviral vectors, allowing transduction of non-dividing cells, production at higher titers and, importantly, a lower risk of insertional mutagenesis (Zhou et al., 2016), making them particularly attractive for certain diseases where long-term therapeutic gene expression is required [reviewed by (Quinonez and Sutton, 2002)]. However, they do not allow high levels of transgene expression and their transgene capacity is relatively low (~9 kb). As for lentiviral vectors, adeno-associated vectors can also transduce dividing and non-dividing cells. Also, their low immunogenicity compared to lentiviral vectors (Vandendriessche et al., 2007) together with the episomal nature of their genome (Duan et al., 1998, Nakai et al., 2001) allows safer long-term transgene expression. However, more recent studies reported that adeno-associated vectors are also able to integrate into the host genome, albeit at low frequencies, highlighting a potential risk of insertional mutagenesis [reviewed by (Deyle and Russell, 2009, McCarty et al., 2004)]. Nevertheless, adeno-associated vectors have shown great success in clinical trials for the treatment of ocular disease (Maguire et al., 2009, Jacobson et al., 2012), haemophilia B (Nathwani et al., 2011) and Parkinson's disease (PD) (LeWitt et al., 2011, Muramatsu et al., 2010) among others. Importantly, in November 2012, the European Medicines Agency approved the first gene therapy product in the Western countries: Glybera, an AAV1-based vector to deliver human LPL cDNA to muscle cells via intramuscular injection for the treatment of lipoprotein lipase deficiency that shows safety and persistent transgene expression (Gaudet et al., 2010). Unfortunately, adeno-associated vectors do not allow high levels of transgene expression, their production is relatively complex, and their low transgene capacity (~4 kb) renders them suitable for only certain pathologies [(Clement and Grieger, 2016) and reviewed by (Lu, 2004)]. Adenoviral vectors, which also transduce dividing and non-dividing cells, bypassed these limitations allowing high levels of transgene expression, long-term transgene expression, higher transgene capacity of up to ~37 kb, production at higher titers, and very low to absent risk

of insertional mutagenesis since they very rarely integrate (Harui et al., 1999, Stephen et al., 2008, Stephen et al., 2010). Conversely, they exhibit high immunogenicity in comparison to other vectors (Stilwell and Samulski, 2004) and toxicity at high doses and can be neutralized by the host pre-existing immunity. Despite some challenges have yet to be overcome, adenoviruses are among the most promising gene transfer vectors of all available vectors, have been used in clinical trials mainly for the treatment of cancer as oncolytic vectors and as vaccines, and are also being tested for a wide range of human diseases such as cardiovascular, ocular, neurologic or inflammatory disease (The Journal of Gene Medicine: Clinical Trial, 2016). Furthermore, the world's first gene therapy product approved was based on an adenoviral vector to treat head and neck squamous cell carcinoma [reviewed by (Peng, 2005, Chen et al., 2014)], highlighting their success as vectors. For their characteristics and their potential, adenoviral vectors are currently on the top choice of vectors for gene therapy clinical trials.

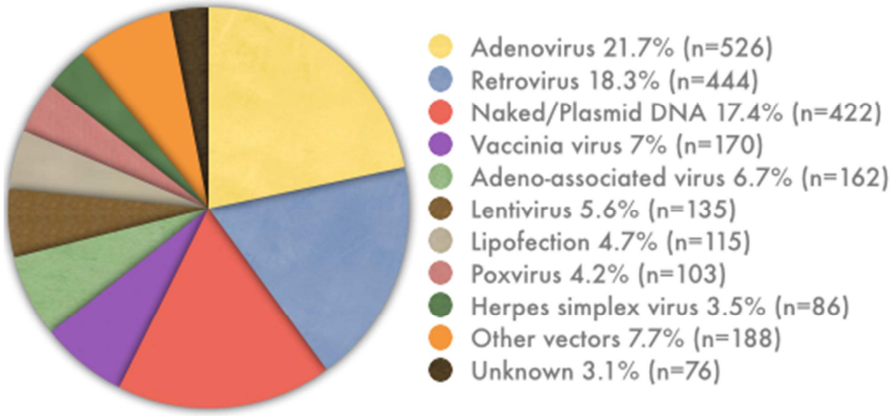

Figure 1-2. Gene transfer vectors used in gene therapy clinical trials. Numbers and percentages for each gene transfer vector are indicated in the figure. Figure reproduced with permission from (The Journal of Gene Medicine: Clinical Trial, 2016).

1.2 Adenovirus

Adenoviruses were first discovered in 1953 during a study attempting to grow human adenoid tissue in the laboratory, when Rowe and colleagues described a cytopathogenic agent that could induce cellular transmittable degeneration (ROWE et al., 1953). Adenovirus belongs to the *Adenoviridae* family of viruses characterized by having a non-enveloped icosahedral capsid that contains a linear double-stranded DNA genome. Adenovirus have been classified into five genera (*Mastadenovirus, Aviadenovirus, Atadenovirus, Siadenovirus and Ichtadenovirus*) based on the host from where they were first isolated (Adenovirus taxonomy, 2016). *Mastadenovirus* (mammalian adenoviruses) were classified into subtypes such as canine, murine or human adenovirus. Human

adenovirus, which originated from human and simian samples, were classified into species A-G and further subclassified into 54 different human serotypes and 33 simian serotypes according to phylogenetic sequence similarity, ability to agglutinate erythrocytes and oncogenic properties and serologic profiles [(Adenovirus taxonomy, 2016, Bailey and Mautner, 1994) and reviewed by (Davison et al., 2003)]. Serotypes belonging to the same species share tropism and clinical properties. Species B, C, D and E have ocular tropism, species A, D, F and G enteric tropism, species A, B, C and E respiratory tropism, and species B and D renal tropism [reviewed by (Arnberg, 2012)] (Table 1-1). Regarding their clinical properties, adenovirus can cause infections in humans that in most cases present with mild symptoms and self-resolve within a few days. Species D can cause epidemic keratoconjunctivitis, species F have been associated with gastroenteritis, species A, B, C and E cause respiratory disease, and species B are responsible for kidney disease [reviewed by (White et al., 2007)]. Unfortunately, some infections can have more severe outcomes such as pneumonia, which has been associated with acute respiratory distress syndrome [reviewed by (Brkic et al., 2002)]. Moreover, adenoviruses can worsen symptoms of established pathologies such as asthma or cystic fibrosis (CF), cause epidemic infections in closed communities, and even be lethal in immunosuppressed individuals [(Gern et al., 2012) and reviewed by (Frickmann et al., 2012, Schaller et al., 2006, Echavarria, 2008, Lion, 2014, Lion et al., 2003, de Mezerville et al., 2006, Chakrabarti et al., 2002)]. Among human adenovirus serotypes, serotype 5 of species C (HAdV-5) is by far the best characterized serotype, with detailed description of its genetic and capsid structure characteristics, tropism *in vitro* and *in vivo*, potential toxicity and associated immune responses when used as a vector *in vivo,* and has shown broad potential in the development of therapeutic vectors in the clinic. For these reasons, HAdV-5 is the serotype of choice in the studies presented in this thesis.

Table 1-1. Classification of human adenovirus serotypes.

Adenovirus species	Adenovirus serotype	Tropism	Receptors [1]	Adapter molecules [1, 5]
A	12, 18, 31	Enteric, respiratory	CAR	FIX[6], FX
B1	3, 7, 16, 21, 50	Ocular, respiratory, renal	CD46[2], DSG2[2], CD80, CD86, HSPG[3]	FX
B2	11, 14, 34, 35	Ocular, respiratory, renal	CD46[2], DSG2[2], CD80, CD86, HSPG[3]	FX
C	1, 2, 5, 6	Ocular, respiratory	CAR, integrins, HSPG, VCAM-1,	DPPC, lactoferrin,

			MHC-I-α2, SR, LRP, CR1,	C4BP, FVII, FIX, FX, PC
D	8, 9, 10, 13, 15, 17, 19, 20, 22, 23, 24, 25, 26, 27, 28, 29, 30, 32, 33, 36, 37, 38, 39, 42, 43, 44, 45, 46, 47, 48, 49, 51, 53, 54	Ocular, enteric, renal	SA, CD46[4], CAR	FX
E	4	Ocular, respiratory	CAR	
F	40, 41	Enteric	CAR	
G	52	Enteric	SA[7], CAR[7]	

[1]Both confirmed and postulated receptors and adapter molecules have been included. Some are not confirmed for all serotypes belonging to the same adenovirus species.
[2]Serotypes 11, 21, 35, and 50 use CD46 (Gaggar et al., 2005, Trinh et al., 2012) and CD46 is a low-affinity receptor for serotypes 3 and 7 and might not be a receptor for serotype 14 (Marttila et al., 2005, Tuve et al., 2006, Trinh et al., 2012). Serotypes 3, 7, 11 and 14 can use DSG2 (Wang et al., 2011c, Trinh et al., 2012).
[3]Serotypes 3 and 35 can bind to HSPG but with low affinity (Tuve et al., 2008).
[4]Only serotypes 26, 37 and 49 from species D have been suggested to use CD46 (Lemckert et al., 2006, Wu et al., 2004, Li et al., 2012).
[5]Refer to (Waddington et al., 2008, Balakireva et al., 2003, Adams et al., 2009, Johansson et al., 2007, Martin et al., 2003, Shayakhmetov et al., 2005b).
[6]Coagulation factor IX (FIX) enhances cell binding and infection of serotypes 18 and 31 but not 12 (Lenman et al., 2011, Jonsson et al., 2009).
Reviewed by (Arnberg, 2012, Zhang and Bergelson, 2005, Arnberg, 2009, Sharma et al., 2009b, Excoffon et al., 2014).
[7](Lenman et al., 2015).
ND; not determined, CAR; coxsackie and adenovirus receptor, HSPG; heparan sulphate proteoglycan, VCAM-1; vascular cell adhesion molecule-1, MHC-I-α2; α2 domain of the major histocompatibility complex-I, LRP; low-density lipoprotein receptor-related protein, SR; scavenger receptor, CR1; complement receptor 1, DPPC; dipalmitoyl phosphatidylcholine, C4BP; C4b-binding protein, DSG2; desmoglein 2, SA; sialic acid-containing glycoproteins, FVII; coagulation factor VII, FX; coagulation factor X.

1.2.1 Human adenovirus structure

1.2.1.1 Adenovirus genome

The human adenovirus genome is a ~34-37 kb linear dsDNA genome that encodes early, intermediate and late genes and contains inverted terminal repeats (ITRs) at each 5' and 3' end as well as the packaging signal, a sequence adjacent to the left ITR that allows genome packaging into the viral capsid (Flint, 1982) (Figure 1-3). Early genes (E1-E4) are implicated in the expression, transcription and replication of viral DNA and the suppression of the host anti-viral immune response and are transcribed from E1A, E1B, E2A, E2B, E3 and E4 transcriptional units. Intermediate genes include protein IX/Mu/μ and IVa2, which are transcribed from separate transcriptional units (Persson et al., 1979). Late genes (L1-L5) encode structural proteins of the capsid or proteins involved in capsid assembly and are transcribed from the major late promoter (MLP) in the major late transcriptional unit (MLTU) [reviewed by (Akusjarvi, 2008)]. Importantly, L4-33K and

L4-22K proteins are expressed from the L4 specific promoter (L4P) at intermediate times of infection and activate the MLP (Morris et al., 2010). A novel open reading frame (ORF), the U exon-24K, is expressed at late times of infection from a unique promoter within the UXP transcriptional unit (located between L5 and E3) (Tollefson et al., 2007, Ying et al., 2010). The adenoviral genome also encodes two viral RNAs: virus-associated RNA I (VA-I) and VA-II, which are involved in the suppression of the host immune response and are expressed from a polymerase III promoter [reviewed by (Mathews, 1995)]. Furthermore, multiple mRNAs can be transcribed from a single gene, which can be subsequently subjected to alternative splicing and differential polyadenylation resulting in viral proteins with different functions [reviewed by (Biasiotto and Akusjarvi, 2015)]. Interestingly, DNA sequence corresponding to protein regions with a key function in maintaining virion structure or completion of viral cycle tend to be conserved among species and serotypes, while sequences corresponding to exposed protein regions associated with immune recognition or without an essential role in stabilsing virion structure exhibit a higher degree of divergence (Chroboczek and Jacrot, 1987, Bailey and Mautner, 1994, Tarassishin et al., 2000). This phenomenon can be also observed in the conservation of genes across genera, thus defining 16 genus-common genes with key functions in DNA replication, encapsidation and virion structure such as the adenoviral DNA polymerase, pre-terminal protein (pTP), ssDNA-binding protein (DBP)/E2A, IVa2, fiber, hexon or pre-protein VI (pVI), and genus-specific genes that were created later in evolution such as the *Mastadenovirus* E4 Orf1 (Davison et al., 2003). Importantly, despite divergence in adenoviral genome sequence and gene content, the organization of common genes in the adenoviral genome has been highly conserved in the course of viral evolution (Tibbetts, 1977, Davison et al., 2003).

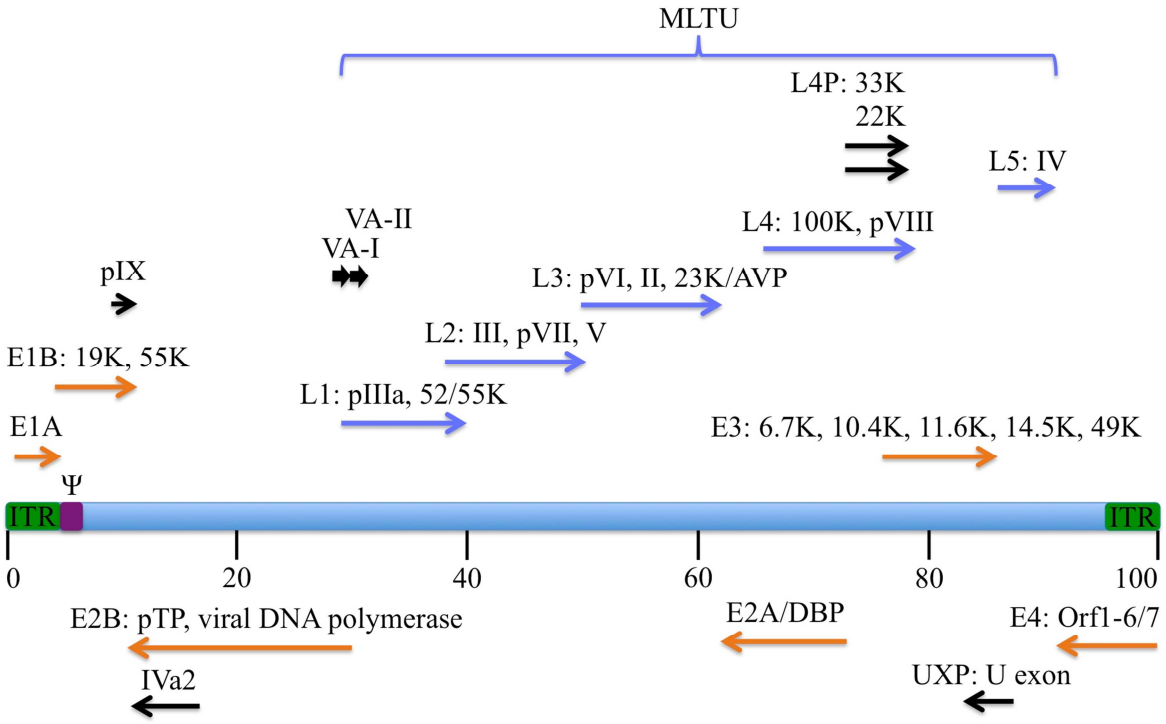

Figure 1-3. Adenoviral genome map. Early genes are shown as orange arrows, intermediate genes as black arrows and late genes as blue arrows. Viral-associated RNAs are shown as thick black arrows. The arrows's tip indicates the orientation of adenoviral genes. Internal terminal repeats (ITR) in green and adenoviral DNA packaging signal (Ψ) in purple. Certain transcripts for each adenoviral gene are indicated. Viral genes have been mapped by superimposing an arbitrary scale of 100 map units. "p" preceding protein names refers to their precursor forms. MLTU; major late transcriptional unit; VA-I and II; virus-associated RNA I and II, respectively, L4P; L4 specific promoter, Orf; open reading frame.

1.2.1.2 Adenovirus capsid composition

The adenoviral capsid is a 90-100 nm non-enveloped capsid of ~150MDa with *pseudo* triangulation number (T) = 25 icosahedral symmetry formed by 20 facets, 30 edges and 12 vertices (World WSM and Horwitz MS, 2007) (Figure 1-4). The main components of the capsid are protein II/hexon (240 homotrimers) and protein IV/fiber (12 homotrimers), which is anchored into protein III/penton base (12 homopentamers) at each of the 12 apexes (van Oostrum and Burnett, 1985). This structure is further stabilized by the cement proteins IIIa, VI, VIII and IX with copy number 60, ~350, 120 and 240, respectively [(Benevento et al., 2014, Reddy and Nemerow, 2014, Reddy et al., 2010) and reviewed by (Russell, 2009) and (Vellinga et al., 2005)]. The capsid also contains DNA-associated proteins V (~157 copies), VII (833 copies), X (100 copies), IVa2 (only a few copies), terminal protein (TP) (2 copies) and the viral cysteine protease L3-23K/AVP (~7 copies) [(Benevento et al., 2014, van Oostrum and Burnett, 1985, Anderson, 1990) and reviewed by (Russell, 2009)] (Figure 1-4A). In particular, each facet of the icosahedral capsid is formed by 9 hexons stabilized by protein IX, which has been termed the Group of Nine (GON), bound to 3 peripentonal hexons (PPHs) that are associated with protein IIIa

(Figure 1-4C left panel and Figure 1-4D left two panels). This gives a total of 12 hexons that are in turn associated with 1 penton base, forming a group of 13 independent polypeptides. A total of 5 PPHs (one from each structure of 13 polypeptides) associate with one penton base, forming what has been termed the Group of Six (GOS) (Figure 1-4C right panel) [(Stewart et al., 1991) and reviewed by (San Martin, 2012)]. Furthermore, four hexons together with one penton base monomer conform the asymmetric unit (AU) (Figure 1-4B-C). Importantly, protein VI and VIII together with V form a complex that associates with PPHs and hexons from the GON to increase capsid stability (Figure 1-4D right two panels) (Reddy et al., 2010, Reddy and Nemerow, 2014).

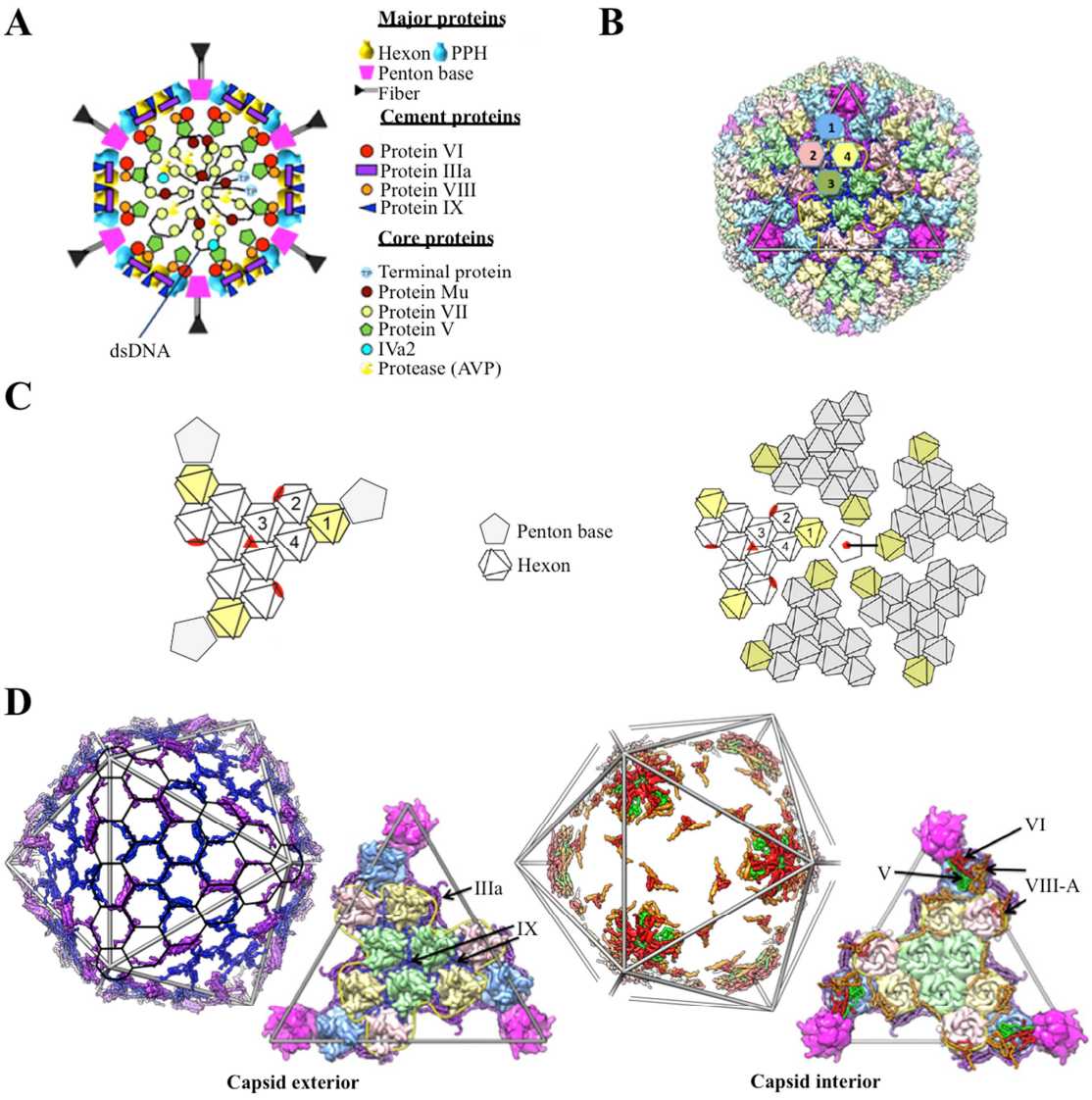

Figure 1-4. Adenoviral capsid structure and organization of capsid proteins. A) Schematic illustration of the organization of dsDNA and major, cement and core proteins in the adenoviral capsid. B) Overall organization of the adenoviral capsid. Hexons within the asymmetric unit (AU) of one facet are indicated with numbers. The outline of the triangular icosahedral facet is indicated as a grey triangle and the Group of Nine (GON), which is formed by 9 hexons in each facet plus three adjacent penton base, with a yellow line. Penton base represented in magenta, outer cement protein IIIa and IX in purple and blue, respectively, and hexons in light blue, light yellow, light green and tan. Fiber is not shown. C) GON (left panel). Group of Six

(GOS) formed by one penton and the five adjacent peripentonal hexons (PPHs) (right panel). Hexon trimers are depicted as hexagons with an overlaid triangle and penton base as pentagons. PPHs are highlighted in yellow. Hexons within the AU of one facet are indicated with numbers. D) Arrangement of cement proteins in the adenoviral capsid. The capsid exterior (left two panels) and interior (right two panels) are shown. The outline of hexons within one facet in the capsid exterior (farthest left panel) is highlighted by black lines. The GON is indicated with a yellow line. Protein IIIa represented in purple, IX in blue, VI in red, VIII in orange, V in green, penton base in magenta and hexons in light blue, light yellow, light green and tan. Figures in (A-B and D) adapted from (Reddy and Nemerow, 2014). Figures in (C) adapted from (San Martin, 2012).

The fiber protein protrudes outwards from the capsid vertex and is composed of 3 monomers, each containing an N-terminal tail, a rod-like shaft region with triple β-spiral repeat motifs, and a C-terminal globular knob domain with three eight-stranded antiparallel β sandwich and exposed loops (Ruigrok et al., 1990, Xia et al., 1994, van Raaij et al., 1999, Stewart et al., 1993) (Figure 1-5C). In the trimeric conformation, the fiber knob domain has a three-bladed propeller structure and contains a central depression (Xia et al., 1994). The fiber protein inserts the fiber shaft and N-terminal domain into the penton base (Liu et al., 2011, Zubieta et al., 2005). The interactions are made via three flexible fiber N-terminal tails with three penton base grooves and with an arginine-glycine-aspartic acid (RGD) motif in the penton base (Figure 1-5J). Also, the fiber shaft interacts with the penton base pore at the top surface (Liu et al., 2011, Zubieta et al., 2005) (Figure 1-5M). The penton base is composed of 5 subunits where each monomer has a basal β-barrel jelly roll domain containing both C and N-terminals facing the inner part of the capsid and a distal irregular insertion domain that contains variable loops (Zubieta et al., 2005) (Figure 1-5B). The penton base N-terminal region interacts with protein IIIa (Liu et al., 2010). The penton base also interacts with the fiber N-terminal tail via three penton base grooves formed between penton subunits and the RGD motif, which is located in one of the penton base monomer variable loops (Zubieta et al., 2005), and also interacts with the fiber shaft via the penton base pore top surface (Liu et al., 2011, Zubieta et al., 2005). The interaction between penton base and hexon involves loops of the jelly roll motifs of both proteins (Fabry et al., 2005) (Figure 1-5L). Regarding the hexon, it is composed of 3 subunits each containing an eight-stranded β-barrel with jelly roll topology and loops connected by α-helixes (Roberts et al., 1986, Rux and Burnett, 2000, Liu et al., 2010) (Figure 1-5A). Importantly, the hexon has 7 hypervariable regions (HVR), 5 of which are exposed on the outer part of the capsid and 2 of which (HVRs 1 and 6) are buried (Crawford-Miksza and Schnurr, 1996, Rux and Burnett, 2000). Both the C and N-terminals of hexon face the inner part of the capsid (Roberts et al., 1986, Liu et al., 2010). Interactions between hexons are made via their C-terminal, the β-barrel structure and the hexon loops (Fabry et al., 2005, Reddy et al., 2010). Interactions of hexons with protein IIIa are made via the hexon N-terminal and with protein VIII via the hexon C or N-terminal (Reddy et al., 2010, Liu et

al., 2010) (Figure 1-5N). Also, the hexons within the GON interact with the C-terminal of protein IX and the PPHs interact with the N-terminal of protein IX (Reddy and Nemerow, 2014) (Figure 1-5K).

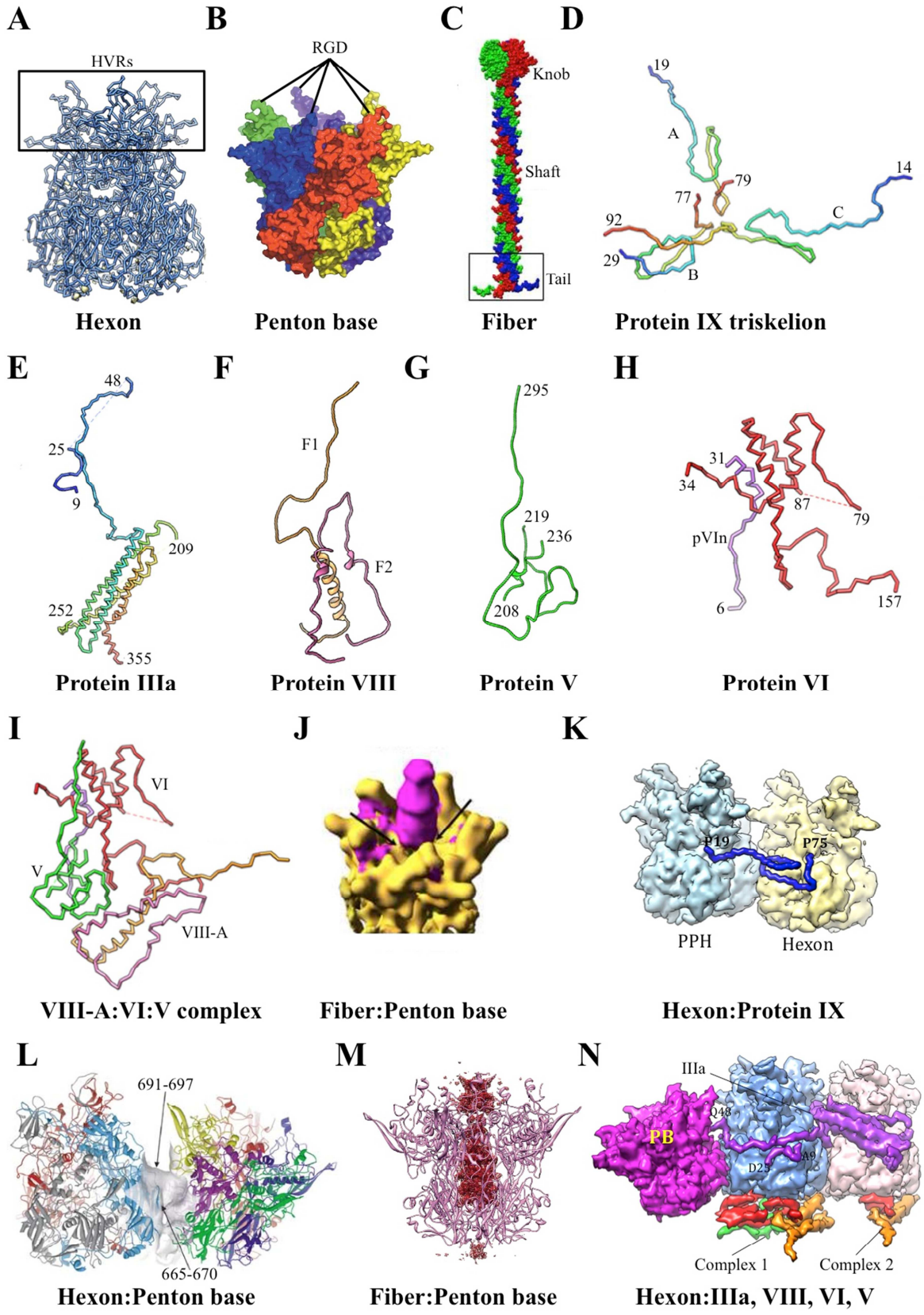

Figure 1-5. Adenoviral capsid structural proteins and their interactions. Ribbon diagram of the ordered segments of hexon (A), protein IX triskelion (D), protein IIIa (E), protein VIII (F), protein V (G), protein VI (H), VIII-A:VI:V complex (I), peripentonal hexon (PPH) and penton base (L) and fiber N-terminal tail and penton base (M). Cryo-Electron Microscopy or X-ray diffraction structure and molecular dynamic flexible fitting (MDFF) simulation of penton base (B) and fiber (C) with each monomer coloured uniquely, and simulation of the interactions between the fiber N-terminal tail and penton base (J), between hexons and protein IX (K) and between hexons, protein IIIa, VIII, VI and V (N). Complex 1 composed of proteins VIII-A, VI and V, and complex 2 of proteins VIII-B and VI are shown (N). Three molecules of protein IX

(labelled as “A”, “B” and “C”) are shown in (D), and fragment 1 (F1) and 2 (F2) of protein VIII in (F). Black arrows in (J) indicate sites of interactions between fiber and penton base. Fiber is represented in magenta in (J) and red in (M), penton base in yellow in (J), light pink in (M), multicolored in the right position in (L) and magenta in (N), hexons in light blue, light yellow or light tan in (K and N) and multicolored in the left position in (L), protein IX in dark blue in (K), protein IIIa in purple in (N), protein V in green (N), protein VI in red (N) and protein VIII in orange (N). Certain protein residues are labelled in (D-H, K and N) and two out of the three interacting hexon loops with the penton base are indicated in (L). HVR; hypervariable regions, RGD; arginine-glycine-glutamic acid residues, pVIn; pre-protein VI cleaved N-terminal, PB; penton base. Figures from (A), (D-I), (K) and (N) adapted from (Reddy and Nemerow, 2014). Figure in (B) adapted from (Zubieta et al., 2005). Figures in (C) and (J) adapted from (Liu et al., 2011). Figures in (L) adapted from (Fabry et al., 2005). Figure in (M) adapted from (Nemerow et al., 2012).

Protein IIIa and IX are the only cement proteins that stabilize the adenovirus capsid from the capsid exterior (Figure 1-4D left two panels). The Protein IIIa structure was shown to be predominantly composed of an α-helix with one 3-stranded β-sheet (Liu et al., 2010). This structure was later updated to a long extended polypeptide forming the N-terminal and an antiparallel very well ordered four-helix bundle structure [originally assigned to protein IX (Liu et al., 2010)], composed of two long helix-turn-helix motifs and a disordered region (Reddy and Nemerow, 2014) (Figure 1-5E). This protein was initially described to be located under the capsid vertices inside the virion (San Martin et al., 2008) but later shown to present its C-terminal on the capsid exterior (Reddy and Nemerow, 2014). Protein IIIa simultaneously interacts via the protein IIIa N-terminal domains with the peripentonal hexons (PPH) reaching the penton base and it has been suggested that it also interacts with another protein IIIa molecule (Liu et al., 2010, Reddy and Nemerow, 2014) (Figure 1-5N). Protein IX is located at the facet edges at the outer part of the capsid (Reddy and Nemerow, 2014). Initial studies showed an exceptionally extended and flexible conformation composed of an N-terminal domain, a rope domain and a long 12-turn helix-bundle domain (Liu et al., 2010). Importantly, a recently updated structure of protein IX reversed the chain direction placing the C-terminal to the capsid exterior and assigned the four-helix bundle to protein IIIa (Reddy and Nemerow, 2014). Based on the initial structure, this protein was described to interact via the C-terminal α-helix of different copies of protein IX with hexon by forming a 4-helix bundle (Fabry et al., 2009, Liu et al., 2010, Saban et al., 2006, Marsh et al., 2006). However, later studies showed these interactions correspond to protein IIIa (Reddy and Nemerow, 2014). Also, different copies of protein IX were shown to interact with each other via the N-terminal β-strand forming trimeric triskelion-like structures at the GON (Furcinitti et al., 1989, Liu et al., 2010). According to the updated model, the triskelion-like structures are formed with the C-terminal and not the N-terminal of protein IX (Figure 1-5D), and while the triskelion-like structures stabilize the hexons within the GON, the N-terminal of each protein IX simultaneously interacts with the PPHs (Reddy and Nemerow, 2014) (Figure 1-5K).

Protein VI, VIII and V act as cement proteins stabilizing the adenovirus capsid from the capsid interior (Figure 1-4D right two panels). Originally, protein VIII was described to be a protein located in the inner part of the capsid composed of an ordered helix, an inverted U-shaped structure and an extended polypeptide chain (Reddy et al., 2010, Liu et al., 2010). Later studies showed that pre-protein VIII is cleaved by AVP into three fragments, which combine to form two structurally distinct copies of protein VIII: VIII-A containing fragments 1 (composed of an ordered helix and an inverted U-shaped structure) and fragment 3 (composed of an extended polypeptide chain), and VIII-B only containing fragment 1 (Reddy and Nemerow, 2014) (Figure 1-5F). This study showed that while protein VIII-A forms a complex with protein VI and V by direct binding (complex 1), VIII-B only binds to protein VI (termed VI-B for convenience) (complex 2) (Figure 1-5I and N). Thus, complex 1 was reported to stabilize PPHs with the GON from underneath the capsid vertex via interactions mediated by protein VIII-A and VI, and complex 2 to stabilize the hexons within the same GON at each facet via interactions with both VIII-B and VI-B (Figure 1-4D right two panels). Protein VI has unstructured C and N-terminals and a helical core and is localized in the inner part of the capsid (Reddy and Nemerow, 2014) (Figure 1-5H). Reddy *et al.* showed that after proteolysis by AVP, the cleaved peptide corresponding to the first 33 N-terminal residues of pre-protein VI is separated from the rest of the molecule but remains bound to the PPH (Reddy and Nemerow, 2014). The same study proposed that the next 34-50 residues of the cleaved protein VI, which are involved in endosomal membrane penetration, can adopt a helical conformation upon contact with endosomal membranes. Also, this region as well as the α-helix and the C-terminal of protein VI were described to interact with PPHs, joining them to the adjacent GON. Interestingly, this study also showed that protein VI can interact with protein V and VIII. As described above, protein VI can stabilize the capside via formation of two different complexes by associating with protein V and VIII-A (complex 1) or only with VIII-B (complex 2) (Figure 1-5I and N). Protein V is a core protein composed of an ordered C-terminal with two α-helix, and a disordered and extended N-terminal (Reddy and Nemerow, 2014) (Figure 1-5G). Via the C-terminal it associates with protein VI and the fragment 3 of VIII-A (Figure 1-5I and N), and via the N-terminal with the viral DNA.

Despite the general capsid architecture being conserved among genera, there are genus-specific proteins that confer unique features to the capsid structure. For instance, *Atadenovirus* lacks proteins V and IX from *Mastadenovirus,* which are replaced by proteins p32k and LH3 (Pantelic et al., 2008). In particular, LH3 confers stability to the adenoviral capsid by binding to hexons from the outer part of the capsid where it locates on

top of hexons (Pantelic et al., 2008). Likewise, non-human adenovirus (NHAdV) canine serotype 2 (CAV-2), a member of the *Mastadenovirus* genera, displays some structural differences compared to human adenovirus. CAV-2 exhibits a smooth structure where many of the external penton base and hexon loops are shorter or absent in comparison to human adenovirus (HAdV) (Schoehn et al., 2008). Conversely, the fiber shows a more complex structure with two bends in the shaft at repeats 4 and 10, and the C-terminal of protein IX is located on the outer part of the capsid (Schoehn et al., 2008). Furthermore, there are also structural differences among HAdV serotypes. One of the clearest differences corresponds to the length and the flexibility of the fiber shaft. While species C have fibers with 18 or 22 shaft repeats, species A have longer and more flexible fibers with 23 shaft repeats and species B, D and E have shorter and more rigid fibers with 6, 8 or 12 fiber shafts, respectively [reviewed by (Arnberg, 2012)]. Interestingly, species F display two different fibers on the capsid, a long one with 21 or 22 fiber shafts and a shorter one of 12 (Kidd et al., 1993, Yeh et al., 1994). Also, two different fibers have been reported in species G, which include a long one of 17 fiber shaft repeats and a shorter one of 9 (Jones et al., 2007). Importantly, the short and long fibers of species F and G bind different host cell receptors (Roelvink et al., 1998, Lenman et al., 2015). Similarly, differences in the penton base have been reported, with species F not containing an RGD motif in contrast to other HAdV serotypes (Albinsson and Kidd, 1999). Capsid protein structure differences might have important implications during host cell receptor recognition, virion internalization or capsid disassembly and assembly processes as well as implications for virion recognition by the anti-viral host immune response.

1.2.2 Human adenovirus “life” cycle

1.2.2.1 Adenovirus internalization

The classical species C HAdV *in vitro* cell entry pathway (Figure 1-6) starts with the attachment to its primary receptor the coxsackie and adenovirus receptor (CAR) (Bergelson et al., 1997, Tomko et al., 1997), which also serves as a receptor for species A, D, E, F and G adenoviruses (Roelvink et al., 1998, Lenman et al., 2015). Binding to CAR is made via interactions between the extracellular domains of CAR and the lateral interface between two adjacent fiber knob domains (Roelvink et al., 1999, Lortat-Jacob et al., 2001, Freimuth et al., 1999, Kirby et al., 2000, Bewley et al., 1999, Excoffon et al., 2005), and this first interaction induces clustering of multiple CAR proteins (Burckhardt et al., 2011). Soon after, the RGD motif in the penton base interacts with $\alpha_v\beta_1$, $\alpha_3\beta_1$, $\alpha_M\beta_2$, $\alpha_v\beta_3$ or $\alpha_v\beta_5$ integrins (Salone et al., 2003, Li et al., 2001, Davison et al., 1997, Wickham et al., 1993,

Chiu et al., 1999, Mathias et al., 1998, Davison et al., 2001, Huang et al., 1996). In particular, binding to CAR gives rise to diffusive and drifting motions that together with virus attachment to immobile integrins promotes the release of fiber from virions and thus the start of capsid disassembly (Nakano et al., 2000, Burckhardt et al., 2011). Interestingly, the released fiber remains associated with the plasma membrane for up to 30 to 60 min (Greber et al., 1993). Also, this first capsid disassembly event results in the exposure of pVI from the capsid (Burckhardt et al., 2011). $\alpha_v\beta_1$, $\alpha_v\beta_3$ and $\alpha_v\beta_5$ integrins act as secondary HAdV-5 receptors to promote viral internalization (Wickham et al., 1993, Wickham et al., 1994, Mathias et al., 1998, Shayakhmetov et al., 2005a, Salone et al., 2003), which takes place 5 min after receptor-recognition (Greber et al., 1993) and is mediated via clathrin-mediated endocytosis and involves the cytosolic GTPase dynamin (Patterson and Russell, 1983, Meier et al., 2002, Wang et al., 1998, Chardonnet and Dales, 1970a). In this process, $\alpha_v\beta_3$ and $\alpha_v\beta_5$ integrins recruit the adaptor complex AP-2 to facilitate viral endocytosis (Honing et al., 2005, Robinson, 2004). Also, binding of HAdV-5 to integrins leads to integrin clustering, which activates signalling pathways such as p85/p110 phosphoinositide-3-OH kinase (PI3K) via the activation of the p85 subunit (Li et al., 1998b, Li et al., 1998a). $PI(3,4)P_2$ and $PI(3,4,5)P_3$ [products of PI3K activation (Simonsen et al., 2001)] activate Rab5 GTPase that regulates endocytosis and homotypic vesicular fusion with early endosomes (Rauma et al., 1999, Zerial and McBride, 2001). Also, peripheral trafficking of endocytic vesicles containing virus requires protein kinase C (PKC) (Nakano et al., 2000), which is activated by $PI(3,4,5)P_3$ (Nakano et al., 2000). In addition, PI3K prepares the host cell for trafficking of endosomes and viral particles along the microtubule network by activating Rac1 and CDC42, members of the Rho family of GTPases that are involved in the polymerization of monomeric actin and reorganization of actin filaments (Li et al., 1998a). Further viral capsid disassembly occurs in the endocytic pathway and, between 40 and 150 min after internalization, the hexon is partially degraded in a process dependent on endosomal and lysosomal proteases (Greber et al., 1993, Greber et al., 1996). Also, protein IIIa and protein VIII detach from the virion in endosomal vesicles within 15 min after adenovirus internalization and, 3 to 5 min later, the penton base dissociates from hexon (Greber et al., 1993). Interestingly, adenovirus was shown to trigger macropinocytosis, coincident with clathrin-mediated viral endocytosis, but its role has not been fully defined yet (Meier et al., 2002). Next, internalized adenoviral particles escape from early endosomes into the cytosol and only 5% of the incoming viruses are degraded in lysosomes (Greber et al., 1993). This process has been associated with protein VI, which penetrates the endosomes via the N-terminal amphipathic α-helix (Wiethoff et al., 2005, Moyer et al., 2011) introducing positive curvature strain to the membrane that

leads to membrane fragmentation (Maier et al., 2010). This process requires cleavage of pVI by AVP and is triggered by two separate signals: activation of AVP by acidification of endosomes and capsid disassembly via RGD-dependent interaction of penton base with integrin receptors (Greber et al., 1996, Shayakhmetov et al., 2005a, Burckhardt et al., 2011, Wang et al., 2000). In particular, $\alpha_v\beta_5$ integrins have been directly associated with the promotion of viral penetration from endosomes (Wickham et al., 1994). Also, PKC has been associated with adenovirus escape from endosomes (Nakano et al., 2000). When adenoviruses access the cytosol, the adenoviral nucleocapsid is mainly composed of hexon partially associated with protein VI and protein IX and contains the adenoviral DNA, which is condensed with proteins V, VII and X, covalently associated with the TP at each 5' DNA end and non-covalently associated with AVP (Wodrich et al., 2010, Xue et al., 2005). Adenoviral nucleocapsids are transported along the microtubule network via a bidirectional movement towards the nucleus (Suomalainen et al., 1999, Mabit et al., 2002, Dales and Chardonnet, 1973) in a process facilitated by the cytoplasmic dynein and dynactin (Suomalainen et al., 1999, Kelkar et al., 2004, Leopold et al., 2000). Also, it was recently reported that a PPxY motif (x being any amino acid) in protein VI recruits Nedd4-family E3 ubiquitin ligases resulting in protein VI ubiquitylation (Wodrich et al., 2010). Via an unknown mechanism, this event mediates the microtubule-dependent transport of protein VI, essential for transport of virions towards the nucleus (Wodrich et al., 2010). Importantly, upon adenovirus uptake, signalling pathways involved in transport of nucleocapsids along the microtubule network are also activated. These include cAMP-dependent protein kinase A (PKA), p38 mitogen-activated protein kinase (MAPK), and MAPKAP kinase 2 (MK2) that depends on MKK6 (Suomalainen et al., 2001, Bhat and Fan, 2002, Tibbles et al., 2002). PKA and P38 MAPK stimulate both the frequency and velocity of minus-end-directed viral motility along microtubules (towards the microtubule organizing centre (MTOC) adjacent to the nucleus), MK2 enhances the frequency of minus-end-directed virus transport, and p38 MAPK suppresses lateral viral motilities thus enhancing nuclear targeting (Suomalainen et al., 2001). Viral particles can be detected at the nuclear membrane by electron microscopy within 45 to 60 min post adenovirus uptake (Dales and Chardonnet, 1973, Greber et al., 1993) and adenoviral DNA and proteins V and VII within 60 to 120 min (Greber et al., 1997, Matthews and Russell, 1998). The mechanism by which adenoviral nucleocapsids dissociate from microtubules to interact with the cell nucleus has not been fully defined yet. However, the nuclear export factor exportin 1 (XPO1)/CRM1, which binds CAN/Nup214, has been proposed to be part of a sensor mechanism that triggers the detachment of nucleocapsids from microtubules proximal to the nucleus, allowing them to interact with the nuclear membrane (Strunze et

al., 2005). Once the nucleocapsid reaches the nuclear membrane, it interacts with CAN/Nup214 at the nuclear pore complex (NPC) (Strunze et al., 2011). Also, despite the majority of protein IX is lost from the capsid in the cytosol, with a 30 min half-time (Greber et al., 1993), it seems that adenoviral nucleocapsids bind to kinesin-1 light-chain (KLC)1 and 2 via protein IX (Strunze et al., 2011). Simultaneously, kinesin-1 heavy-chain KIF5c interacts with the nucleoporin Nup358, which is attached to the Nup214:Nup88 complex, mediating capsid disassembly and displacement of Nup214, Nup358 and Nup62 from the NPC towards the cell periphery (plus-end-directed motility), which in turn causes NPC disruption and thus increases nuclear envelope permeability (Greber et al., 1997, Strunze et al., 2011). These interactions recruit nuclear histone H1 via an unknown mechanism, and H1 binds to hexon (Trotman et al., 2001). Also, DNA-associated protein VII binds to H1 import factors importin α, importin β, importin 7 and transportin via nuclear localization signal (NLS)-containing regions present in protein VII (Wodrich et al., 2006, Hindley et al., 2007). As a result, H1-hexon complexes are imported into the nucleus leading to complete capsid disassembly and delivery of viral DNA, protein V, protein VI, protein VII and TP into the nucleus where DNA replication occurs (Trotman et al., 2001, Strunze et al., 2011, Greber et al., 1997, Xue et al., 2005, Wodrich et al., 2006, Hindley et al., 2007, Chatterjee et al., 1986, Matthews and Russell, 1998, Le et al., 2006, Fredman and Engler, 1993, Schreiner et al., 2012). Hsc70 has also been associated with import of viral DNA *in vitro* but its role has not been confirmed yet (Saphire et al., 2000). More recently it was reported that a significant fraction of the incoming viral genomes (~25%) is misdelivered to the cytosol as a consequence of virus docking and disassembly at the NPC and only a 6% to 48% is imported into the nucleus, a percentage that increases at higher viral multiplicity of infection (MOI) (Wang et al., 2013). Once the viral DNA is internalized into the nucleus, the TP forms a complex with the cellular CAD pyrimidine synthesis enzyme allowing correct location of adenoviral DNA for replication (Fredman and Engler, 1993, Angeletti and Engler, 1998). According to several reports, replication and transcription of early genes requires only viral DNA, protein VI and protein VII, and protein V may be dispensable (Xue et al., 2005, Haruki et al., 2006, Chatterjee et al., 1986, Schreiner et al., 2012), which is in agreement with the observed earlier dissociation of protein V from DNA in comparison to that of protein VII (Le et al., 2006, Puntener et al., 2011, Chatterjee et al., 1986). Replication-deficient adenoviral vectors (*E1A*-deficient) do not replicate their DNA and instead remain episomal in the nucleus of host cells or rarely integrated into the host genome (Harui et al., 1999, Stephen et al., 2008, Stephen et al., 2010). In the case of wild type adenovirus, replication of viral DNA and production of

viral proteins gives rise to a new generation of virions ready to lyse host cells and start a new viral cycle.

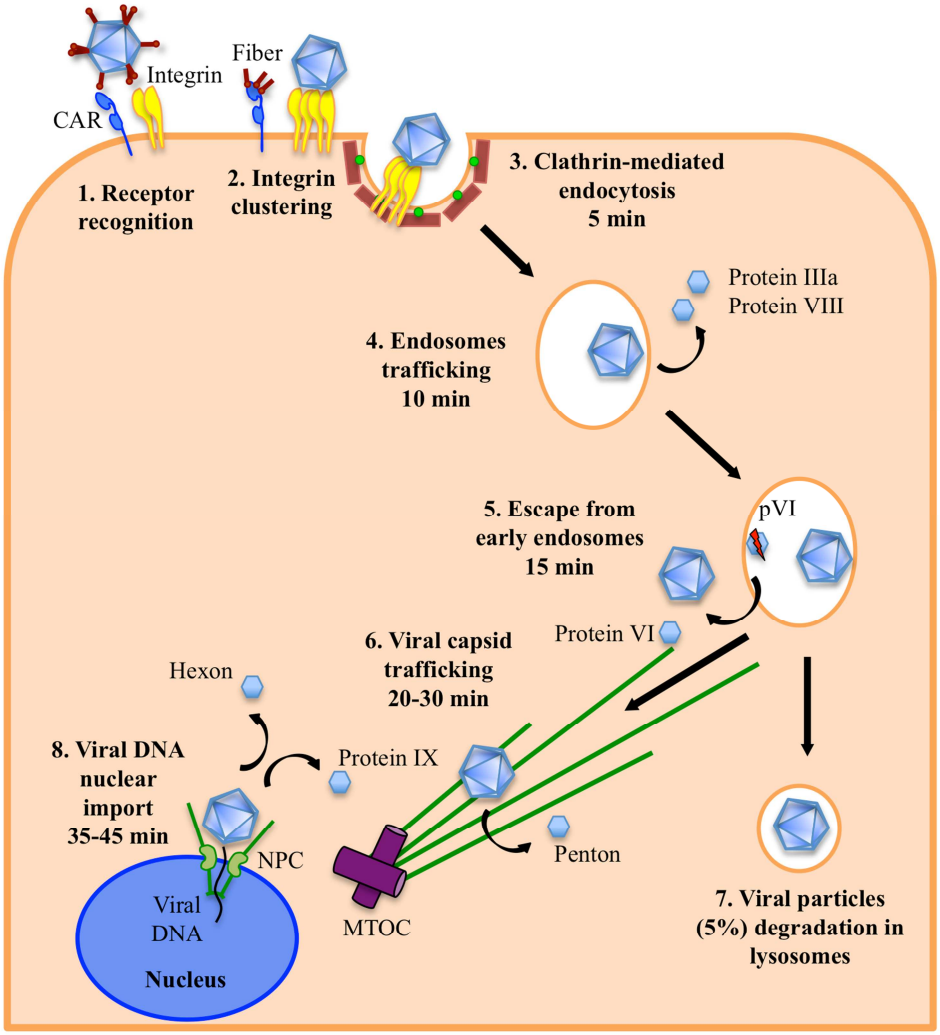

Figure 1-6. Classical species C human adenovirus *in vitro* transduction pathway. 1. Adenovirus attaches to the plasma membrane via CAR and $\alpha_v\beta_1$, $\alpha_3\beta_1$, $\alpha_M\beta_2$, $\alpha_v\beta_3$ and $\alpha_v\beta_5$ integrins. **2.** Adenovirus binding to integrins promotes integrin clustering leading to the activation of signalling pathways within the host cell. **3.** Adenoviral binding to $\alpha_v\beta_1$, $\alpha_v\beta_3$ and $\alpha_v\beta_5$ integrins promotes internalization of viral particles via clathrin-mediated endocytosis within 5 min after receptor recognition. **4.** Protein IIIa and protein VIII dissociate from viral capsids in the endosomes 10 min after receptor recognition. **5.** Adenoviral capsids escape from early endosomes 15 min after receptor recognition in a process mediated by protein VI that results in the partial degradation of pre-protein VI (pVI). **6.** Viral capsids travel along the microtubule network towards the nucleus and the penton dissociates from capsids during this process. **7.** A total of 5% of the incoming adenoviruses get degraded in the lysosomes. **8.** Protein IX dissociates from the viral capsid at the nuclear pore complex (NPC) and adenoviral DNA is imported into the nucleus along with proteins V, VI and VII and terminal protein (TP). MTOC; microtubule-organizing centre.

Importantly, other receptors have also been associated with HAdV-5 cell transduction. These include vascular cell adhesion molecule-1 (VCAM-1) (Chu et al., 2001), α2 domain of the major histocompatibility complex-I (MHC-I-α2) (Hong et al., 1997, Davison et al., 1999), scavenger receptor (SR) (Khare et al., 2012), low-density lipoprotein receptor-related protein (LRP) (Shayakhmetov et al., 2005b) and complement receptor (CR)1

(Carlisle et al., 2009) (Table 1-1). Moreover, the use of adaptor molecules such as dipalmitoyl phosphatidylcholine (DPPC) (Balakireva et al., 2003), lactoferrin (Adams et al., 2009, Johansson et al., 2007), C4b-binding protein (C4BP) (Martin et al., 2003, Shayakhmetov et al., 2005b) or coagulation factors (see section 1.3.4.2) has also been reported (Table 1-1). The diversity of HAdV-5 interactions with host proteins together with the existence of other receptors such as desmoglein 2 (DSG2), sialic acid-containing glycoproteins, CD46, CD80 or CD86 that can be used by other adenovirus species [reviewed by (Arnberg, 2009, Arnberg, 2012, Hall et al., 2010)] (Table 1-1) and with the existence of species or serotype-specific endocytic pathways such as macropinocytosis (Amstutz et al., 2008, Kalin et al., 2010) and trafficking kinetics (Miyazawa et al., 2001, Chardonnet and Dales, 1970b, Shayakhmetov et al., 2003) demonstrates the high versatility of adenovirus to infect host cells within different environments.

1.2.2.2 Adenoviral DNA transcription and replication

Following delivery of viral DNA, proteins V, VI and VII and TP into the nucleus of the host cell, adenoviral genomes associate with promyelocytic leukemia-nuclear bodies (PML-NBs) and form viral replication centres (Puvion-Dutilleul and Puvion, 1990, Doucas et al., 1996). To repress incoming viral genomes from successful replication, a network of cellular processes get activated (see section 1.2.3). In return, early viral genes are expressed. Early proteins have two major roles during the infection process: they counteract the anti-viral immune response (see section 1.2.4) and induce the infected cell into the S-phase of cell cycle (synthesis phase) to support adenoviral DNA replication (Spitkovsky et al., 1996). Initiation of viral gene expression is mediated by protein VI, which via the PPxY motif activates the adenovirus E1A promoter for *E1A* expression (Schreiner et al., 2012). E1A binds to retinoblastoma tumor suppressor (pRb) (Buchkovich et al., 1990, Giordano et al., 1991, Dyson et al., 1989) leading to its dissociation from the transcription factor E2F and thus induction of progression into the S-phase (Bagchi et al., 1990). E1A also enhances the expression of cell division cycle 25A (CDC25A) and cyclin E, which are involved in the G1/S-phase transition (Spitkovsky et al., 1996), and regulates effectors of cyclin dependent kinase 2 (CDK2) (Alevizopoulos et al., 1998). Moreover, a role for E1A in epigenetic reprogramming for induction of the S-phase has been reported (Horwitz et al., 2008, Ferrari et al., 2008). In addition, during the early phase, E1A activates E1B and E2 early promoters for expression of *E1B* (Wu et al., 1987) and *E2* (Reichel et al., 1988). *E3* and *E4* expression is also activated by E1A through its interaction with ring finger protein 20 (RNF20), which recruits Paf1/RNA polymerase II

complex component (PAF1) to early genes enabling transcription (Jones and Shenk, 1979, Fonseca et al., 2013). Also, protein X was shown to bind to viral DNA (Anderson et al., 1989), and pre-protein X was reported to target the nucleolus and was associated with the accumulation of E2 early proteins via modulation of mRNA biogenesis (Lee et al., 2004). Mature viral transcripts of early genes are then exported from the nucleus into the cytoplasm, where protein synthesis occurs, in a XPO1-dependent manner (Schmid et al., 2012). Interestingly, E1A promotes expression of viral genes that can cooperate with E1A in inducing cells into the S-phase. This is the case of E1B 55K, which has been involved in the enhancement of cyclin E expression (Zheng et al., 2008). However, as a result of *E1A* expression, p53 is stabilized and subsequently induces cell cycle arrest at G_1 or cell apoptosis via the activation of downstream proteins (Lowe and Ruley, 1993, Debbas and White, 1993). To prevent death of the infected cell, E1B 19K and E1B 55K antagonize E1A-triggered p53-mediated apoptosis (Sabbatini et al., 1995, Teodoro and Branton, 1997, Debbas and White, 1993). In particular, E1B 55K interacts with p53 (Kao et al., 1990) and represses transcriptional activation of p53-inducible genes (Yew et al., 1994, Martin and Berk, 1998, Martin and Berk, 1999). Also, E1B 55K forms a complex with E4 open reading frame 6 (E4 Orf6)/E4 34K that acts as an E3 ubiquitin ligase and mediates proteasomal degradation of p53 (Harada et al., 2002, Querido et al., 2001). Moreover, SUMOylation of E1B 55K allows E1B 55K to be imported into the nucleus, associate with PML-NBs and in turn SUMOylate p53 to promote its association with PML-NBs and thus its displacement from target sites (Endter et al., 2005, Endter et al., 2001, Muller and Dobner, 2008, Pennella et al., 2010, Wimmer et al., 2010). E4 Orf3/E4 11K has also been associated with the blockade of p53-dependent transcription of host proteins by inducing epigenetic changes on p53 target promoters and thus preventing p53 DNA-binding (Soria et al., 2010). Thus, via the action of viral proteins, adenoviruses block the anti-viral intracellular immune response and proceed to replicate their genome.

Adenoviral DNA replication involves adenoviral DNA polymerase, pTP, E2A and cellular proteins nuclear factor (NF)I and III [reviewed by (Challberg and Kelly, 1989, Stillman, 1989)] (Figure 1-7). The process is initiated with the formation of a complex between pTP and the adenoviral DNA polymerase (Parker et al., 1998, Brenkman et al., 2002) and the binding of pTP to the terminal dCMP of either ITR of the viral DNA, where it serves as a viral protein primer (Challberg et al., 1980, Rekosh et al., 1977). This DNA region is defined as the origin of replication (Tamanoi and Stillman, 1983, Challberg and Rawlins, 1984, Rawlins et al., 1984, Lally et al., 1984, Wides et al., 1987). NFI transcription factor binds to viral DNA in close proximity to the origins of replication and to the adenoviral

DNA polymerase and stabilizes the adenoviral DNA polymerase:pTP complex (Mul and Van der Vliet, 1992, Nagata et al., 1982, Bosher et al., 1990, Chen et al., 1990), stimulating initiation of replication (Leegwater et al., 1985, Rosenfeld et al., 1987, Nagata et al., 1983b). E2A enhances the rate of initiation of viral DNA replication by facilitating binding of NFI to viral DNA and is the primary determinant of the efficiency of DNA replication (Cleat and Hay, 1989, Stuiver and van der Vliet, 1990, Jones et al., 1987, Caravokyri and Leppard, 1996, Mul and van der Vliet, 1993). Furthermore, NFIII can also bind to viral DNA and stimulate DNA replication (Pruijn et al., 1986, Rosenfeld et al., 1987, O'Neill et al., 1988). The transition from initiation of replication to elongation of viral DNA takes place by a jumping back mechanism that is based on the formation of a pTP-CAT intermediate following pTP binding to dCMP, that is next coupled with an internal GTA triplet that jumps back from three positions forward [reviewed by (King and van der Vliet, 1994)]. This process ends with the dissociation of pTP from the adenoviral DNA polymerase (King et al., 1997). Next, the adenoviral DNA polymerase elongates the nascent DNA chains while E2A binds to and protects the exposed ssDNA (Nass and Frenkel, 1980, van der Vliet et al., 1978, Fowlkes et al., 1979, Lindenbaum et al., 1986). Of note, the topoisomerase NFII is required for replication of long DNA templates (Guggenheimer et al., 1984, Nagata et al., 1983a), and the host cell protein nucleophosmin (NPM1), which is relocated from the nucleolus to the nucleoplasm in a protein V-dependent manner, has also been associated with viral DNA replication (Ugai et al., 2012).

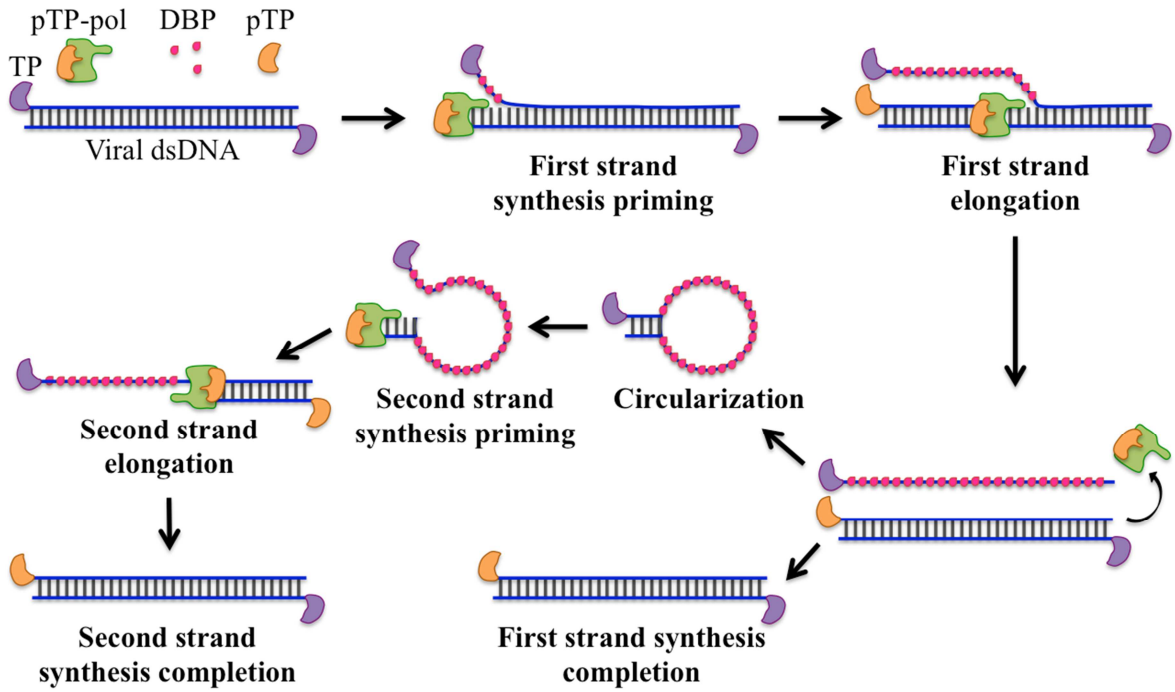

Figure 1-7. Adenovirus dsDNA replication mechanism. DBP; ssDNA-binding protein/E2A, pTP; pre-terminal protein, pol; adenoviral DNA polymerase.

When viral DNA replication is completed, newly synthetized dsDNA is transported to the periphery of the viral replication centres to serve as a template for expression of three different transcriptional units: protein IX, IVa2 and the MLTU for late gene expression (Pombo et al., 1994). Despite the majority of protein VII is removed from viral DNA upon entry into the nucleus, some molecules remain bound to DNA during the early phase of infection (Ross et al., 2011). These DNA-bound protein VII subsequently dissociate from viral DNA as a consequence of the transcription process via a mechanism that involves a structural change in the viral chromatin (Schreiner et al., 2013, Chen et al., 2007). IVa2 has been associated with the activation of transcription of late genes through the formation of a complex with L4-33K (Tribouley et al., 1994, Lutz and Kedinger, 1996, Pardo-Mateos and Young, 2004, Ali et al., 2007, Farley et al., 2004). The long primary transcript produced from MLTU accumulates in interchromatin granules and Cajal bodies (CBs) rosettes together with transcription and splicing factors, where it is processed and spliced for production of the viral late mRNAs (Aspegren et al., 1998, James et al., 2010, Bridge et al., 1995, Gama-Carvalho et al., 2003). The splicing process has been associated with E4 Orf4, L4-33K and L4-22K, as well as with cellular proteins PKA, DNA-dependent protein kinase (DNA-PK) and protein phosphatase IIA (PP2A) [(Brestovitsky et al., 2011, Morris and Leppard, 2009) and reviewed by (Biasiotto and Akusjarvi, 2015)]. The resultant transcripts are then exported into the cytoplasm in a process that is selective for viral transcripts mediated by the E1B 55K:E4 Orf6 complex and the cellular nuclear RNA export factor 1 (NXF1) (Woo and Berk, 2007, Blanchette et al., 2008, Yatherajam et al., 2011, Bridge and Ketner, 1990). Next, late mRNAs are translated in a process mediated by the viral L4-100K protein (Hayes et al., 1990), and newly synthetized late proteins are imported into the nucleus for virion assembly.

1.2.2.3 Adenoviral DNA packaging and capsid maturation

Adenoviral late proteins are synthetized in the cytoplasm. While the majority of viral proteins assemble independently in the cytoplasm, hexon trimers need the assistance of L4-100K, which binds to hexon monomers via one of the L4-100K globular domains and acts as a chaperone for hexon folding and self-assembly (Hong et al., 2005, Oosterom-Dragon and Ginsberg, 1981, Cepko and Sharp, 1982). Subsequently, viral proteins are imported into the nucleus for virion assembly. Unlike fiber and penton base oligomers, hexon trimers require the association with pVI to be imported into the nucleus (Kauffman and Ginsberg, 1976, Wodrich et al., 2003). Once in the nucleus, adenoviral structural proteins assemble to form a procapsid. Next, the newly synthetized adenoviral dsDNA is inserted

into the procapsid in a process dependent on the presence of an adenoviral DNA packaging signal and viral proteins IVa2 and L4-22K. The packaging signal is an A/T-rich sequence located at nucleotides 194 to 358 in HAdV-5 adjacent to the left ITR (Hearing et al., 1987). IVa2 is able to bind to the packaging signal and mediate DNA packaging into capsids via a mechanism that requires hydrolysis of ATP (Zhang and Imperiale, 2000, Ostapchuk et al., 2005, Ostapchuk et al., 2011, Ostapchuk and Hearing, 2008). In this process, L4-22K binds to and forms a complex with IVa2 that enhances IVa2 binding to the packaging signal (Ewing et al., 2007). Moreover, L1-52/55K, which is located beneath the vertex (Condezo et al., 2015), can bind to IVa2 (Perez-Romero et al., 2006) and also to the packaging signal in an IVa2 and sequence-independent manner (Perez-Romero et al., 2005, Zhang and Arcos, 2005) and play a role in viral DNA packaging (Gustin and Imperiale, 1998, Perez-Romero et al., 2005, Hasson et al., 1989). Furthermore, protein IIIa can also bind to the packaging signal and interact with L1-52/55K (Ma and Hearing, 2011), and protein VII and pre-protein VII (pVII) can bind to IVa2 and L1-52/55K as well as to viral DNA in a non-specific manner (Zhang and Arcos, 2005). Since protein IIIa is located at the capsid vertex, a possible role in signalling the position for viral DNA to be encapsidated has been proposed (Ma and Hearing, 2011). L4-33K, which is expressed at the early stages of the late phase of infection and localizes to the nucleus, was also shown to have a role in DNA packaging and to function as an alternative RNA splicing factor for pIIIa, pVI and fiber transcripts (Fessler and Young, 1999, Wu et al., 2013). Final maturation of the procapsid into infectious adenoviral particles requires the action of AVP, which moves along the viral DNA (McGrath et al., 2001a) until it finds a particular protein consensus sequence (Diouri et al., 1996) on the precursor of protein IIIa, VI, VII, VIII, X, TP and L1-52/55K and cleaves them to generate mature proteins (Tremblay et al., 1983, Boudin et al., 1980, Perez-Berna et al., 2014). Of note, the cleavage sequence is found in residue 570 of protein IIIa, residues 33 and 239 of VI, residues 13 and 24 of VII, residues 111, 131 and 157 of VIII, residues 27, 32 and 51 of X, residues 36, 66, 124, 275, 300, 351, 382 and 398 of L1-52/55K and residues 175, 183, 316 and 349 of TP [reviewed by (Mangel and San Martin, 2014)]. This event was found essential for successful infection of host cells, since viral capsids containing the precursor capsid proteins instead of the corresponding mature forms exhibit a more ordered and stable structure that impairs capsid disassembly (Silvestry et al., 2009, Perez-Berna et al., 2009). Also, the release of L1-52/55K from the capsid via proteolytic processing by the AVP was shown to facilitate genome release during capsid disassembly (Condezo et al., 2015). Moreover, it was reported that activation of AVP requires two events (Gupta et al., 2004, Mangel et al., 1993): first, AVP binds to viral DNA in a sequence-independent manner leading to a conformational change in AVP and

thus its partial activation (Mangel et al., 1993). Partially activated AVP cleaves pVI at the C-terminal and the cleaved peptide covalently binds to AVP resulting in a second conformational change that leads to its complete activation (Mangel et al., 1993, McGrath et al., 2003, McGrath et al., 2001b). Once mature infectious virions are formed, AVP prepares infected cells for viral progeny release by cleaving cytokeratin and thus inducing changes in the cell cytoskeleton (Chen et al., 1993b). In this process, actin was shown to bind to and activate AVP (Brown et al., 2002). Next, E3-11.6K/adenovirus death protein (ADP), which accumulates in infected cells towards the late stages of infection, induces lysis of infected cells via an unidentified mechanism involving the cellular protein MAD2 mitotic arrest deficient-like 2 (MAD2L2)/MAD2B (Tollefson et al., 1996b, Tollefson et al., 1996a, Ying and Wold, 2003) and thus allows virions release. Interestingly, fiber, penton base and hexon proteins are produced in excess during adenovirus late gene expression (Boulanger and Puvion, 1973, Rebetz et al., 2009). The excess protein produced was shown to promote the spread of progeny viruses to neighbouring cells by mediating disruption of cell-cell junctions in a process involving fiber:penton base:hexon complexes binding to basolateral CAR of infected and neighbouring cells (Walters et al., 2002, Zhang et al., 2015).

1.2.3 Anti-viral host immune response against adenovirus

The immune system is prepared to combat the biological threats that an organism may be subjected to. The first line of defence is based on mechanical barriers (e.g: skin or mucous membranes), on chemical barriers including anti-microbial substances that inhibit bacteria growth (e.g: salivary lysozyme), digestive enzymes, extreme pH or α-defensins secreted by Paneth cells, and on microbiological barriers such as the microbial flora, which produces bacteriocins and other anti-microbial peptides. The second line of defence is composed of the innate immunity, a conjunction of different cells and mechanisms (macrophages, mast cells, dendritic cells (DC), natural killer (NK) cells, the complement system, pattern recognition receptors (PRRs), etc.) that can trigger a non-specific acute inflammation process mediated by pro-inflammatory cytokines and chemokines, upon detection of threats. Finally, if the threat persists, phagocytes such as DCs migrate to the lymph nodes and activate adaptive immune responses, the third line of defence, which is mainly composed of B and T cells. Effector B cells and $CD8^+$ T cells or also called cytotoxic T lymphocytes (CTLs) are able to generate antigen-specific receptors (BCR or TCR, respectively) upon binding to specific antigens and reception of activation signals in a process mediated by Th2 or Th1-type $CD4^+$ T cells, which in turn require the presence of

active antigen presenting cells (APCs) or DCs to promote the expression of co-stimulatory molecules. As a result, effector B cells generate antigen-specific antibodies to neutralize microorganisms and viruses and $CD8^+$ T cells mediate cytolytic killing of infected cells. In particular, the anti-viral response is based on mechanisms to prevent infection of host cells such as neutralizing antibodies and complement, and on immune cells that eliminate infected cells such as NK cells or CTLs, which are driven by the release of interferon (IFN) and tumor necrosis factor (TNF)-α (reviewed by (Fensterl and Sen, 2009, Warren and Smyth, 1999, Lopez-Gordo et al., 2014a, Andersen et al., 2006) (Figure 1-8).

Neutralizing IgG antibodies (NAbs) can recognize specific epitopes on adenoviral capsid proteins (Sumida et al., 2005, Gall et al., 1996) such as the hexon (Roberts et al., 2006, Abe et al., 2009, Shiratsuchi et al., 2010, Bradley et al., 2012b, Hong et al., 2003), the fiber (Myhre et al., 2007, Bradley et al., 2012a, Yu et al., 2013, Hong et al., 2003, Gahery-Segard et al., 1998, Parker et al., 2009) or the penton base (Yu et al., 2013, Hong et al., 2003, Gahery-Segard et al., 1998), and form immune complexes that can be phagocytosed by macrophages via antibody constant fraction receptors (FcR) or recognized by FcR on NK cells [reviewed by (Gattoni et al., 2006, Warren and Smyth, 1999)]. These interactions also result in the production of type I (α and β) IFN and the maturation of caspase-dependent interleukin (IL)-1β (Zaiss et al., 2009). Moreover, adenovirus recognition by anti-hexon and anti-penton base antibodies results in the accumulation of virions in endocytic vesicles (Wohlfart, 1988). Similarly, circulating IgM antibodies negatively correlate with liver transduction (Khare et al., 2013). This is partly due to resident macrophages in the liver [Kupffer cells (KC)], which have FcR that can bind to IgM antibodies on virions (Xu et al., 2008), and partly due to complement component 3 (C3) receptor CRIg-dependent KC recognition of virions that have been opsonised by the complement system (He et al., 2013). Also, KC can bind to adenoviral capsids via scavenger receptors such as scavenger receptor A (SR-A)-II (Xu et al., 2008, Haisma et al., 2008, Khare et al., 2012) and undergo cell death following phagocytosis in a process dependent on adenovirus capsid disassembly and endosomal membrane penetration (Manickan et al., 2006, Smith et al., 2008). Another defence mechanisms dependent on the Fc portion of IgM or IgG antibodies is the cytosolic tripartite motif-containing protein 21 (TRIM21), which is a RING finger E3-ubiquitin ligase that depends on the host AAA ATPase valosin-containing protein (VCP) and the proteasome to degrade viral capsids (Mallery et al., 2010, Hauler et al., 2012). Furthermore, a recent report showed that upon IgM binding to virions and subsequent opsonisation of capsids by complement proteins *in vitro* (Cichon et al., 2001), receptor-ligand interactions of virions with host cells gets

blocked (Xu et al., 2013). Interestingly, while the classical complement pathway (IgM-mediated) plays a critical role in opsonizing virions *in vitro* (Xu et al., 2013), both the classical and non-classical pathways are apparent *in vivo* (Tian et al., 2009, Xu et al., 2008, Jiang et al., 2004), indicating that in the absence of IgM antibodies adenoviral capsids can activate and be opsonized by the complement system. Also, the complement system is involved in other processes such as adenovirus-induced thrombocytopenia, which is dependent on factor B and C3 of the alternative complement pathway and results in the induction of the nuclear factor-kappa B (NF-κB) upon C3 binding to adenoviral capsids (Appledorn et al., 2008a, Kiang et al., 2006). Furthermore, adenoviral DNA can trigger an innate immune response. Plasmacytoid DCs (pDCs) can recognize non-methylated viral CpG-containing DNA in the endosomes through Toll-like receptor (TLR)9, which via the myeloid differentiation primary response 88 (MYD88) results in the expression of pro-inflammatory genes and secretion of IL-6 and IL-12 (Yamaguchi et al., 2007, Zhu et al., 2007). Also, the activation of pDC by certain adenovirus serotypes such as HAdV-35 can lead to IFN-α production in a TLR9-dependent manner and subsequent NK cell activation (Pahl et al., 2012, Zhu et al., 2008), and immune complexes can induce DC maturation via TLR9 agonist motifs present in the adenoviral genome (Perreau et al., 2012). Furthermore, adenoviral DNA can also trigger TLR-independent responses on conventional DCs (cDCs) and macrophages (Basner-Tschakarjan et al., 2006, Zhu et al., 2007). Macrophages can detect adenoviral DNA in a TLR9-independent manner leading to the maturation of pro-IL-1β via a mechanism mediated by NOD-like receptor family pyrin domain containing 3 (NLRP3) and apoptosis-associated speck-like protein containing a caspase-recruitment domain (ASC), components of the innate cytosolic molecular complex called the inflammasome (Muruve et al., 2008), and that requires penetration of endosomal membranes (Barlan et al., 2011b, Barlan et al., 2011a). Also, binding of macrophage β_3 integrins with the adenovirus RGD motif promotes secretion of IL-1α (Di Paolo et al., 2009a). TLR2 has also been associated with NF-κB activation and humoral responses to adenovirus (Appledorn et al., 2008b). Moreover, the RNA sensor melanoma differentiation-associated protein 5 (MDA5) and cytosolic adenoviral DNA sensors such as absent in melanoma 2 (AIM2), TRAF family member-associated NF-κB activator (TANK)-binding kinase 1 (TBK1), DEAD-box helicase 41 (DDX41), DNA-dependent activator of IRFs (DAI), cyclic GMP-AMP synthase (cGAS), or the complex formed by NLRP3 with ASC and caspase-1, can lead to cytokine production (mainly type I IFN) upon adenovirus infection (Schulte et al., 2013, Stein and Falck-Pedersen, 2012, Steinstraesser et al., 2011, Nociari et al., 2007, Muruve et al., 2008, Lam et al., 2014). Interestingly,

adenovirus-induced rupture of endosomal membranes activates the NLRP3 inflammasome (Barlan et al., 2011b, Barlan et al., 2011a). Other proteins such as DDX58/retinoic acid-inducible gene I (RIG-I), which recognizes VA-I and II, have also been associated with adenoviral-induced innate immune responses (Minamitani et al., 2011). Also, other cell types such as erythrocytes or neutrophils contribute to anti-adenoviral immune responses through interactions with adenovirus capsids via CAR, CR1 or FcR (Carlisle et al., 2009, Cotter et al., 2005). Importantly, the production of type I IFN by infected cells or immune cells such as DC or macrophages promotes an anti-viral state in neighbouring non-infected cells by triggering the expression of anti-viral enzymes such as MxA, 2',5'-oligoadenylate synthase and eukaryotic translation initiation factor 2 α kinase 2 (EIF2AK2)/protein kinase RNA-activated (PKR) via Jak-STAT signalling (Katze et al., 2002). Also, type I IFN leads to the maturation of DC by up-regulating the expression of co-stimulatory molecules such as CD80, CD86 and CD40 (Vujanovic et al., 2009). The production of type II IFN (IFN-γ) by NK cells also contributes to the promotion of an anti-viral state, for instance, by inducing the expression of major histocompatibility complex class I (MHC-I) on non-immune cells as well as MHC-II on professional APC [reviewed by (Gattoni et al., 2006)], which use it to present antigens to naive $CD4^+$ T cells TCR and thus initiate an adaptive immune response. Furthermore, IFN-γ and TNF-α inhibit early adenovirus transgene expression via a transcription-related mechanism (Mestan et al., 1986, Sung et al., 2001). TNF-α, which is produced by macrophages and lymphocytes, is also able to induce apoptosis of infected cells by binding to its receptors TNF-related apoptosis-inducing ligand (TRAIL) 1 and 2 (Wong and Goeddel, 1986, Nagata, 1997). Activated macrophages and DC also release IL-12, which leads to the differentiation of naive $CD4^+$ T cells into T helper (Th)1-type $CD4^+$ T cells and contributes to IFN-γ secretion by Th1-type $CD4^+$ T and $CD8^+$ T cells [(Akira, 2000) and reviewed by (Jankovic et al., 2001)] and thus further enhances the overall immune response. However, for complete T $CD8^+$ cells activation, both the presence of Th1 or Th2-type $CD4^+$ T cells and antigen presentation by DCs via MHC-I are needed (Albert et al., 1998, Ekkens et al., 2007, Schumacher et al., 2004). Effector $CD8^+$ T cells can then produce a cytotoxic response towards the infected cell that ends with apoptosis. Also, NK cell activation *in vitro* relies on the contribution of T cells (Pahl et al., 2012), suggesting a reciprocal interaction between immune cells for their activation. On the other hand, upon interaction of Th2-type $CD4^+$ T cells TCR with MHC-II:antigen complex from B cells that have previously recognized and internalised an antigen via their BCR, Th2-type $CD4^+$ T cell gets activated and produces cytokines that in turn initiate a process of BCR isotype switching on the B cell resulting in its maturation towards a plasma antibody-producing B cell [reviewed by (Jankovic et al., 2001)]. Also, B

cells as well as neutrophils, macrophages, and T cells express α-defensins [reviewed by (Selsted and Ouellette, 2005)], which have been postulated to bind to the adenoviral capsid in a RGD motif-dependent manner based on cryoEM and molecular dynamic flexible fitting (MDFF) simulations (Flatt et al., 2013) and block the disassembly of capsids (Smith and Nemerow, 2008, Smith et al., 2010, Snijder et al., 2013).

Finally, non-immune cells can also activate immune responses upon adenovirus infections. For instance, epithelial cells and renal epithelium-derived cells (REC) can activate the immune system in a CAR or RGD-dependent manner, respectively (Tamanini et al., 2006, Liu et al., 2005), and induce the expression of CXCL10/IFN-inducible protein 10 (IP-10) via NF-κB signalling. Also, epithelial cells and mucosal tissue can release β-defensins (Pazgier et al., 2006).

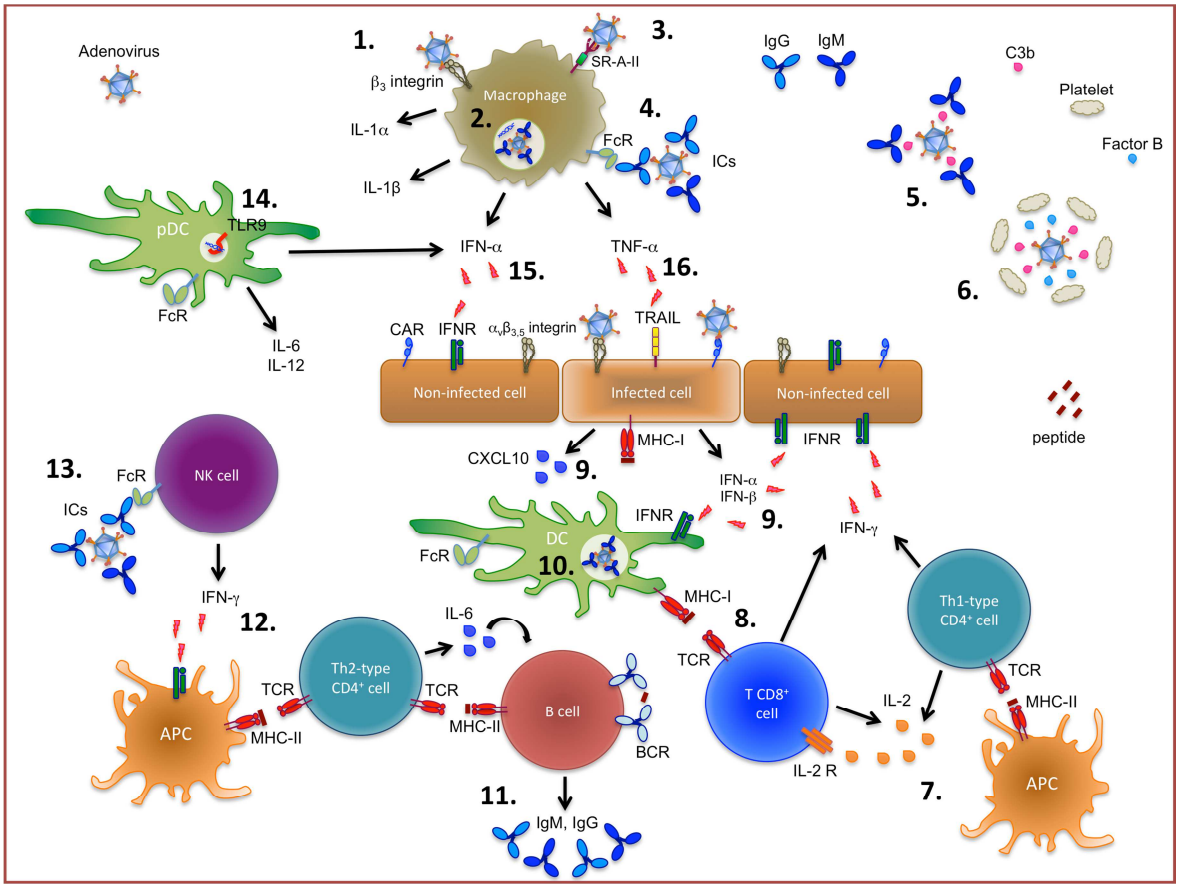

Figure 1-8. Innate and adaptive anti-adenoviral immune response. 1. Maturation of interleukin (IL)-1α upon binding of macrophage β_3 integrins to adenovirus penton base RGD motif. **2.** Maturation of IL-1β upon recognition of adenoviral dsDNA by macrophages. **3.** Binding to adenoviral capsid via scavenger receptor A (SR-A)-II. **4.** Macrophage maturation upon phagocytosis of immune complexes (ICs) via antibody constant fraction receptors (FcR). **5.** Adenovirus neutralization via the IgM-mediated classical complement pathway. **6.** Thrombocytopenia resulting from the activation of the alternative complement pathway on adenoviral capsids. **7.** Production of IL-2 by Th1-type $CD4^+$ T cells upon antigen presentation by antigen presenting cells (APCs) via major histocompatibility complex class II (MHC-II), and IL-2-mediated activation of $CD8^+$ T cells. **8.** Activation of $CD8^+$ T cells as a result of antigen presentation by dendritic cells (DC) via MHC-I. **9.** Secretion of interferon (IFN)-α and β by infected cells and expression of CXCL10 upon adenovirus

binding to CAR or $\alpha_v\beta_{3,5}$ integrins. **10.** Maturation of DCs via phagocytosis of ICs. **11.** B cell maturation and isotype switching following antigen presentation to Th2-type $CD4^+$ T cells. **12.** IFN-γ-mediated induction of MHC-II on APCs and antigen presentation to Th2-type $CD4^+$ T cells. **13.** Recognition of ICs via FcR on NK cells. **14.** Secretion of IL-6 and 12 by plasmacytoid dendritic cell (pDC) upon adenoviral dsDNA recognition via Toll-like receptor (TLR)9. **15.** Secretion of IFN-α upon macrophage or pDC activation leading to the induction of an anti-viral state on non-infected cells. **16.** Secretion of tumor necrosis factor (TNF)-α upon macrophage activation resulting in TNF-related apoptosis-inducing ligand (TRAIL) 1 and 2-mediated apoptosis of infected cells. CAR; coxsackie virus and adenovirus receptor, C3b; complement component 3b, IFNR; interferon receptor; BCR; B cell receptor, TCR; T cell receptor. Figure adapted from (Lopez-Gordo et al., 2014b).

1.2.4 Adenovirus evasion of host immune response

Despite the high complexity and efficiency of the immune system to stop viral infections, adenoviruses evolved to attenuate the anti-viral innate immune response and even to benefit from it to boost infection events. The key players are adenoviral proteins E1, E3 and E4 together with protein VI, protein VII and adenoviral RNAs (Table 1-2).

In addition to controlling viral gene expression, the cell cycle and apoptosis, E1A protein also has a role in other processes such as immune suppression (Ferrari et al., 2008). Taking a focus on the latter, E1A blocks the response to IFN-α by inhibiting the binding of IFN-stimulated gene factor 3 (ISGF3) transcriptional complex to the interferon-stimulated response element (ISRE), which is in turn required for ISGF3 expression (Gutch and Reich, 1991, Kalvakolanu et al., 1991). The mechanism by which E1A inhibits ISGF3 binding to ISRE was found to involve E1A blocking binding of the signal transducer and activator of transcription (STAT)2 domain of ISGF3 to acetyltransferase p300 and/or CREB-binding protein (CBP) (Bhattacharya et al., 1996). Since p300 and CBP are transcription adaptors for ISGF3, the inhibition of their binding to ISGF3 results in the repression of STAT2 transactivation (Bhattacharya et al., 1996). Interestingly, the conserved region (CR)1 of E1A was found indispensable in this process (Gutch and Reich, 1991, Kalvakolanu et al., 1991, Ackrill et al., 1991). E1A can also inhibit IFN-stimulated gene (ISG) expression by binding to the RNF20 complex, which catalyses histone 2B (H2B) monoubiquitination for activation of gene expression as a response to IFN (Fonseca et al., 2012). Moreover, E1A was reported to inhibit the induction of MHC-II by IFN-γ as well as the production of IFN-β in response to dsRNA (Ackrill et al., 1991). In order to block the presentation of peptides to the immunoproteasome, E1A interacts with the immunoproteasome subunit beta (PSMB)10/MECL1 and modulates STAT1 phosphorylation, which results in the downregulation of the IFN-γ-induced PSMB10, PSMB9/LMP2 and PSMB8/LMP7 expression (Berhane et al., 2011b). Likewise, E1B is also involved in attenuating immune responses. E1B 19K blocks TNF-α-induced apoptosis by binding to the apoptosis inducers BAK and BAX and thus preventing them from

forming functional oligomers (Chiou et al., 1994, White et al., 1992, Sundararajan and White, 2001). E1B 55K represses transcription of ISGs allowing the formation of viral replication centres (Chahal et al., 2012, Chahal et al., 2013). E1B 55K also inhibits expression of genes that induce synthesis of IFN such as DDX58, MDA5, interferon regulatory factor (IRF)7 and MYD88 (Miller et al., 2009). Moreover, it was shown that E1B 55K interacts with E4 Orf6 and cellular proteins cullin (CUL)5, RBX1 and elongins B and C to assemble an SCF (Skp, CUL, F-box)-like E3-ubiquitin ligase complex (Harada et al., 2002, Querido et al., 2001) that triggers proteasome-mediated degradation of p53 (Harada et al., 2002, Querido et al., 2001), MRE11 (Stracker et al., 2002), DNA ligase IV (Baker et al., 2007), Bloom helicase (BLM) (Orazio et al., 2011), integrin α3 (Dallaire et al., 2009) and TIP60 (Gupta et al., 2013). Via the degradation of DNA ligase IV, which is responsible for non-homologous end joining (NHEJ) (Grawunder et al., 1998), and the degradation of MRE11 that is a component of the MRE11-RAD50-NBS1 (MRN) complex involved in double strand break (DSB) repair and formation of viral genome concatemers, adenovirus prevents the induction of DNA damage signalling during viral replication and viral genome concatenation that would otherwise interfere with the packaging of viral DNA into virions (Weiden and Ginsberg, 1994). TIP60 is an acetyltransferase involved in histone acetylation to regulate gene expression, DNA damage response (DDR), apoptosis and cell cycle and it binds to the E1A promoter and acetylates histone 4 (H4) to suppress *E1A* gene expression (Sun et al., 2009, Gupta et al., 2013). Degradation of TIP60 by the E1B 55K:E4 Orf6 complex allows viral early gene transcription (Gupta et al., 2013). Furthermore, the E1B 55K:E4 Orf6 complex triggers proteasome-mediated degradation of SPOC1 (Schreiner et al., 2013), which is involved in chromatin condensation and in the DDR to DSBs and leads to the repression of viral gene expression at the level of transcription (Schreiner et al., 2013, Mund et al., 2012). Finally, E1B 55K also mediates proteasomal degradation of death domain-associated protein (DAXX) by acting as a CUL5-dependent E3-ubiquitin-ligase in a process that is independent of E4 Orf6 (Schreiner et al., 2010). Since DAXX forms a complex with ATP-dependent helicase (ATRX) [reviewed by (Salomoni and Khelifi, 2006)] and represses viral replication by silencing viral gene expression (Tavalai et al., 2008), degradation of DAXX allows viral DNA replication.

E3 proteins play a key role in the modulation of the anti-viral immune response [reviewed by (Lichtenstein et al., 2004)]. E3 19K has two main functions: inhibition of T cell recognition of infected cells and inhibition of NK cell activation. To prevent $CD8^+$ T cell activation, E3 19K inhibits transport of MHC-I to the plasma membrane by retaining this

molecule in the endoplasmic reticulum (ER) (Burgert and Kvist, 1985, Burgert et al., 1987, Cox et al., 1991). Via E1A and p300-dependent (Routes et al., 2005) or E1A-independent mechanisms (Tomasec et al., 2007), adenovirus transduction results in the upregulation of proteins that can bind to the killer cell lectin like receptor C1 (KLRC1)/NKG2D, which is a receptor expressed on NK cells and T cells (Bauer et al., 1999). To counteract this process, E3 19K sequesters KLRC1 ligands such as the MHC-I chain-related protein A and B (MICA and MICB) in the ER and thus prevents their expression on the plasma membrane and subsequent recognition by KLRC1 (McSharry et al., 2008). Moreover, a complex formed by E3 10.4K/receptor internalization and degradation (RID)-α and E3 14.5K/RID-β (Stewart et al., 1995, Gooding et al., 1991, Tollefson et al., 1991) induces internalization and degradation of death-domain-containing receptors of the TNFR superfamily such as Fas cell surface death receptor (FAS) (Burgert et al., 2002, Elsing and Burgert, 1998, Hilgendorf et al., 2003, Tollefson et al., 1998, McNees et al., 2002) or the epidermal growth factor receptor (EGFR) (Hilgendorf et al., 2003, Carlin et al., 1989, Tollefson et al., 1991). Also, E3 10.4K:E3 14.5K complex together with E3 6.7K inhibits ligand-induced apoptosis in infected cells by down-regulating TRAIL 1 and 2 (Burgert et al., 2002, Benedict et al., 2001, Hilgendorf et al., 2003). Furthermore, E3 14.7K supresses the cytolytic and pro-inflammatory functions of TNF-α (Burgert et al., 2002, Horton et al., 1991).

In similarity to E4 Orf6, E4 Orf3 can associate with E1B 55K and form a complex that prevents concatemer formation (Weiden and Ginsberg, 1994). Also, it was reported that both E4 Orf6 and 3 can bind to DNA-PK, which is involved in the DSB repair response [reviewed by (Jeggo et al., 1995)], and thus inhibit viral genome concatenation (Boyer et al., 1999). The E1B 55K:E4 Orf3 complex also mediates SUMOylation of cellular proteins (Sohn and Hearing, 2012). Moreover, E4 Orf3 has been associated with the disruption of PML spherical nuclear bodies, which localize adjacent to viral replication centres and respond to IFN [(Stadler et al., 1995, Grotzinger et al., 1996) and reviewed by (Regad and Chelbi-Alix, 2001)], and their reorganization into track-like structures (Doucas et al., 1996, Stracker et al., 2002, Carvalho et al., 1995). In particular, E4 Orf3 was reported to interact with PMLII, an isoform of PML protein (Hoppe et al., 2006, Leppard et al., 2009), and this interaction was necessary for PML-NB reorganization into track-like structures (Hoppe et al., 2006). Simultaneously, E4 Orf3 also interacts and relocates cellular proteins such as speckled protein 100kDa (Sp100) (Carvalho et al., 1995), TIF1α (Yondola and Hearing, 2007), or the MRN complex (Stracker et al., 2002, Evans and Hearing, 2005, Carson et al., 2009, Stracker et al., 2005) into these structures. Since Sp100 is an IFN-inducible protein

with a role in activation and repression of transcription (Grotzinger et al., 1996), re-localization of Sp100 may prevent its anti-viral action. The role of TIF1α in an anti-viral immune response is unclear (Yondola and Hearing, 2007).

Other viral proteins such as protein VI, protein VII and TP have also been associated with the evasion of anti-viral immune responses. Protein VI prevents DAXX-mediated repression of viral gene expression by interacting with and displacing DAXX from the PML-NB and translocating it into the cytoplasm (Schreiner et al., 2012). Binding of protein VII to adenovirus genomes prevents DNA sensing and activation of the MRN complex during viral DNA replication, which would otherwise lead to viral genome concatenation (Karen and Hearing, 2011), as well as activation of SPOC1 (Schreiner et al., 2013). Also, a recent study reported that protein VII can associate with cellular histones and form complexes with nucleosomes following post-translational modification (Avgousti et al., 2016). In particular, this study showed that protein VII binds to high mobility group box 1 (HMGB1) and retains it in the chromatin. Since HMGB1 is secreted from immune cells (Lotze and Tracey, 2005, Kang et al., 2014), its retention in the chromatin prevents HMGB1-associated immune responses (Avgousti et al., 2016). Furthermore, adenoviral RNA VA-I blocks activation of the IFN-inducible EIF2AK2, which represses protein synthesis in response to dsRNA [(O'Malley et al., 1986) and reviewed by (Mathews and Shenk, 1991)], and is involved in selective translation of viral mRNAs over host cell protein (O'Malley et al., 1989). VA-I and II are also processed to 5’ and 3’ small viral RNAs (svaRNAs) (Andersson et al., 2005), and svaRNAs of VA-I can interact with argonaute 2 (AGO2), a member of the RNA-induced silencing complex (RISC), to inhibit gene expression (Aparicio et al., 2006).

Interestingly, not only adenovirus can evade the anti-viral immune response but also use it to its benefit. For instance, IL-8 induces expression of adenoviral receptors $\alpha_v\beta_3$ integrin and human CAR (hCAR) to the apical side of polarized cells via the activation of Src-family tyrosine kinases or the activation of AKT/S6K and inhibition of glycogen synthase kinase 3 (GSK3)β, respectively (Lutschg et al., 2011, Kotha et al., 2015). Also, IL-8 promotes the adhesion of transmigrating neutrophils at the apical surface of polarized epithelium and that process has been associated with the enhancement of adenovirus transduction via a yet unidentified mechanism (Kotha et al., 2015). Importantly, the mechanisms mediating evasion of the anti-viral immune response differ between adenovirus serotypes. For instance, HAdV-4 and HAdV-12 E4 Orf3 do not relocate MRE11 to track-like structures and thus fail to prevent the accumulation of MRN complex

at viral replication centres and subsequent DNA concatenation (Stracker et al., 2005). Also, differences on the components forming the E1B 55K:E4 Orf6 complex from different serotypes have been reported. While HAdV-34/B2, HAdV-9/D and HAdV-4/E form E1B 55K:E4 Orf6 complexes composed of CUL5 in similarity to HAdV-5, HAdV-12/A and HAdV-40/F associate with CUL2, and HAdV-16/B1 seems to bind both CUL2 and 5 (Cheng et al., 2011). Moreover, not only they differ in structure but also in their function, since only HAdV-5, 12 and 40 E1B 55K:E4 Orf6 complexes are able to degrade p53, MRE11 or integrin α3. In contrast, HAdV-9, 16 and 34 E1B 55K:E4 Orf6 complexes are unable to degrade p53 or integrin α3, and HAdV-4 E1B 55K:E4 Orf6 complex is unable to degrade p53 or MRE11 (Cheng et al., 2011). These data suggest either the existence of complementary viral mechanisms to target degradation of cellular proteins or serotype-specific cellular mechanisms mediating the anti-viral immune response. Also, while HAdV-5 E1B 55K:E4 Orf3 complex can mediate SUMOylation of NBS1 and MRE11, E1B 55K:E4 Orf3 complexes from other serotypes such as HAdV-3, 4, 9 and 12 are not able to do so (Sohn and Hearing, 2012). Furthermore, there are mechanisms of evasion of the anti-viral immune response that belong to unique serotypes, as is the case for HAdV-19a E3 49K protein (Windheim et al., 2013). E3 49K is proteolytically cleaved and the large ectodomain sec49K is secreted from infected cells for binding to protein tyrosine phosphatase receptor type C (PTPRC)/CD45 on leukocytes, resulting in the inhibition of NK cell activation and cytotoxicity as well as T cell activation and cytokine production (Windheim et al., 2013). Such mechanisms have not yet been described for other serotypes. Serotype-specific differences in the mechanisms dictating evasion of the anti-viral immune response have direct implications for adenoviral vector development, since they may lead researchers towards serotype-directed strategies to increase gene transfer efficiency (see section 1.3.5).

Table 1-2. Adenovirus evasion of host immune responses by adenoviral proteins.

Adenoviral protein	Function	Mechanism
E1A	Blockade of IFN-α response.	Inhibition of ISGF3 transcriptional complex binding to ISRE. Binding of E1A to RNF20 complex.
	Inhibition of MHC-II induction.	
	Inhibition of dsRNA-mediated IFN-β production.	
	Blockade of peptide presentation to the immunoproteasome.	Interaction of E1A with PSMB10/MECL1 leading to downregulation of PSMB10, PSMB9/LMP2 and PSMB8/LMP7.
E1B and E4	Blockade of TNF-α-induced apoptosis.	Binding of E1B 19K to BAK and BAX to prevent oligomer formation.
	Repression of ISGs transcription.	E1B 55K-mediated.
	Relieve of silencing of viral gene expression to allow viral DNA replication.	E1B 55K-mediated degradation of DAXX.
	Repression of IFN synthesis.	E1B 55K-mediated inhibition of DDX58, MDA5, IRF7, MYD88 expression.
	Prevention of E1A-triggered apoptosis.	E1B 19K-mediated modulation of p53-mediated apoptosis. E1B 55K-mediated repression of transcriptional activation of p53-inducible genes and SUMOylation of p53 for its displacement from PML-NBs. E1B 55K:E4 Orf6 complex-mediated degradation of p53. E4 Orf3-mediated epigenetic regulation of p53 target promoters to prevent p53 DNA-binding.
	Inhibition of the induction of DNA damage signalling during viral replication and of viral DNA concatenation.	E1B 55K:E4 Orf6 complex-mediated degradation of DNA ligase IV and MRE11.
	Prevention of DDR and relieve of E1A gene expression repression to allow viral early gene transcription.	E1B 55K:E4 Orf6 complex-mediated degradation of TIP60.
	Relieve of viral gene expression repression.	E1B 55K:E4 Orf6 complex-mediated degradation of SPOC1.
	Prevention of DSB repair response and thus DNA	E1B 55K:E4 Orf3 complex-mediated.

	concatenation.	E4 Orf3 and 6 bind to and inhibit DNA-PK.
	Inhibition of IFN response.	E4 Orf3-mediated disruption of IFN-responsive PML-NB and re-localization of Sp100 and MRN complex.
E3	Inhibition of T cell activation.	E3 19K-mediated inhibition of MHC-I transport to the plasma membrane.
	Prevention of T cell and NK cell killing of infected cells via KLRC1/NKG2D receptors.	Sequestration of MICA and MICB in the ER to prevent their plasma membrane localizaiton.
	Prevention of CTL and FAS or EGF-R-mediated apoptosis.	E3 10.4K:E3 14.5 K complex-mediated internalization and degradation of FAS and EGF-R.
	Inhibition of ligand-induced apoptosis.	E3 10.4K:E3 14.5 K complex and E3 6.7K-mediated downregulation of TRAIL 1 and 2.
	Suppression of the cytolytic and pro-inflammatory functions of TNF-α.	E3 14.7K-mediated.
Protein VI	Relieve of silencing of viral gene expression to allow viral DNA replication.	Interaction of protein VI with DAXX and displacement from the PML-NB into the cytoplasm.
Protein VII	Prevention of DNA sensing and activation of the MRN complex during viral DNA replication and thus concatenation.	Binding of protein VII to viral DNA.
	Relieve of viral gene expression repression.	Binding of protein VII to SPOC1.
	Prevention of HMGB1-mediated immune responses.	Binding of protein VII to HMGB1 for its retention in the chromatin and thus inhibition of its secretion from immune cells.
Adenoviral RNA	Inhibition of protein synthesis repression in response to dsRNA.	Blockade of the activation of IFN-inducible EIF2AK2.
	Inhibition of gene expression for certain cellular proteins.	Interaction of svaRNAs of VA-I with AGO2.

ISGF3; IFN-stimulated gene factor 3, ISRE; interferon-stimulated response element, RNF20; ring finger protein 20, PSMB10; immunoproteasome subunit beta 10, TNF; tumor necrosis factor, ISG; IFN-stimulated gene, IRF; interferon regulatory factor, DDR; DNA damage response, DAXX; death domain-associated protein, DSB; double strand break, DNA-PK; DNA-dependent protein kinase, PML-NB; promyelocytic leukemia-nuclear bodies, Sp100; speckled protein 100kDa, MRN; MRE11-RAD50-NBS1, MHC; major histocompatibility complex, KLRC1; killer cell lectin like receptor C1, MICA and MICB; MHC-I chain-related protein A and B, ER; endoplasmic reticulum, FAS; Fas cell surface death receptor, EGF-R; epidermal growth factor receptor, TRAIL; TNF-related apoptosis-inducing ligand, HMGB1; high mobility group box 1, svaRNA; small viral RNA, AGO2; argonaute 2.

1.3 Adenoviruses as gene therapy vectors

To date, the use of adenoviral vectors in clinical trials represents 21.7% of all vectors used (The Journal of Gene Medicine: Clinical Trial, 2016). Despite the percentage has decreased in the last few years due to the optimization of lentiviral and adeno-associated vectors and the emergence of novel vectors, overall, adenoviral vectors still hold the highest percentage of individual vectors being used. Adenoviral vectors are very attractive vectors for several reasons: they can infect dividing and quiescent cells, exhibit very low risk of insertional mutagenesis since they remain episomal, have a considerably large packaging capacity allowing the insertion of long transgenes, achieve high levels of transient transgene expression and long-term transgene expression, have a wide tropism, can be easily engineered, can be produced at high titers under Good Manufacturing Practice (GMP) and are stable, which allows their manipulation, storage and distribution to clinics [reviewed by (Lusky, 2005)].

1.3.1 Evolution of adenoviral vectors

Adenoviruses can be genetically engineered to generate replication-deficient adenoviral vectors able to transduce host cells but unable to replicate inside of them, a key feature for gene transfer vehicles. Three generations of adenoviral vectors have been developed: first, second, and third generation (Figure 1-9). The first generation vectors have the *E1* and/or *E3* genes deleted from the adenoviral genome but retain the ITRs, the packaging signal and the remaining viral genes [reviewed by (Danthinne and Imperiale, 2000)]. This particular deletion allows the introduction of up to ~8 kb of foreign DNA, which can be expressed under the control of a heterologous promoter. Due to the lack of the *E1* gene, which is involved in the initiation of viral DNA replication by activating the expression of *E2* gene (Reichel et al., 1988), these vectors can transduce host cells but do not replicate. For this reason, they need to be produced in packaging cell lines such as HEK-293 cells (Graham et al., 1977) engineered to provide the *E1* gene *in trans* and thus allow vector amplification. However, researchers soon observed that replication-competent adenoviruses were generated in these packaging cell lines since the adenoviral genome was able to undergo homologous recombination with the adenoviral DNA within the cell genome and regain the *E1* gene (Lochmuller et al., 1994, Hehir et al., 1996). Thus, optimized packaging cell lines such as Per.C6® cells with only the exact sequence corresponding to the *E1* gene with no flanking adenoviral sequences were generated, ensuring the replication-deficient nature and safety of adenoviral vectors (Fallaux et al., 1998). Moreover, since the *E1* gene

also induces the expression of *E3* and *E4* genes, these vectors exhibit reduced expression of viral proteins and thus reduced stimulation of the anti-viral immune response to viral antigens in comparison to wild type adenovirus. However, the presence of E1-like proteins in host cells able to promote the expression of viral genes can result in antigen-related toxicity and allow replication of vectors (Reichel et al., 1987). Also, increasing knowledge on the adenovirus biology highlighted additional issues associated with the *E1* gene deletion. Since *E2* and *E3* genes are involved in intrinsic defence mechanisms against the intracellular immune response, *E1* gene deletion results in disarmed vectors that trigger the host cell immune response to transduced cells (Poller et al., 1996). These characteristics highly limit the duration of transgene expression and cause toxicity. With the aim to prevent viral DNA replication in host cells, reduce the anti-viral immune response to viral antigens and increase transgene capacity, second generation adenoviral vectors were generated by removing the *E2* and/or *E4* regions in addition to *E1* and *E3* [(Amalfitano et al., 1998) and reviewed by (Wang and Finer, 1996)]. Of note, new packaging cell lines expressing *E1*, viral DNA polymerase and pTP had to be engineered for successful vector production (Amalfitano and Chamberlain, 1997). This new generation of vectors increased the transgene capacity to ~14 kb, achieved longer transgene expression and decreased vector-associated inflammatory responses (Dedieu et al., 1997, Wang et al., 1997). Further genetic manipulation of adenoviral vectors gave rise to a further sophisticated version, the third generation helper-dependent (HD) or also called gutless vectors [reviewed by (Cots et al., 2013, Alba et al., 2005)]. These vectors are devoid of viral genes and only retain the ITRs and the packaging signal, thus they allow the insertion of particularly long transgenes of up to ~37 kb (Kochanek et al., 1996). Due to the lack of suitable packaging cell lines, HD vectors require a first or second generation helper adenoviral vector that complements the viral genes involved in viral DNA replication and packaging and capsid assembly *in trans* (Kochanek et al., 1996). Despite allowing long-term transgene expression since the lack of viral coding sequences highly diminished immunogenicity (Maione et al., 2001, Ehrhardt and Kay, 2002, Dudley et al., 2004, Kim et al., 2001), the presence of helper vector contaminants limits their potential. To reduce this contamination, several strategies based on the Cre-loxP or Flp-FRT systems were developed to prevent the generation of helper virions during the production process [reviewed by (Cots et al., 2013, Alba et al., 2005, Segura et al., 2008)]. These strategies consist of the addition of locus of X-over P1 (loxP) or flippase recognition target (FRT) sequences flanking the helper packaging signal. The production of these vectors in cell lines expressing the recombinase Cre or Flp, respectively, allows the excision of the helper packaging signal and thus prevents packaging of helper vector DNA. However, due to the reversible nature of these systems

and induced toxicity (Loonstra et al., 2001), other strategies such as the addition of attB/attP-φC31 sequences flanking the helper packaging signal are currently being developed (Alba et al., 2007, Alba et al., 2011). The presence of attB/attP-φC31 sequences retards helper vector DNA packaging, which reduces the amount of helper virions generated at collection time-points during the production process. Also, this strategy is often combined with the reversion of the orientation of the DNA packaging signal sequence of the helper vector to avoid homologous recombination events between helper and HD vector genomes (Palmer and Ng, 2003). However, since these vectors are composed of stuffer DNA in place of viral gene sequences to maintain optimum vector size and thus ensure genetic stability (Bett et al., 1993, Parks and Graham, 1997, Smith et al., 2009, Shayakhmetov et al., 2004a), the activation of innate immune mechanisms upon recognition of dsDNA have been observed (Cerullo et al., 2007). The promotion of immune responses to HD capsids upon intravenous administration has also been reported (Brunetti-Pierri et al., 2004, Mane et al., 2006).

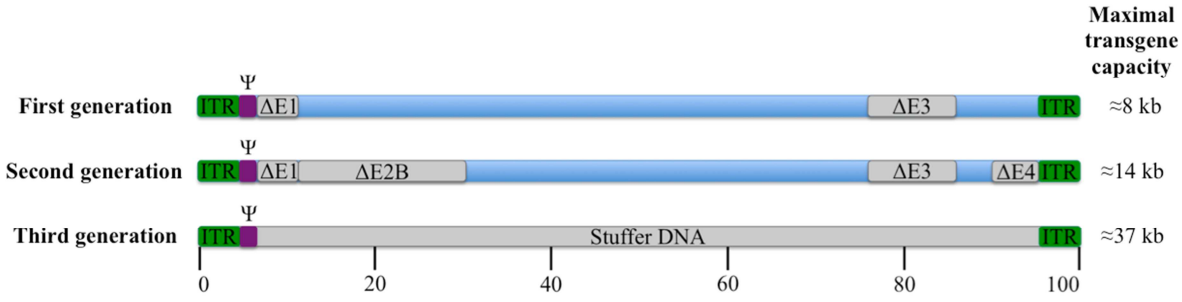

Figure 1-9. Genome map of first, second and third generation adenoviral vectors. The location of deleted viral genes and maximal transgene capacity for each type of vector are indicated. Adenoviral genes have been mapped by superimposing an arbitrary scale of 100 map units. Internal terminal repeats (ITR) in green, adenoviral DNA packaging signal (Ψ) in purple and genetic engineering in grey.

1.3.2 Adenoviral vectors in the clinic

Adenoviral vectors have shown promise as oncolytic vectors, as vaccines and in gene therapy. Oncolytic adenoviral vectors are replication-competent adenoviral vectors that have particular mutations in their genome to selectively and exclusively replicate in cancer cells leading to the lysis and thus death of the transduced cancer cell and the production of new virions able to transduce and kill neighbouring cancer cells [reviewed by (Rosewell Shaw and Suzuki, 2016, Fukuhara et al., 2016)]. Also, oncolytic adenoviral vectors have been employed to deliver transgenes encoding immune modulatory molecules selectively to cancer cells and thus modulate the immune response towards cancer cells [reviewed by (Rosewell Shaw and Suzuki, 2016, Fukuhara et al., 2016)]. The rationale behind using

adenoviruses for vaccine vector development lies on their capability to induce a potent T and B cell response to antigens encoded as transgenes and thus provide immunity to a particular disease [(Yang et al., 2003) and reviewed by (Majhen et al., 2014)]. As for adenoviral oncolytic vectors, adenovirus-based vaccines have reached the clinical stage, showing promising results against bacteria, viruses and protozoans in clinical trials (The Journal of Gene Medicine: Clinical Trial, 2016, Clinical Trials, 2016). Since these approaches differ from the focus of the studies presented in this thesis, oncolytic adenoviral vectors and adenovirus-based vaccines will not be further discussed. Regarding the use of adenoviral vectors in gene therapy, increasing knowledge of adenovirus biology has allowed remarkable progress in their optimization as vectors, which has directly translated into a growing interest in adenovirus-based gene therapy. To date, there have been over 500 clinical trials based on adenoviral vectors for the treatment of cardiovascular, ocular, neurologic or inflammatory disease, as well as cancer with some of them reaching phase II and III (The Journal of Gene Medicine: Clinical Trial, 2016). As an example, a phase III clinical trial is being conducted in the USA using an adenovirus-based approach to deliver a transgene encoding VEGF via a perivascular collagen collar device for stenosis prevention in end-stage renal disease (ID#[1] US-0854). Another ongoing clinical trial is employing an adenoviral vector to deliver a p21 gene via intraocular administration to the subconjunctival space prior to trabeculectomy for the treatment of glaucoma, currently on phase I (ID# US-0589). A clinical trial in phase I using HAdV-5 encoding fibroblast growth factor (FGF) for the treatment of peripheral artery occlusive disease Fontaine stage III is currently taking place in the UK (ID# UK-0026). Importantly, the world's first gene therapy product approved by a government agency for clinical use was an adenoviral vector encoding p53 for the treatment of head and neck squamous cell carcinoma (Gendicine), which was licensed in China in October 2003 [reviewed by (Peng, 2005, Chen et al., 2014)]. The product is also currently been used in a phase II multi-center clinical trial for patients with recurrent head and neck squamous cell carcinoma in the USA (ID# US-0226), and other adenoviral vectors based on the p53 transgene as a therapeutic agent have also been developed and used in clinical trials for hepatocellular carcinoma (ID# US-0189), adenocarcinoma of the prostate (ID# US-0192), breast cancer (ID# US-0216) or metastatic bladder cancer (ID# US-0219) among others (The Journal of Gene Medicine: Clinical Trial, 2016).

[1]Gene therapy clinical Trial identification number as cataloged in The Journal of Gene Medicine: Clinical Trial, 2016.

1.3.3 Limitations of adenoviral vectors

Despite the promising results shown, however, there are still pitfalls that need to be further addressed to develop safe and efficient adenoviral gene transfer vectors. The main limiting factors for the use of HAdV-5 in gene therapy are the liver and spleen-associated toxicity induced following intravascular administration of vectors that can lead to systemic inflammatory response syndrome and multiorgan failure (see section 1.3.4), the existence of pre-existing immunity that neutralizes virions preventing them from reaching the target tissue, and the induction of immune responses elicited by transduced cells that leads to their elimination and thus the termination of transgene expression (see section 1.2.3). For the treatment of certain diseases a finite expression of the therapeutic transgene can be sufficient such as in the case of suicide gene therapy for the treatment of prostate cancer (Kubo et al., 2015) or even advantageous such as the induction of vasculogenesis for the treatment of coronary artery disease (Grines et al., 2003). However, for other diseases such as Duchenne muscular dystrophy (DMD) (Kawano et al., 2008) or CF (Potash et al., 2013), where replacement gene therapy is needed to restore protein deficiencies, persistent expression of transgene is an essential requisite. Also, certain diseases require re-administration of the gene therapy vector. Thus, even when pre-existing immunity is absent when the vector is administered for the first time, new neutralizing antibodies are generated against virions following the first administration, precluding future re-administration of vectors (Ye et al., 2000, Haegel-Kronenberger et al., 2004). In order to bypass neutralization of virions by pre-existing immunity, alternative strategies such as *ex vivo* approaches have been developed. For instance, one study reported the success of an adenoviral vector-based gene therapy *ex vivo* approach to deliver the tissue inhibitor of metalloproteinases-3 (TIMP-3) to retard intimal thickening in autologous porcine arteriovenous interposition grafts in the long-term (3 months) (George et al., 2011). This study highlights the translational potential for *ex vivo* gene therapy. Unfortunately, *ex vivo* approaches are limited to certain pathologies and are not suitable for most diseases. Thus, alternative strategies to bypass pre-existing immunity and evade the anti-viral immune response are being under study (see section 1.3.5). Finally, one study reported that the adenoviral genome is not exempt from recombination events with the host cell genome and that this can lead to vector genome integration *in vitro* and *in vivo* (Stephen et al., 2010, Stephen et al., 2008). Despite such integration events are very rare [homologous recombination: ~$2x10^{-5}$ (*in vitro*) and ~$4x10^{-7}$ (*in vivo*) per vector molecule per cell, heterologous recombination: ~$3x10^{-3}$ (*in vitro*) and ~$7x10^{-5}$ (*in vivo*) per vector molecule

per cell (Stephen et al., 2010, Stephen et al., 2008)], this represents a safety risk and thus it is a concern that should be further addressed.

1.3.4 Liver tropism and detargeting strategies for HAdV-5-based vectors

1.3.4.1 Receptor-mediated HAdV-5 gene transfer

The treatment of many diseases such as cardiovascular disease or metastatic cancer requires administration of the adenoviral vector via the vasculature or with potential exposure to the bloodstream. However, upon intravascular delivery, HAdV-5-based vectors exhibit high hepatic tropism, which can result in toxicity and the activation of immune responses (Lozier et al., 2002, Raper et al., 2002, Atencio et al., 2006, Morral et al., 2002). Importantly, these side effects can even lead to fatal consequences, as exemplified by a participant in a phase I clinical trial for ornithine transcarbamylase (OTC) deficiency with a HAdV-5-based approach, who suffered from severe systemic inflammatory response syndrome and died 98 h following intravascular vector administration (Raper et al., 2003). The anatomical architecture of liver sinusoids results in the sequestration of adenoviral particles in the space of Disse (Di Paolo et al., 2009b, Shayakhmetov et al., 2004b), the area beneath and between sinusoidal endothelial cells and the hepatocyte surface. Moreover, adenoviral particles are trapped by liver residential macrophages (KC) (Alemany et al., 2000, Di Paolo et al., 2009b, Tao et al., 2001). KCs can be depleted by the use of clodronate liposomes, which are ingested by KC causing their death (van Rooijen and van Kesteren-Hendrikx, 2003). However, even in the absence of KCs, intravascular administration of high doses of HAdV-5 still results in efficient liver transduction (Wolff et al., 1997, Di Paolo et al., 2009b), indicating that adenovirus interacts with cellular receptors to mediate hepatocyte cell transduction.

In an attempt to identify the receptors that dictate HAdV-5 liver tropism, the receptors involved in the classical *in vitro* transduction pathway (CAR and $\alpha_v\beta_{3,5}$ integrins) were assessed. Mutations in the fiber or penton base to ablate HAdV-5 interactions with CAR or $\alpha_v\beta_{3,5}$ integrins, respectively, (Leissner et al., 2001, Alemany and Curiel, 2001, Smith et al., 2002, Smith et al., 2003b, Martin et al., 2003, Einfeld et al., 2001, Mizuguchi et al., 2002, Smith et al., 2003a, Bradshaw et al., 2012) (Figure 1-10) or the combination of both ablating mutations (Koizumi et al., 2003, Martin et al., 2003, Smith et al., 2003b) successfully impaired adenoviral transduction *in vitro* but failed to significantly reduce *in vivo* liver transduction. However, there is some controversy with other studies showing

700-fold reduced mouse liver transduction (Einfeld et al., 2001) or 509-fold reduced rat liver transduction (Nicol et al., 2004) with HAdV-5 vectors ablated for both CAR and $\alpha_v\beta_{3,5}$ integrin-binding. Other studies investigated the role of heparan sulphate (HS) in liver transduction and reported that HAdV-5 binding to heparan sulphate glycosaminoglycans (HS-GAG) is sufficient to mediate liver transduction (Dechecchi et al., 2001, Smith et al., 2003a). Mutant adenovirus lacking binding to HS (91KKTK94[2] mutated to 91GAGA94 in the fiber shaft) exhibited decreased liver transduction in non-human primates (Smith et al., 2003a). Another study assessing the 91GAGA94 mutation only resulted in a moderate decrease in liver transduction in rats (Nicol et al., 2004). Other mutations were assessed such as the replacement of the HAdV-5 fiber shaft (containing the 91KKTK94 motif) with the fiber shaft from HAdV-31 or from HAdV-41, which do not contain this motif (Di Paolo et al., 2007). However, no liver de-targeting was observed in this study. The combination of 91GAGA94 mutation with CAR-binding ablating mutations achieved 1000-fold decreased liver transduction in mice (Smith et al., 2003b). Ablation of CAR and $\alpha_v\beta_{3,5}$ integrin-binding together with the replacement of HAdV-5 fiber shaft with the non-KKTK-containing fiber shaft from HAdV-25 resulted in a >30,000-fold decrease in mouse liver transduction (Koizumi et al., 2003). Other studies report that 91GATK94 mutation alone or in combination with CAR-ablating point mutation Y477A achieved the same extent of liver de-targeting in mice (Bayo-Puxan et al., 2006). However, in the later study, they suggest that fiber shaft mutations may alter the fiber structure conferring rigidity and thus hampering simultaneous binding of HAdV-5 to CAR and $\alpha_v\beta_{3,5}$ integrins. Further work reported that the 91GAGA94 mutation does not negatively affect adenovirus binding to host cells but instead it interferes with virus trafficking at a post-attachment stage blocking cell transduction (Kritz et al., 2007). Studies based on mutating HAdV-5 capsid proteins to impair HAdV-5:HS interaction have not succeeded in de-targeting HAdV-5 from the liver. However, HS has been associated with HAdV-5 transduction in several studies that used heparin lyases I, II and III to remove HS from cultured cells (Dechecchi et al., 2000, Dechecchi et al., 2001) or $HS^{positive}$ and $HS^{negative}$ cell lines (Dechecchi et al., 2001).

[2]Numbers refer to amino acid residue position in the protein.

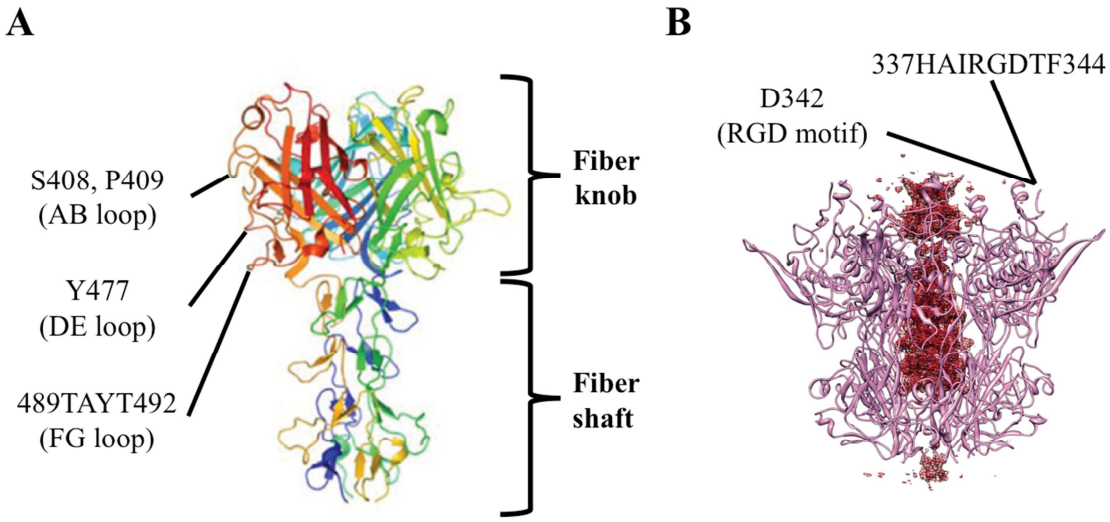

Figure 1-10. HAdV-2 fiber and HAdV-5 penton base receptor-binding sites. Ribbon diagram of fiber knob and shaft domains (4 last repeats) (A) or penton base (light pink) (B). Contact sites between fiber knob and coxsackie and adenovirus receptor (CAR) (Roelvink et al., 1999) or penton base and $\alpha_v\beta_{3,5}$ integrins (Bradshaw et al., 2012, Smith et al., 2003b) that have been targeted for mutation are indicated. S; serine, P; proline; Y; tyrosine, T; threonine, A; alanine. Figure in (A) adapted from (Hall et al., 2010) and figure in (B) adapted from (Nemerow et al., 2012).

1.3.4.2 Interactions of HAdV-5 with blood components: erythrocytes, platelets and blood proteins

Following intravascular administration, HAdV-5-based vectors not only interact with components of the immune response (see section 1.2.3), but also with other cells and proteins in the bloodstream that can affect vector persistence in blood and biodistribution and toxicity profiles.

Human but not mouse or rhesus macaque erythrocytes were reported to bind HAdV-5 virions via interactions of CAR with the fiber knob domain (Seiradake et al., 2009) (Figure 1-11). Also, human but not mouse erythrocytes can interact with HAdV-5 virions via CR1 in the presence of C1q and antibodies and affect the persistence of virions in blood (Carlisle et al., 2009) (Figure 1-11). Incorporation of CAR-binding ablating mutations into HAdV-5 vectors successfully abolished agglutination of virions with human and rat erythrocytes (Nicol et al., 2004) but failed to prevent agglutination with erythrocytes in human plasma (Carlisle et al., 2009). Interestingly, it was recently reported that binding of HAdV-5 to erythrocytes is a reversible process and does not prevent extravasation and organ transduction after intravascular administration (Rojas et al., 2016). HAdV-5 has been consistently reported to cause transient thrombocytopenia between 5 and 24 h following intravenous administration of vectors that depends on vector dose (Lozier et al., 2002, Cichon et al., 1999, Varnavski et al., 2005, Othman et al., 2007). Thrombocytopenia was shown to take place as a consequence of HAdV-5 virions binding to and activating

platelets through interactions with CAR (Othman et al., 2007) (Figure 1-11). Activated platelets subsequently express cell adhesion molecule P-selectin, which binds its ligand P-selectin glycoprotein ligand-1 (PSGL-1) on leukocytes to form platelet-leukocyte aggregates. Also, adenoviral vectors induce release of ultra-large molecular weight Von Willebrand factor (VWF), which can bind to platelets (Bernardo et al., 2005), from endothelial cells *in vivo* and expression of VCAM-1 *in vitro* (Othman et al., 2007), which potentially contributes to platelet-leukocyte aggregates rolling and transendothelial migration [reviewed by (Carlos and Harlan, 1994)]. As a consequence of these events, platelet-leukocyte aggregates are cleared from the circulation by scavenger macrophages in the liver (Stone et al., 2007, Bondanza et al., 2000). Also, adenovirus-induced thrombocytopenia was associated with factor B and C3 of the alternative complement pathway (Appledorn et al., 2008a, Kiang et al., 2006).

In 2005 Shayakhmetov *et al.* used *ldlr*$^{-/-}$ mice together with the LRP and HSPG-binder lactoferrin, heparinase I and mutant HAdV-5 vectors with impaired binding to CAR, to demonstrate that LRP and HSPGs could serve as HAdV-5 receptors both *in vitro* and *in vivo* (Shayakhmetov et al., 2005b). Moreover, C4BP and coagulation factor IX (FIX) were identified as fiber knob domain-interacting blood proteins and were shown to confer CAR-independent HAdV-5 transduction of HSPG and LRP-expressing cell lines and primary human hepatocytes. Thus, they proposed a novel pathway for HAdV-5 cell entry consisting of C4BP and FIX bridging HAdV-5 to cellular receptors such as LRP and HSPGs (Figure 1-11). Interestingly, CAR-binding-ablated HAdV-5 exhibited similar liver transduction levels in *FIX*$^{-/-}$ mice than those of wild type HAdV-5, suggesting that C4BP and FIX were not the only blood proteins contributing to liver tropism (Shayakhmetov et al., 2005b). Further studies identified other vitamin K-dependent coagulation factors such as coagulation factor VII (FVII), coagulation factor X (FX) and protein C (PC) as able to enhance hepatocyte transduction *in vitro* (Parker et al., 2006) (Figure 1-11). Importantly, these coagulation factors share a common protein structure that comprises a non-catalytic glutamic acid (GLA) domain, two epidermal growth factor (EGF)-like domains and a serine protease (SP) domain: GLA-EGF1-EGF2-SP [reviewed by (Furie and Furie, 1988, Patthy, 1985)] (Figure 1-12A). Conversely, HAdV-5 transduction was not enhanced by vitamin K-dependent coagulation factors that do not have this structure such as coagulation factor XI (FXI) and coagulation factor XII (FXII) or by prothrombin/FII, which has "kringle" (KR) domains in place of the EGF-like domains [reviewed by (Furie and Furie, 1988, Patthy, 1985)]. The same study also reported that treating mice with warfarin, which is an anticoagulant that inhibits the γ-carboxylation of GLA residues of vitamin K-

dependent zymogens, prior to vector administration led to a substantially reduced liver transduction. Thus, they reported that the ability of vitamin K-dependent coagulation factors to enhance transduction was related to their particular protein domain structure (Parker et al., 2006). Further studies using surface plasmon resonance (SPR) confirmed interactions of HAdV-5 virions with FVII, FIX, FX and PC (Kalyuzhniy et al., 2008).

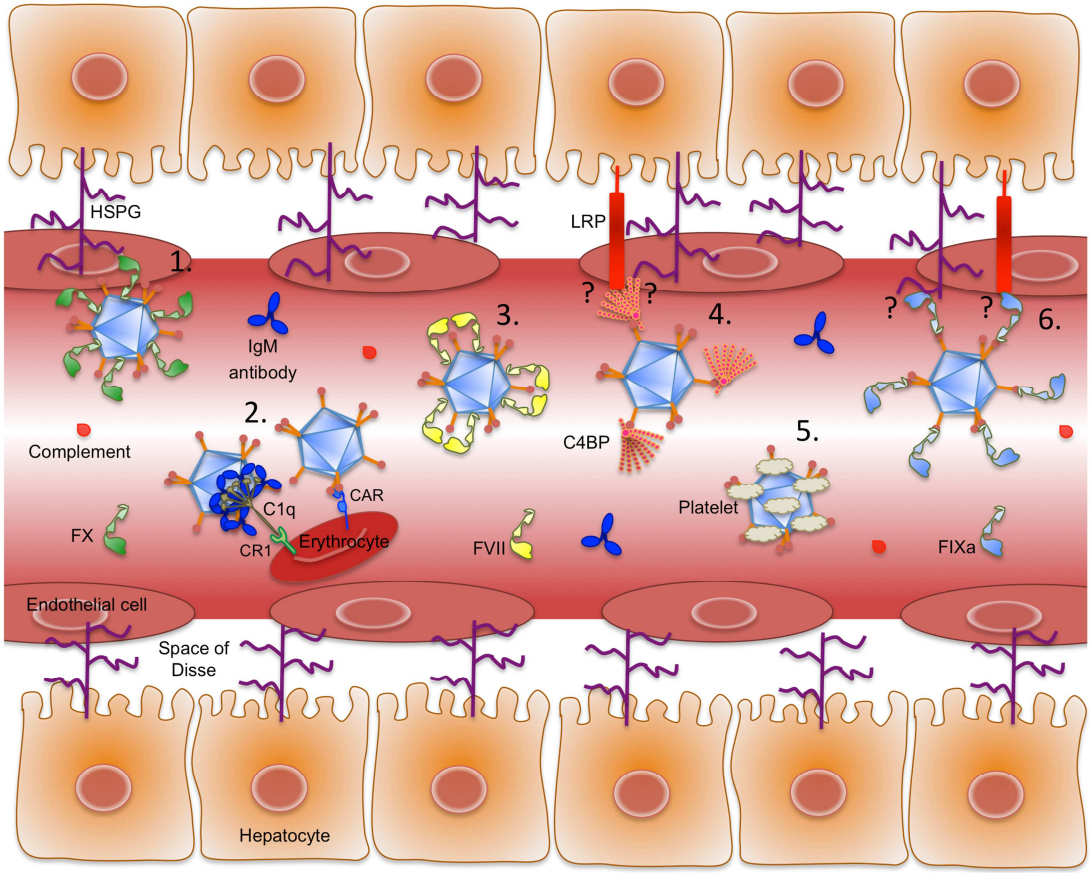

Figure 1-11. HAdV-5 interactions with blood proteins. 1. FX-mediated transduction through heparan sulphate proteoglycans (HSPGs). **2.** HAdV-5 interactions with erythrocytes via complement receptor (CR)1 and coxsackie and adenovirus receptor (CAR). **3.** HAdV-5:FVII complexes. **4.** HAdV-5:complement-4 binding protein (C4BP) complexes and proposed transduction via HSPGs or low-density lipoprotein receptor-related protein (LRP). **5.** HAdV-5 interactions with platelets. **6.** HAdV-5:FIXa complex and proposed transduction via HSPGs or LRP. FX; coagulation factor X, FVII; coagulation factor VII, FIXa; activated coagulation factor IX. Figure adapted from (Lopez-Gordo et al., 2014a).

Later reports showed that HAdV-5 could not only make use of FX to facilitate liver transduction upon exposure to the bloodstream, but also for transduction of other tissues such as the adrenal glands, where there is absent expression of CAR (Tran et al., 2013). Similarly, FIX and FX mediated binding of HAdV-5 virions to human epithelial cells via HS (Jonsson et al., 2009). Importantly, other adenovirus serotypes can also exploit coagulation factors for host cell transduction. For instance, HAdV-31 can use FIX but not FX to transduce epithelial cells via HS-GAG (Jonsson et al., 2009), HAdV-18 transduction of epithelial cells from the airways or intestine is enhanced by FIX (Lenman et al., 2011)

and FX can enhance HAdV-35 binding in SPR analysis and transduction *in vivo* in the absence of its primary receptor CD46 (Greig et al., 2009). However, these properties are not necessarily shared between serotypes belonging to the same adenovirus species. For instance, while FIX can enhance HAdV-18 and 31 transduction, it has no effect on HAdV-12, another member of species A adenovirus (Lenman et al., 2011). Furthermore, binding affinities between adenovirus and coagulation factors or between adenovirus:coagulation factor complexes and host cell receptors can also differ among serotypes, as observed for HAdV-31 binding to FIX with a higher affinity than that of HAdV-5, and for HAdV-31:FIX complex binding to less sulphated and more *N*-acetylated HS domains than the HAdV-5:FIX complex (Lenman et al., 2011). Finally, it was demonstrated that activation of FIX to FIXa exposes a binding site for LRP that allows FIXa:LRP binding in a heparin and calcium-dependent manner (Neels et al., 2000).

1.3.4.2.1 FX-mediated HAdV-5 cell entry

Interestingly, only recombinant human FX (hFX) fully rescued liver transduction of mice administered warfarin, highlighting a key role for FX in HAdV-5 hepatic tropism (Parker et al., 2006). Parker *et al.* reported that FX binds to HAdV-5 in a calcium-dependent manner since addition of EDTA was able to dissociate HAdV-5:FX interactions in SPR analysis (Parker et al., 2006). This finding also accounts for the fact that the γ-carboxylation of GLA residues of vitamin K-dependent zymogens, which is inhibited by warfarin, is necessary for Ca^{2+} binding (Venkateswarlu et al., 2002). The affinity constant of HAdV-5:FX binding was determined to be $1.9x10^5$ viral particles (vp)/ml (Parker et al., 2006). Later studies reported an association rate constant (ka) of $1.2x10^6$ M^{-1} s^{-1} and a dissociation rate constant (kd) of $2.23x10^{-3}$ s^{-1}, with an overall equilibrium dissociation constant (K_D) of $1.83x10^{-9}$ M (Waddington et al., 2008). Another group reported similar values: ka of $3.37x10^5$ M^{-1} s^{-1}, kd of $7.71x10^{-5}$ s^{-1} and K_D of $228.7x10^{-9}$ M (Kalyuzhniy et al., 2008).

To identify the adenovirus proteins involved in HAdV-5:FX interactions, mutant HAdV-5 were generated. The use of fiberless HAdV-5 demonstrated that HAdV-5:FX interaction was not dependent on the fiber (Waddington et al., 2008). Three-dimensional reconstructions calculated from cryoelectron micrographs of HAdV-5:FX complexes revealed that one FX molecule binds to one hexon trimer at the central depression at the top of each trimer (Waddington et al., 2008) (Figure 1-12B-D). These data are in agreement with data obtained from affinity chromatography assays of HAdV-5:FX

complexes (Kalyuzhniy et al., 2008). Furthermore, studies on a range of 22 adenovirus serotypes with high, weak or no FX-binding indicated that the differences in HAdV-5 binding affinity to FX depends on the hexon HVRs (Waddington et al., 2008) (Figure 1-12E). Further studies suggested that HVR 5 was involved in hexon HAdV-5:FX interactions (Kalyuzhniy et al., 2008) and that disruption of HVR 5 by inserting a biotin acceptor peptide (BAP) or glycine-alanine residues could reduce hepatocyte transduction and liver damage or binding to FX and liver transduction, respectively (Shashkova et al., 2009, Vigant et al., 2008). However, alignment of hexon amino acid sequences from FX-binding and non-FX-binding adenoviruses revealed no correlation between the capacity to bind to FX and the presence of conserved amino acids within HVR 5 (Kalyuzhniy et al., 2008). Instead, the amino acid residues TDT in HAdV-3 and 21 HVR 3 and amino acids 423TET425 in HAdV-5 HVR 7 and TDT in HAdV-2, 4, 16 and 41 HVR 7 were associated with hexon binding to FX (Kalyuzhniy et al., 2008). In agreement, another study defined 423TET425 in HVR 7 as the amino acid motif involved in hexon HAdV-5:FX interaction (Doronin et al., 2012) (Figure 1-12F). Further phylogenetic analysis together with high-resolution models of HAdV-5:FX complexes identified the critical amino acid E451 in the HVR 7 of FX-binding adenoviruses, which was replaced by Q451 in non-FX-binders (Alba et al., 2009). Generation of a mutant HAdV-5 (hereafter referred to as AdT*) containing the mutations I421G, T423N, E424S, L426Y, E451Q in HVR 7 and T270P and E271G in HVR 5 was shown to reduce FX-binding to negligible levels (Alba et al., 2009). Importantly, AdT* exhibited extremely low liver transduction and induced lower levels of inflammatory cytokines and chemokines compared to those of HAdV-5 (Alba et al., 2010, Bradshaw et al., 2012, Alba et al., 2012, Alba et al., 2009). Successful abrogation of binding of HAdV-5 to FX was also achieved by introducing the point mutation T425A in HAdV-5 HVR 7 (Doronin et al., 2012).

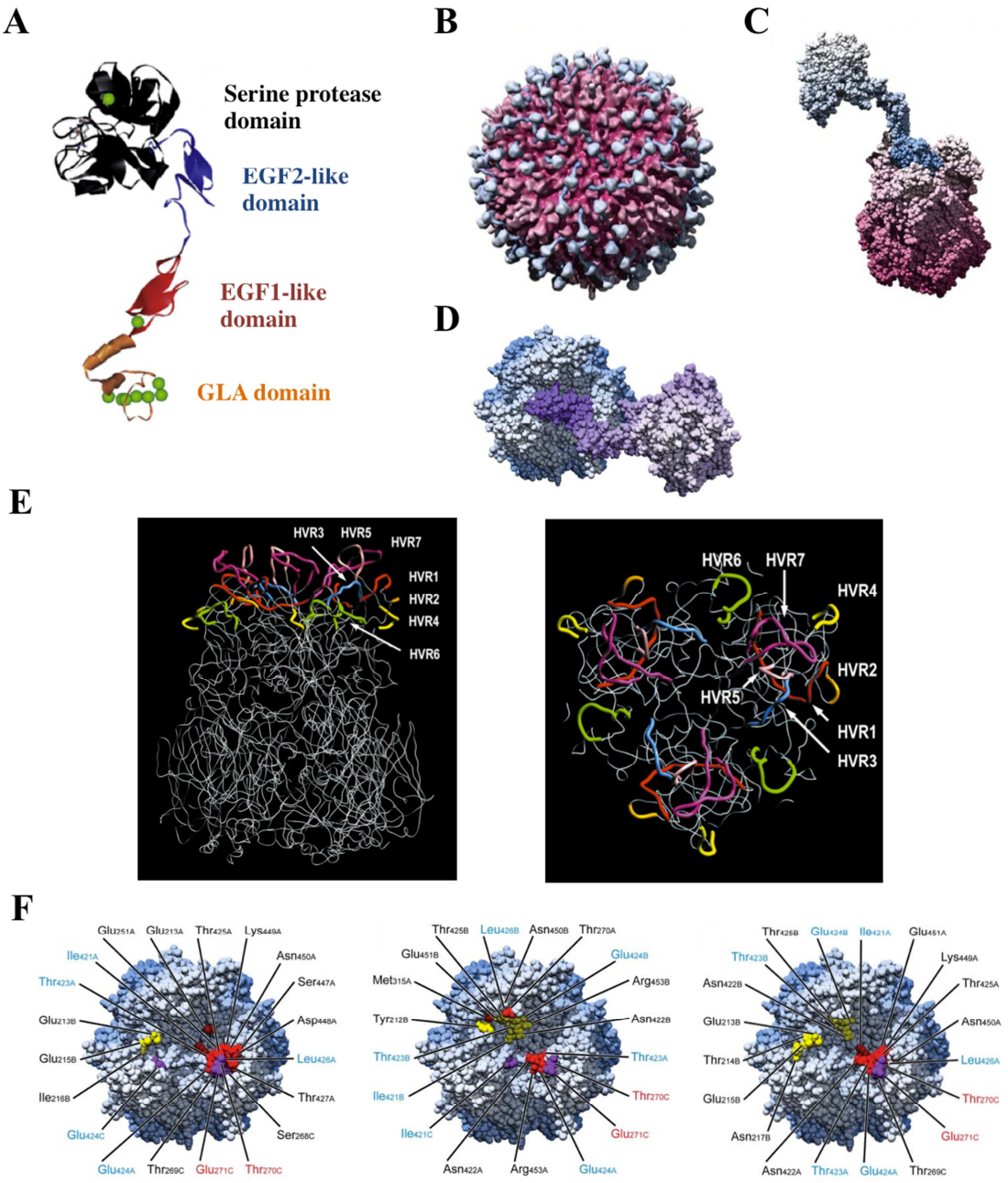

Figure 1-12. HAdV-5:FX complexes and HAdV-5 amino acid residues involved in HAdV-5:FX interaction. A) Ribbon diagram of FX structure. Ca^{2+} is represented as green balls. B-C) HAdV-5:FX interaction. Hexon protein shown in magenta and FX in blue. D) HAdV-5 hexon:FX complex. Hexon protein shown in blue and FX in purple. E) HAdV-5 hexon hypervariable regions (HVRs). HVR 1 shown in red, HVR 2 in orange, HVR 3 in blue, HVR 4 in yellow, HVR 5 in pink, HVR 6 in green and HVR 7 in magenta. F) Top side view of HAdV-5 hexon. Amino acid residues that interact with FX are indicated in each of the three models calculated (Alba et al., 2009). Amino acid residues coloured correspond to those targeted for mutation in a mutant FX-binding deficient HAdV-5 (AdT*) (Alba et al., 2009). EGF; epidermal growth factor receptor, GLA; glutamic acid. Figure in (A) adapted from (Waddington et al., 2008), Figure in (B-C) reproduced with permission from (Lowenstein, 2008). Figure in (D) reproduced with permission from (Alba et al., 2009). Figures in (E) reproduced with permission from (Rux and Burnett, 2000). Figure in (F) reproduced with permission from (Alba et al., 2009).

Regarding the domain from FX involved in HAdV-5:FX interaction, the use of GLA domainless recombinant hFX, hFXa lacking the GLA-EGF1 domains, and the FX GLA-binder and FX inhibitor X-bp, which belongs to the C-type lectin superfamily (Atoda et al.,

1998) (Figure 1-13F), showed that the FX GLA domain is required for FX binding to HAdV-5 hexon (Waddington et al., 2008, Kalyuzhniy et al., 2008, Corjon et al., 2011). MDFF simulations defined amino acid K10 in the GLA domain as the one responsible for interactions with the amino acid motif 423TET425 in HAdV-5 HVR 7 (Doronin et al., 2012) (Figure 1-13A-D). The domain from FX involved in binding to HSPG was also investigated. The anticoagulants NAPc2 from the hematophagous nematode *Ancylostoma caninum* and Ixolaris from the tick salivary gland, which inhibit FX by binding to the heparin-binding exosite of FX (exosite II) with high affinity (Murakami et al., 2007, Monteiro et al., 2005), blocked FX-dependent HAdV-5 transduction *in vitro* and *in vivo* (Waddington et al., 2008). These data indicate that HAdV-5:FX complexes bind to HSPG through the FX exosite II, which is located in the SP domain (Rezaie, 2000). Other studies *in vitro* and *ex vivo* using FX containing mutations in the conserved amino acid residues within the FX exosite II [R424, K420, K351, R347, K276, R273, R306 of the mature peptide (Waddington et al., 2008)] confirmed that the FX SP domain interacts with HSPG (Duffy et al., 2011) (Figure 1-13E). HSPGs are glycoproteins composed of a core protein (proteoglycan) to which one or more HS-GAG side chains are covalently linked. HS-GAGs are composed of units of *N*-acetylated or *N*-sulphated *N*-acetylglucosamine (GlcN) and D-glucuronic acid (GlcA) or the *O*-sulphated and epimerized GlcA that results in L-iduronic acid (IdoA) (Hacker et al., 2005, Esko and Lindahl, 2001). Liver HS are characterized by having high levels of *N* and *O*-linked sulphate groups (Vongchan et al., 2005) and in particular hepatocytes contain trisulphated disaccharides (Lawrence et al., 2008). Competition experiments with highly sulphated heparins or HS *in vitro* and *ex vivo*, as well as experiments on cells lacking 2-*O*-sulphate groups, or cells treated with the chemical HSPG sulphation inhibitor sodium chlorate, demonstrated the role of *N* and *O*-sulphation from HS side chains of HSPG in binding to FX (Bradshaw et al., 2010). In summary, coagulation FX mediates HAdV-5 liver transduction by binding to HAdV-5 hexon HVRs via the FX GLA domain while simultaneously interacting with *N* and *O*-linked sulphate groups of cellular HSPG through the FX SP domain.

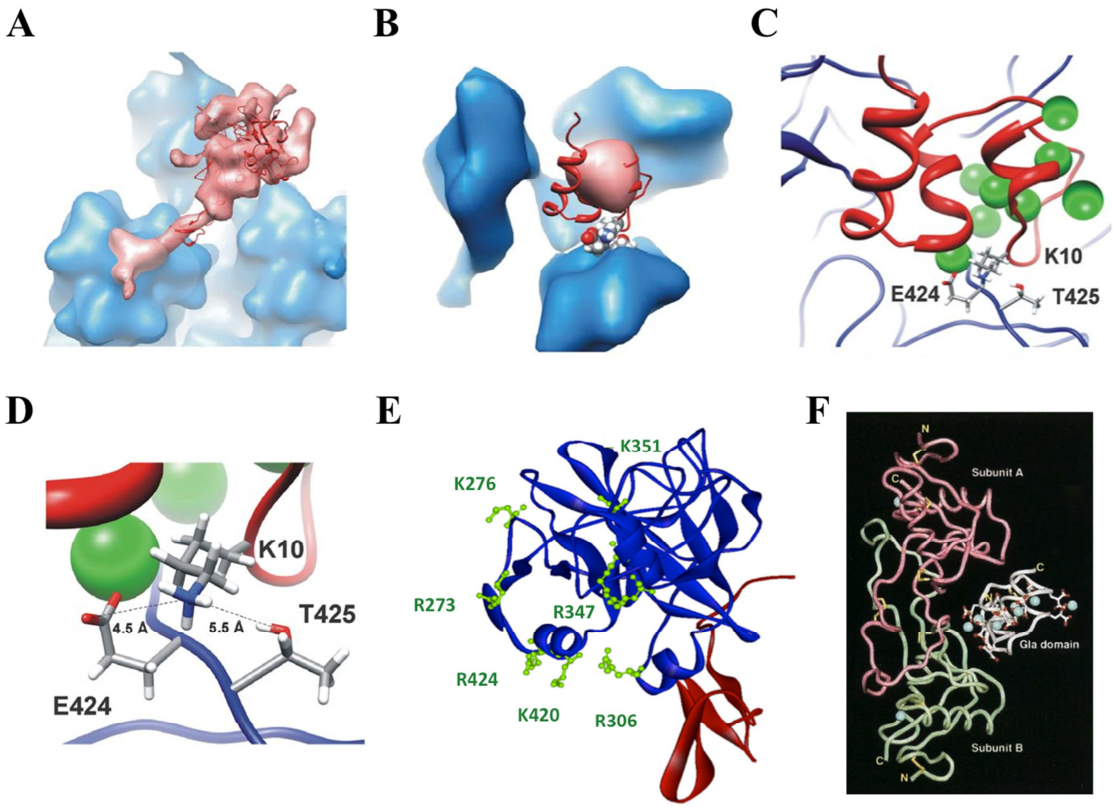

Figure 1-13. FX interaction with HAdV-5 hexon and HSPG. A-D) Cryo-Electron Microscopy structure and molecular dynamic flexible fitting simulation of HAdV-5:FX complex. Amino acid residue K10 in FX (red ribbon) GLA domain interacts with the amino acids motif 423TET425 in HAdV-5 hexon hypervariable region (HVR) 7. Cryo-Electron Microscopy density for FX is shown in light pink in (A-B). 423TET425 side chains are shown in space-filling representation and coloured by element in (C-D). Ca^{2+} is represented as green balls in (C-D). E) Ribbon diagram of the FX serine protease (SP) and epidermal growth factor-like (EGF)2 domains. SP shown in blue and EGF2 in red. Amino acid residues that interact with heparan sulphate proteoglycans (HSPG) are indicated and shown in green. F) Ribbon diagram of the FX inhibitor X-bp and its binding to FX GLA domain. Subunits A and B of X-bp are shown and indicated. Figures in (A-D) reproduced with permission from (Doronin et al., 2012). Figure in (E) adapted from (Duffy et al., 2011). Figue in (F) reproduced with permission from (Mizuno et al., 2001). Copyright (2001) National Academy of Sciences, U.S.A.

For the generation of safe HAdV-5-based vectors, in addition to de-targeting HAdV-5 vectors from the liver (transductional de-targeting), it is essential to reduce off-target effects that can arise from transgene expression in off-target tissues or residual virion accumulation in the liver. With this aim, transcriptional de-targeting, which consists in decreasing transgene expression in a tissue-specific manner, can be achieved by using silencers of transcriptionally regulated tissue-specific markers (Kanai et al., 1996) or via tissue-specific miRNA-mediated post-transcriptional suppression (Bennett et al., 2012, Suzuki et al., 2008, Card et al., 2012). Thus, by the combination of both transductional and transcriptional de-targeting strategies, the availability of the adenoviral vector for the target tissue can be increased while reducing toxicity and off-target effects.

1.3.4.2.2 Implications for HAdV-5:FX interaction in immunity

A role for FX in protecting HAdV-5 capsids against attack by the immune system in mice *in vivo* or after incubation of virions with mouse or human serum *in vitro* has been described (Xu et al., 2013, Ma et al., 2015, Duffy et al., 2016) (Figure 1-14). In the absence of FX, natural IgM antibodies recognize epitopes on the HAdV-5 capsid and activate the classical complement pathway, which via the opsonisation of HAdV-5 capsid by C3b complement protein leads to blockade of virion binding to host cells *in vitro* and thus cell transduction (Xu et al., 2013). In this process, complement protein C1q and complement component 4 (C4) were also identified as mediators of *in vitro* adenovirus neutralization (Xu et al., 2013). In contrast, IgM antibodies binding to virions is blocked in the presence of FX (Duffy et al., 2016) as well as covalent association of C3b with the adenoviral capsid (Xu et al., 2013), resulting in inhibition of *in vitro* adenovirus neutralization. Importantly, the HAdV-5 hexon HVRs, which are the capsid region targeted for FX-binding (Alba et al., 2009), were identified as the neutralization targeted epitopes (Ma et al., 2015). Interestingly, FX-binding deficient AdT* was able to bind to human IgM (hIgM) antibodies (Duffy et al., 2016), indicating that hIgM might not only recognize FX binding sites but also other hexon HVRs and thus suggesting that the mechanism by which FX blocks binding of hIgM antibodies to virions might be based on steric blocking rather than competition for binding sites. In contrast, FX did not block human IgG (hIgG) antibodies binding to HAdV-5 viral capsids (Duffy et al., 2016). Moreover, lack of binding to FX does not necessarily correlate with the presence of adenovirus neutralization as seen with the non-FX-binders HAdV-26 and 48, which despite not binding to FX are protected from *in vitro* neutralization in the presence of mouse serum (Ma et al., 2015). Furthermore, the ability of virions to bind to FX does not correlate with the presence of adenovirus neutralization in the absence of such binding. This is the case for the FX-binders HAdV-35 and HAdV-50, which are not neutralized *in vitro* in the presence of mouse serum and absence of FX-binding (Ma et al., 2015). The effects of HAdV-5 neutralization were also observed *in vivo.* Transduction of liver, lung, kidney, heart and spleen was negligible with FX-binding deficient HAdV-5 mutants (Xu et al., 2013). Moreover, while IgM antibodies, C1q and C4 were found responsible for the suppression of liver transduction, HAdV-5 neutralization in lung also required C3 (Xu et al., 2013). The exact mechanism by which FX protects HAdV-5 against *in vitro* and *in vivo* neutralization and the implications that binding to FX may have on different adenovirus serotypes have not been fully described yet. Also, whether FX also directly blocks interactions of C3b with viral capsids has not been investigated.

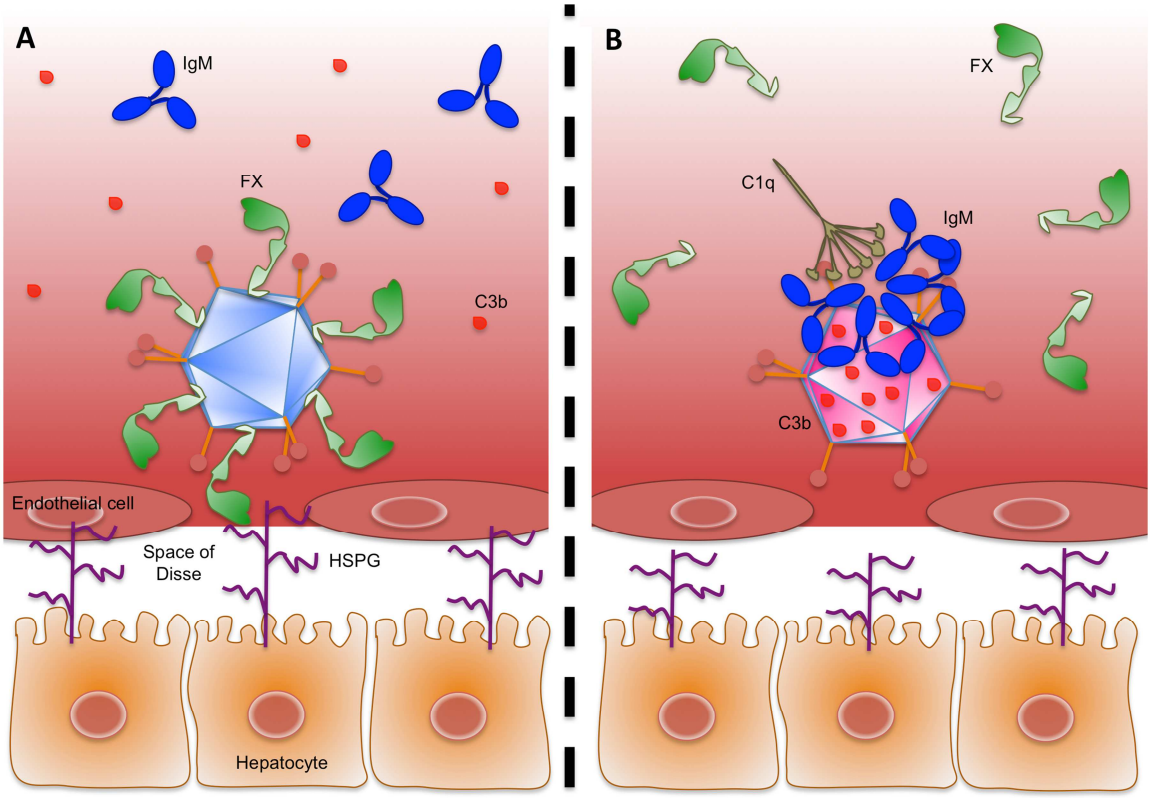

Figure 1-14. HAdV-5 interactions with the classical complement pathway *in vivo*. A) FX protects HAdV-5 from neutralization by the IgM antibody-mediated classical complement pathway and mediates transduction of hepatocytes. B) In the absence of FX or absence of HAdV-5 binding to FX, HAdV-5 is neutralized by natural IgM antibodies, which activate the classical complement pathway. Opsonization of HAdV-5 virions by C3b blocks HAdV-5 binding to host cells and thus cell transduction. FX; coagulation factor X, HSPG; heparan sulphate proteoglycan, C3; complement protein 3. Figure reproduced with permission from (Lopez-Gordo et al., 2014a).

1.3.5 Strategies to circumvent immune responses to human adenoviral vectors

The activation of immune responses against adenoviral vectors precludes efficient gene transfer and thus is still one of the main limitations for their use in gene therapy. In particular, several studies have reported toxicity and activation of anti-viral immune responses following intravascular delivery of HAdV-5 vectors, which has been mainly associated with their liver and spleen tropism (Lozier et al., 2002, Raper et al., 2002, Atencio et al., 2006, Morral et al., 2002, Bradshaw et al., 2012). Also, multiple interactions of adenoviral capsids or adenoviral DNA with DCs, NK cells, $CD4^+$ and $CD8^+$ T cells, NAbs and mechanisms of the innate immune response such as the complement system have also been reported (see sections 1.2.3 and 1.3.4.2.2). Thus, designing adenoviral vectors able to evade the immune response is key to increase their safety and gene transfer efficiency for their use in gene therapy.

NAbs can be directed to different components of the virion such as the hexon (Roberts et al., 2006, Abe et al., 2009, Shiratsuchi et al., 2010, Bradley et al., 2012b, Hong et al., 2003), the fiber (Myhre et al., 2007, Bradley et al., 2012a, Yu et al., 2013, Hong et al., 2003, Gahery-Segard et al., 1998, Parker et al., 2009) or the penton base (Yu et al., 2013, Hong et al., 2003, Gahery-Segard et al., 1998). Importantly, it was shown that the specificity of NAbs depends on the route of exposure to virions. While natural adenoviral infections result in antibodies mainly to the fiber protein, exposure to adenoviral vectors through vaccination results in antibodies that are largely directed to the hexon and/or penton base (Cheng et al., 2010, Sumida et al., 2005). The epitopes that are recognized by antibodies are primarily the hexon HVRs (Roberts et al., 2006, Abe et al., 2009, Shiratsuchi et al., 2010, Bradley et al., 2012a, Bradley et al., 2012b, Yu et al., 2013), the knob domain of the fiber (Myhre et al., 2007, Bradley et al., 2012a, Yu et al., 2013) and the RGD motif in the penton base (Hong et al., 2003). Several studies have either modified adenoviral capsid proteins or exchanged them with those of low-seroprevalent serotypes (pseudotyping) to remove neutralization epitopes and thus bypass the humoral immune response to adenoviral vectors (Figure 1-15). To achieve successful pseudotyping of adenoviral capsids, it is essential to first determine the viability of capsid protein replacements based on structural and biochemical constraints. Regarding the hexon, the exchange of only a subset of HAdV-5 hexon HVRs with those of HAdV-48 demonstrated that NAbs can recognize multiple HVRs and thus highlighted the importance of targeting all HVRs for genetic engineering to completely circumvent pre-existing immunity (Bradley et al., 2012b). Indeed, the exchange of all HAdV-5 hexon HVRs with those of HAdV-48 successfully evaded recognition of virions by NAbs in both mice and rhesus monkeys (Roberts et al., 2006). Other studies also reported evasion of pre-existing immunity in mice using HAdV-5 vectors with whole hexon or hexon HVRs replaced with those of serotypes 3, 4, 9, 12 or 43 (Roy et al., 1998, Ostapchuk and Hearing, 2001, Wu et al., 2002, Bruder et al., 2012). Importantly, a later study by Coughlan and colleagues showed that despite evading neutralizing antibodies, recombinant HAdV-5 vectors containing HAdV-48 hexon HVRs triggered a robust pro-inflammatory response that differed from that of HAdV-5 or HAdV-48 parental vectors (Coughlan et al., 2012). This study indicates that modification of capsid proteins can lead to unexpected effects that cannot be predicted from parental vectors. Given that anti-fiber NAbs represent a considerable proportion of the anti-adenovirus NAbs population and that seroprevalence is tightly associated with serotype, the design of chimeric adenoviral vectors by replacing the fiber of high-seroprevalent serotypes with that of low-seroprevalent serotypes is also a promising strategy to evade pre-existing immunity. Importantly, the high similarity of the

N-terminal region of the fiber (fiber tail) among serotypes facilitates fiber-pseudotyping strategies (Tarassishin et al., 2000). A study on the seroprevalence of a range of serotypes in the Belgian population reported a high number of NAbs to species A, C and E and a low number to species B and D, of which HAdV-11, 34, 35 and 50 (species B) and HAdV-43 and 48 (species D) exhibited the lowest values (Vogels et al., 2003). These data indicate that such serotypes may be a good choice for fiber-pseudotyping strategies. Following this approach, chimeric vectors such as HAdV-5/F3[3] (Haviv et al., 2002, Kanerva et al., 2002, Volk et al., 2003, Ulasov et al., 2007), HAdV-5/F11 (Havenga et al., 2001, Stone et al., 2005, Wang et al., 2011b), HAdV-5/F16 (Havenga et al., 2001) and HAdV-5/F35 (Havenga et al., 2001) were generated. Despite HAdV-5/F11 and HAdV-5/F35 showing reduced toxicity and induction of inflammatory cytokines in mice and baboons (Ni et al., 2005), HAdV-5/F35 exhibited tropism for $CD34^+$ human hematopoietic stem cells (Shayakhmetov et al., 2000), monocytes, granulocytes and blast cells of human bone marrow (Rogozhin et al., 2011), and $CD4^+$ and $CD8^+$ T lymphocytes (Zhang et al., 2013) that while conferring unique targeting properties, might also trigger an unpredicted immune response. Thus, in-depth characterization of novel chimeric adenoviral vectors and the associated immune response *in vivo* should be done before conducting further studies in humans. Other strategies to bypass anti-fiber pre-existing immunity such as the truncation of the fiber knob domain or its replacement with foreign trimerization motifs fused to the fiber shaft (fiber deknobbing) [reviewed by (Coughlan et al., 2010)] have been also assessed and shown success in evading NAbs (Myhre et al., 2007, Gaden et al., 2004, Magnusson et al., 2001, Izumi et al., 2005) (Figure 1-15). Despite the promising results obtained by pseudotyping or deknobbing adenoviral vectors, these strategies are limited by the formation of nonviable virions and the generation of virions with a lower number of fiber copies that can result in lower vector titers and infectivity (Youil et al., 2002, Legrand et al., 1999, Falgout and Ketner, 1988, Von Seggern et al., 1999, Kupgan et al., 2014). To avoid infectivity issues associated with genetic engineering of viral capsid proteins, vectors have been developed from low-seroprevalent serotypes such as HAdV-6 (Capone et al., 2006), HAdV-7 (Nan et al., 2003), HAdV-11 (Holterman et al., 2004, Stone et al., 2005), HAdV-35 (Gao et al., 2003, Sakurai et al., 2003, Seshidhar Reddy et al., 2003, Vogels et al., 2003, Barouch et al., 2004, McVey et al., 2010) or HAdV-49 (Lemckert et al., 2006) and have showed successful evasion of NAbs (Figure 1-15). Nevertheless, since seroprevalence to adenovirus serotypes is determined by exposure to virions (Thorner et al., 2006, Nwanegbo et al., 2004, Ludwig et al., 1998), seroprevalence should be assessed

[3]"F" stands for adenovirus fiber and the preceeding number refers to the adenovirus serotype to which the fiber belongs.

by age and geographical location to allow smart choice of serotypes for the development of vectors able to evade pre-existing immunity. The use of NHAdVs such as simian (Roy et al., 2005, Belousova et al., 2010), canine (Lau et al., 2012, Ord et al., 2013), bovine (Sharma et al., 2009a, Tandon et al., 2012), porcine (Bangari et al., 2005, Sharma et al., 2009a), fowl (Logunov et al., 2004, Shashkova et al., 2005), ovine (Hofmann et al., 1999, Voeks et al., 2002) or murine (Robinson et al., 2009) has also been proposed as an alternative to current strategies, since NHAdVs can circumvent NAbs targeted against HAdVs (Figure 1-15). Also, NHAdVs have other advantages over HAdVs such as having absent or very low pathogenicity, being unable to replicate in human cells and tolerate insertions of long transgenes [reviewed by (Lopez-Gordo et al., 2014b)]. However, many challenges such as potential cross-reactivity of NAbs against human antigens with non-human antigens due to structural similarity between HAdVs and NHAdVs, or occurrence of interspecies adaptation have yet to be overcome for NHAdV to be safely used as gene therapy vectors [reviewed by (Lopez-Gordo et al., 2014b)].

In addition to NAbs, $CD4^+$ and $CD8^+$ T cells can also limit efficiency of gene transfer with adenoviral vectors *in vivo* (see section 1.2.3). Since $CD4^+$ and $CD8^+$ T cells mainly recognize epitopes in the hexon (Leen et al., 2004, Olive et al., 2002, Tang et al., 2006, Onion et al., 2007), genetic engineering of hexon epitopes or hexon-pseudotyping might be an attractive approach to evade the anti-viral T cell response. Moreover, CTL-mediated killing of cells partially relies on the detection of antigenic peptides on transduced cells, which result from processing of capsid proteins of the incoming virions and from the leaky expression of adenoviral genes from the vector genome (Yang et al., 1994). To reduce the CTL response to transduced cells, third generation HD vectors, which are devoid of viral gene sequences in their genome, were generated (Kochanek et al., 1996). Importantly, their low immunogenicity allowed long-term transgene expression (Maione et al., 2001, Ehrhardt and Kay, 2002, Dudley et al., 2004). However, since these vectors are composed of stuffer DNA in place of viral gene sequences to maintain optimum vector size (Bett et al., 1993, Parks and Graham, 1997, Smith et al., 2009), the activation of innate immune mechanisms upon recognition of dsDNA has been observed. For instance, a TLR9-dependent innate immune response, which is activated upon recognition of non-methylated CpG-containing viral DNA (Bauer et al., 2001), was observed both *in vitro* and *in vivo* to HD vectors (Cerullo et al., 2007). Also, one study reported that the nature of stuffer DNA has important effects on the T cell response against transduced cells (Parks et al., 1999). Importantly, despite the potential shown by HD vectors [reviewed by (Cots et al., 2013)], HD capsids can stimulate an immune response upon intravenous administration that is

equivalent to first and second generation adenoviral vectors and that is characterized by the production of pro-inflammatory cytokines such as IL-6 and TNF-α (Brunetti-Pierri et al., 2004, Mane et al., 2006). Thus, other strategies aimed at blocking interactions between adenoviral capsid proteins and components of the immune system to further attenuate the anti-viral immune response might be essential to achieve efficient gene transfer with adenoviral vectors. Interestingly, blockade of interactions between HAdV-5 virions and SRs on KCs (Xu et al., 2008, Haisma et al., 2008, Khare et al., 2012) or between HAdV-5 virions and complement proteins (Xu et al., 2008) blocked vector clearance by KCs *in vitro* and *in vivo*. Depletion of KCs with clodronate liposomes (van Rooijen and van Kesteren-Hendrikx, 2003) or gadolinium chloride, which forms a colloidal precipitate that can be phagocytosed by macrophages and lead to cell death (Hardonk et al., 1992), are approaches that have been assessed in experimental models. Moreover, interaction of the RGD motif in the penton base with macrophage β_3 integrin results in the secretion of IL-1α (Di Paolo et al., 2009a) and the RGD motif has also been proposed as the region targeted for binding to α-defensins (Flatt et al., 2013), which block capsid disassembly (Smith and Nemerow, 2008, Smith et al., 2010, Snijder et al., 2013). Mutation of the HAdV-5 RGD motif to arginine-glycine-glutamic acid (RGE) achieved a reduction in spleen uptake following intravascular administration and in the associated immune response (Bradshaw et al., 2012). Also, since DCs have been reported to interact with the adenovirus fiber shaft region via a heparin-sensitive receptor (Cheng et al., 2007), mutations in the fiber shaft region may help reducing DC-mediated immune responses.

Other interactions between virions and non-immune cells have also been associated with the promotion of immune responses, limiting gene transfer efficiency. For instance, interactions between HAdV-5 fiber and CAR have been shown to stimulate an immune response in human respiratory cells, which is characterized by the activation of mitogen-activated protein kinase 3 (MAPK3)/ERK1 MAPK, MAPK1/ERK2 MAPK, MAPK8/c-Jun N-terminal kinase (JNK) MAPK and NF-κB and the induction of expression of chemokines IL-8, growth-related oncogene (GRO)-α and γ, C-C motif chemokine ligand 5 (CCL5)/RANTES and CXCL10/IP-10 (Tamanini et al., 2006). HAdV-5 binding to CAR on platelets has also been associated with the formation of virion-platelet-leukocyte aggregates that are cleared from the circulation by macrophages in the liver (Stone et al., 2007, Othman et al., 2007). CAR-binding ablating mutations might reduce CAR-mediated immune responses and virion clearance (Figure 1-15). Furthermore, immune recognition of virions can facilitate interactions of vectors with non-immune cells. This is the case for

human but not mouse erythrocytes, which can detect HAdV-5 virions via CR1 in the presence of C1q and antibodies (Carlisle et al., 2009).

An alternative approach has been reported by several groups who have attempted to coat the adenoviral capsid with cationic polymers or lipid molecules, with the aim of preventing immune recognition of capsid proteins by IgG or IgM antibodies, complement proteins, α-defensins or immune cells, and with the aim of hampering binding of virions to receptors on non-immune cells that may trigger the immune response and lead to toxicity (Wonganan and Croyle, 2010) (Figure 1-15). Initial studies performed chemical modifications of virions with polyethylene glycol (PEG) (Romanczuk et al., 1999), but later studies also showed promising results with multivalent copolymers of poly[*N*-(2-hydroxypropyl)methacrylamide] (pHPMA) (Green et al., 2004). Both polymer coating approaches achieved protection of virions from NAbs *in vitro* (Romanczuk et al., 1999, Wang et al., 2011a, Eto et al., 2004) and led to lower production of NAbs *in vivo* (Eto et al., 2010). PEGylation of virions impaired virion-engulfment by macrophages *in vitro* or KCs *in vivo*, reducing the expression of IL-6 in both settings (Mok et al., 2005). PEGylation also prevented thrombocytopenia and abrogated neutrophil infiltration to the liver resulting in reduced toxicity, reduced spleen transduction, and decreased expression of pro-inflammatory cytokines (De Geest et al., 2005). Coating of HAdV-5 virions with pHPMA increased persistence of virions in the bloodstream and substantially reduced liver transduction and associated toxicity (Green et al., 2004). Interestingly, in addition to preventing immune recognition of virions and interactions of virions with host cell receptors (removal of native tropism), this strategy also offers retargeting possibilities, since targeting molecules can be chemically attached to polymer chains (Stevenson et al., 2007, Morrison et al., 2008, Parker et al., 2005, Morrison et al., 2009). Nevertheless, it has to be taken into account that an IgM-mediated immune response is activated towards PEG molecules that depends on the length of PEG chains (Shimizu et al., 2012). Therefore, further characterization of the immune response elicited by polymer coated adenoviral vectors and the implications for gene transfer efficiency should be done for their safe use in gene therapy.

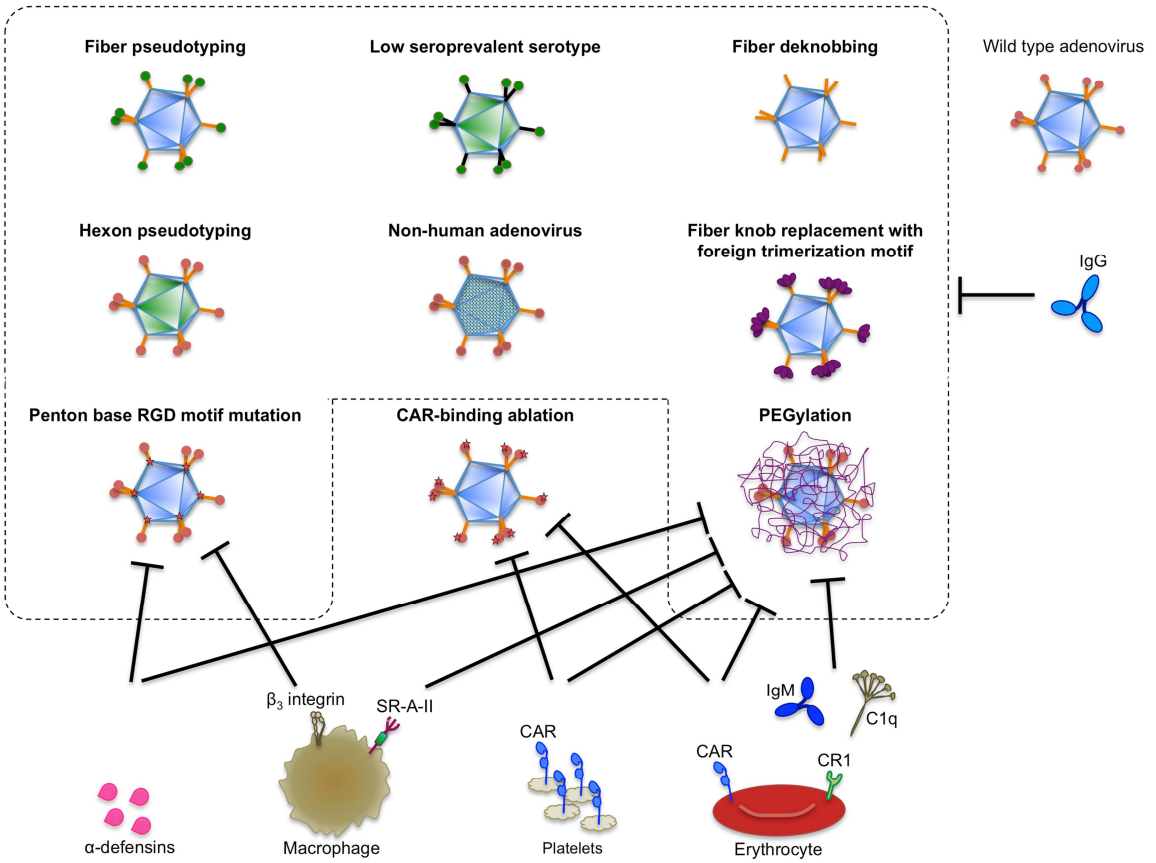

Figure 1-15. Strategies to circumvent the immune response to adenoviral vectors. Genetic pseudotyping of adenovirus capsid proteins (fiber or hexon) with those of low-seroprevalent serotypes, use of low-seroprevalent adenovirus serotypes or non-human adenoviral vectors, fiber deknobbing or removal of fiber knob domain and replacement with foreign trimerization motifs, genetic engineering to remove epitopes in capsid proteins (fiber knob domain or penton base), and PEGylation of adenoviral virions, are illustrated. Blunt arrows indicate the interactions between adenoviral capsid proteins and host proteins that are inhibited due to each strategy. Adenovial capsid proteins represented in green indicate proteins from low-seroprevalent serotypes. Red stars indicate mutation sites on adenoviral capsid proteins. RGD; arginine-glycine-glutamic acid residues, CAR; coxsackie virus and adenovirus receptor, SR-A-II; scavenger receptor A-II, CR1; complement receptor 1.

1.3.6 Adenoviral retargeting strategies

Multiple strategies have been deployed to generate adenoviral vectors that selectively target the cell type where the gene therapy is required. These strategies are based on transcriptional or transductional re-targeting. Transcriptional retargeting is aimed at limiting adenovirus replication or transgene expression to the target tissue via genetic complementation (Fueyo et al., 2000) or through the use of tissue-specific promoters/enhancer systems (Rodriguez et al., 1997, Wu et al., 2001), respectively. Transductional retargeting is aimed at limiting adenovirus cell entry to a specific cell type and can be achieved by incorporating genetic mutations into the adenoviral capsid to modify tropism [e.g: fiber serotype swap (genetic pseudotyping) (Haviv et al., 2002, Kanerva et al., 2002, Ulasov et al., 2007, Volk et al., 2003, Havenga et al., 2001, Raki et al., 2008, Shayakhmetov et al., 2000, Ni et al., 2005); knobless fiber shaft fusions

(Magnusson et al., 2001, Belousova et al., 2003, Izumi et al., 2005, Li et al., 2006); adapter ligand complexes such as bispecific antibodies (Nettelbeck et al., 2001, Miller et al., 1998, Nettelbeck et al., 2004), conjugated antibody fragments (Korokhov et al., 2003, Li et al., 2007) or recombinant bispecific fusion proteins (Harvey et al., 2010); or insertion of heterologous binding ligands into adenoviral proteins (Dmitriev et al., 1998)]. Transductional retargeting can also be achieved by modifying the adenoviral capsid via covalent or non-covalent fusion of adapter ligands with the capsid [reviewed by (Coughlan et al., 2010)]. The retargeting strategies used in adenoviral vectors that are currently undergoing clinical assessment are genetic pseudotyping [e.g: clinical trial with 21 patients using HAdV-5 with the fiber knob replaced with that of HAdV-3 and encoding GMCSF to stimulate an anti-tumor immune response (Koski et al., 2010)] and, predominantly, the insertion of heterologous binding ligands [e.g: clinical trial with 21 patients using HAdV-5 with the RGD motif-containing CDCRGDCFC peptide inserted into the fiber knob HI loop for enhanced targeting of cancer cells in solid tumors (Nokisalmi et al., 2010)]. These studies showed anti-tumor activity with mild side effects including thrombocytopenia, transaminitis, hyponatremia, fever and fatigue (Koski et al., 2010, Nokisalmi et al., 2010), and thus highlight the potential of such strategies in the clinic.

The insertion of heterologous binding ligands consists of selecting heterologous peptides that home to the *in vivo* target tissue and incorporating them into the adenoviral capsid. The selected peptide should not need any major post-translational modification in the ER to maintain binding to the target protein, since adenoviral proteins are translated in the cytosol under non-reducing conditions and they do not go to the ER before virus assembly in the nuclei. These peptides can be found by rational design or by technologies such as phage display (Figure 1-16), which allows the isolation of candidate peptides from peptide libraries as highly efficient and selective binders of specific proteins expressed on target cells [reviewed by (Azzazy and Highsmith, 2002, Pande et al., 2010)]. Heterologous peptides have been inserted into the C-terminal of the fiber (Kurachi et al., 2007b, Kurachi et al., 2007a, Wickham et al., 1997, Gonzalez et al., 1999, Ranki et al., 2007, Rein et al., 2004, Staba et al., 2000), the penton base (Wickham et al., 1996, Einfeld et al., 1999), certain hexon HVRs (Vigne et al., 1999, Wu et al., 2005) or the capsid protein IX (Dmitriev et al., 2002, Campos et al., 2004, Vellinga et al., 2004). The insertion of heterologous peptides should not disrupt the interactions necessary for adenovirus assembly. The HAdV-5 knob domain at the C-terminal of the fiber is composed of an eight-stranded antiparallel β sandwich with interspersing exposed loop regions (Xia et al., 1994). The loop regions comprise 8-55 amino acid residues (Xia et al., 1994) and are the

preferable location for peptide incorporation due to their flexibility, exposure and non-conserved characteristics. The HI loop, which is not involved in fiber interactions with HAdV-5 native receptors, has been reported as the most suitable surface exposed loop for peptide incorporation (Figure 1-16) since fiber trimerization, capsid structure and viral titer is maintained after the introduction of peptides (Krasnykh et al., 1998). The first heterologous peptide that was successfully introduced into the HI loop was the RGD motif-containing CDCRGDCFC peptide, which successfully targeted $\alpha_v\beta_{3,5}$ integrin-expressing primary ovarian cancer cells (Dmitriev et al., 1998), pancreatic carcinoma cells (Wesseling et al., 2001), non-hematopoietic human tumor cell lines and primary melanoma cells (Nagel et al., 2003). Also, the RGD motif-containing ACDCRGDCFCD peptide enhanced transduction of $\alpha_v\beta_{3,5}$ integrin-positive cells that do not express CAR (Kurachi et al., 2007a). Interestingly, the targeting efficacy of RGD motif-containing peptides was demonstrated *in vivo* via increased transgene expression in liver, lung, spleen and kidney following intravenous delivery (Reynolds et al., 1999). Moreover, a HAdV-5 encoding the peptide motif NGR in the HI loop targeted aminopeptidase N-expressing rhabdomyosarcoma cells *in vitro* (Majhen et al., 2006). Another peptide successfully incorporated into the HI loop is A20FMDV2 (derived from VP1 of foot-and-mouth disease virus) to target $\alpha_v\beta_6$ integrin (Coughlan et al., 2009). A20FMDV2 peptide showed targeting and cytotoxicity on a panel of $\alpha_v\beta_6$ integrin-expressing human carcinoma cells and enhanced tumor virion uptake following systemic delivery (Coughlan et al., 2009). The incorporation of the YSA peptide into the HI loop achieved selective targeting of Ephrin A2 receptor (EphA2R)-positive cells and human pancreatic cancer cells *in vitro* but failed to show transduction of human pancreatic cells *in vivo* after intravascular administration (van Geer et al., 2009). *In vitro* phage display technology has made it possible to identify heterologous peptides that target human tracheal glandular cells (Gaden et al., 2004), endothelial cells (Nicklin et al., 2001), human transferrin receptor (hTfR) on brain microcapillary endothelium (Xia et al., 2000) or neuroglial cells (Joung et al., 2005), smooth muscle cells (Work et al., 2004) or gastric cancer tissues (Zhang et al., 2012) *in vitro*. One study introduced an endothelial cell-targeting peptide that had been found by *in vitro* phage display, into the HI loop of the HAdV-5 fiber and showed selectivity for endothelial cells *in vitro* and for blood vessels following intravascular delivery into mice (Nicklin et al., 2004). Another study generated an HAdV-5 with an heterologous peptide found by *in vitro* phage display that selectively targeted human a colorectal cancer cell line *in vitro*, but failed to show selective targeting in mice (Rittner et al., 2007). *In vivo* phage display has also led to selection of peptides that home to mouse lung, skin, pancreas, intestine, uterus, adrenal gland or retina (Rajotte et al., 1998), mouse

brain or kidney blood vessels (Pasqualini and Ruoslahti, 1996), mouse white fat vasculature by targeting prohibitin (Kolonin et al., 2004), or rat kidney (Denby et al., 2007). In the latter study, the identified kidney-targeting peptides were incorporated into the HI loop of HAdV-19p and the resultant vectors showed selectivity for rat kidney tubular epithelium or rat glomeruli (Denby et al., 2007). These studies show the potential of incorporating heterologous peptides into the HI loop of the fiber knob domain as a strategy to selectively retarget adenoviral vectors to tissues for gene therapy applications.

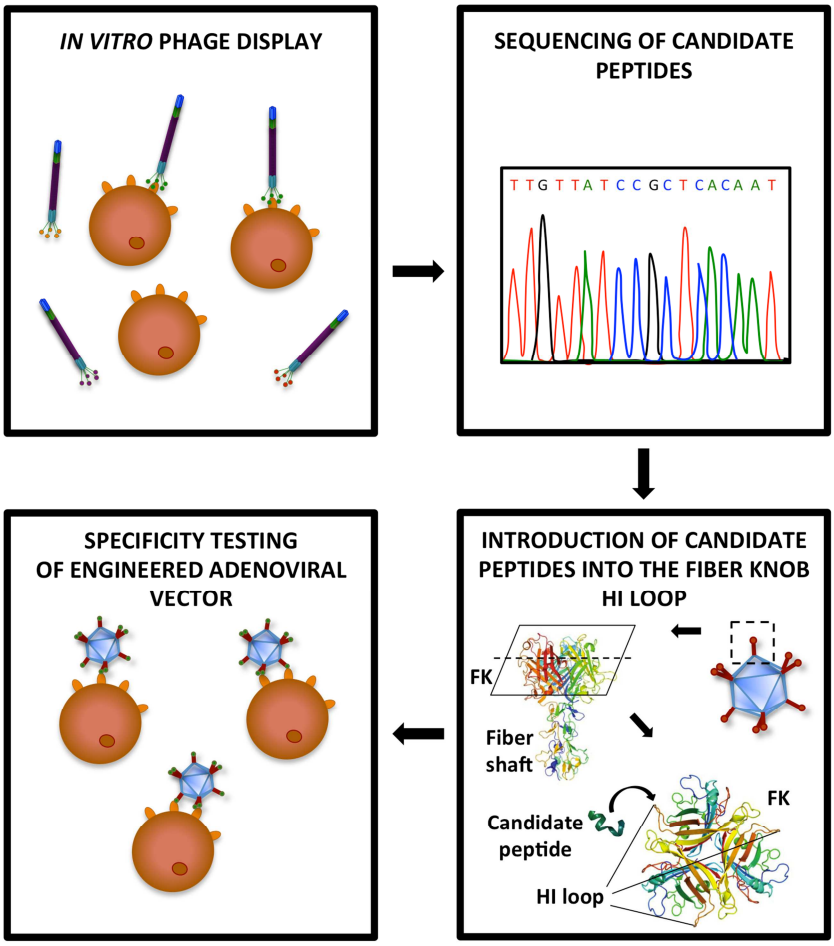

Figure 1-16. Re-targeting of adenoviral vectors via the incorporation of heterologous peptides found by *in vitro* phage display, into the HI loop of the fiber knob domain. Candidate peptides for binding to a particular ligand are selected from *in vitro* phage display libraries and their corresponding DNA is sequenced. The DNA sequence is inserted into the adenoviral genome corresponding to the HI loop sequence in the fiber ORF. Recombinant adenoviral vectors are produced and tested *in vitro* for their specificity for cells expressing the targeted ligand. FK; fiber knob. Ribbon diagram of fiber and fiber knob images on the lower right square reproduced with permission from (Hall et al., 2010).

1.4 Aims of this thesis

The studies presented in this thesis were conducted to gain further understanding of the mechanisms mediating HAdV-5 virion neutralization by the host innate immune response and hepatic and splenic tropism of HAdV-5-based vectors following intravascular delivery. To this end, the interactions of HAdV-5 virions with blood components and host cell receptors were investigated. The hypothesis of this thesis was that HAdV-5-based vectors can use FX for protection against neutralization and for liver transduction following administration of vectors through the vasculature, but that in the absence of FX-binding and neutralization, HAdV-5 can follow alternative pathways for liver and spleen transduction via CAR and $\alpha_v\beta_{3,5}$ integrins and via interactions with other blood proteins. It was also hypothesized that FX-binding deficient HAdV-5 vectors can be retargeted to specific tissues. Thus, this thesis is divided into three studies encompassing four questions:

What are the mechanisms by which natural IgM antibodies, complement and FX mediate HAdV-5 virion neutralisation or protection from neutralisation *in vitro* and *in vivo?* Wild type and FX-binding deficient HAdV-5 vector transduction was assessed in mouse models lacking different components of the immune response, and in *in vitro* cell culture models in the presence of purified serum from individual mouse strains.

Do FX, CAR and $\alpha_v\beta_{3,5}$ integrins mediate the hepatic and splenic tropism of HAdV-5 following intravascular delivery? Do alternative transduction pathways exist for HAdV-5 *in vitro* and are they relevant *in vivo?* FX, CAR and $\alpha_v\beta_{3,5}$ integrin-binding deficient HAdV-5 vectors were administered through the vasculature to immunocompromised mice unable to neutralize FX-binding deficient virions and liver and spleen transduction was evaluated. HAdV-5 transduction of cell culture models was assessed after exposure of virions to purified mouse serum.

Does FX binding to HAdV-5 influence the efficiency of cell uptake and endosomal membrane penetration of the virion? These processes were investigated in the presence of FX by microscopic assessment of fluorescently labelled virions at the single cell level.

Can HAdV-5 vectors be selectively retargeted to relevant cells of the kidney by genetic modification of the capsid? HAdV-5 vectors were engineered to incorporate renal targeting peptides identified by *in vitro* phage display into the HI loop of the fiber knob domain, and assessed for their efficiency in mediating specific gene delivery *in vitro*.

Chapter 2 Materials and Methods

2.1 Materials

All chemicals were obtained from Sigma-Aldrich (Poole, UK) and of the highest quality available unless otherwise stated. All primers were purchased from Eurofins Genomics (Wolverhampton, UK) unless otherwise stated. All antibodies were purchased from Thermo Fisher Scientific (Renfrew, UK) unless otherwise stated. All cell culture reagents were obtained from GIBCO® by Life Technologies (Paisley, UK) unless otherwise stated. The DNA plasmids used can be found in the appendix.

2.1.1 Oligonucleotides

The primers used in experimental procedures are summarised in Table 2-1.

Table 2-1. Oligonucleotides used in experimental procedures.

Name (probe type)	DNA sequence (5'→3')	Application
Hexon-F	CCCGCTTTCCAAGATGGCTA	PCR
Hexon-R	GTTGGCGGGTATAGGGTAGA	PCR
Fiber-F	ACTGCCACTGGTAGCTTGGG	PCR
Fiber-R	TGGCCAGCTGGTTTAGGATG	PCR
Penton base-F	ATGAGGAAGGTCCTCCTCCC	PCR
Penton base-R	CCCCAGCCTGTGTTATTGCT	PCR
Hexon_HVR 5/HVR 7	CTCAGTGGTACGAAACTGAA	Sequencing
Hexon_HVR 7	CTATGTGGAATCAGGCTGTT	Sequencing
Fiber Knob_HI loop	ACTGAAGGCACAGCC	Sequencing
Fiber Knob_AB loop_KO1	AATGCACCAAACACAAATCC	Sequencing
Penton base_RGE	CATTCCCGCACTGTTGGATG	Sequencing
***LacZ*-F**	ATCTGACCACCAGCGAAATGG	qPCR
***LacZ*-R**	CATCAGCAGGTGTATCTGCCG	qPCR
Claudin 16_Mm00475025_m1 (FAM_MGB probe)	-	TaqMan®
18s_Hs03928985_g1 (VIC_MGB probe)	-	TaqMan®
Oligo_NotIASFPPAFNotI5-3	GCGGCCGCc<u>GCGAGTTTTCCGC CGGCGTTT</u>GCGGCCGC[1]	Cloning
Oligo_NotIASFPPAFNotI3-5	GCGGCCGCAAACGCCGGCGGA AAACTCGCGGCGGCCGC	Cloning
Oligo_NotIYAAHRSHNotI5-3	GCGGCCGCc<u>TATGCTGCGCATC GTTCTCAT</u>GCGGCCGC[1]	Cloning
Oligo_NotIYAAHRSHNotI3-5	GCGGCCGCATGAGAACGATGC GCAGCATAGGCGGCCGC	Cloning

[1]*Not*I sites are shown in upper case, additional cytosine to maintain the fiber ORF in lower case, and nucleotides corresponding to ASFPPAF or YAAHRSH peptides, respectively, in upper case and underlined. All oligonucleotides were purchased from Eurofins MWG Operon by Eurofins Genomics with the exception of TaqMan® probes, which were purchased from Thermo Fisher Scientific. PCR; polymerase chain reaction, qPCR; quantitative Real-Time polymerase chain reaction.

2.1.2 DNA plasmids

The DNA plasmids used in experimental procedures were based on the AdEasy, E1/E3 deleted HAdV-5 adenoviral vector system (Stratagene by Agilent Technologies) (Luo et al., 2007) and are summarised in Table 2-2.

Table 2-2. DNA plasmids used in experimental procedures.

Name	Encoded reporter and/or fiber genes	Antibiotic resistance gene	Source of reference
pAdEasy1	wt HAdV-5 fiber	Amp^R	Agilent Technologies
pAdT*	*E.coli* LacZ, wt HAdV-5 fiber	Neo^R/Kan^R	(Alba et al., 2009)
pAdT*KO1	*E.coli* LacZ, HAdV-5 fiber KO1	Neo^R/Kan^R	Dr. Angela C. Bradshaw[1]
pAdT*RGE	*E.coli* LacZ		(Bradshaw et al., 2012)
pShuttle-CMV-*LacZ*	*E.coli* LacZ	Neo^R/Kan^R	Agilent Technologies
pShuttle-KO1-AAA	HAdV-5 fiber KO1 AAA	Sm^R	Agilent Technologies
pShuttle-KO1	HAdV-5 fiber KO1	Sm^R	Generated in this study
pShuttle-KO1-AAA-AAASFPPAF	HAdV-5 fiber KO1 AAAASFPPAFAAA	Sm^R	Generated in this study
pShuttle-KO1-AAA-AAAYAAHRSH	HAdV-5 fiber KO1 AAAYAAHRSHAAA	Sm^R	Generated in this study
pAdEasy1-CMV-*LacZ*	*E.coli* LacZ, wt HAdV-5 fiber	Neo^R/Kan^R	Generated in this study
pAdEasy1-CMV-*LacZ*-KO1	*E.coli* LacZ, HAdV-5 fiber KO1	Neo^R/Kan^R	Generated in this study
pAdT*KO1-AAA	*E.coli* LacZ, HAdV-5 fiber KO1 AAA	Neo^R/Kan^R	Generated in this study
pAdT*KO1-AAA-AAAASFPPAF	*E.coli* LacZ, HAdV-5 fiber KO1 AAAASFPPAFAAA	Neo^R/Kan^R	Generated in this study
pAdT*KO1-AAA-AAAYAAHRSH	*E.coli* LacZ, HAdV-5 fiber KO1 AAAYAAHRSHAAA	Neo^R/Kan^R	Generated in this study

Genetic maps of all the plasmids used in the studies presented in this thesis are shown in the appendix. HAdV-5; human adenovirus serotype 5, Amp^R; ampicillin resistance, Neo^R; neomycin resistance, Kan^R; kanamycin resistance, Sm^R; streptomycin resistance, wt; wild type.
[1]pAdT*KO1 was a kind gift from Dr. Angela C. Bradshaw (University of Glasgow, UK).

2.1.3 Antibodies

The antibodies used in experimental procedures are summarised in Table 2-3 and Table 2-4. Primary mouse anti-human Giantin IgG1 antibody was kindly provided by Professor Hans-Peter Hauri (Biocentre of the University of Basel, Switzerland).

Table 2-3. Primary antibodies used in experimental procedures.

Antibody reactivity	Host species	Clonality	Working concentration	Application	Provider (Catalogue number)
Anti-adenovirus fiber IgG2a	Mouse	Monoclonal (Clone: 4D2)	0.2 μg/ml	WB	Abcam (ab3233)
Anti-β-galactosidase-DIG Digoxigenin	Mouse	Monoclonal	0.5 μg/ml	ELISA	Roche (provided in the kit)
Anti-CAR IgG1	Mouse	Monoclonal (Clone: RmcB)	5 μg/ml	FCM	Upstate, NY (05-644)
Anti-pericentrin	Rabbit	Polyclonal	5 μg/ml	ICC	Abcam (ab4448)
Anti-Alexa Fluor 488	Rabbit	Polyclonal	1 μg/ml	SLO	Thermo Fisher Scientific (A-11094)
Anti-human Giantin IgG1	Mouse	Monoclonal (Clone: G1/133)	33.33 μg/ml	SLO	Enzo Life Sciences (ALX-804-600-C100)
Anti-β-galactosidase	Rabbit	Polyclonal	5 μg/ml	IHC	MP Biomedicals LLC (08559761)
Mouse IgG (isotype control)	Mouse	N/A	Matched		Thermo Fisher Scientific (10400C)
Rabbit IgG (isotype control)	Rabbit	N/A	Matched		Thermo Fisher Scientific (10500C)

WB; western blotting, FCM; flow cytometry, ICC; immunocytochemistry, IHC; immunohistochemistry, SLO; SLO penetration assay, N/A; not applicable. "Matched" refers to a concentration equivalent to that of the primary antibody used in each assay.

Table 2-4. Secondary antibodies used in experimental procedures.

Antibody reactivity	Host species	Clonality	Working concentration	Application	Provider (Catalogue number)
Anti-mouse IgG HRP	Rabbit	Polyclonal	1.3 µg/ml	WB	Dako (P0260)
Anti-DIG-POD Fab fragment Peroxidase	Sheep	Polyclonal	0.26 U/ml	ELISA	Roche (provided in the kit)
Anti-mouse IgG Alexa Fluor 488	Goat	Polyclonal	4 µg/ml	FCM	Thermo Fisher Scientific (A-11001)
Anti-rabbit IgG Alexa Fluor 546	Goat	Polyclonal	4 µg/ml	ICC	Thermo Fisher Scientific (A-11035)
Anti-rabbit IgG Alexa Fluor 594	Goat	Polyclonal	4 µg/ml	SLO	Thermo Fisher Scientific (A-11037)
Anti-mouse IgG Alexa Fluor 680	Goat	Polyclonal	4 µg/ml	SLO	Thermo Fisher Scientific (A-21058)
Anti-rabbit IgG Alexa Fluor 488	Goat	Polyclonal	4 µg/ml	IHC	Thermo Fisher Scientific (A-11008)

HRP; horseradish peroxidase, Fab; fragment antigen-binding, WB; western blotting, FCM; flow cytometry, ICC; immunocytochemistry, IHC; immunohistochemistry, SLO; SLO penetration assay, N/A; not applicable.

2.1.4 Bacterial cells

The *Escherichia coli* (*E. coli*) strains used are summarised in Table 2-5.

Table 2-5 Bacterial strains used.

Bacterial strain	Genotype	Transformation characteristics
JM109	*end*A1, *rec*A1, *gyr*A96, *thi*, *hsd*R17 (r_k–, m_k+), *rel*A1, *sup*E44, Δ(*lac-pro*AB), [F´ *tra*D36, *pro*AB, *laq*I^qZΔM15]	Chemically-competent
BJ5183	*endA1, sbcBC, recBC, galK, met, thi-1, bioT, hsdR.* Sm^R.	Electroporation-competent

JM109 cells were purchased from Promega and BJ5183 from Stratagene by Agilent Technologies. Sm^R; streptomycin resistance.

2.1.5 Immortalised cell lines

The immortalised cell lines used, cell characteristics, medium used and culture requirements are described in Table 2-6. K562CLDN16 cells were kindly provided by Justin Roth (Case Western Reserve University, Cleveland, Ohio, USA). CHO-CAR cells were a kind gift from Dr. George Santis (King's College London School of Medicine, London, UK) (Bergelson et al., 1997). SKOV3-CAR cells were generated by transfecting a RFP-hCAR plasmid that has been described before (Farmer et al., 2009). They were a kind gift from Dr. Katie White (University of Glasgow, UK).

Table 2-6. Immortalised cell lines used.

Cell line	Cellular origin and characteristics	Cell culture medium and supplements
HEK-293	Human Embryonic Kidney (Graham et al., 1977), adherent cell line.	MEM supplemented with PCN, Sm, FCS, NaP and L-Gln.
Per.C6®	Human embryonic retina (HER) from Crucell (Leiden, The Netherlands) (Fallaux et al., 1998), adherent cell line.	DMEM 5.55 mM D-Glucose, 4 mM L-Gln and 1 mM NaP supplemented with PCN, Sm, FCS and 0.01 M $MgCl_2$.
A549	Human lung carcinoma, adherent cell line.	RPMI-1640 supplemented with PCN, Sm, FCS, NaP and L-Gln.
SKOV3	Human ovary adenocarcinoma, adherent cell line.	RPMI-1640 supplemented with PCN, Sm, FCS, NaP and L-Gln.
SKOV3-CAR	SKOV3 cells stably overexpressing RFP-tagged hCAR and Neo^R gene *neo*, adherent cell line.	RPMI-1640 supplemented with PCN, Sm, FCS, NaP and L-Gln and geneticin.
CHO-K1	Chinese hamster ovary, adherent cell line.	Ham's F-10 Nutrient Mixture medium 1 mM L-Gln and 1 mM NaP supplemented with PCN, Sm and FCS.
CHO-CAR	CHO cells stably expressing hCAR (Bergelson et al., 1997), adherent cell line.	Ham's F-10 Nutrient Mixture medium 1 mM L-Gln and 1 mM NaP supplemented with PCN, Sm and FCS.
HeLa	Human cervix adenocarcinoma, adherent cell line.	MEM supplemented with PCN, Sm, FCS, NaP and L-Gln.
HepG2	Human liver hepatocellular carcinoma, adherent cell line.	MEM supplemented with PCN, Sm, FCS, NaP and L-Gln.
ACHN	Human kidney adenocarcinoma, adherent cell line.	RPMI-1640 supplemented with PCN, Sm, FCS, NaP and L-Gln.
MCF7	Human breast adenocarcinoma, adherent cell line.	RPMI-1640 supplemented with PCN, Sm, FCS, NaP and L-Gln.
K562	Human bone marrow chronic myelogenous leukemia, suspension cell line.	DMEM 5.55 mM D-Glucose, 4 mM L-Gln and 1 mM NaP supplemented with PCN, Sm, and FCS.
K562CLDN16	K562 cells stably expressing claudin 16 and $PURO^R$ gene *pac* under the MND promoter, suspension cell line.	DMEM 5.55 mM D-Glucose, 4 mM L-Gln and 1 mM NaP supplemented with PCN, Sm, FCS and puromycin.

Supplements concentration used: PCN (100 U/ml), Sm (100 µg/ml), FCS (10% (v/v)), NaP (1 mM) and L-Gln (2 mM), geneticin (1000 ng/µL), puromycin (5 µg/ml).
Abbreviations: MEM; Minimum Essential Medium, RPMI; Roswell Park Memorial Institute, DMEM; Dulbecco's Modified Eagle Medium, FCS; foetal calf serum, PCN; penicillin, Sm; streptomycin, NaP; sodium pyruvate, Gln; glutamine, hCAR; human coxsackie and adenovirus receptor, RFP; red fluorescent protein, Neo^R; neomycin resistance gene, $PURO^R$; puromycin resistance gene.
Supplier: MEM, DMEM, RPMI-1640, Ham's F-10 Nutrient Mixture medium, PCN/Sm mix, geneticin and puromycin were purchased from GIBCO® by Life Technologies, FCS was purchased from PAA Laboratories, NaP from Sigma-Aldrich and L-Gln from Invitrogen by Life Technologies.

2.1.6 Adenoviral vectors

All adenoviral vectors used in experimental procedures are replication-deficient adenoviral vectors designed and generated in-house with the exception of Alexa Fluor 488 labelled HAdV-2 ts1, which was kindly provided by Professor Urs Greber (University of Zurich, Switzerland). Adenoviral vectors were based on the AdEasy, E1/E3 deleted HAdV-5 adenoviral vector system (Stratagene by Agilent Technologies) (Luo et al., 2007) and encode the *E.coli LacZ* reporter gene for expression of the bacterial cytoplasmic β-galactosidase, in place of the viral E1 early adenovirus gene under the cytomegalovirus immediate-early promoter (CMV-IEP). Adenoviral vectors' genetic characteristics and mutations are specified in Table 2-7, Table 2-8 and Figure 2-1.

Table 2-7. Adenoviral vectors' genetic characteristics.

Adenoviral vector	Hexon mutation	Penton base mutation	Fiber mutation	Targeting peptide into FK HI loop[1]
HAdV-5 (Waddington et al., 2008)	-	-		-
AdT* (Alba et al., 2009)	T*	-	-	-
HAdV-5 RGE (Bradshaw et al., 2012)	-	RGE		-
HAdV-5 KO1	-	-	KO1	-
AdT*RGE (Bradshaw et al., 2012)	T*	RGE	-	-
AdT*KO1 AAA	T*	-	KO1	544AAA546
AdT*KO1 AAAASFPPAF	T*	-	KO1	544AAAASFPPAFAAA556
AdT*KO1 AAAYAAHRSHAAA	T*	-	KO1	544AAAYAAHRSHAAA556

[1]Numbers refer to amino acid residue position in the protein.
FK; fiber knob domain.

Table 2-8. Genetic mutations in adenoviral capsid.

Mutation	Protein for ablated binding	AdV protein targeted for mutation: region or domain mutated	Genetic mutations on protein residues
T*	FX	Hexon: HVR 5 and 7	HVR 5: T270P, E271G HVR 7: I421G, T423N, E424S, L426Y, E451Q (Alba et al., 2009)
RGE	$\alpha_v\beta_{3,5}$ integrins	Penton base	D342E (Bai et al., 1993)
KO1	CAR	Fiber: AB loop region of the fiber knob domain	S408E, P409A (Roelvink et al., 1999, Jakubczak et al., 2001)

FX; coagulation factor X, HVR; hypervariable region, CAR; coxsackie and adenovirus receptor.

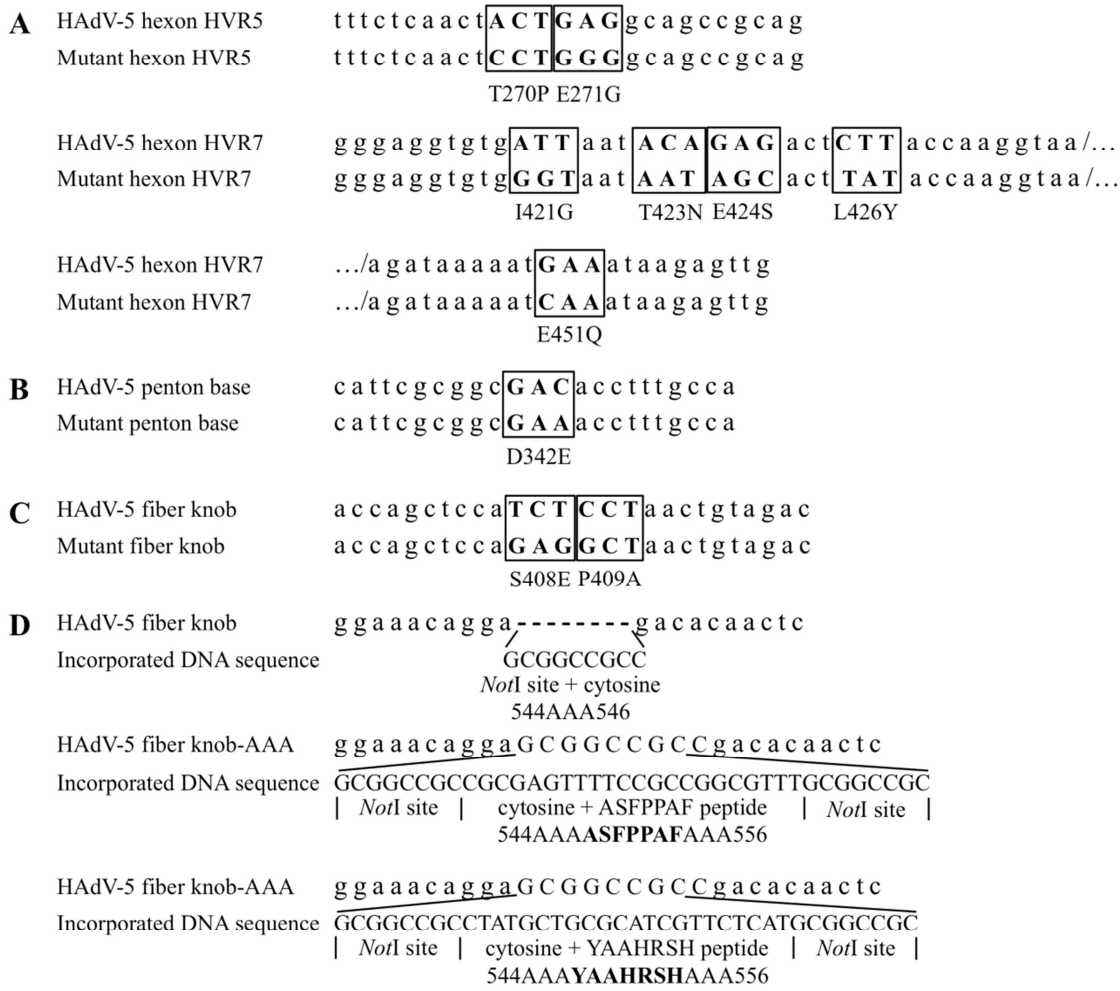

Figure 2-1. Genetic modifications introduced on adenoviral vectors. A-C) Nucleotide alignment between parental HAdV-5 genome and HAdV-5 genome with the T* mutations in the hexon HVRs (A), the RGE mutation in the penton base (B) or the KO1 mutation in the fiber knob domain (C). Mutated nucleotides are bolded capital letters and the corresponding mutated amino acid residues are boxed and indicated below each nucleotide triplet. D) Heterologous DNA sequences incorporated into the HI loop sequence of the fiber ORF are indicated below the parental HAdV-5 genome, with the corresponding heterologous peptide sequence indicated below. Candidate peptide sequences are bolded and restriction sites indicated. Numbers refer to amino acid residue position in the protein.

2.1.7 Mouse strains and husbandry

The mouse strains used were C57BL/6 (Harlan Laboratories, UK), Rag $2^{-/-}$ (B6(Cg)-*Rag2*$^{tm1.1Cgn}$/J, on a C57BL/6 genetic background) kindly provided by Dr. Alison M. Michie (Glasgow University, UK) and NSG (NOD.Cg-*Prkdc*^{scid} *Il2rg*^{tm1Wjl}/SzJ) kindly provided by Professor James Brewer and Dr. Chris Hansell (Glasgow University, UK). Rag $2^{-/-}$ mice are deficient in *Rag-2* gene, which is necessary for the somatic DNA rearrangement V(D)J recombination (Shinkai et al., 1992, Alt et al., 1992). As a result, they are unable to differentiate B and T lymphocytes to a mature state, which leads to a lack of production of natural IgM antibodies (Shinkai et al., 1992, Alt et al., 1992). NSG mice have the severe combined immune deficiency (*scid*) mutation (*Prkdc*^{null}), a complete

null mutation in the *IL2RG* gene and 2 base pair (bp) deletion in the haemolytic complement (*Hc*) gene. They lack mature B and T lymphocytes [no IgM production (Shultz et al., 2005)], are defective in dendritic cell and macrophage cytokine production and haemolytic complement protein 5 (C5), and have extremely low NK cell cytotoxic activity (Shultz et al., 2005, Zhou et al., 2014, Ito et al., 2002, Shultz et al., 1995). A summary of the mouse strains characteristics can be found in Table 2-9. All animals were housed in the Central Research Facility (Glasgow, UK) under controlled environmental conditions maintained at ambient temperature with 12 h light/dark cycles. Mice were fed standard chow and water was provided *ad libitum.* Rag $2^{-/-}$ and NSG mice were maintained in a pathogen-free environment in microisolator individually ventilated (PIV) caging. All animal experiments were approved by the University of Glasgow Animal Procedures and Ethics Committee and performed under UK Home Office licence (PPL 60/4429) in strict accordance with UK Home Office guidelines.

Table 2-9. Summary of the immune system characteristics of mouse strains.

Mouse strain	Genotype	Phenotype
C57BL/6	Wild type	Immunocompetent.
Rag $2^{-/-}$	*Rag-2* ^{null}	Immature B and T lymphocytes.
NSG	*Prkdc* ^{null} and *IL2RG* ^{null}	Immature B and T lymphocytes. Deficient dendritic cell and macrophage cytokine production. Deficient complement protein 5. Low NK cell cytotoxic activity.

2.2 Methods

2.2.1 Cell culture

Adherent cell lines were cultured at 37^{o}C / 5% or 10% CO_2 in the case of Per.C6® cells (Crucell) (Fallaux et al., 1998). Suspension cell lines were grown in tissue culture flasks siting in a vertical steady position at 37^{o}C / 5% CO_2. Adherent cells were passaged when 80% confluence was reached to prevent overgrowth. Suspension cells were passaged approximately every 3 days and seeded again at a concentration of $3.3x10^3$ cells/ml in 30 ml of complete fresh medium. When passaging adherent cells, cells were washed once with Dulbecco's calcium and magnesium free PBS (DPBS) and incubated with trypsin-ethylenediamine tetra-acetic acid (trypsin-EDTA) 0.05% (Invitrogen by Life Technologies) at 37^{o}C until cells detached from the flask surface. Next, cells were added to 5 ml of complete medium, subjected to centrifugation at 480 g for 5 min and resuspended

into 10 ml of fresh complete culture medium. A total of 2 ml (1/5 dilution) of cell suspension was added to 13 ml of fresh medium and cultured at 37^{o}C / 5% or 10% CO_2. When seeding of a known number of cells per well was required, cells were counted from cell suspensions using a haemocytometer (Hausser Scientific, PA, USA). The volume of cell suspension containing that specific number of cells was calculated with the following formula ([Volume (ml) = N x n / (A x 1x10^4)], where N = number of wells to seed, n = number of cells required per well, A = average number of cells per block of squares in the haemocytometer) and topped with fresh complete medium up to the required volume (number of wells to seed x volume per well). When passaging suspension cells, cells were subjected to centrifugation at 480 g for 5 min, resuspended into 10 ml of fresh complete culture medium and counted using a haemocytometer. The volume of cell suspension containing 1x10^5 cells was calculated as described before, topped with fresh complete medium up to 30 ml, and transferred into a 150 cm^2 tissue culture flask.

2.2.2 Cryopreservation of cell lines

A total of 1x10^6 cells were resuspended in 1 ml of fresh medium with 10% dimethyl sulphoxide (DMSO) (Fisher Scientific by Thermo Fisher Scientific), aliquoted into a cryopreservation vial, frozen down to -80^{o}C in isopropanol to keep a cooling constant of -1^{o}C/min and stored in liquid nitrogen. For recovery of cryopreserved cells, vials were thawed at 37^{o}C and cell suspensions added to 10 ml fresh medium in a universal container. After 5 min centrifugation at 480 g, pellets were resuspended in fresh medium, transferred to a 75 or 150 cm^2 tissue culture flask and incubated at 37^{o}C / 5% or 10% CO_2.

2.2.3 Cell lines testing

2.2.3.1 RNA extraction from cultured cells

Total RNA was extracted from K562 or K562CLDN16 suspension cells using the miRNeasy Mini kit (QIAGEN, Manchester, UK). Cells were subjected to centrifugation at 480 g for 5 min, resuspended in 10 ml of PBS, and counted using a haemocytometer (Hausser Scientific, PA, USA). The volume of cell suspension containing 3x10^6 cells was calculated as described in section 2.2.1, subjected to centrifugation at 480 g for 5 min, and resuspended in 700 µl of QIAzol Lysis Reagent, a solution of phenol that contains guanidine thiocyanate used for cell lysis and inhibition of RNases. Samples were homogenized using a vortex and incubated for 5 min at room temperature. Next, proteins were removed from the lysate by organic extraction adding 140 µl of chloroform, shaking

the samples for 15 sec and incubating them at room temperature for 3 min, followed by 15 min centrifugation at 12000 g at 4^{o}C. The upper aqueous phase was transferred to a fresh tube and 1.5 volumes of absolute ethanol were added and mixed by pipetting to precipitate RNA. Samples were transferred into an RNeasy Mini silica-membrane column in a 2 ml collection tube and subjected to centrifugation at 8000 g for 15 sec at room temperature for RNA binding to the membrane. Next, 700 µl of buffer RWT, also containing guanidine thiocyanate, were added to the column and subjected to centrifugation for 15 sec at 8000 g. The column was washed with 500 µl of buffer RPE to remove salts and subjected to centrifugation as before. RNA was eluted in a new 1.5 ml microcentrifuge tube with 30 µl of RNase-free water by centrifugation at 8000 g for 1 min and elution was repeated using the same water to maximise RNA elution yield. RNA was stored at -80^{o}C.

2.2.3.2 Reverse transcription of RNA

Complementary DNA was generated from total RNA that had been extracted from K562 or K562CLDN16 suspension cells as described in section 2.2.3.1, using the Reverse Transcription kit (Applied Biosystems by Life Technologies, UK). A total of 1 µg of RNA was added to 2 µl 10X RT buffer, 5.5 mM $MgCl_2$, 0.5 mM each deoxyribonucleotide triphosphates (dNTPs), 1 µl random hexamers, 0.4 µl RNase inhibitor and 0.5 µl Multiscribe Reverse Transcriptase, and topped up to 20 µl with RNase-free water, in a 96-well plate. Thermal cycler conditions used as follows: 25^{o}C for 10 min (DNA annealing); 48^{o}C for 30 min (cDNA extension); 95^{o}C for 5 min (reverse transcriptase inactivation). Resultant cDNA was kept at -20^{o}C for storage.

2.2.3.3 TaqMan® Real-Time PCR

Claudin 16 gene expression from K562 and K562CLDN16 suspension cells was quantified by TaqMan® Real-Time PCR. This method consists in the use of a set of forward and reverse primers specific for the gene of interest and a TaqMan® oligonucleotide probe labelled with a reporter fluorophore at the 5' end and a quencher at the 3' end that prevents fluorescent emission by the fluorophore while both are attached to the probe. The TaqMan® probe recognizes and binds to a sequence on the cDNA downstream of the forward primer. The 5'→3' exonuclease activity of Taq polymerase allows cleavage of the TaqMan® probe upon product amplification, resulting in the separation of the fluorophore and the quencher and thus emission of fluorescence, the intensity of which is proportional to the amount of product generated. Fluorescence intensity is acquired during the

exponential PCR phase and the value it reaches when crossing an arbitrary threshold situated on the exponential phase [cycle threshold (CT)] is indicative of the amount of original cDNA in the samples, thus allowing comparative studies. Also, a housekeeping gene, the expression levels of which remain constant, is used for normalization of the reads, correcting for errors in cDNA content between samples.

A total of 1.5 μl of cDNA, 5 μl 2X Universal TaqMan® mastermix II (containing buffer, dNTPs with dUTP, AmpliTaq Gold® DNA Polymerase and ROX^{TM} Passive Reference) (Applied Biosystems by Life Technologies, UK), 0.5 μl TaqMan® probe, and 8.5 μl nuclease-free water were added in triplicate to a 384-well plate. A negative control containing nuclease-free water instead of cDNA controled for DNA contaminations in any of the reagents. Claudin 16 mRNA probe (Table 2-1): Mm00475025_m1 conjugated to the fluorochrome FAM (Life Technologies by Thermo Fisher Scientific, UK); 18S ribosomal RNA probe as housekeeping gene (Table 2-1): Hs03928985_g1 conjugated to the fluorochrome VIC (Life Technologies by Thermo Fisher Scientific, UK). Thermal cycler conditions used as follows: 50^{o}C for 2 min; 95^{o}C for 10 min (DNA denaturation); 95^{o}C for 15 sec and 60^{o}C for 1 min (DNA denaturation, annealing and extension) repeated 40 times. The $2^{(CT\ gene\ of\ interest\ -\ CT\ housekeeping\ gene)}$ method (Livak and Schmittgen, 2001) was followed for graphical representation of results. The 7900HT Sequence Detection System v2.3 (Applied Biosystems, California, USA) was used for analysis.

2.2.3.4 Flow cytometry

Expression levels of CAR protein on the plasma membrane were measured by flow cytometry. Flow cytometry allows the classification of cells in solution by measurement of size (FSC; forward scatter) and granularity or internal complexity (SSC; side scatter), which are determined by how the cell scatters incident laser light. Also, cells expressing a specific protein can be quantified by detection with a fluorescently labelled antibody.

Cultured cells were washed with DPBS, dissociated with citric saline and resuspended in ice-cold serum-free (SF) medium to a concentration of $4x10^6$ cells/ml. A total of $2x10^5$ cells (50 μl of cell suspension) were added to FACS tubes and incubated with an equal volume of mouse anti-CAR IgG1 primary antibody (clone: RmcB, Upstate, NY, Sigma-Aldrich) or mouse IgG (Life Technologies by Thermo Fisher Scientific) as an isotype control (5 μg/ml in ice-cold SF medium) for 30 min at 4^{o}C in triplicate. Next, cells were washed twice with SF medium, incubated with the secondary antibody (Alexa Fluor 488-

conjugated goat anti-mouse IgG, Life Technologies by Thermo Fisher Scientific) for 30 min at 4°C (4 μg/ml in ice-cold SF medium), washed twice with SF medium and resuspended in 150 μl of ice-cold SF medium for analysis. BD FACS Canto II flow cytometer and BD FACSDiva v6.1.3 software were used for analysis with 1-laser configuration (488 nm) and FlowJo single cell analysis v10.1 software for graphical representation. Cells were gated on the basis of forward and side light scatter profiles, with a minimum of 10,000 gated events analysed per sample. Results are shown as a percentage of the parental population and expressed as the mean of technical triplicates +/- standard error of the mean (SEM).

2.2.4 Adenoviral vector genome cloning

2.2.4.1 Growth and cryopreservation of *Escherichia coli*

E. coli were grown in Luria Broth (LB) (Sigma-Aldrich, UK) at 37°C with shaking at 200 rpm in an Innova® 44 incubator shaker (Eppendorf, Hamburg, Germany) or spread on LB agar plates (Luria Agar Base, Miller, Sigma-Aldrich). When bacterial selection was required, ampicillin (50 μg/ml), kanamycin (50 μg/ml) or streptomycin (100 μg/ml) were added to LB or LB agar plates. Bacterial cultures, originating from single clones and carrying a particular DNA plasmid, were stored in 15% (v/v) glycerol LB at -80°C.

2.2.4.2 Plasmid DNA transformation into chemically competent *Escherichia coli*

To amplify plasmid DNA, a total of 50 ng plasmid DNA were added to 50 μl of JM109 chemically competent bacteria cells (Table 2-5) (Promega, UK) on ice and samples were incubated on ice for 30 min. Next, samples were placed into a 42°C water bath for 30 sec to perform heat shock and, immediately after, placed on ice for 2 min. Next, samples were incubated in 450 μl super optimal broth with catabolite repression (S.O.C) medium (Invitrogen by Life Technologies, UK) in a 1.5 μl microcentrifuge tube for 60 min at 37°C with shaking at 200 rpm using an Innova® 44 incubator shaker (Eppendorf). Following incubation, 100 μl of sample were spread on LB agar plates (see section 2.2.4.1) and incubated at 37°C overnight.

2.2.4.3 Plasmid DNA transformation into electrocompetent *Escherichia coli*

To perform homologous recombination between two DNA plasmids ("transfer vector" and "plasmid vector"), 50 µl of BJ5183 electrocompetent bacteria cells (Table 2-5) (Stratagene by Agilent Technologies) were mixed with a (transfer vector):(plasmid vector) ratio of 1:0, 1:3, 1:6 and 1:9 on ice, where 1 stands for 100 ng DNA. The ratio 1:0 was used as a background control. The mix was added to a chilled 2 mm electroporation cuvette (Cell Projects, UK), tapped gently to remove any air bubble and incubated on ice for 3 min. Next, the sample was subjected to a pulse at 200Ω 2.5kV 25µF, subsequently added to 500 µl ice-cold S.O.C medium (Invitrogen by Life Technologies, UK) in a 1.5 µl microcentrifuge tube, and incubated for 60 min at 37^{o}C with shaking at 200 rpm in an Innova® 44 incubator shaker (Eppendorf). Cells were subjected to centrifugation at 400 g for 1 min, resuspended in 50 µl of S.O.C medium and spread on LB agar plates (see section 2.2.4.1) and incubated at 37^{o}C overnight.

2.2.4.4 Plasmid DNA isolation

Plasmid DNA was isolated from bacteria grown in 3 ml of LB (Sigma-Aldrich, UK) using a PureLink® Quick Plasmid Miniprep kit (Invitrogen by Life Technologies) if low amounts of DNA (≤ 30 µg DNA) were required ("miniprep") or from bacteria grown in 200 ml using a PureLink® HiPure Plasmid Filter Purification kit (Invitrogen by Life Technologies) if high amounts of DNA (≤ 850 µg DNA) were required ("maxiprep"), following the manufacturer's instructions. In both kits, cells are lysed using an alkaline/sodium dodecyl sulphate (SDS) procedure and DNA is bound to a silica membrane and eluted. For minipreps, the elution step was repeated using the same original volume of elution buffer to increase DNA elution yield. For maxipreps, 250 ml Nalgene® centrifuge bottles (Sigma-Aldrich) in a JA-10 rotor (Beckman Coulter) with an Avanti J-26XP centrifuge (Beckman Coulter) were used to subject the bacterial culture to centrifugation. DNA was eluted from the DNA Binding Column into a 50 ml Nalgene® centrifuge tube and, to precipitate the eluted DNA, a JA-20 rotor (Beckman Coulter) with an Avanti J-26XP centrifuge (Beckman Coulter) were used. The concentration of plasmid DNA isolated from either kit was quantified using a NanoDrop 1000 Spectrophotometer (Thermo Scientific, Loughborough, UK) as described in section 2.2.4.5, and DNA was stored at -20^{o}C.

2.2.4.5 Nucleic acid quantification

The concentration of DNA and RNA from samples was quantified using a NanoDrop 1000 Spectrophotometer (Thermo Scientific, Loughborough, UK). Samples were subjected to a 260 nm UV light beam and absorbance was measured. DNA or RNA concentration was calculated using the Beer-Lambert law: $A = \varepsilon \times c \times l$, where A = absorbance of the sample, ε = molar absorptivity (constant for a given solution), c = nucleic acid concentration, l = path length of solution passed through by the light beam. Taking into account that proteins can absorb light at 280 nm, EDTA, guanidine HCl and other contaminants at 230 nm, and phenol at 230 nm and 270 nm, sample purity was examined by calculating the ratio $A_{260\ nm}$ / $A_{280\ nm}$ and $A_{260\ nm}$ / $A_{230\ nm}$. Samples with an $A_{260\ nm}$ / $A_{280\ nm}$ ratio higher than 1.8 for DNA or 2 for RNA, or with a $A_{260\ nm}$ / $A_{230\ nm}$ ratio higher than 2 were considered pure and used for further analysis.

2.2.4.6 Restriction endonuclease digestion of plasmid DNA

For screening of bacterial colonies carrying a specific DNA plasmid, DNA was extracted from single colonies (see section 2.2.4.4), digested with restriction endonucleases, and the amount and size of DNA bands were verified by agarose gel electrophoresis (see section 2.2.4.7). With this purpose, 1 μg DNA was digested with 5 units of restriction endonuclease with the addition of buffer and bovine serum albumin (BSA), as per manufacturer's instructions (New England Biolabs), in a final volume of 20 μl in nuclease-free water, and incubated overnight at 37^{o}C.

When enzymatic digestion of plasmid DNA was required for subsequent cloning (e.g: homologous recombination of DNA plasmids or ligation of DNA plasmids) or transfection into eukaryotic cells, the required amount of plasmid DNA to be digested was chosen and digested in 50 μl final volume in nuclease-free water. A total of 5 units of restriction endonuclease per 1 μg DNA were used (volume of restriction endonuclease never exceeding 10% of final volume) along with buffer and BSA as indicated by the manufacturer (New England Biolabs). Samples were incubated overnight at 37^{o}C. When enzymatic digestion was completed, restriction endonucleases were inactivated at 65^{o}C for 20 min or as indicated by the manufacturer.

2.2.4.7 Agarose gel electrophoresis

UltraPure™ Agarose (Invitrogen by Life Technologies) was dissolved in UltraPure™ TBE buffer [0.1 M Tris, 0.09 M boric acid, 0.001 M EDTA] (Life Technologies by Thermo Fisher Scientific) at 0.8% (w/v) by heating, with the addition of 0.5 μg/ml ethidium bromide (Sigma-Aldrich). DNA samples (≥1 μg) with the addition of Blue/Orange loading dye [0.4% orange G, 0.03% blomophenol blue, 0.03% xylene cyanol FF, 15% Ficoll® 400, 10 mM Tris-HCl pH 7.5, 50 mM EDTA pH 8.0] (Promega, UK) were loaded into the agarose wells along with 1 μg of 1 kb DNA ladder (Promega, UK), which was used as a marker of molecular weight. DNA fragments were separated by electrophoresis in TBE at a constant voltage of 100 V at room temperature, and visualized using a ChemiDoc™ XRS+ System with Image Lab™ software.

2.2.4.8 Isolation and purification of DNA fragments from agarose gel

DNA fragments were separated by agarose gel electrophoresis and extracted from the agarose gel using the Wizard® SV Gel and PCR Clean-Up System (Promega, UK), which uses a silica membrane SV Minicolumn to bind the extracted DNA, following the manufacturer's instructions. DNA bands were visualized using a transilluminator (UVP) and the elution step was repeated using the same original volume of nuclease-free water to increase DNA extraction yield. Isolated DNA was stored at -20^{o}C until further use.

2.2.4.9 Plasmid DNA 5' end dephosphorylation

To prevent self-ligation reactions of enzymatically digested DNA plasmids at a single site that would lead to recircularization, 5' end of plasmids were dephosphorylated. The amount of enzymatically digested plasmid DNA to be dephosphorylated was chosen according to the amount of DNA required for subsequent cloning steps, and diluted up to 30 μl in nuclease-free water. A total of 2 units of Antarctic Phosphatase (AP) (New England Biolabs, UK) were used per μg of digested plasmid DNA. The following formula was used to calculate the amount of buffer required for each reaction: Total reaction volume (Y) = 30 μl digested plasmid DNA + volume AP in μl (X) + volume of buffer in μl (Y/10), where X is a known value. Samples were incubated for 15 min at 37^{o}C and AP was subsequently inactivated by incubation of samples at 65^{o}C for 5 min.

2.2.4.10 DNA precipitation

DNA was mixed by vortexing with 3 M acetic acid pH 4.8 to a final concentration of 2.44% (v/v) and with ethanol absolute (pre-cooled at -20^{o}C) to a final concentration of 73.17%, and incubated at -20^{o}C for 60 min. Next, the sample was subjected to centrifugation at 16000 g for 5 min, the supernatant was removed, and DNA was air dried for 10 min and resuspended in DNase-free water.

2.2.4.11 DNA ligation

Backbone plasmid DNA and insert DNA were ligated at molar ratios 1:1 and 1:3, where 1 stands for 50 ng backbone DNA. One µl T4 DNA ligase (New England Biolabs) was added to a total of 20 µl of 1X buffer in nuclease-free water containing both the backbone and the insert, and incubated overnight at 16^{o}C. A background control was included, where the insert was replaced with nuclease-free water. When enzymatic ligation was completed, T4 DNA ligase was inactivated at 65^{o}C for 10 min as indicated by the manufacturer, and 5 µl of reaction was transformed into JM109 chemically competent bacteria cells (see section 2.2.4.2).

2.2.4.12 DNA sequencing

Specific DNA sequences within the adenoviral hexon, penton base or fiber ORFs were sequenced to verify the presence of mutations that had been introduced into the adenoviral vector's genome by genetic engineering. The BigDye® Terminator v3.1 Cycle Sequencing kit (Applied Biosystems by Life Technologies) was used to perform Sanger Sequencing. This method uses dNTPs and 2',3'-dideoxyribonucleotide triphosphates (ddNTP), which lack a 3'-hydroxyl group and are labelled to a specific fluorescent dye depending on their nitrogenous base. Both nucleotides are incorporated into the nascent DNA, but when a ddNTP is incorporated, elongation is terminated. DNA products are separated by size by capillary electrophoresis and passed through a laser beam that allows the discrimination between the 4 different nitrogenous bases and, therefore, identification of DNA nucleotide sequence.

A total of 200 ng of purified DNA amplicons (see section 2.2.5.16) or extracted plasmid DNA (see section 2.2.4.4), together with 4 µl of BigDye Terminator sequencing buffer 5X, 1 µl Terminator Ready Reaction Mix and 2 µl of 2 µM sequencing primers (final concentration of 0.2 µM) (Table 2-1) were used per reaction in a 96-well plate as indicated

by the manufacturer. Sequencing reaction mix was adjusted to 20 µl with deionized water. Thermal cycler conditions used as follows: 96^{o}C for 45 sec (DNA denaturation); 96^{o}C for 45 sec (DNA denaturation), 50^{o}C for 25 sec (DNA annealing) and 60^{o}C for 4 min (DNA extension) repeated 24 times. Samples were purified immediately after or stored at 4^{o}C and purified on the next day.

Purification of the DNA extension products was performed using Agencourt® CleanSEQ® (Beckman Coulter), which is based on Solid Phase Reversible Immobilization (SPRI) technology, where DNA is purified by binding to magnetic beads. The purification process was performed following the manufacturer's instructions. A total of 40 µl nuclease-free water were used to resuspend DNA:magnetic bead complexes and, of those, 20 µl were transferred to a MicroAmp Optical 96-well reaction plate (Applied Biosystems by Thermo Fisher Scientific). DNA extension products were separated by capillary electrophoresis in a 3730 DNA Analyzer (Applied Biosystems by Thermo Fisher Scientific) using 3730 Data collection v3.0 software. The obtained DNA sequences were analysed with Sequencing Analysis v5.2 software.

2.2.5 Adenoviral vector amplification and quality control

2.2.5.1 Adenoviral DNA transfection into HEK-293 cells

Adenoviral vector genomes were linearized with *Pac*I and the restriction endonuclease was subsequently heat-inactivated (65^{o}C for 20 min) prior to transfection into eukaryotic cells (see section 2.2.4.6). A total of 4 µg of digested plasmid DNA were transfected per well into low passage HEK-293 packaging cells in a 6-well plate at 70% confluence (6x10^{5} cells/well) using Lipofectamine 2000 as per manufacturer's instructions (Invitrogen by Life Technologies, USA). Since HEK-293 cells have the adenoviral E1 gene incorporated into their genome, they complement the E1 deficiency from adenoviral vectors and thus allow adenovirus propagation (Graham et al., 1977). After 5 h of incubation at 37^{o}C / 5% CO_2, 2 ml of fresh medium were added per well and, 24 h post-transfection, the medium was completely replaced with fresh medium. Medium was changed every 2-3 days and, 10 days post-transfection, cells were collected and freeze-thawed to release the adenoviral vectors. Transfection of circular PD10-GFP plasmid was used as a control for transfection and as an indicator of transfection efficiency.

2.2.5.2 Adenoviral DNA transfection into Per.C6® cells

Adenoviral vector genomes were linearized with *Pac*I and restriction endonuclease was subsequently heat-inactivated prior to transfection into eukaryotic cells (see section 2.2.4.6). A total of 8 μg were transfected into $3x10^6$ cells Per.C6® (Crucell) packaging cells grown overnight in a T25 cm^2 culture flask using Lipofectamine 2000 as per manufacturer's instructions (Invitrogen by Life Technologies, USA). Per.C6® cells contain the adenoviral E1 gene into their genome to allow adenovirus propagation (Fallaux et al., 1998). After 5 h of incubation at 37°C / 5% CO_2, 3 ml of fresh medium were added and, 24 h post-transfection, the medium was completely replaced with fresh medium. Medium was changed every 2-3 days and 8 days post-transfection cells were collected and freeze-thawed to release the adenoviral vectors.

2.2.5.3 Generation of crude adenoviral vector stocks

Rescued adenoviral vectors and pure adenoviral vector preparations were propagated in HEK-293 packaging cells or Per.C6® packaging cells (Crucell) (HAdV-5 KO1). When cytopathic effect (CPE) was observed, cells were detached from the culture flask by tapping, subjected to centrifugation at 480 g for 5 min, resuspended in DPBS (1 ml for early amplification steps and 6 ml when cells from 25 T150 cm^2 culture flasks were pooled together), and lysed with 1,1,2-trichloro-1,2,2-trifluoroethane (ArkloneP) (Sigma-Aldrich) (see section 2.2.5.4). When 25 T150 cm^2 culture flasks were used, one T150 cm^2 culture flask was treated individually to generate a seed stock: cell resuspension in 1 ml of DPBS and lysis with ArkloneP. The seed stock was aliquoted into 100 μl aliquots and used for future adenovirus preparations.

2.2.5.4 Adenoviral vector extraction from eukaryotic cells

Adenoviral vectors were extracted from cellular suspensions using the organic dissolvent ArkloneP (Sigma-Aldrich) for cell lysis. An equal volume of ArkloneP was added to cells re-suspended in DPBS. The container was inverted for 30 sec followed by gentle shaking for 10 sec, and this process was repeated 4 times. After centrifugation at 750 g for 15 min at room temperature, the DPBS fraction containing the adenoviral vectors was collected and stored at -80°C.

2.2.5.5 Generation of pure adenoviral vector preparations by purification via double CsCl gradient ultracentrifugation

Purification of adenovirus preparations allows concentration of the adenoviral vector and removal of empty adenovirus particles and contaminants such as cell debris or media components. Ultracentrifuge clear tubes (Beckman Coulter, UK) were rinsed with 70% ethanol and sterile water and a first CsCl gradient was generated by adding 2.5 ml of 1.25 g/ml CsCl and 2.5 ml of 1.40 g/ml CsCl at the bottom. The crude adenoviral lysate from 25X T150 cm^2 culture flasks production was added gently on top of the CsCl gradient, topped up with DPBS and subjected to ultracentrifugation in a SW40 Ti rotor at 90000 g and 18^oC for 1.5 h. On completion of the spin, two distinct white bands were observed between the two CsCl fractions: the upper band containing pure immature adenoviral vectors and the lower band pure mature adenoviral vectors (Figure 2-2A). The lower band was collected in the minimal volume possible by piercing the tube underneath the adenovirus layer with a 19 gauge needle. Extracted adenoviral vectors were added to a fresh ultracentrifuge tube containing 5 ml 1.34 g/ml CsCl solution and topped up with DPBS. After 18 h ultracentrifugation at 90000 g and 18^oC in a SW40 Ti rotor, a unique adenovirus white band was obtained (Figure 2-2B) and collected with a 21 gauge needle in less than 1 ml and injected for dialysis into a Slide-A-Lyzer Dialysis Cassette G2 (molecular weight cut-off of 10000 Da) (Perbio Science by Thermo Scientific, UK) that had been previously hydrated in TE buffer [0.01 M Tris pH 8, 0.001 M EDTA]. The adenoviral vector solution was dialysed by two rounds of 2 h in 2 litres TE followed by an overnight dialysis in 2 litres TE 10% (v/v) glycerol. The adenoviral vector solution (pure adenoviral vector preparation) was extracted from the cassette and stored at -80^oC.

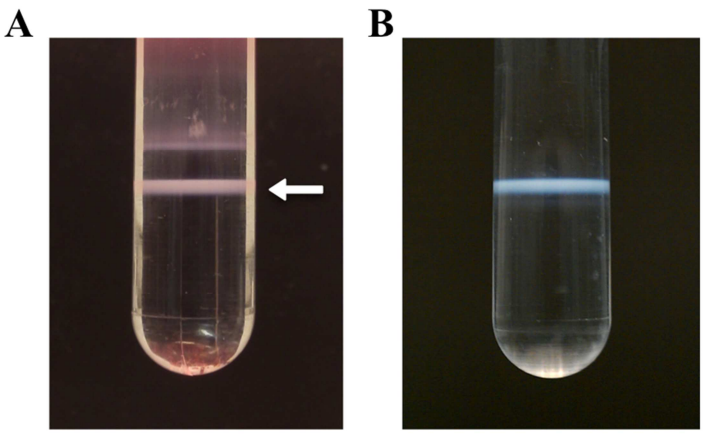

Figure 2-2. Purification of a HAdV-5 preparation by double CsCl gradient ultracentrifugation. A) Crude adenoviral lysate after the first ultracentrifugation step. The upper band corresponds to immature adenovirus particles, the lower band to mature adenovirus particles, and cell debris is found on top of the

upper band. Arrow indicates the band that is collected for the second gradient. B) Mature adenovirus particles after the second ultracentrifugation step.

2.2.5.6 X-Gal staining

Expression of β-galactosidase reporter gene was detected from cells transduced with adenoviral vectors that encode the *LacZ* reporter gene, using 5-bromo-4-chloro-3-indolyl-β-D-galactoside (X-Gal) as a substrate for β-galactosidase. X-Gal is a synthetic organic compound composed of a galactose and an indole that when hydrolysed generates an insoluble blue product, allowing the identification of active β-galactosidase (Horwitz et al., 1964).

Cells were washed once with DPBS, fixed in 2% (w/v) paraformaldehyde (PFA) (100 µL/well for 96-well plates and 1 ml/well for 6-well plates) at room temperature for 10 min, washed with DPBS twice and stained with X-Gal staining solution [0.1 M phosphate buffer, pH 7.3, 1.3 mM $MgCl_2$, 3 mM $K_3F_3(CN)_6$, 3 mM $K_4Fe(CN_6)_6$, 1 mg/ml X-gal] (200 µL/well for 96-well plates and 3 ml/well for 6-well plates) at 37^{o}C overnight.

When staining for β-galactosidase expressed in whole mouse organs, organs (liver, spleen, lungs, intestine, kidney, heart and pancreas) that had been fixed in 2% (w/v) PFA overnight at 4^{o}C were washed twice in 5 ml DPBS and stained with 5 ml X-Gal staining solution at 37^{o}C overnight. Stained organs were stored in 70% ethanol at 4^{o}C.

2.2.5.7 Replication-competent adenovirus (RCA) assessment

Replication-competent adenoviruses (RCA) are adenoviral particles that can replicate in non-permissive ($E1^{-/-}$) cells and can result from the use of HEK-293 packaging cells for vector propagation (Lochmuller et al., 1994, Hehir et al., 1996). HEK-293 cells have an integrated 4344 bp fragment of the left end of the HAdV-5 genome containing the left inverted terminal repeat (LITR), the packaging signal and *E1* and *pIX* genes (Louis et al., 1997, Graham et al., 1977). Presence of HAdV-5 sequences flanking the *E1* gene in the packaging cell line can result in homologous recombination events between HAdV-5-based genomes and the cell genome and lead to the production of $E1^+$ viral genomes and thus RCAs (Hehir et al., 1996, Lochmuller et al., 1994). In contrast, since Per.C6® cells contain only E1A and E1B-coding sequences (HAdV-5 nucleotides 459-3510), their use for vector propagation does not result in RCAs (Fallaux et al., 1998). A maximum of 1 RCA per $3x10^{10}$ vp is accepted by FDA guidelines (FDA Gene Therapy Letter, 2000).

The presence of RCA was tested from pure adenoviral preparations by transducing non-permissive HeLa cells at a density of 50-60% with 100 µl of the same adenovirus dilutions prepared for the titer determination of adenoviral plaque forming units (pfu) (see section 2.2.5.9). Medium was changed to fresh complete medium every 2-3 days for a total of 8 days. The presence of CPE or individual viral plaques was carefully checked during the process.

2.2.5.8 Titre determination of physical adenoviral particles

The concentration of physical adenoviral particles from pure adenovirus preparations was calculated using the micro bicinchoninic acid (BCA) Protein Assay (Pierce, Thermo Fisher Scientific, USA). This assay is based on the detection of Cu^{+1}, generated when protein reduces Cu^{2+} in an alkaline environment. Two molecules of BCA chelate one molecule of Cu^{+1} producing a soluble purple product that absorbs light at 562 nm and thus can be quantified by colorimetric detection. The increase in absorbance directly correlates to the amount of protein present in the samples. The amount of protein present per unit volume is used as an indicative of the amount of adenovirus in the sample tested.

BSA standards were prepared at concentrations ranging from 0.5 µg/ml to 200 µg/ml according to the manufacturer's instructions. Adenovirus samples were diluted 1/150, 3/150 and 5/150 in a final volume of 300 µl of DPBS and 150 µl of sample, BSA standards or DPBS (blank control) were added in duplicate in a 96-well culture plate. Next, an equal volume of BCA working reagent (solutions A, B and C in a ratio 25:24:1) was added to all wells and plate was incubated at 37^{o}C for 2 h. Following incubation, the absorbance was assessed at 562 nm using a VICTOR^{TM} X3 Multilabel Plate Reader (PerkinElmer). Protein concentration was calculated by extrapolating from the standard curve after subtracting the absorbance from the blank control, and the number of adenoviral particles per unit volume (vp/ml) was determined using the formula: 1 µg protein = $4x10^{9}$ vp, which is based on the HAdV-5 particle molecular weight of ~150 MDa (World WSM and Horwitz MS, 2007).

2.2.5.9 Titre determination of infectious adenoviral particles by end-point dilution assay

The ratio vp/pfu is a quality control indicator of how infective an adenovirus preparation is, where a high ratio corresponds to lower quality and poorly infective preparations, which can be due to the presence of a high quantity of immature non-infective adenovirus particles [reviewed by (Vellinga et al., 2014)]. This value becomes essential when the

preparation is going to be administered *in vivo* in order to diminish toxicity. Also, the vp/pfu ratio is useful to detect possible propagation deficiency when producing novel mutant adenoviral vectors. However, vp/pfu values should be considered carefully since the intrinsic infectivity may vary between adenovirus serotypes or mutants. Thus, acceptable vp/pfu values should be determined for each particular adenoviral vector. For recombinant HAdV-5 vectors to be used in gene therapy and in particular in *in vivo* studies, the FDA Advisory Committee recommends a vp/pfu ratio of 30 (FDA Gene Therapy Letter, 2000) in order to diminish associated toxicity issues.

Pure adenovirus preparations were diluted in complete medium in ten-fold serial dilutions and 100 μl were added to 50-60% confluent HEK-293 packaging cells or Per.C6® packaging cells (Crucell) in the case of HAdV-5 KO1 in a 96-well plate with ten replicates of each dilution. Medium was changed after 16-18 h incubation at 37^{o}C / 5% CO_2 (HEK-293 cells) or 10%CO_2 (Per.C6® cells) and replaced with fresh complete medium every 2-3 days until CPE was apparent. After 8 days, the number of wells with visible plaques for each dilution were counted and fitted into the following equations to determine the titre of the adenoviral vector preparation in pfu/ml: Proportionate distance = (% positive wells from dilution with above 50% positive wells - 50%) / (% positive wells from dilution with above 50% positive wells - % positive wells from dilution with below 50% positive wells). Log ID_{50} (infectivity dose) = [(-1) / (dilution above 50% positive wells)] - proportionate distance. Viral tissue culture ID_{50} ($TCID_{50}$) / ml = 1 / [$10^{(\log ID50)}$] x 10 (conversion factor). Pfu/ml = 0.7 x $TCID_{50}$/ml.

Adenoviral plaques were not clearly visible when Per.C6® (Crucell) cells were used. Therefore, transduced cells (β-galactosidase-positive cells) were stained with X-Gal staining solution (see section 2.2.5.6) to ensure that all wells with plaques were considered for the calculations. In order to fairly compare adenoviral infectivity for the different pure adenoviral vector preparations, all titers of adenoviral pfu/ml were assessed both by eye and by X-Gal staining. Also, AdT*KO1 AAA and AdT*KO1 AAAASFPPAFAAA failed to form plaques. Thus, titers of these two vectors were determined in infectious units (IU)/ml by assessing the presence or absence of individual transduced cells in the wells by X-Gal staining following the same equations as above.

2.2.5.10 Nanoparticle Tracking Analysis (NTA)

The laser-based Nanoparticle Tracking Analysis (NTA) by NanoSight is a technology that through individual visualization of nanoscale particles in solution in real-time, it allows the generation of high-resolution particle size distribution profiles (detection limit of 10 nm) and particles quantification (Figure 2-3). This technology was used to characterize the size of adenoviral particles from pure preparations, and identify the possible presence of aggregates.

Pure adenoviral vector preparations were diluted 1/100 or 1/1000 in DPBS to a total of 700 µl in order to have an approximate concentration of $1x10^{7}$-$1x10^{10}$ vp/ml as indicated by the manufacturer, and loaded into the instrument with a 1 ml syringe. Adenoviral particles in solution were recorded and analysed with Nanosight NTA v2.3 software.

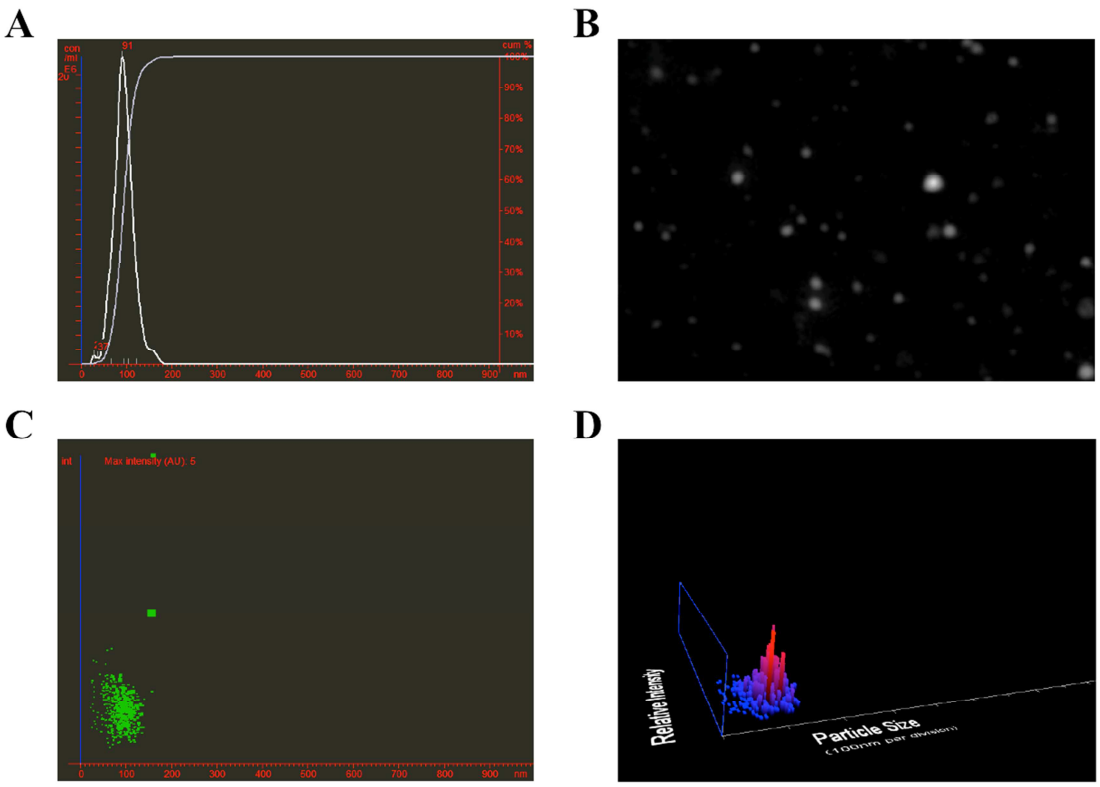

Figure 2-3. NanoSight output of a pure HAdV-5 preparation. A) Concentration (vp/ml) vs. particle size (nm). B) Nanoparticle Tracking Analysis (NTA) video frame of adenoviral particles. C) Intensity of the scattered light [arbitrary units (AU)] vs. particle size (nm). D) 3D representation of (C) where Z axis represents the amount of adenoviral particles for each (X,Y) coordenate.

2.2.5.11 Sodium dodecyl sulphate polyacrylamide gel electrophoresis (SDS-PAGE)

A polyacrylamide gel composed of a 12% resolving gel [40% (v/v) Acrylamide/Bis Solution 30% (BIO-RAD, UK), 0.375 M Tris pH 8.8, 0.1% (w/v) sodium dodecyl sulphate (SDS) in ultrapure water] and a 4% stacker gel [13.3% (v/v) Acrylamide/Bis Solution 30% (BIO-RAD, UK), 0.125 M Tris pH 6.8, 0.1% (w/v) SDS in ultrapure water] was prepared. For polyacrylamide polymerization, 0.438 M ammonium persulphate (APS) (Thermo Fisher Scientific) was added to a final concentration of 1% (v/v) and N,N,N',N'-tetramethylethylenediamine (TEMED) (Sigma-Aldrich) was added to a final concentration of 0.1% (v/v). A total of $5x10^{10}$ adenoviral particles from pure adenoviral vector preparations were mixed with loading buffer 5X [10% (v/v) Tris-HCl pH 6.8, 10% (w/v) SDS, 30% (v/v) glycerol, 0.1% (w/v) bromophenol blue, 2% (v/v) β-mercaptoethanol] in a total volume of 100 μl in PBS. β-mercaptoethanol is used to reduce disulphide bonds in proteins and SDS to denature proteins and confer an overall negative charge to allow the separation of proteins uniquely by size (Laemmli, 1970). Samples were also heated to 95^{o}C for 10 min to completely denature proteins. Samples, along with 20 μl of rainbow ladder (Amersham Bioscience UK Ltd, UK), which was used as a marker of molecular weight, were loaded into the polyacrylamide gel and electrophoresed at 100 V in running buffer [25 mM Tris-HCl, 0.2 M glycine, 0.1% (w/v) SDS pH 8.3] until the samples reached the resolving gel and then at 200 V until the dye front reached the bottom of the gel.

2.2.5.12 Silver staining

Adenoviral capsid composition and integrity of capsid structure of pure adenoviral vector preparations were confirmed by silver staining (Thermo Scientific by Life Technologies) performed on a polyacrylamide gel after electrophoretic separation of proteins (see section 2.2.5.11), according to the manufacturer's instructions. In this assay, proteins bind to silver ions that, when reduced, allow the visualization of such proteins. Gels were scanned using a ChemiDoc^{TM} XRS+ System with Image Lab^{TM} software.

2.2.5.13 Western blotting analysis

The presence of heterologous peptides into the HI loop of the adenovirus fiber knob domain was confirmed by western blotting. After electrophoretic separation of proteins on a polyacrylamide gel (see section 2.2.5.11), the gel was washed with Transfer buffer [0.2 M glycine, 25 mM Tris, 20% methanol, 0.01% (w/v) SDS] for 10 min and protein bands

were transferred to a hydrophobic Amersham Hybond-P 0.45 μm polyvinylidene difluoride (PVDF) membrane (GE Healthcare Life Sciences, UK) at 90 mV overnight at 4°C. The membrane was pre-treated by incubation in methanol for 10 sec, followed by 5 min in ultrapure water and 10 min in Transfer buffer. After protein transfer, the membrane was blocked with TBS-Tween (TBST) [150 mM NaCl, 50 mM Tris, 0.1% (v/v) Tween-20] with the addition of 10% (w/v) fat-free milk powder for 3 h at 4°C. Next, the membrane was incubated with mouse anti-adenovirus fiber IgG2a primary antibody (clone: 4D2, Abcam®) at 37°C for 60 min on an orbital shaker (0.2 μg/ml), washed twice with blocking buffer for 5 min each, incubated with secondary antibody (HRP-conjugated rabbit anti-mouse IgG (Abcam®)) for 60 min at room temperature with shaking (1 μg/ml), and washed 4 times with blocking buffer for 15 min each and twice with TBST for 15 min each. Protein bands were visualized using Amersham™ ECL™ Prime western blotting chemiluminescent detection reagent (GE Healthcare Life Sciences, UK), by which the membrane was incubated for 5 min at room temperature with a mix of Solution A (luminol as the chemiluminescent substrate) and Solution B (peroxide as the oxidizing agent) in equal proportions. Next, the membrane was drained from excess detection reagent, wrapped in clear cling film and placed on a Kodak Medical X-ray film General Purpose Blue/MXBE (Carestream, USA). The film was developed using a Kodak X-OMAT 1000 developer and scanned using a ChemiDoc™ XRS+ System with Image Lab™ software.

2.2.5.14 Adenoviral DNA extraction

Adenoviral DNA was extracted from 1 μl pure adenoviral vector preparations or crude adenoviral vector stocks (see sections 2.2.5.5 and 2.2.5.3) using the QIAamp® UltraSens™ Virus kit (QIAGEN, Manchester, UK) according to the manufacturer's instructions. In this assay, samples are mixed with buffer containing a proprietary reagent that forms complexes with nucleic acids, which can then be sedimented by low-g-force centrifugation (QIAGEN, 2016). Next, DNA is bound to a silica-membrane QIAamp spin column, washed and eluted. The elution step was repeated using the same original volume of elution buffer to increase DNA extraction yield and isolated DNA was stored at -20°C until further use.

2.2.5.15 Polymerase chain reaction (PCR)

PCR was performed to amplify specific DNA sequences within the adenoviral hexon, penton base or fiber ORFs for their subsequent sequencing, using adenoviral DNA

extracted from pure adenoviral vector preparations or crude adenoviral vector stocks (see section 2.2.5.14) following the GoTaq® G2 DNA Polymerase protocol provided by Promega. A total of 200 ng DNA, 10 µl colourless GoTaq reaction buffer (7.5 mM $MgCl_2$) along with additional 2.5 µl of 1.25 mM $MgCl_2$ for a final $MgCl_2$ concentration of 2.75 mM, 0.2 mM each dNTPs, 1.25 units GoTaq DNA polymerase, 5 µl of 2 µM forward and reverse primers (final concentration of 0.2 µM) (Table 2-1) and nuclease-free water up to a total reaction volume of 50 µL, were used per reaction in a 96-well plate. A negative control without the addition of DNA was done for each set of primers to assess for DNA contaminations in any of the reagents. Thermal cycler conditions used as follows: 95^{o}C for 2 min (DNA initial denaturation); 95^{o}C for 1 min (DNA denaturation), 55^{o}C for 1 min (DNA annealing) and 72^{o}C for 3 min (DNA extension) repeated 30 times; 72^{o}C for 5 min. Samples were subsequently purified and stored at 4^{o}C.

2.2.5.16 DNA purification of PCR amplicons

PCR amplicons were purified prior to sequencing to eliminate primers, excess of dNTPs, salts, DNA polymerase and other components from the PCR reaction (see section 2.2.5.15). Purification was performed using the Agencourt® AMPure® XP PCR purification system (Beckman Coulter, UK) following the manufacturer's instructions. This system is based on the Agencourt's solid-phase paramagnetic bead technology, by which DNA is purified by binding to magnetic beads. After DNA purification, samples were immediately sequenced (see section 2.2.4.12) or kept overnight at 4^{o}C to be sequenced on the following day.

2.2.6 Adenoviral vector experiments

2.2.6.1 *In vitro* transduction assay with suspension cells

K562 or K562CLDN16 suspension cells were seeded at 2x10^{6} cells/well and incubated with 5000 vp/cell in SF medium in 6 well-plates at 37^{o}C / 5% CO_2 for 3 h on an orbital shaker at 90 rpm. Following incubation, cells were transferred to individual sterile 2 ml microcentrifuge tubes, subjected to centrifugation at 100 g for 5 min, resuspended in 2 ml fresh complete medium, transferred to new 6 well-plates and further incubated at 37^{o}C for 48 h. Following incubation, cells were transferred to individual 2 ml microcentrifuge tubes, subjected to centrifugation at 100 g for 5 min, resuspended in 2 ml DPBS, subjected to centrifugation again at 100 g for 5 min and resuspended in 200 µl of Reporter lysis buffer

[20 mM K_3PO_4 pH 7.8, 0.04% (v/v) Triton X-100] (Promega, USA). Wells were assessed for β-galactosidase activity (see section 2.2.6.5).

2.2.6.2 *In vitro* coagulation factor X transduction assay

A total of $1x10^4$ cells/well seeded on a 96-well culture plate were incubated for 3 h at 37°C / 5% CO_2 with 1000 vp/cell in SF medium with or without recombinant hFX at a working concentration of 10 μg/ml (Haematologic Technologies). Next, the medium was replaced with fresh complete medium and cells incubated for further 48 h at 37°C / 5% CO_2. When indicated, 50 μl SF medium containing 10 μg/ml of hFX was pre-incubated at 56°C for 30 min before the addition of $2x10^{10}$ vp/ml adenoviral vector and incubation for 30 min at 37°C. In that case, adenovirus suspensions were diluted 200-fold in SF medium following incubation, 1000 vp/cell were added onto cells (previously washed with SF medium) and cells incubated at 37°C / 5% CO_2 for 2 h. After the 2 h incubation, medium was replaced with 2% fetal calf serum (FCS)-containing medium, and cells were further incubated for ~20 h at 37°C / 5% CO_2. In all conditions, cells were washed with DPBS following incubation and lysed with 100 μl of Reporter lysis buffer [20 mM K_3PO_4 pH 7.8, 0.04% Triton X-100] (Promega, USA), and wells were assessed for β-galactosidase activity (see section 2.2.6.5).

2.2.6.3 *In vitro* adenovirus neutralization assay

A total of $1x10^4$ cells/well were plated on 96-well culture plates and incubated overnight at 37°C / 5% CO_2. As previously described (Xu et al., 2013), adenoviral vectors ($2x10^{10}$ vp/ml) were incubated for 30 min at 37°C with 50 μl SF medium, 90% fresh male mouse serum or serum pre-incubated with X-bp (40 μg/ml) at room temperature for 10 min to inhibit HAdV-5-based adenoviral vectors binding to FX. Pure mouse IgM antibodies were added to mouse serum when indicated [50, 150 or 300 μg/ml, as per previous reports (Xu et al., 2013)] and incubated for 10 min at room temperature prior to addition of X-bp. Where indicated, mouse serum was pre-incubated at 56°C for 30 min before the addition of X-bp to inhibit the complement system, as described previously (Xu et al., 2013). Following 30 min incubation at 37°C, adenoviral vector suspensions were diluted 200-fold in SF medium, 1000 vp/cell were added onto cells (previously washed with SF medium) and cells incubated at 37°C / 5% CO_2 for 2 h. When IgM antibodies were used, volumes of all samples were equalized with SF medium to maintain adenovirus concentration constant across samples prior to diluting the samples by 200-fold. After the 2 h incubation at 37°C,

medium was replaced with 2% FCS-containing medium, and cells were further incubated for ~20 h at 37°C / 5% CO_2. Cells were washed with DPBS and lysed with 100 µl of Reporter lysis buffer [20 mM K_3PO_4 pH 7.8, 0.04% Triton X-100] (Promega, USA), and wells were assessed for β-galactosidase activity (see section 2.2.6.5).

2.2.6.4 *In vitro* fiber knob competition assay

A total of $1x10^4$ cells/well were plated on 96-well culture plates and incubated overnight at 37°C / 5% CO_2. Cells were washed with SF medium and incubated for 30 min at 4°C with 1 µg/well (as per Lynda Coughlan's unpublished observation) of recombinant fiber knob (FK) (Coughlan et al., 2009) or FK* [Y477A[4] point mutation in the fiber DE loop to impair binding to CAR (Roelvink et al., 1999, Kirby et al., 2000, Alemany and Curiel, 2001)] (kindly provided by Lynda Coughlan, University of Glasgow, UK) in 50 µl of SF medium per well. HAdV-5 ($2x10^{10}$ vp/ml) was incubated for 30 min at 37°C with 50 µl SF medium, 90% fresh male mouse serum or serum pre-incubated with X-bp (40 µg/ml) at room temperature for 10 min to inhibit HAdV-5 binding to FX, as previously described (Xu et al., 2013). Where indicated, HAdV-5 was incubated in 50 µl SF medium with hFX at a working concentration of 10 µg/ml (Haematologic Technologies) for 30 min at 37°C. After the 30 min incubation at 37°C, adenoviral vector suspensions were diluted 100-fold in SF medium, 50 µl were added onto cells (1000 vp/cell) that had been pre-incubated with FK or FK* and cells were incubated for 2 h at 37°C / 5% CO_2. In experiments where the only condition tested was HAdV-5 on FK or FK*-treated cells, 1000 vp/cell in 50 µl SF medium ($2x10^8$ vp/ml) were added onto cells that had been pre-incubated with FK or FK* as described before, and cells were incubated for 2 h at 37°C / 5% CO_2. In all the conditions, medium was replaced with 2% FCS-containing medium after the 2 h incubation at 37°C, cells were further incubated for ~20 h at 37°C / 5% CO_2, washed with DPBS and lysed with 100 µl of Reporter lysis buffer [20 mM K_3PO_4 pH 7.8, 0.04% Triton X-100] (Promega, USA), and wells were assessed for β-galactosidase activity (see section 2.2.6.5).

[4]Numbers refer to amino acid residue position in the protein.

2.2.6.5 β-galactosidase transgene expression quantification for *in vitro* experiments

β-galactosidase expression levels were quantified by Galacto-Light Plus β-galactosidase reporter gene assay (Life Technologies by Thermo Fisher Scientific, UK). This assay makes use of the enzymatic activity of β-galactosidase, which in the presence of Galacton-Plus® substrate releases chemiluminescence. The level of chemiluminescence is directly related to the amount of β-galactosidase in the sample.

Cells were washed with DPBS, lysed with 100 or 200 µL/well (as indicated in each case) of 1X Reporter lysis buffer [20 mM K_3PO_4pH 7.8, 0.04% (v/v) Triton X-100] (Promega, USA) and plate was freeze-thawed to ensure intracellular content was completely released. A total of 20 µl of sample from each well was transferred to a white 96-well plate and 70 µl of Tropix Galacton-Plus substrate (diluted 1/100 in 100 mM NaH_2PO_4, 1 mM $MgCl_2$, pH 8) were added per well and incubated at room temperature in the dark for 60 min. Next, 100 µl of Tropix Accelerator II were added per well and the chemiluminescence produced was immediately read using a VICTOR^{TM} X3 Multilabel Plate Reader (PerkinElmer). β-galactosidase activity in relative light units (RLU) was normalized to the total amount of protein in 20 µl of sample, which was measured by the BCA Protein assay (see section 2.2.6.6), thus obtaining β-galactosidase activity in RLU/mg protein.

2.2.6.6 Bicinchoninic acid (BCA) Protein assay

Total amount of protein from cellular extracts or purified protein samples was assessed using the BCA Protein Assay (Pierce, Thermo Scientific, USA). BSA standards were prepared at concentrations ranging from 25 µg/ml to 2000 µg/ml according to manufacturer's instructions. A total of 20 µl of samples, BSA standards or DPBS as a blank control were added in duplicate in a 96-well culture plate. Next, 150 µl of BCA working reagent (solutions A and B in a ratio 50:1) was added to all wells and plate was incubated at 37^{o}C for 30 min. Next, absorbance was read at 562 nm using a VICTOR^{TM} X3 Multilabel Plate Reader (PerkinElmer). Protein concentration was calculated by extrapolating the blank-subtracted measurements from the standard curve and expressed as mg protein/ml.

2.2.6.7 Adenoviral vector labelling

To label adenoviral vectors with Alexa Fluor 488 Dye, the Alexa Fluor® 488 Antibody Labeling kit (Molecular Probes by Thermo Fisher Scientific) was used. First, a volume corresponding to 500 μg of adenoviral vector ($2x10^{12}$ vp, assuming 1 μg protein = $4x10^{9}$ vp) from pure preparations was loaded into a 10000 Da molecular weight cut-off (MWCO) Slide-A-Lyzer Dialysis Cassette G2 (Perbio Science by Thermo Scientific, UK) that had been previously hydrated in PBS [1.37 M NaCl, 27 mM KCl, 100 mM Na_2HPO_4, 18 mM KH_2PO_4]. Next, the adenoviral vector solution was dialysed by two rounds of 2 h in 2 litres PBS and then transferred to a 1.5 ml microcentrifuge tube, where 84 μg/ml sodium bicarbonate was added to a final concentration of 10% (v/v) in order to increase the pH for efficient labelling. The adenoviral vector mix was transferred to a vial containing Alexa Fluor 488 Dye as powder and a magnetic stir bar, and stirred on a magnetic stirrer for 15 min at room temperature in the dark. Next, the adenoviral vector solution mix was injected into a new pre-wetted 10000 Da MWCO Slide-A-Lyzer Dialysis Cassette G2, dialysed in 5 litres of TE [0.01 M Tris pH 8, 0.001 M EDTA] overnight, and dialysed in 2 litres of TE 10% (v/v) glycerol for 4 h. The adenoviral vector solution was extracted from the cassette and stored at -80^{o}C.

2.2.6.8 Adenoviral vector trafficking assay

The adenoviral vector trafficking assay allows the assessment of adenoviral vector internalization into host cells and trafficking towards the nucleus. In this assay, cells are incubated with labelled adenoviral vector and subsequently subjected to immunocytochemistry for colocalization analysis of adenoviral particles with cellular components. A549 and SKOV3 cells were plated in 8-well chamber slides at a density of $5x10^{4}$ cells/chamber in a total volume of 500 μL/chamber, and incubated overnight at 37^{o}C / 5% CO_2. Cells were washed once with DPBS, 1 ml of ice-cold SF medium was added per well, and cells were incubated on ice at 4^{o}C for 30 min. Following incubation, the medium was removed from wells and 150 μl of Alexa Fluor 488 labelled adenoviral vector (HAdV-5 or AdT*) in SF medium ($1x10^{5}$ vp/cell) were added to each well with or without hFX (Haematologic Technologies) (10 μg/ml) while the culture plate was still on ice. Cells were incubated for 60 min on ice at 4^{o}C in the dark. Next, to assess adenovirus binding to cell membrane (“0 min” condition), cells were washed once with DPBS, fixed with 4% (w/v) PFA for 10 min at room temperature, washed twice with DPBS and subjected to immunocytochemistry (see section 2.2.6.9). To assess adenovirus internalization into cells

("60 min" condition), cells were washed once with DPBS after the cold incubation, 500 µl of SF medium was added to each well, and cells were incubated at 37°C / 5% CO_2 for 60 min. Next, cells were washed once with DPBS, fixed with 4% (w/v) PFA for 10 min at room temperature, washed twice with DPBS for 5 min each, and subjected to immunocytochemistry (see section 2.2.6.9).

2.2.6.9 Immunocytochemistry (ICC) assay

Following completion of the adenoviral vector trafficking assay (see section 2.2.6.8), cells were fixed with 4% (w/v) PFA, washed with DPBS, and permeabilized in PBST 0.1% (v/v) for 10 min at room temperature. Next, cells were rinsed three times in PBS for 5 min and blocked for 30 min in 10% normal goat serum (Vector Laboratories Inc., USA) in PBST 0.1% (v/v) to reduce nonspecific binding of secondary antibody. Sections were washed in PBST 0.1% (v/v) for 5 min at room temperature and incubated overnight at 4°C with rabbit anti-pericentrin (Abcam®, USA) primary antibody or isotype control (rabbit IgG, Invitrogen by Thermo Fisher Scientific) to control for background noise (5 µg/ml in 1% normal goat serum in PBST 0.01% (v/v)). Next, sections were rinsed three times with PBS for 5 min each and incubated with Alexa Fluor 546-conjugated goat anti-rabbit IgG secondary antibody (Life Technologies by Thermo Fisher Scientific) for 60 min at room temperature in the dark (4 µg/ml in PBS). Following incubation, sections were rinsed three times with PBS for 5 min each in the dark and slides were mounted with ProLong Gold Antifade Reagent with 4',6-diamidino-2-penylindole (DAPI) (Molecular Probes by Life Technologies) for nuclei visualization. Immunofluorescence was captured using a Zeiss confocal imaging system LSM 510 META using LSM image acquisition software (Carl Zeiss, Welwyn Garden City, UK) with a 40x objective (water immersion, numerical aperture: 1) and excitations at 405 nm for DAPI, 488 nm for adenoviral vector and 543 nm for secondary antibody. Adjustments were applied equally to all acquired images.

2.2.6.10 SLO penetration assay

In this assay, the bacterial toxin streptolysin O (SLO) is used to generate pores in the plasma membrane, and these pores allow access of antibodies to the cytosol of the host cell (Suomalainen et al., 2013). For studies on the FX-mediated pathway of adenovirus transduction, $4x10^4$ A549 cells were cultured per well for two days on Alcian blue-coated coverslips in 24-well plates, washed with serum-free RPMI-1640 medium without $NaHCO_3$ (Sigma-Aldrich), and incubated with FK (Coughlan et al., 2009) at 0.4 µg/ml in

RPMI-BSA (RPMI-1640 medium without $NaHCO_3$ supplemented with 0.2% BSA, 20mM HEPES, 100 U/ml penicillin and 100 μg/ml streptomycin) for 30 min at 4°C to avoid virus entry into host cells through the CAR-mediated pathway. Next, cells were incubated with Alexa Fluor 488 labelled HAdV-5 and hFX (10 μg/ml) on ice for 60 min in RPMI-BSA. A dose of $2.46x10^8$ vp/well of Alexa Fluor 488 labelled HAdV-5 pre-determined from pilot experiments was used, resulting in 10 to 200 bound vp/cell and thus allowing single particle quantification. As a control, the CAR-pathway was also analysed using $7.04x10^9$ vp/well of Alexa Fluor 488 labelled HAdV-5 (10 to 200 bound vp/cell) without the addition of hFX or FK. When indicated, cells were incubated with Alexa Fluor 488 labelled HAdV-2 ts1 in the presence of FK and hFX ($3x10^8$ vp/well) or in the absence of FK and hFX ($2x10^9$ vp/well).

After the cold incubation, unbound virus was removed by washing the cells monolayer with RPMI-BSA. To verify that FX-coated Alexa Fluor 488 labelled HAdV-5 was efficiently detected by rabbit anti-Alexa Fluor 488 primary antibody (Life Technologies by Thermo Fisher Scientific), one well at "0 min" condition was incubated with rabbit anti-Alexa Fluor 488 primary antibody (Life Technologies by Thermo Fisher Scientific) in RPMI-BSA for 60 min on ice (1 μg/ml) after unbound virus was washed away. Following incubation, cells were washed three times in RPMI-BSA and once with PBS [1.37 M NaCl, 27 mM KCl, 100 mM Na_2HPO_4, 18 mM KH_2PO_4] and fixed with 3% (w/v) PFA in PBS for 20 min at room temperature. For the rest of the conditions, after washing unbound virus away, cells were incubated for 45 min at 37°C in a water bath to allow virus internalization. When the FX-mediated pathway was studied, FK was added again (0.4 μg/ml) prior to the incubation at 37°C.

Next, to assess the percentage of viral particles remaining on the plasma membrane after the 45 min incubation (plasma membrane-associated viral particles), cells were subsequently incubated with rabbit anti-Alexa Fluor 488 primary antibody (Life Technologies by Thermo Fisher Scientific) in RPMI-BSA on ice for 60 min, washed three times with RPMI-BSA and once with PBS and fixed with 3% (w/v) PFA in PBS for 20 min at room temperature. To assess the percentage of viral particles localized in the cytoplasm, cells that had been incubated for 45 min at 37°C were subsequently subjected to membrane permeabilization with SLO. First, cells were washed twice with SLO binding buffer (25 mM HEPES-KOH pH7.4, 110 mM potassium acetate, 2.5 mM magnesium acetate, 0.2 mM calcium chloride, 1 mM EGTA, 1mM dithiothreitol (DTT)) and SLO (2.48 μg per well, Sigma-Aldrich) was pre-activated by incubation in SLO binding buffer

at room temperature for 5 min just before use. Next, SLO was bound to the plasma membrane at 4^{o}C for 10 min, unbound SLO was washed away and cells were covered in binding buffer and incubated at 37^{o}C for 5 min to allow SLO oligomerization and pore formation. Next, cells were washed with SLO binding buffer once and twice with SLO internalization buffer (25 mM HEPES-KOH pH7.4, 110 mM potassium acetate, 2.5 mM magnesium acetate, 2 mM EGTA), and incubated with rabbit anti-Alexa Fluor 488 primary antibody (Life Technologies by Thermo Fisher Scientific) (1 μg/ml) in internalization buffer on ice for 60 min. When indicated, mouse anti-human Giantin IgG1 primary antibody [clone: G1/133; kindly provided by professor Hans-Peter Hauri, Biocentre of the University of Basel, Switzerland (Linstedt and Hauri, 1993)] was added to the antibody mix at 33.33 μg/ml to confirm correct SLO pore formation. Following incubation, cells were washed three times with internalization buffer and fixed with 3% (w/v) PFA in transport buffer (25 mM HEPES-KOH pH7.4, 110 mM potassium acetate, 2.5 mM magnesium acetate) for 20 min at room temperature. For all the conditions ("0 min", "45 min non-SLO-treated" and "45 min SLO-permeabilized"), cells were washed once in PBS after the fixation step, quenched with 25 mM ammonium chloride in PBS for 10 min, washed again in PBS, and permeabilized with 0.5% Triton X-100 in PBS for 5 min at room temperature. Next, cells were washed once in PBS, blocked in 10% goat serum for 5 min at room temperature and incubated for 30 min at room temperature with Alexa Fluor 594-conjugated goat anti-rabbit IgG secondary antibody (Life Technologies by Thermo Fisher Scientific) at 4 μg/ml and DAPI for nuclear detection. Alexa Fluor 680-conjugated goat anti-mouse IgG secondary antibody (Life Technologies by Thermo Fisher Scientific) (4 μg/ml) was also used along with Alexa Fluor 594-conjugated goat anti-rabbit IgG secondary antibody and DAPI for samples that had been previously incubated with mouse anti-human Giantin IgG1 primary antibody. Following incubation, cells were washed three times in PBS for 4 min each and fixed again in 3% (w/v) PFA in PBS, quenched as specified before, washed in PBS and washed in distilled water just before mounting.

Samples were imaged with the Leica SP5 confocal laser scanning microscope with a 63x objective (oil immersion, numerical aperture: 1.4), excitations were at 405 nm for DAPI, 488 nm for adenoviral vector and 561 nm, 594 nm or 633 nm for secondary antibody (excitation was at 561 nm or 594 nm when Alexa Fluor 594 was used and 633 nm when Alexa Fluor 680 was used), and stacks were recorded at 0.5 μm intervals using 4x averaging and sequential acquisition for the individual channels. Maximal projections of confocal stacks were analyzed by a custom-programmed MatLab (The Mathworks) routine

to score and quantify individual viral particles (Alexa Fluor 488-positive) and of those, whether they are antibody-positive (goat anti-rabbit IgG Alexa Fluor 594-positive) or antibody-negative (goat anti-rabbit IgG Alexa Fluor 594-negative), as well as quantify antibody signal on virus particles. The threshold value for positive antibody signal was determined by placing a virus image on an antibody image obtained from non-infected cells and taking the highest virus-associated antibody signal as a cutoff value. It has been previously reported that following this procedure less than 3.5% of particles have values within 20% of the threshold value indicating that errors due to data analysis are minimal (Suomalainen et al., 2013). Representative images were processed with ImageJ applying the same parameters of brightness and contrast to all images per group.

The calculations applied to determine the number of plasma membrane-associated, cytosolic or endosomal viral particles as well as uptake and penetration efficiencies can be found in Table 2-10.

Table 2-10. Calculations applied to classify adenoviral particles.

Vp classification (%) or process	Classification method / calculations
Plasma membrane-associated vp [A]	Alexa Fluor 488 and antibody-positive vp in intact cells
Plasma membrane-associated plus cytosolic vp [B]	Alexa Fluor 488 and antibody-positive vp in SLO-permeabilized cells
Cytosolic vp	[B] – [A]
Endosomal vp	100 - [B] – [A]
Uptake efficiency	100 – [A]
Endosomal membrane penetration efficiency	([B] – [A]) / (100 – [A]) x 100

"Intact cells" refers to non-permeabilized cells. "Antibody-positive" refers to viral particles positive for anti-rabbit Alexa Fluor 594. Vp; viral particle.

2.2.7 Animal experiments

2.2.7.1 *In vivo* adenoviral vector delivery

For the first adenoviral biodistribution study in C57BL/6 and Rag $2^{-/-}$ mice, male mice aged 10-15 weeks were administered 150 µl of DPBS or $1x10^{11}$ vp/mouse of HAdV-5 (Prep. 1), AdT* (Prep. 1), HAdV-5 RGE, AdT*RGE or HAdV-5 KO1 (Prep. 2) [C57BL/6 mice] or HAdV-5 (Prep. 2), AdT* (Prep. 1), HAdV-5 RGE, AdT*RGE or HAdV-5 KO1 (Prep. 1) [Rag $2^{-/-}$ male] by intravascular tail vein injection in a total volume of 150 µl of DPBS. n = 5 C57BL/6 mice/group, n = 6 Rag $2^{-/-}$ mice/group or 7 (AdT*).

For the second biodistribution experiment in Rag $2^{-/-}$ and NSG mice mice, 9-13 weeks old male Rag $2^{-/-}$ and NSG mice were administered 150 µl of DPBS or $1x10^{11}$ vp/mouse HAdV-5 (Prep. 3) or AdT* (Prep. 2) in 150 µl of DPBS by intravascular tail vein injection. n = 5 for adenoviral vectors groups or 6 (HAdV-5 in Rag $2^{-/-}$ mice), n = 3 for the DPBS groups.

For the third biodistribution experiment in Rag $2^{-/-}$ and NSG mice, 19-21 weeks old male Rag $2^{-/-}$ and NSG mice were administered 150 µl of DPBS or $1x10^{11}$ vp/mouse HAdV-5 (Prep. 3), AdT* (Prep. 2) or AdT*RGE in 150 µl of DPBS by intravascular tail vein injection. n = 3 for all groups or 2 (AdT*RGE in Rag $2^{-/-}$ mice). Blood was collected 6 h post adenoviral vector injections as described in section 2.2.7.2, to be used in cytokine profiling assays.

Mice were sacrificed in all the experiments 48 h after adenoviral vector administration and perfused with DPBS. Organs (liver, spleen, lungs, intestine, kidney, heart and pancreas) were either collected and fixed in 2% (w/v) PFA overnight at 4^oC, frozen in $N_{2(l)}$ or embedded in Optimal Cutting Temperature compound (O.C.T) in cryomolds (Tissue-Tek, USA) and frozen at -80^oC.

2.2.7.2 Preparation of mouse serum

Male mouse blood was collected from C57BL/6, Rag$2^{-/-}$ or NSG mice by heart puncture post-mortem. Fresh serum was separated from whole blood by centrifugation at 6000 g for 10 min at 4^oC after formation of clot in a BD capillary blood collection microtainer tube (Fisher Scientific, UK) and stored at 4^oC. Of note, only fresh serum from male mice was used since the mouse classical complement pathway is highly unstable (Goldman et al., 1978) and there are sexual dimorphic differences in the titre of complement proteins (Baba et al., 1984, Hansen et al., 1974, Lachmann et al., 1975).

When serum was required for cytokine profiling assays, blood was collected using a microvette® CB 300 Z container (SARSTEDT, Germany) and subjected to centrifugation at 10000 g for 5 min at room temperature to separate serum from whole blood. Samples were stored at -80^oC.

2.2.7.3 Protein extraction from mouse tissue

When extracting protein from mouse tissue, approximately 25 mg of frozen liver or 10 mg of frozen spleen were placed in a 2 ml microcentrifuge tube containing 1 ml of lysis buffer provided in the anti-β-galactosidase enzyme-linked immunosorbent assay (ELISA) kit (Roche, Welwyn Garden City, UK) and 2 stainless steel beads (3 mm). Tissues were homogenized using a TissueLyser II (QIAGEN, Manchester, UK) for 1 min at 25 mHz twice, tissue lysates were subjected to centrifugation at 24000 g for 1 min at 4^{o}C and supernatant was transferred to a clean 1.5 ml microcentrifuge tube for storage at -80^{o}C.

2.2.7.4 DNA extraction from mouse tissue

DNA was extracted from mouse tissue samples (~25 or 10 mg of frozen liver or spleen, respectively) using QIAamp DNA Mini kit (QIAGEN, Manchester, UK), which is based on the use of QIAamp Spin Columns that bind DNA following lysis of tissue samples and protein degradation with proteinase K. The kit was used following the manufacturer's instructions. DNA was eluted with 200 µl or 100 µl nuclease-free water for livers or spleens, respectively. A second elution step was done using the same water to maximize DNA elution yield and DNA samples were stored at -20^{o}C until further use.

2.2.7.5 SYBR Green based Quantitative Real-Time polymerase chain reaction (qPCR)

Adenoviral genomes were extracted from frozen liver and spleen mouse tissue samples as described in section 2.2.7.4 and quantified by SYBR Green based qPCR. SYBR Green is an asymmetric cyanine dye that becomes brightly fluorescent when bound to dsDNA. Thus, when used in PCR, its fluorescence is proportional to the amount of DNA product generated. Fluorescence intensity is quantified during the exponential PCR phase and the value it reaches when crossing an arbitrary threshold situated on the exponential phase [cycle threshold (CT)] is indicative of the amount of original DNA in the sample. The comparison of CT values from samples with CT values from standards, which contain a known amount of adenoviral genomes, enables the determination of the amount of adenoviral genomes present in the samples.

Adenoviral DNA standards were generated from pure HAdV-5 encoding *LacZ* reporter gene, ranging from 1.6 to 1.6x10^{6} vp/µl in ten-fold serial dilutions in nuclease-free water, and DNA samples were diluted to 6 or 16 ng/µL, as indicated in each case, into a total of

25 µl nuclease-free water. A total of 6.25 µl of diluted samples (37.5 or 100 ng DNA, as indicated in each case) or adenoviral DNA standards (ranging from 10 vp to $1x10^7$ vp in ten-fold serial dilutions) were added in triplicate to a 384-well plate. A volume of 6.25 µl of Power SYBR Green 2X (Applied Biosystems by Life Technologies) containing buffer, dNTPs, thermostable hot-start DNA polymerase and SYBR Green dye, was added per well, along with 0.05 µl of 100 µM forward and reverse *LacZ* primers (final concentration of 0.4 µM) (Table 2-1). A negative control containing nuclease-free water instead of DNA was performed to assess for non-specific DNA amplification such as primer-dimer formation and its possible impact on the analysis of data. Thermal cycler conditions used as follows: 50°C for 2 min; 95°C for 10 min (DNA denaturation); 95°C for 15 sec and 60°C for 1 min (DNA denaturation, annealing and extension) repeated 40 times; 95°C for 15 sec, 60°C for 15 sec and 95°C for 15 sec (dissociation curve). The number of adenoviral genomes was calculated extrapolating CT values for each sample from the standard curve using SDS v2.3 software, assuming 1 adenoviral genome corresponds to 1 vp.

2.2.7.6 Anti-β-galactosidase ELISA

Protein homogenates were prepared from liver and spleen mouse tissue as described in section 2.2.7.3 and the amount of β-galactosidase present in the samples was determined by anti-β-galactosidase ELISA (Roche, Welwyn Garden City, UK) following the manufacturer's instructions. In this assay, β-galactosidase specifically binds to anti-β-galactosidase antibodies bound to a microplate surface and to a mouse anti-β-galactosidase-DIG primary antibody conjugated to digoxigenin, following the sandwich ELISA principle. A sheep anti-DIG-POD Fab fragment secondary antibody conjugated to peroxidase recognizes digoxigenin from anti-β-galactosidase-DIG primary antibody and, upon addition of 2,2'-azino-bis(3-ethylbenzothiazoline-6-sulphonic acid) (ABTS) substrate, a green coloured product is generated, allowing β-galactosidase quantification.

Samples were diluted into sample buffer as appropriate to fit into the standard curve (concentrations ranging from 78 pg/ml to 1250 pg/ml). Absorbance was measured at 405 nm using a VICTOR™ X3 Multilabel Plate Reader (PerkinElmer). The concentration of β-galactosidase present in the samples (pg/ml) was calculated by extrapolating the blank-subtracted measurements from the standard curve, and corrected by the dilution performed to each protein sample. The values were then normalized by the protein concentration in the samples (mg/ml) measured by the BCA Protein assay (see section 2.2.6.6), obtaining pg β-galactosidase/mg protein.

2.2.7.7 Immunohistochemistry (IHC) assay

Tissue sections were cut at 6 μm from frozen samples [embedded in O.C.T] using a Shandon Cryotome™ SME 77200227 Issue 4 Microtome Cryostat (Thermo Scientific). Sections were fixed for 10 min in 4% (w/v) PFA at room temperature, rinsed twice in PBS [1.37 M NaCl, 27 mM KCl, 100 mM Na_2HPO_4, 18 mM KH_2PO_4] for 5 min each, permeabilized in PBST 0.1% (v/v) for 10 min at room temperature, rinsed three times in PBS for 5 min and blocked for 30 min in PBST 0.1% (v/v) with 10% normal goat serum (Vector Laboratories Inc., USA) to reduce nonspecific binding of the secondary antibody. Next, sections were washed in PBST 0.1% (v/v) for 5 min at room temperature and incubated with rabbit anti-β-galactosidase primary antibody (MP Biomedicals LLC, USA) or isotype control (rabbit IgG, Invitrogen by Thermo Fisher Scientific) to control for background noise, overnight at 4°C (5 μg/ml in 1% normal goat serum in PBST 0.01% (v/v)). After the overnight incubation, sections were rinsed three times with PBS for 5 min and incubated with Alexa Fluor 488-conjugated goat anti-rabbit IgG secondary antibody (Life Technologies by Thermo Fisher Scientific) for 60 min at room temperature in the dark (4 μg/ml in PBS). Next, sections were rinsed three times with PBS for 5 min in the dark and slides were mounted with ProLong Gold Antifade Reagent with DAPI (Molecular Probes by Life Technologies) to counterstain the nuclei. Immunofluorescence was captured using a Zeiss confocal imaging system LSM 510 META using LSM image acquisition software (Carl Zeiss, Welwyn Garden City, UK) with a 40x objective (water immersion, numerical aperture: 1) and excitations at 405 nm for DAPI and 488 nm for secondary antibody. Adjustments were applied equally to all acquired images.

2.2.7.8 Cytokine profiling

Cytokine levels were quantified from serum samples from Rag $2^{-/-}$ and NSG mice (see section 2.2.7.2) using the Cytokine mouse 20-Plez Panel for Luminex Platform assay (Life Technologies by Thermo Fisher Scientific, UK) following the manufacturer's instructions. This cytokine panel is designed for the quantitative determination of FGF-basic, GM-CSF, IFN-γ, IL-1α, IL-1β, IL-2, IL-4, IL-5, IL-6, IL-10, IL-12 (p40/p70), IL-13, IL-17, CXCL10 (IP-10), KC, MCP-1, MIG, MIP-1α, TNF-α and VEGF in serum. In this assay, a range of cytokine-specific antibodies are conjugated to polystyrene beads, which are internally dyed with red and infrared fluorophores of differing intensities and assigned a bead region (unique number) that allows their differentiation. These antibodies are added to samples, standards and controls. Following the sandwich ELISA principle, cytokine-

specific antibodies recognize cytokines from samples. These cytokines are also recognized by cytokine-specific biotinylated antibodies, which are in turn recognized by fluorescent R-Phycoerythrin (RPE)-conjugated streptavidin (streptavidin-RPE). The plate is analysed with the Luminex detection system (using a Bio-Rad Bio-Plex 100 Luminex analyser) that determines the concentration of the different cytokines by detecting the fluorescence of RPE and associating it with each bead region, which according to their spectral properties can be assigned to a particular cytokine. The concentration of each cytokine (pg protein/ml) in the samples was determined from the standard curve using curve fitting Bio-Plex Manager v5.0 software. For values out of range (OOR) below the lowest standard, a zero value was assigned.

2.2.8 Statistical analysis

Data from experiments performed *in vitro* are either shown as the mean of values +/- SEM or shown as a percentage of one of the conditions (specified for each experiment) and expressed as the mean of the normalized values per experiment +/- SEM. n = 1-3 biological replicates per condition with 3-4 technical replicates in experiments with adenoviral vectors *in vitro*. n = 1 biological replicate with 1 technical replicate in trafficking assays. n = 1-2 biological replicates (depending on condition) with 1 technical replicate in SLO penetration assays. n = 3 technical replicates in TaqMan® Real-Time PCR and flow cytometry analysis.

Data from *in vivo* experiments are represented as the mean +/- SEM. n = 2-7 mice in groups administered adenoviral vectors, n = 3-6 mice in groups administered DPBS. n = 3 technical replicates in SYBR green based qPCR analysis. n = 1 technical replicate in the ELISA assay. n = 2-3 mice per group with one technical replicate in immunohistochemistry analysis. n = 2-3 mice per group with 1 technical replicate in cytokine profiling assays.

Statistical analysis was performed in GraphPad Prism v5.0 (GraphPad Software, San Diego, CA, USA). Unpaired Student's T-test, two-tailed Mann-Whitney *U* test, one-way ANOVA and Tukey's range test for *post hoc* pairwise comparisons of groups, or repeated measures ANOVA and Tukey's range test, were applied for significance assessment as specified for each analysis. $p<0.05$ was considered statistically significant.

Chapter 3 HAdV-5 neutralization and tropism *in vitro* and *in vivo* in immunocompetent and immunocompromised mice

3.1 Introduction

Intravascular delivery of vectors based on HAdV-5 leads to the sequestration of adenoviral particles in the liver as a result of the anatomical architecture of liver sinusoids and the presence of resident macrophages (Kupffer cells) (Di Paolo et al., 2009b, Shayakhmetov et al., 2004b, Alemany et al., 2000, Tao et al., 2001). Furthermore, intravascular delivery of HAdV-5 vectors leads to the transduction of hepatocytes via HAdV-5 interactions with cellular receptors. These processes result in high hepatic tropism, which cause toxicity and activation of immune responses (Lozier et al., 2002, Raper et al., 2002, Atencio et al., 2006, Morral et al., 2002). Moreover, intravascular delivery of HAdV-5 results in high tropism for the spleen, which has also been associated with the activation of immune responses against adenoviral vectors (Bradshaw et al., 2012).

CAR, $\alpha_v\beta_{3,5}$ integrins and HSPG were investigated as potential HAdV-5 receptors for liver and spleen transduction. Studies are, however, highly controversial. While the majority of studies reported that ablation of HAdV-5 interactions with CAR had no effect on liver transduction (Leissner et al., 2001, Alemany and Curiel, 2001, Martin et al., 2003, Smith et al., 2002, Smith et al., 2003a, Smith et al., 2003b, Zaiss et al., 2015), other studies sustained the opposite (Einfeld et al., 2001). Also, while some studies found that $\alpha_v\beta_{3,5}$ integrins are not required for liver transduction (Smith et al., 2003a, Mizuguchi et al., 2002, Bradshaw et al., 2012), others showed significantly reduced liver transduction with $\alpha_v\beta_{3,5}$ integrin-binding ablated vectors (Einfeld et al., 2001, Smith et al., 2003b). Furthermore, while ablation of CAR-binding failed to significantly reduce spleen transduction for the most part (Leissner et al., 2001, Alemany and Curiel, 2001, Martin et al., 2003, Smith et al., 2002, Smith et al., 2003a, Einfeld et al., 2001), other studies observed a moderate reduction on spleen transduction (Smith et al., 2003b). Also, some studies assessing the role of $\alpha_v\beta_{3,5}$ integrins in spleen transduction showed a significant reduction with $\alpha_v\beta_{3,5}$ integrin-binding ablated vectors (Smith et al., 2003a, Bradshaw et al., 2012), while others found not significant effect (Einfeld et al., 2001, Mizuguchi et al., 2002). The effect of simultaneous deletion of HAdV-5 interaction with CAR and $\alpha_v\beta_{3,5}$ integrins on liver and spleen transduction was also assessed and despite some studies showed decreased liver and/or spleen transduction (Smith et al., 2003b, Einfeld et al., 2001, Koizumi et al., 2003), others failed to find a significant effect (Martin et al., 2003). Mutation of the putative HSPG binding motif in the HAdV-5 fiber shaft (Smith et al., 2003a, Nicol et al., 2004) or the combination of such mutations with CAR and $\alpha_v\beta_{3,5}$ integrin-binding ablating mutations (Smith et al., 2003b, Koizumi et al., 2003) reduced

liver transduction in mice, rats and non-human primates, but the effects were subsequently shown to be likely due to defects in adenoviral particle trafficking associated with fiber shaft mutations (Bayo-Puxan et al., 2006, Kritz et al., 2007). In agreement, a recent study showed that HSPGs are dispensable for mouse liver transduction with HAdV-5 vectors (Zaiss et al., 2015). Interestingly, new mechanisms of HAdV-5 transduction consisting of blood factors bridging HAdV-5 to cellular receptors were identified (Shayakhmetov et al., 2005b, Parker et al., 2006) and FX was shown to be the key factor responsible for liver but not spleen transduction (Parker et al., 2006, Alba et al., 2010, Alba et al., 2009, Xu et al., 2013, Alba et al., 2012).

In addition to the role that FX plays in HAdV-5 hepatic tropism, recent work revealed an alternative role for FX in protecting HAdV-5 virions against "immune attack" or adenovirus neutralization (Xu et al., 2013) (Figure 3-1). This study showed that HAdV-5 neutralization *in vitro* is mediated by both natural IgM antibodies and the complement system, and that covalent modification of virions with C3b blocks binding of virions to host cells (Cichon et al., 2001, Xu et al., 2013). This data supports previous studies showing that activation of the classical complement pathway for adenovirus neutralization *in vitro* involves IgM antibodies (Tian et al., 2009). Conversely, other studies reported that both the classical and alternative complement pathways mediate adenovirus neutralization *in vitro* (Xu et al., 2008, Jiang et al., 2004). Moreover, it was discovered that HAdV-5 neutralization *in vivo* involves natural IgM antibodies and the complement system and results in negligible liver and spleen transduction (Xu et al., 2013). These data are in agreement with another study, which reported that circulating IgM antibodies negatively correlate with liver transduction (Khare et al., 2013). Other reports, however, show that *in vivo* adenovirus neutralization involves both the classical and non-classical complement pathways, thus indicating that IgM antibodies may be dispensable for *in vivo* adenovirus neutralization (Tian et al., 2009). Binding of FX to HAdV-5 capsid prevented binding of IgM antibodies to virions and the activation of C3 convertase, thus inhibiting adenovirus opsonisation with C3b and allowing adenovirus transduction (Xu et al., 2013, Duffy et al., 2016).

Interestingly, mice lacking the mediators of adenovirus neutralization exhibited high liver transduction when FX-binding deficient adenoviral vectors were administered through the vasculature (Xu et al., 2013) indicating that FX is not required for liver transduction in immunocompromised mice and suggesting that other pathways of cell entry may be available. In agreement, mice lacking *Ext1*, an enzyme required for HS biosynthesis

(McCormick et al., 1998), exhibited high levels of HAdV-5 liver transduction indicating that alternative pathways of HAdV-5 transduction are present when the FX-mediated pathway is not available (Zaiss et al., 2015). Whether these alternative pathways involve HAdV-5 engaging with cellular receptors or serum proteins that bridge HAdV-5 to such receptors remains unknown.

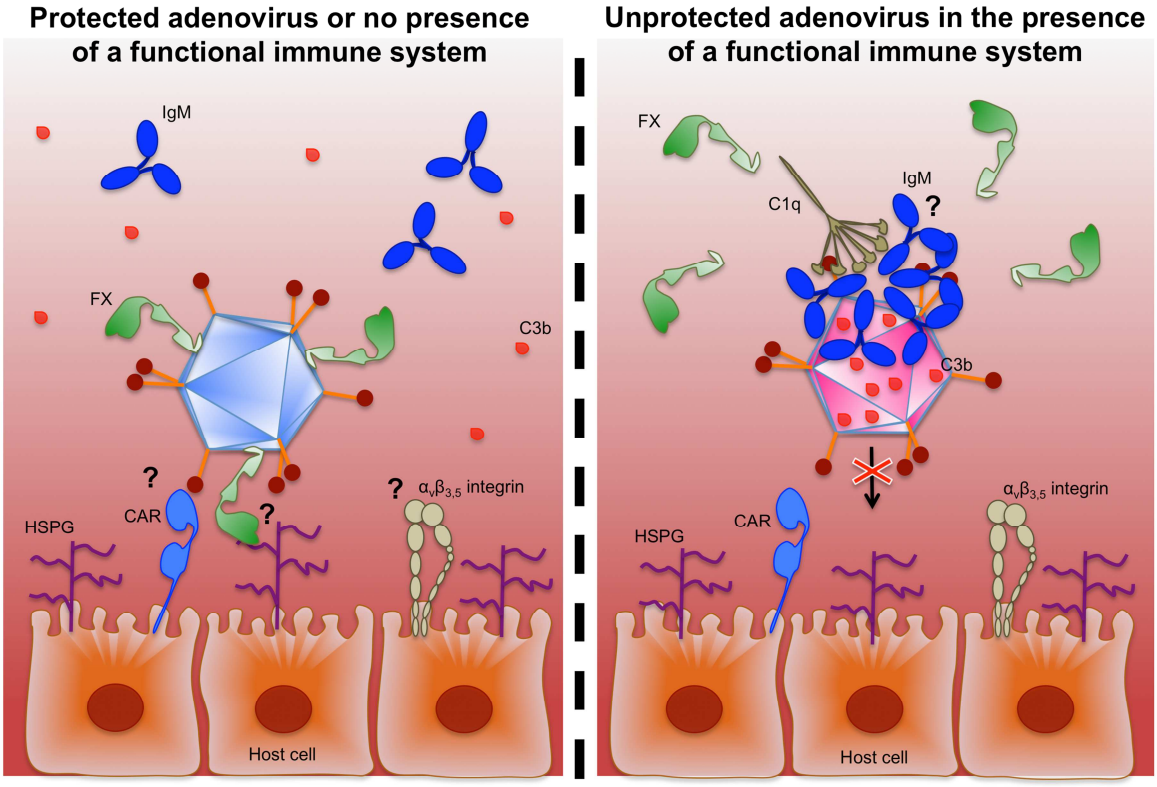

Figure 3-1. HAdV-5 *in vivo* neutralization and cell transduction following intravascular delivery. FX-mediated host cell transduction and protection against neutralization by natural IgM antibodies and the complement system (left panel). Suggested role for CAR and $\alpha_v\beta_{3,5}$ integrins in liver and spleen transduction. Blockade of HAdV-5 cell transduction by neutralization of virions in the absence of FX-binding (right panel). Question marks indicate interactions yet to be confirmed. FX; coagulation factor X, CAR; coxsackie and adenovirus receptor, HSPG; heparan sulphate proteoglycan, C3; complement protein 3. Figure adapted from (Lopez-Gordo et al., 2014a).

Here, the mechanisms dictating *in vitro* and *in vivo* HAdV-5 neutralization and the role of FX in protecting HAdV-5 from this process were investigated (Figure 3-1). The role of FX in HAdV-5 hepatic and splenic tropism in the absence of adenovirus neutralization following intravascular delivery was also assessed, and CAR and $\alpha_v\beta_{3,5}$ integrins were evaluated as possible receptors mediating FX-independent HAdV-5 liver and spleen transduction in this setting (Figure 3-1). Finally, the hypothesis that HAdV-5 can use alternative FX-independent pathways for cell transduction *in vitro* after exposure of virions to mouse serum that may be relevant *in vivo*, was also assessed.

3.2 Aims

The aims of the present study were:

- To describe the mechanisms mediating *in vitro* and *in vivo* HAdV-5 neutralization by the host innate immune response and the role of FX in this process.
- To investigate the role of FX, CAR and $\alpha_v\beta_{3,5}$ integrins in HAdV-5 hepatic and splenic tropism in the absence of adenovirus neutralization following intravascular delivery.
- To define alternative HAdV-5 FX-independent pathways for cell transduction *in vitro* after exposure of virions to mouse serum.

3.3 Results

3.3.1 Generation and validation of adenoviral vectors

Adenoviral vectors used in this study were replication-deficient HAdV-5-based adenoviral vectors encoding the *E.coli LacZ* gene (β-galactosidase). A summary of the adenoviral vectors' genetic and receptor recognition characteristics is shown in section 2.1.6.

3.3.1.1 Cloning strategy to generate HAdV-5 KO1 adenoviral vector

The genome of HAdV-5 KO1 (pAdEasy1-CMV-*LacZ*-KO1) was engineered in order to incorporate specific genetic modifications in the fiber knob domain to alter receptor recognition characteristics (Figure 3-2). Briefly, pAdEasy1-CMV-*LacZ*-KO1 was generated by the homologous recombination of pAdEasy1-CMV-*LacZ* with pShuttle-KO1. pAdEasy1-CMV-*LacZ* was the resultant of the homologous DNA recombination between pAdEasy1 and pShuttle-CMV-*LacZ*. pShuttle-KO1 was the resultant of the enzymatic ligation of pShuttle-KO1-AAA with pAdT*KO1.

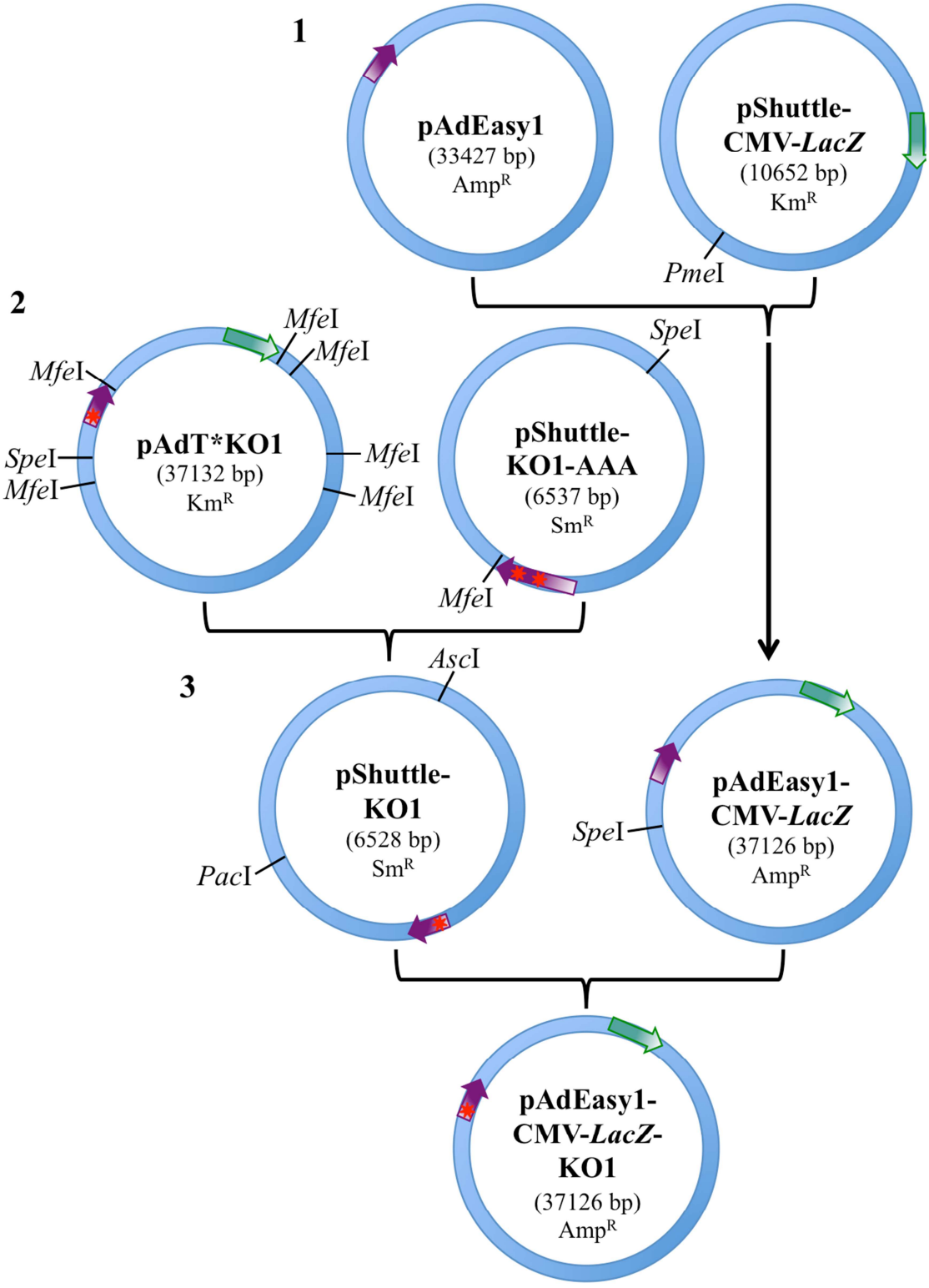

Figure 3-2. Cloning strategy to generate HAdV-5 KO1 genome (pAdEasy1-CMV-*LacZ* KO1). 1. First cloning step where pAdEasy1 and pShuttle-CMV-*LacZ* are subjected to homologous DNA recombination to generate pAdEasy1-CMV-*LacZ*. **2.** Second cloning step involving enzymatic ligation between the fiber ORF from AdT*KO1 with the backbone from pShuttle-KO1-AAA, to obtain pShuttle-KO1. **3.** Third cloning step to generate pAdEasy1-CMV-*LacZ*-KO1 by homologous DNA recombination between pShuttle-KO1 and pAdEasy1-CMV-*LacZ*. Features in green represent *LacZ*, features in purple represent the fiber ORF, and stars in red represent genetic mutations (AAA peptide and KO1 mutation in pShuttle-KO1-AAA or only KO1 mutation in the other plasmids). Amp^R; ampicillin resistance, Km^R; kanamycin resistance, Sm^R; streptomycin resistance.

The first cloning step involved generating pAdEasy1-CMV-*LacZ* by introducing the reporter gene *LacZ* under the control of the CMV-IEP promoter (from pShuttle-CMV-*LacZ*) into pAdEasy1 genome. pShuttle-CMV-*LacZ* was transformed into chemically competent *E. coli* for plasmid amplification. Plasmid DNA (pDNA) was extracted from single kanamycin resistant colonies, enzymatically digested with *Pac*I and subsequently electrophoresed for plasmid confirmation (Figure 3-3A). To prepare pShuttle-CMV-*LacZ* for homologous DNA recombination, the plasmid was linearized with *Pme*I, the 5' ends were de-phosphorylated, and *Pme*I-digested pDNA was electrophoresed (Figure 3-3B) and subsequently extracted from the agarose gel for DNA purification. Homologous DNA recombination was performed by transforming purified *Pme*I-digested pShuttle-CMV-*LacZ* into electrocompetent $recA^+$ *E. coli* together with the transfer circular vector pAdEasy1 (amplified in bacteria as before and verified by digestion with *Pac*I or *Asc*I (Figure 3-3C). pAdEasy1-CMV-*LacZ* was extracted from single ampicillin resistant colonies, confirmed by enzymatic digestion with *Pac*I (Figure 3-3D), and transformed into chemically competent *E. coli* to amplify pDNA in a recA1 system unable to recombine DNA, thus conferring stability to the plasmid. A large-scale preparation of pAdEasy1-CMV-*LacZ* was obtained from a single positive colony and confirmed by enzymatic digestion with *Pac*I or *Spe*I (Figure 3-3E-F).

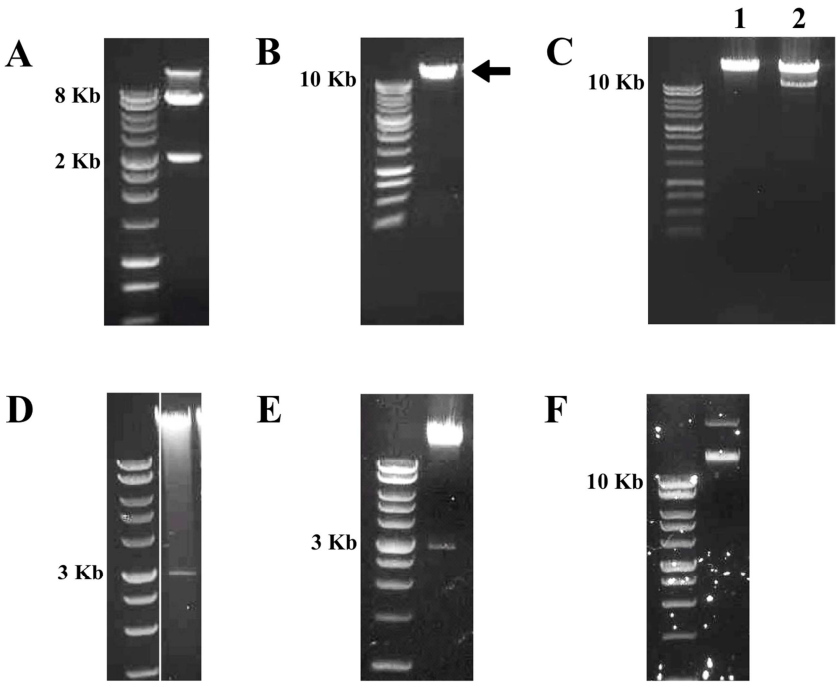

Figure 3-3. pAdEasy1-CMV-*LacZ* KO1 first cloning step. A) *Pac*I-digested pShuttle-CMV-*LacZ* maxiprep (7730 bp, 2930 bp). B) *Pme*I-digested pShuttle-CMV-*LacZ* (10660 bp). C) *Pac*I-digested (1) or *Asc*I-digested (2) pAdEasy1 maxiprep. Bands 37126 bp (1) or 27506 bp and 9620 bp (2). D) *Pac*I-digested pAdEasy1-CMV-*LacZ* miniprep from $recA^+$ bacteria (34196 bp, 2930 bp). E) *Pac*I-digested pAdEasy1-CMV-*LacZ* maxiprep (34196 bp, 2930 bp). F) *Spe*I-digested pAdEasy1-CMV-*LacZ* maxiprep. Arrow

indicates the DNA band extracted from the agarose gel. 1 kb DNA ladder (Invitrogen, UK) used in (A) and 1 kb DNA ladder (Promega, UK) used in (B-F).

In the second cloning step, pShuttle-KO1 was obtained by enzymatic ligation of the fiber ORF from pAdT*KO1 (containing the KO1 mutation) with the backbone pShuttle-KO1-AAA, from which the fiber ORF [containing the KO1 mutation and an extra *Not*I site + cytosine (AAA peptide)] had been removed. See section 5.3.1.1 for more details on the latter plasmid. To prepare pAdT*KO1 and pShuttle-KO1-AAA for ligation, the fiber ORF from both plasmids was extracted by enzymatic digestion with *Mfe*I and *Spe*I. The digests were electrophoresed and the DNA bands corresponding to the pAdT*KO1 fiber ORF and the pShuttle-KO1-AAA backbone were extracted from the agarose gel (Figure 3-4A-B). Enzymatic ligation was performed between both DNA fragments and the ligation product was transformed into chemically competent *E. coli*. A large-scale preparation of pShuttle-KO1 was obtained from a single positive streptomycin resistant colony and confirmed by enzymatic digestion with *Mfe*I and *Spe*I (Figure 3-4C). Absence of the extra *Not*I site in the fiber knob HI loop sequence was confirmed by sequencing.

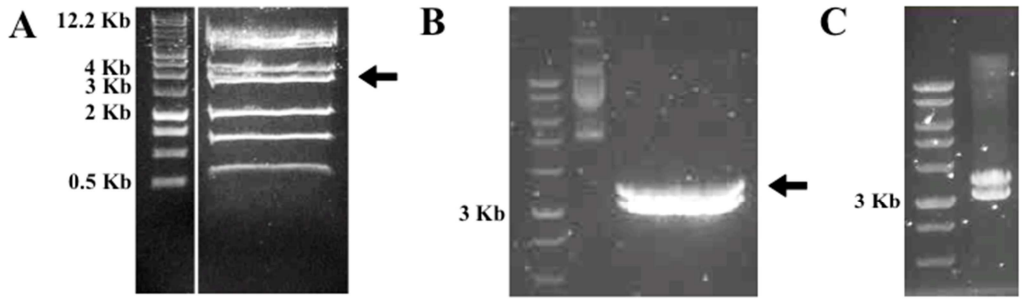

Figure 3-4. pAdEasy1-CMV-*LacZ* KO1 second cloning step. A) *Mfe*I and *Spe*I-digested pAdT*KO1 maxiprep (16412 bp, 10359 bp, 4091 bp, 3088 bp, 1615 bp, 1038 bp, 529 bp). B) *Mfe*I and *Spe*I-digested pShuttle-KO1-AAA maxiprep (3440 bp, 3097 bp). C) *Mfe*I and *Spe*I-digested pShuttle-KO1 maxiprep (3440 bp, 3088 bp). Arrows indicates the DNA bands extracted from the agarose gel. 1 kb DNA ladder (Invitrogen, UK) used in (A) and 1 kb DNA ladder (Promega, UK) used in (B-C).

The third cloning step involved generating the final HAdV-5 KO1 genome (pAdEasy1-CMV-*LacZ*-KO1). Homologous DNA recombination was performed between pAdEasy1-CMV-*LacZ* and pShuttle-KO1 to exchange the pAdEasy1-CMV-*LacZ* fiber ORF with the fiber ORF from pShuttle-KO1, which contained the KO1 mutation. To prepare the plasmids, pAdEasy1-CMV-*LacZ* was linearized with *Spe*I (Figure 3-5A), the 5' ends were de-phosphorylated and pDNA was purified by DNA precipitation. pShuttle-KO1 was enzymatically digested with *Asc*I and *Pac*I, electrophoresed, and the band containing the "fiber KO1" was extracted from the agarose gel (Figure 3-5B). Homologous DNA recombination was performed as before and positive ampicillin resistant colonies were

confirmed by sequencing. pDNA from one of the positive colonies was transformed into chemically competent recA1 *E. coli* as before and a large-scale preparation for pAdEasy1-CMV-*LacZ*-KO1 was obtained from positive clones which were sequenced to confirm presence of the KO1 mutation in the fiber ORF. To confirm homologous recombination had taken place only via the left homology arm of the DNA plasmids (see section 5.3.1.1 for detailed principle explanation), the final pAdEasy1-CMV-*LacZ*-KO1 was confirmed by enzymatic digestion with *Xho*I (Figure 3-5D). As a further quality control, pAdEasy1-CMV-*LacZ*-KO1 was enzymatically digested with a range of restriction endonucleases as shown in Figure 3-5C-D.

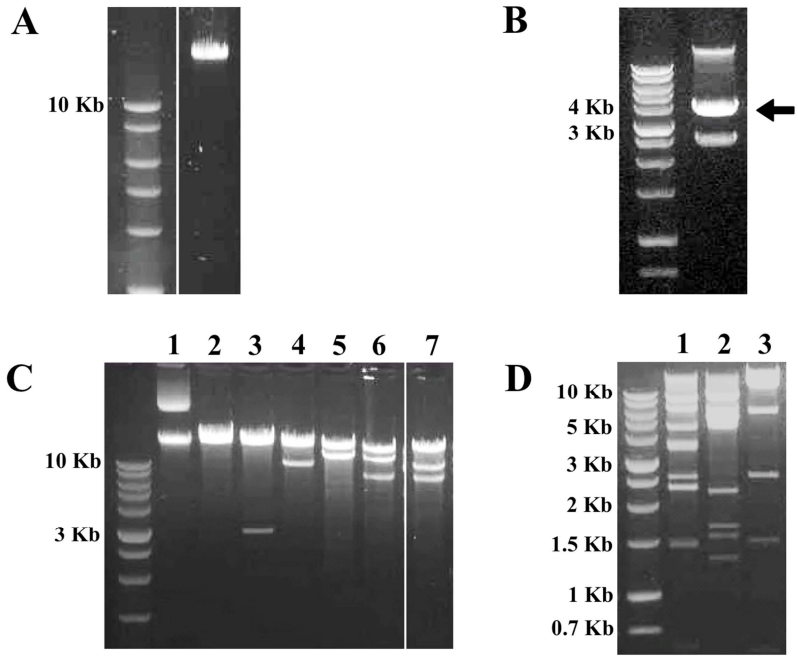

Figure 3-5. pAdEasy1-CMV-*LacZ* KO1 third cloning step. A) *Spe*I-digested pAdEasy1-CMV-*LacZ* maxiprep. B) *Asc*I and *Pac*I-digested pShuttle-KO1 maxiprep (3440 bp, 3088 bp). C) uncut pAdEasy1-CMV-*LacZ*-KO1 maxiprep (1), pAdEasy1-CMV-*LacZ*-KO1 maxiprep digested with *Spe*I, (2), *Pac*I (3), *Asc*I (4), *Eco*RI (5), *Bam*HI (6) or *Sal*I (7). Bands 37126 bp (2), 34196 bp, 2930 bp (3), 27506 bp, 9620 bp (4), 24282 bp, 12844 bp (5), 18456 bp, 11734 bp, 6936 bp (6), or 20413 bp, 9431 bp, 6903 bp, ***379 bp*** (7). D) pAdEasy1-CMV-*LacZ*-KO1 maxiprep digested with *Sma*I (1), *Bgl*II (2), *Xho*I (3). Bands 8370 bp, 6478 bp, 4456 bp, 3540 bp, 3386 bp, 2463 bp, 2278 bp, 2262 bp, 1455 bp, ***1398 bp***, 630 bp, ***230 bp, 180 bp*** (1), 8895 bp, 6180 bp, 5415 bp, 5178 bp, 4645 bp, 2151 bp, 1625 bp, 1497 bp, 1268 bp, ***272 bp*** (2), 14500 bp, 12376 bp, 5744 bp 2466 bp, 1445 bp, ***595 bp*** (3). Arrows indicates the DNA bands extracted from the agarose gel. 1 kb DNA ladder (Promega, UK) used. Bolded and in italics DNA band sizes in figure legend correspond to bands that are not visible in the image but that were visible in the agarose gel using a transilluminator (UVP).

3.3.1.2 Adenoviral vectors amplification and quality control

HAdV-5, AdT* and HAdV-5 RGE were amplified from pure adenoviral vector preparations originated from a single plaque. Due to a lack of available pure adenoviral vector preparations, AdT*RGE was produced by transfecting the *Pac*I-linearized adenoviral genome pAdT*RGE into eukaryotic permissive HEK-293 cells for vector

amplification and generation of crude adenoviral vector stocks. Since HAdV-5 KO1 exhibited propagation difficulties in HEK-293 cells, the genome of HAdV-5 KO1 (pAdEasy1-CMV-*LacZ*-KO1) was linearized with *Pac*I and transfected into eukaryotic permissive Per.C6® cells (Crucell), which allow higher levels of adenovirus production than those from HEK-293 cells (Fallaux et al., 1998), and rescued HAdV-5 KO1 were subsequently propagated in Per.C6® cells. Pure adenoviral vector preparations were generated for all adenoviral vectors above and tested for their quality (safety, genetic stability, concentration and infectivity, transgene expression, and adenovirus particles aggregation, protein composition and integrity) as indicated below.

The absence of RCAs was confirmed for the pure adenoviral vector preparations generated in this study, ensuring safety of adenoviral preparations. Vector genetic stability was confirmed by sequencing the adenoviral vectors' genome for each amplification step. With this aim, adenoviral DNA was extracted from adenovirus particles and sequences corresponding to the hexon, penton base or fiber ORFs were amplified by PCR. PCR amplicons were purified and analysed by sequencing to confirm the presence of the introduced genetic modifications. The concentration of adenovirus particles (vp/ml) and infectivity (pfu/ml) of pure adenoviral vector preparations were also assessed. The expected vp/ml and vp/pfu ratios for wild type and mutant HAdV-5 vectors according to historical values following the manufacturing process available in our laboratory facilities were obtained (from around 40 to 150, with the exception of HAdV-5 KO1 that exhibited high vp/pfu ratios, being those higher than 6000) (Table 3-1). Of note, adenoviral vectors presented vp/pfu ratios that slightly differed from the recommended values by the FDA (see section 2.2.5.9). Since a high ratio for HAdV-5 KO1 might merely result from the lack of binding to CAR due to the KO1 mutation (Leissner et al., 2001, Jakubczak et al., 2001, Roelvink et al., 1999) and not be associated with impaired adenovirus propagation, vp/pfu ratios obtained were considered acceptable for a safe use of the adenoviral vectors in *in vivo* studies.

Table 3-1. Adenoviral vectors quality control.

Adenoviral vector	Titre (vp/ml)	Titer (pfu/ml)	Vp/pfu	Vp diameter (nm)
HAdV-5 (Prep. 1)	$1.55x10^{12}$	$1.88x10^{10}$	82.45	91
HAdV-5 (Prep. 2)	$1.66x10^{12}$	$1.11x10^{10}$	149.55	95
HAdV-5 (Prep. 3)	$3.27x10^{12}$	$2.61x10^{10}$	125.29	103
AdT* (Prep. 1)	$2.55x10^{12}$	$1.76x10^{10}$	144.89	86

AdT* (Prep. 2)	$3.85x10^{12}$	$8.81x10^{10}$	43.70	88
HAdV-5 RGE	$1.60x10^{12}$	$3.20x10^{10}$	50	94
HAdV-5 KO1 (Prep. 1)	$8.75x10^{11}$	$1.40x10^{8}$	6250	100
HAdV-5 KO1 (Prep. 2)	$7.73x10^{12}$	$1.16x10^{9}$	6663.79	90
AdT*RGE	$5.34x10^{12}$	$3.62x10^{10}$	147.51	109

Plaque forming units (pfu/ml) values shown were obtained with the pfu observed after performing X-Gal staining. Values of viral particle (vp) diameter by Nanoparticle Tracking Analysis (NanoSight) are the mean of technical triplicates. "Prep." followed by a number refers to the individual pure adenovirus preparations generated. HAdV-5; human adenoviral vector serotype 5.

The absence of virion aggregates in pure adenoviral vector preparations was confirmed by assessing the adenovirus capsid size. Adenovirus capsid diameter values were similar to the historical values for HAdV-5-based vectors [90-100 nm (Norrby, 1969, Goosney and Nemerow, 2003)] (Table 3-1). HAdV-5 KO1 capsid protein composition and integrity of capsid structure was confirmed by silver staining (Figure 3-6), indicating that the KO1 mutation did not interfere with capsid assembly and maturation. Silver staining of HAdV-5, AdT*, HAdV-5 RGE and AdT*RGE have been previously demonstrated (Alba et al., 2009, Bradshaw et al., 2012).

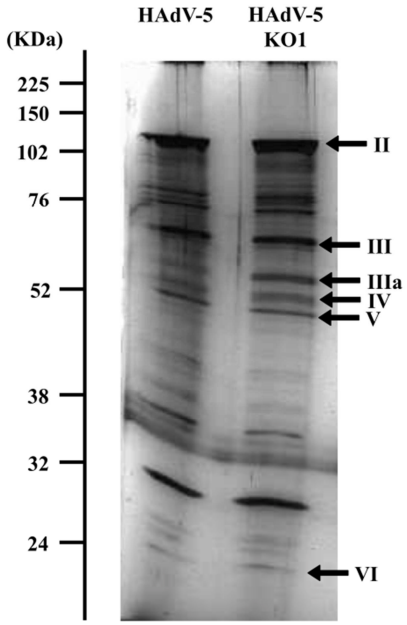

Figure 3-6. Adenovirus capsid protein composition of HAdV-5 KO1. A total of $5x10^{10}$ denatured HAdV-5 or HAdV-5 KO1 particles were loaded in a 12% SDS-polyacrylamide gel and proteins were visualized by silver staining (Life Technologies). Rainbow ladder (Amersham Bioscience UK Ltd, UK) was used as a marker for molecular weight. Numbers on the right indicate polypeptides of viral particles and their designations. Mw (kDa): 109 (protein II/hexon), 63.3 (protein III/penton base and IIIa), 62 (protein IV/fiber), 41.6 (protein V) and 23.4 (protein VI) (San Martin and Burnett, 2003).

Next, the ability of FX to enhance cell transduction of HAdV-5 but not FX-binding deficient AdT*-based vectors was confirmed by assessing adenoviral transduction of CAR^{high} A549 or CAR^{low} SKOV3 cells in the presence or absence of hFX. As expected,

transduction with HAdV-5-based vectors was significantly enhanced by hFX in both cell lines while transduction with AdT*-based vectors remained unaffected or minimally enhanced (Figure 3-7). As previously reported (Bradshaw et al., 2012), HAdV-5 RGE and AdT*RGE were able to transduce A549 and SKOV3 cells in the absence of hFX despite lacking $\alpha_v\beta_{3,5}$ integrin-binding (Figure 3-7). HAdV-5 KO1 exhibited extremely low transduction levels of A549 cells in the absence of hFX (Figure 3-7) in agreement with previous reports (Jakubczak et al., 2001, Smith et al., 2003b, Smith et al., 2002). In contrast, HAdV-5 KO1 showed similar transduction levels to HAdV-5 in CAR^{low} SKOV3 cells (Figure 3-7).

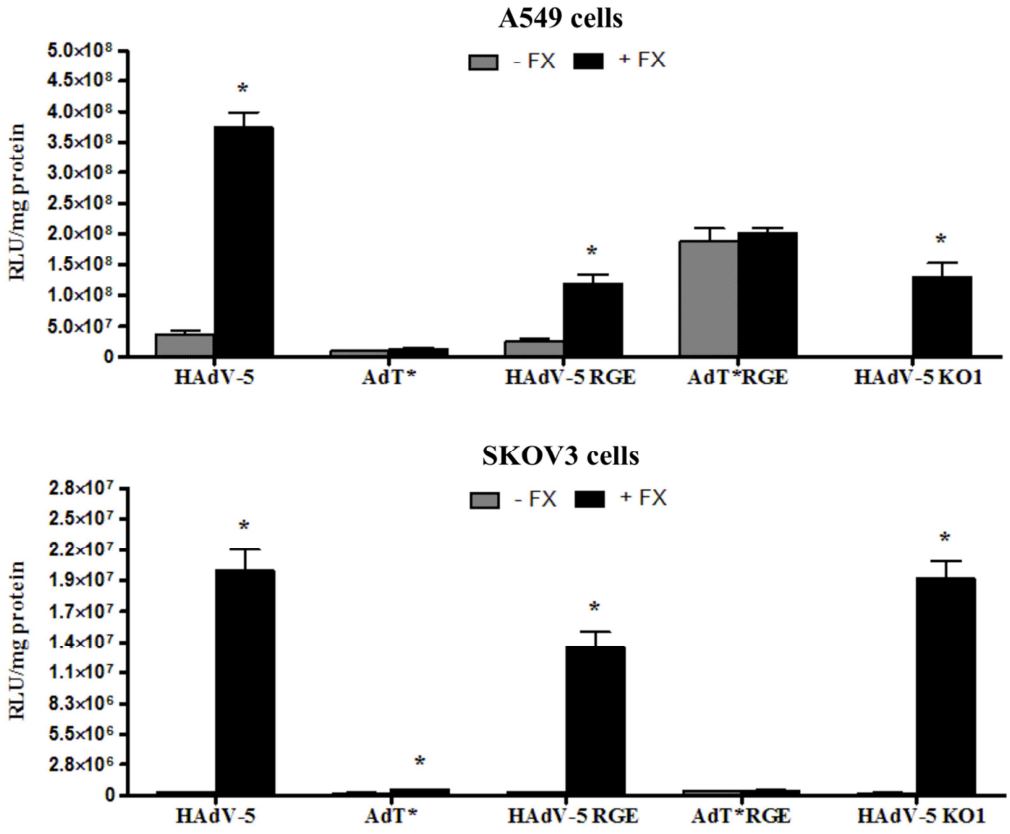

Figure 3-7. Sensitivity to FX on adenoviral transduction. A549 or SKOV3 cells were incubated with pure adenoviral vector preparations (1000 vp/cell) at 37°C for 3 h in the presence or absence of human recombinant FX (10 μg/ml), washed with 10% FCS RPMI-1640 medium and incubated at 37°C for further 48 h. β-galactosidase expression levels were quantified as relative light units (RLU) and normalized to total mg of protein. n = 4 technical replicates per condition. Data from a single adenoviral preparation for each wild type or mutant adenoviral vector is shown as a representative. Values are shown as the mean of values +/- SEM. Unpaired Student's T-test applied. *$p<0.05$ vs. matched controls.

3.3.2 Validation of mouse models

Since immunocompromised Rag $2^{-/-}$ (Shinkai et al., 1992, Alt et al., 1992) and NSG (Zhou et al., 2014, Shultz et al., 2005, Shultz et al., 1995, Ito et al., 2002) mice lack IgM antibodies (section 2.1.7), one of the reported mediators of *in vitro* and *in vivo* adenovirus neutralization (Xu et al., 2013), these mice were used in *in vivo* studies to bypass the adenovirus neutralization associated with FX-binding deficient adenoviral vectors and thus allow tropism studies with such vectors. To confirm Rag $2^{-/-}$ and NSG mice are unable to neutralize HAdV-5 virions, HAdV-5 transduction of A549 cells was assessed following pre-incubation of HAdV-5 with Rag $2^{-/-}$ or NSG serum. Serum from immunocompetent C57BL/6 mice was used as a control. Transduction occurred at low levels in the presence of SF medium alone due to the low MOI (adenoviral particles/cell) used in the assay (Figure 3-8). The presence of C57BL/6 serum produced a significant enhancement in HAdV-5 transduction (2.4-fold) indicating the presence of a factor(s) in the serum able to contribute to HAdV-5 transduction (Figure 3-8A). Pre-incubation of C57BL/6 serum with X-bp, a molecule that binds to FX GLA domain impairing HAdV-5:FX interaction (Atoda et al., 1998), resulted in the inhibition of HAdV-5 transduction (Figure 3-8A), suggesting the presence of adenovirus neutralization in the absence of FX-binding. Both Rag $2^{-/-}$ and NSG sera significantly enhanced HAdV-5 transduction by 3.5-fold and 3.2-fold, respectively (Figure 3-8A). In contrast to C57BL/6 serum, Rag $2^{-/-}$ and NSG serum pre-incubated with X-bp did not reduce HAdV-5 transduction in comparison to the SF media condition (Figure 3-8A) suggesting an absence of adenovirus neutralization and thus validating the immunocompromised mouse models chosen for *in vivo* experiments. Interestingly, Rag $2^{-/-}$ and NSG serum pre-incubated with X-bp enhanced HAdV-5 transduction to levels similar to those observed in the absence of X-bp (Figure 3-8A). These results suggest that HAdV-5 transduces A549 cells predominantly via a FX-independent mechanism in the presence of immunocompromised mouse serum. Next, FX-binding deficient AdT* was used to confirm results. C57BL/6 serum inhibited AdT* transduction both in the presence and absence of X-bp (Figure 3-8B), again supporting a role for FX in protecting HAdV-5 from neutralization. However, both Rag $2^{-/-}$ and NSG sera enhanced AdT* transduction by 2.4-fold and 1.8-fold, respectively (Figure 3-8B), although this was only significant for Rag $2^{-/-}$ serum, confirming lack of adenovirus neutralization and FX-independency in mouse serum-enhanced transduction in the presence of immunocompromised mouse serum.

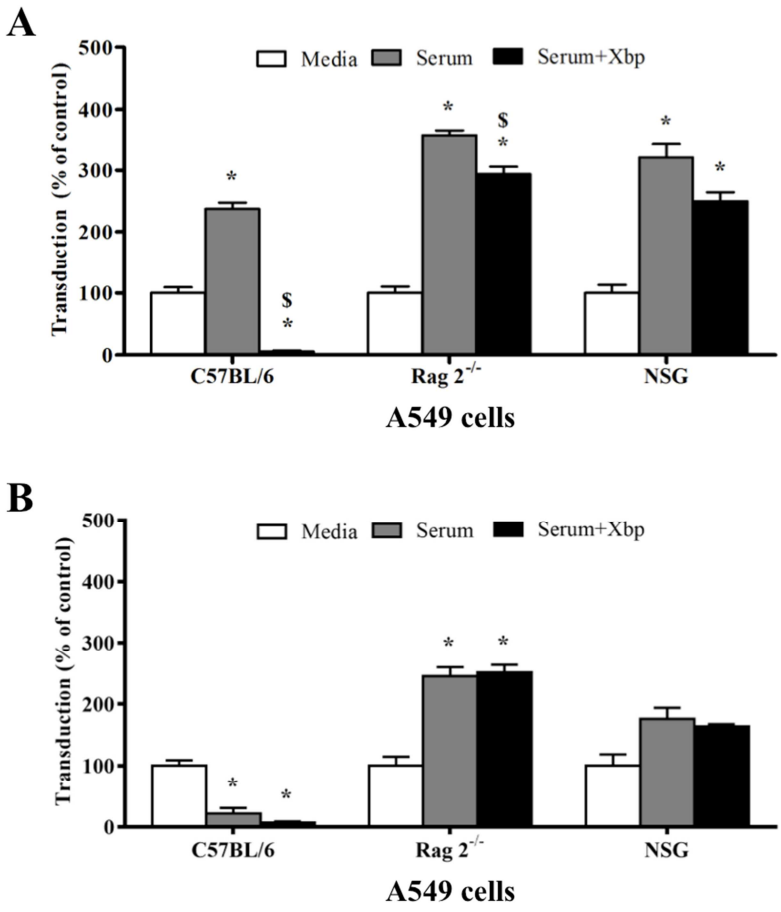

Figure 3-8. Effect of mouse serum on adenoviral transduction. HAdV-5 (A) or AdT* (B) ($2x10^{10}$ vp/ml) were incubated for 30 min at 37°C with serum-free (SF) RPMI-1640 media or 90% C57BL/6, Rag $2^{-/-}$ or NSG serum in the presence or absence of X-bp (40 μg/ml). Adenovirus suspensions were diluted 200-fold in SF media and added to A549 cells (1000 vp/cell) and incubated at 37°C for 2 h. Then, media was replaced with 2% FCS RPMI and cells incubated for further 20 h. β-galactosidase expression levels were quantified as relative light units (RLU) and normalized to total mg of protein. n = 7 (C57 BL/6), n = 6 (Rag $2^{-/-}$), n = 3 (NSG) biological replicates per condition with 4 technical replicates. Values are shown as a percentage of the SF media alone condition and expressed as the mean of the normalized values per experiment +/- SEM. Repeated measures ANOVA and *post hoc* Tukey's range test applied. *$p<0.05$ vs. matched controls, \$$p<0.05$ vs. matched serum.

These data indicate that while FX is critical in protecting HAdV-5 from neutralization, FX may only partially mediate HAdV-5 transduction *in vitro* in the presence of immunocompromised Rag $2^{-/-}$ or NSG serum, suggesting that other mechanisms of HAdV-5 transduction might be present in this setting.

3.3.2.1 Role of IgM antibodies on HAdV-5 neutralization by mouse serum *in vitro*

To assess the specific role of IgM antibodies on HAdV-5 neutralization *in vitro*, A549 cells were incubated with HAdV-5 in the presence of immunocompromised Rag $2^{-/-}$ serum with the addition of pure mouse IgM antibodies. X-bp was added when indicated to inhibit HAdV-5:FX interaction and thus expose HAdV-5 to neutralization. C57BL/6 serum was

used as a control. C57BL/6 serum significantly enhanced HAdV-5 transduction 2.5-fold and pre-incubation of C57BL/6 serum with X-bp decreased transduction (Figure 3-9) as previously observed (Figure 3-8). In contrast, Rag $2^{-/-}$ serum pre-incubated with X-bp enhanced HAdV-5 transduction 2.5-fold confirming the lack of adenovirus neutralization (Figure 3-9). A range of three different concentrations of IgM were used according to previous reports (Xu et al., 2013). Addition of IgM to Rag $2^{-/-}$ serum that had been pre-incubated with X-bp to expose HAdV-5 to possible neutralization, had no effect on HAdV-5 serum-enhanced transduction (Figure 3-9). These data suggest that IgM may not be involved in adenovirus neutralization by Rag $2^{-/-}$ serum but is in disagreement with previous reports (Xu et al., 2013).

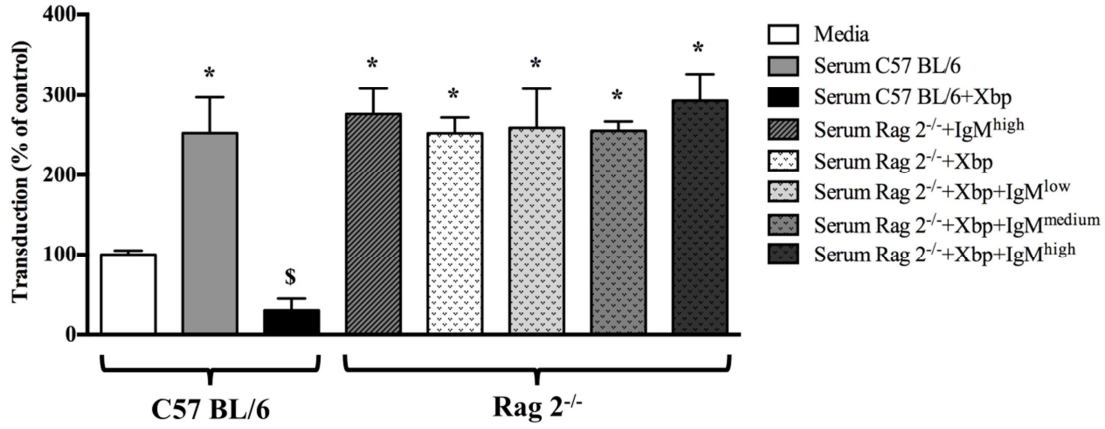

Figure 3-9. Role of IgM antibodies on adenovirus neutralization. HAdV-5 ($2x10^{10}$ vp/ml) was incubated for 30 min at 37°C with serum-free (SF) RPMI-1640 media or 90% C57 BL/6 or Rag $2^{-/-}$ serum in the presence or absence of X-bp (40 μg/ml) or IgM antibodies (low: 50, medium: 150 or high: 300 μg/ml). Adenovirus suspensions were diluted 200-fold in SF media and added to A549 cells (1000 vp/cell) and incubated at 37°C for 2 h. Then, media was replaced with 2% FCS RPMI and cells incubated for further 20 h. β-galactosidase expression levels were quantified as relative light units (RLU) and normalized to total mg of protein. n = 3 biological replicates per condition with 4 technical replicates. Values are shown as a percentage of the SF media alone condition and expressed as the mean of the normalized values per experiment +/- SEM. Repeated measures ANOVA and post hoc Tukey's range test applied. *$p<0.05$ vs. media, \$$p<0.05$ vs. matched serum.

3.3.2.2 Role of complement on HAdV-5 neutralization by mouse serum *in vitro*

Next, the role of complement on adenovirus neutralization *in vitro* in the presence of mouse serum was studied by performing transduction assays with HAdV-5 on A549 cells using immunocompetent C57BL/6 serum that had been pre-incubated at 56°C to inhibit the complement system. Immunocompromised Rag $2^{-/-}$ serum was used as a non-neutralizing control serum. Unheated C57BL/6 and Rag $2^{-/-}$ serum significantly enhanced HAdV-5 transduction (2.2-fold and 3.3-fold, respectively) and X-bp inhibited HAdV-5 transduction when added to unheated C57BL/6 serum (Figure 3-10) as observed before (Figure 3-8).

Interestingly, heat-treated C57BL/6 and heat-treated Rag $2^{-/-}$ sera were unable to enhance HAdV-5 transduction (Figure 3-10), suggesting that the factors in serum involved in such enhancement may be heat-labile and thus unable to enhance HAdV-5 transduction after exposure to high temperatures. Furthermore, heated C57BL/6 serum pre-incubated with X-bp failed to inhibit HAdV-5 transduction (Figure 3-10A), similar to that observed with heated Rag $2^{-/-}$ serum with X-bp (Figure 3-10B).

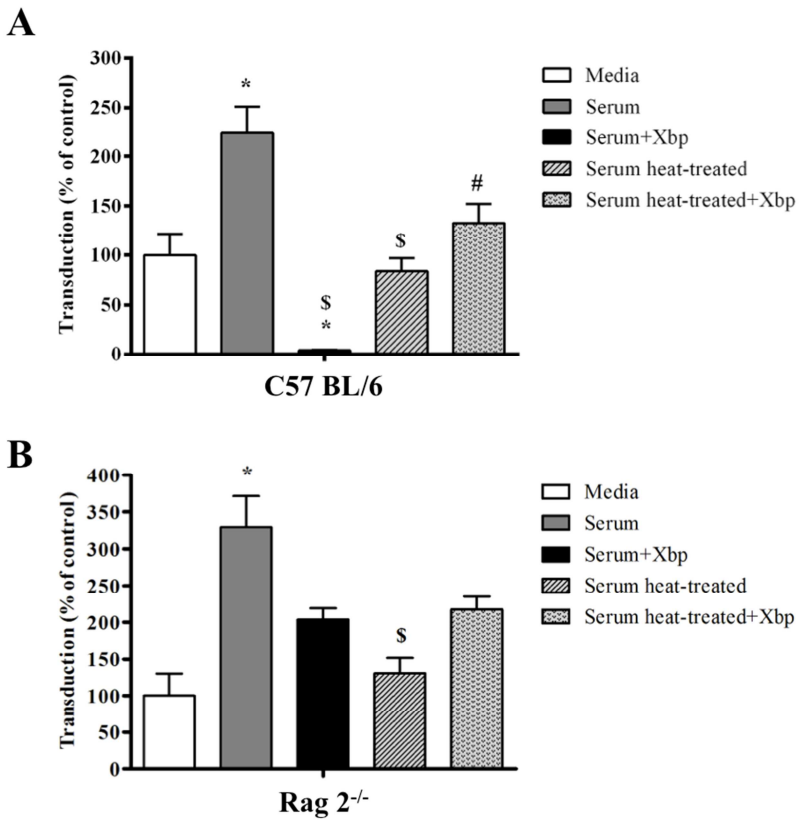

Figure 3-10. Effect of heat-treated serum on adenoviral transduction. HAdV-5 ($2x10^{10}$ vp/ml) was incubated for 30 min at 37°C with serum-free (SF) RPMI-1640 media or 90% C57 BL/6 (A) or Rag $2^{-/-}$ (B) serum in the presence or absence of X-bp (40 μg/ml). When indicated, mouse serum was pre-incubated at 56°C for 30 min before the addition of X-bp. Adenovirus suspensions were diluted 200-fold in SF media and added to A549 cells (1000 vp/cell) and incubated at 37°C for 2 h. Then, media was replaced with 2% FCS RPMI and cells incubated for further 20 h. β-galactosidase expression levels were quantified as relative light units (RLU) and normalized to total mg of protein. n = 3 biological replicates per condition with 4 technical replicates. Values are shown as a percentage of the SF media alone condition and expressed as the mean of the normalized values per experiment +/- SEM. Repeated measures ANOVA and *post hoc* Tukey's range test applied. *$p<0.05$ vs. media, \$$p<0.05$ vs. serum, #$p<0.05$ vs. serum+X-bp.

These results indicate that exposing C57BL/6 serum to high temperatures (56°C) impairs the adenovirus neutralizing properties of C57BL/6 serum in the absence of FX-binding and the transduction enhancing properties of mouse serum, suggesting a role for heat-labile factors in adenovirus neutralization and transduction.

3.3.3 HAdV-5 neutralization and role of FX, $\alpha_v\beta_{3,5}$ integrins and CAR in tropism in C57BL/6 and Rag $2^{-/-}$ mice

Next, the role of FX, CAR and $\alpha_v\beta_{3,5}$ integrins as possible receptors for HAdV-5 transduction *in vivo* was evaluated. To study receptor usage for HAdV-5 transduction *in vivo* a series of HAdV-5 mutants were used with impaired binding to FX (AdT*) (Alba et al., 2009), $\alpha_v\beta_{3,5}$ integrins (HAdV-5 RGE) (Bradshaw et al., 2012) or CAR (HAdV-5 KO1), and a mutant lacking binding to both FX and $\alpha_v\beta_{3,5}$ integrins (AdT*RGE) (Bradshaw et al., 2012) to dismiss the possibility of FX being sufficient for HAdV-5 RGE to transduce cells despite lacking $\alpha_v\beta_{3,5}$ integrin-binding. A total of $1x10^{11}$ vp of HAdV-5, AdT*, HAdV-5 RGE, AdT*RGE or HAdV-5 KO1 vectors were administered to C57BL/6 and IgM antibody-deficient Rag $2^{-/-}$ mice via intravascular delivery and accumulation of viral genomes and transduction levels were quantified in liver and spleen 48 h post-administration (Figure 3-11).

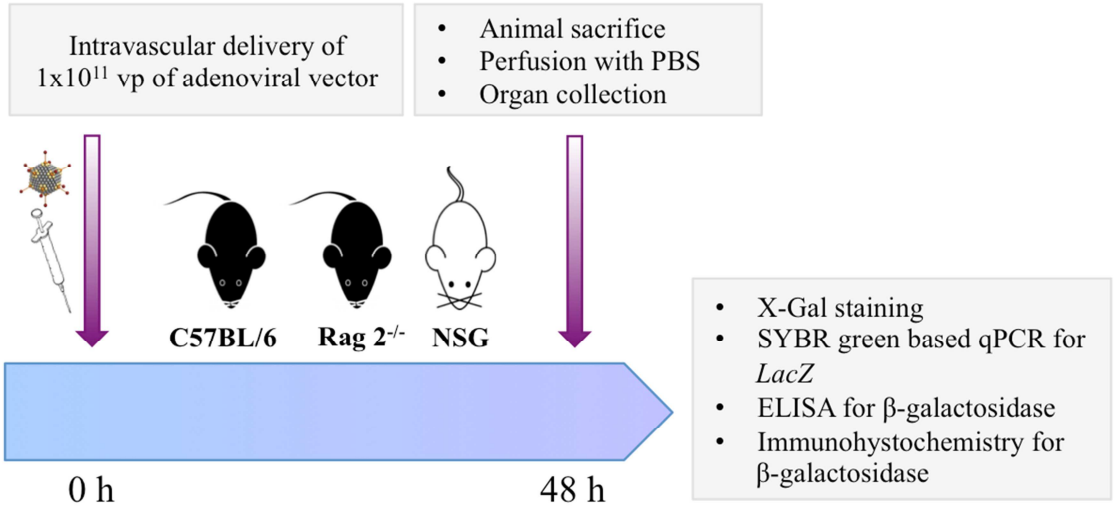

Figure 3-11. Timeline diagram of *in vivo* experiments. Mice were administered $1x10^{11}$ vp of adenoviral vector per animal via tail vein injection. Mice were sacrificed 48 h post-injections and organs were analysed for adenovirus genome content and transduction levels.

In agreement with the X-Gal staining (Figure 3-12A), quantification of viral genomes and adenoviral transduction levels in C57BL/6 mice liver revealed that AdT*-based vectors (AdT* or AdT*RGE) were at significantly lower levels (191-fold and 6774-fold for AdT* and 10.5-fold and 25-fold for AdT*RGE, respectively) than those of HAdV-5 or HAdV-5 RGE controls (Figure 3-12C-D), confirming a role for FX in protecting HAdV-5 from neutralization. Also, AdT*RGE genomes were at statistically significant higher levels (8-fold) than those of AdT* (Figure 3-12C). Levels of HAdV-5 RGE genomes and transduction in C57BL/6 liver were significantly decreased (2-fold and 12-fold,

respectively) compared to those of HAdV-5 (Figure 3-12C-D), suggesting a role for $\alpha_v\beta_{3,5}$ integrins in liver transduction. Whilst significantly lower levels of HAdV-5 KO1 transduction were also detected in the liver (4-fold) (Figure 3-12D), suggesting a role for CAR in liver transduction of C57BL/6 mice, HAdV-5 KO1 genomes were found at similar levels to those of HAdV-5 (Figure 3-12C). Analysis of C57BL/6 spleens revealed that AdT* genomes and transduction levels were significantly lower than those of HAdV-5 (6-fold and 5-fold, respectively) (Figure 3-12E-F) supporting again the presence of adenovirus neutralization of FX-binding deficient AdT* vectors. Surprisingly, despite the lack of FX-binding, AdT*RGE genome and transduction levels in C57BL/6 spleen were found comparable to those of HAdV-5 RGE (Figure 3-12E-F). Also, AdT*RGE genome and transduction levels in C57BL/6 spleen were significantly higher (8.9-fold and 6.2-fold, respectively) than those of AdT* (Figure 3-12E-F). HAdV-5 RGE and HAdV-5 KO1 genomes and transduction levels in C57BL/6 spleen were comparable to those of HAdV-5 (Figure 3-12E-F), indicating no involvement of $\alpha_v\beta_{3,5}$ integrins or CAR in spleen transduction. Similar levels of X-Gal staining were observed in spleens of C57BL/6 mice for all administered vectors (Figure 3-12B). The pattern of liver and spleen transduction following immunohistochemistry analysis for β-galactosidase was similar to that of genome and transduction levels for all vectors (Figure 3-13). Interestingly, both HAdV-5 RGE and AdT*RGE localized in the spleen marginal zone (MZ) (Figure 3-13B), the area between the red and the white pulp. Together with previous reports, these results indicate that AdT*-based vectors are neutralized by the immune system of C57BL/6 mice. The data also shows that $\alpha_v\beta_{3,5}$ integrins and CAR might be involved in liver but not spleen transduction of C57BL/6 mice, and that lack of binding to $\alpha_v\beta_{3,5}$ integrins seems to increase localization of adenoviral vectors to the spleen MZ and liver and spleen transduction in FX-binding deficient vectors.

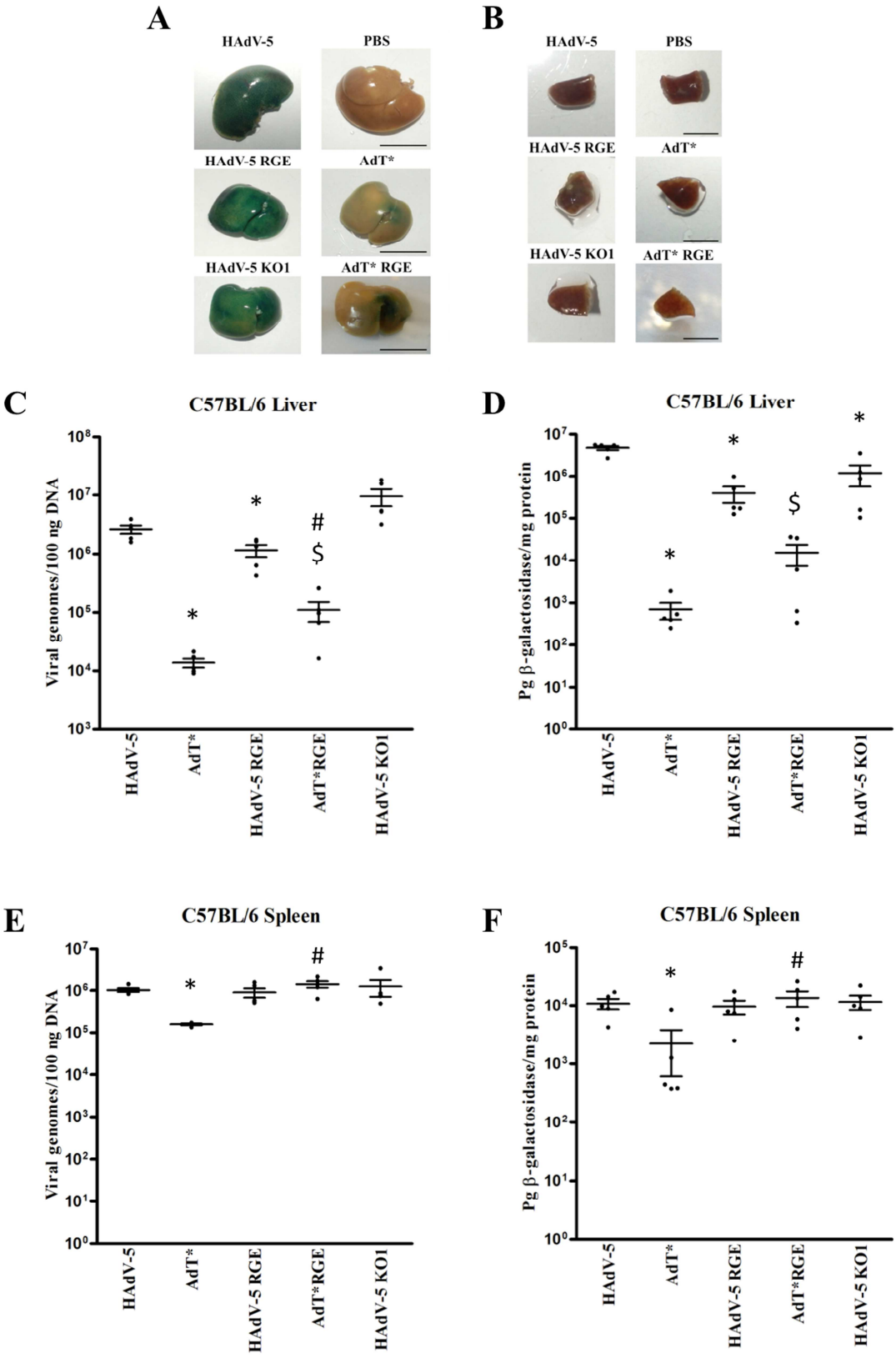

Figure 3-12. Adenoviral genomes accumulation and transduction in C57BL/6 mice. C57BL/6 mice were administered DPBS or $1x10^{11}$ vp/mouse HAdV-5, AdT*, HAdV-5 RGE, AdT*RGE or HAdV-5 KO1 (n = 5 mice/group) by intravascular delivery and sacrificed and perfused 48 h post-injection. A-B) β-galactosidase expression in C57BL/6 mice by X-Gal staining following organ fixation in 2% paraformaldehyde. Representative images of liver (A) and spleen (B) are shown. Scale bar 1 cm (A) or 0.25 cm (B). C-F) Viral genome content was quantified by SYBR green based qPCR analysis in liver (C) and spleen (E). β-galactosidase expression was quantified by ELISA in liver (D) and spleen (F) and normalised to total mg of protein. Values are expressed as the mean +/- SEM. Unpaired Student's T-test applied. *p<0.05 vs. HAdV-5, #p<0.05 vs. AdT*, $p<0.05 vs. HAdV-5 RGE.

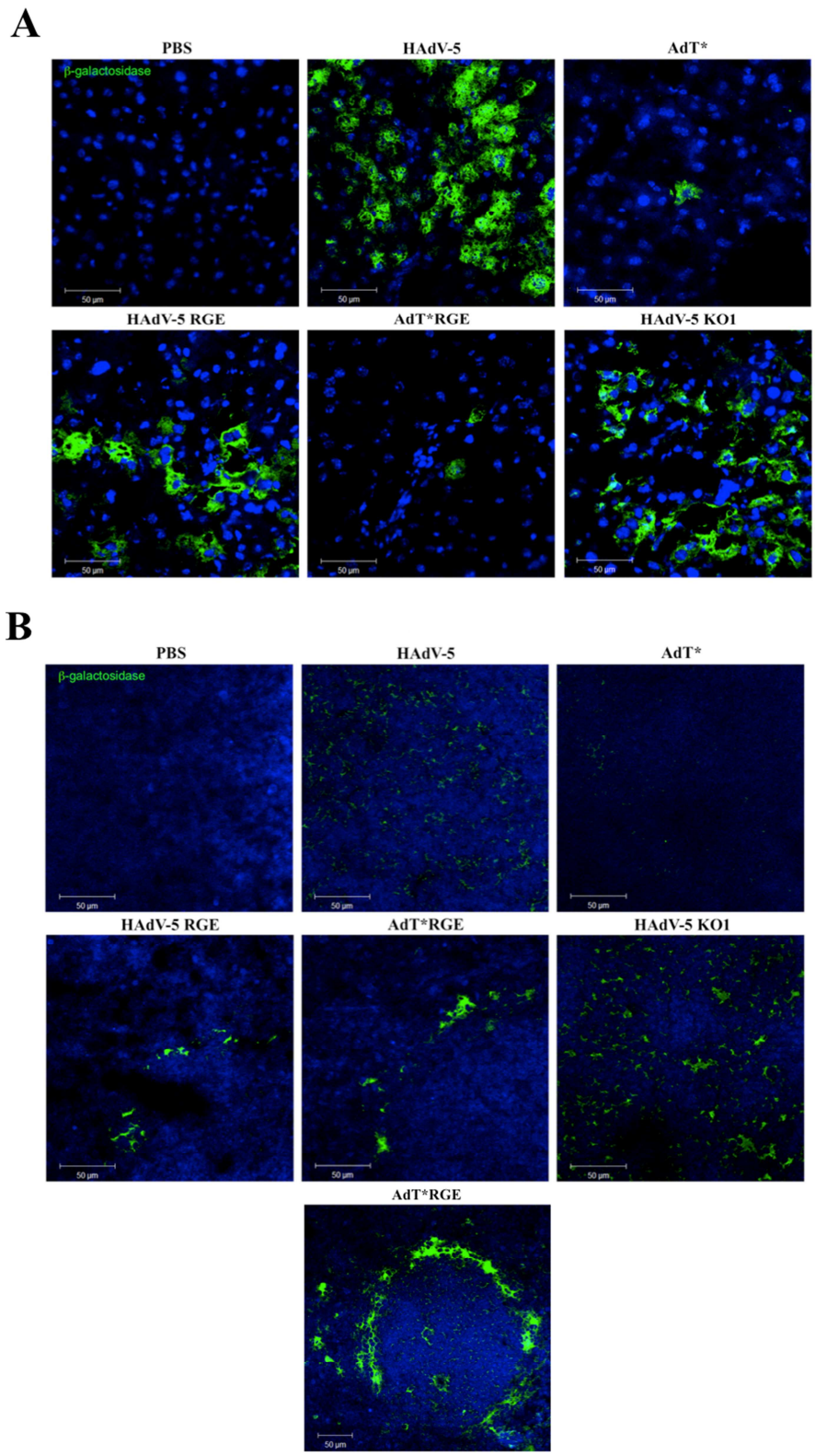

Figure 3-13. Immunohistochemistry analysis of β-galactosidase in C57BL/6 mice. Representative merged images of 6 µm frozen liver (A) and spleen (B) sections from C57BL/6 mice 48 h following intravascular administration of DPBS or $1x10^{11}$ vp/mouse HAdV-5, AdT*, HAdV-5 RGE, AdT*RGE or HAdV-5 KO1 (n = 5 mice/group). Rabbit anti-β-galactosidase primary antibody and Alexa Fluor 488-conjugated goat anti-rabbit IgG secondary antibody (green) were used. Nuclei were counterstained with DAPI (blue). n = 3 mice analysed per group with 1 technical replicate. Magnification 40x or 25x for the lower AdT*RGE image in (B). Scale bars 50 µm.

Next, liver and spleen transduction of immunocompromised Rag $2^{-/-}$ mice was evaluated. Accumulation of genomes in Rag $2^{-/-}$ liver was lower for AdT* compared to HAdV-5 (6-fold) (Figure 3-14C) but it did not reach statistical significance. AdT* liver transduction levels were significantly lower (23-fold) than those of HAdV-5 (Figure 3-14D), in agreement with immunohistochemistry analysis on liver sections (Figure 3-15A). Moreover, AdT*RGE genome and transduction levels in Rag $2^{-/-}$ liver were significantly lower (2.3-fold and 2.6-fold, respectively) than those of HAdV-5 RGE (Figure 3-14C-D), as observed in immunohistochemistry analysis on liver sections (Figure 3-15A). Since Rag $2^{-/-}$ mice are unable to neutralize adenovirus *in vitro* (section 3.3.2), these results suggest a role for FX in liver transduction of these mice. HAdV-5 RGE and HAdV-5 KO1 showed levels of accumulated genomes and liver transduction similar to those of HAdV-5 (Figure 3-14C-D), suggesting $\alpha_v\beta_{3,5}$ integrins and CAR are not involved in liver tropism in Rag $2^{-/-}$ mice. No differences in β-galactosidase activity were detected in livers subjected to X-Gal staining (Figure 3-14A). Interestingly, immunohistochemistry analysis on liver sections revealed lower levels of β-galactosidase detection in Rag $2^{-/-}$ mice administered HAdV-5 RGE and HAdV-5 KO1 than those of HAdV-5 (Figure 3-15A). Regarding the spleen, significantly higher levels of AdT*RGE transduction were detected in comparison to those of AdT* or HAdV-5 RGE (293-fold and 82-fold, respectively) (Figure 3-14F), in agreement with X-Gal staining (Figure 3-14B) and immunohistochemistry analysis on spleen sections (Figure 3-15B). Together, these data suggest that in contrast to $\alpha_v\beta_{3,5}$ integrins and CAR, FX might be involved in liver transduction of immunocompromised Rag $2^{-/-}$ mice, and that lack of $\alpha_v\beta_{3,5}$ integrins binding on a FX-binding deficient vector might increase liver and spleen transduction.

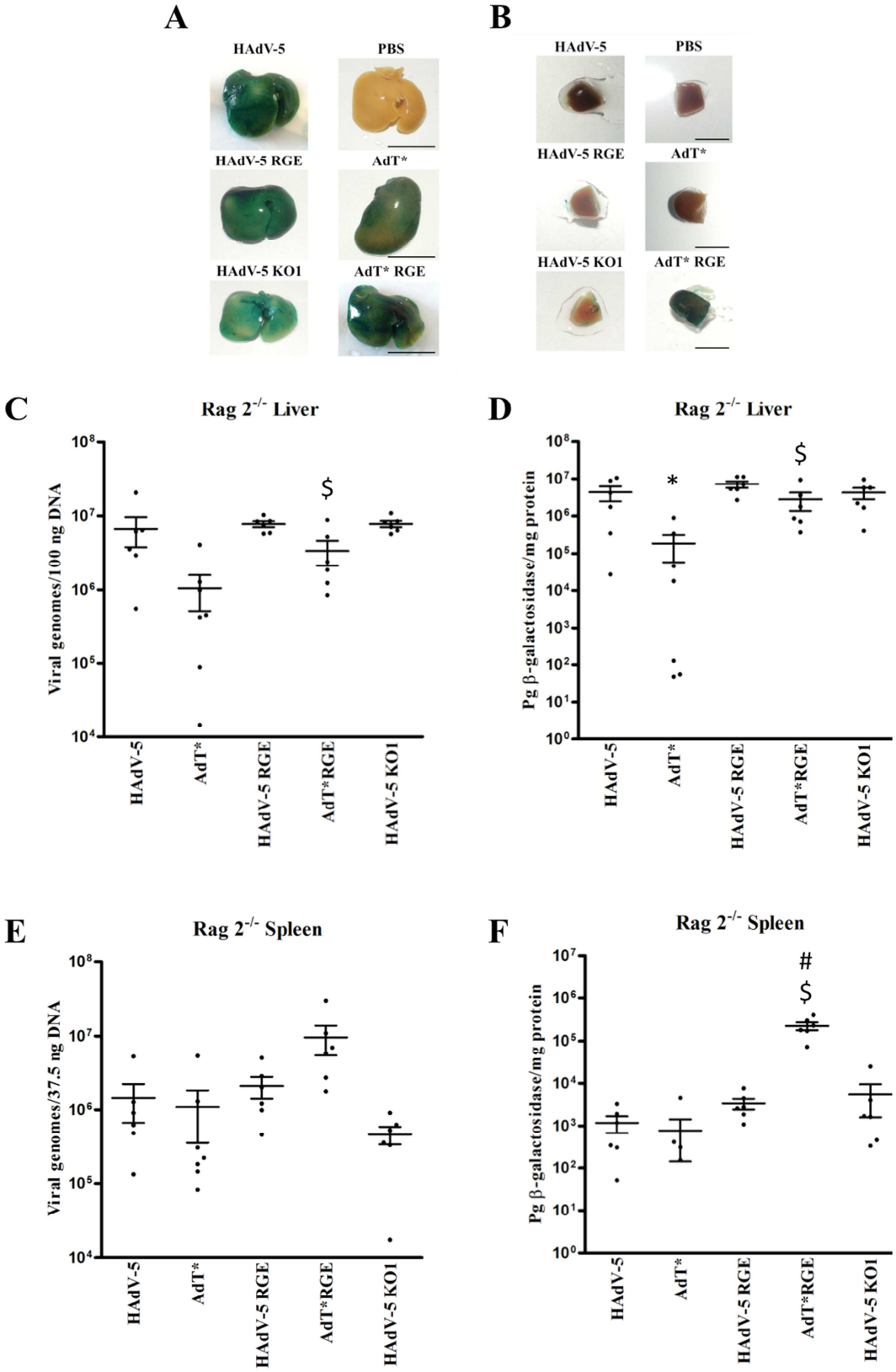

Figure 3-14. Adenoviral genomes accumulation and transduction in Rag 2$^{-/-}$ mice. Rag 2$^{-/-}$ mice were administered DPBS (n = 6) or 1x10^{11} vp/mouse HAdV-5 (n = 6), AdT* (n = 7), HAdV-5 RGE (n = 6), AdT*RGE (n = 6) or HAdV-5 KO1 (n = 6) by intravascular delivery and sacrificed and perfused 48 h post-injection. A-B) β-galactosidase expression in Rag 2$^{-/-}$ mice by X-Gal staining following organ fixation in 2% paraformaldehyde. Representative images of liver (A) and spleen (B) are shown. Scale bar 1 cm (A) or 0.25 cm (B). C-F) Viral genome content was quantified by SYBR green based qPCR analysis in liver (C) and spleen (E). β-galactosidase expression was quantified by ELISA in liver (D) and spleen (F) and normalised to total mg of protein. Values are expressed as the mean +/- SEM. Unpaired Student's T-test applied. *p<0.05

vs. HAdV-5, #p<0.05 vs. AdT*, $p<0.05 vs. HAdV-5 RGE. Values ≤ 1 have been omitted from the graphical representation but considered for statistical analysis.

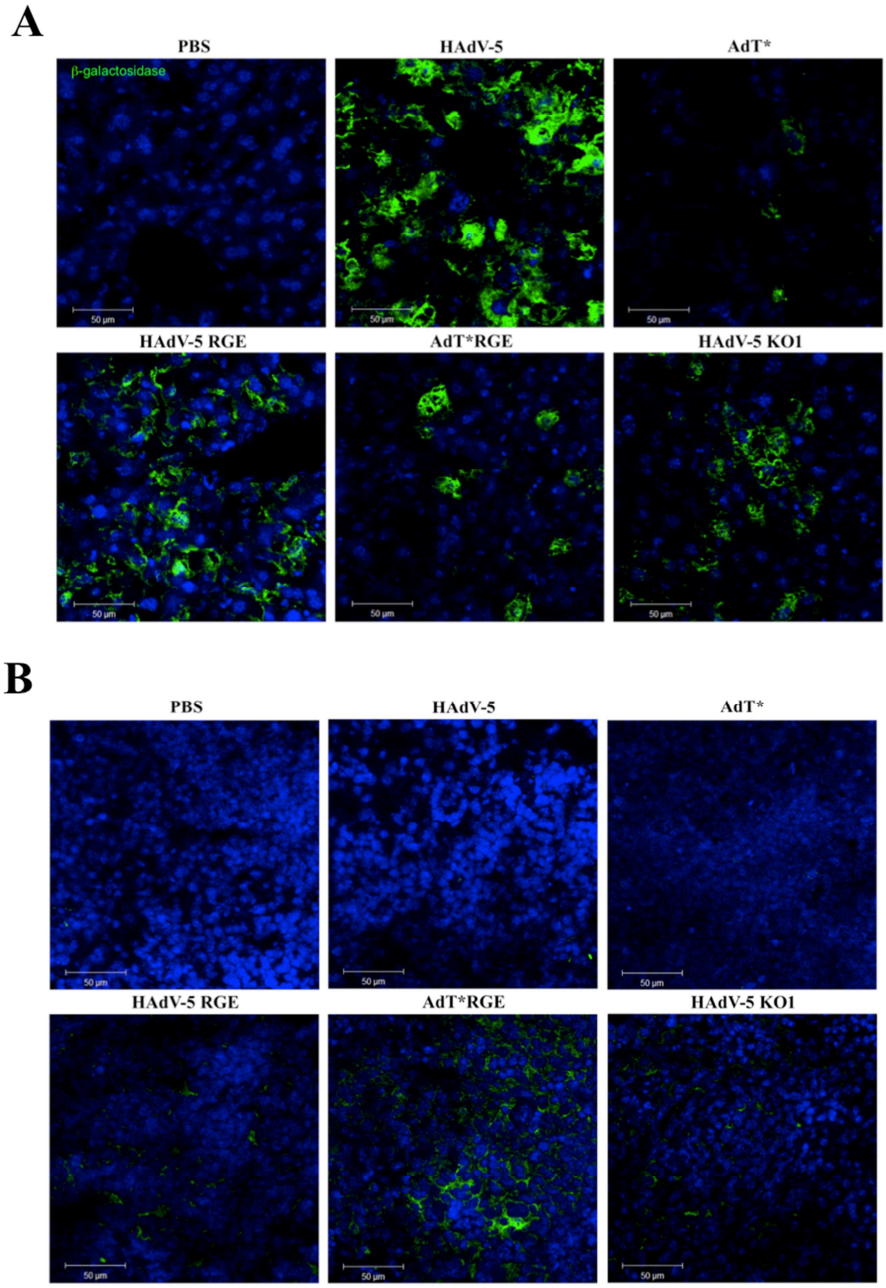

Figure 3-15. Immunohistochemistry analysis of β-galactosidase in Rag 2$^{-/-}$ mice. Representative merged images of 6 µm frozen liver (A) and spleen (B) sections from Rag 2$^{-/-}$ mice 48 h following intravascular administration of DPBS (n = 6) or 1x10^{11} vp/mouse HAdV-5 (n = 6), AdT* (n = 7), HAdV-5 RGE (n = 6), AdT*RGE (n = 6) or HAdV-5 KO1 (n = 6). Rabbit anti-β-galactosidase primary antibody and Alexa Fluor 488-conjugated goat anti-rabbit IgG secondary antibody (green) were used. Nuclei were counterstained with DAPI (blue). n = 3 mice analysed per group with 1 technical replicate. Magnification 40x. Scale bars 50 µm.

3.3.4 Role of FX in tropism in NSG mice

To confirm a role of FX in liver transduction in immunocompromised mice, HAdV-5 and AdT* vectors were administered to NSG mice as before (Figure 3-11) and Rag 2$^{-/-}$ mice were used as a control.

Quantification of viral genomes and adenoviral transduction in Rag $2^{-/-}$ mice liver revealed significantly lower levels of AdT* than those of HAdV-5 (4-fold and 7-fold, respectively) (Figure 3-16A-B) in agreement with immunohistochemistry analysis of β-galactosidase on liver sections (Figure 3-17B), and thus confirming previous results (Figure 3-14C-D and Figure 3-15A). X-Gal staining in Rag $2^{-/-}$ mice livers showed no visual differences between vectors (Figure 3-17A). Slightly higher levels of AdT* genomes and transduction were found in Rag $2^{-/-}$ spleen (4-fold and 6-fold, respectively) (Figure 3-16C-D), consistent with X-Gal staining of spleen (Figure 3-17A) and immunohistochemistry analysis of β-galactosidase on spleen sections (Figure 3-17B), but they did not reach statistical significance.

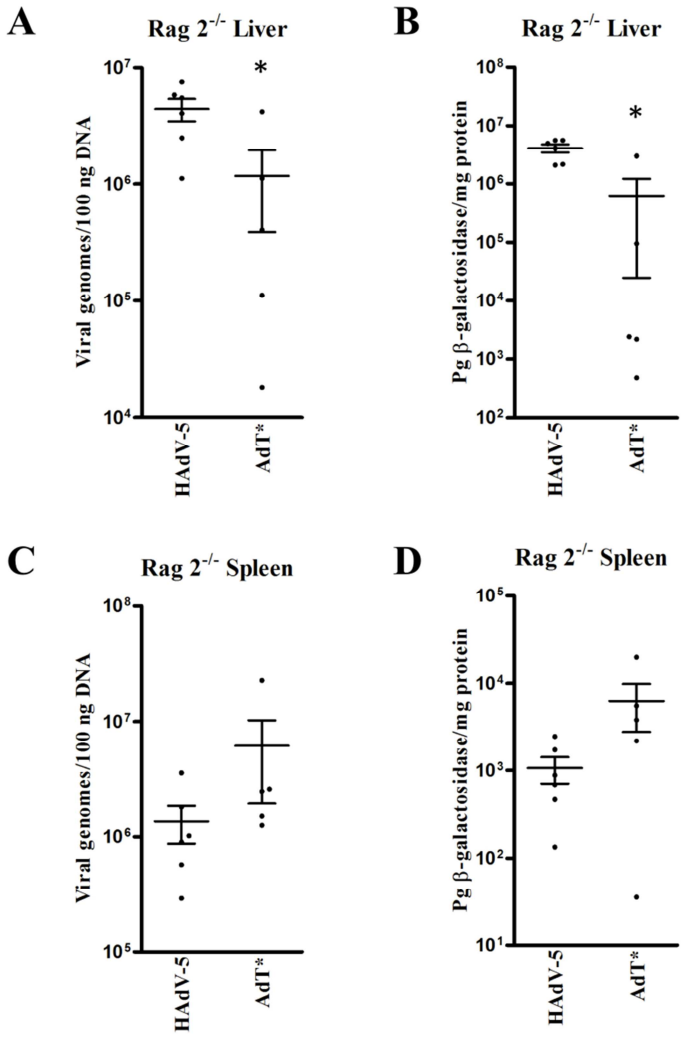

Figure 3-16. Adenoviral transduction and genomes accumulation in Rag $2^{-/-}$ mice. Rag $2^{-/-}$ mice were administered $1x10^{11}$ vp/mouse HAdV-5 (n = 6) or AdT* (n = 5) by intravascular delivery and sacrificed and perfused 48 h post-injection. Viral genome content was quantified by SYBR green based qPCR analysis in liver (A) and spleen (C). β-galactosidase expression was quantified by ELISA in liver (B) and spleen (D) and normalised to total mg of protein. Values are expressed as the mean +/- SEM. Unpaired Student's T-test applied. *$p<0.05$ vs. HAdV-5.

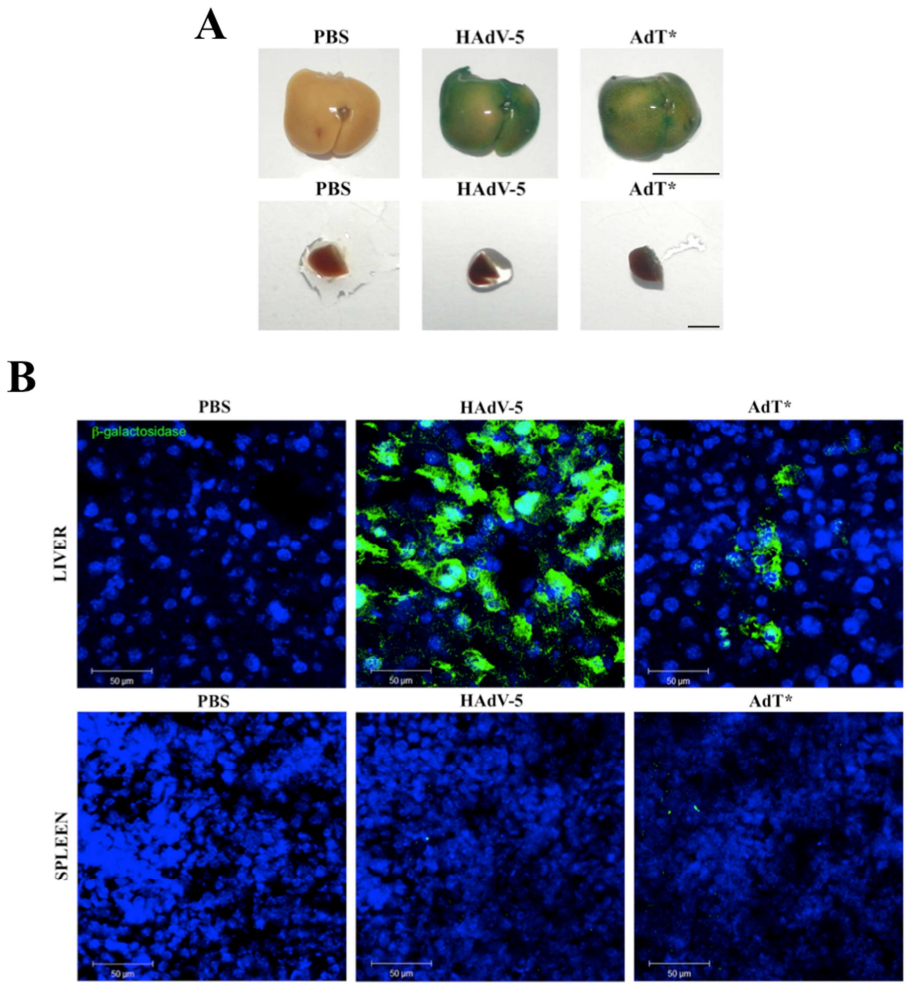

Figure 3-17. β-galactosidase expression in Rag 2$^{-/-}$ mice liver and spleen. Rag 2$^{-/-}$ mice were administered DPBS (n = 3) or 1x10^{11} vp/mouse HAdV-5 (n = 6) or AdT* (n = 5) by intravascular delivery and sacrificed and perfused 48 h post-injection. A) Representative images of X-Gal staining of liver (top panel) and spleen (bottom panel) fixed in 2% paraformaldehyde are shown. Scale bar 1 cm (upper panel) or 0.25 cm (lower panel). B) Immunohistochemistry analysis of β-galactosidase on 6 µm frozen liver and spleen sections from Rag 2$^{-/-}$ mice. Rabbit anti-β-galactosidase primary antibody and Alexa Fluor 488-conjugated goat anti-rabbit IgG secondary antibody (green) were used. Nuclei were counterstained with DAPI (blue). n = 3 mice analysed per group with 1 technical replicate. Representative merged images are shown. Magnification 40x. Scale bars 50 µm.

In NSG mice, AdT* genome and transduction levels in liver were similar to those of HAdV-5 (Figure 3-18A-B), suggesting FX is not involved in liver tropism in NSG mice, which is in sharp contrast to Rag 2$^{-/-}$ mice (Figure 3-14C-D and Figure 3-16A-B). Also, no differences were found in X-Gal staining of liver or immunohistochemistry analysis for β-galactosidase in liver sections (Figure 3-19). Quantification of genomes and transduction in spleen showed statistically significant higher levels of AdT* than those of HAdV-5 (5-fold and 13-fold, respectively) (Figure 3-18C-D), in agreement with X-Gal staining of spleen (Figure 3-19A), suggesting that lack of binding to FX results in a change in HAdV-5 biodistribution towards the spleen in these mice. No differences were found in immunohistochemistry analysis for β-galactosidase in spleen sections (Figure 3-19B).

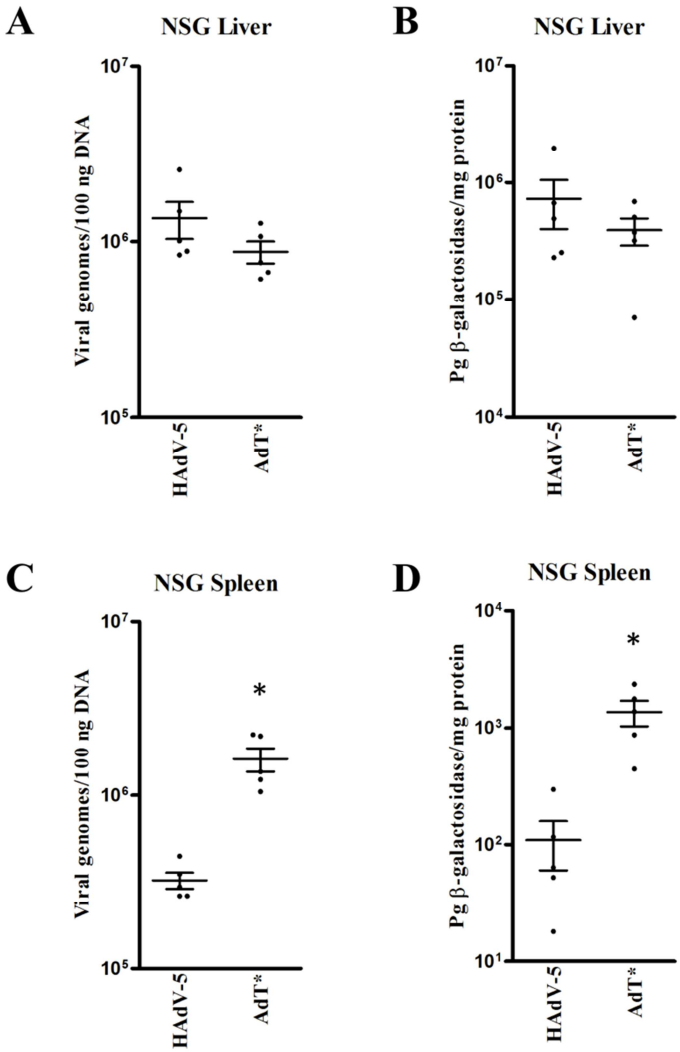

Figure 3-18. Adenoviral genomes accumulation and transduction in NSG mice. NSG mice were administered $1x10^{11}$ vp/mouse HAdV-5 (n = 5) or AdT* (n = 5) by intravascular delivery and sacrificed and perfused 48 h post-injection. Viral genome content was quantified by SYBR green based qPCR analysis in liver (A) and spleen (C). β-galactosidase expression was quantified by ELISA in liver (B) and spleen (D) and normalised to total mg of protein. Values are expressed as the mean +/- SEM. Unpaired Student's T-test applied. *$p<0.05$ vs. HAdV-5.

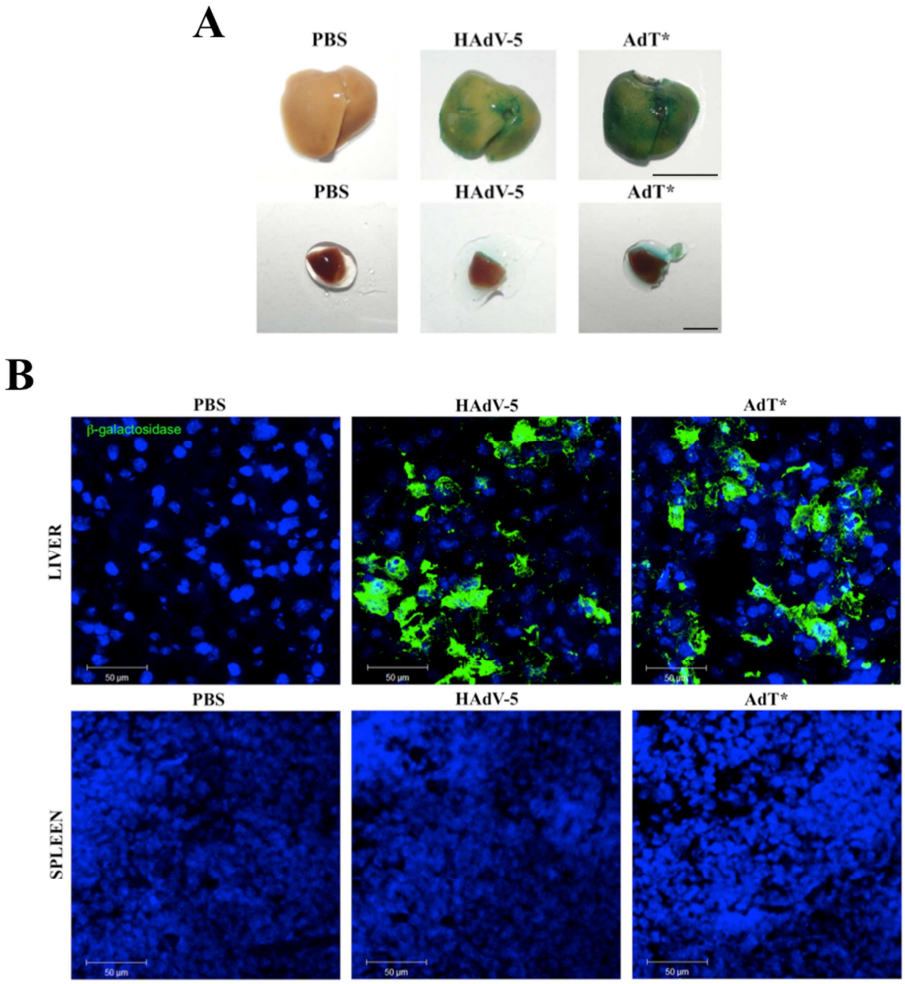

Figure 3-19. β-galactosidase expression in NSG mice liver and spleen. NSG mice were administered DPBS (n = 3) or $1x10^{11}$ vp/mouse HAdV-5 (n = 5) or AdT* (n = 5) by intravascular delivery and sacrificed and perfused 48 h post-injection. A) Representative images of X-Gal staining of liver (top panel) and spleen (bottom panel) fixed in 2% paraformaldehyde are shown. Scale bar 1 cm (upper panel) or 0.25 cm (lower panel). B) Immunohistochemistry analysis of β-galactosidase on 6 μm frozen liver and spleen sections from NSG mice. Rabbit anti-β-galactosidase primary antibody and Alexa Fluor 488-conjugated goat anti-rabbit IgG secondary antibody (green) were used. Nuclei were counterstained with DAPI (blue). n = 3 mice analysed per group with 1 technical replicate. Representative merged images are shown. Magnification 40x. Scale bars 50 μm.

3.3.5 Role of $\alpha_v\beta_{3,5}$ integrins in tropism in NSG mice

The lack of $\alpha_v\beta_{3,5}$ integrins-binding in a FX-binding deficient vector (AdT*RGE) resulted in an increase in liver and spleen transduction in both immunocompetent C57BL/6 and immunocompromised Rag $2^{-/-}$ mice (see section 3.3.3). Whether this effect was also present in other immunocompromised mouse strains and whether the increased transduction would result in an immune response against the adenoviral vector was investigated. HAdV-5, AdT* and AdT*RGE vectors were administered to NSG mice as before, Rag $2^{-/-}$ mice were used as a control, and cytokine production was evaluated from mouse serum 6 h post adenovirus injections (Figure 3-20). Of note, one Rag $2^{-/-}$ mouse administered AdT*RGE was excluded from data analysis due to technical reasons (n = 2).

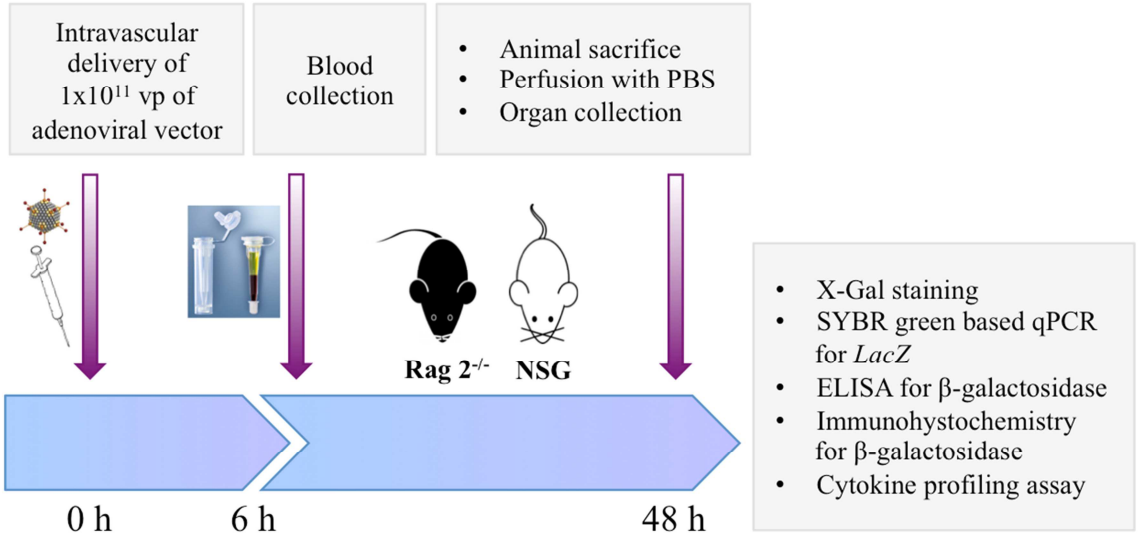

Figure 3-20. Timeline diagram of *in vivo* experiment. Mice were administered $1x10^{11}$ vp of adenoviral vector per animal via tail vein injection and, after 6 h, blood was collected for cytokine profiling assays. Mice were sacrificed 48 h post-injections and organs were analysed for adenovirus genome content and transduction levels.

The analysis of livers and spleens of Rag $2^{-/-}$ mice administered HAdV-5, AdT* or AdT*RGE (Figure 3-21 and Figure 3-22) showed results consistent with those described previously (section 3.3.3). AdT* genome and transduction levels in liver were significantly lower than those of HAdV-5 (4-fold and 97-fold, respectively) (Figure 3-21A-B). Despite the low number of animals administered AdT*RGE (n = 2) did not allow statistical significance assessment, AdT*RGE genome and transduction levels in liver and spleen were found higher than those of AdT* (Figure 3-21 and Figure 3-22), as observed previously (Figure 3-14 and Figure 3-15).

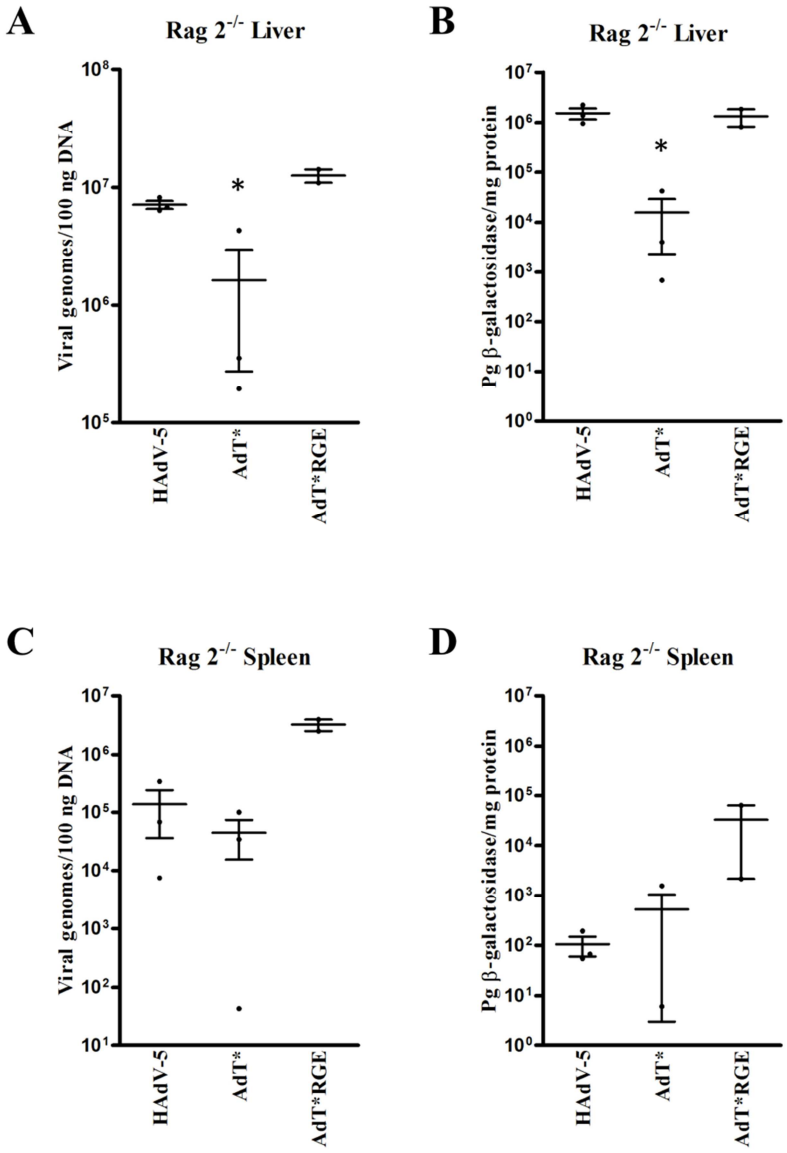

Figure 3-21. Adenoviral genomes accumulation and transduction in Rag 2$^{-/-}$ mice. Rag 2$^{-/-}$ mice were administered 1x10^{11} vp/mouse HAdV-5 (n = 3), AdT* (n = 3) or AdT*RGE (n = 2) by intravascular delivery and sacrificed and perfused 48 h post-injection. Viral genome content was quantified by SYBR green based qPCR analysis in liver (A) and spleen (C). β-galactosidase expression was quantified by ELISA in liver (B) and spleen (D) and normalised to total mg of protein. Values are expressed as the mean +/- SEM. Unpaired Student's T-test applied. *$p<0.05$ vs. HAdV-5. Values ≤ 1 have been omitted from the graphical representation but considered for statistical analysis.

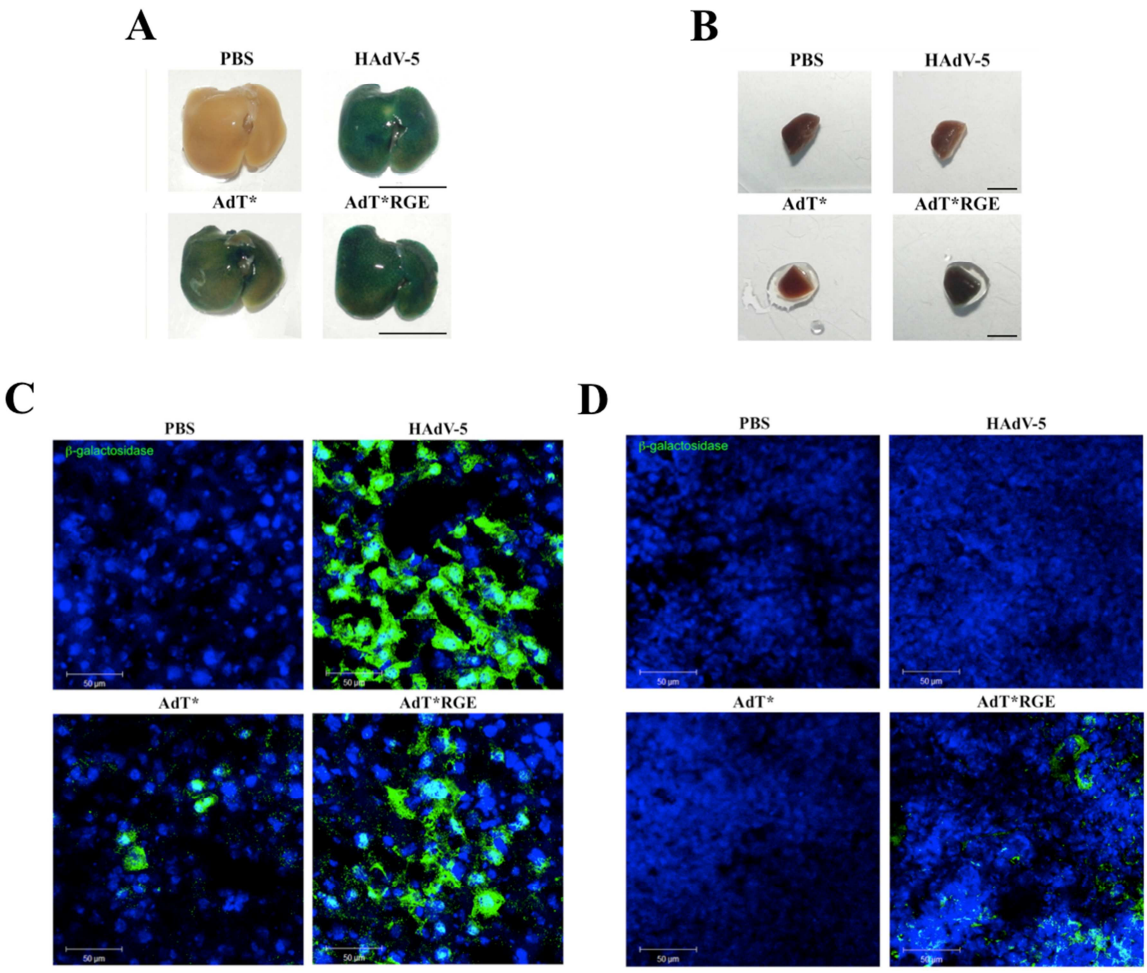

Figure 3-22. β-galactosidase expression in Rag 2$^{-/-}$ mice liver and spleen. Rag 2$^{-/-}$ mice were administered DPBS (n = 3) or 1x10^{11} vp/mouse HAdV-5 (n = 3), AdT* (n = 3) or AdT*RGE (n = 2) by intravascular delivery and sacrificed and perfused 48 h post-injection. A) Representative images of X-Gal staining of liver (A) and spleen (B) fixed in 2% paraformaldehyde are shown. Scale bar 1 cm (A) or 0.25 cm (B). C-D) Immunohistochemistry analysis of β-galactosidase on 6 μm frozen liver (C) and spleen (D) sections from Rag 2$^{-/-}$ mice. Rabbit anti-β-galactosidase primary antibody and Alexa Fluor 488-conjugated goat anti-rabbit IgG secondary antibody (green) were used. Nuclei were counterstained with DAPI (blue). n = 3 mice analysed per group with 1 technical replicate, with the exception of AdT*RGE samples (n = 2). Representative merged images are shown. Magnification 40x. Scale bars 50 μm.

In the NSG mice, genome and transduction levels (Figure 3-23A-B), X-Gal staining (Figure 3-24A) and immunohistochemistry analysis for β-galactosidase in liver (Figure 3-24C) showed no differences between the administered vectors, as observed previously (Figure 3-18A-B and Figure 3-19), and thus confirming FX is not involved in liver tropism in NSG mice and suggesting $\alpha_v\beta_{3,5}$ integrins do not serve as receptors for liver transduction in the absence of FX-binding. In the spleen, AdT* exhibited slightly higher levels of transduction than those of HAdV-5 (18-fold) (Figure 3-23D) as observed previously (Figure 3-18D). Also, higher genome and transduction levels (122–fold and 14-fold, respectively) (Figure 3-23C-D), X-Gal staining (Figure 3-24B) and β-galactosidase detection in immunohistochemistry analysis (Figure 3-24D) were found for AdT*RGE in comparison to AdT* in spleen. These data suggest that lack of binding to $\alpha_v\beta_{3,5}$ integrins in

a non-FX-binding vector has an enhancing effect on NSG mice spleen transduction, as observed in C57BL/6 and Rag $2^{-/-}$ mice (section 3.3.3).

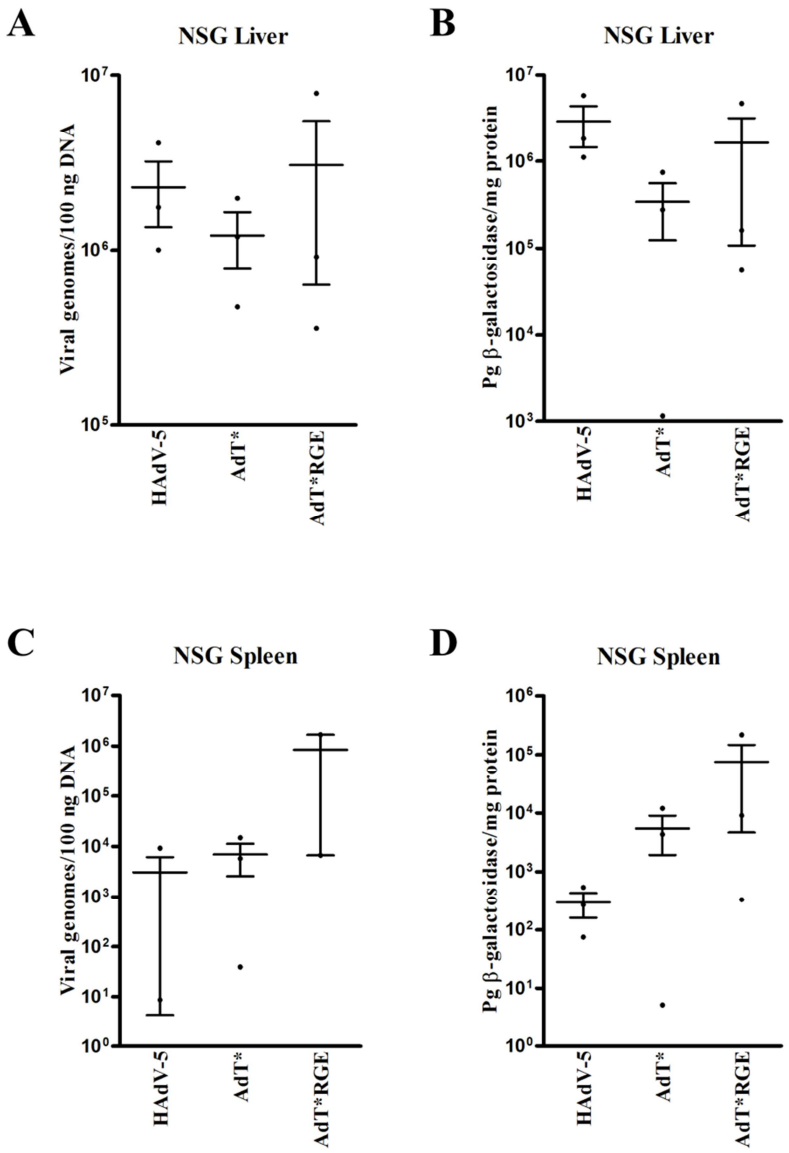

Figure 3-23. Adenoviral genomes accumulation and transduction in NSG mice. NSG mice were administered $1x10^{11}$ vp/mouse HAdV-5, AdT* or AdT*RGE (n = 3 mice/group) by intravascular delivery and sacrificed and perfused 48 h post-injection. Viral genome content was quantified by SYBR green based qPCR analysis in liver (A) and spleen (C). β-galactosidase expression was quantified by ELISA in liver (B) and spleen (D) and normalised to total mg of protein. Values are expressed as the mean +/- SEM. Unpaired Student's T-test applied. Values ≤ 1 have been omitted from the graphical representation but considered for statistical analysis.

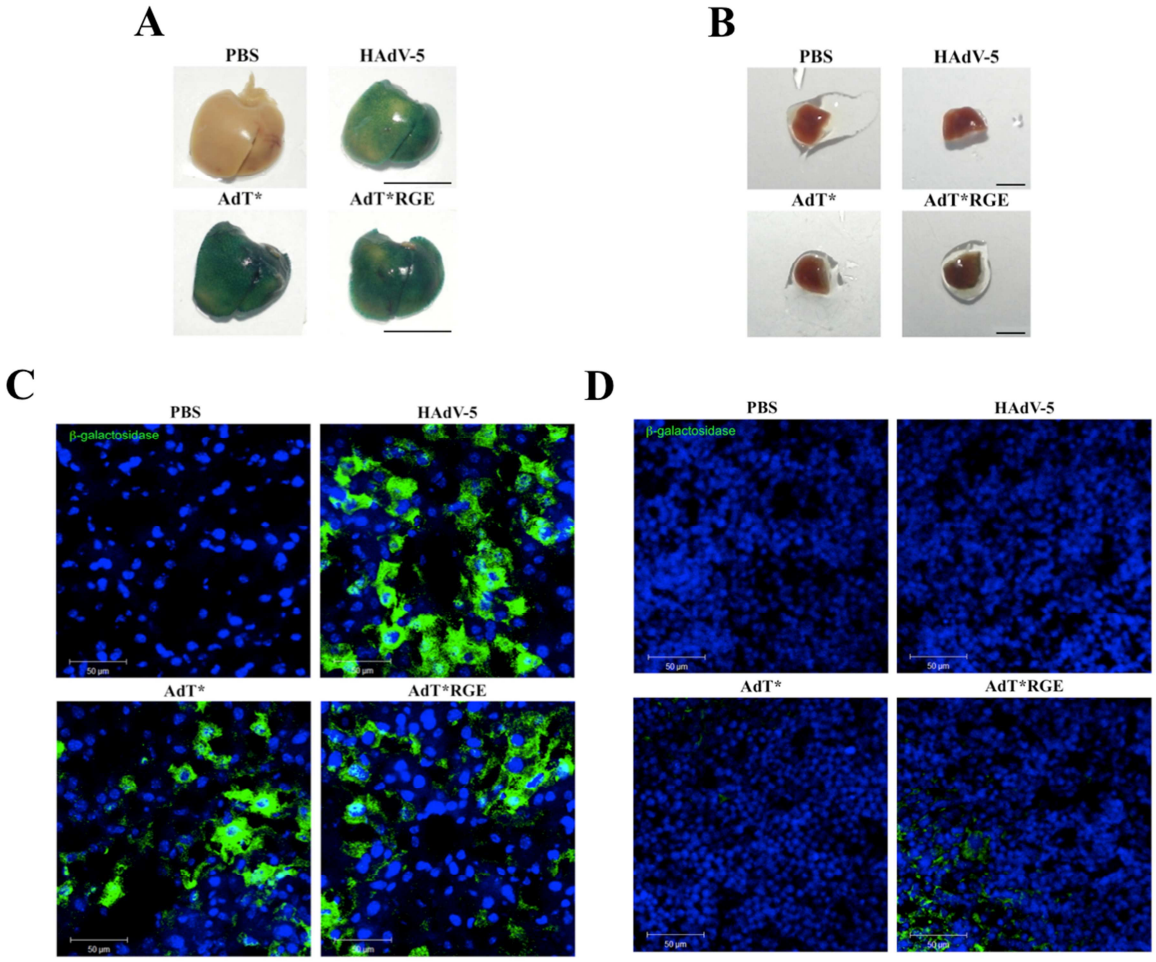

Figure 3-24. β-galactosidase expression in NSG mice liver and spleen. NSG mice were administered DPBS or $1x10^{11}$ vp/mouse HAdV-5, AdT* or AdT*RGE (n = 3 mice/group) by intravascular delivery and sacrificed and perfused 48 h post-injection. A) Representative images of X-Gal staining of liver (A) and spleen (B) fixed in 2% paraformaldehyde are shown. Scale bar 1 cm (A) or 0.25 cm (B). C-D) Immunohistochemistry analysis of β-galactosidase on 6 µm frozen liver (C) and spleen (D) sections from NSG mice. Rabbit anti-β-galactosidase primary antibody and Alexa Fluor 488-conjugated goat anti-rabbit IgG secondary antibody (green) were used. Nuclei were counterstained with DAPI (blue). n = 3 mice analysed per group with 1 technical replicate. Representative merged images are shown. Magnification 40x. Scale bars 50 µm.

3.3.5.1 Cytokine profiling of FX and $\alpha_v\beta_{3,5}$ integrin-binding deficient HAdV-5 vectors in Rag $2^{-/-}$ and NSG mice

To assess the immune response to HAdV-5, AdT* and AdT*RGE vectors in Rag $2^{-/-}$ and NSG mice, cytokine production was evaluated from blood 6 h post administration of vectors using a Mouse Cytokine 20-Plex Panel for Luminex® Platform which includes FGF-basic, GM-CSF, IFN-γ, IL-1α, IL-1β, IL-2, IL-4, IL-5, IL-6, IL-10, IL-12 (p40/p70), IL-13, IL-17, CXCL10 (IP-10), KC, MCP-1, MIG, MIP-1α, TNF-α and VEGF.

Of the analysed cytokines, only NSG mice administered AdT*RGE showed statistically significant lower levels of IL-4 in comparison to those administered AdT* (Figure 3-25B). However, the values detected for this cytokine were negligible for all the animals and

AdT*RGE showed lower levels than control NSG mice administered DPBS (Figure 3-25B).

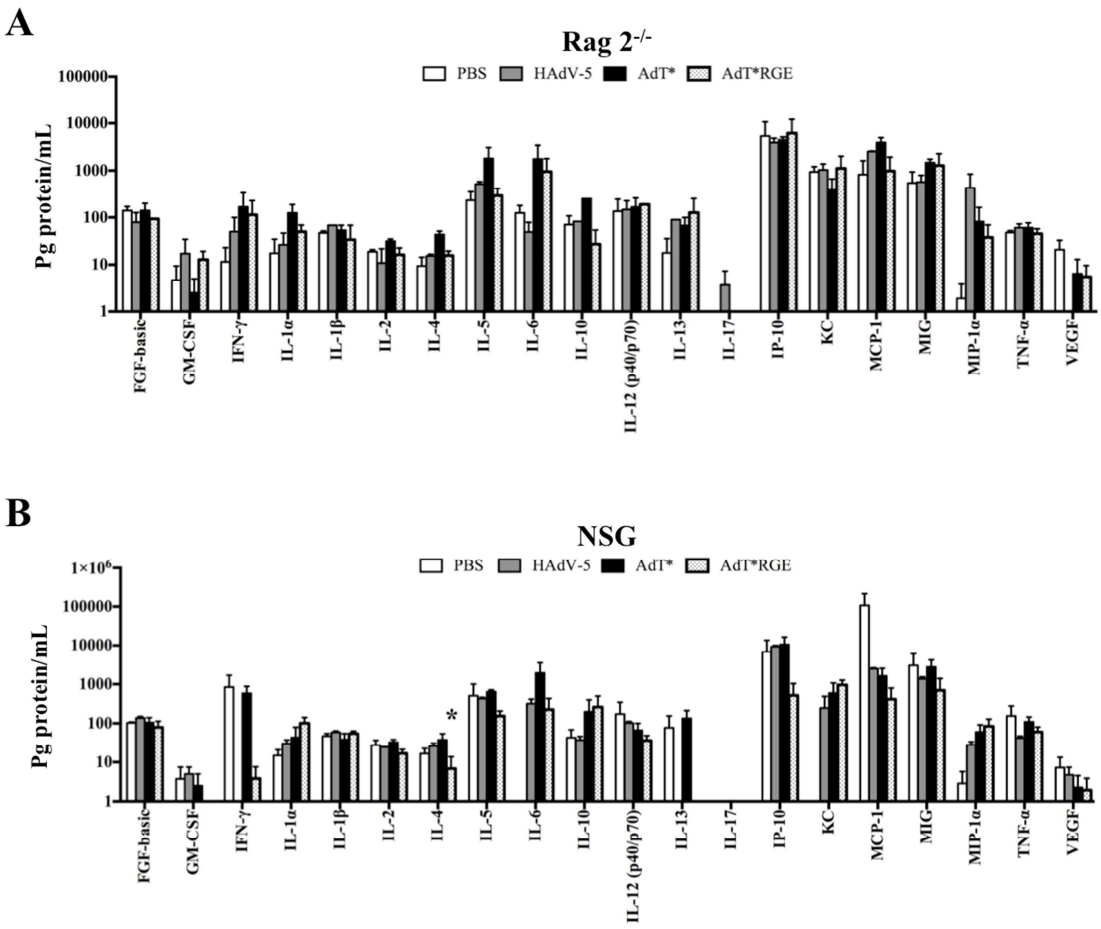

Figure 3-25. Cytokine profiling of Rag $2^{-/-}$ and NSG mice serum after adenoviral vector administration. Cytokine concentrations detected in Rag $2^{-/-}$ (A) and NSG (B) serum 6 h following intravascular administration of DPBS (n = 3) or $1x10^{11}$ vp/mouse HAdV-5 (n = 3), AdT* (n = 3) or AdT*RGE (n = 2) (A) or DPBS or $1x10^{11}$ vp/mouse HAdV-5, AdT* or AdT*RGE (n = 3 mice/group) (B). Values are shown as the mean of values (pg cytokine/ml) +/- SEM. n = 2-3 mice analysed per group with one measurement per sample with a readout of n = 1-3 (Rag $2^{-/-}$ serum samples) or n = 2-3 (NSG serum samples). One-way ANOVA and *post hoc* Tukey's range test applied. *$p<0.05$ vs. AdT*. This assay was performed by Dr. Julio Alonso Padilla (University of Glasgow, UK) with the assistance of Dr. Ashley Miller (University of Glasgow, UK), who helped in data analysis and interpretation of results.

3.3.6 Identification of FX-independent pathways of HAdV-5 transduction in the presence of mouse serum *in vitro*

Experiments *in vivo* indicate that FX-independent pathways for transduction of immunocompromised NSG mice liver are present (see section 3.3.4). Moreover, transduction experiments *in vitro* suggest the existence of FX-independent mechanisms driving transduction after exposure of HAdV-5 to immunocompromised Rag $2^{-/-}$ or NSG serum (see section 3.3.2). Here, alternative FX-independent pathways for HAdV-5 transduction *in vitro* that might be relevant *in vivo* were investigated.

3.3.6.1 Role of CAR in FX-independent HAdV-5 transduction in the presence of mouse serum *in vitro*

To assess the role of CAR in mouse serum-enhanced HAdV-5 transduction, HAdV-5 transduction of $CAR^{negative}$ CHO-K1 and CHO cells stably expressing hCAR (CHO-CAR cells) (Bergelson et al., 1997) was assessed in the presence of immunocompromised Rag $2^{-/-}$ serum with or without X-bp.

First, flow cytometry was performed on CHO-K1 and CHO-CAR cells to assess CAR-expression. 91.3±3.8% of CHO-CAR cells expressed CAR in contrast to only 0.6±0.05% of CHO-K1 cells (Figure 3-26A). Transduction of CHO-K1 cells with HAdV-5 or AdT* in SF media alone was negligible (Figure 3-26B) as previously reported (Di et al., 2012). Rag $2^{-/-}$ serum did not enhance HAdV-5 or AdT* transduction of CHO-K1 cells (Figure 3-26B), suggesting that the cell receptor(s) involved in the enhancement of transduction produced by serum is not present in this cell line. These results are in agreement with previous reports showing no enhancement of HAdV-5 transduction of CHO cells in the presence of mouse FX (mFX), which is consistent with the presence of low levels of HSPG on these cells (Zaiss et al., 2011). Conversely, CHO-CAR cells exhibited higher levels of basal HAdV-5 transduction than those of CHO-K1 cells in the presence of SF media alone, Rag $2^{-/-}$ serum significantly enhanced HAdV-5 transduction by 3-fold and pre-incubation of serum with X-bp had no effect on the enhanced transduction (Figure 3-26C). Also, Rag $2^{-/-}$ serum significantly enhanced AdT* transduction by 2.7-fold (Figure 3-26C) despite the lack of FX-binding. These data suggests that, in similarity to A549 cells, a FX-independent pathway for HAdV-5 transduction is present in CHO cells expressing hCAR, suggesting a possible role for CAR in this setting.

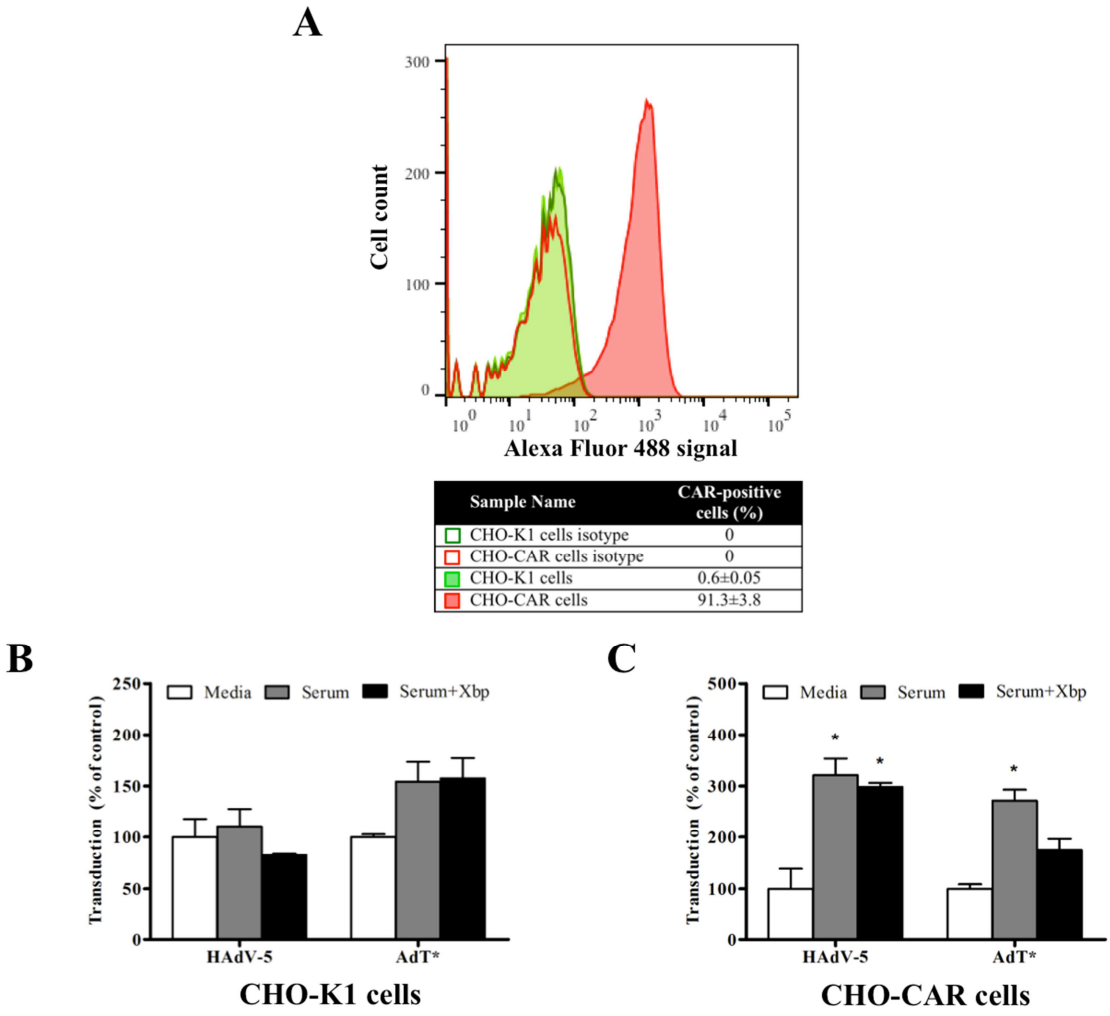

Figure 3-26. Adenoviral transduction in the presence of immunocompromised mouse serum in CHO cells engineered to express CAR. A) CAR expression levels on cell plasma membrane were tested by flow cytometry in CHO-K1 and CHO-CAR cells. Mouse anti-CAR IgG1 primary antibody and Alexa Fluor 488-conjugated goat anti-mouse IgG secondary antibody were used. CAR-positive cells are shown as a percentage of the parental population and expressed as the mean of technical triplicates +/- SEM. A representative image is shown. B-C) HAdV-5 or AdT* ($2x10^{10}$ vp/ml) were incubated for 30 min at 37°C with serum-free (SF) F-10 media or 90% Rag $2^{-/-}$ serum in the presence or absence of X-bp (40 µg/ml). Adenovirus suspensions were diluted 200-fold in SF media and added to CHO-K1 (B) or CHO-CAR (C) cells (1000 vp/cell) and incubated at 37°C for 2 h. Then, media was replaced with 2% FCS F-10 media and cells incubated for further 20 h. β-galactosidase expression levels were quantified as relative light units (RLU) and normalized to total mg of protein. n = 3 biological replicates per condition with 4 technical replicates. Values are shown as a percentage of the SF media alone condition and expressed as the mean of the normalized values per experiment +/- SEM. Repeated measures ANOVA and *post hoc* Tukey's range test applied. *p<0.05 vs. matched controls.

To further assess the role of CAR in the observed mouse serum-enhanced transduction, transduction experiments in the presence of Rag $2^{-/-}$ serum were performed in CAR^{low} SKOV3 cells and SKOV3 cells stably expressing hCAR (SKOV3-CAR).

Via flow cytometry only 1.3±0.05% of SKOV3 cells expressed CAR, while 63.9±0.3% of SKOV3-CAR cells was positive for CAR (Figure 3-27A). Rag $2^{-/-}$ serum significantly enhanced HAdV-5 transduction of SKOV3 cells by 8-fold and addition of X-bp inhibited the transduction enhancing properties of Rag $2^{-/-}$ serum (Figure 3-27B). These data

indicates that serum-enhanced transduction in SKOV3 cells is predominantly mediated by FX, as previously reported (Ma et al., 2015). Moreover, Rag $2^{-/-}$ serum enhanced AdT* transduction minimally (Figure 3-27B), confirming that HAdV-5 transduction of SKOV3 cells in the presence of immunocompromised Rag $2^{-/-}$ serum is mainly dependent on FX. Similar to that seen in A549 cells, Rag $2^{-/-}$ serum significantly enhanced SKOV3-CAR cell transduction by 3.5-fold, and addition of X-bp had minimal effect on the enhanced transduction (Figure 3-27C). Furthermore, AdT* transduction was significantly enhanced by 3.1-fold in the presence of Rag $2^{-/-}$ serum in SKOV3-CAR cells (Figure 3-27C), showing that a FX-independent transduction mechanism is also present in SKOV3-CAR cells as observed for A549 and CHO-CAR cells.

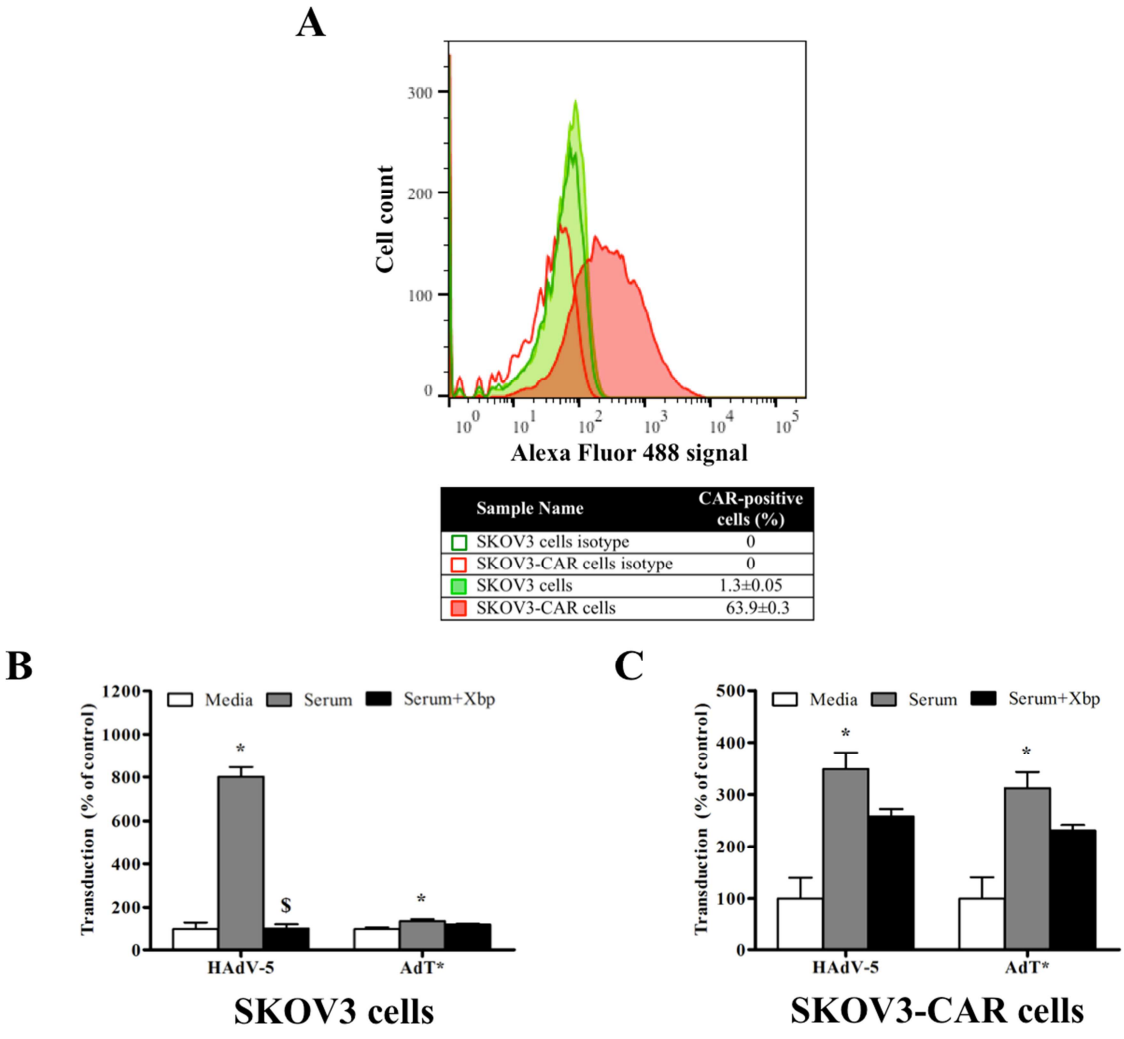

Figure 3-27. Adenoviral transduction in the presence of immunocompromised mouse serum in SKOV3 cells engineered to express CAR. A) CAR expression levels on cell plasma membrane were tested by flow cytometry in SKOV3 and SKOV3-CAR cells. Mouse anti-CAR IgG1 primary antibody and Alexa Fluor 488-conjugated goat anti-mouse IgG secondary antibody were used. CAR-positive cells are shown as a percentage of the parental population and expressed as the mean of technical triplicates +/- SEM. A representative image is shown. B-C) HAdV-5 or AdT* ($2x10^{10}$ vp/ml) were incubated for 30 min at 37°C with serum-free (SF) RPMI-1640 media or 90% Rag $2^{-/-}$ serum in the presence or absence of X-bp (40 µg/ml). Adenovirus suspensions were diluted 200-fold in SF media and added to SKOV3 (B) or SKOV3-CAR (C) cells (1000 vp/cell) and incubated at 37°C for 2 h. Then, media was replaced with 2% FCS RPMI-

1640 (B) or 2% FCS 1000 ng/µl geneticin RPMI-1640 (C) media and cells incubated for further 20 h. β-galactosidase expression levels were quantified as relative light units (RLU) and normalized to total mg of protein. n = 4 (B), n = 3 (C) biological replicates per condition with 4 technical replicates. Values are shown as a percentage of the SF media alone condition and expressed as the mean of the normalized values per experiment +/- SEM. Repeated measures ANOVA and *post hoc* Tukey's range test applied. *p<0.05 vs. matched controls, $p<0.05 vs. matched serum.

To further interrogate HAdV-5 receptor usage in the presence of mouse serum, the availability of CAR during cell transduction was blocked using soluble recombinant HAdV-5 fiber knob (FK) (Coughlan et al., 2009). FK*, which has the point mutation Y477A in the fiber DE loop to impair CAR-binding (Roelvink et al., 1999, Kirby et al., 2000, Alemany and Curiel, 2001), was used as a control. First, the ability of FK to block CAR was confirmed by assessing HAdV-5 transduction of A549 cells pre-incubated with FK or FK* (Figure 3-28). Pre-incubation of A549 cells with FK significantly decreased HAdV-5 transduction 12-fold compared to the FK* control (Figure 3-28). Of note, FK* significantly increased HAdV-5 transduction of A549 cells (Figure 3-28). Next, A549 cells were incubated with HAdV-5 in the presence of C57BL/6 (Figure 3-29A) or Rag $2^{-/-}$ (Figure 3-29B) serum. Pre-incubation of A549 cells with FK decreased basal HAdV-5 transduction in the presence of SF media alone, while FK* had no effect (Figure 3-29A-B). Both C57BL/6 and Rag $2^{-/-}$ sera enhanced HAdV-5 transduction (Figure 3-29A-B) as observed before, and while pre-incubation of C57BL/6 serum with X-bp resulted in a decrease in transduction (Figure 3-29A), it had minimal effect on Rag $2^{-/-}$ serum-enhanced transduction (Figure 3-29B). Importantly, pre-incubation of cells with FK significantly reduced the enhancing properties of C57BL/6 serum from 6.9–fold (+FK*) to 2.9–fold (+FK) and of Rag $2^{-/-}$ serum from 7.4–fold (+FK*) to 1.5–fold (+FK) (Figure 3-29A-B). These results show that blockade of CAR on A549 cells has a direct impact on HAdV-5 transduction in the presence of mouse serum, confirming a role for CAR in this context.

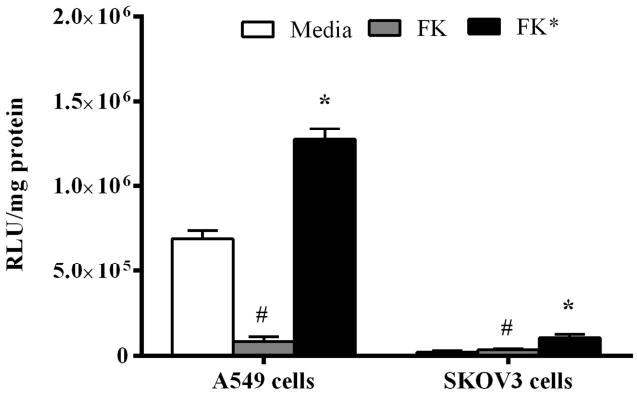

Figure 3-28. Effect of soluble recombinant HAdV-5 fiber knob (FK) on adenoviral transduction. HAdV-5 (1000 vp/cell) was added on A549 or SKOV3 cells that had been pre-incubated with SF media, FK or FK* (Y477A point mutation to impair binding to CAR) at 1 µg/well. After 2 h incubation at 37°C, media

was replaced with 2% FCS RPMI media and cells were incubated for further 20 h. β-galactosidase expression levels were quantified as relative light units (RLU) and normalized to total mg of protein. Background chemoluminescence was subtracted from all values. n = 4 technical replicates per condition. Values are shown as the mean of values +/- SEM. One-way ANOVA and *post hoc* Tukey's range test applied. *p<0.05 vs. matched controls, #p<0.05 vs. "+FK*" condition.

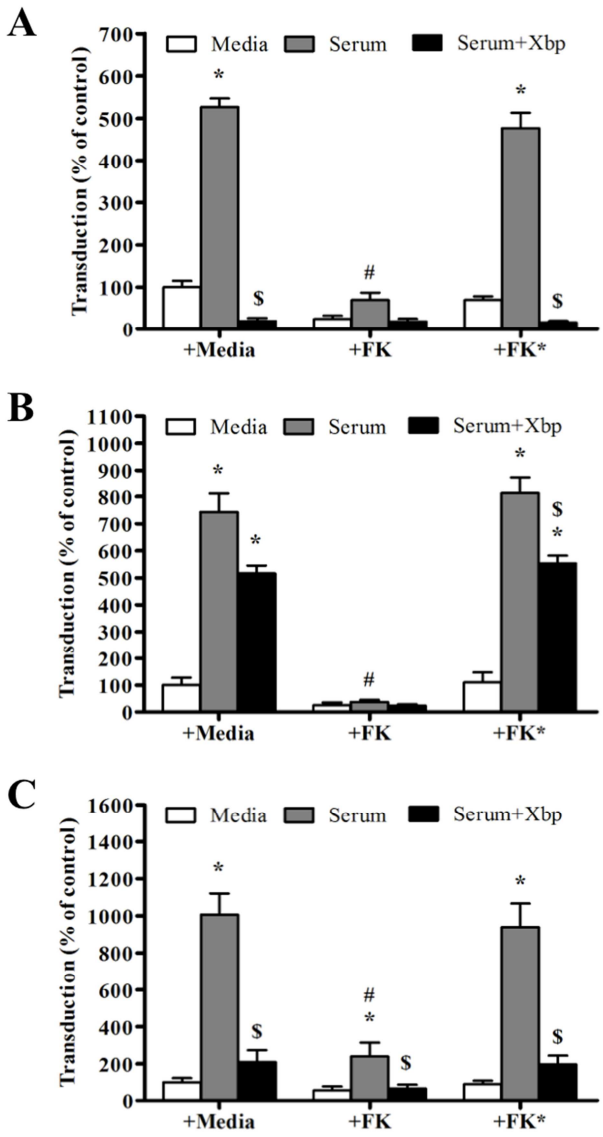

Figure 3-29. CAR-dependency of adenoviral transduction in the presence of mouse serum. HAdV-5 ($2x10^{10}$ vp/ml) was incubated for 30 min at 37°C with serum-free (SF) RPMI-1640 media, 90% C57BL/6 (A) or Rag $2^{-/-}$ (B-C) mouse serum in the presence or absence of X-bp (40 μg/ml). Adenovirus suspensions were diluted 100-fold in SF media and added to A549 (A-B) or SKOV3 (C) cells (1000 vp/cell) that had been pre-incubated with an equal volume of SF media, soluble recombinant fiber knob (FK) or FK* (Y477A point mutation to impair binding to CAR) at 1 μg/well. After 2 h incubation at 37°C, media was replaced with 2% FCS RPMI and cells were incubated for further 20 h. β-galactosidase expression levels were quantified as relative light units (RLU) and normalized to total mg of protein. n = 3 biological replicates per condition with 4 technical replicates. Values are shown as a percentage of the SF media alone condition and expressed as the mean of the normalized values per experiment +/- SEM. Repeated measures ANOVA and *post hoc* Tukey's range test applied. *p<0.05 vs. matched controls, $p<0.05 vs. matched serum, #p<0.05 vs. serum + FK*. Statistical significance was reached between the fold-change enhancement produced by serum in the presence of FK vs. that in the presence of FK* in (A-C) (paired Student's T-test, p<0.05).

Surprisingly, despite the presence of FX in mouse serum, C57BL/6 and Rag $2^{-/-}$ serum failed to significantly enhance HAdV-5 transduction in the presence of FK (Figure 3-29A-

B), suggesting that HAdV-5 might not follow the FX-mediated pathway in the presence of mouse serum when the FX-independent and CAR-mediated pathway is unavailable. To evaluate whether the FX-mediated pathway of HAdV-5 transduction in the presence of mouse serum is affected by the presence of soluble FK, HAdV-5 transduction experiments with Rag $2^{-/-}$ serum and FK were performed in SKOV3 cells, which are transduced predominantly in a FX-dependent manner in the presence of Rag $2^{-/-}$ serum. First, FK was confirmed to have no effect on basal HAdV-5 transduction of CAR^{low} SKOV3 cells in the presence of SF media alone (Figure 3-28). As observed in A549 cells (Figure 3-28), FK* significantly increased HAdV-5 transduction in SKOV3 cells (Figure 3-28). Next, HAdV-5 transduction of SKOV3 cells was assessed in the presence of Rag $2^{-/-}$ serum and FK or FK* (Figure 3-29C). Rag $2^{-/-}$ serum produced a significant enhancement in HAdV-5 transduction in the presence of FK (4.3-fold) that was inhibited by X-bp (Figure 3-29C), indicating HAdV-5 was able to transduce SKOV3 cells via the FX-mediated pathway. However, this enhancement was significantly lower than that in the presence of FK*, which was 10.6-fold (Figure 3-29C). Since only 1.3±0.05% of SKOV3 cells were shown to express CAR in flow cytometry assays (Figure 3-27A), these results suggest that presence of FK might affect the use of the FX-mediated pathway in the presence of Rag $2^{-/-}$ serum. To further investigate whether the observed effects of FK on the FX-mediated pathway of HAdV-5 transduction are evident only in the presence of Rag $2^{-/-}$ serum, HAdV-5 transduction of A549 cells was assessed in the presence of FK or FK* with or without the addition of hFX in the absence of mouse serum. Addition of hFX enhanced HAdV-5 transduction by 3-fold but, unexpectedly, it did not reach statistical significance (Figure 3-30). Presence of FK slightly reduced FX-enhanced transduction and FK* slightly increased FX-enhanced transduction but did not reach statistical significance (Figure 3-30). Together, these data show a trend for FK but not FK* to negatively affect HAdV-5 transduction via the FX-mediated pathway.

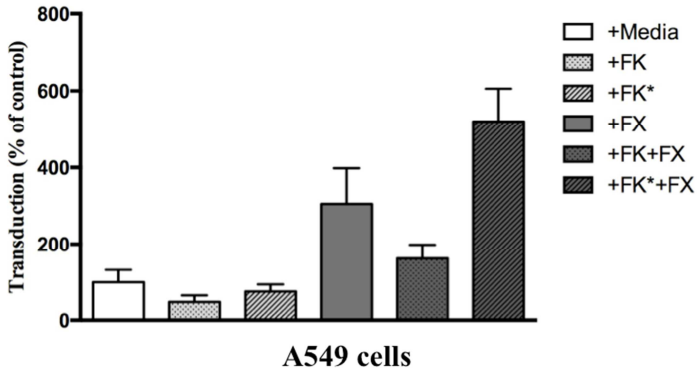

Figure 3-30. Effect of soluble recombinant fiber knob (FK) and FX on adenoviral transduction. HAdV-5 ($2x10^{10}$ vp/ml) was incubated for 30 min at 37°C with serum-free (SF) RPMI-1640 media in the absence or presence of recombinant human FX (10 μg/ml). Adenovirus suspensions were diluted 100-fold in SF media and added to A549 cells (1000 vp/cell) that had been pre-incubated with an equal volume of SF media, FK or FK* (Y477A point mutation to impair binding to CAR) at 1 μg/well. After 2 h incubation at 37°C, media was replaced with 2% RPMI media and cells were incubated for further 20 h. β-galactosidase expression levels were quantified as relative light units (RLU) and normalized to total mg of protein. n = 3 biological replicates per condition with 4 technical replicates. Values are shown as a percentage of the SF media alone condition and expressed as the mean of the normalized values per experiment +/- SEM. Repeated measures ANOVA and *post hoc* Tukey's range test applied ($p<0.05$).

Together, these data support a role for CAR in HAdV-5 transduction *in vitro* in the presence of immunocompetent or immunocompromised mouse serum. Moreover, the data suggests that HAdV-5 may not transduce A549 cells via alternative pathways such as the FX-mediated pathway when the FX-independent and CAR-mediated pathway is unavailable.

3.3.6.2 Direct HAdV-5 fiber knob interaction with CAR is not required for transduction in the presence of immunocompromised mouse serum

The presence of mouse serum is required to enhance HAdV-5 transduction via a CAR-mediated pathway. The mechanisms behind this effect might involve a mouse serum protein either able to bridge HAdV-5 to CAR on the plasma membrane or to enhance transduction by stabilizing HAdV-5:CAR interactions. To assess whether the CAR-mediated pathway of HAdV-5 transduction in the presence of mouse serum occurs via a direct interaction between the HAdV-5 fiber knob and CAR, transduction assays were performed in the presence of Rag $2^{-/-}$ serum using the CAR-binding deficient HAdV-5 KO1. HAdV-5 was used as a control.

HAdV-5 KO1 transduction of A549 cells was enhanced 2.8–fold in the presence of Rag $2^{-/-}$ serum (Figure 3-31), and pre-incubation of Rag $2^{-/-}$ serum with X-bp had no effect on the enhanced transduction (Figure 3-31), indicating that HAdV-5 KO1 transduced A549 cells in a FX-independent manner, as observed for HAdV-5 (Figure 3-31). These results suggest

that a direct interaction of HAdV-5 fiber knob with CAR is not required for transduction in the presence of Rag $2^{-/-}$ serum, suggesting the CAR-mediated pathway might involve a serum protein bridging HAdV-5 to CAR.

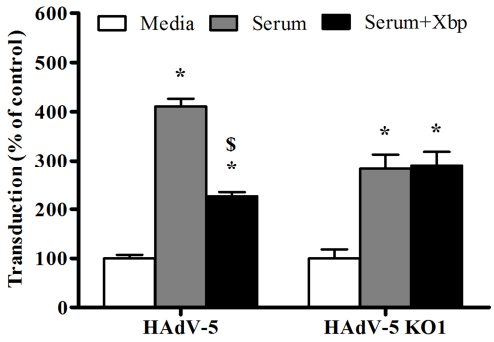

Figure 3-31. Effect of immunocompromised mouse serum on CAR-binding deficient HAdV-5 transduction. HAdV-5 or HAdV-5 KO1 ($2x10^{10}$ vp/ml) were incubated for 30 min at 37°C with serum-free (SF) RPMI-1640 media or 90% Rag $2^{-/-}$ mouse serum in the presence or absence of X-bp (40 μg/ml). Adenovirus suspensions were diluted 200-fold in SF media and added to A549 cells (1000 vp/cell) and incubated at 37°C for 2 h. Then, media was replaced with 2% FCS RPMI and cells incubated for further 20 h. β-galactosidase expression levels were quantified as relative light units (RLU) and normalized to total mg of protein. n = 4 biological replicates per condition with 4 technical replicates. Values are shown as a percentage of the SF media alone condition and expressed as the mean of the normalized values per experiment +/- SEM. Repeated measures ANOVA and *post hoc* Tukey's range test applied. *$p<0.05$ vs. matched controls, \$$p<0.05$ vs. matched serum.

3.3.6.3 Effect of heat on the FX-mediated pathway for HAdV-5 transduction

Next, the mouse serum proteins that might be involved in the observed enhancement on HAdV-5 transduction in the presence of mouse serum were investigated. As discussed in section 3.3.2.2, exposure of C57BL/6 or Rag $2^{-/-}$ serum to high temperatures (56°C) inhibited the transduction enhancing properties of mouse serum, suggesting that the factors involved in both FX-mediated and FX-independent HAdV-5 transduction in the presence of mouse serum are heat-labile. To confirm that FX is heat-labile, transduction experiments were performed with HAdV-5 on A549 cells in the presence or absence of hFX that had been pre-exposed to 56°C. As expected, HAdV-5 transduction was significantly enhanced in the presence of hFX by 2.9-fold (Figure 3-32). However, heat-exposed hFX failed to enhance HAdV-5 transduction (Figure 3-32), confirming that heat inhibits the enhancing properties of hFX.

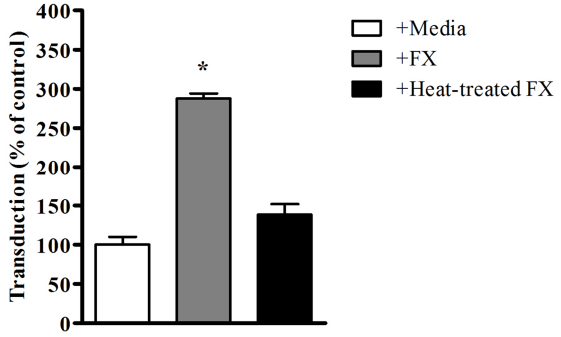

Figure 3-32. Effect of heat on the HAdV-5 transduction enhancing properties of FX *in vitro*. HAdV-5 ($2x10^{10}$ vp/ml) was incubated for 30 min at 37°C with recombinant human FX (hFX) or heat-treated hFX (10 μg/ml) in serum-free (SF) RPMI-1640 media. Adenovirus suspensions were diluted 200-fold in SF media and added to A549 cells (1000 vp/cell) and incubated at 37°C for 2 h. Then, media was replaced with 2% FCS RPMI media and cells incubated for further 20 h. β-galactosidase expression levels were quantified as relative light units (RLU) and normalized to total mg of protein. n = 3 biological replicates per condition with 4 technical replicates. Values are shown as a percentage of the SF media alone condition and expressed as the mean of values +/- SEM. Repeated measures ANOVA and *post hoc* Tukey's range test applied. *$p<0.05$ vs. "Media" condition.

3.3.6.4 HAdV-5 transduction in the presence of immunocompromised mouse serum in a series of high and low CAR-expressing cell lines

To investigate whether the CAR-mediated pathway in the presence of mouse serum is also present in other high CAR-expressing cell lines (determined from NCI60 database, retrieved from http://biogps.org/#goto=welcome), transduction experiments were performed in the presence of immunocompromised Rag $2^{-/-}$ serum with or without X-bp in HeLa and HepG2 cells. Flow cytometry assays confirmed a high percentage of HeLa and HepG2 cells expressing CAR on the cell plasma membrane, 79.9±4.6% and 71±0.3% respectively (Figure 3-33A). Both cell lines exhibited an HAdV-5 transduction profile similar to that observed in A549 cells, where Rag $2^{-/-}$ serum significantly enhanced HAdV-5 transduction (4.7-fold in HeLa cells and 2.2-fold in HepG2 cells) and X-bp had minimal or inexistent effect on the enhanced transduction (Figure 3-33B-C). AdT* transduction was significantly enhanced by Rag $2^{-/-}$ serum in HeLa cells both in the presence or absence of X-bp by 4.7-fold and 3.3-fold, respectively (Figure 3-33B). However, despite a 2-fold transduction enhancement was observed for AdT* in HepG2 cells with and without X-bp, it did not reach statistical significance (Figure 3-33C). These results indicate that FX-independent pathways of HAdV-5 transduction in the presence of Rag $2^{-/-}$ serum are also present in other CAR^{high} cell lines such as HeLa and HepG2 cells.

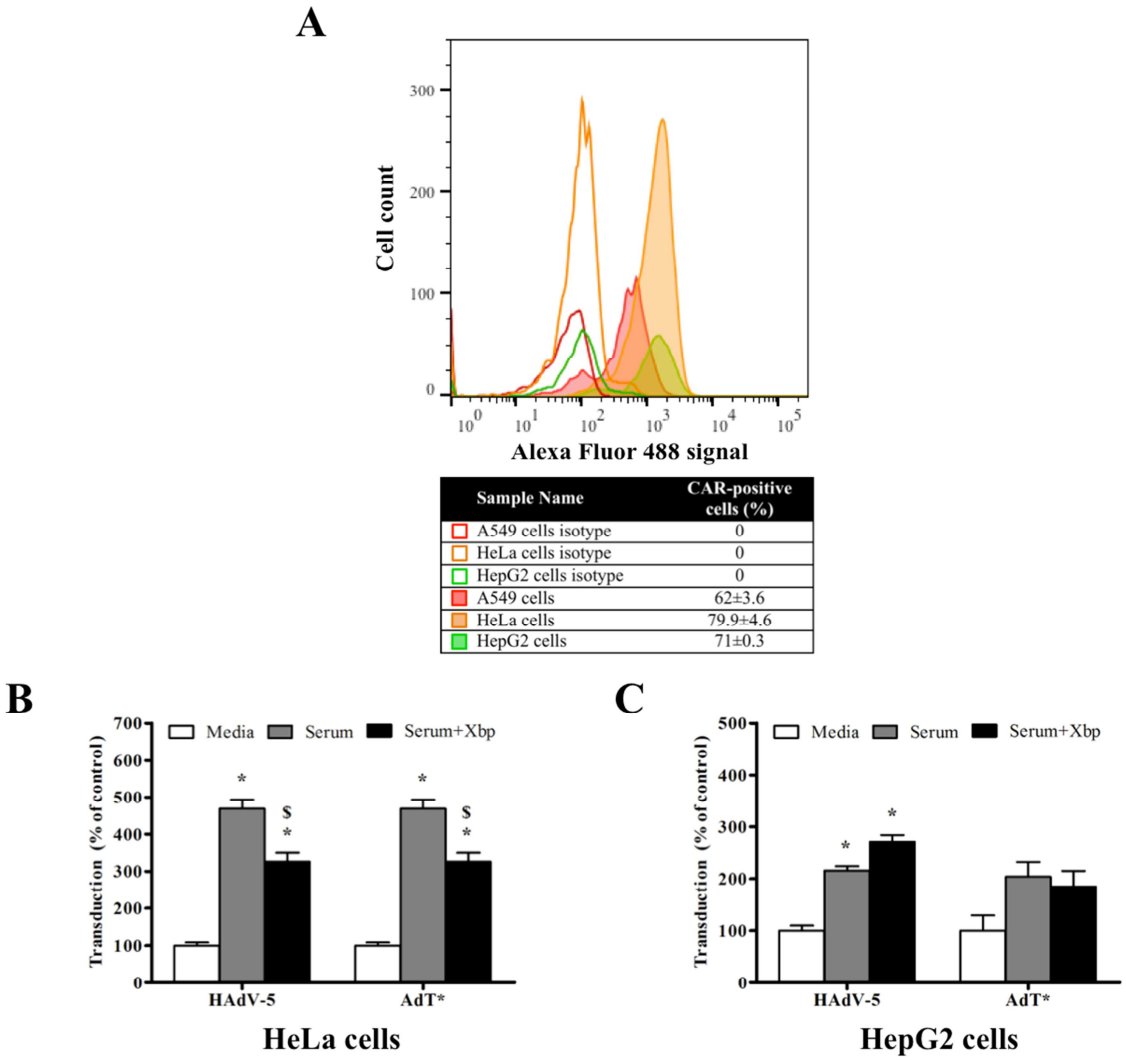

Figure 3-33. Adenoviral transduction in the presence of immunocompromised mouse serum in high CAR-expressing cell lines. A) CAR expression levels on cell plasma membrane were tested by flow cytometry in HeLa and HepG2 cells. Mouse anti-CAR IgG1 primary antibody and Alexa Fluor 488-conjugated goat anti-mouse IgG secondary antibody were used. CAR-positive cells are shown as a percentage of the parental population and expressed as the mean of technical triplicates +/- SEM. A representative image is shown. B-C) HAdV-5 or AdT* ($2x10^{10}$ vp/ml) were incubated for 30 min at 37°C with serum-free (SF) MEM media or 90% Rag $2^{-/-}$ serum in the presence or absence of X-bp (40 µg/ml). Adenovirus suspensions were diluted 200-fold in SF media and added to HeLa (B) or HepG2 (C) cells (1000 vp/cell) and incubated at 37°C for 2 h. Then, media was replaced with 2% FCS MEM media and cells incubated for further 20 h. β-galactosidase expression levels were quantified as relative light units (RLU) and normalized to total mg of protein. n = 6 (B), n = 3 (C) biological replicates per condition with 4 technical replicates. Values are shown as a percentage of the SF media alone condition and expressed as the mean of the normalized values per experiment +/- SEM. Repeated measures ANOVA and *post hoc* Tukey's range test applied. *p<0.05 vs. matched controls, $p<0.05 vs. matched serum.

Next, whether other low CAR-expressing cell lines (determined from NCI60 database, retrieved from http://biogps.org/#goto=welcome) such as ACHN or MCF7 are transduced by HAdV-5 via the FX-mediated pathway in the presence of Rag $2^{-/-}$ serum, as observed in SKOV3 cells, was assessed. The levels of CAR on the cell plasma membrane were assessed by flow cytometry, and only 3.5±0.5% of ACHN and 0.3±0.08% of MCF7 cells were positive for CAR (Figure 3-34A). Rag $2^{-/-}$ serum significantly enhanced HAdV-5

transduction by 3.6-fold in ACHN and 2.9-fold in MCF7 cells (Figure 3-34B-C). The presence of X-bp reduced serum-enhanced HAdV-5 transduction in ACHN cells but unexpectedly this reduction did not reach statistical significance (Figure 3-34B). X-bp had minimal effect on the enhanced transduction in MCF7 cells (Figure 3-34C). Moreover, Rag $2^{-/-}$ serum significantly enhanced AdT* transduction by 2.1-fold in ACHN and 2.5-fold in MCF7 in the presence and absence of X-bp (Figure 3-34B-C). These data indicate that FX-independent pathways of HAdV-5 transduction in the presence of Rag $2^{-/-}$ serum are also present in CAR^{low} ACHN and $CAR^{negative}$ MCF7 cells.

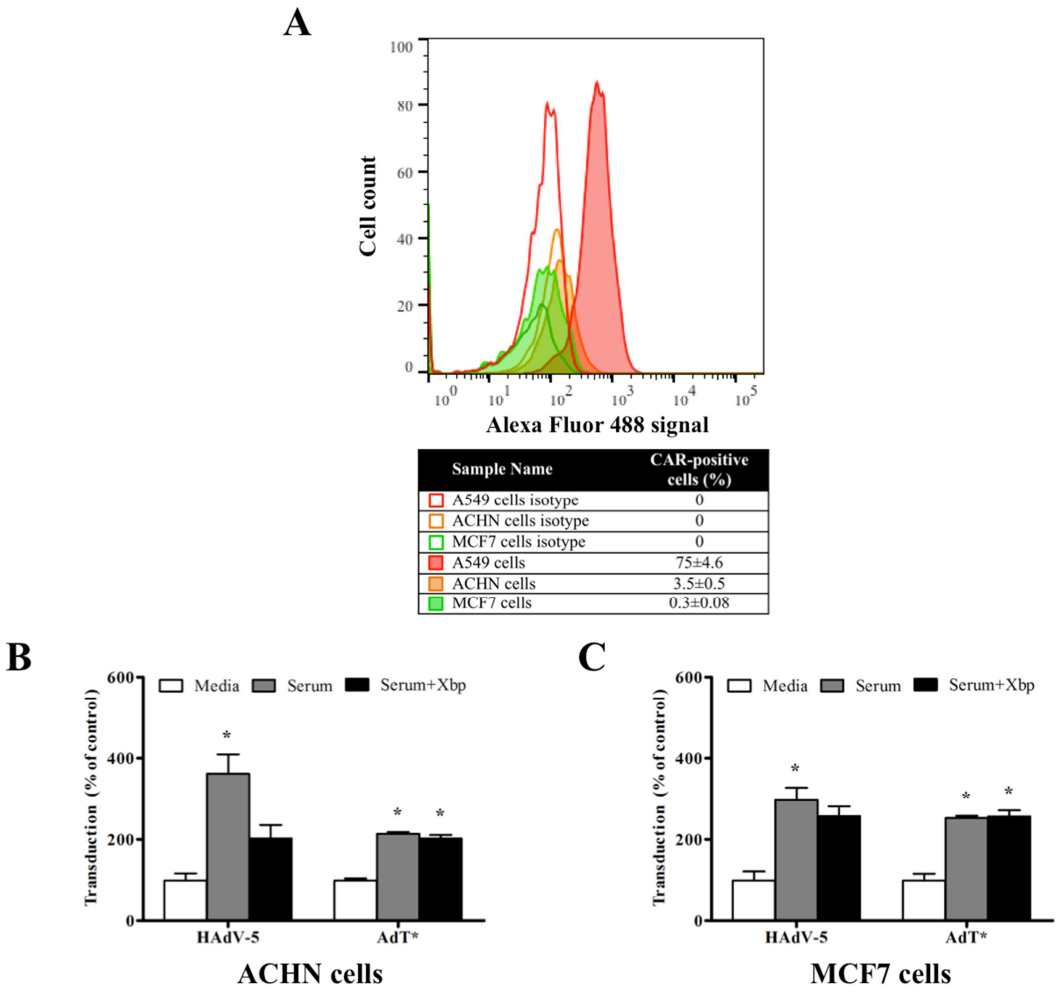

Figure 3-34. Adenoviral transduction in the presence of immunocompromised mouse serum in low CAR-expressing cell lines. A) CAR expression levels on cell plasma membrane were tested by flow cytometry in ACHN and MCF7 cells. Mouse anti-CAR IgG1 primary antibody and Alexa Fluor 488-conjugated goat anti-mouse IgG secondary antibody were used. CAR-positive cells are shown as a percentage of the parental population and expressed as the mean of technical triplicates +/- SEM. A representative image is shown. B-C) HAdV-5 or AdT* ($2x10^{10}$ vp/ml) were incubated for 30 min at 37°C with serum-free (SF) RPMI-1640 media or 90% Rag $2^{-/-}$ serum in the presence or absence of X-bp (40 µg/ml). Adenovirus suspensions were diluted 200-fold in SF media and added to ACHN (B) or MCF7 (C) cells (1000 vp/cell) and incubated at 37°C for 2 h. Then, media was replaced with 2% FCS RPMI media and cells incubated for further 20 h. β-galactosidase expression levels were quantified as relative light units (RLU) and normalized to total mg of protein. n = 3 biological replicates per condition with 4 technical replicates. Values are shown as a percentage of the SF media alone condition and expressed as the mean of

the normalized values per experiment +/- SEM. Repeated measures ANOVA and *post hoc* Tukey's range test applied. *p<0.05 vs. matched controls.

Together, these results suggest that HAdV-5 can transduce different cell lines in a FX-independent manner in the presence of immunocompromised Rag $2^{-/-}$ serum, independently of CAR expression levels.

3.4 Discussion

Here, the mechanisms mediating *in vitro* and *in vivo* HAdV-5 neutralization were assessed. Moreover, the use of FX-independent pathways for HAdV-5 liver and spleen transduction following intravascular delivery were investigated and novel pathways of HAdV-5 transduction *in vitro* after exposure of virions to mouse serum were defined. The data indicate that while natural IgM antibodies and the complement system are required for adenovirus neutralization *in vitro* after exposure to mouse serum, innate immunity alone might be sufficient to mediate neutralization *in vivo.* FX was identified as critical in protecting HAdV-5 from neutralization by mouse serum both *in vitro* and *in vivo* but dispensable for liver and spleen transduction in immunocompromised NSG mice. CAR and $\alpha_v\beta_{3,5}$ integrins were shown to have no role in liver or spleen tropism in immunocompromised Rag $2^{-/-}$ and $\alpha_v\beta_{3,5}$ integrins in immunocompromised NSG mice (CAR not assessed), while CAR and $\alpha_v\beta_{3,5}$ integrins appeared to be involved in immunocompetent C57BL/6 mice liver transduction. Both immunocompetent and immunocompromised mouse serum enhanced HAdV-5 transduction *in vitro* in a FX-independent manner on high CAR-expressing cell lines via a mechanism involving a blood factor bridging HAdV-5 to CAR. In contrast, HAdV-5 transduction of low CAR-expressing cell lines in the presence of immunocompromised mouse serum was either FX-dependent or via other FX and CAR-independent pathways, depending on cell type. Therefore, Figure 3-35 summarizes our suggested model of HAdV-5 *in vitro* neutralization and cell transduction in the presence of mouse serum.

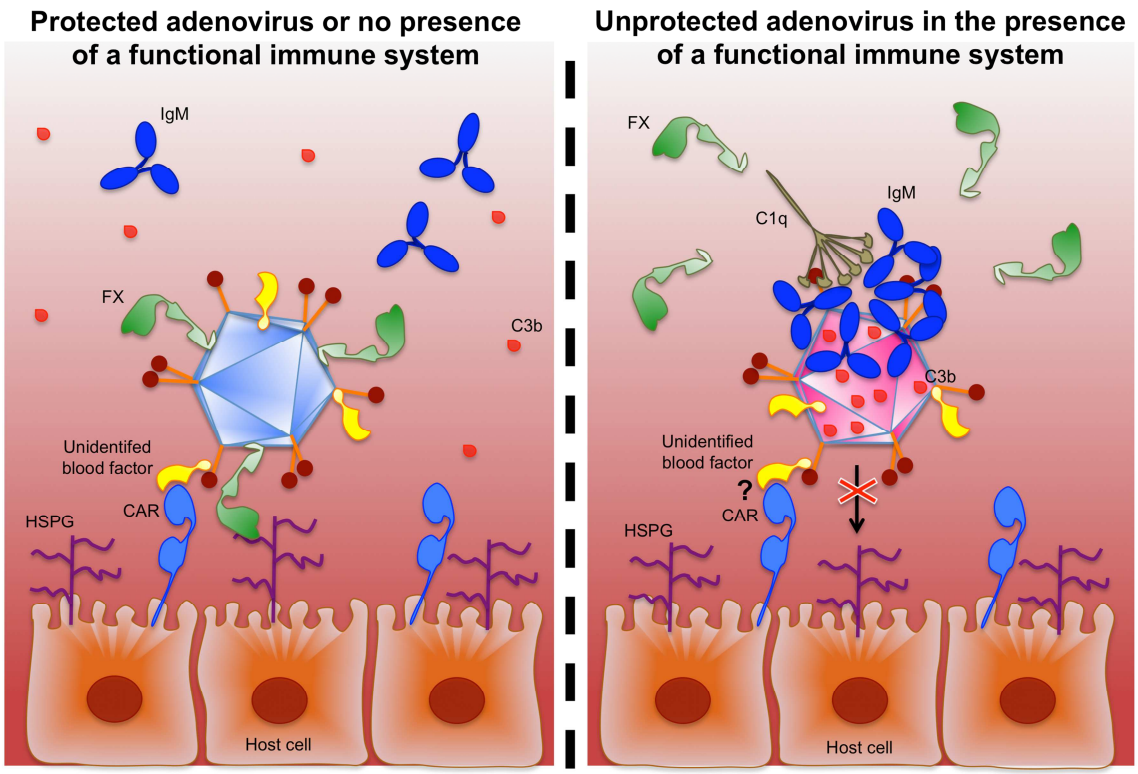

Figure 3-35. Suggested model of HAdV-5 *in vitro* neutralization and cell transduction in the presence of mouse serum. HAdV-5 can use FX for protection against neutralization in the presence of immunocompetent mouse serum. In the absence of adenovirus neutralization and presence of mouse serum, HAdV-5 can transduce host cells via a FX-mediated pathway or through a FX-independent mechanism that involves an unidentified blood protein bridging HAdV-5 to CAR. FX; coagulation factor X, CAR; coxsackie and adenovirus receptor, HSPG; heparan sulphate proteoglycan, C3; complement protein 3. Figure adapted from (Lopez-Gordo et al., 2014a).

3.4.1 *In vitro* and *in vivo* adenovirus neutralization

First, immunocompromised Rag $2^{-/-}$ mice (IgM antibodies-deficient) (Shinkai et al., 1992, Alt et al., 1992) and NSG mice (IgM antibodies and C5-deficient) (Zhou et al., 2014, Shultz et al., 2005, Ito et al., 2002, Shultz et al., 1995) were confirmed to lack the ability to neutralize HAdV-5 *in vitro* in the absence of FX-binding, in contrast to immunocompetent C57BL/6 mice, revealing a role for IgM antibodies in *in vitro* HAdV-5 neutralization and a role for FX in protecting HAdV-5 from it. However, complementation of IgM antibodies in Rag $2^{-/-}$ serum failed to rescue *in vitro* HAdV-5 neutralization. The finding that IgM antibodies might not be involved in HAdV-5 *in vitro* neutralization in the presence of Rag $2^{-/-}$ serum is in contrast with a previous report (Xu et al., 2013). This study showed that complementation of Rag $1^{-/-}$ serum with mouse IgM antibodies purified from BALB/c mice rescued HAdV-5 neutralization *in vitro*. Here, Rag $2^{-/-}$ serum was complemented with pure mouse IgM antibodies that had been isolated from BALB/c serum. Rag $1^{-/-}$ and Rag $2^{-/-}$ mice are both strains derived from C57BL/6 mice by mutation of *Rag-1* or *Rag-2* genes respectively (Mombaerts et al., 1992, Shinkai et al., 1992), which are involved in the

somatic DNA rearrangement V(D)J recombination (Alt et al., 1992). Since these two mouse strains have a very similar phenotype (Mombaerts et al., 1992, Shinkai et al., 1992), it was presumed the mechanisms of adenovirus neutralization might also be closely related. Furthermore, Rag $2^{-/-}$ mice only lack IgM production in comparison to its background strain C57BL/6 mice, which can neutralize HAdV-5 *in vitro* when not bound to FX (Xu et al., 2013). Thus, lack of adenovirus neutralization by IgM-complemented Rag $2^{-/-}$ serum might be due to strain incompatibilities, where the complement system from Rag $2^{-/-}$ serum is unable to bind BALB/c IgM antibodies to initiate the classical complement cascade on the HAdV-5 capsid. Also, BALB/c IgM antibodies were not tested for binding to HAdV-5 vectors neither in the absence nor the presence of Rag $2^{-/-}$ serum. Confirmation of these interactions by techniques such as NanoSight, ELISA or SPR would help in assessing the reason behind the controversial results. To further dissect the underlying mechanisms of adenovirus neutralization by mouse serum *in vitro*, the role of complement was assessed. Transduction assays in the presence of C57BL/6 serum that had been heat-treated resulted in the impairment of HAdV-5 neutralization when not bound to FX, indicating that a heat-labile protein is involved in HAdV-5 neutralization. Based on previous data (Xu et al., 2013), it was presumed this was the complement system. However, further experiments should be performed to draw definite conclusions since other heat-labile proteins might be present in C57BL/6 serum and be the ones involved in HAdV-5 *in vitro* neutralization.

Next, liver transduction was assessed in C57BL/6, Rag $2^{-/-}$ and NSG mice. FX-binding deficient AdT* exhibited a significantly lower liver transduction than that of HAdV-5 in C57BL/6 mice in contrast to NSG mice, which had equivalent levels of liver transduction with these two vectors. Interestingly, Rag $2^{-/-}$ mice had a significantly lower AdT* liver transduction compared to that of HAdV-5, albeit this reduction was less pronounced than in C57BL/6 mice. These results suggest that while FX might play a role in protecting HAdV-5 against neutralization in C57BL/6 mice, its role in liver tropism in immunocompromised NSG mice is minimal, which is in agreement with previous data suggesting that FX-independent pathways can mediate liver transduction (Zaiss et al., 2015). Interestingly, FX might be involved in liver tropism in immunocompromised Rag $2^{-/-}$ mice, indicating that strain-specific processes may dictate adenovirus liver tropism. For instance, the effect of both CAR and integrin-binding ablating mutations on HAdV-5 vectors on liver transduction was highly variable between mouse and rat and between different rat strains (Nicol et al., 2004), suggesting that indeed intrinsic differences in the use of adenoviral receptors for liver transduction may be present between strains. However, the lower liver transduction found in Rag $2^{-/-}$ mice could be the result of

adenovirus neutralization, albeit at lower levels than those found in C57BL/6 mice. Here, it was suggest that the mechanisms for adenovirus neutralization *in vivo* may differ from those *in vitro*: IgM antibodies may be required for *in vitro* neutralization but dispensable *in vivo.* Thus, while neither Rag $2^{-/-}$ or NSG mice serum can neutralize HAdV-5 *in vitro* in the absence of FX-binding because they lack IgM antibodies, the intact innate immunity of Rag $2^{-/-}$ mice might be sufficient to mediate adenovirus neutralization *in vivo*. Under this hypothesis, since NSG mice are defective in both the adaptive and innate immune response, they would not be able to mediate adenovirus neutralization *in vivo.* Supporting our hypothesis, one study demonstrated that while *in vitro* neutralization requires IgM antibodies and the classical complement pathway, both the classical and non-classical pathways are apparent *in vivo* (Tian et al., 2009), indicating that *in vitro* and *in vivo* adenovirus neutralization is mediated by different mechanisms. Furthermore, this study showed that C3 is activated *in vivo* in Rag $1^{-/-}$ mice following adenovirus administration but not *in vitro* after exposure of HAdV-5 to Rag $1^{-/-}$ serum, in agreement with our findings. Also, a more recent study using Rag $1^{-/-}$ mice showed lower levels of liver transduction after administration of FX-binding deficient HAdV-5 or HAdV-5 with X-bp, in contrast to C57BL/6 mice (Xu et al., 2013). However, although these data might suggest that HAdV-5 can be neutralized in mice lacking IgM antibodies, they suggested the lower transduction might be due to FX being involved in liver tropism to some extent in Rag $1^{-/-}$ mice (Xu et al., 2013). Nevertheless, data from other studies assessing *in vitro* adenovirus neutralization are highly controversial. For instance, one report showed that although HAdV-5 is mainly opsonized by the IgM-mediated classical complement pathway *in vitro*, there are other antibody-independent pathways that can opsonize HAdV-5 *in vitro* (Xu et al., 2008). In particular, this study showed that HAdV-5 was opsonized by C3b when incubated with Rag $1^{-/-}$ serum despite lacking IgM antibodies (Xu et al., 2008), which is in agreement with another study showing that in the absence of IgM antibodies the alternative complement pathway can be activated *in vitro* (Jiang et al., 2004). These findings are however in contrast with our data showing that *in vitro* HAdV-5 neutralization requires the presence of IgM antibodies and with more recent reports showing similar results (Xu et al., 2013). Thus, further studies should be done to describe the mechanisms behind *in vitro* and *in vivo* adenovirus neutralization and confirm the involvement or dispensability of IgM antibodies in this process. In any case, if the innate immunity alone is sufficient to neutralize adenovirus *in vivo*, differences in the presence of proteins from the innate immune response in NSG and Rag $2^{-/-}$ mice may dictate the capacity or incapacity to neutralize adenovirus in the bloodstream and thus account for the differences observed in liver transduction with HAdV-5 and AdT* vectors in these mouse strains. For instance,

while both NSG and Rag $2^{-/-}$ mice can produce C1q and C4, complement proteins that have been associated with adenovirus neutralization *in vitro* and *in vivo* (Xu et al., 2013), NSG mice lack C5 (Baxter and Cooke, 1993), which is a downstream mediator of both the classical and non-classical complement pathways. Thus, absence of C5 might impair NSG mice from neutralizing FX-binding deficient vectors. Also, the levels of C4 differ between mouse strains (Hansen et al., 1974, Lachmann et al., 1975) and, interestingly, the levels of C4 have been shown to be elevated in the intestine of Rag $1^{-/-}$ mice although unaffected in the liver (Jima et al., 2009). Since C4 is a mediator of adenovirus neutralization (Xu et al., 2013), the levels of C4 might directly affect adenovirus neutralization. More studies would be required to investigate whether the differences observed in liver transduction between immunocompromised Rag $2^{-/-}$ and NSG mice with FX-binding deficient vectors are due to strain-specific mechanisms dictating tropism or differences in HAdV-5 neutralization due to intrinsic strain-specific differences in the components of the innate immune system. Regarding the spleen, AdT* exhibited a higher transduction than that of HAdV-5 in NSG mice. Taking into account that NSG mice are defective in macrophage response (Ito et al., 2002, Shultz et al., 1995), these observations are in agreement with previous work showing that macrophage depletion in MF1 mice results in higher spleen transduction with AdT* compared to HAdV-5 vectors (Alba et al., 2010, Bradshaw et al., 2012). Further experiments are needed to investigate the reason behind this observation. NSG mice are a well stablished highly immunocompromised mouse model that supports engraftment with a functional human immune system (Brehm et al., 2010, Pearson et al., 2008) and thus allows investigation of the *in vivo* function of the human immune system (Shultz et al., 2007). Here, NSG mice were used to study adenovirus tropism in the absence of adenovirus neutralization. However, it should be taken into account that neutrophils and monocytes remain functional in NSG mice and, therefore, they could have an effect on the biodistribution of adenoviral vectors.

3.4.2 Cellular receptors mediating liver and spleen transduction

In the assessment of receptors for HAdV-5 liver and spleen transduction, it was found that both CAR and $\alpha_v\beta_{3,5}$ integrins seem to play a role in liver tropism in C57BL/6 mice but not in Rag $2^{-/-}$ mice or NSG mice in the case of $\alpha_v\beta_{3,5}$ integrins (CAR not assessed). CAR and $\alpha_v\beta_{3,5}$ integrins did not seem to be involved in spleen transduction in neither C57BL/6 or Rag $2^{-/-}$ mice and $\alpha_v\beta_{3,5}$ integrins were not involved in NSG mice spleen transduction (CAR not assessed). Previous studies using HAdV-5 with mutations in the fiber knob domain such as S408E, P409A, Y491D, A494D, A503D, Y477A or K417A successfully

impaired interactions with CAR but did not achieve liver de-targeting in C57BL/6, BALB/c and CD-1 mice or non-human primates (Leissner et al., 2001, Alemany and Curiel, 2001, Smith et al., 2002, Smith et al., 2003b, Martin et al., 2003, Zaiss et al., 2015, Smith et al., 2003a), suggesting that CAR is not involved in liver transduction. The effect of mutations impairing interaction of HAdV-5 with $\alpha_v\beta_{3,5}$ integrins on liver and spleen transduction have also been studied. The substitution of the RGD motif in the penton base with an influenza HA epitope to impair binding to $\alpha_v\beta_{3,5}$ integrins had little effect on liver or spleen transduction in BALB/c mice (Einfeld et al., 2001). Deletion of RGD motif in the penton base was also tested but resulted in no differences on liver or spleen transduction in C57BL/6 mice (Mizuguchi et al., 2002, Martin et al., 2003). The PD1 mutation, which consists of a substitution of amino acids 337HAIRGDTF344[5] with amino acids SRGYPYDVPDYAGTS in the penton base, significantly reduced liver transduction in C57BL/6 mice and also decreased spleen transduction (Smith et al., 2003b). In non-human primates, the PD1 mutation produced levels of liver transduction similar to HAdV-5 but lower levels of transduction in the spleen (Smith et al., 2003a). Moreover, a previous study using HAdV-5 RGE revealed no role of $\alpha_v\beta_{3,5}$ integrins on MF1 mice liver transduction in contrast to the spleen, where it produced a 5-fold reduction in transduction (Bradshaw et al., 2012). The impact of simultaneously ablating CAR-binding and $\alpha_v\beta_{3,5}$ integrins on liver and spleen transduction has also been assessed. Incorporation of an influenza HA epitope into the HI loop of the fiber knob domain and in place of the penton base RGD motif to simultaneously ablate interactions with CAR and $\alpha_v\beta_{3,5}$ integrins, respectively, reduced liver transduction 700-fold in BALB/c mice (Einfeld et al., 2001). Also, the combination of PD1 and KO1 mutations produced a moderate effect on liver and spleen transduction in C57BL/6 mice (Smith et al., 2003b) and the deletion of amino acids 489TAYT492 in the FG loop of the fiber knob to ablate binding to CAR together with a deletion of the RGD motif produced a 270-fold lower liver transduction (Koizumi et al., 2003). However, liver transduction of C57BL/6 mice was not altered by the combination of K417A in the fiber knob and the deletion of RGD in the penton base (Martin et al., 2003). Despite the moderate effect that CAR and $\alpha_v\beta_{3,5}$ integrin-binding ablating mutations produced in liver transduction in some of the studies above, ablation of HAdV-5 interactions with CAR or $\alpha_v\beta_{3,5}$ integrins for the most par failed to significantly reduce liver transduction. This is in agreement with our data from Rag $2^{-/-}$ mice but in contrast to our observations in C57BL/6 mice. The reason behind these differences should be further investigated. Nevertheless, it is important to bear in mind that when assessing CAR or

[5]Numbers refer to amino acid residue position in the protein.

$\alpha_v\beta_{3,5}$ integrin-binding ablating mutations it might be necessary to simultaneously ablate interactions with FX or block the use of HSPGs to prevent HAdV-5 from using compensatory pathways for transduction, such as the FX-mediated pathway, when CAR or $\alpha_v\beta_{3,5}$ integrins are unavailable. Studies on spleen transduction are more controversial, but a tendency for $\alpha_v\beta_{3,5}$ integrins to be involved in spleen transduction has been reported in several studies. This is in contrast with our data, where neither C57BL/6 nor Rag $2^{-/-}$ mice spleen transduction levels were reduced by the $\alpha_v\beta_{3,5}$ integrin-binding ablating mutation RGE. Interestingly, this mutation enhanced localization of vectors to the spleen MZ, where phagocytic cells such as MARCO-positive scavenging macrophages and Moma-1 (CD169)-positive marginal metallophilic macrophages have been shown to trap HAdV-5 particles at early time-points following adenovirus administration (Di Paolo et al., 2009a). Also, it was found that the presence of the RGE mutation in FX-binding deficient vectors (AdT*RGE) enhanced liver and spleen transduction in C57BL/6, Rag $2^{-/-}$ and NSG mice. These data is in contrast with one study using the same vector that showed no differences on liver or spleen transduction in MF1 mice compared to the control vector (Bradshaw et al., 2012). However, these differences might be due to strain-specific processes. Previous studies reported that macrophage β3 integrins can interact with the adenovirus RGD motif and induce an innate antiviral immune response via production of IL-1β (Di Paolo et al., 2009a). The lack of binding to β3 integrins in RGD-mutated vectors might impair adenovirus recognition and engulfment by macrophages via the β3 integrin-mediated pathway, resulting in an increase in the amount of adenovirus available to transduce non-immune cells in tissues such as liver and spleen. However, although this effect might be more evident when using low viral doses (1 to $3x10^{10}$ vp/mouse), which are completely taken up by immune cells (Tao et al., 2001), the use of a high viral dose ($1x10^{11}$ vp/mouse) in our studies that saturates resident macrophages in the liver (Tao et al., 2001) would have been expected to attenuate the effects associated with macrophage sequestration. Nevertheless, the immune response against AdT*RGE was investigated in Rag $2^{-/-}$ and NSG mice. No significant differences were found in any of the cytokines analysed. However, since the innate immune response decreases with age (Grolleau-Julius et al., 2006, Wong et al., 2010, Pereira et al., 2011, Wong and Goldstein, 2013, Zacca et al., 2015) and the mice used in this experiment were 19-21 weeks old, the response might have been slightly attenuated. Assessment of cytokine levels in liver and spleen tissue could help in detecting subtle changes between groups that might not be detectable in serum. Also, increasing the sample size of the experimental groups would help in increasing the experimental power and confirming results. Finally, further experiments would be necessary to draw conclusions on the involvement of CAR and $\alpha_v\beta_{3,5}$ integrins on mouse

liver and spleen transduction and to determine the influence of the $\alpha_v\beta_{3,5}$ integrin-binding ablating RGE mutation on AdT* vectors and the resulting effects on liver and spleen transduction.

3.4.3 Pathways of *in vitro* HAdV-5 transduction after exposure of virions to mouse serum

Together with previous reports (Xu et al., 2013, Zaiss et al., 2015, Martin et al., 2003), evidence that FX, CAR and $\alpha_v\beta_{3,5}$ integrins might be dispensable for liver transduction in immunocompetent and immunocompromised mice suggests that alternative pathways of adenovirus transduction are present *in vivo*. Moreover, transduction experiments *in vitro* revealed that HAdV-5 can follow FX-independent pathways for cell transduction after exposure to immunocompetent and immunocompromised mice serum. Interestingly, evidence of such pathways in the presence of serum from different strains of immunocompromised mice suggests that these pathways might be conserved across mouse strains. Also, the use of FX-independent pathways in this setting was confirmed for several cell lines, suggesting that these pathways might be widely used. Interestingly, they were also observed in hepatocyte-derived HepG2 cells, indicating that HAdV-5 might potentially use these pathways for hepatocyte transduction *in vivo*. Here, it was found that in this setting HAdV-5 can use CAR via an indirect mechanism that involves a mouse serum protein able to bridge HAdV-5 to CAR (Figure 3-35). The biological relevance of CAR as a receptor for HAdV-5 transduction has historically been quite controversial. CAR has been reported as a receptor for adenovirus species A, C, D, E, F and G (Roelvink et al., 1998, Lenman et al., 2015). However, the localization of CAR on the basolateral side of the plasma membrane (Walters et al., 1999, Cohen et al., 2001) hinders its use as a receptor for replicating adenovirus infecting intact epithelium and for non-replicating adenoviruses. The CAR amino acid sequence is highly conserved, with a 83% homology and conservative amino acid substitutions in differing positions between human and mouse CAR (Tomko et al., 1997, Bergelson et al., 1998). hCAR is a 46 kDa transmembrane glycoprotein that belongs to the immunoglobulin (Ig) superfamily and is composed of a leader sequence (LS), two Ig-like domains (D1 and D2), a transmembrane domain and a cytoplasmic domain containing a class I PSD95/DlgA/ZO-1 (PDZ)-binding domain involved in interactions with several proteins (Bergelson et al., 1997, Cohen et al., 2001, Excoffon et al., 2010). The D1 distal domain is involved in direct binding to adenovirus (Roelvink et al., 1999, Lortat-Jacob et al., 2001, Freimuth et al., 1999, Kirby et al., 2000, Bewley et al., 1999), while D2 domain facilitates D1:HAdV-5 interaction (Excoffon et al.,

2005). hCAR is encoded by the highly conserved gene *CXADR* composed of 8 exons (Bowles et al., 1999), which via alternative splicing results in three soluble isoforms and two transmembrane isoforms (Thoelen et al., 2001, Dorner et al., 2004). The transmembrane isoforms (CAR^{Ex7} and CAR^{Ex8}) are both composed of LS, D1, D2 and transmembrane domains but they differ in the last 26 (CAR^{Ex7}) or 13 (CAR^{Ex8}) amino acids of the cytoplasmic domain (Excoffon et al., 2010). Recent studies show that the isoform that localizes to the basolateral side of polarized epithelia with a role in cell-cell adhesion corresponds to CAR^{Ex7}, the most abundant isoform. Interestingly, CAR^{Ex8} isoform has been reported to localize to the apical membrane and be negatively regulated by basolateral hCAR (CAR^{Ex7}) through interactions with the membrane-associated guanylate kinase inverted 1 (MAGI-1)b (Excoffon et al., 2010). Also, the expression of apical hCAR (CAR^{Ex8}) is stimulated by the pro-inflammatory cytokine and neutrophil chemoattractant IL-8, which is in turn induced by HAdV-5 fiber binding to CAR (Tamanini et al., 2006), through activation of AKT/S6K and inhibition of GSK3β (Kotha et al., 2015). Apical hCAR enhances the adhesion of transmigrating neutrophils at the apical surface of polarized epithelium and the presence of neutrophils on the apical surface has been associated with the promotion of adenovirus entry to host cells (Kotha et al., 2015). Of note, IL-8 also induces re-localization of $\alpha_v\beta_3$ integrin to the apical side of polarized cells via activation of Src-family tyrosine kinases enabling HAdV-5 transduction (Lutschg et al., 2011). These studies suggest that adenovirus evolved to stimulate the expression of its own receptors to allow infection of intact epithelium from the apical side and support a possible role for the apical hCAR isoform on adenovirus transduction. Moreover, it was reported that the intrinsic expression levels of basolateral and apical hCAR can vary between tissues (Shaw et al., 2004) and, in particular, while basolateral hCAR was poorly expressed in liver, apical hCAR was mainly expressed in liver over heart, brain and lung (Excoffon et al., 2010). Evidence that apical hCAR is highly expressed in liver and that HAdV-5 can follow a CAR-mediated mechanism for *in vitro* transduction after exposure to mouse serum might begin to unravel the high liver tropism found when administering HAdV-5 through the vasculature. Furthermore, since the use of CAR as a receptor for cell transduction by HAdV-5 has been shown to stimulate the immune response by inducing transcription of inflammatory genes (Tamanini et al., 2006), future studies should address whether this response is also promoted upon HAdV-5 following the CAR-mediated pathway in the presence of mouse serum.

Interestingly, while the CAR-mediated pathway was found as the predominant route for HAdV-5 transduction in the presence of immunocompromised mouse serum in high CAR-

expressing cell lines, a partial response to the FX-inhibitor X-bp was also observed, suggesting that the FX-mediated and the CAR-mediated HAdV-5 transduction pathways may be available simultaneously. These results suggest that availability of cellular receptors such as CAR or HSPG might determine which transduction pathway is followed in the presence of mouse serum. This observation is in agreement with previous studies showing that other receptors such as CD46 might compete with FX for binding to other adenovirus serotypes such as HAdV-35 (Greig et al., 2009). Moreover, it was unexpectedly found that blockade of CAR decreased FX-mediated transduction, suggesting that HAdV-5 attachment to CAR might also facilitate the use of the FX-mediated pathway at some level. A previous report showed that while optimal adenovirus transport to the MTOC via FX-mediated cell uptake requires the post-attachment internalisation signal provided by integrins, it does not require CAR (Bradshaw et al., 2010). However, the influence of CAR on other processes such as adenovirus binding to host cells in the presence of FX was not assessed. Alternatively, when the CAR-mediated pathway is unavailable due to limited access to CAR on the plasma membrane, our data indicates that HAdV-5 can use other pathways for cell entry. Here, HAdV-5 transduced CAR^{low} SKOV3 cells via the FX-mediated pathway in the presence of Rag $2^{-/-}$ serum, as previously reported (Ma et al., 2015). Furthermore, other mechanisms of HAdV-5 cell transduction in the presence of mouse serum might be present. For instance, HAdV-5 transduced CAR^{low} ACHN and $CAR^{negative}$ MCF7 cells in the presence of Rag $2^{-/-}$ serum via a mechanism independent of FX and CAR. These mechanisms might involve other receptors that have been described to interact with species C adenovirus such as $\alpha_v\beta_{3,5}$ integrins, VCAM-1 (Chu et al., 2001), MHC-I-α2 (Hong et al., 1997, Davison et al., 1999), SR (Khare et al., 2012), LRP (Shayakhmetov et al., 2005b) or CR1 (Carlisle et al., 2009). The potential existence of several FX-independent pathways for HAdV-5 transduction *in vitro* in the presence of mouse serum brings into discussion how many mechanisms of HAdV-5 transduction are yet to be identified and whether they might be relevant *in vivo.* It remains unclear what factors determine which pathway of HAdV-5 transduction is followed after exposure to mouse serum. Previous work suggested that the levels of expression of specific cellular receptors or their relative abundance on susceptible cells might dictate which transduction pathway is used for adenoviral transduction (Zaiss et al., 2011). Also, the affinity of the adenoviral capsid for individual components of the different transduction pathways (e.g: receptors, bridging molecules, etc.) might also determine the route of entry. For instance, a previous report showed that the ability of HAdV-5:hFX or HAdV-5:mFX complexes to enhance transduction *in vitro* was determined by their affinity for HSPG (Zaiss et al., 2011). Evidence that several FX-independent transduction pathways exist in the presence

of mouse serum and that HAdV-5 can potentially use different pathways to transduce a single cell line has direct implications on our study. For instance, it highlights the need for further experiments to confirm that HAdV-5 KO1 is able to use the CAR-mediated pathway in the presence of mouse serum and it does not use other FX-independent pathways in this setting, which is key to confirm the existence of a bridging mechanism for CAR-mediated transduction.

3.4.4 Mouse serum factor(s) mediating *in vitro* HAdV-5 transduction after exposure of virions to mouse serum

The mouse serum factor involved in CAR-mediated HAdV-5 transduction in the presence of mouse serum (Figure 3-35) has not been identified yet. However, several mouse serum proteins have been reported to interact with HAdV-5 and potentially enhance transduction. These include FVII (Parker et al., 2006), FIX (Parker et al., 2006, Shayakhmetov et al., 2005b, Kalyuzhniy et al., 2008), C4BP (Shayakhmetov et al., 2005b) and PC (Parker et al., 2006, Kalyuzhniy et al., 2008). One study shows that FVII might slightly enhance HAdV-5 transduction (Parker et al., 2006). As found for HAdV-5:FX interaction, FVII can bind to HAdV-5 amino acid motif 423TET425 in the HVR 7 through the residue R28 in FVII GLA domain (Irons et al., 2013). However, despite FVII contains a heparin-binding exosite (Martinez-Martinez et al., 2011, Irons et al., 2013), another study shows that FVII is unable to interact with HSPG due to the formation of dimers between the SP domains (Irons et al., 2013). FIX was reported to bind to HAdV-5 (Kalyuzhniy et al., 2008) and to contain a heparin-binding exosite in similarity to that in FVII that could potentially be used for binding to HS on the plasma membrane (Yang et al., 2002, Johnson et al., 2010). FIX enhanced HAdV-18 binding to and infection of epithelial cells (Lenman et al., 2011) and HAdV-31 binding to and infection of epithelial cells via HS-GAG (Jonsson et al., 2009, Lenman et al., 2011). Interestingly, FIX enhanced HAdV-5 transduction of mouse hepatocytes and Kupffer cells *in vitro* and *in vivo*, and human hepatocytes *in vitro* (Shayakhmetov et al., 2005b). C4BP allowed primary human hepatocyte transduction *in vitro* in a CAR-independent manner (Shayakhmetov et al., 2005b), and PC mediated CAR-independent HAdV-5 transduction of HepG2 cells (Parker et al., 2006). Moreover, it would be interesting to investigate other vitamin K-dependent coagulation factors such as prothrombin or protein S, which contain GLA domains that might potentially bind to HAdV-5 and mediate cell transduction in the presence of mouse serum. Here, it was found that both hFX and the factor(s) involved in FX-independent mouse serum-enhanced HAdV-5 transduction are heat-labile. Transduction assays in the presence of heat-treated

recombinant mFX should be done to confirm results. Also, pull-down assays such as tandem affinity purification (TAP), co-immunoprecipitation using an anti-adenovirus antibody, SPR, cross-linking or mass spectrometry performed on HAdV-5 after incubation with mouse serum would help in identifying the mouse blood factor involved in the CAR-mediated pathway.

Finally, future experiments using more translationally relevant animal models would provide valuable information on the interplay between adenovirus immune recognition and cellular uptake mechanisms and how the data obtained from mouse experimentation may translate into humans. A recent study showed high variability on the effect of human serum (with no pre-existing neutralising hIgG antibodies) on HAdV-5 neutralization and transduction *in vitro* (Duffy et al., 2016). This study demonstrated a protective role for FX binding to HAdV-5 capsids against neutralization in 56% of human serum samples analysed and of the remaining 44% that did not neutralize HAdV-5 in the absence of FX-binding some enhanced transduction in a complete FX-dependent manner and others in a partial FX-dependent manner (Duffy et al., 2016). Understanding of the complex adenovirus biology is essential for the optimization and development of adenoviral vectors for gene therapy.

Chapter 4 Investigating the effect of FX:HAdV-5 interaction on virion uptake and endosomal membrane penetration

4.1 Introduction

HAdV-5 exploits interactions with blood components such as FX for host cell transduction and protection against virion neutralization (Parker et al., 2006, Xu et al., 2013). In particular, binding of HAdV-5 hexon to FX facilitates access to HSPG on the plasma membrane of host cells (Parker et al., 2006, Kalyuzhniy et al., 2008, Waddington et al., 2008, Alba et al., 2009, Bradshaw et al., 2010). The interactions that take place between HAdV-5 and FX have been carefully described both *in vitro* and *in vivo*, as well as the interactions between FX and HSPG (Waddington et al., 2008, Alba et al., 2009, Bradshaw et al., 2010, Duffy et al., 2011, Doronin et al., 2012). However, the effect of FX on the different stages of the HAdV-5 cell entry pathway (virion binding to plasma membrane, uptake, escape from endosomal vesicles, trafficking towards the nucleus and nuclear import) and whether interaction of virions with additional co-receptors is required for FX-mediated transduction has not been defined in detail yet (Figure 4-1). FX was reported to increase binding of virions to host cells (Alba et al., 2009, Bradshaw et al., 2012). Another study addressed whether the presence of CAR or α_v integrins might be necessary for FX-mediated cell entry *in vitro* and reported that HAdV-5 vectors ablated for α_v integrin-binding had a delayed cell entry in contrast to CAR-binding deficient HAdV-5 vectors (Bradshaw et al., 2010). This suggests that an efficient post-attachment internalisation signal might be necessary for HAdV-5 optimal transport to the nucleus following FX-mediated cell surface attachment. No other studies have assessed whether FX remains bound to HAdV-5 capsids during viral cell entry or the influence that the presence of FX might have on capsid disassembly, uptake of virions, escape from endosomal vesicles, transport of nucleocapsids along the microtubule network and docking onto the NPC.

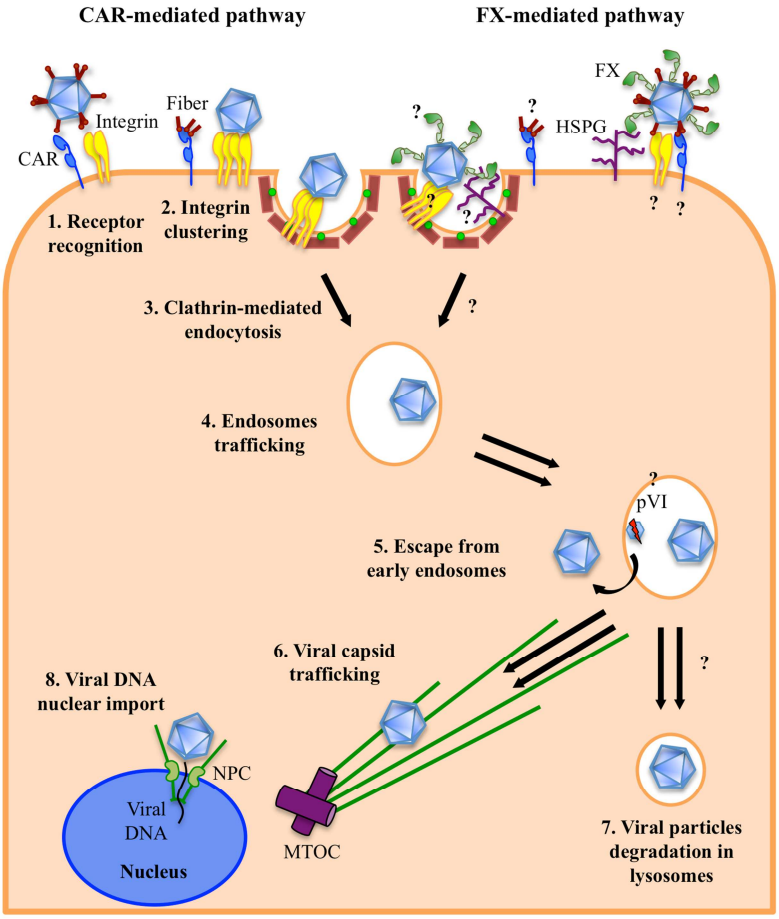

Figure 4-1. Species C adenovirus *in vitro* transduction pathways. 1. Adenovirus attaches to the plasma membrane via CAR and $\alpha_v\beta_1$, $\alpha_M\beta_2$, $\alpha_v\beta_3$ and $\alpha_v\beta_5$ integrins. **2.** Adenovirus binding to integrins promotes integrins clustering. **3.** Adenoviral binding to $\alpha_v\beta_1$, $\alpha_v\beta_3$ and $\alpha_v\beta_5$ integrins promotes internalization of viral particles via clathrin-mediated endocytosis. **4.** Viral capsids traffic in the endosomes. **5.** Adenoviral capsids escape from early endosomes in a process mediated by pre-protein VI (pVI). **6.** Viral capsids travel along the microtubule network towards the nucleus. **7.** A percentage of incoming adenoviruses get degraded in the lysosomes. **8.** Adenoviral DNA is imported into the nucleus. CAR; coxsackie and adenovirus receptor, HSPG; heparan sulphate proteoglycan, FX; coagulation factor X, MTOC; microtubule-organizing centre, TP; terminal protein, NPC; nuclear pore complex.

With the aim of studying these processes at the single cell level, new methods such as the SLO penetration assay emerged (Suomalainen et al., 2013). The SLO penetration assay was developed to allow the study of adenovirus uptake and endosomal membrane penetration (Figure 4-2A). In this assay, cells are incubated with Alexa Fluor 488-labelled viral vectors and pores are subsequently generated in the plasma membrane of transduced cells using the bacterial toxin SLO. This protein is a thiol-activated cholesterol-dependent cytolysin toxin from *Streptococcus pyogenes* (Tweten, 2005, Hotze and Tweten, 2012) that binds as a monomer to cholesterol in the plasma membrane and via oligomerization of 50-80 subunits can form pores of variables sizes (up to ~30 nm diameter) (Bhakdi et al., 1985, Palmer et al., 1998, Niedermeyer, 1985, Hugo et al., 1986, Sekiya et al., 1993). A representation of a SLO monomer is shown in Figure 4-2B. The formation of SLO pores on the plasma membrane allows access of antibodies into the cell cytosol that recognize

Alexa Fluor 488 dye on cytosolic viral particles. In contrast, viral particles located in the endosomes remain inaccessible to antibody recognition. Thus, viral particles can be classified into plasma membrane-associated plus cytosolic viral particles (Alexa Fluor 488 and antibody-positive) or endosomal viral particles (Alexa Fluor 488-positive and antibody-negative). Via the classification and quantification of viral particles, virus uptake and endosomal membrane penetration efficiencies can be determined. Furthermore, the use of penetration-deficient HAdV-2 ts1 allows the assessment of endosome integrity within the experimental conditions. HAdV-2 ts1 is a HAdV-2 vector belonging to species C that has the P137L mutation in the AVP (Rancourt et al., 1995), which is located in a surface-exposed loop in proximity to 3 cysteine residues (C104, C122 and C126) that are important for enzyme activity (Rancourt et al., 1994). This point mutation prevents correct protein folding and incorporation of the AVP into the adenoviral capsid (Rancourt et al., 1995). Since AVP is involved in degradation of the capsid-stabilizing pVI (Rancourt et al., 1995, Weber, 1976, Greber et al., 1996, Ruzindana-Umunyana et al., 2002) to allow penetration from endosomes (Maier et al., 2010, Moyer et al., 2011, Wiethoff et al., 2005), HAdV-2 ts1 gets trapped in the endosomes and degraded in lysosomes (Greber et al., 1996, Imelli et al., 2009, Gastaldelli et al., 2008).

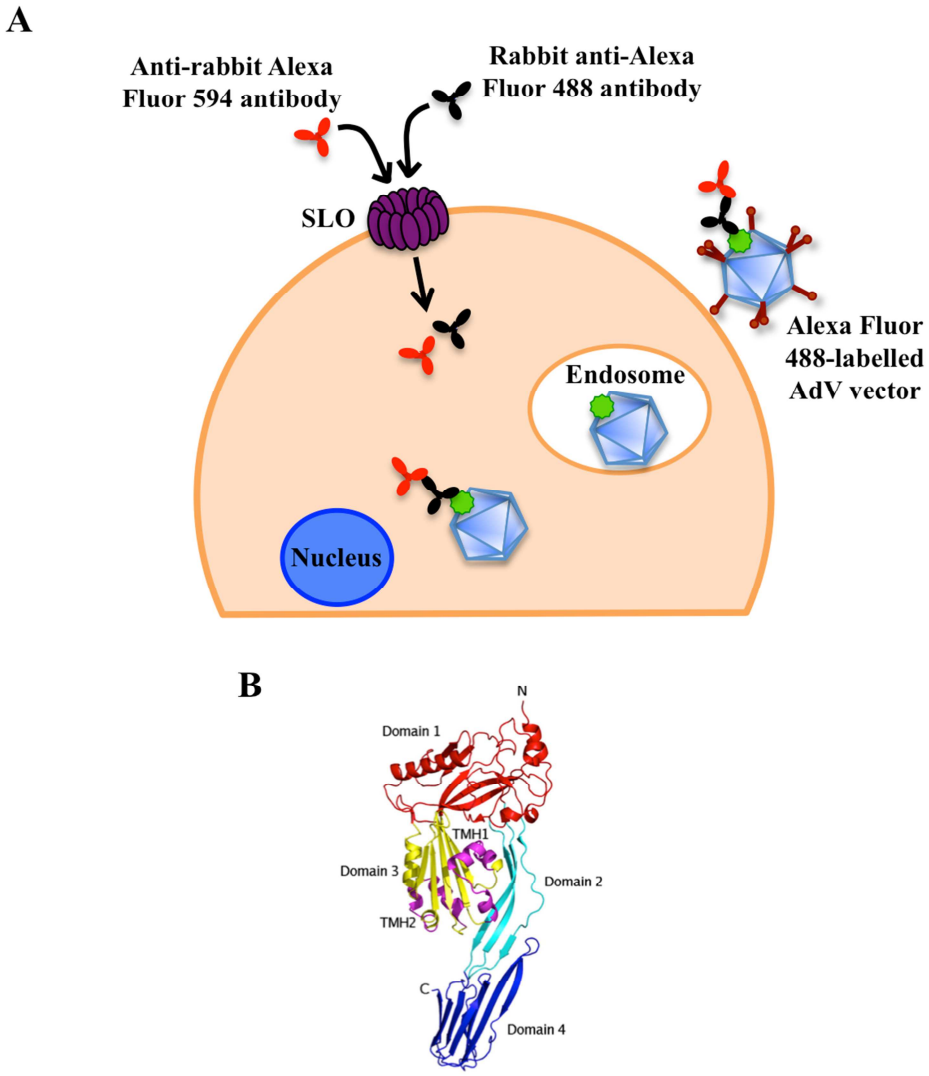

Figure 4-2. SLO penetration assay. A) Graphical representation of the SLO penetration assay that allows measurement of virus uptake and endosomal membrane penetration into the cytosol of host cells. Viral particles are classified as plasma membrane-associated plus cytosolic (Alexa Fluor 488 and antibody-positive) or endosomal (Alexa Fluor 488-positive and antibody-negative). Alexa Fluor 488 (green), primary antibody (black) and secondary antibody (red). B) Ribbon diagram of the crystal structure of SLO [with permission from (Feil et al., 2014)]. Domain 1 (red), domain 2 (cyan), domain 3 (yellow), domain 4 (dark blue), and TMH1 and TMH2 regions (magenta). N; NH_2-terminal, AdV; adenovirus.

Here, the effect of FX binding to HAdV-5 capsid on adenovirus uptake and endosomal membrane penetration was investigated by performing the SLO penetration assay. This work was undertaken in the Institute of Molecular Life Sciences at the University of Zurich under the supervision of Professor Urs Greber and Dr. Maarit Suomalainen as part of the Marie Curie ITN ADVance programme.

4.2 Aims

The aims of the present study were:

- To investigate the effect of FX binding to HAdV-5 capsid on adenovirus uptake.
- To investigate the effect of FX binding to HAdV-5 capsid on adenovirus endosomal membrane penetration.

4.3 Results

4.3.1 Generation and validation of adenoviral vectors

Adenoviral vectors used in this study were replication-deficient HAdV-5-based adenoviral vectors encoding the *E.coli LacZ* gene (β-galactosidase). A summary of the adenoviral vectors' genetic and receptor recognition characteristics is shown in section 2.1.6.

Adenoviral vectors were amplified from pure adenoviral vector preparations originated from a single plaque and the resultant pure adenoviral vector preparations were confirmed for the absence of RCAs, presence of genetic modifications and absence of virion aggregates (Table 4-1), as before (see section 3.3.1.2).

Table 4-1. Quality control of adenoviral vectors.

Adenoviral vector	Titre (vp/ml)	Titer (pfu/ml)	Vp/pfu	Vp diameter (nm)
HAdV-5	$4.33x10^{12}$	N/T	N/T	102
HAdV-5-Alexa Fluor 488	$7.04x10^{11}$	$1.39x10^{9}$	506.47	106
AdT*	$5.90x10^{12}$	N/T	N/T	99
AdT*-Alexa Fluor 488	$3.25x10^{12}$	$1.35x10^{10}$	240.74	113
HAdV-2 ts1-Alexa Fluor 488	$2x10^{12}$	N/A	N/A	N/T

Plaque forming units (pfu/ml) values shown were obtained with the pfu observed after performing X-Gal staining. Values of viral particle (vp) diameter by Nanoparticle Tracking Analysis (NanoSight) are the mean of technical triplicates. HAdV-5; human adenoviral vector serotype 5, N/T; not tested, N/A; not applicable.

In order to perform the SLO penetration assay to study HAdV-5 uptake and endosomal membrane penetration in the presence of FX, HAdV-5 was fluorescently-labelled with Alexa Fluor 488 dye (Figure 4-3), which reacts with primary amines on the adenoviral capsid proteins. The FX-binding deficient control vector AdT* was also fluorescently-labelled with Alexa Fluor 488 dye. Alexa Fluor 488 labelled HAdV-2 ts1 was kindly provided by Professor Urs Greber (University of Zurich, Switzerland). Pure Alexa Fluor

488-labelled adenoviral vector preparations were assessed for their viral particle concentration (vp/ml) and infectivity (pfu/ml), and vp/pfu ratios of 506.47 and 240.74 were obtained for Alexa Fluor 488-labelled HAdV-5 and AdT*, respectively (Table 4-1).

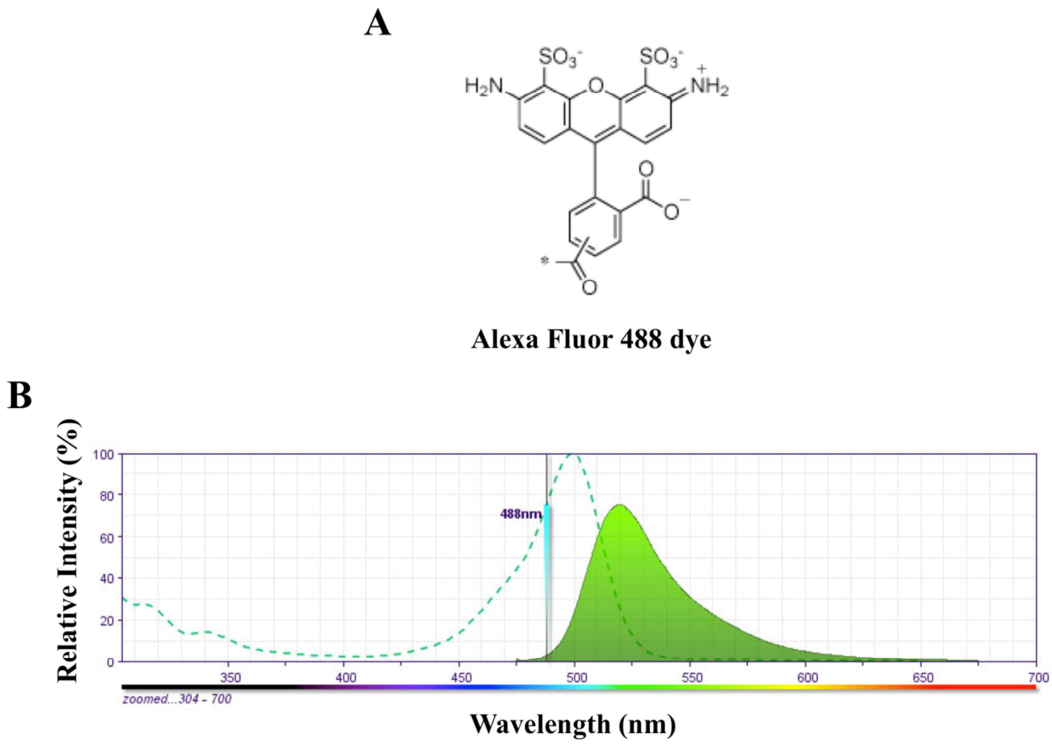

Figure 4-3. Alexa Fluor 488 dye. A) Chemical structure of Alexa Fluor 488 fluorophore. B) Fluorescence spectra of Alexa Fluor 488 dye. Absorption spectral profile (dotted line) and emission spectral profile (green filled area). Image reproduced from BD Biosciences.

4.3.1.1 Effect of FX on Alexa Fluor 488-labelled HAdV-5

To confirm that the ability of FX to bind to HAdV-5 and enhance cell binding and transduction was preserved on Alexa Fluor 488-labelled HAdV-5, CAR^{high} A549 or CAR^{low} SKOV3 cells were incubated with Alexa Fluor 488-labelled HAdV-5 in the presence or absence of hFX at 0^{o}C for 60 min ("0 min" condition) to assess cell binding or subsequently incubated at 37^{o}C for 60 min ("60 min" condition) to allow virion internalization and transport along the microtubules towards the MTOC and the nucleus, a process that takes around 45 min to be completed (Greber et al., 1993). Alexa Fluor 488-labelled AdT* was used as a negative control, since it lacks binding to FX and thus cell binding and transduction is not affected by the presence of FX. After the incubation time, cells were subjected to immunocytochemistry using antibodies that specifically recognize pericentrin, which is an integral component of the MTOC, to enable colocalization analysis. As expected, both HAdV-5 and AdT* colocalized with the MTOC in A549 and SKOV3 cells in the "60 min" condition both in the presence or absence of FX (Figure 4-4).

In contrast, colocalization was not observed in cells in the “0 min” condition with or without FX (Figure 4-4). Presence of FX increased HAdV-5 binding and transduction of A549 cells (Figure 4-4A) and SKOV3 cells (Figure 4-4B). As expected, AdT* binding and transduction of A549 (Figure 4-4A) and SKOV3 (Figure 4-4B) cells was unaffected in the presence of FX. IgG isotype controls for antibodies confirmed specificity (Figure 4-4C).

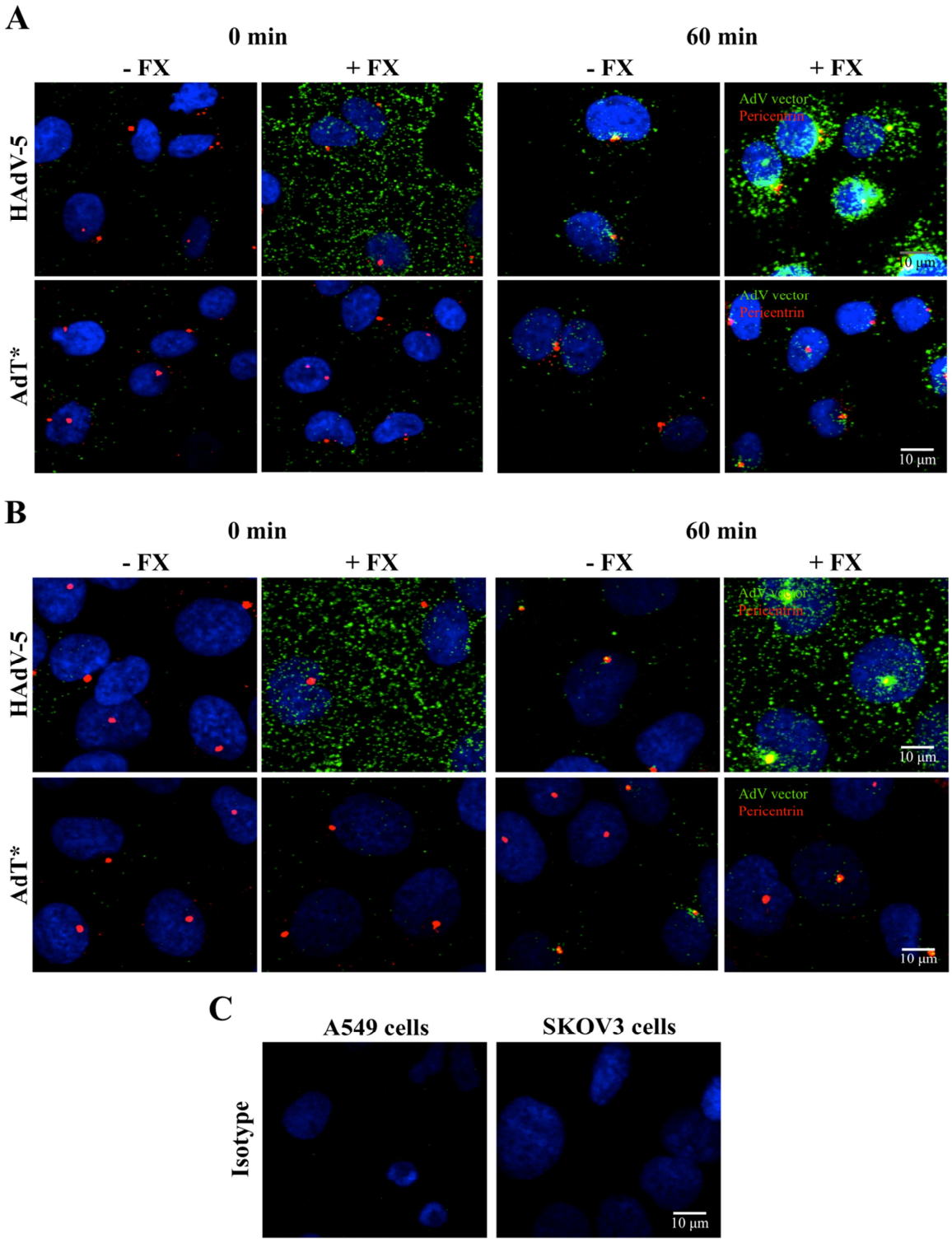

Figure 4-4. Effect of FX on adenoviral cell binding and transduction. A549 (A) or SKOV3 (B) cells were incubated with Alexa Fluor 488-labelled HAdV-5 or AdT* ($1x10^5$ vp/cell) for 60 min at 0^oC ("0 min" condition) or further incubated for 60 min at 37^oC ("60 min" condition) in the presence or absence of recombinant human FX (10 µg/ml). Alexa Fluor 488-labelled HAdV-5 (green). Rabbit anti-pericentrin primary antibody and Alexa Fluor 546-conjugated goat anti-rabbit IgG secondary antibody were used to stain the microtubule-organizing centre (MTOC) (red). Nuclei were counterstained with DAPI (blue). n = 1 biological replicate with 1 technical replicate. Representative merge images are shown. Yellow indicates viral particles colocalizing with MTOC. Scale bar 10 µm. AdV; adenovirus, FX; coagulation factor X.

4.3.2 HAdV-5 uptake and endosomal membrane penetration via the CAR-mediated pathway *in vitro*

4.3.2.1 Assessment of correct pore formation by SLO on the cell surface

First, it was confirmed that SLO pores can be successfully formed on the surface of A549 cells under the experimental conditions, resulting in plasma membrane permeabilization and thus allowing access of antibodies into the cytosol for adenovirus recognition. A549 cells were incubated with Alexa Fluor 488-labelled HAdV-5 on ice for 60 min to synchronize adenovirus internalization and subsequently at 37°C for 45 min, permeabilized with SLO and stained for Giantin, a Golgi membrane protein conserved in several mammalian cell types (Linstedt and Hauri, 1993). Giantin was successfully stained in SLO-treated cells in the presence of HAdV-5 (Figure 4-5A left panel) in similarity to SLO-treated cells in the absence of adenovirus, which were used as a control (Figure 4-5C), indicating that the primary antibody was able to access the cytosol and thus confirming A549 cells can be SLO-permeabilized.

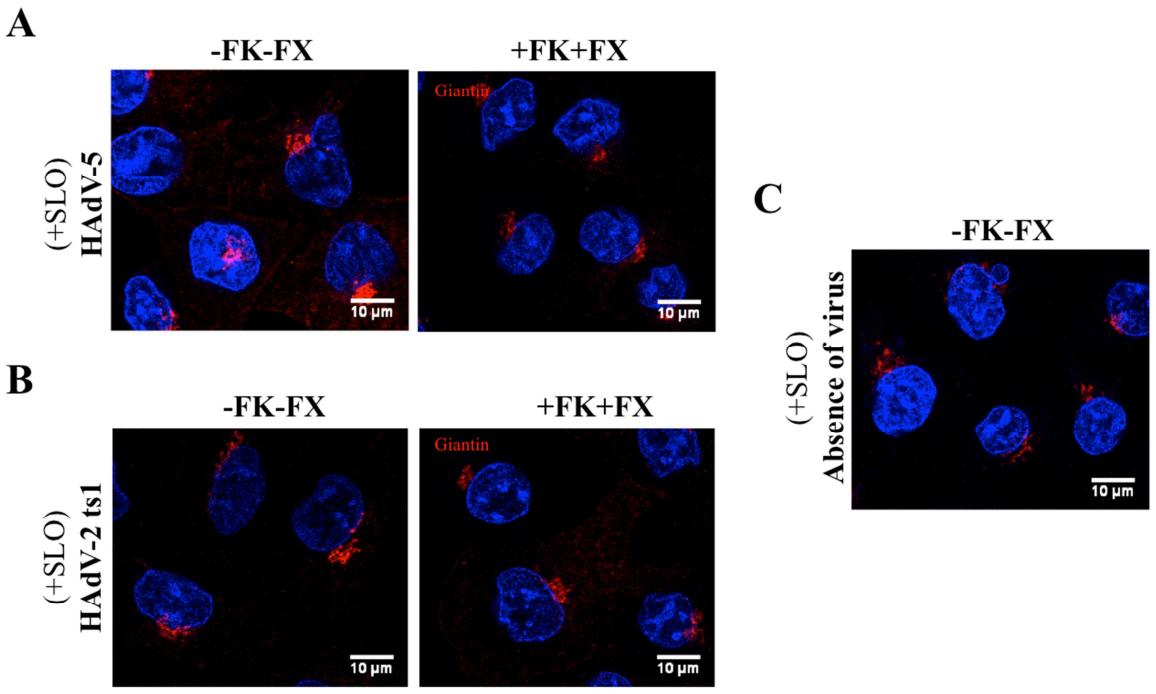

Figure 4-5. SLO pores formation in A549 cells. Cells were incubated with Alexa Fluor 488-labelled HAdV-5 (A), Alexa Fluor 488-labelled HAdV-2 ts1 (B) or serum-free media (C) for 45 min at 37°C in the presence or absence of soluble recombinant HAdV-5 fiber knob (FK) (0.4 µg/ml) and recombinant human FX (10 µg/ml) and permeabilized with SLO (2.48 µg/well). Mouse anti-human Giantin IgG1 primary antibody and Alexa Fluor 680-conjugated goat anti-mouse IgG secondary antibody were used to stain Giantin (red). Nuclei were counterstained with DAPI (blue). n = 1 biological replicate with 1 technical replicate. Representative images of maximum projections of individual confocal stacks are shown. Scale bar 10 µm.

4.3.2.2 HAdV-5 uptake and endosomal membrane penetration *in vitro*

Once the correct formation of SLO pores on A549 cells was confirmed, uptake and endosomal membrane penetration of HAdV-5 particles following the CAR-mediated pathway was investigated. A549 cells were incubated with Alexa Fluor 488-labelled HAdV-5 for 45 min at 37°C and intact (non-permeabilized) or SLO-permeabilized cells were incubated with rabbit anti-Alexa Fluor 488 antibody to detect adenoviral particles.

To study HAdV-5 uptake, antibody-positive viral particles on intact A549 cells after 45 min incubation (plasma membrane-associated viral particles) were imaged (Figure 4-6) and quantified (Figure 4-7). For the first independent experiment performed, 4.2% of viral particles were detected by the antibody (Figure 4-7A), indicating that 4.2% of viral particles remained on the surface after virus internalization. These results indicate that HAdV-5 uptake efficiency via the CAR-mediated pathway was 95.8%. For the second independent experiment performed, it was found that 4.8% of viral particles were membrane-associated viral particles (Figure 4-7B), resulting in a HAdV-5 uptake efficiency via the CAR-mediated pathway of 95.2%.

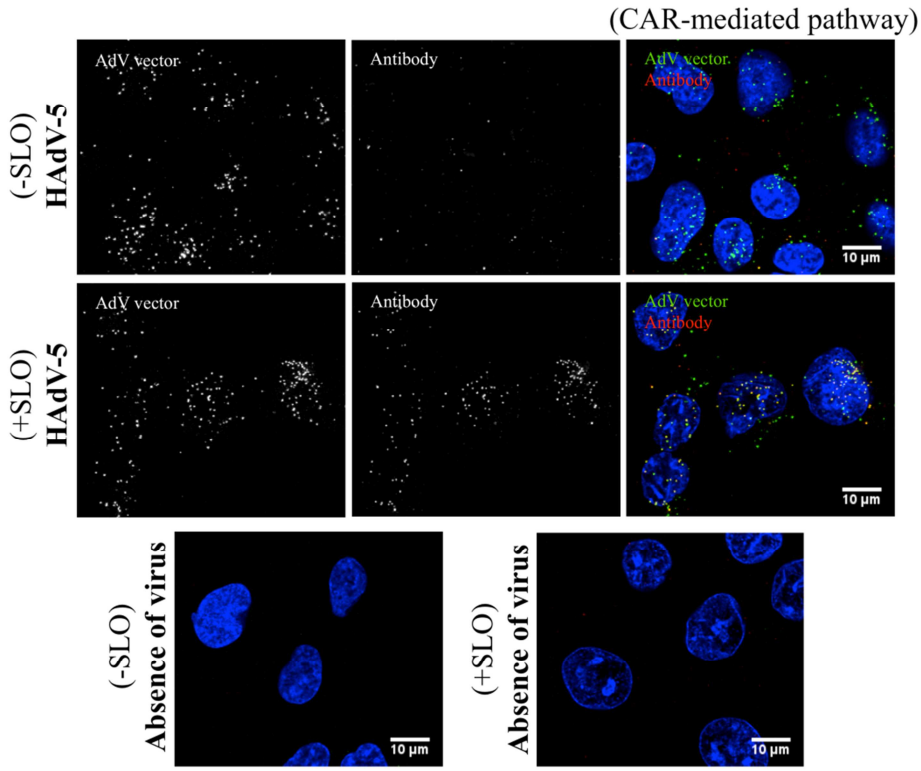

Figure 4-6. HAdV-5 internalization via the CAR-mediated pathway *in vitro*. Cells were incubated with Alexa Fluor 488-labelled HAdV-5 for 45 min at 37°C and permeabilized or not with SLO (2.48 µg/well). Rabbit anti-Alexa Fluor 488 primary antibody and Alexa Fluor 594-conjugated goat anti-rabbit IgG secondary antibody were used. Alexa Fluor 488-labelled HAdV-5 (green). Alexa Fluor 594-conjugated goat anti-rabbit IgG secondary antibody puncta (red) correspond to plasma membrane-associated (-SLO) or

plasma membrane-associated plus cytosolic (+SLO) viral particles. Nuclei were counterstained with DAPI (blue). n = 2 biological replicates with 1 technical replicate. Representative images of maximum projections of individual confocal stacks are shown. In the merge image, yellow indicates viral particles double-positive for Alexa Fluor 488 and Alexa Fluor 594-conjugated goat anti-rabbit IgG antibody. Scale bar 10 µm. AdV; adenovirus, CAR; coxsackie and adenovirus receptor.

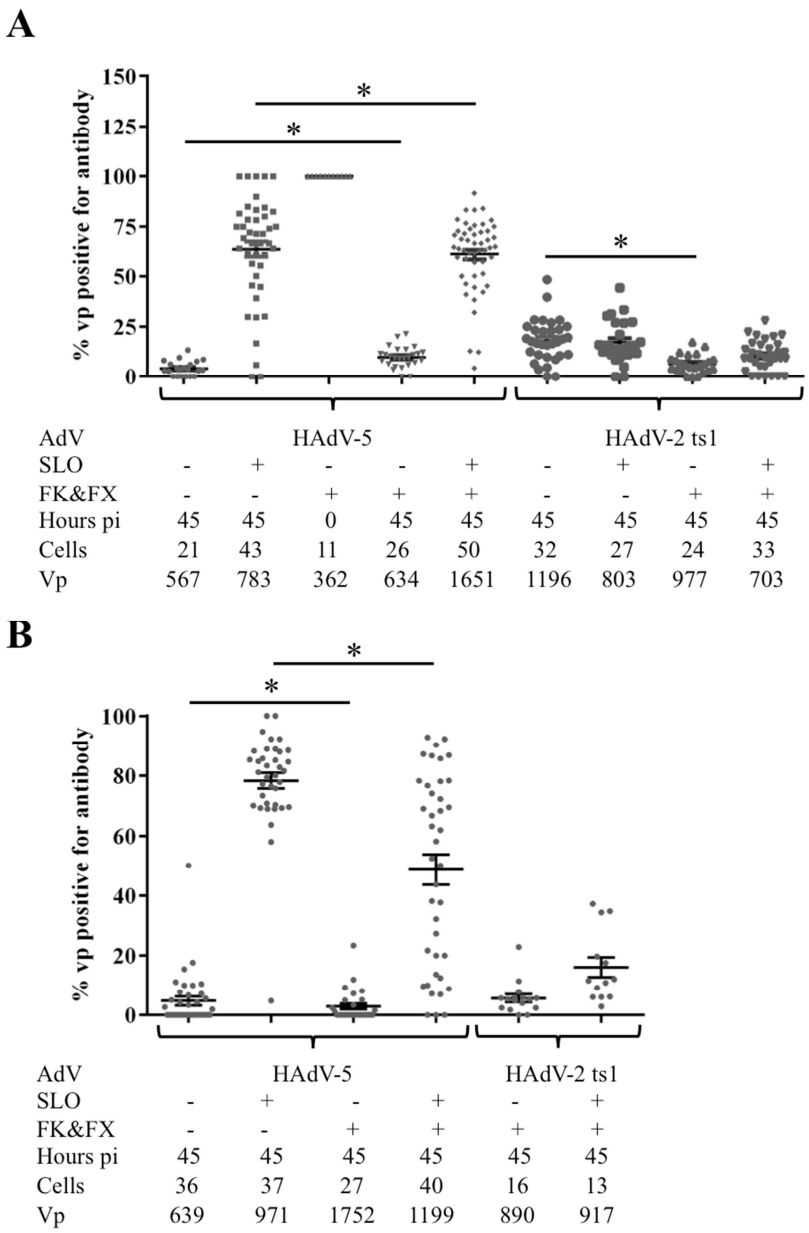

Figure 4-7. Quantification of antibody-positive HAdV-5 particles following the CAR or the FX-mediated pathway *in vitro*. Cells were incubated with Alexa Fluor 488-labelled HAdV-5 or Alexa Fluor 488-labelled HAdV-2 ts1 for 45 min at 37°C with or without soluble recombinant fiber knob (FK) (0.4 µg/ml) and recombinant human FX (10 µg/ml) and permeabilized or not with SLO (2.48 µg/well). Rabbit anti-Alexa Fluor 488 primary antibody and Alexa Fluor 594-conjugated goat anti-rabbit IgG secondary antibody were used for viral particles detection. Maximal projections of confocal stacks were analysed by a custom-programmed MatLab (The Mathworks) routine to score and quantify individual virus particles (vp). The plots show the percentages of Alexa Fluor 594-conjugated goat anti-rabbit IgG secondary antibody-positive vp in two independent experiments [first independent experiment (A), second independent experiment (B)] with 1 technical replicate per condition. Each dot represents one cell and numbers of cells and viruses analysed per condition are indicated. Values are expressed as the mean +/- SEM. Two-tailed Mann-Whitney *U* test applied. *p<0.05. pi; post-start of incubation of cells with adenovirus at 37°C (time of internalization).

To study HAdV-5 endosomal membrane penetration, viral particles were classified as plasma membrane-associated plus cytosol-associated (Alexa Fluor 488 and antibody-positive) or endosomal (Alexa Fluor 488-positive but antibody-negative) in SLO-permeabilized cells after 45 min incubation at 37^{o}C and imaged (Figure 4-6) and quantified (Figure 4-7). Following the CAR-mediated pathway, 63.7% of viral particles were plasma membrane-associated plus cytosolic viral particles for the first independent experiment (Figure 4-7A). Since 4.2% of viral particles remained on the surface after virus internalization (Figure 4-7A), 59.5% of viral particles were classified as cytosolic. The remaining 36.3% of viral particles were classified as endosomal. These results indicate that of 95.8% of viral particles that were internalized into A549 cells, 62.1% penetrated the endosomes into the cytosol (penetration efficiency of 62.1%). For the second independent experiment, it was found that 78.4% of viral particles were plasma membrane-associated plus cytosolic viral particles (Figure 4-7B). Since 4.8% were plasma membrane-associated viral particles (Figure 4-7B), 73.6% of viral particles were classified as cytosolic and the remaining 21.6% as endosomal. These results indicate the endosomal membrane penetration efficiency was 77.3%. Table 4-2 contains a summary of the obtained results.

Table 4-2. Uptake and endosomal membrane penetration efficiencies for HAdV-5 following the CAR-mediated or the FX-mediated pathway *in vitro*.

Cell entry pathway	Plasma membrane-associated vp (%)	Cytosolic vp (%)	Endosomal vp (%)	Uptake efficiency (%)	Endosomal membrane penetration efficiency (%)
CAR-mediated (Exp. 1)	4.2	59.5	36.3	95.8	62.1
CAR-mediated (Exp. 2)	4.8	73.6	21.6	95.2	77.3
FX-mediated (Exp. 1)	9.7	51.2	39.1	90.3	56.7
FX-mediated (Exp. 2)	2.9	45.8	51.3	97.1	47.2

"Exp." followed by a number refers to the individual independent experiment performed. Vp; viral particles.

4.3.3 HAdV-5 uptake and endosomal membrane penetration following the FX-mediated pathway *in vitro*

4.3.3.1 Assessment of Alexa Fluor 488 dye signal intensity

Since the fluorescence emitted by Alexa Fluor 488 fluorophore is used to detect adenoviral particles for quantitative and comparative analysis, it was first confirmed that the different

Alexa Fluor 488-labelled adenoviral preparations to be used in the experiments (HAdV-5 and HAdV-2 ts1) emitted a similar level of fluorescence intensity. The fluorescence signal from Alexa Fluor 488 dye was assessed after detection of viral particles with the antibodies in intact (non-permeabilized) A549 cells that had been incubated for 45 min at 37^{o}C with Alexa Fluor 488-labelled HAdV-5 or Alexa Fluor 488-labelled HAdV-2 ts1. Since the antibodies cannot access the inside of intact cells, they only recognize the few viral particles remaining on the plasma membrane after the incubation time. Thus, the majority of viral particles, which have been internalized into cells, are Alexa Fluor 488-positive but antibody-negative, enabling quantification of Alexa Fluor 488 fluorescence signal intensity with no interference from the antibody fluorophore. The peak of fluorescence was around 3x10^{4} relative fluorescence units (RFU) for Alexa Fluor 488-labelled HAdV-5, slightly lower than that of Alexa Fluor 488-labelled HAdV-2 ts1, which was around 4.2x10^{4} RFU (Figure 4-8). However, it was considered they were within acceptable levels of similarity to perform comparative uptake and endosomal membrane penetration assays.

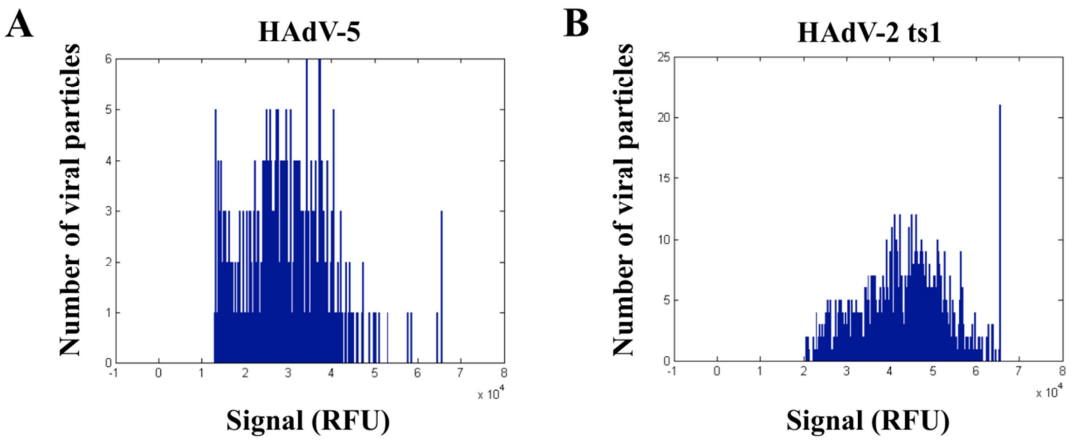

Figure 4-8. Level of Alexa Fluor 488 emitted fluorescence from Alexa Fluor 488-labelled adenoviral particles. Histograms show the intensity of emitted fluorescence for Alexa Fluor 488 fluorophore on labelled HAdV-5 (A) or HAdV-2 ts1 (B) in the absence of Alexa Fluor 488 recognition by rabbit anti-Alexa Fluor 488 primary antibody. Signal of emitted fluorescence was analysed by a custom-programmed MatLab (the Mathworks) routine. n = 1 biological replicate with 1 technical replicate per virus. RFU; relative fluorescence units.

4.3.3.2 Blockade of CAR for HAdV-5 transduction with soluble recombinant HAdV-5 fiber knob

For experiments assessing the FX-mediated pathway for HAdV-5 transduction, FK was used to block access to CAR on the cell surface and thus prevent virus from using the CAR-mediated pathway. Therefore, under this condition, quantification analysis for uptake and endosomal membrane penetration studies only reflects HAdV-5 using the FX-mediated pathway. To confirm a concentration of 0.4 μg/ml of FK (based on previous

dose-finding experiments) can successfully block the use of CAR by HAdV-5 within the experimental conditions, A549 cells that had been pre-incubated with FK were incubated with Alexa Fluor 488-labelled HAdV-5 for 45 min at 37°C to allow virus internalization. Of note, the same dose of Alexa Fluor 488-labelled HAdV-5 than that used for quantification studies on the FX-mediated pathway was used in this assay. Adenoviral particles were detected in intact or SLO-permeabilized A549 cells with the antibodies as before and classified as membrane-associated viral particles (intact cells) or membrane-associated plus cytosolic viral particles (SLO-permeabilized cells). Only few HAdV-5 particles (Alexa Fluor 488-positive) were detected in intact and SLO-permeabilized cells (Figure 4-9). Of those, very few viral particles were antibody-positive in intact A549 cells (Figure 4-9 upper panel), indicating that only few viral particles remained on the plasma membrane. In SLO-permeabilized A549 cells there were also only few viral particles either antibody-positive or negative, indicating that only few were internalized (Figure 4-9 lower panel), and thus confirming that FK successfully blocked the use of CAR for adenovirus transduction within the experimental conditions.

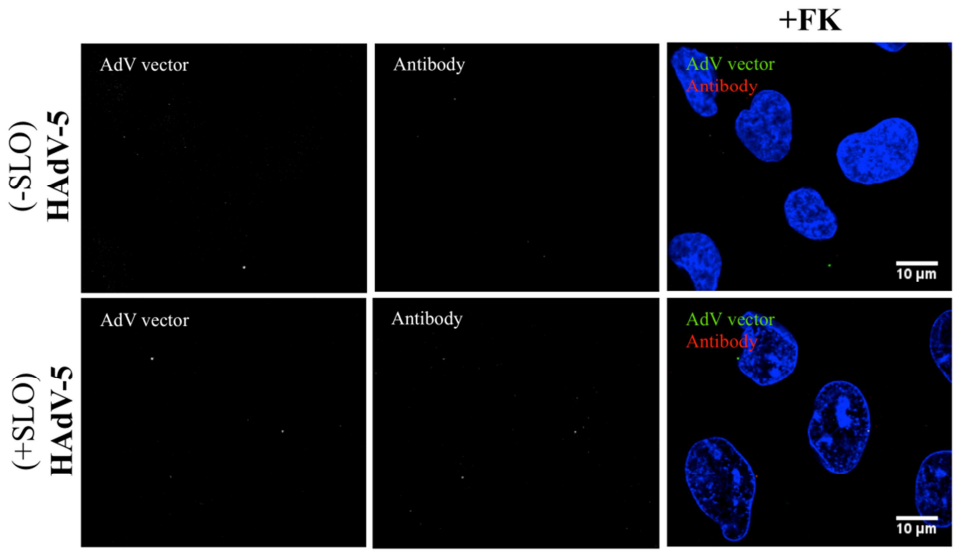

Figure 4-9. Blockade of *in vitro* HAdV-5 transduction with soluble recombinant HAdV-5 fiber knob (FK). Cells were incubated with Alexa Fluor 488-labelled HAdV-5 for 45 min at 37°C in the presence of FK (0.4 µg/ml) and permeabilized or not with SLO (2.48 µg/well). Rabbit anti-Alexa Fluor 488 primary antibody and Alexa Fluor 594-conjugated goat anti-rabbit IgG secondary antibody were used. Alexa Fluor 488-labelled HAdV-5 (green). Alexa Fluor 594-conjugated goat anti-rabbit IgG secondary antibody puncta (red) correspond to plasma membrane-associated (-SLO) or plasma membrane-associated plus cytosolic (+SLO) viral particles. Nuclei were counterstained with DAPI (blue). n = 1 biological replicate with 1 technical replicate. Representative images of maximum projections of individual confocal stacks are shown. In the merge image, yellow indicates viral particles double-positive for Alexa Fluor 488 and Alexa Fluor 594-conjugated goat anti-rabbit IgG antibody. Scale bar 10 µm. AdV; adenovirus.

4.3.3.3 Assessment of correct pore formation by SLO on cell surface in the presence of FX

Next, it was confirmed that A549 cells are successfully SLO-permeabilized in the presence of FX, allowing access of antibodies into the cytosol for adenovirus recognition. A549 cells were incubated with the different Alexa Fluor 488-labelled adenovirus to be used in the experiments (HAdV-5 and HAdV-2 ts1) for 45 min at 37^{o}C in the presence of FK and hFX. Then, cells were permeabilized with SLO and stained for Giantin. Giantin was successfully stained in SLO-treated cells in the presence of either virus under the experimental conditions (Figure 4-5A-B right panel) in similarity to SLO-treated control cells (absence of adenovirus, FK or FX) (Figure 4-5C), indicating that the primary antibody was able to access the cytosol and thus confirming that SLO can form functional pores on the plasma membrane in the presence of FX.

4.3.3.4 Assessment of FX-coated HAdV-5 recognition by anti-Alexa Fluor 488 antibody

To confirm that Alexa Fluor 488-labelled HAdV-5 is efficiently recognized by rabbit anti-Alexa Fluor 488 primary antibody in the presence of FX, A549 cells that had been pre-incubated with FK were incubated with Alexa Fluor 488-labelled HAdV-5 for 60 min on ice in the presence of FK and hFX. After the incubation time, viral particles attached to the plasma membrane were detected on intact A549 cells with the antibodies as before. Cells were imaged (Figure 4-10) and antibody-positive viral particles quantified (Figure 4-7). One hundred per cent of viral particles was detected by the antibody (Figure 4-7), indicating that FX binding to viral capsids does not interfere with antibody detection of viral capsids.

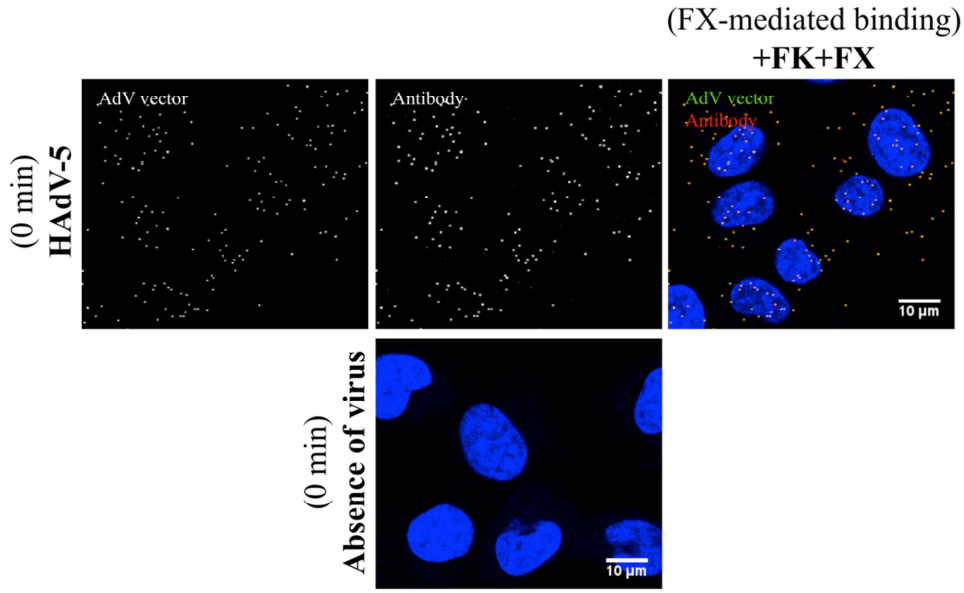

Figure 4-10. HAdV-5 *in vitro* cell binding in the presence of FX. Cells were incubated with Alexa Fluor 488-labelled HAdV-5 on ice for 60 min in the presence of soluble recombinant HAdV-5 fiber knob (FK) (0.4 µg/ml) and recombinant human FX (10 µg/ml). Rabbit anti-Alexa Fluor 488 primary antibody and Alexa Fluor 594-conjugated goat anti-rabbit IgG secondary antibody were used. Alexa Fluor 488-labelled HAdV-5 (green). Alexa Fluor 594-conjugated goat anti-rabbit IgG secondary antibody puncta (red) correspond to plasma membrane-associated viral particles. Nuclei were counterstained with DAPI (blue). n = 1 biological replicate with 1 technical replicate. Representative images of maximum projections of individual confocal stacks are shown. In the merge image, yellow indicates viral particles double-positive for Alexa Fluor 488 and Alexa Fluor 594-conjugated goat anti-rabbit IgG antibody. Scale bar 10 µm. AdV; adenovirus.

4.3.3.5 Assessment of endosome integrity in the presence of FX

To investigate HAdV-5 endosomal membrane penetration in the presence of FX, it is essential to ensure that the endosomes remain intact under the experimental conditions. Thus, to assess whether adenovirus-bound FX may increase endosomal permeability itself, lack of endosomal membrane penetration was confirmed for the penetration-deficient and FX-binding HAdV-2 ts1 (Rancourt et al., 1995, Waddington et al., 2008) in the presence of hFX. A549 cells were incubated with Alexa Fluor 488-labelled HAdV-2 ts1 for 45 min at 37^{o}C in the presence of FK and hFX and viral particles were detected in intact or SLO-permeabilized cells with the antibodies as before. As a control, endosomal membrane penetration was also assessed in intact and SLO-permeabilized A549 cells for Alexa Fluor 488-labelled HAdV-2 ts1 in the absence of FK and hFX. Antibody-positive viral particles were imaged (Figure 4-11) and quantified (Figure 4-7).

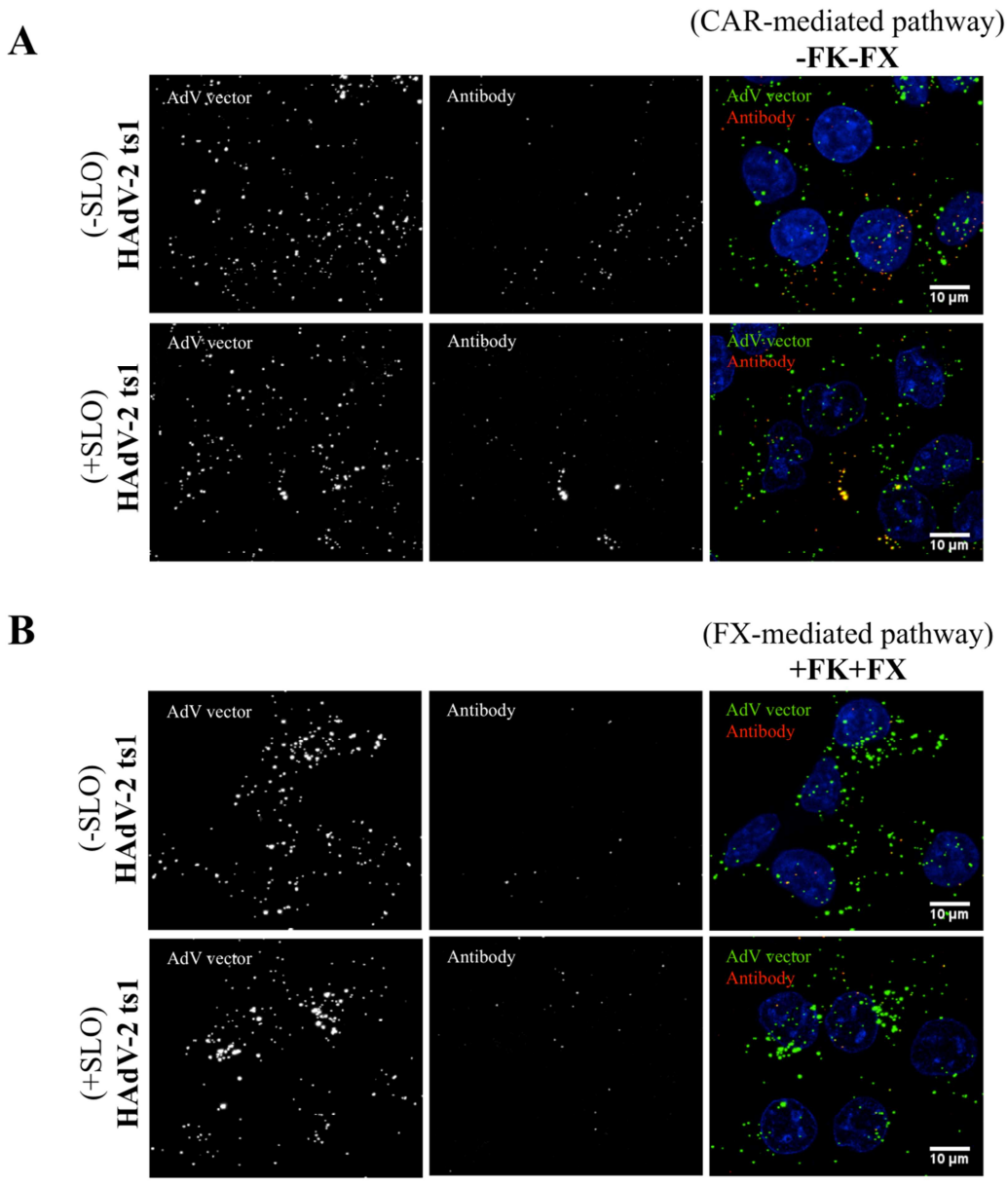

Figure 4-11. Endosome integrity in the presence of FX. Cells were incubated with Alexa Fluor 488-labelled HAdV-2 ts1 for 45 min at 37°C in the presence (B) or absence (A) of soluble recombinant HAdV-5 fiber knob (FK) (0.4 µg/ml) with (B) or without (A) recombinant human FX (10 µg/ml) and permeabilized or not with SLO (2.48 µg/well). Rabbit anti-Alexa Fluor 488 primary antibody and Alexa Fluor 594-conjugated goat anti-rabbit IgG secondary antibody were used. Alexa Fluor 488-labelled HAdV-5 (green). Alexa Fluor 594-conjugated goat anti-rabbit IgG secondary antibody puncta (red) correspond to plasma membrane-associated (-SLO) or plasma membrane-associated plus cytosolic (+SLO) viral particles. Nuclei were counterstained with DAPI (blue). n = 1 (A) or 2 (B) biological replicates with 1 technical replicate. Representative images of maximum projections of individual confocal stacks are shown. In the merge image, yellow indicates viral particles double-positive for Alexa Fluor 488 and Alexa Fluor 594-conjugated goat anti-rabbit IgG antibody. Scale bar 10 µm. AdV; adenovirus.

Following the CAR-mediated pathway (in the absence of FK and FX), 18% of viral particles were found at the plasma membrane in intact cells (uptake efficiency of 82%) and 17.2% of viral particles were antibody-positive in SLO-permeabilized cells (plasma membrane-associated plus cytosolic viral particles) (Figure 4-7A). These results indicate

that the majority of antibody-positive particles in SLO-permeabilized cells corresponded to plasma membrane-associated viral particles. Thus, internalized HAdV-2 ts1 particles were mainly located in the endosomes (82% of incoming viruses), resulting in an endosomal membrane penetration efficiency of 0%. These results confirm that endosomes remain intact during the assay in the absence of FK and FX.

Following the FX-mediated pathway (in the presence of FK and FX), 6.5% of viral particles were associated with the plasma membrane of intact cells for the first independent experiment (Figure 4-7A), resulting in an uptake efficiency of 93.5%. In SLO-permeabilized cells, the percentage of plasma membrane-associated plus cytosolic viral particles was 10.4% (Figure 4-7A). Since 6.5% of viral particles were on the plasma membrane after the 45 min incubation (Figure 4-7A), 3.9% of viral particles were classified as cytosolic and the remaining 89.6% as endosomal. These results indicate the endosomal membrane penetration efficiency for HAdV-2 ts1 in the presence of FK and FX was 4.2%. For the second independent experiment, it was found that 5.7% of viral particles associated with the plasma membrane of intact cells (Figure 4-7B) in the presence of FK and FX (uptake efficiency of 94.3%). In SLO-permeabilized cells, the percentage of plasma membrane-associated plus cytosolic viral particles was 16% (Figure 4-7B). Since 5.7% were plasma membrane-associated viral particles (Figure 4-7B), 10.3% of viral particles were classified as cytosolic and the remaining 84% as endosomal, resulting in an endosomal membrane penetration efficiency of 11%. Table 4-3 contains a summary of the obtained results.

Table 4-3. Uptake and endosomal membrane penetration efficiencies for HAdV-2 ts1 following the CAR-mediated or the FX-mediated pathway *in vitro*.

Cell entry pathway	Plasma membrane-associated vp (%)	Cytosolic vp (%)	Endosomal vp (%)	Uptake efficiency (%)	Endosomal membrane penetration efficiency (%)
CAR-mediated (Exp. 1)	18	0	82	82	0
FX-mediated (Exp. 1)	6.5	3.9	89.6	93.5	4.2
FX-mediated (Exp. 2)	5.7	10.3	84	94.3	11

"Exp." followed by a number refers to the individual independent experiment performed. Vp; viral particles.

Statistical analysis was performed on the percentage of HAdV-2 ts1 particles that remained bound to the plasma membrane of intact cells after the 45 min incubation following the

CAR or FX-mediated pathway, to assess statistical significance of the uptake efficiency via these transduction pathways. Uptake efficiency of HAdV-2 ts1 following the FX-mediated pathway was significantly higher than that following the CAR-mediated pathway (Figure 4-7A), indicating that binding to FX might facilitate HAdV-2 ts1 internalization into A549 cells. As expected, viral particles did not penetrate the endosomal membrane following the CAR-mediated pathway (Figure 4-7A). In contrast, few viral particles penetrated the endosomes into the cytosol following the FX-mediated pathway (Figure 4-7), suggesting that the integrity of endosomes could have been slightly compromised in the presence of FX. Figure 4-12 shows a summary of the mean values for the data obtained from the two independent experiments.

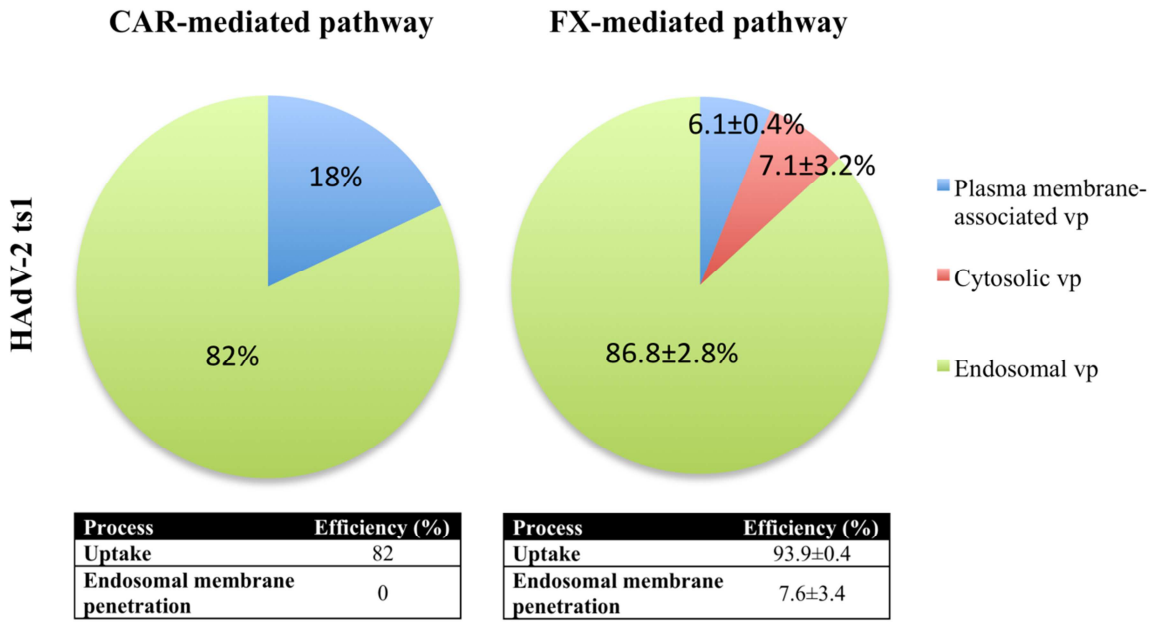

Process	Efficiency (%)
Uptake	82
Endosomal membrane penetration	0

Process	Efficiency (%)
Uptake	93.9±0.4
Endosomal membrane penetration	7.6±3.4

Figure 4-12. Classification of HAdV-2 ts1 particles by localization in host cells, and uptake and endosomal membrane penetration efficiencies. The mean of values +/- SEM from two independent experiments is shown for the FX-mediated pathway. Vp; viral particles.

4.3.3.6 HAdV-5 uptake and endosomal membrane penetration *in vitro*

Once the correct formation of SLO pores and endosome integrity on A549 cells in the presence of FX was confirmed, as well as the correct detection of FX-coated HAdV-5 with anti-Alexa Fluor 488 antibody, HAdV-5 uptake and endosomal membrane penetration following the FX-mediated pathway was investigated. A549 cells that had been pre-incubated with FK were incubated with Alexa Fluor 488-labelled HAdV-5 for 45 min at 37^{o}C in the presence of FK and hFX to allow virus internalization. Intact or SLO-permeabilized A549 cells were incubated with the antibodies to detect adenoviral particles

as before and antibody-positive viral particles were imaged (Figure 4-13) and quantified (Figure 4-7).

For the first independent experiment, a total of 9.7% (Figure 4-7A) of viral particles remained on the surface of intact cells after the 45 min incubation, indicating that HAdV-5 uptake efficiency via the FX-mediated pathway was 90.3%. In SLO-permeabilized cells, 60.9% (Figure 4-7A) of viral particles were either plasma membrane-associated or cytosolic. Since 9.7% (Figure 4-7A) of viral particles were on the plasma membrane after the 45 min incubation, 51.2% were classified as cytosolic and the remaining 39.1% as endosomal. These data indicate that the endosomal membrane penetration efficiency was 56.7%. For the second independent experiment, it was found that 2.9% of viral particles were plasma membrane-associated viral particles (Figure 4-7B) (uptake efficiency of 97.1%). In SLO-permeabilized cells, 45.8% of viral particles were plasma membrane-associated plus cytosolic viral particles (Figure 4-7B). Since 2.9% were plasma membrane-associated viral particles (Figure 4-7B), 45.8% of viral particles were classified as cytosolic and the remaining 51.3% as endosomal, resulting in an endosomal membrane penetration efficiency of 47.2%. Table 4-2 contains a summary of the results obtained.

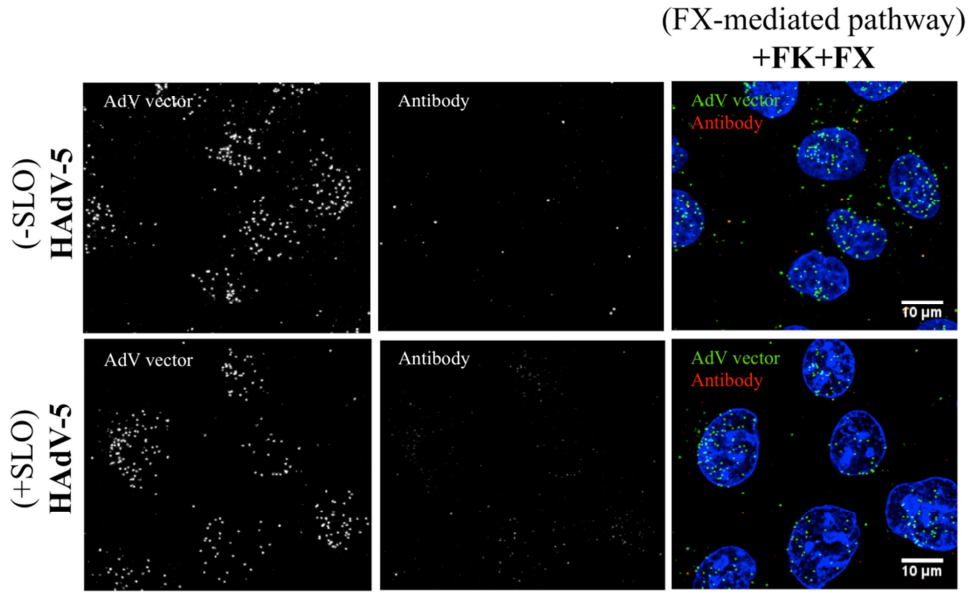

Figure 4-13. HAdV-5 internalization via the FX-mediated pathway *in vitro*. Cells were incubated with Alexa Fluor 488-labelled HAdV-5 for 45 min at 37°C in the presence of soluble recombinant HAdV-5 fiber knob (FK) (0.4 µg/ml) and recombinant human FX (10 µg/ml) and permeabilized or not with SLO (2.48 µg/well). Rabbit anti-Alexa Fluor 488 primary antibody and Alexa Fluor 594-conjugated goat anti-rabbit IgG secondary antibody were used. Alexa Fluor 488-labelled HAdV-5 (green). Alexa Fluor 594-conjugated goat anti-rabbit IgG secondary antibody puncta (red) correspond to plasma membrane-associated (-SLO) or plasma membrane-associated plus cytosolic (+SLO) viral particles. Nuclei were counterstained with DAPI (blue). n = 2 biological replicates with 1 technical replicate. Representative images of maximum projections

of individual confocal stacks are shown. In the merge image, yellow indicates viral particles double-positive for Alexa Fluor 488 and Alexa Fluor 594-conjugated goat anti-rabbit IgG antibody. Scale bar 10 μm. AdV; adenovirus.

Unexpectedly, a lower level of fluorescence intensity was detected for Alexa Fluor 594-conjugated goat anti-rabbit IgG secondary antibody in SLO-permeabilized cells in the presence of FK and FX for the second independent experiment performed in comparison with the rest of the conditions tested (representative images shown in Figure 4-13). A lower intensity signal can lead to the underestimation of the percentage of antibody-positive viral particles and have an impact on data quantification analysis. To assess whether this observed effect was a single isolated case or the result of treating the cells with SLO in the presence of FK and FX, Alexa Fluor 594 fluorescence signal intensity was assessed in SLO-permeabilized cells incubated with HAdV-5 in the presence of FK and FX for both independent experiments and compared to a positive and a negative control (Figure 4-14). Alexa Fluor 594 fluorescence signal intensity from SLO-permeabilized cells after 45 min incubation with HAdV-5 in the absence of FK and FX were used as a positive control, since a high percentage of HAdV-5 (59.5% or 73.6% from two independent experiments) is located in the cytosol and thus recognized by the antibody (Figure 4-7). SLO-permeabilized cells incubated with HAdV-2 ts1 in the presence of FK and FX was used as a negative control, since the majority of HAdV-2 ts1 (89.6% or 84% from two independent experiments) localizes in the endosomes and thus is not recognized by the antibody. For the first independent experiment, the peak of Alexa Fluor 594 fluorescence intensity in the negative control was found around 100 RFU and around 300 RFU for the positive control (Figure 4-14A). The peak of Alexa Fluor 594 fluorescence intensity in the test sample (SLO-permeabilized cells incubated with HAdV-5 in the presence of FK and FX) was found within acceptable levels of similarity to the positive control, at approximately 250 RFU (Figure 4-14A). In the second experiment however, while the negative control showed a fluorescence intensity of approximately 0 RFU and the positive control ~$1.5x10^4$ RFU (Figure 4-14B), fluorescence intensity in the test sample was found at approximately $3x10^3$ RFU (Figure 4-14B), slightly lower than that in the positive control and in agreement with the images shown in Figure 4-13.

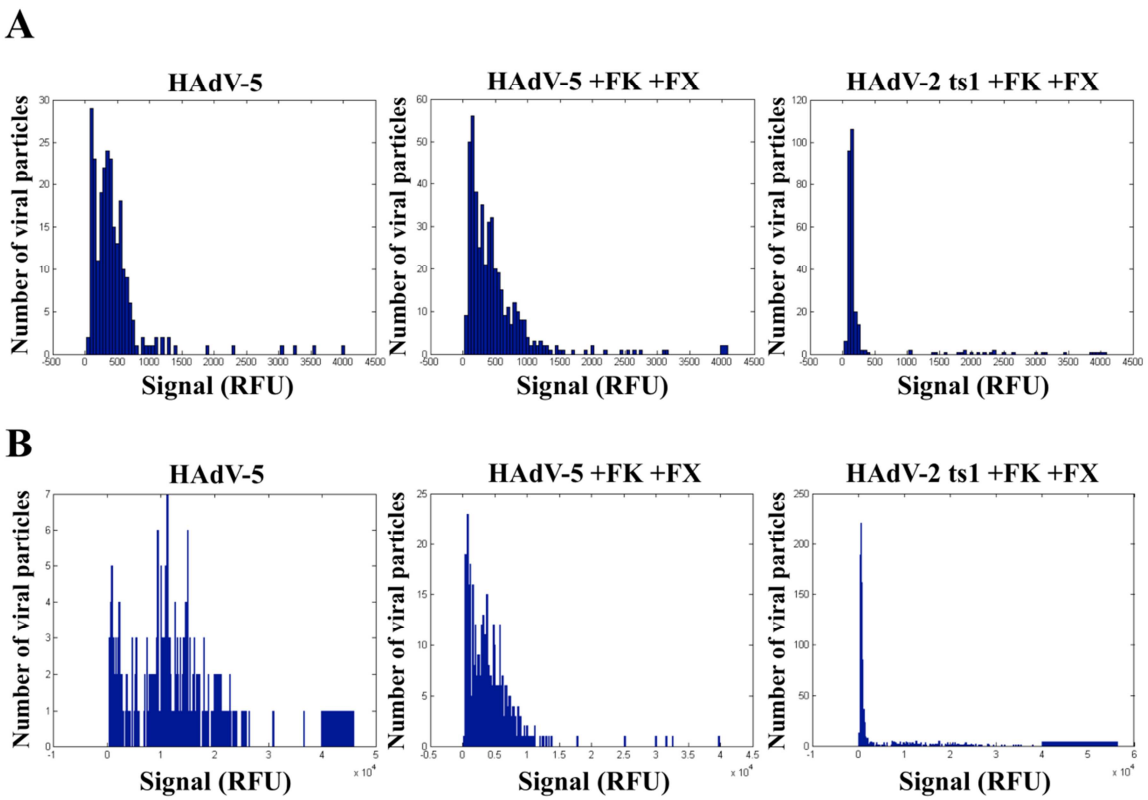

Figure 4-14. Level of Alexa Fluor 594 emitted fluorescence. Cells were incubated with Alexa Fluor 488-labelled HAdV-5 for 45 min at 37°C in the presence or absence of soluble recombinant HAdV-5 fiber knob (FK) (0.4 µg/ml) and recombinant human FX (10 µg/ml) and permeabilized with SLO (2.48 µg/well). Rabbit anti-Alexa Fluor 488 primary antibody and Alexa Fluor 594-conjugated goat anti-rabbit IgG secondary antibody were used. Histograms show the intensity of emitted fluorescence for Alexa Fluor 594 fluorophore on Alexa Fluor 594-conjugated goat anti-rabbit IgG antibody for two independent experiments [first independent experiment (A), second independent experiment (B)] with 1 technical replicate per condition. Positive control (left panel), negative control (right panel) and test sample (centre panel). Signal of emitted fluorescence was analysed by a custom-programmed MatLab (the Mathworks) routine. RFU; relative fluorescence units, FK; soluble recombinant fiber knob, FX; coagulation factor X.

4.3.4 Comparison of HAdV-5 uptake and endosomal membrane penetration efficiencies following the CAR or FX-mediated pathways *in vitro*

Statistical analysis was performed on the percentage of HAdV-5 particles that remained bound to the plasma membrane and thus not internalized in intact cells after 45 min incubation at 37°C, following the CAR or FX-mediated pathway. For the first independent experiment, uptake efficiency of HAdV-5 following the FX-mediated pathway was significantly lower than that via the CAR-mediated pathway (Figure 4-7A). In contrast, uptake efficiency via the FX-mediated pathway was significantly higher in the second independent experiment (Figure 4-7B). Figure 4-15 shows a summary of the mean values for the data obtained from the two independent experiments.

To analyse statistical significance for endosomal membrane penetration efficiencies for HAdV-5 following the FX or CAR-mediated pathways, the statistical test is applied on the percentage of antibody-positive viral particles in SLO-permeabilized cells (plasma membrane-associated plus cytosolic viral particles). The test is applied with the assumption that the percentage of antibody-positive viral particles that are located at the plasma membrane of SLO-permeabilized cells after 45 min incubation at 37^{o}C in the presence of FK and FX (FX-mediated pathway) is very similar to that in the absence of FK and FX (CAR-mediated pathway). In this study, these percentages were 4.2% following the CAR-mediated pathway and 9.7% via the FX-mediated pathway for the first independent experiment and 4.8% following the CAR-mediated pathway and 2.9% via the FX-mediated pathway for the second independent experiment (Figure 4-7). Thus, since the percentage of membrane-associated viral particles were very similar in both conditions, the percentage of membrane-associated plus cytosolic viral particles was compared to determine statistical significance on the endosomal membrane penetration efficiencies via the CAR or FX-mediated pathway. This comparison was done in each independent experiment, and both experiments showed significantly lower penetration efficiency following the FX-mediated pathway compared to that via the CAR-mediated pathway (Figure 4-7). Figure 4-15 shows a summary of the mean values for the data obtained from the two independent experiments.

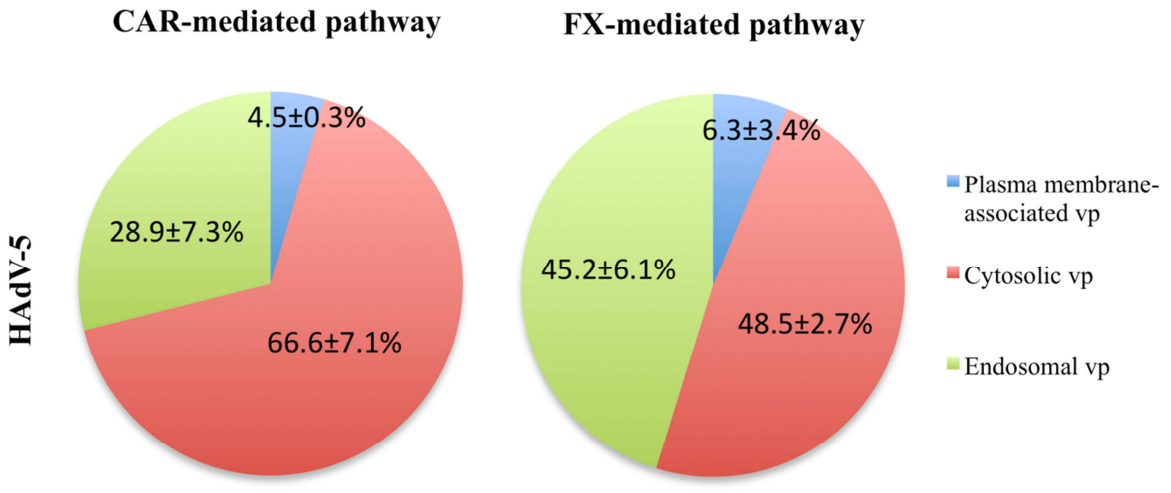

Process	Efficiency (%)
Uptake	95.5±0.3
Endosomal membrane penetration	69.7±7.6

Process	Efficiency (%)
Uptake	93.7±3.4
Endosomal membrane penetration	51.9±4.8

Figure 4-15. Classification of HAdV-5 particles by localization in host cells, and uptake and endosomal membrane penetration efficiencies. The mean of values +/- SEM from two independent experiments is shown. Vp; viral particles.

4.4 Discussion

Here, the effect of FX binding to the HAdV-5 capsid on HAdV-5 uptake and endosomal membrane penetration was investigated at the single cell level performing the SLO penetration assay (Suomalainen et al., 2013). Our results indicate that binding of FX to certain adenovirus serotypes might facilitate virion internalization into host cells, as seen for the penetration-deficient HAdV-2 ts1. However, uptake efficiency for HAdV-5 following the FX-mediated pathway was very similar to that via the CAR-mediated pathway. Moreover, the presence of FX itself slightly affected the integrity of endosomes, increasing membrane permeability and thus virion leakage into the cytosol. Interestingly, however, it decreased HAdV-5 endosomal membrane penetration efficiency, restricting the amount of HAdV-5 virions able to access the cytosol.

4.4.1 FX-mediated HAdV-5 cell binding

The most evident finding was related to the viral dose required for quantification of individual viral particles. The optimal MOI to allow imaging of individual viral particles is approximately 10 to 200 viral particles bound per cell. Also, it is important to use a similar MOI for the different conditions tested to avoid any additional effects merely related to the amount of virus transducing the host cells at a given time. In this study, a similar number of viral particles bound per cell were present in each of the conditions tested; however, to obtain these MOIs, the viral dose used for studies of the FX-mediated pathway ($2.46x10^8$ vp/well) was 28.6 times lower than that when assessing the CAR-mediated pathway ($7.04x10^9$ vp/well) (see section 2.2.6.10). This suggests that the main advantage of following the FX-mediated pathway for cell transduction might be an increase in binding to host cells, which is in agreement with our data assessing cell binding and with previous reports (Alba et al., 2009, Bradshaw et al., 2012). This increase in HAdV-5 binding in the presence of FX indicates that the FX-mediated pathway may involve higher affinity or stable interactions compared to those between HAdV-5 and CAR. Therefore, in the presence of CAR and FX, viral particles might predominantly use the FX-mediated pathway.

4.4.2 HAdV-5 uptake following the FX-mediated pathway

Analysis of HAdV-5 uptake revealed similar efficiencies via the CAR-mediated and FX-mediated pathways, indicating that internalization of HAdV-5 particles after binding to HSPG via FX might be as efficient as after binding to CAR. HSPG has multiple roles on

cellular processes such as ligand-receptor clustering and signalling, basement membrane organization and provision of a matrix for cell migration, cell adhesion and packing of granular content for secretion, and it can also bind to cytokines, chemokines and growth factors to protect them against proteolysis, or bind to proteases and protease inhibitors for their spatial distribution and activity [reviewed by (Christianson and Belting, 2014, Sarrazin et al., 2011, Lin, 2004, Dreyfuss et al., 2009)]. Whether HAdV-5 uses HSPG only for attachment to host cells or whether HAdV-5 is also internalized via an HSPG-dependent mechanism is still unknown. Interestingly, HSPGs have been associated with ligand-induced endocytosis of molecules for clearance [(Wittrup et al., 2009) and reviewed by (Christianson and Belting, 2014, Belting, 2003)]. Also, it has been observed that HSPGs cluster during endocytosis via a conserved GxxxG dimerization motif in the transmembrane domain (Dews and Mackenzie, 2007, Chen and Williams, 2013). Moreover, depending on the cellular context and type of extracellular ligand, HSPG-mediated internalization can take place in a lipid-raft-dependent or independent manner (Fuki et al., 2000, Tkachenko et al., 2004, Zimmermann et al., 2005, Wittrup et al., 2010, Payne et al., 2007, Fuki et al., 1997, Chen and Williams, 2013, Capurro et al., 2012) and can end up with the degradation of HSPG and its cargo in the lysosomes (Fuki et al., 2000, Burbach et al., 2003, Sarrazin et al., 2010). Alternatively, HSPG can work in conjunction with integrins, which can be used for adenovirus internalization into host cells (Wickham et al., 1993, Wickham et al., 1994, Mathias et al., 1998, Salone et al., 2003, Shayakhmetov et al., 2005a, Patterson and Russell, 1983, Meier et al., 2002, Wang et al., 1998, Chardonnet and Dales, 1970a). According to previous reports, extracellular matrix components can bind to HSPG and simultaneously to $\alpha_v\beta_3$, $\alpha_v\beta_5$, $\alpha_2\beta_1$ or $\alpha_6\beta_4$ integrins via RGD motifs to mediate intracellular signalling (Saoncella et al., 1999, Woods et al., 2000, Beauvais et al., 2004, McQuade et al., 2006, Hozumi et al., 2006). Importantly, it was shown that after HAdV-5 attachment to HSPG via FX, virus engagement with α_v integrins is necessary for efficient viral trafficking towards the MTOC (Bradshaw et al., 2010), suggesting that while FX allows adenovirus attachment to HSPG, viral particles might need to interact with co-receptors such as α_v integrins to facilitate virus internalization. Future studies should address whether adenovirus endocytosis is mediated by HSPG or if, on the contrary, HSPG only serve as attachment receptors and virus endocytosis is mediated by integrins. Also, studies to describe the exact mechanism mediating virus endocytosis (clathrin or caveolin-dependent or clathrin and caveolin-independent) after attachment to HSPG should be performed.

4.4.3 HAdV-5 endosomal membrane penetration following the FX-mediated pathway

Regarding HAdV-5 endosomal membrane penetration efficiency, differences were found between the CAR-mediated and FX-mediated pathways. The use of HAdV-2 ts1 (Rancourt et al., 1995) revealed that FX might slightly affect the integrity of endosomes by increasing membrane permeability. However, when analysing HAdV-5 endosomal membrane penetration after attachment to HSPG, the penetration efficiency was found significantly reduced in both independent experiments compared to that after attachment to CAR. These results suggest that the presence of FX might negatively affect the capacity of HAdV-5 to penetrate the endosomes and access the cytosol. Although no further studies were performed to elucidate the reason behind this observation, it was hypothesized FX might remain bound to HAdV-5 hexon, be internalized along with the incoming virions, and hamper capsid disassembly by increasing capsid stability. Alternatively, since FK was used in our experimental setting to block CAR-mediated HAdV-5 uptake when studying the FX-mediated pathway, decreased endosomal membrane penetration efficiency via the FX-mediated pathway could have been associated, not with the presence of FX itself, but with the lack of binding to CAR. Since binding to CAR is required for capsid disassembly, which starts with the loss of fiber from viral capsids and thus exposure of pVI (Nakano et al., 2000, Burckhardt et al., 2011) for penetration from endosomes (Wiethoff et al., 2005, Moyer et al., 2011, Maier et al., 2010), lack of binding to CAR might have increased capsid stability and thus hindered penetration from endosomes. As an alternative, assessment of endosomal membrane penetration via the FX-mediated pathway could be done using CAR-binding deficient HAdV-5 vectors instead of FK. In either case, an increase in capsid stability may result in a delay of capsid disassembly to late endosomes, where a lower pH could facilitate this process. Importantly, delayed capsid disassembly could lead to retrograde transport of viral capsids to the cell surface, as observed previously for HAdV-5 vectors carrying species B HAdV-35 fiber knob (Shayakhmetov et al., 2003), which would result in a lower endosomal membrane penetration efficiency and delivery of viral genomes to the nucleus. However, delayed capsid disassembly might still result in efficient nuclear delivery of viral genomes, in similarity to species A, B and D adenoviruses, which access the nucleus from late endosomes and lysosomes in a fiber knob-dependent manner (Defer et al., 1990, Miyazawa et al., 2001, Miyazawa et al., 1999, Chardonnet and Dales, 1970b, Shayakhmetov et al., 2003, Teigler et al., 2014). It should however be taken into account that although these adenovirus species successfully reach the nucleus via a lysosomal trafficking pathway following endocytosis, this process takes

longer than the classical species C adenovirus trafficking pathway via early endosomes after endocytosis and it can stimulate endosomal acidification-dependent anti-viral immune mechanisms (Teigler et al., 2014). In particular, one study reported that species B HAdV-7 DNA accumulated in the nucleus at 220 min post-receptor attachment in comparison with HAdV-5, which only took 40 min (Miyazawa et al., 2001). Therefore, while analysis of antibody-positive and negative viral particles in SLO penetration assays 45 min post-receptor attachment may allow studies on HAdV-5 penetration from early endosomes, studies on HAdV-5 penetration from late endosomes might require to be done at later time points, since at 45 min viral capsids may still locate to the endosomes and not have accessed the cytosol. Future experiments assessing HAdV-5 intracellular localization at different time points (kinetic assays) would allow determination of how long internalization, penetration from endosomes, trafficking and access to the nucleus may take when HAdV-5 follows the FX-mediated pathway. Also, further studies assessing whether FX remains bound to HSPG or the adenoviral capsid during virus endocytosis and vesicular trafficking would help in studying the possible implications FX-binding may have on virus internalization and endosomal membrane penetration. Moreover, further studies on whether the absence of binding to CAR affects viral capsid stability and thus endosomal membrane penetration could be done, for instance, by assessing the exposure efficiency of pVI from CAR-binding deficient HAdV-5 vectors using antibodies specific for pVI. Finally, the lower endosomal membrane penetration efficiency observed when HAdV-5 follows the FX-mediated pathway may not be associated with increased capsid stability but instead with the mechanism mediating uptake of viral particles. As stated above, viral particles may be internalized in a HSPG-dependent manner via a clathrin-independent mechanism, which might result in lower endosomal membrane penetration efficiency due to slower vesicular trafficking kinetics compared to that of clathrin-mediated endocytosis. For instance, a study reported that while non-HSPG-binding mutant AAV2 was internalized via clathrin-mediated endocytosis, HSPG-binding AAV2 was internalized in a clathrin- and caveolin-independent manner that resulted in less efficient nuclear delivery of viral genomes (Uhrig et al., 2012). The observation that binding or lack of binding to HSPG on other viruses such as AAV can lead to the use of different internalization pathways with different efficiencies of nuclear delivery of viral genomes suggests that different mechanisms might also mediate CAR-dependent or HSPG-dependent adenovirus internalization. Again, if attachment to HSPG promotes clathrin-independent adenoviral endocytosis that takes longer to deliver viral capsids to the nucleus than the described clathrin-mediated endocytosis following the CAR-mediated pathway,

studies of endosomal membrane penetration might require to be done at later time points, when viral particles have had sufficient time to access the cytosol.

4.4.4 Implications of the FX-mediated pathway on cell signalling and immunity

Adenoviral vectors might also exploit interactions with HSPG to activate signalling pathways within the host cell that may indirectly facilitate adenovirus transduction. A role for HSPG in the activation of signalling pathways by retaining and stabilizing ligands, transporting ligands or facilitating ligand-receptor interactions has been described [reviewed by (Christianson and Belting, 2014, Sarrazin et al., 2011, Lin, 2004, Dreyfuss et al., 2009, Hacker et al., 2005)]. Although HSPG has not yet been associated with promotion of signalling pathways after binding to the FX:HAdV-5 complex, this possibility should be investigated. Also, it would be interesting to address whether the presence of FX may also have additional effects on viral transduction aside from mediating attachment of viral capsids to HSPG, such as activation or inhibition of particular cellular processes within the cell that facilitate adenovirus transduction. To investigate these possibilities, uptake and endosomal membrane penetration could be assessed in cells incubated with the FX-binding deficient AdT* vector, which follows the CAR-mediated pathway in the presence of FX. This would allow assessment of additional effects that the presence of FX itself or FX binding to HSPG could have on adenoviral internalization of HAdV-5 based vectors. Moreover, FX might prevent the activation of intracellular immune responses to adenoviral capsids. Since FX blocks viral capsid recognition and binding to IgM antibodies (Duffy et al., 2016), intracellular defence mechanisms such as the TRIM21-dependent dismantling of viral capsids and degradation in the proteasome that depends on the association of viral capsids with IgG or IgM antibodies (Mallery et al., 2010, Hauler et al., 2012) might not take place in the presence of FX and absence of IgG antibodies. Furthermore, if FX remains bound to viral capsids during virus internalization and transport to the nucleus, it might also protect the virus against host cell presentation of viral peptides via MHC-I to immune cells or recognition via TLRs. Further studies should address these questions.

4.4.5 Limitations of the study

It is important to note that the high scatter of data in the quantification of antibody-positive viral particles in SLO-permeabilized cells both in the presence and absence of FX reflects a high cell-to-cell variability in the assay. This observation indicates that the stability of cells

could have been slightly compromised during the assay. Analysis on a higher number of cells might reduce the observed variability. Also, to score and quantify the amount of antibody-positive viral particles from imaged samples with the custom-programmed MatLab (The Mathworks) routine, it is essential to choose the threshold signal intensity value that discriminates between antibody-positive and antibody-negative viral particles (background intensity). To assess whether the thresholding procedure efficiently detects most of the antibody-positive viruses within the cell, a control sample can be done, where all internalized adenoviruses are also antibody-positive. This control sample can be SLO-permeabilized cells incubated with HAdV-5 and treated with Triton X-100 before addition of antibodies. Triton permeabilizes cell membranes leaving endosomal viral particles accessible for the antibody and thus ensuring recognition of all viral particles (Suomalainen et al., 2013). The threshold signal intensity value chosen should be lower than the antibody fluorescence intensity to allow detection of all viral particles in the control sample, since they are all antibody-positive viral particles. If the threshold does not allow classification of 100% of viral particles as antibody-positive in the control sample, the threshold should be adjusted. Moreover, the main limitation on analysing statistical significance on endosomal membrane penetration efficiencies is that it is done based on the percentage of total antibody-positive viral particles in SLO-permeabilized cells 45 min post-receptor attachment, which not only includes cytosolic but also membrane-associated viral particles. Thus, comparisons between endosomal membrane penetration efficiencies via the CAR or FX-mediated pathways require a similar number of particles remaining on the plasma membrane following one or the other pathway after 45 min incubation. This allows comparability and reduction of the error associated with the method applied (custom-programmed MatLab (The Mathworks) routine) for analysis and quantification of individual viral particles. Since only two independent experiments were done, the experiments from this study should be repeated for confirmation of initial results. Furthermore, while HAdV-2 ts1 is often used as a penetration-deficient vector, studies show that HAdV-2 ts1 capsids still contain 2 to 3 copies of the AVP, which despite being a lower number of copies than in wild type HAdV-2 [~7 copies (Benevento et al., 2014)], can still result in HAdV-2 ts1 particles being able to penetrate from endosomes (Anderson, 1990). Moreover, HAdV-5 capsids have been reported to associate with the MTOC during cell transduction and accumulate at high viral doses (Bailey et al., 2003, Bradshaw et al., 2010). No visible accumulation of viral particles at the MTOC was observed when using low HAdV-5 MOIs in the SLO penetration assays regardless of the presence of FX. However, addition of FX to a higher input viral dose in HAdV-5 trafficking assays resulted in a clear accumulation of viral particles in the MTOC. These results indicate that the

behaviour of viral particles during cell transduction might also depend on the viral dose used, highlighting the importance of studies using different MOIs for more translational conclusions.

Finally, different adenovirus trafficking patterns have been associated with cell type (e.g: due to different expression of adenoviral receptors), the environment around the host cell or the physiologic state within the host cell, as well as different trafficking patterns based on adenovirus serotype [reviewed by (Leopold and Crystal, 2007)]. Thus, study of the FX-mediated pathway of adenovirus transduction should not be limited to one specific adenovirus serotype or host cell type. Assessment of this pathway for FX-binding serotypes with different affinities for FX belonging to different adenovirus species such as HAdV-2, 7, 16, 18, 49 or 50 (Waddington et al., 2008) would provide useful mechanistic data, increasing our knowledge on the biological processes mediating the different pathways for adenovirus transduction of host cells, and thus helping in the optimization of adenoviral vectors for gene therapy with increased transgene transfer efficiencies.

Chapter 5 Designing adenoviral vectors for kidney-specific gene therapy

5.1 Introduction

A wide range of heritable or acquired kidney diseases are incurable to date and require renal replacement therapy by dialysis or transplantation as they progress to an advanced stage. For instance, chronic kidney disease (CKD), which is defined as a gradual loss of kidney function (decreased glomerular filtration rate (GFR) and increased proteinuria) over time (National Kidney, 2002, Levey et al., 2005), is recognised as a global public health problem with an increasing prevalence of end-stage renal failure (ESRF) in the more developed countries [(Foley and Collins, 2007, Rutkowski, 2000, Coresh et al., 2007) and reviewed by (Jha et al., 2013)]. Furthermore, there is a tight association between a low GFR and raised albuminuria with an increased risk of cardiovascular disease and a reduction in life expectancy (Go et al., 2004, Chronic Kidney Disease Prognosis et al., 2010, van der Velde et al., 2011, Kottgen et al., 2007, Wattanakit et al., 2007, Astor et al., 2006, Alonso et al., 2011, Kokubo et al., 2009). The main described causes of CKD are hypertension and diabetes mellitus (DM) (Coresh et al., 2007, Marumo et al., 2015, Guyton et al., 1972, Wadei and Textor, 2012, Fox et al., 2012, de Boer et al., 2011, Berhane et al., 2011a), which are also risk factors for cardiovascular disease (Franco et al., 2007, Loukine et al., 2011, Franco et al., 2005). Moreover, CKD has been reported to cause hypertension (Kokubo et al., 2009), which can also lead to cardiovascular diseases. However, other conditions such as glomerulonephritis (GN), inherited diseases affecting the kidneys (e.g: polycystic kidney disease, autosomal dominant tubulointerstitial kidney disease ADTKD, etc), immune diseases such as lupus, kidney infections or malformations can also cause CKD [reviewed by (Jha et al., 2013, Eckardt et al., 2013)]. Importantly, the incidence of diabetic nephropathy (DN) has dramatically increased in the past decade in the more developed Asian countries, and GN is the leading cause of ESRF for the less developed countries (Couser et al., 2011). Current therapy to retard progression of renal damage is based on lifestyle interventions such as controlling the diet (high sodium and restricted protein intake to reduce blood pressure or cardiovascular events, respectively) and increasing physical activity to reduce albuminuria, and on pharmacological interventions such as using hypertensive agents to treat high blood pressure (e.g: angiotensin-converting enzyme inhibitors (ACEIs) and angiotensin II receptor blockers (ARBs) to inhibit the renin-angiotensin-aldosterone system (RAAS), which also lowers albuminuria), lowering lipid content to reduce cardiovascular events or administering oral glucose-lowering drugs in CKD patients with DM [(Fouque and Aparicio, 2007) and reviewed by (Gansevoort et al., 2013, Wiggins and Kelly, 2009)]. However, despite the success of current therapy for preventing progression of kidney disease (Ruggenenti et al.,

2008), there are limitations yet to be overcome such as the high costs associated with dialysis or the insufficient supply of renal allografts for transplantation in the most advanced cases. Also, due to the high diversity of causes and risk factors that can lead to kidney disease as well as the heterogeneity of mechanisms mediating specific subgroups or stages of kidney disease [reviewed by (Gansevoort et al., 2013)], there is a lack of subgroup-directed therapeutic interventions. Thus, the use of a gene therapy approach such as adenoviral vectors that can target specific renal cell subsets in the kidney to deliver a therapeutic drug or restore genetic deficiencies might help in reducing morbidity and mortality associated with particular subtypes of kidney disease. Several studies in swine, rat or dog using *ex vivo* or *in vivo* approaches with delivery to the kidney via the renal artery or aorta successfully achieved adenovirus-mediated gene transfer to the renal cortex and inner and outer medulla, renal vasculature, glomerular cells, proximal tubular cells, distal tubular and pyelic epithelial cells, tubular cells from the papilla and medulla, epithelial cysts, interstitial fibroblasts, mesangial cells, podocytes or parietal epithelial cells of the Bowman's capsule of the glomerulus (Heikkila et al., 1996, Heikkila et al., 2001, Moullier et al., 1994, Zhu et al., 1996, Fujishiro et al., 2005, Chetboul et al., 2001, Nahman et al., 2000, Bhatt et al., 2002, Sandovici et al., 2006, Denby et al., 2007). Importantly, therapeutic effect was observed in a model of salt-induced renal damage where systemically administered adenoviral vectors expressing kallikrein partially reversed salt-induced glomerular hypertrophy, reduced urinary protein and blood urea nitrogen levels, reduced collagen and reticular deposition, supressed superoxide generation and restored nitric oxide production. (Bledsoe et al., 2006).

In the last decade, several de-targeting and re-targeting strategies have been developed to generate adenoviral vectors that selectively target the cell type where the gene therapy is required, while having minimal off-target effects (see sections 1.3.4 and 1.3.6). Targeting of specific renal cell subsets in the kidney with adenoviral vectors requires the identification of particular proteins selectively expressed on those cell subsets. Here, I focused on claudin 16 and nephrin. Claudin 16 is a tight junction protein located in the thick ascending limb of loop of Henle (Figure 5-1) with a major role in the regulation of magnesium reabsorption [reviewed by (Hou and Goodenough, 2010)]. Nephrin is located at the slit diaphragm area of the glomerular podocyte (Ruotsalainen et al., 1999, Mundel and Shankland, 2002) (Figure 5-1) and it has been associated with cell adhesion and signalling [reviewed by (Ristola and Lehtonen, 2014)]. Targeting of the thick ascending limb of loop of Henle or the nephron is of special interest for the treatment of diseases affecting those areas. These include diseases associated with the thick ascending limb of

loop of Henle such as ADTKD-*UMOD* (Bleyer and Hart, 1993) or medullary cystic kidney disease type 1 (MCKD1) (Kirby et al., 2013) or diseases affecting the glomerulus such as diffuse mesangial sclerosis (DMS), congenital nephrotic syndrome of the Finnish type (CNSF), Alport's syndrome and variants, minimal change disease (MCD), focal segmental glomerulosclerosis (FSGS) and collapsing glomerulonephropathy, immune and inflammatory glomerulonephropathies, hypertensive nephropathy, diabetic glomerulonephropathy and age-associated glomerulonephropathy [reviewed by (Wiggins, 2007)].

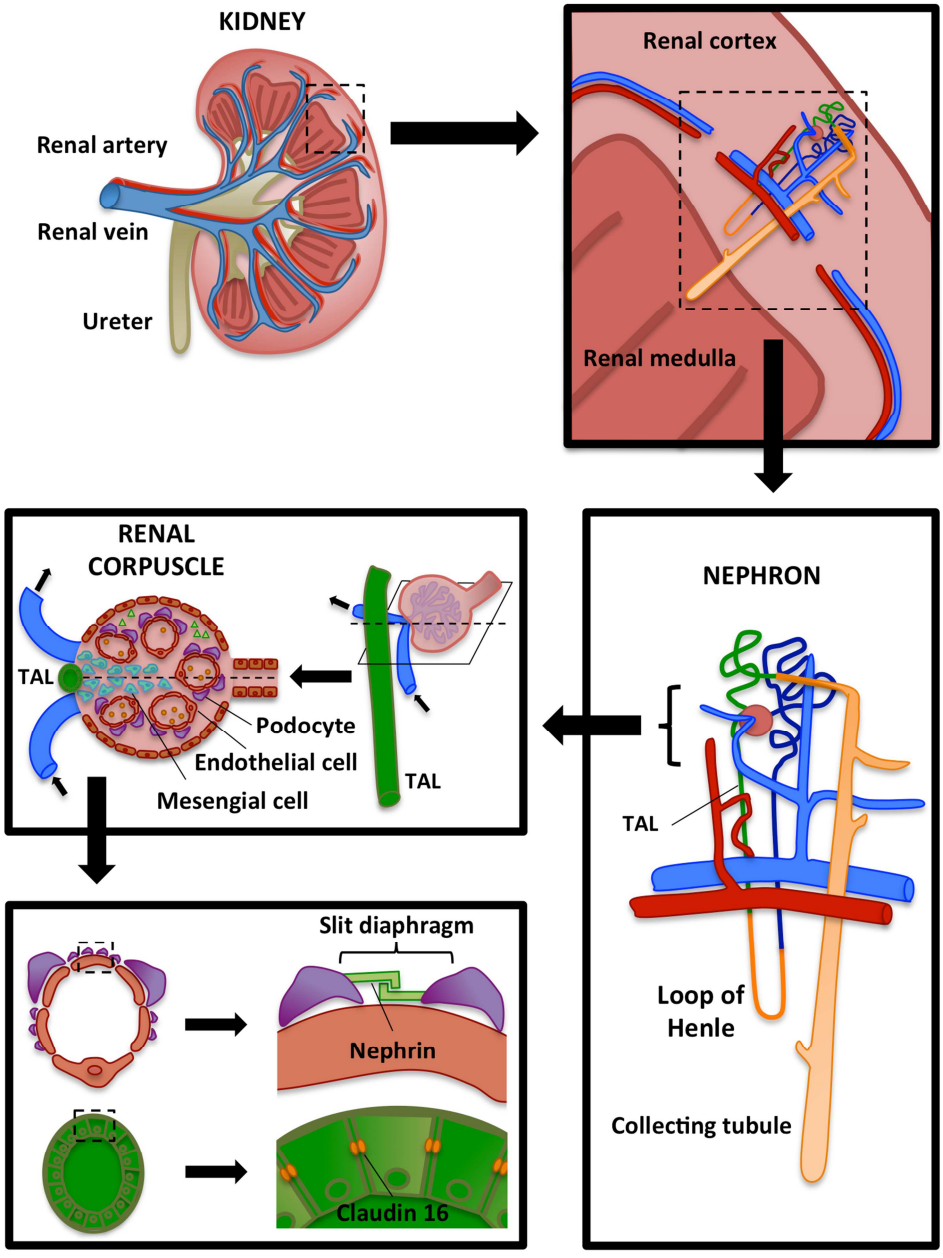

Figure 5-1. Nephrin and claudin 16 location in the kidney. Nephrons are the functional units of the kidney and locate within the renal cortex and renal medulla. Nephrons are composed of a renal corpuscle and a renal tubule and are involved in blood filtration and reabsorption. They are connected to blood vessels and to the collecting tubule, which collects urine for excretion. The renal corpuscle is composed of different cell types such as endothelial cells, mesengial cells and podocytes. Nephrin is located in the slit diaphragm area of

podocytes. Claudin 16 is a tight junction protein located in the thick ascending limb of loop of Henle (TAL), which is a component of the renal tubule.

In this study, HAdV-5-based vectors were engineered by introducing heterologous peptides found by *in vitro* phage display into the HI loop of the fiber knob domain with the aim of targeting distinct marker proteins in the kidney such as claudin 16 or nephrin. Also, specific genetic mutations were added to the engineered adenoviral vectors to reduce liver transduction and thus possible off-target effects and toxicity problems as well as the activation of immune responses, which have been associated with intravascular administration of HAdV-5-based vectors (Lozier et al., 2002, Raper et al., 2002, Atencio et al., 2006, Morral et al., 2002).

5.2 Aims

The aim of the present study was:

- To generate liver de-targeted adenoviral vectors with specific targeting of claudin 16 or nephrin-expressing cells for kidney-specific gene therapy.

5.3 Results

5.3.1 Generation of adenoviral vectors

Adenoviral vectors used in this study (AdT*KO1 AAA, AdT*KO1 AAAASFPPAFAAA and AdT*KO1 AAAYAAHRSHAAA) are replication-deficient HAdV-5-based adenoviral vectors encoding the *E.coli LacZ* gene (β-galactosidase). These vectors have FX-binding ablating mutations in the hexon HVR 5 and 7 (Alba et al., 2009), the CAR-binding ablating KO1 mutation into the fiber knob domain (Leissner et al., 2001, Jakubczak et al., 2001, Roelvink et al., 1999) and AAA, AAAASFPPAFAAA or AAAYAAHRSHAAA heterologous peptides (found by *in vitro* phage display), respectively, into the HI loop of the fiber knob domain. A summary of the adenoviral vectors' genetic and receptor recognition characteristics is shown in section 2.1.6.

5.3.1.1 Cloning strategy to generate kidney-specific adenoviral vectors

The genomes of AdT*KO1 AAA, AdT*KO1 AAAASFPPAFAAA and AdT*KO1 AAAYAAHRSHAAA (pAdT*KO1-AAA, pAdT*KO1-AAA-AAAASFPPAF and pAdT*KO1-AAA-AAAYAAHRSH, respectively) were engineered to incorporate specific genetic modifications in the hexon and fiber knob domain to alter receptor recognition

characteristics (Figure 5-2). Briefly, ASFPPAF and YAAHRSH peptides were identified after 4 rounds of *in vitro* phage display [7-mer linear peptide library fused to pIII N-terminal on bacteriophage M13KE (Noren and Noren, 2001)] as binders to claudin 16 on K562CLDN16 suspension cells (K562 cells stably expressing claudin 16) or nephrin on K562NPHN suspension cells (K562 cells stably expressing nephrin), respectively. The DNA sequences corresponding to ASFPPAF and YAAHRSH peptides flanked by *Not*I sites were cloned into the *Not*I site from pShuttle-KO1-AAA, which has the KO1 mutation (Leissner et al., 2001, Jakubczak et al., 2001, Roelvink et al., 1999) in the fiber ORF and an additional AAA peptide (*Not*I site + cytosine at *Not*I site 3' end) incorporated into the HI loop of the fiber knob domain. Of note, the additional cytosine was added to maintain the fiber ORF after the addition of the *Not*I site. The 5'→3' and complementary 3'→5' ssDNA oligonucleotides for ASFPPAF or YAAHRSH peptides (Oligo_NotIASFPPAFNotI5-3 and Oligo_NotIASFPPAFNotI3-5 or Oligo_NotIYAAHRSHNotI5-3 and Oligo_NotIYAAHRSHNotI3-5, respectively) were mixed at a 1:1 ratio in nuclear-free water to generate dsDNA. Of note, as a result of the enzymatic ligation, a new *Not*I site is generated in the plasmid. Again, to avoid disruption of the fiber ORF, an additional cytosine was added at the 3' end of the first *Not*I site in Oligo_NotIASFPPAFNotI5-3 and Oligo_NotIYAAHRSHNotI5-3 oligonucleotides, thus resulting in a new AAA peptide. Next, the dsDNA sequences were enzymatically digested with *Not*I restriction enzyme and enzymatically ligated into *Not*I-digested pShuttle-KO1-AAA. As a result, pShuttle-KO1-AAA-AAAASFPPAF and pShuttle-KO1-AAA-AAAYAAHRSH were generated, which encode the KO1 mutation and AAAASFPPAFAAA or AAAYAAHRSHAAA peptides, respectively. This work was performed by Dr. Laura Denby (University of Glasgow, UK) and funded by Myrovylitis Trust. pShuttle-KO1-AAA-AAAASFPPAF, pShuttle-KO1-AAA-AAAYAAHRSH or pShuttle-KO1-AAA were then recombined by homologous DNA recombination with pAdT* (Alba et al., 2009) to generate pAdT*KO1-AAA-AAAASFPPAF, pAdT*KO1-AAA-AAAYAAHRSH or pAdT*KO1-AAA (control vector), respectively.

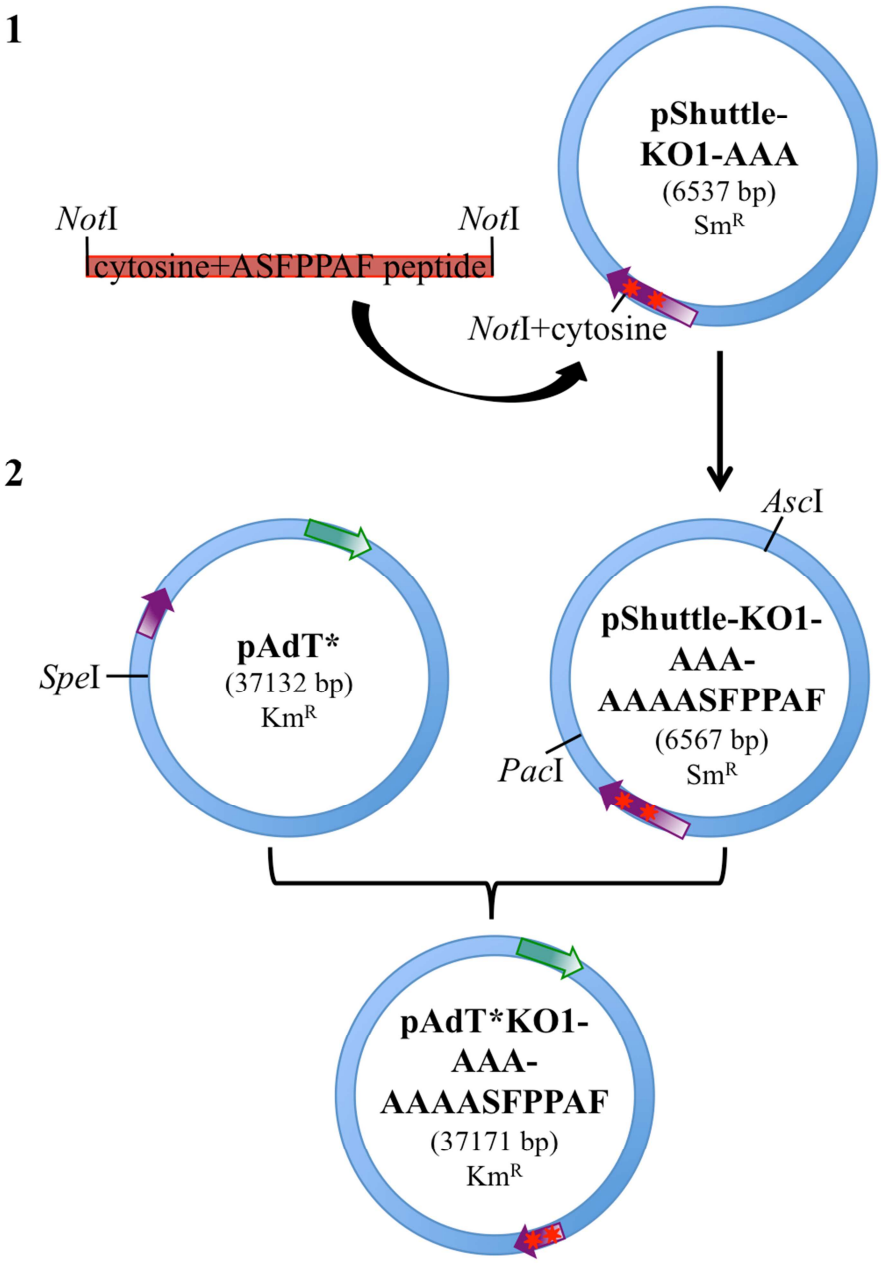

Figure 5-2. Cloning strategy to generate AdT*KO1 AAAASFPPAFAAA genome (pAdT*KO1-AAA-AAAASFPPAF). 1. First cloning step consisting in the insertion of the DNA sequence corresponding to the heterologous peptide into the HI loop sequence of the fiber ORF from pShuttle-KO1-AAA. **2.** Second cloning step where pAdT* and pShuttle-KO1-AAA-AAAASFPPAF are subjected to homologous DNA recombination to generate pAdT*KO1-AAA-AAAASFPPAF. The cloning strategy to generate AdT*KO1 AAA and AdT*KO1 AAAYAAHRSHAAA genomes (pAdT*KO1-AAA and pAdT*-KO1-AAAYAAHRSH, respectively) are identical to the represented one with the exception of the DNA sequence corresponding to the heterologous peptide. Features in green represent *LacZ*, features in purple represent the fiber ORF, and stars in red represent genetic mutations (AAA peptide and KO1 mutation in pShuttle-KO1-AAA, or AAAASFPPAFAAA peptide and KO1 mutation in pShuttle-KO1-AAA-AAAASFPPAF and pAdT*KO1-AAA-AAAASFPPAF). Sm^R; streptomycin resistance, Km^R; kanamycin resistance.

To perform the homologous recombination, pShuttle-KO1-AAA-AAAASFPPAF, pShuttle-KO1-AAA-AAAYAAHRSH and pShuttle-KO1-AAA were transformed into chemically competent *E. coli* for plasmid amplification and a pDNA large-scale preparation was generated from one of the streptomycin resistant positive colonies. To prepare the plasmids for recombination, pAdT* was linearized with *Spe*I (Figure 5-3A),

the 5' ends were de-phosphorylated and pDNA was purified by DNA precipitation. pShuttle-KO1-AAA, pShuttle-KO1-AAA-AAAASFPPAF and pShuttle-KO1-AAA-AAAYAAHRSH were enzymatically digested with *Asc*I and *Pac*I, electrophoresed, and the band containing the "fiber KO1 with the peptide sequence" was extracted from the agarose gel for each of the plasmids (Figure 5-3B).

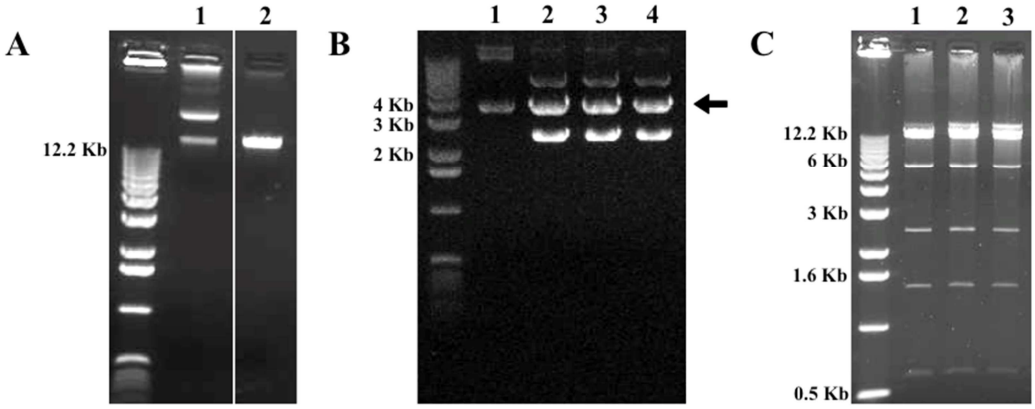

Figure 5-3. pAdT*KO1-AAA, pAdT*KO1-AAA-AAAASFPPAF and AdT*KO1-AAA-AAAYAAHRSH second cloning step. A) Circular pAdT* (1) and *Spe*I-digested pAdT* (2) (37132 bp). B) Circular pShuttle-KO1-AAA (1), *Asc*I and *Pac*I-digested pShuttle-KO1-AAA (2), *Asc*I and *Pac*I-digested pShuttle-KO1-AAA-AAAASFPPAF (3) and *Asc*I and *Pac*I-digested pShuttle-KO1-AAA-AAAYAAHRSH (4). Bands 4038 bp and 2499 bp (2) or 4068 bp and 2499 bp (3 and 4). C) *Xho*I-digested pAdT*KO1-AAA (1), pAdT*KO1-AAA-AAAASFPPAF (2) and pAdT*KO1-AAA-AAAYAAHRSH (3). Bands 14500 bp, 12391 bp, 5744 bp, 2466 bp, 1445 bp and 595 bp (1) or 14500 bp, 12421 bp, 5744 bp, 2466 bp, 1445 bp and 595 bp (2 and 3). Arrow indicates the DNA band extracted from the agarose gel. 1 kb DNA ladder (Invitrogen, UK) used.

Of note, pAdT* and pShuttle-KO1-based plasmids share two homologous DNA regions (Figure 5-4A). However, homologous DNA recombination between pAdT* and pShuttle-KO1-based plasmids must happen via only the left homology arm in order to exclusively mutate pAdT* fiber ORF by introducing the mutated fiber ORF from pShuttle-KO1-based plasmids. Homologous DNA recombination via both the left and right homology arms would result in a deletion of 2717 base pairs from pAdT* genome in the resultant plasmid (exchange of a 2899 bp DNA fragment from pAdT* with a 182 bp DNA fragment from pShuttle-KO1-based plasmids) (Figure 5-4A). Thus, digestion of pShuttle-KO1-based plasmids with *Asc*I and *Pac*I removed the right homology arm.

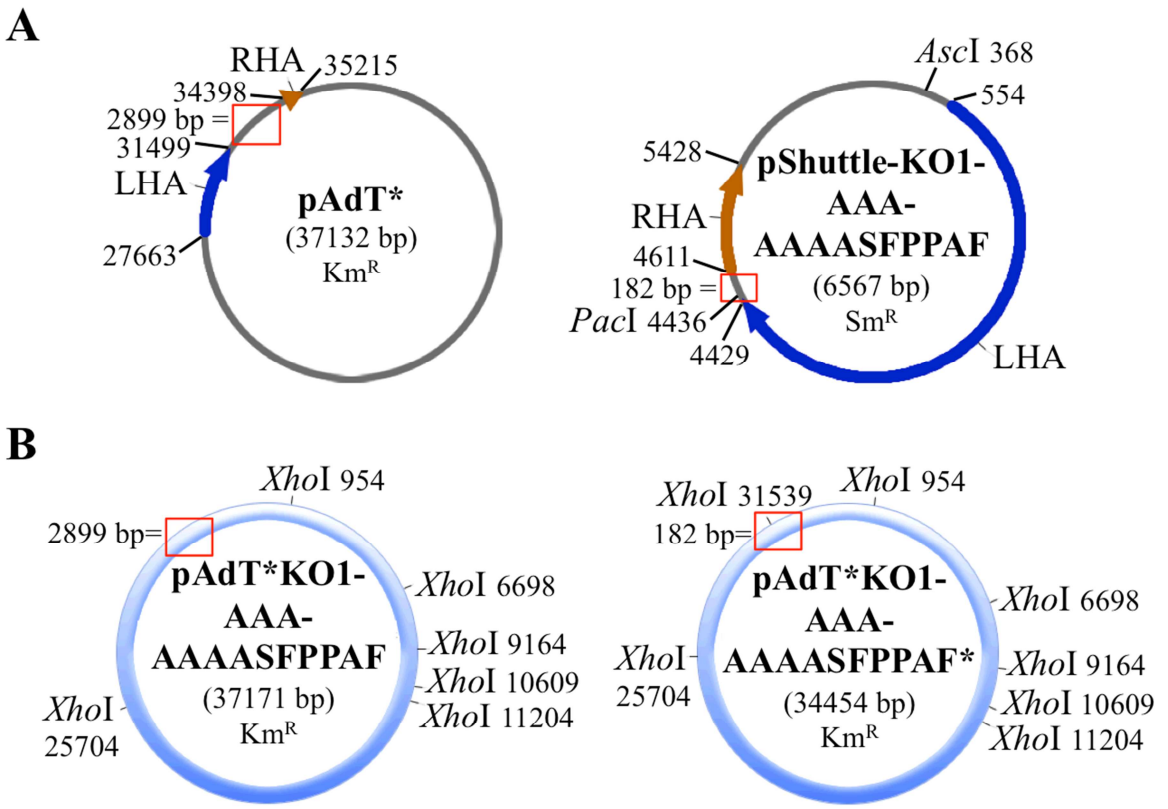

Figure 5-4. Homologous recombination between pAdT* and pShuttle-KO1-AAA-AAAASFPPAF. pShuttle-KO1-AAA-AAAASFPPAF has been used in this representation as an example of the pShuttle-KO1 plasmids used in this study. A) DNA sequence homology between pAdT* and pShuttle-KO1-AAA-AAAASFPPAF. Left homology arm (LHR) in blue and right homology arm (RHA) in orange. Numbers indicate the base pair position in the genome for each feature. B) pAdT*KO1-AAA-AAAASFPPAF resultant from the homologous recombination between pAdT* and pShuttle-KO1-AAA-AAAASFPPAF via the LHA (left panel), and pAdT*KO1-AAA-AAAASFPPAF* resultant from the homologous recombination via the LHA and the RHA (right panel). The red square corresponds to the DNA region between the LHR and RHA (A) or the non-homologous DNA region between pAdT*KO1-AAA-AAAASFPPAF and pAdT*KO1-AAA-AAAASFPPAF* (B). Sm^R; streptomycin resistance gene, Km^R; kanamycin resistance gene.

Homologous DNA recombination was performed by transforming purified *Asc*I and *Pac*I-digested pShuttle-KO1-AAA, *Asc*I and *Pac*I-digested pShuttle-KO1-AAA-AAAASFPPAF, or *Asc*I and *Pac*I-digested pShuttle-KO1-AAA-AAAYAAHRSH into electrocompetent $recA^+$ *E. coli* together with purified *Spe*I-digested pAdT*. The resultant pAdT* KO1-AAA, pAdT*KO1-AAA-AAAASFPPAF or pAdT*KO1-AAA-AAAYAAHRSH were extracted from single kanamycin resistant colonies, confirmed by enzymatic digestion with *Xho*I, and transformed into chemically competent *E. coli* to amplify pDNA in a recA1 system unable to recombine DNA, thus conferring stability to the plasmid. Large-scale preparations of pAdT* KO1-AAA, pAdT*KO1-AAA-AAAASFPPAF or pAdT*KO1-AAA-AAAYAAHRSH were obtained from single positive colonies. Plasmids were confirmed by enzymatic digestion with *Xho*I (Figure 5-3C) to ensure that homologous DNA recombination had taken place between *Spe*I-digested pAdT* and *Asc*I and *Pac*I-digested pShuttle-KO1-based plasmids via only the left

homology arm. *Xho*I was chosen since there is a *Xho*I restriction site in the region between the left and right homology arms in pShuttle-KO1-based plasmids (region removed from pShuttle-KO1-based plasmids by digestion with *Asc*I and *Pac*I) that is not present in pAdT* genome (Figure 5-4B). This quality control was performed in case partially digested or non-digested molecules of pShuttle-KO1-based plasmids remained in the sample used for plasmid recombination. As a further quality control, the resultant plasmids (pAdT*KO1-AAA, pAdT*KO1-AAA-AAAASFPPAF and pAdT*KO1-AAA-AAAYAAHRSH) were sequenced to confirm the presence of the genetic mutations in the hexon HVRs, the KO1 mutation in the fiber knob domain, and the AAA, AAAASFPPAF or AAAYAAHRSHAAA peptides in the fiber HI loop, respectively.

5.3.2 Adenoviral vectors amplification and quality control

AdT*KO1 AAA, AdT*KO1 AAAASFPPAFAAA and AdT*KO1 AAAYAAHRSHAAA genomes were linearized with *Pac*I and transfected into eukaryotic permissive HEK-293 cells and PD10-GFP plasmid was used as a control of transfection (Figure 5-5A). Rescued adenoviral vectors were collected from cells and propagated in HEK-293 packaging cells. Four rounds of amplification (T25, T150, 4 T150, 25 T150) were required for obtaining sufficient amount of virus to generate pure adenoviral vector preparations. Of note, amplification of AdT*KO1 AAA, AdT*KO1 AAAASFPPAFAAA and AdT*KO1 AAAYAAHRSHAAA was done simultaneously and cells were collected when CPE was observed in the control AdT*KO1 AAA vector. Unfortunately, in contrast to AdT*KO1 AAAASFPPAFAAA vector that produced CPE in similarity to AdT*KO1 AAA at collection time points, AdT*KO1 AAAYAAHRSHAAA did not show CPE in any round of amplification. To assess whether AdT*KO1 AAAYAAHRSHAAA had propagation deficiencies, an arbitrary volume of 50 µl of the collected virus from each round of amplification (virus from each round collected in an equal volume of DPBS) was incubated with HEK-293 cells. A dramatic decrease in the number of transduced cells (β-galactosidase-positive) was observed with each round of amplification (Figure 5-5B), suggesting a loss of AdT*KO1 AAAYAAHRSHAAA infectivity during propagation. Therefore, amplification of AdT*KO1 AAAYAAHRSHAAA was not continued. Pure adenoviral vector preparations were generated for AdT*KO1 AAA and AdT*KO1 AAAASFPPAFAAA.

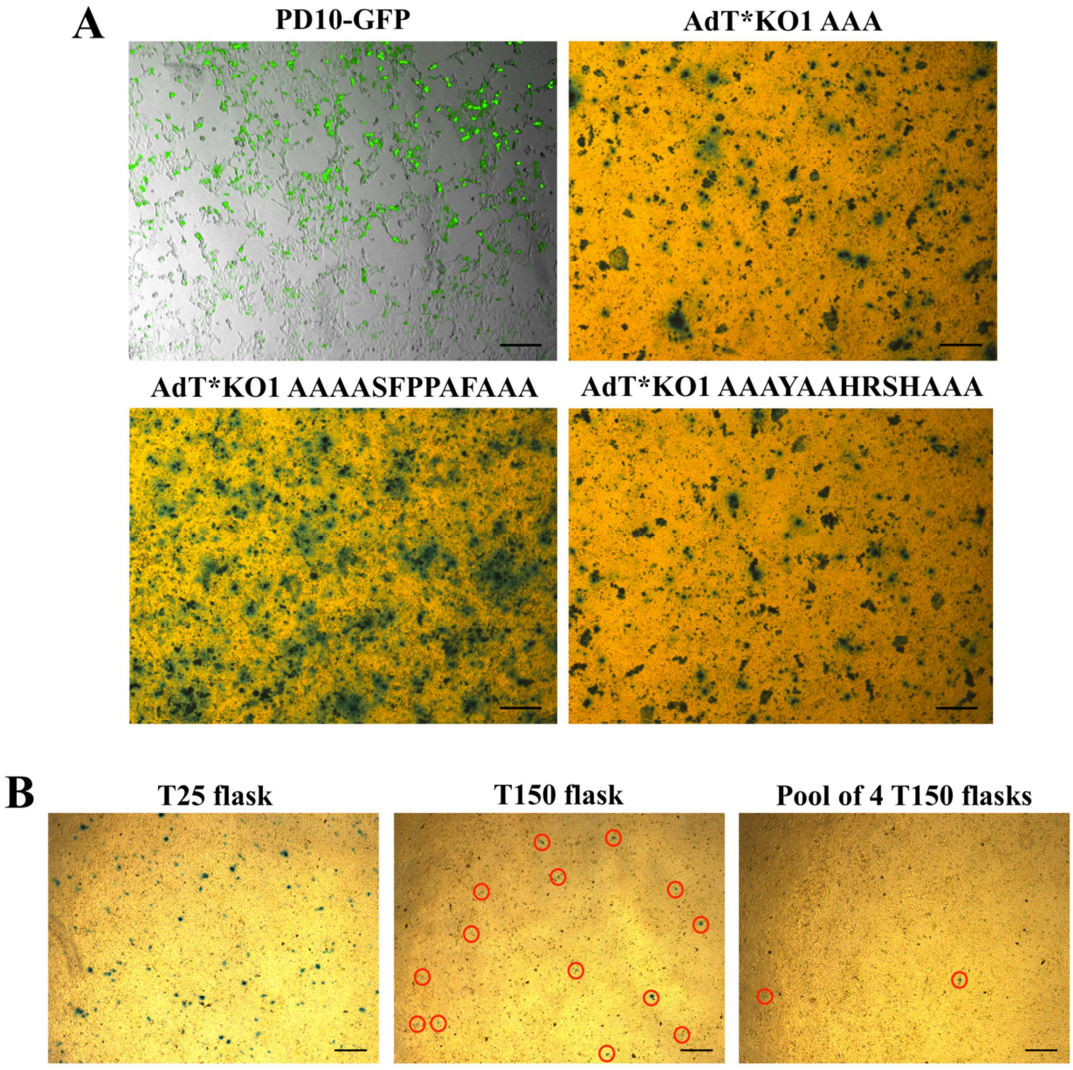

Figure 5-5. Amplification of kidney-targeted AdT*KO1-based vectors. A) Kidney-targeted AdT*KO1 AAA, AdT*KO1 AAAASFPPAFAAA or AdT*KO1 AAAYAAHRSHAAA genomes (pAdT*KO1-AAA, pAdT*KO1-AAA-AAAASFPPAF or pAdT*KO1-AAA-AAAYAAHRSH, respectively) were transfected into HEK-293 cells. GFP-positive cells (green) 24 h after transfection of PD10-GFP control plasmid into HEK-293 cells. β-galactosidase expression by X-Gal staining of HEK-293 cells after fixation with 2% paraformaldehyde 10 days post-transfection. B) β-galactosidase expression by X-Gal staining of HEK-293 cells incubated for 20 h with 50 µl of AdT*KO1 AAAYAAHRSHAAA from three different rounds of amplification (T25, T150 or 4 T150). Representative images are shown. β-galactosidase-positive cells are highlighted with a red circle in images corresponding to T150 and 4 T150 to facilitate their visualization. Scale bars = 250 µM.

The absence of RCAs was confirmed for the pure adenoviral vector preparations generated in this study, ensuring safety of adenoviral preparations. Also, adenoviral DNA was sequenced after each amplification step to verify vector genetic stability and confirm the presence of the T* mutations in the hexon HVRs, the KO1 mutation in the fiber knob domain and the heterologous peptides in the HI loop of the fiber knob domain.

The concentration of adenovirus particles (vp/ml) and infectivity (pfu/ml) of pure adenoviral vector preparations were also tested (Table 5-1). In this study, no visual

presence of plaques was found when assessing infectivity of AdT*KO1 AAA or AdT*KO1 AAAASFPPAFAAA preparations, thus making it impossible to determine the infectivity by detection of pfu. Thus, HEK-293 cells from infectivity assays were subjected to X-Gal staining at completion of the assay and visual detection of individual β-galactosidase-positive cells was used to determine the infectivity in IU/ml. AdT*KO1 AAA and AdT*KO1 AAAASFPPAFAAA preparations exhibited extremely high vp/IU ratios (1924554 vp/IU and 2237205 vp/IU, respectively) (Table 5-1).

Table 5-1. Kidney-targeted adenoviral vectors quality control.

Adenoviral vector	Adenovirus titre (vp/ml)	Adenovirus titer (IU/ml)	Vp/IU	Vp diameter (nm)
AdT*KO1 AAA	$6.91x10^{11}$	$3.59x10^{5}$	1924554	109
AdT*KO1 AAAASFPPAFAAA	$8.03x10^{11}$	$3.59x10^{5}$	2237205	114

Infectious units (IU)/ml values shown were obtained from β-galactosidase-positive cells observed by X-Gal staining. Values of vp diameter by Nanoparticle Tracking Analysis (NanoSight) are the mean of technical triplicates. Vp; viral particle.

To assess whether the low infectivity of AdT*KO1 AAA or AdT*KO1 AAAASFPPAFAAA preparations was the result of adenovirus aggregation, pure adenovirus preparations were tested for the presence of adenovirus aggregates using the laser-based NTA by NanoSight, a technology that allows visualization and size determination of adenovirus particles. HAdV-5 capsids are around 90-100 nm in diameter (Norrby, 1969, Goosney and Nemerow, 2003). AdT*KO1 AAA and AdT*KO1 AAAASFPPAFAAA capsids were found to be 109 nm and 114 nm, respectively, confirming the absence of adenovirus aggregates (Table 5-1).

Next, whether the genetic modification incorporated in these vectors might interfere with capsid assembly and maturation and thus infectivity of vectors was investigated by performing silver staining on AdT*KO1 AAA and AdT*KO1 AAAASFPPAFAAA preparations electrophoresed in a polyacrylamide gel. AdT* was used as a control in this assay. Despite the presence of the major adenovirus capsid proteins (hexon, penton base and fiber) was confirmed for AdT*KO1 AAA and AdT*KO1 AAAASFPPAFAAA, a slightly different pattern of bands was observed for these vectors in comparison to AdT* control vector (Figure 5-6). These results suggest that adenovirus capsid protein composition and integrity might be affected in these vectors.

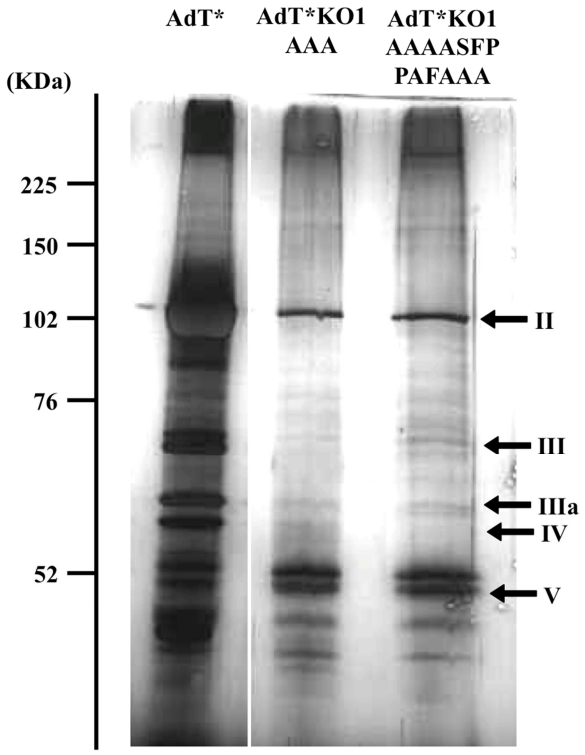

Figure 5-6. Adenovirus capsid composition of kidney-targeted AdT*KO1-based vectors analysed by silver staining. A total of $5x10^{10}$ denatured AdT*, AdT*KO1 AAA or AdT*KO1 AAAASFPPAFAAA particles were loaded in a 12% SDS-polyacrylamide gel and proteins were visualized by silver staining (Life Technologies). Rainbow ladder (Amersham Bioscience UK Ltd, UK) was used as a marker for molecular weight. Numbers on the right indicate polypeptides of viral particles and their designations. Mw (kDa): 109 (protein II/hexon), 63.3 (protein III/penton base and IIIa), 62 (protein IV/fiber) and 41.6 (protein V) (San Martin and Burnett, 2003).

Finally, whether the difference in fiber mass between AdT*KO1 AAA and AdT*KO1 AAAASFPPAFAAA associated with the incorporation of the heterologous peptide into the HI loop of the fiber knob domain could be detected as a shift in fiber mobility in a polyacrylamide gel was investigated, using HAdV-5 and AdT* as controls. HAdV-5 fiber monomer has a mass of 62 kDa (San Martin and Burnett, 2003), the AAA peptide of 231.25 Da and the AAAASFPPAFAAA peptide of 1.1623 kDa. Thus, the expected fiber monomer mass from AdT*KO1 AAA is 62.23125 kDa and from AdT*KO1 AAAASFPPAFAAA is 63.1623 kDa. A similar mobility was observed for HAdV-5, AdT* and AdT*KO1 AAA fiber monomers (Figure 5-7). A slight shift in fiber monomer mobility was observed for AdT*KO1 AAAASFPPAFAAA in comparison to the control vectors (Figure 5-7).

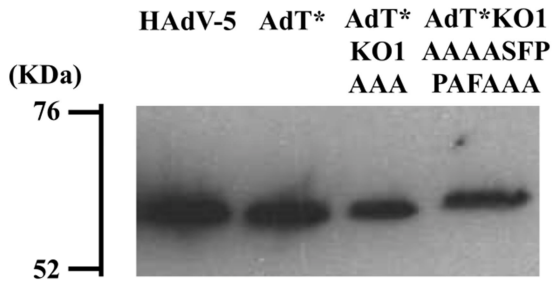

Figure 5-7. Western blotting analysis of adenovirus fiber monomers from kidney-targeted AdT*KO1-based vectors. Fiber monomers from $5x10^{10}$ denatured HAdV-5, AdT*, AdT*KO1 AAA or AdT*KO1 AAAASFPPAFAAA particles visualized on a 12% SDS-polyacrylamide gel. Mouse anti-adenovirus fiber IgG2a primary antibody and HRP-conjugated rabbit anti-mouse IgG secondary antibody were used. Rainbow ladder (Amersham Bioscience UK Ltd, UK) was used as a marker for molecular weight. Fiber monomer mass: 62 kDa (HAdV-5 or AdT*), 62.23 kDa (AdT*KO1 AAA) and 63.16 (AdT*KO1 AAAASFPPAFAAA).

5.3.3 Specificity of claudin16-targeted AdT*KO1 AAAASFPPAFAAA for claudin16-expressing cells *in vitro*

Since ASFPPAF peptide was selected by *in vitro* phage display as a specific binder to claudin 16 expressed on K562CLDN16 suspension cells, the specificity of AdT*KO1 AAAASFPPAFAAA for K562CLDN16 cells was investigated. To confirm that K562CLDN16 cells express claudin 16 in contrast to K562 cells, total RNA was extracted from K562CLDN16, complementary DNA (cDNA) was generated, and the amount of claudin 16 mRNA was quantified by TaqMan® Real-Time PCR. K562CLDN16 cells showed expression of claudin 16 mRNA in contrast to K562 cells (Figure 5-8A).

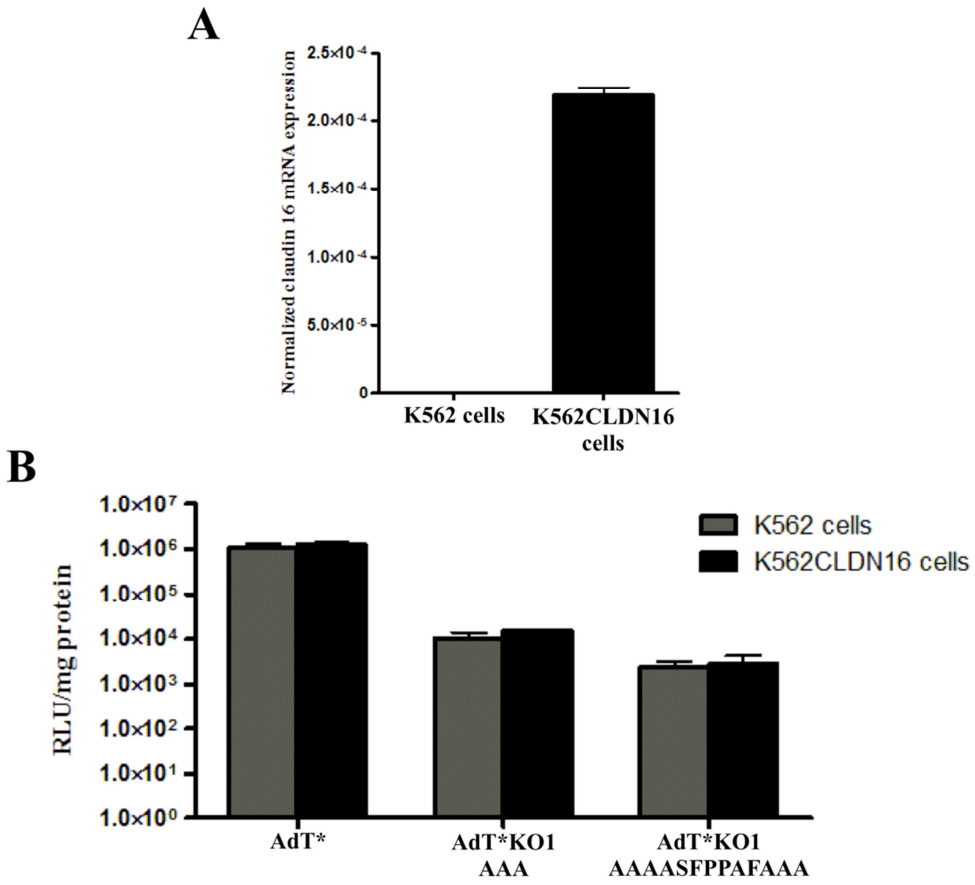

Figure 5-8. Specificity of claudin 16-targeted adenoviral vector for claudin 16-expressing cells *in vitro*. A) Claudin 16 mRNA expression in K562CLDN16 and K562 cells was determined by TaqMan® Real-Time PCR. Data represented as the mean of technical triplicates +/- SEM following the $2^{\Delta CT}$ method (Livak and Schmittgen, 2001) and normalized to 18S rRNA expression. B) K562CLDN16 and K562 cells were incubated with AdT*, AdT*KO1 AAA or AdT*KO1 AAAASFPPAFAAA (5000 vp/cell) at 37°C for 3 h, washed with 10% FCS DMEM media and incubated for further 48 h. β-galactosidase expression levels were quantified as relative light units (RLU) and normalized to total mg of protein. n = 2 biological replicates per condition with 3 technical replicates. Values corresponding to one representative experiment are shown and expressed as the mean of values +/- SEM. Unpaired Student's T-test applied.

Next, K562CLDN16 cells were incubated with AdT*, AdT*KO1 AAA or AdT*KO1 AAAASFPPAFAAA and K562 cells were used as a control. AdT*KO1 AAA and AdT*KO1 AAAASFPPAFAAA transduction of control K562 cells was 103-fold or 455-fold lower than that of AdT*, respectively (Figure 5-8B). Transduction of K562CLDN16 cells was comparable to that of K562 cells for all the adenoviral vectors tested (Figure 5-8B).

5.4 Discussion

With the aim of developing novel adenoviral vectors that specifically target the kidney for gene therapy applications, two mutant adenoviral vectors (AdT*KO1 AAAASFPPAFAAA and AdT*KO1 AAAYAAHRSHAAA) that lack binding to CAR and FX and have candidate heterologous peptides into the HI loop of the fiber knob domain for targeting of the kidney were designed. Also, a control vector (AdT*KO1 AAA) was designed in this study. AdT*KO1 AAAYAAHRSHAAA was successfully produced after transfection of adenoviral genomes into packaging cells; however, viral particles were not able to propagate. AdT*KO1 AAA and AdT*KO1 AAAASFPPAFAAA were successfully generated and showed reporter gene expression, lack of RCAs, presence of genetic mutations and lack of adenovirus aggregates. However, both vectors exhibited extremely low infectivity and a slightly different pattern of protein bands on silver staining performed on adenoviral capsids compared to the control adenoviral vector. Moreover, AdT*KO1 AAAASFPPAFAAA failed to specifically target K562 cells expressing claudin 16, the target for ASFPPAF.

5.4.1 Limitations of the engineered adenoviral vectors

The lack of AdT*KO1 AAAYAAHRSHAAA propagation suggests that the genetic modifications incorporated in this vector might have interfered with capsid assembly and maturation processes affecting capsid protein composition and integrity and thus infectivity of vectors. The low infectivity of AdT*KO1 AAA and AdT*KO1 AAAASFPPAFAAA vectors in HEK-293 cells is in agreement with the requirement of several rounds of amplification to produce sufficient adenovirus for the generation of pure adenoviral vector preparations and with the relatively low vp/ml titers obtained after adenovirus purification. The low infectivity of these vectors could be partly associated with their deficiency in CAR-binding as previously reported for CAR-positive cells transduced with adenoviral vectors with the KO1 mutation (Jakubczak et al., 2001, Smith et al., 2003b, Smith et al., 2002). However, these vectors also exhibited low transduction levels of low CAR-expressing K562 cells (Ebbinghaus et al., 2001, Shayakhmetov et al., 2000) and a slightly different pattern of protein bands on silver staining of adenovirus capsids. Moreover, previous reports have successfully generated adenoviral vectors that combine the KO1 mutation with the introduction of heterologous peptides (Nicklin et al., 2001, Nicklin et al., 2004, Uusi-Kerttula et al., 2016). Also, despite a negative correlation between the introduced peptide size and viral infectivity has been reported, peptides of up to 83 amino-

acids in length have been successfully incorporated (Belousova et al., 2002), suggesting that the 13 amino-acid AAAASFPPAFAAA peptide used in our study is within an appropriate length. Together, the data suggests that the incorporation of AAA or AAAASFPPAFAAA peptides in particular into the fiber knob of these mutant vectors might have affected the formation of mature capsids at a certain degree and led to low infective adenoviral particles, which could have been due to a hampered internalization into host cells or trafficking towards the nucleus, or even to the presence of virus degradation in the endosomes or lysosomal recycling of viral particles. Nevertheless, the presence of immature non-infective viral particles as a result of the adenovirus purification process cannot be dismissed. On the other hand, the lack of AdT*KO1 AAAASFPPAFAAA specificity for the target cells suggests that ASFPPAF peptide might have lost its binding properties to claudin 16 once incorporated into the adenoviral capsid. It is important to consider that there might be several reasons behind this observation. For instance, the specificity of AAAASFPPAFAAA peptide for claudin 16 might differ from that of ASFPPAF. Also, the loss of specificity of ASFPPAF peptide might be due to changes in its spatial conformation as a result of it being constrained when fused with the fiber. Moreover, even if the peptide spatial conformation is maintained after fusion with the fiber, binding of ASFPPAF peptide to claudin 16 might be influenced by fiber residues in close proximity. To confirm whether the lack of AdT*KO1 AAAASFPPAFAAA specificity for claudin $16^{positive}$ K562CLDN16 cells results from an impaired binding of AAAASFPPAFAAA-containing fiber to claudin 16, binding of AdT*KO1 AAAASFPPAFAAA to K562CLDN16 cells should be assessed at low temperatures, which only allow virus binding but not virus internalization. Also, it is to notice that a better control adenoviral vector in this study would be an AdT*KO1 with an AAAAAA peptide incorporated into the HI loop instead of the AAA peptide it was designed with, since the mutant kidney-targeted AdT*KO1 vectors have a total of 6 additional alanine residues in the HI loop (3 alanine residues flanking each end of the candidate peptide). Furthermore, it would also be advisable to confirm whether claudin 16 mRNA is successfully translated into protein and whether it successfully locates to the plasma membrane on K562CLDN16 cells.

5.4.2 Alternative re-targeting strategies

Despite incorporation of heterologous peptides into the HI loop of the fiber knob domain being a very promising strategy and proven very useful for adenoviral vectors' selective targeting, problems associated with the conservation of peptide conformation and target-

binding properties once inserted into the fiber knob domain can limit its success. Strategies to bypass these problems have been developed. For instance, one study performed *in vitro* phage display employing a functional HAdV-5 fiber knob domain with a collection of ligands in the HI loop as a peptide library and screened for candidates on a mouse fibroblast cell line, successfully resulting in three candidate peptides (Fontana et al., 2003). The main advantage is that following this strategy the candidate peptides are screened based on the conformation and binding properties they have once into the HI loop. In our setting, the construction of custom phage display libraries using the fiber knob with random heterologous peptides into the HI loop flanked by AAA peptides might help in better screening for candidates for specific targeting. Other strategies to bypass these problems include the use of affibody libraries. Affibodies are engineered proteins based on the Z-domain derived from the immunoglobulin-binding region of staphylococcal protein A, a 58 amino acids-peptide that folds into a three-helical bundle structure (Uhlen et al., 1984). Affibody libraries are constructed by the combinatorial randomization of 13 amino acid positions from the molecule and can be employed for phage display (Nord et al., 1995, Nord et al., 1997). Next, affibodies can be inserted into the HI loop (Magnusson et al., 2007, Myhre et al., 2009). As before, following this strategy the spatial conformation of candidate peptides is maintained throughout the whole process. Alternatively, other locations are available for insertion of candidate peptides such as other loops in the C-terminal of the fiber, the fiber shaft, the penton base, the hexon HVRs or protein IX, which also allow correct viral assembly and effective targeting (Kurachi et al., 2007b, Kurachi et al., 2007a, Wickham et al., 1997, Gonzalez et al., 1999, Ranki et al., 2007, Rein et al., 2004, Staba et al., 2000, Wickham et al., 1996, Einfeld et al., 1999, Vigne et al., 1999, Wu et al., 2005, Dmitriev et al., 2002, Campos et al., 2004, Vellinga et al., 2004, Li et al., 2006). Nonetheless, peptide sequence could also influence whether the candidate peptide maintains its targeting properties once inserted into the adenoviral protein. For instance, incorporation of certain peptides into the hexon HVR 5 achieved target-binding in contrast to other peptides (Vigne et al., 1999, Kurachi et al., 2007a). If the targeting peptides are not functional as fiber insertions, adapter ligand complexes can be generated, which are comprised of a protein that binds to the adenoviral vector (soluble ectodomain of CAR (sCAR), FX GLA domain, antibody fragments (Fab) specific for adenoviral proteins etc.) and a protein that specifically binds to the therapeutic target (peptide ligand, protein domain, single-chain variable fragment (scFv) antibody, etc.) [reviewed by (Barnett et al., 2002, Coughlan et al., 2010)]. Once the adapter ligand complexes are generated, they are used to coat the adenoviral vector prior to its use. Finally, other re-targeting strategies not involving heterologous peptides might be particularly useful for kidney-targeting with

adenoviral vectors such as genetic pseudotyping, which consists of modifying tropism by exchanging adenoviral proteins from the adenoviral vector with those from a different adenovirus serotype to generate a chimeric vector. Human adenovirus serotypes 7, 11, 21, 34, 35 and 37 have been associated with acute haemorrhagic cystitis and nephritis in humans (Asim et al., 2003, Shields et al., 1985, Ambinder et al., 1986, Harnett et al., 1982, Liles et al., 1993, Murphy et al., 1993). Thus, these serotypes could be used for development of chimeric adenoviral vectors for kidney targeting. Also, some of these serotypes (e.g: HAdV-11, 34, 35) have low seroprevalence of neutralizing antibodies in the human population (Thorner et al., 2006, Vogels et al., 2003) making them particularly attractive for gene therapy since they evade pre-existing immunity. Since the fiber N-terminal region or fiber tail, which is bound to penton base protein, presents high homology amongst diverse adenovirus species (Tarassishin et al., 2000), the fiber has been the main target for pseudotyping. However, chimeric adenovirus should be carefully designed, since capsid proteins other than fiber have been shown to influence tropism. For instance, HAdV-11 kidney tropism in mice was shown to be independent of the fiber (Stone et al., 2005). Thus, the generation of kidney-targeted chimeric adenovirus is a promising strategy as an alternative to the incorporation of heterologous peptides into adenoviral proteins.

Increasing knowledge on adenovirus biodistribution and emerging strategies for vector re-targeting and de-targeting together with the identification of disease-specific biomarkers will potentially allow the development of tissue-specific adenoviral vectors with improved efficacy able to bypass toxicity and host immune responses when administered systemically for gene therapy.

Chapter 6 General discussion and future perspectives

The studies presented in this thesis were focused on investigating the interactions of HAdV-5-based vectors with host cell receptors and blood components following intravascular administration, and defining their role in hepatic and splenic tropism *in vivo* as well as in the immune response against virions. Moreover, the generation of kidney-specific adenoviral vectors for gene therapy was assessed.

The success of gene therapy to treat human diseases relies on the use of delivery vectors able to efficiently introduce genetic material into affected host cells. The ideal vector should be specific for the target tissue, able to deliver short or large therapeutic transgenes into the host cell, enable transient or sustained transgene expression as required without causing insertional mutagenesis, be non-immunogenic or able to evade immune responses, be easily produced and manufactured, and have sufficient storage stability for distribution to clinics (Somia and Verma, 2000). Through time, adenoviruses have evolved to become very efficient biological machines able to deliver genetic material into susceptible eukaryotic cells in a very elegant manner via complex but, at the same time, simple mechanisms that have been optimized and adapted to different environments to ensure their survival and endurance. Interestingly, not only have they developed mechanisms to evade deleterious interactions with host cells such as those with components of the anti-viral immune response but also they have developed mechanisms to benefit from certain interactions and enhance infectious events. A clear example is FX, which by binding to the HAdV-5 capsid is exploited to facilitate interactions with host cell receptors for cell transduction as well as to protect virions against attack by the immune system (Parker et al., 2006, Waddington et al., 2008, Xu et al., 2013). Moreover, given that one of the routes of entry of HAdV-5 into susceptible hosts is via the respiratory tract and that respiratory epithelial cells can produce FVII and FX upon tissue damage (Perrio et al., 2007), it makes evolutionary sense for HAdV-5 to use coagulation factors to facilitate infection of host cells and subsequent virus spread. In particular, FX binds to the HAdV-5 hexon protein and mediates transduction through cellular HSPG (Parker et al., 2006, Kalyuzhniy et al., 2008, Waddington et al., 2008, Alba et al., 2009, Bradshaw et al., 2010, Duffy et al., 2011, Doronin et al., 2012). Simultaneously, FX prevents binding of natural IgM antibodies to HAdV-5 capsids thus blocking the activation of the classical complement pathway on virions that would otherwise lead to virion neutralization (Xu et al., 2013, Ma et al., 2015). The use of HAdV-5-based vectors in gene therapy following intravascular delivery, which is the preferable administration route for many diseases such as cardiovascular disease or metastatic cancer, is limited by the high hepatic tropism these vectors exhibit that has been associated with toxicity and the activation of immune responses (Lozier et al., 2002, Raper

et al., 2002, Atencio et al., 2006, Morral et al., 2002). The ability of FX to bridge HAdV-5 virions to HSPG on the surface of hepatocytes and thus drive liver transduction has become a clear target to fully define the responsible capsid regions to allow ablation of this interaction and thus reduce liver transduction and associated toxicity. Genetic manipulation of key amino acid residues in the HAdV-5 hexon led to the generation of HAV-5-based adenoviral vectors unable to bind to FX that consequently exhibited substantially reduced liver transduction in immunocompetent mice (Alba et al., 2010, Alba et al., 2009, Bradshaw et al., 2012). Unfortunately, recent studies using FX-binding deficient HAdV-5 vectors in immunocompromised mice lacking the mediators for adenovirus neutralization (Xu et al., 2013) or mice lacking HS biosynthesis (Zaiss et al., 2015) revealed the dual function of FX in protecting virions from neutralization and that alternative pathways of HAdV-5 liver transduction are present when the FX-mediated pathway is not available. Moreover, these studies also highlighted the need of further research to unravel the mechanisms mediating liver transduction and immune attack and their implications for the use of HAdV-5 vectors in gene therapy.

Here, assessment of liver transduction in immunocompetent and immunocompromised mice intravenously administered wild type or FX-binding deficient HAdV-5-based vectors confirmed the role of FX in protecting HAdV-5 from *in vitro* and *in vivo* neutralization. Interestingly, it was found that IgM antibodies might not be required for *in vivo* adenovirus neutralization. Conversely, assessment of HAdV-5 neutralization *in vitro* following exposure of virions to immunocompetent or immunocompromised mouse serum revealed that IgM antibodies are essential for *in vitro* HAdV-5 neutralization, suggesting that *in vitro* and *in vivo* adenovirus neutralization is mediated by different mechanisms. Neutralization of virions has been poorly characterized and data from studies both *in vitro* and *in vivo* is controversial. While some authors have reported adenovirus neutralization via the classical and alternative pathways *in vitro* (Xu et al., 2008, Jiang et al., 2004), others have only detected activation of the IgM-mediated classical pathway (Xu et al., 2013). Moreover, while some authors report lack of HAdV-5 neutralization by the complement system in the absence of IgM antibodies *in vivo* (Xu et al., 2013), others sustain the opposite (Tian et al., 2009). Unfortunately, in the time frame imposed by this study these controversies could not be resolved. Further studies to clarify the mechanisms mediating *in vitro* and *in vivo* neutralization of virions are required and are fundamental for the development of adenoviral vectors able to evade immune responses when administered intravascularly. For instance, the use of mouse models lacking different components of the immune response, including complement proteins [e.g: $C1q^{-/-}$ (Botto, 1998), $C3^{-/-}$ (Wessels

et al., 1995), $C4^{-/-}$ (Fischer et al., 1996), $Bf/C2^{-/-}$ (Taylor et al., 1998)], T and/or B cell response [e.g: B and T cell deficient SCID (reviewed by (Bosma and Carroll, 1991)) or Rag $1^{-/-}$ (Mombaerts et al., 1992); B cell deficient *Igh-6*$^{-/-}$ (Kitamura et al., 1991) or J_HD mice (Chen et al., 1993a) ; T cell deficient athymic nude mice (Flanagan, 1966, Groscurth and Kistler, 1975); secreted immunoglobulins deficient "mIg Tg" mice (Hannum et al., 2000)] or other components of the innate immune response including macrophage and natural killer-associated responses [e.g: NSG mice (Zhou et al., 2014, Shultz et al., 2005, Shultz et al., 1995, Ito et al., 2002)], and the development of novel immunocompromised mouse models lacking other key components of the anti-viral immune response would help in addressing these questions. Furthermore, the use of inhibitors for specific components of the complement system such as "C1 inhibitor", which affects C1r and C1s proteases of the C1 complex and can be used *in vitro* and *in vivo* (Rossi et al., 2010, Patston et al., 1991, Landsem et al., 2013, Tradtrantip et al., 2014, Tillou et al., 2010), among others [reviewed by (Wouters and Zeerleder, 2015)], would provide valuable information in defining the mechanism mediating neutralization. Also, soluble recombinant CR1 can be employed to inhibit both the classical and alternative complement pathways (Yazdanbakhsh and Scaradavou, 2004, Yazdanbakhsh et al., 2003), and thus further confirm the role of the complement system in adenovirus neutralization. Since FX has been identified as essential to protect HAdV-5 vectors from neutralization (Xu et al., 2013, Ma et al., 2015, Duffy et al., 2016), it might be advisable to maintain HAdV-5:FX interactions when designing HAdV-5-based adenoviral vectors for gene therapy. In this scenario, however, additional strategies to block HAdV-5:FX complexes from binding to HSPG might be required to reduce liver tropism and associated toxicity as well as FX-mediated transduction of tissues or cells where the gene therapy is not required (Jonsson et al., 2009, Tran et al., 2013). Alternatively, HAdV-5-based vectors could be genetically engineered by mutating only the key amino acid residues involved in neutralization and thus protect virions against immune attack regardless of FX-binding, as has been observed for HAdV-26 and 48, which despite not binding to FX are intrinsically protected from *in vitro* neutralization in the presence of mouse serum (Ma et al., 2015). Alternative approaches to prevent FX from facilitating HAdV-5 liver transduction while also protecting HAdV-5 virions from neutralization and simultaneously exploiting FX-binding as a retargeting strategy have also been explored. For instance, a study coating HAdV-5 capsids with the FX GLA domain fused to scFv antibodies specific for receptors such as Her2, EGFR or the stem cell marker ATP-binding cassette protein G2 (ABCG2) demonstrated retargeting to cells expressing these receptors both *in vitro* and *in vivo* (Chen et al., 2010). However, these vectors still showed high levels of liver transduction due to binding to endogenous FX. Importantly, while pre-

treatment of mice with warfarin resulted in substantially reduced liver transduction, it still partially maintained the retargeting characteristics of these vectors, indicating that coating of capsids with FX GLA domain may partially protect virions against neutralization and allow retargeting of vectors. A recent study showed that position-specific PEGylation of HAdV-5 hexon HVR1 protected virions from IgM antibody and complement-mediated neutralization and scavenging of virions by macrophages *in vitro,* and prolonged circulation of virions in blood (Krutzke et al., 2016). However, this study also reported high liver transduction with a HVR1 PEGylated and FX and CAR-binding deficient HAdV-5 vector. Nevertheless, other studies demonstrated that tissue-specific targeting with FX-binding deficient HAdV-5 vectors can still be achieved in the absence of additional strategies to protect virions against the detrimental consequences of neutralization (Vigant et al., 2008, Shashkova et al., 2009, Alba et al., 2010). Collectively, these studies suggest that neutralization of virions might not be as crucial when using HAdV-5 vectors provided with mechanisms to target specific cell types, when the required therapeutic transgene levels can be achieved with low amount of vector reaching the target tissue or when using oncolytic vectors able to replicate in the target cell and amplify the therapeutic effect. Finally, only one study has assessed both adenovirus neutralization by human serum with no pre-existing neutralising hIgG antibodies and the role of FX in this process (Duffy et al., 2016). This study showed high heterogeneity across samples, where some individual serums neutralized HAdV-5 in the absence of FX-binding (56%) while others failed to neutralize regardless of FX (44%). These results differ from those obtained from studies performed in mice and presented in this thesis, where all serum samples from immunocompetent mice led to HAdV-5 virion neutralization in the absence of FX-binding. These differences between humans and animal models represents one of the main limitations of vector development, causing failure of a high number of clinical trials, since on some occasions the observations from pre-clinical studies in animal models do not translate into the clinical setting. Thus, the use of human primary cell cultures, *ex vivo* approaches with human tissue or the development of appropriate *in vitro* systems using human samples and translationally relevant animal models might be essential to determine the effects of HAdV-5 binding to blood components upon systemic delivery of vectors in humans.

The *in vivo* studies presented in this thesis with FX-binding deficient HAdV-5 in immunocompromised mice confirmed the existence of alternative FX-independent pathways of liver transduction in the absence of FX-binding, supporting previous reports (Zaiss et al., 2015, Xu et al., 2013). This finding was also corroborated by performing

transduction experiments *in vitro* in the presence of immunocompromised mouse serum and absence of FX-binding, either using FX-binding deficient HAdV-5-based vectors or the FX inhibitor X-bp (Atoda et al., 1998). These studies confirmed the existence of FX-independent mechanisms able to enhance HAdV-5 cell transduction in this setting. These data are also consistent with previous reports showing that HAdV-5 can use mouse serum proteins such as FVII, FIX or C4BP to access host cell receptors such as LRP or HSPGs both *in vitro* and *in vivo* (Shayakhmetov et al., 2005b). Together, these findings support the assertion that FX is not the only bridging molecule that can facilitate HAdV-5 cell transduction *in vivo* or in the presence of mouse serum *in vitro*. Importantly, several studies have investigated the role of CAR and $\alpha_v\beta_{3,5}$ integrins as possible host cell receptors for liver transduction in mice following intravascular administration of HAdV-5-based vectors (Leissner et al., 2001, Alemany and Curiel, 2001, Smith et al., 2002, Smith et al., 2003b, Martin et al., 2003, Einfeld et al., 2001, Mizuguchi et al., 2002, Smith et al., 2003a, Bradshaw et al., 2012, Koizumi et al., 2003). Despite some differences between the individual studies, ablation of HAdV-5 binding to CAR or $\alpha_v\beta_{3,5}$ integrins for the most part failed to reduce liver transduction in immunocompetent mice. Here, it was hypothesised that this might have been the result of HAdV-5 using FX as a compensatory pathway for liver transduction in the absence of CAR or $\alpha_v\beta_{3,5}$ integrin-binding. To date, only one study investigated the role of CAR in HAdV-5 liver tropism when the FX-mediated pathway was unavailable for cell transduction, which was performed by depleting mice of HSPG expression as opposed to using FX-binding ablated mutant HAdV-5 (Zaiss et al., 2015). This strategy allowed the study of the role of FX in tropism in immunocompetent mice while still maintaining its function in protecting virions from neutralization. This study reported that CAR does not serve as a receptor for hepatocyte transduction in immunocompetent mice following intravascular administration of vectors. Currently, no studies have been done to assess the role of $\alpha_v\beta_{3,5}$ integrins in HAdV-5 liver tropism in a setting where the FX-mediated pathway of cell transduction is not available and HAdV-5 virions cannot be neutralized. Here, liver tropism of HAdV-5 vectors simultaneously ablated for FX and $\alpha_v\beta_{3,5}$ integrin-binding to prevent HAdV-5 from using compensatory pathways for transduction was assessed in immunocompromised NSG mice lacking the mediators for neutralization (Zhou et al., 2014, Shultz et al., 2005, Shultz et al., 1995, Ito et al., 2002) and thus bypassing the associated virion neutralization in the absence of FX-binding. In similarity to findings for CAR (Zaiss et al., 2015), the data in this thesis suggest that $\alpha_v\beta_{3,5}$ integrins do not serve as receptors for hepatocyte transduction in immunocompromised mice following intravascular administration of vectors. Future experiments delivering $\alpha_v\beta_{3,5}$ integrin-binding deficient HAdV-5-based vectors to

immunocompetent HSPG-deficient mice (Zaiss et al., 2015) would help in confirming results. In an attempt to identify the reported FX-independent mechanisms driving liver transduction, the existence of alternative transduction pathways *in vitro* was investigated following exposure of virions to immunocompromised mouse serum. The use of a range of immortalized cell lines expressing high, low or absent levels of CAR together with the use of engineered cell lines stably expressing hCAR, soluble recombinant HAdV-5 fiber knob to block access to CAR for cell binding and CAR-binding deficient HAdV-5 vector, demonstrated the existence of a FX-independent cell transduction mechanism in the presence of mouse serum involving the use of CAR as a host cell receptor but not relying on direct interactions between HAdV-5 virions and CAR. Importantly, the presence of FX-independent transduction pathways in this setting was also confirmed for hepatocyte-derived HepG2 cells, indicating that HAdV-5 might potentially use this pathway for hepatocyte transduction *in vivo*. Whether CAR is involved in HepG2 cell transduction in the presence of mouse serum is yet to be investigated. To my knowledge, this is the first study describing a specific FX-independent pathway for adenovirus cell transduction following pre-incubation of virions with mouse serum involving CAR as a cellular receptor. Future experiments should focus on identifying the mouse blood factor(s) responsible for CAR-mediated HAdV-5 transduction *in vitro* in the presence of mouse serum as well as the adenovirus capsid protein(s) and the amino acid residues involved in interactions with such blood factor(s). To address these questions, several strategies can be employed such as pull-down assays or co-immunoprecipitation, competition assays with recombinant HAdV-5 capsid proteins, SPR, cross-linking or mass spectrometry performed on HAdV-5 after incubation with mouse serum.

Interestingly, it was observed that when CAR is available, the CAR-mediated pathway is the predominant route for cell transduction in the presence of mouse serum, suggesting that the use of CAR as a host cell receptor might be particularly beneficial over other available receptors, including HSPGs. However, a partial response to the FX-inhibitor X-bp was also observed in the presence of immunocompromised mouse serum, indicating that HAdV-5 might also be able to simultaneously use the FX-mediated pathway in this setting. Furthermore, transduction assays on immortalised cell lines with low or absent levels of CAR on the plasma membrane revealed two different patterns of HAdV-5 transduction in the presence of mouse serum when CAR is unavailable. HAdV-5 either transduced cells via the FX-mediated pathway or via yet unknown FX and CAR-independent mechanisms. These results highlight the high versatility of viruses in transducing cells within different environments and bring into question how many pathways HAdV-5 vectors can use for

cell entry in the presence of mouse serum and whether they are relevant *in vivo*. With the aim of further investigating the beneficial effect of the different transduction pathways on HAdV-5 cell entry, HAdV-5 cell binding, uptake and endosomal membrane penetration in the presence of FX was assessed at the single cell level. Here, FX-binding was found to minimally affect HAdV-5 virion uptake into host cells and the main advantage for HAdV-5 following the FX-mediated pathway for cell entry was increased binding to host cells, confirming previous reports (Alba et al., 2009, Bradshaw et al., 2012). Interestingly, HAdV-5 endosomal membrane penetration efficiency was decreased in the presence of FX within the experimental conditions, restricting virions from accessing the cytosol for trafficking towards the cell nucleus. Therefore, the use of certain pathways for cell transduction might present both advantages and disadvantages for HAdV-5 and it might depend on the cellular context, the differential affinity of the adenoviral capsid for individual components of the transduction pathway, and/or the type of cellular receptor available which determines the transduction pathway used in a particular setting. Further experiments assessing the reason behind these observations, as well as investigating the benefits of using the CAR-mediated pathway in the presence of mouse serum at the single cell level would provide valuable data to gain a greater depth of understanding of the complex adenovirus biology, as well as contribute to the development of liver de-targeted adenoviral vectors. Also, it is important to bear in mind that *in vitro* studies or studies *in vivo* with animal models do not always translate to humans. For instance, differences have been found in the capability of HAdV-5 to bind to mouse, rhesus macaque or human erythrocytes that can result from differential expression of HAdV-5 receptors on these cells (Seiradake et al., 2009, Carlisle et al., 2009). Similarly, while the species B receptor CD46 is expressed ubiquitously in humans [(Johnstone et al., 1993) and reviewed by (Liszewski et al., 1991)], its expression in mice, rat and guinea pig is predominantly located in the testes (Miwa et al., 1998, Tsujimura et al., 1998, Hosokawa et al., 1996) and in leukocytes, erythrocytes and endothelial and epithelial cells in pigs (Toyomura et al., 1997). Also, assessment of HAdV-5 transduction of cultured cells in the presence of human serum samples with no pre-existing neutralising hIgG antibodies revealed that of those samples unable to neutralize HAdV-5, some enhanced HAdV-5 transduction of CAR-expressing A549 cells in a FX-dependent and some in a FX-independent manner, showing high heterogeneity between samples (Duffy et al., 2016). These results differ from those obtained in the studies presented in this thesis, where incubation of HAdV-5 with A549 cells in the presence of immunocompromised mouse serum resulted in FX-independent cell transduction regardless of the mouse sample used. Thus, these studies highlight the limitations of using animal models and the need of better systems to investigate the effects

of HAdV-5 binding to blood components and host cell receptors upon intravascular delivery in humans. Nevertheless, our findings further increase the knowledge of the interactions of HAdV-5 vectors with host proteins and their implications for systemic gene therapy and provide a model for a novel mechanism of HAdV-5 transduction in the presence of mouse serum that may be relevant *in vivo*, putting researchers one step closer towards achieving generation of efficient and safe tissue-specific HAdV-5 vectors.

6.1 Concluding remarks

The studies presented in this thesis highlight the complexity of adenovirus biology and the capacity of adenovirus to adapt to different environments by binding to host factors and cell receptors to achieve efficient cell transduction. Despite evidence showing that CAR and $\alpha_v\beta_{3,5}$ integrins might not be essential for liver tropism following intravascular administration and instead interactions with host factors might represent the main mechanisms of liver transduction, it might still be beneficial to engineer CAR-binding deficient vectors given that CAR is highly expressed in a wide range of mouse and human tissues (Shaw et al., 2004, Excoffon et al., 2010, Tomko et al., 1997). Furthermore, it has also been reported that thrombocytopenia is caused by interaction between CAR on platelets and virions (Othman et al., 2007), and that sequestration of virions by erythrocytes in the bloodstream, which greatly reduces the circulating half-life of the vector, is mediated by CAR (Nicol et al., 2004). Moreover, the results presented in this thesis investigating the existence and implications of as yet unidentified interactions together with previous work indicate that avoiding HAdV-5 interaction with proteins present in the bloodstream that enhance undesired tropism should be the next focus in generating safe HAdV-5-based vectors for gene therapy with limited adenovirus-associated toxicity. With this aim, de-targeting strategies combined with additional strategies to reduce the anti-viral immune response should be developed and assessed in a relevant pre-clinical setting. Once de-targeting and evasion of immune responses to virions is achieved, the next step would be to develop re-targeting strategies to design tissue-specific vectors able to efficiently target the desired tissue with minimal side effects. Here, the design of liver de-targeted and kidney-specific HAdV-5-based vectors for gene therapy was assessed, but unfortunately it did not achieve specificity for the target cells or preserve virus functionality. In particular, these vectors exhibited very low infectivity and capsid integrity problems, highlighting the limitations of current re-targeting strategies and the importance of performing detailed studies on the viability of capsid protein replacements

or mutations and extensive quality control assays on engineered vectors before pre-clinical testing.

In summary, the discovery of the role of FX in liver tropism and immune protection for HAdV-5 was a major advance in the generation of adenoviral vectors for gene therapy and changed the view from simple viral capsid protein:cell receptor interactions to a more complex system where multiple interactions can take place simultaneously to mediate adenoviral transduction. The work presented in this thesis confirms previous findings on the role of FX in protecting HAdV-5 virions against attack from the immune system while also contributing to tropism and provides a novel model of FX-independent HAdV-5 transduction involving as yet unidentified mouse serum proteins.

Together, adenoviral vectors based on HAdV-5 still present pitfalls that need to be further addressed for their use in gene therapy. However, refinement in the resolution of existing techniques such as X-ray crystallography and electron microscopy that allows detailed study of adenoviral capsid proteins and their interactions within the capsid, emergence of new technologies such as single cell based assays that enable precise characterization of cellular processes, and improved genome editing strategies and analytical techniques for in-depth characterization of protein:protein interactions, gene expression and *in vivo* immune responses, has certainly expanded current knowledge and allowed major recent advances that will hopefully translate into successful development of safe, efficient, specific, potent, long-lasting and economically and socially accessible adenoviral-based gene therapy products in the coming years.

List of References

ABE, S., OKUDA, K., URA, T., KONDO, A., YOSHIDA, A., YOSHIZAKI, S., MIZUGUCHI, H., KLINMAN, D. & SHIMADA, M. 2009. Adenovirus type 5 with modified hexons induces robust transgene-specific immune responses in mice with pre-existing immunity against adenovirus type 5. *J Gene Med,* 11**,** 570-9.

ACKRILL, A. M., FOSTER, G. R., LAXTON, C. D., FLAVELL, D. M., STARK, G. R. & KERR, I. M. 1991. Inhibition of the cellular response to interferons by products of the adenovirus type 5 E1A oncogene. *Nucleic Acids Res,* 19**,** 4387-93.

ADAMS, W. C., BOND, E., HAVENGA, M. J., HOLTERMAN, L., GOUDSMIT, J., KARLSSON HEDESTAM, G. B., KOUP, R. A. & LORE, K. 2009. Adenovirus serotype 5 infects human dendritic cells via a coxsackievirus-adenovirus receptor-independent receptor pathway mediated by lactoferrin and DC-SIGN. *J Gen Virol,* 90**,** 1600-10.

ADENOVIRUS TAXONOMY. 2016. *Available at* http://www.vmri.hu/~harrach/AdVtaxshort.htm [Online]. [Accessed].

AKIRA, S. 2000. The role of IL-18 in innate immunity. *Curr Opin Immunol,* 12**,** 59-63.

AKUSJARVI, G. 2008. Temporal regulation of adenovirus major late alternative RNA splicing. *Front Biosci,* 13**,** 5006-15.

ALBA, R., BOSCH, A. & CHILLON, M. 2005. Gutless adenovirus: last-generation adenovirus for gene therapy. *Gene Ther,* 12 Suppl 1**,** S18-27.

ALBA, R., BRADSHAW, A. C., COUGHLAN, L., DENBY, L., MCDONALD, R. A., WADDINGTON, S. N., BUCKLEY, S. M., GREIG, J. A., PARKER, A. L., MILLER, A. M., WANG, H., LIEBER, A., VAN ROOIJEN, N., MCVEY, J. H., NICKLIN, S. A. & BAKER, A. H. 2010. Biodistribution and retargeting of FX-binding ablated adenovirus serotype 5 vectors. *Blood,* 116**,** 2656-64.

ALBA, R., BRADSHAW, A. C., MESTRE-FRANCES, N., VERDIER, J. M., HENAFF, D. & BAKER, A. H. 2012. Coagulation factor X mediates adenovirus type 5 liver gene transfer in non-human primates (Microcebus murinus). *Gene Ther,* 19**,** 109-13.

ALBA, R., BRADSHAW, A. C., PARKER, A. L., BHELLA, D., WADDINGTON, S. N., NICKLIN, S. A., VAN ROOIJEN, N., CUSTERS, J., GOUDSMIT, J., BAROUCH, D. H., MCVEY, J. H. & BAKER, A. H. 2009. Identification of coagulation factor (F)X binding sites on the adenovirus serotype 5 hexon: effect of mutagenesis on FX interactions and gene transfer. *Blood,* 114**,** 965-71.

ALBA, R., COTS, D., OSTAPCHUK, P., BOSCH, A., HEARING, P. & CHILLON, M. 2011. Altering the Ad5 packaging domain affects the maturation of the Ad particles. *PLoS One,* 6**,** e19564.

ALBA, R., HEARING, P., BOSCH, A. & CHILLON, M. 2007. Differential amplification of adenovirus vectors by flanking the packaging signal with attB/attP-PhiC31 sequences: implications for helper-dependent adenovirus production. *Virology,* 367**,** 51-8.

ALBERT, M. L., SAUTER, B. & BHARDWAJ, N. 1998. Dendritic cells acquire antigen from apoptotic cells and induce class I-restricted CTLs. *Nature,* 392**,** 86-9.

ALBINSSON, B. & KIDD, A. H. 1999. Adenovirus type 41 lacks an RGD alpha(v)-integrin binding motif on the penton base and undergoes delayed uptake in A549 cells. *Virus Res,* 64**,** 125-36.

ALEMANY, R. & CURIEL, D. T. 2001. CAR-binding ablation does not change biodistribution and toxicity of adenoviral vectors. *Gene Ther,* 8**,** 1347-53.

ALEMANY, R., SUZUKI, K. & CURIEL, D. T. 2000. Blood clearance rates of adenovirus type 5 in mice. *J Gen Virol,* 81**,** 2605-9.

ALEVIZOPOULOS, K., CATARIN, B., VLACH, J. & AMATI, B. 1998. A novel function of adenovirus E1A is required to overcome growth arrest by the CDK2 inhibitor p27(Kip1). *EMBO J,* 17**,** 5987-97.

ALI, H., LEROY, G., BRIDGE, G. & FLINT, S. J. 2007. The adenovirus L4 33-kilodalton protein binds to intragenic sequences of the major late promoter required for late phase-specific stimulation of transcription. *J Virol,* 81**,** 1327-38.

ALONSO, A., LOPEZ, F. L., MATSUSHITA, K., LOEHR, L. R., AGARWAL, S. K., CHEN, L. Y., SOLIMAN, E. Z., ASTOR, B. C. & CORESH, J. 2011. Chronic kidney disease is associated with the incidence of atrial fibrillation: the Atherosclerosis Risk in Communities (ARIC) study. *Circulation,* 123**,** 2946-53.

ALT, F. W., RATHBUN, G., OLTZ, E., TACCIOLI, G. & SHINKAI, Y. 1992. Function and control of recombination-activating gene activity. *Ann N Y Acad Sci,* 651**,** 277-94.

AMALFITANO, A. & CHAMBERLAIN, J. S. 1997. Isolation and characterization of packaging cell lines that coexpress the adenovirus E1, DNA polymerase, and preterminal proteins: implications for gene therapy. *Gene Ther,* 4**,** 258-63.

AMALFITANO, A., HAUSER, M. A., HU, H., SERRA, D., BEGY, C. R. & CHAMBERLAIN, J. S. 1998. Production and characterization of improved adenovirus vectors with the E1, E2b, and E3 genes deleted. *J Virol,* 72**,** 926-33.

AMBINDER, R. F., BURNS, W., FORMAN, M., CHARACHE, P., ARTHUR, R., BESCHORNER, W., SANTOS, G. & SARAL, R. 1986. Hemorrhagic cystitis associated with adenovirus infection in bone marrow transplantation. *Arch Intern Med,* 146**,** 1400-1.

AMSTUTZ, B., GASTALDELLI, M., KALIN, S., IMELLI, N., BOUCKE, K., WANDELER, E., MERCER, J., HEMMI, S. & GREBER, U. F. 2008. Subversion of CtBP1-controlled macropinocytosis by human adenovirus serotype 3. *EMBO J,* 27**,** 956-69.

ANDERSEN, M. H., SCHRAMA, D., THOR STRATEN, P. & BECKER, J. C. 2006. Cytotoxic T cells. *J Invest Dermatol,* 126**,** 32-41.

ANDERSON, C. W. 1990. The proteinase polypeptide of adenovirus serotype 2 virions. *Virology,* 177**,** 259-72.

ANDERSON, C. W., YOUNG, M. E. & FLINT, S. J. 1989. Characterization of the adenovirus 2 virion protein, mu. *Virology,* 172**,** 506-12.

ANDERSSON, M. G., HAASNOOT, P. C., XU, N., BERENJIAN, S., BERKHOUT, B. & AKUSJARVI, G. 2005. Suppression of RNA interference by adenovirus virus-associated RNA. *J Virol,* 79**,** 9556-65.

ANGELETTI, P. C. & ENGLER, J. A. 1998. Adenovirus preterminal protein binds to the CAD enzyme at active sites of viral DNA replication on the nuclear matrix. *J Virol,* 72**,** 2896-904.

APARICIO, O., RAZQUIN, N., ZARATIEGUI, M., NARVAIZA, I. & FORTES, P. 2006. Adenovirus virus-associated RNA is processed to functional interfering RNAs involved in virus production. *J Virol,* 80**,** 1376-84.

APPLEDORN, D. M., MCBRIDE, A., SEREGIN, S., SCOTT, J. M., SCHULDT, N., KIANG, A., GODBEHERE, S. & AMALFITANO, A. 2008a. Complex interactions with several arms of the complement system dictate innate and humoral immunity to adenoviral vectors. *Gene Ther,* 15**,** 1606-17.

APPLEDORN, D. M., PATIAL, S., MCBRIDE, A., GODBEHERE, S., VAN ROOIJEN, N., PARAMESWARAN, N. & AMALFITANO, A. 2008b. Adenovirus vector-induced innate inflammatory mediators, MAPK signaling, as well as adaptive immune responses are dependent upon both TLR2 and TLR9 in vivo. *J Immunol,* 181**,** 2134-44.

ARNBERG, N. 2009. Adenovirus receptors: implications for tropism, treatment and targeting. *Rev Med Virol,* 19**,** 165-78.

ARNBERG, N. 2012. Adenovirus receptors: implications for targeting of viral vectors. *Trends Pharmacol Sci,* 33**,** 442-8.

ASIM, M., CHONG-LOPEZ, A. & NICKELEIT, V. 2003. Adenovirus infection of a renal allograft. *Am J Kidney Dis,* 41**,** 696-701.

ASPEGREN, A., RABINO, C. & BRIDGE, E. 1998. Organization of splicing factors in adenovirus-infected cells reflects changes in gene expression during the early to late phase transition. *Exp Cell Res,* 245**,** 203-13.

ASTOR, B. C., CORESH, J., HEISS, G., PETTITT, D. & SARNAK, M. J. 2006. Kidney function and anemia as risk factors for coronary heart disease and mortality: the Atherosclerosis Risk in Communities (ARIC) Study. *Am Heart J,* 151**,** 492-500.

ATENCIO, I. A., GRACE, M., BORDENS, R., FRITZ, M., HOROWITZ, J. A., HUTCHINS, B., INDELICATO, S., JACOBS, S., KOLZ, K., MANEVAL, D., MUSCO, M. L., SHINODA, J., VENOOK, A., WEN, S. & WARREN, R. 2006. Biological activities of a recombinant adenovirus p53 (SCH 58500) administered by hepatic arterial infusion in a Phase 1 colorectal cancer trial. *Cancer Gene Ther,* 13**,** 169-81.

ATODA, H., ISHIKAWA, M., MIZUNO, H. & MORITA, T. 1998. Coagulation factor X-binding protein from Deinagkistrodon acutus venom is a Gla domain-binding protein. *Biochemistry,* 37**,** 17361-70.

AVGOUSTI, D. C., HERRMANN, C., KULEJ, K., PANCHOLI, N. J., SEKULIC, N., PETRESCU, J., MOLDEN, R. C., BLUMENTHAL, D., PARIS, A. J., REYES, E. D., OSTAPCHUK, P., HEARING, P., SEEHOLZER, S. H., WORTHEN, G. S., BLACK, B. E., GARCIA, B. A. & WEITZMAN, M. D. 2016. A core viral protein binds host nucleosomes to sequester immune danger signals. *Nature,* 535**,** 173-7.

AZZAZY, H. M. & HIGHSMITH, W. E., JR. 2002. Phage display technology: clinical applications and recent innovations. *Clin Biochem,* 35**,** 425-45.

BABA, A., FUJITA, T. & TAMURA, N. 1984. Sexual dimorphism of the fifth component of mouse complement. *J Exp Med,* 160**,** 411-9.

BAGCHI, S., RAYCHAUDHURI, P. & NEVINS, J. R. 1990. Adenovirus E1A proteins can dissociate heteromeric complexes involving the E2F transcription factor: a novel mechanism for E1A trans-activation. *Cell,* 62**,** 659-69.

BAI, M., HARFE, B. & FREIMUTH, P. 1993. Mutations that alter an Arg-Gly-Asp (RGD) sequence in the adenovirus type 2 penton base protein abolish its cell-rounding activity and delay virus reproduction in flat cells. *J Virol,* 67**,** 5198-205.

BAILEY, A. & MAUTNER, V. 1994. Phylogenetic relationships among adenovirus serotypes. *Virology,* 205**,** 438-52.

BAILEY, C. J., CRYSTAL, R. G. & LEOPOLD, P. L. 2003. Association of adenovirus with the microtubule organizing center. *J Virol,* 77**,** 13275-87.

BAKER, A., ROHLEDER, K. J., HANAKAHI, L. A. & KETNER, G. 2007. Adenovirus E4 34k and E1b 55k oncoproteins target host DNA ligase IV for proteasomal degradation. *J Virol,* 81**,** 7034-40.

BALAKIREVA, L., SCHOEHN, G., THOUVENIN, E. & CHROBOCZEK, J. 2003. Binding of adenovirus capsid to dipalmitoyl phosphatidylcholine provides a novel pathway for virus entry. *J Virol,* 77**,** 4858-66.

BANGARI, D. S., SHUKLA, S. & MITTAL, S. K. 2005. Comparative transduction efficiencies of human and nonhuman adenoviral vectors in human, murine, bovine, and porcine cells in culture. *Biochem Biophys Res Commun,* 327**,** 960-6.

BARLAN, A. U., DANTHI, P. & WIETHOFF, C. M. 2011a. Lysosomal localization and mechanism of membrane penetration influence nonenveloped virus activation of the NLRP3 inflammasome. *Virology,* 412**,** 306-14.

BARLAN, A. U., GRIFFIN, T. M., MCGUIRE, K. A. & WIETHOFF, C. M. 2011b. Adenovirus membrane penetration activates the NLRP3 inflammasome. *J Virol,* 85**,** 146-55.

BARNETT, B. G., CREWS, C. J. & DOUGLAS, J. T. 2002. Targeted adenoviral vectors. *Biochim Biophys Acta,* 1575**,** 1-14.

BAROUCH, D. H., PAU, M. G., CUSTERS, J. H., KOUDSTAAL, W., KOSTENSE, S., HAVENGA, M. J., TRUITT, D. M., SUMIDA, S. M., KISHKO, M. G., ARTHUR, J. C., KORIOTH-SCHMITZ, B., NEWBERG, M. H., GORGONE, D. A., LIFTON, M. A., PANICALI, D. L., NABEL, G. J., LETVIN, N. L. & GOUDSMIT, J. 2004. Immunogenicity of recombinant adenovirus serotype 35 vaccine in the presence of pre-existing anti-Ad5 immunity. *J Immunol,* 172**,** 6290-7.

BASNER-TSCHAKARJAN, E., GAFFAL, E., O'KEEFFE, M., TORMO, D., LIMMER, A., WAGNER, H., HOCHREIN, H. & TÜTING, T. 2006. Adenovirus efficiently transduces plasmacytoid dendritic cells resulting in TLR9-dependent maturation and IFN-alpha production. *J Gene Med,* 8**,** 1300-6.

BAUER, S., GROH, V., WU, J., STEINLE, A., PHILLIPS, J. H., LANIER, L. L. & SPIES, T. 1999. Activation of NK cells and T cells by NKG2D, a receptor for stress-inducible MICA. *Science,* 285**,** 727-9.

BAUER, S., KIRSCHNING, C. J., HACKER, H., REDECKE, V., HAUSMANN, S., AKIRA, S., WAGNER, H. & LIPFORD, G. B. 2001. Human TLR9 confers responsiveness to bacterial DNA via species-specific CpG motif recognition. *Proc Natl Acad Sci U S A,* 98**,** 9237-42.

BAXTER, A. G. & COOKE, A. 1993. Complement lytic activity has no role in the pathogenesis of autoimmune diabetes in NOD mice. *Diabetes,* 42**,** 1574-8.

BAYO-PUXAN, N., CASCALLO, M., GROS, A., HUCH, M., FILLAT, C. & ALEMANY, R. 2006. Role of the putative heparan sulfate glycosaminoglycan-binding site of the adenovirus type 5 fiber shaft on liver detargeting and knob-mediated retargeting. *J Gen Virol,* 87**,** 2487-95.

BEAUVAIS, D. M., BURBACH, B. J. & RAPRAEGER, A. C. 2004. The syndecan-1 ectodomain regulates alphavbeta3 integrin activity in human mammary carcinoma cells. *J Cell Biol,* 167**,** 171-81.

BELOUSOVA, N., KOROKHOV, N., KRENDELSHCHIKOVA, V., SIMONENKO, V., MIKHEEVA, G., TRIOZZI, P. L., ALDRICH, W. A., BANERJEE, P. T., GILLIES, S. D., CURIEL, D. T. & KRASNYKH, V. 2003. Genetically targeted adenovirus vector directed to CD40-expressing cells. *J Virol,* 77**,** 11367-77.

BELOUSOVA, N., KRENDELCHTCHIKOVA, V., CURIEL, D. T. & KRASNYKH, V. 2002. Modulation of adenovirus vector tropism via incorporation of polypeptide ligands into the fiber protein. *J Virol,* 76**,** 8621-31.

BELOUSOVA, N., MIKHEEVA, G., XIONG, C., SOGHOMONIAN, S., YOUNG, D., LE ROUX, L., NAFF, K., BIDAUT, L., WEI, W., LI, C., GELOVANI, J. & KRASNYKH, V. 2010. Development of a targeted gene vector platform based on simian adenovirus serotype 24. *J Virol,* 84**,** 10087-101.

BELTING, M. 2003. Heparan sulfate proteoglycan as a plasma membrane carrier. *Trends Biochem Sci,* 28**,** 145-51.

BENEDICT, C. A., NORRIS, P. S., PRIGOZY, T. I., BODMER, J. L., MAHR, J. A., GARNETT, C. T., MARTINON, F., TSCHOPP, J., GOODING, L. R. & WARE, C. F. 2001. Three adenovirus E3 proteins cooperate to evade apoptosis by tumor necrosis factor-related apoptosis-inducing ligand receptor-1 and -2. *J Biol Chem,* 276**,** 3270-8.

BENEVENTO, M., DI PALMA, S., SNIJDER, J., MOYER, C. L., REDDY, V. S., NEMEROW, G. R. & HECK, A. J. 2014. Adenovirus composition, proteolysis, and disassembly studied by in-depth qualitative and quantitative proteomics. *J Biol Chem,* 289**,** 11421-30.

BENNETT, D., SAKURAI, F., SHIMIZU, K., MATSUI, H., TOMITA, K., SUZUKI, T., KATAYAMA, K., KAWABATA, K. & MIZUGUCHI, H. 2012. Further reduction

in adenovirus vector-mediated liver transduction without largely affecting transgene expression in target organ by exploiting microrna-mediated regulation and the Cre-loxP recombination system. *Mol Pharm,* 9**,** 3452-63.

BERGELSON, J. M., CUNNINGHAM, J. A., DROGUETT, G., KURT-JONES, E. A., KRITHIVAS, A., HONG, J. S., HORWITZ, M. S., CROWELL, R. L. & FINBERG, R. W. 1997. Isolation of a common receptor for Coxsackie B viruses and adenoviruses 2 and 5. *Science,* 275**,** 1320-3.

BERGELSON, J. M., KRITHIVAS, A., CELI, L., DROGUETT, G., HORWITZ, M. S., WICKHAM, T., CROWELL, R. L. & FINBERG, R. W. 1998. The murine CAR homolog is a receptor for coxsackie B viruses and adenoviruses. *J Virol,* 72**,** 415-9.

BERHANE, A. M., WEIL, E. J., KNOWLER, W. C., NELSON, R. G. & HANSON, R. L. 2011a. Albuminuria and estimated glomerular filtration rate as predictors of diabetic end-stage renal disease and death. *Clin J Am Soc Nephrol,* 6**,** 2444-51.

BERHANE, S., ARESTE, C., ABLACK, J. N., RYAN, G. B., BLACKBOURN, D. J., MYMRYK, J. S., TURNELL, A. S., STEELE, J. C. & GRAND, R. J. 2011b. Adenovirus E1A interacts directly with, and regulates the level of expression of, the immunoproteasome component MECL1. *Virology,* 421**,** 149-58.

BERNARDO, A., BALL, C., NOLASCO, L., CHOI, H., MOAKE, J. L. & DONG, J. F. 2005. Platelets adhered to endothelial cell-bound ultra-large von Willebrand factor strings support leukocyte tethering and rolling under high shear stress. *J Thromb Haemost,* 3**,** 562-70.

BETT, A. J., PREVEC, L. & GRAHAM, F. L. 1993. Packaging capacity and stability of human adenovirus type 5 vectors. *J Virol,* 67**,** 5911-21.

BEWLEY, M. C., SPRINGER, K., ZHANG, Y. B., FREIMUTH, P. & FLANAGAN, J. M. 1999. Structural analysis of the mechanism of adenovirus binding to its human cellular receptor, CAR. *Science,* 286**,** 1579-83.

BHAKDI, S., TRANUM-JENSEN, J. & SZIEGOLEIT, A. 1985. Mechanism of membrane damage by streptolysin-O. *Infect Immun,* 47**,** 52-60.

BHAT, N. R. & FAN, F. 2002. Adenovirus infection induces microglial activation: involvement of mitogen-activated protein kinase pathways. *Brain Res,* 948**,** 93-101.

BHATT, U. Y., SFERRA, T. J., JOHNSON, A., WILLIAMS, C., SHIREY, K., VENEMA, T., NUOVO, G. J. & NAHMAN, N. S., JR. 2002. Glomerular beta-galactosidase expression following transduction with microsphere-adenoviral complexes. *Kidney Int,* 61**,** S68-72.

BHATTACHARYA, S., ECKNER, R., GROSSMAN, S., OLDREAD, E., ARANY, Z., D'ANDREA, A. & LIVINGSTON, D. M. 1996. Cooperation of Stat2 and p300/CBP in signalling induced by interferon-alpha. *Nature,* 383**,** 344-7.

BIASIOTTO, R. & AKUSJARVI, G. 2015. Regulation of human adenovirus alternative RNA splicing by the adenoviral L4-33K and L4-22K proteins. *Int J Mol Sci,* 16**,** 2893-912.

BLAESE, R. M., CULVER, K. W., MILLER, A. D., CARTER, C. S., FLEISHER, T., CLERICI, M., SHEARER, G., CHANG, L., CHIANG, Y., TOLSTOSHEV, P., GREENBLATT, J. J., ROSENBERG, S. A., KLEIN, H., BERGER, M., MULLEN, C. A., RAMSEY, W. J., MUUL, L., MORGAN, R. A. & ANDERSON, W. F. 1995. T lymphocyte-directed gene therapy for ADA- SCID: initial trial results after 4 years. *Science,* 270**,** 475-80.

BLANCHETTE, P., KINDSMULLER, K., GROITL, P., DALLAIRE, F., SPEISEDER, T., BRANTON, P. E. & DOBNER, T. 2008. Control of mRNA export by adenovirus E4orf6 and E1B55K proteins during productive infection requires E4orf6 ubiquitin ligase activity. *J Virol,* 82**,** 2642-51.

BLEDSOE, G., SHEN, B., YAO, Y., ZHANG, J. J., CHAO, L. & CHAO, J. 2006. Reversal of renal fibrosis, inflammation, and glomerular hypertrophy by kallikrein gene delivery. *Hum Gene Ther,* 17**,** 545-55.

BLEYER, A. J. & HART, P. S. 1993. Autosomal Dominant Tubulointerstitial Kidney Disease, UMOD-Related (ADTKD-UMOD). *In:* PAGON, R. A., ADAM, M. P., ARDINGER, H. H., WALLACE, S. E., AMEMIYA, A., BEAN, L. J. H., BIRD, T. D., FONG, C. T., MEFFORD, H. C., SMITH, R. J. H. & STEPHENS, K. (eds.) *GeneReviews(R).* Seattle (WA).

BONDANZA, A., SABBADINI, M. G., PELLEGATTA, F., ZIMMERMANN, V. S., TINCANI, A., BALESTRIERI, G., MANFREDI, A. A. & ROVERE, P. 2000. Anti-beta2 glycoprotein I antibodies prevent the De-activation of platelets and sustain their phagocytic clearance. *J Autoimmun,* 15**,** 469-77.

BOSHER, J., ROBINSON, E. C. & HAY, R. T. 1990. Interactions between the adenovirus type 2 DNA polymerase and the DNA binding domain of nuclear factor I. *New Biol,* 2**,** 1083-90.

BOSMA, M. J. & CARROLL, A. M. 1991. The SCID mouse mutant: definition, characterization, and potential uses. *Annu Rev Immunol,* 9**,** 323-50.

BOTTO, M. 1998. C1q knock-out mice for the study of complement deficiency in autoimmune disease. *Exp Clin Immunogenet,* 15**,** 231-4.

BOUDIN, M. L., D'HALLUIN, J. C., COUSIN, C. & BOULANGER, P. 1980. Human adenovirus type 2 protein IIIa. II. Maturation and encapsidation. *Virology,* 101**,** 144-56.

BOULANGER, P. A. & PUVION, F. 1973. Large-scale preparation of soluble adenovirus hexon, penton and fiber antigens in highly purified form. *Eur J Biochem,* 39**,** 37-42.

BOWLES, K. R., GIBSON, J., WU, J., SHAFFER, L. G., TOWBIN, J. A. & BOWLES, N. E. 1999. Genomic organization and chromosomal localization of the human Coxsackievirus B-adenovirus receptor gene. *Hum Genet,* 105**,** 354-9.

BOYER, J., ROHLEDER, K. & KETNER, G. 1999. Adenovirus E4 34k and E4 11k inhibit double strand break repair and are physically associated with the cellular DNA-dependent protein kinase. *Virology,* 263**,** 307-12.

BRADLEY, R. R., LYNCH, D. M., IAMPIETRO, M. J., BORDUCCHI, E. N. & BAROUCH, D. H. 2012a. Adenovirus serotype 5 neutralizing antibodies target both hexon and fiber following vaccination and natural infection. *J Virol,* 86**,** 625-9.

BRADLEY, R. R., MAXFIELD, L. F., LYNCH, D. M., IAMPIETRO, M. J., BORDUCCHI, E. N. & BAROUCH, D. H. 2012b. Adenovirus serotype 5-specific neutralizing antibodies target multiple hexon hypervariable regions. *J Virol,* 86**,** 1267-72.

BRADSHAW, A. C., COUGHLAN, L., MILLER, A. M., ALBA, R., VAN ROOIJEN, N., NICKLIN, S. A. & BAKER, A. H. 2012. Biodistribution and inflammatory profiles of novel penton and hexon double-mutant serotype 5 adenoviruses. *J Control Release,* 164**,** 394-402.

BRADSHAW, A. C., PARKER, A. L., DUFFY, M. R., COUGHLAN, L., VAN ROOIJEN, N., KAHARI, V. M., NICKLIN, S. A. & BAKER, A. H. 2010. Requirements for receptor engagement during infection by adenovirus complexed with blood coagulation factor X. *PLoS Pathog,* 6**,** e1001142.

BREHM, M. A., CUTHBERT, A., YANG, C., MILLER, D. M., DIIORIO, P., LANING, J., BURZENSKI, L., GOTT, B., FOREMAN, O., KAVIRAYANI, A., HERLIHY, M., ROSSINI, A. A., SHULTZ, L. D. & GREINER, D. L. 2010. Parameters for establishing humanized mouse models to study human immunity: analysis of human hematopoietic stem cell engraftment in three immunodeficient strains of mice bearing the IL2rgamma(null) mutation. *Clin Immunol,* 135**,** 84-98.

BRENKMAN, A. B., BREURE, E. C. & VAN DER VLIET, P. C. 2002. Molecular architecture of adenovirus DNA polymerase and location of the protein primer. *J Virol,* 76**,** 8200-7.

BRESTOVITSKY, A., SHARF, R., MITTELMAN, K. & KLEINBERGER, T. 2011. The adenovirus E4orf4 protein targets PP2A to the ACF chromatin-remodeling factor and induces cell death through regulation of SNF2h-containing complexes. *Nucleic Acids Res,* 39**,** 6414-27.

BRIDGE, E. & KETNER, G. 1990. Interaction of adenoviral E4 and E1b products in late gene expression. *Virology,* 174**,** 345-53.

BRIDGE, E., XIA, D. X., CARMO-FONSECA, M., CARDINALI, B., LAMOND, A. I. & PETTERSSON, U. 1995. Dynamic organization of splicing factors in adenovirus-infected cells. *J Virol,* 69**,** 281-90.

BRKIC, S., VUKOBRATOV, Z., PREVEDEN, T., JOVANOVIC, J., VUKADINOV, J. & KOVACEVIC, N. 2002. [Clinical importance of adenoviral infections]. *Med Pregl,* 55**,** 337-41.

BROWN, M. T., MCBRIDE, K. M., BANIECKI, M. L., REICH, N. C., MARRIOTT, G. & MANGEL, W. F. 2002. Actin can act as a cofactor for a viral proteinase in the cleavage of the cytoskeleton. *J Biol Chem,* 277**,** 46298-303.

BRUDER, J. T., SEMENOVA, E., CHEN, P., LIMBACH, K., PATTERSON, N. B., STEFANIAK, M. E., KONOVALOVA, S., THOMAS, C., HAMILTON, M., KING, C. R., RICHIE, T. L. & DOOLAN, D. L. 2012. Modification of Ad5 hexon hypervariable regions circumvents pre-existing Ad5 neutralizing antibodies and induces protective immune responses. *PLoS One,* 7**,** e33920.

BRUNETTI-PIERRI, N., PALMER, D. J., BEAUDET, A. L., CAREY, K. D., FINEGOLD, M. & NG, P. 2004. Acute toxicity after high-dose systemic injection of helper-dependent adenoviral vectors into nonhuman primates. *Hum Gene Ther,* 15**,** 35-46.

BUCHKOVICH, K., DYSON, N., WHYTE, P. & HARLOW, E. 1990. Cellular proteins that are targets for transformation by DNA tumour viruses. *Ciba Found Symp,* 150**,** 262-71; discussion 271-8.

BURBACH, B. J., FRIEDL, A., MUNDHENKE, C. & RAPRAEGER, A. C. 2003. Syndecan-1 accumulates in lysosomes of poorly differentiated breast carcinoma cells. *Matrix Biol,* 22**,** 163-77.

BURCKHARDT, C. J., SUOMALAINEN, M., SCHOENENBERGER, P., BOUCKE, K., HEMMI, S. & GREBER, U. F. 2011. Drifting motions of the adenovirus receptor CAR and immobile integrins initiate virus uncoating and membrane lytic protein exposure. *Cell Host Microbe,* 10**,** 105-17.

BURGERT, H. G. & KVIST, S. 1985. An adenovirus type 2 glycoprotein blocks cell surface expression of human histocompatibility class I antigens. *Cell,* 41**,** 987-97.

BURGERT, H. G., MARYANSKI, J. L. & KVIST, S. 1987. "E3/19K" protein of adenovirus type 2 inhibits lysis of cytolytic T lymphocytes by blocking cell-surface expression of histocompatibility class I antigens. *Proc Natl Acad Sci U S A,* 84**,** 1356-60.

BURGERT, H. G., RUZSICS, Z., OBERMEIER, S., HILGENDORF, A., WINDHEIM, M. & ELSING, A. 2002. Subversion of host defense mechanisms by adenoviruses. *Curr Top Microbiol Immunol,* 269**,** 273-318.

BURLEVA, E. P. & BABUSHKINA, Y. V. 2016. [Administration of Neovasculgen agent for treatment of a patient with neuroischaemic form of diabetic foot syndrome]. *Angiol Sosud Khir,* 22**,** 47-51.

CAMPOS, S. K., PARROTT, M. B. & BARRY, M. A. 2004. Avidin-based targeting and purification of a protein IX-modified, metabolically biotinylated adenoviral vector. *Mol Ther,* 9**,** 942-54.

CAPONE, S., MEOLA, A., ERCOLE, B. B., VITELLI, A., PEZZANERA, M., RUGGERI, L., DAVIES, M. E., TAFI, R., SANTINI, C., LUZZAGO, A., FU, T. M., BETT, A., COLLOCA, S., CORTESE, R., NICOSIA, A. & FOLGORI, A. 2006. A novel adenovirus type 6 (Ad6)-based hepatitis C virus vector that

overcomes preexisting anti-ad5 immunity and induces potent and broad cellular immune responses in rhesus macaques. *J Virol,* 80**,** 1688-99.
CAPURRO, M. I., SHI, W. & FILMUS, J. 2012. LRP1 mediates Hedgehog-induced endocytosis of the GPC3-Hedgehog complex. *J Cell Sci,* 125**,** 3380-9.
CARAVOKYRI, C. & LEPPARD, K. N. 1996. Human adenovirus type 5 variants with sequence alterations flanking the E2A gene: effects on E2 expression and DNA replication. *Virus Genes,* 12**,** 65-75.
CARD, P. B., HOGG, R. T., GIL DEL ALCAZAR, C. R. & GERARD, R. D. 2012. MicroRNA silencing improves the tumor specificity of adenoviral transgene expression. *Cancer Gene Ther,* 19**,** 451-9.
CARLIN, C. R., TOLLEFSON, A. E., BRADY, H. A., HOFFMAN, B. L. & WOLD, W. S. 1989. Epidermal growth factor receptor is down-regulated by a 10,400 MW protein encoded by the E3 region of adenovirus. *Cell,* 57**,** 135-44.
CARLISLE, R. C., DI, Y., CERNY, A. M., SONNEN, A. F., SIM, R. B., GREEN, N. K., SUBR, V., ULBRICH, K., GILBERT, R. J., FISHER, K. D., FINBERG, R. W. & SEYMOUR, L. W. 2009. Human erythrocytes bind and inactivate type 5 adenovirus by presenting Coxsackie virus-adenovirus receptor and complement receptor 1. *Blood,* 113**,** 1909-18.
CARLOS, T. M. & HARLAN, J. M. 1994. Leukocyte-endothelial adhesion molecules. *Blood,* 84**,** 2068-101.
CARSON, C. T., ORAZIO, N. I., LEE, D. V., SUH, J., BEKKER-JENSEN, S., ARAUJO, F. D., LAKDAWALA, S. S., LILLEY, C. E., BARTEK, J., LUKAS, J. & WEITZMAN, M. D. 2009. Mislocalization of the MRN complex prevents ATR signaling during adenovirus infection. *EMBO J,* 28**,** 652-62.
CARVALHO, T., SEELER, J. S., OHMAN, K., JORDAN, P., PETTERSSON, U., AKUSJARVI, G., CARMO-FONSECA, M. & DEJEAN, A. 1995. Targeting of adenovirus E1A and E4-ORF3 proteins to nuclear matrix-associated PML bodies. *J Cell Biol,* 131**,** 45-56.
CATTOGLIO, C., PELLIN, D., RIZZI, E., MARUGGI, G., CORTI, G., MISELLI, F., SARTORI, D., GUFFANTI, A., DI SERIO, C., AMBROSI, A., DE BELLIS, G. & MAVILIO, F. 2010. High-definition mapping of retroviral integration sites identifies active regulatory elements in human multipotent hematopoietic progenitors. *Blood,* 116**,** 5507-17.
CEPKO, C. L. & SHARP, P. A. 1982. Assembly of adenovirus major capsid protein is mediated by a nonvirion protein. *Cell,* 31**,** 407-15.
CERULLO, V., SEILER, M. P., MANE, V., BRUNETTI-PIERRI, N., CLARKE, C., BERTIN, T. K., RODGERS, J. R. & LEE, B. 2007. Toll-like receptor 9 triggers an innate immune response to helper-dependent adenoviral vectors. *Mol Ther,* 15**,** 378-85.
CHAHAL, J. S., GALLAGHER, C., DEHART, C. J. & FLINT, S. J. 2013. The repression domain of the E1B 55-kilodalton protein participates in countering interferon-induced inhibition of adenovirus replication. *J Virol,* 87**,** 4432-44.
CHAHAL, J. S., QI, J. & FLINT, S. J. 2012. The human adenovirus type 5 E1B 55 kDa protein obstructs inhibition of viral replication by type I interferon in normal human cells. *PLoS Pathog,* 8**,** e1002853.
CHAKRABARTI, S., MAUTNER, V., OSMAN, H., COLLINGHAM, K. E., FEGAN, C. D., KLAPPER, P. E., MOSS, P. A. & MILLIGAN, D. W. 2002. Adenovirus infections following allogeneic stem cell transplantation: incidence and outcome in relation to graft manipulation, immunosuppression, and immune recovery. *Blood,* 100**,** 1619-27.
CHALLBERG, M. D., DESIDERIO, S. V. & KELLY, T. J., JR. 1980. Adenovirus DNA replication in vitro: characterization of a protein covalently linked to nascent DNA strands. *Proc Natl Acad Sci U S A,* 77**,** 5105-9.

CHALLBERG, M. D. & KELLY, T. J. 1989. Animal virus DNA replication. *Annu Rev Biochem,* 58**,** 671-717.

CHALLBERG, M. D. & RAWLINS, D. R. 1984. Template requirements for the initiation of adenovirus DNA replication. *Proc Natl Acad Sci U S A,* 81**,** 100-4.

CHARDONNET, Y. & DALES, S. 1970a. Early events in the interaction of adenoviruses with HeLa cells. I. Penetration of type 5 and intracellular release of the DNA genome. *Virology,* 40**,** 462-77.

CHARDONNET, Y. & DALES, S. 1970b. Early events in the interaction of adenoviruses with HeLa cells. II. Comparative observations on the penetration of types 1, 5, 7, and 12. *Virology,* 40**,** 478-85.

CHATTERJEE, P. K., VAYDA, M. E. & FLINT, S. J. 1986. Adenoviral protein VII packages intracellular viral DNA throughout the early phase of infection. *EMBO J,* 5**,** 1633-44.

CHEN, C. Y., MAY, S. M. & BARRY, M. A. 2010. Targeting adenoviruses with factor x-single-chain antibody fusion proteins. *Hum Gene Ther,* 21**,** 739-49.

CHEN, G. X., ZHANG, S., HE, X. H., LIU, S. Y., MA, C. & ZOU, X. P. 2014. Clinical utility of recombinant adenoviral human p53 gene therapy: current perspectives. *Onco Targets Ther,* 7**,** 1901-9.

CHEN, J., MORRAL, N. & ENGEL, D. A. 2007. Transcription releases protein VII from adenovirus chromatin. *Virology,* 369**,** 411-22.

CHEN, J., TROUNSTINE, M., ALT, F. W., YOUNG, F., KURAHARA, C., LORING, J. F. & HUSZAR, D. 1993a. Immunoglobulin gene rearrangement in B cell deficient mice generated by targeted deletion of the JH locus. *Int Immunol,* 5**,** 647-56.

CHEN, K. & WILLIAMS, K. J. 2013. Molecular mediators for raft-dependent endocytosis of syndecan-1, a highly conserved, multifunctional receptor. *J Biol Chem,* 288**,** 13988-99.

CHEN, M., MERMOD, N. & HORWITZ, M. S. 1990. Protein-protein interactions between adenovirus DNA polymerase and nuclear factor I mediate formation of the DNA replication preinitiation complex. *J Biol Chem,* 265**,** 18634-42.

CHEN, P. H., ORNELLES, D. A. & SHENK, T. 1993b. The adenovirus L3 23-kilodalton proteinase cleaves the amino-terminal head domain from cytokeratin 18 and disrupts the cytokeratin network of HeLa cells. *J Virol,* 67**,** 3507-14.

CHENG, C., GALL, J. G., KONG, W. P., SHEETS, R. L., GOMEZ, P. L., KING, C. R. & NABEL, G. J. 2007. Mechanism of ad5 vaccine immunity and toxicity: fiber shaft targeting of dendritic cells. *PLoS Pathog,* 3**,** e25.

CHENG, C., GALL, J. G., NASON, M., KING, C. R., KOUP, R. A., ROEDERER, M., MCELRATH, M. J., MORGAN, C. A., CHURCHYARD, G., BADEN, L. R., DUERR, A. C., KEEFER, M. C., GRAHAM, B. S. & NABEL, G. J. 2010. Differential specificity and immunogenicity of adenovirus type 5 neutralizing antibodies elicited by natural infection or immunization. *J Virol,* 84**,** 630-8.

CHENG, C. Y., GILSON, T., DALLAIRE, F., KETNER, G., BRANTON, P. E. & BLANCHETTE, P. 2011. The E4orf6/E1B55K E3 ubiquitin ligase complexes of human adenoviruses exhibit heterogeneity in composition and substrate specificity. *J Virol,* 85**,** 765-75.

CHETBOUL, V., KLONJKOWSKI, B., LEFEBVRE, H. P., DESVAUX, D., LAROUTE, V., ROSENBERG, D., MAUREY, C., CRESPEAU, F., ADAM, M., ADNOT, S., ELOIT, M. & POUCHELON, J. L. 2001. Short-term efficiency and safety of gene delivery into canine kidneys. *Nephrol Dial Transplant,* 16**,** 608-14.

CHIOU, S. K., TSENG, C. C., RAO, L. & WHITE, E. 1994. Functional complementation of the adenovirus E1B 19-kilodalton protein with Bcl-2 in the inhibition of apoptosis in infected cells. *J Virol,* 68**,** 6553-66.

CHIU, C. Y., MATHIAS, P., NEMEROW, G. R. & STEWART, P. L. 1999. Structure of adenovirus complexed with its internalization receptor, alphavbeta5 integrin. *J Virol,* 73**,** 6759-68.

CHRISTIANSON, H. C. & BELTING, M. 2014. Heparan sulfate proteoglycan as a cell-surface endocytosis receptor. *Matrix Biol,* 35**,** 51-5.

CHROBOCZEK, J. & JACROT, B. 1987. The sequence of adenovirus fiber: similarities and differences between serotypes 2 and 5. *Virology,* 161**,** 549-54.

CHRONIC KIDNEY DISEASE PROGNOSIS, C., MATSUSHITA, K., VAN DER VELDE, M., ASTOR, B. C., WOODWARD, M., LEVEY, A. S., DE JONG, P. E., CORESH, J. & GANSEVOORT, R. T. 2010. Association of estimated glomerular filtration rate and albuminuria with all-cause and cardiovascular mortality in general population cohorts: a collaborative meta-analysis. *Lancet,* 375**,** 2073-81.

CHU, Y., HEISTAD, D., CYBULSKY, M. I. & DAVIDSON, B. L. 2001. Vascular cell adhesion molecule-1 augments adenovirus-mediated gene transfer. *Arterioscler Thromb Vasc Biol,* 21**,** 238-42.

CICHON, G., BOECKH-HERWIG, S., SCHMIDT, H. H., WEHNES, E., MULLER, T., PRING-AKERBLOM, P. & BURGER, R. 2001. Complement activation by recombinant adenoviruses. *Gene Ther,* 8**,** 1794-800.

CICHON, G., SCHMIDT, H. H., BENHIDJEB, T., LOSER, P., ZIEMER, S., HAAS, R., GREWE, N., SCHNIEDERS, F., HEEREN, J., MANNS, M. P., SCHLAG, P. M. & STRAUSS, M. 1999. Intravenous administration of recombinant adenoviruses causes thrombocytopenia, anemia and erythroblastosis in rabbits. *J Gene Med,* 1**,** 360-71.

CLEAT, P. H. & HAY, R. T. 1989. Co-operative interactions between NFI and the adenovirus DNA binding protein at the adenovirus origin of replication. *EMBO J,* 8**,** 1841-8.

CLEMENT, N. & GRIEGER, J. C. 2016. Manufacturing of recombinant adeno-associated viral vectors for clinical trials. *Mol Ther Methods Clin Dev,* 3**,** 16002.

CLINICAL TRIALS. 2016. *Clinical Trials: A service of the U.S National Institutes of Health. Available at:* https://clinicaltrials.gov/ [Online]. [Accessed].

COHEN, C. J., SHIEH, J. T., PICKLES, R. J., OKEGAWA, T., HSIEH, J. T. & BERGELSON, J. M. 2001. The coxsackievirus and adenovirus receptor is a transmembrane component of the tight junction. *Proc Natl Acad Sci U S A,* 98**,** 15191-6.

CONDEZO, G. N., MARABINI, R., AYORA, S., CARAZO, J. M., ALBA, R., CHILLON, M. & SAN MARTIN, C. 2015. Structures of Adenovirus Incomplete Particles Clarify Capsid Architecture and Show Maturation Changes of Packaging Protein L1 52/55k. *J Virol,* 89**,** 9653-64.

CORESH, J., SELVIN, E., STEVENS, L. A., MANZI, J., KUSEK, J. W., EGGERS, P., VAN LENTE, F. & LEVEY, A. S. 2007. Prevalence of chronic kidney disease in the United States. *JAMA,* 298**,** 2038-47.

CORJON, S., GONZALEZ, G., HENNING, P., GRICHINE, A., LINDHOLM, L., BOULANGER, P., FENDER, P. & HONG, S. S. 2011. Cell entry and trafficking of human adenovirus bound to blood factor X is determined by the fiber serotype and not hexon:heparan sulfate interaction. *PLoS One,* 6**,** e18205.

COTS, D., BOSCH, A. & CHILLON, M. 2013. Helper dependent adenovirus vectors: progress and future prospects. *Curr Gene Ther,* 13**,** 370-81.

COTTER, M. J., ZAISS, A. K. & MURUVE, D. A. 2005. Neutrophils interact with adenovirus vectors via Fc receptors and complement receptor 1. *J Virol,* 79**,** 14622-31.

COUGHLAN, L., ALBA, R., PARKER, A. L., BRADSHAW, A. C., MCNEISH, I. A., NICKLIN, S. A. & BAKER, A. H. 2010. Tropism-modification strategies for targeted gene delivery using adenoviral vectors. *Viruses,* 2**,** 2290-355.

COUGHLAN, L., BRADSHAW, A. C., PARKER, A. L., ROBINSON, H., WHITE, K., CUSTERS, J., GOUDSMIT, J., VAN ROIJEN, N., BAROUCH, D. H., NICKLIN, S. A. & BAKER, A. H. 2012. Ad5:Ad48 hexon hypervariable region substitutions lead to toxicity and increased inflammatory responses following intravenous delivery. *Mol Ther,* 20**,** 2268-81.

COUGHLAN, L., VALLATH, S., SAHA, A., FLAK, M., MCNEISH, I. A., VASSAUX, G., MARSHALL, J. F., HART, I. R. & THOMAS, G. J. 2009. In vivo retargeting of adenovirus type 5 to alphavbeta6 integrin results in reduced hepatotoxicity and improved tumor uptake following systemic delivery. *J Virol,* 83**,** 6416-28.

COUSER, W. G., REMUZZI, G., MENDIS, S. & TONELLI, M. 2011. The contribution of chronic kidney disease to the global burden of major noncommunicable diseases. *Kidney Int,* 80**,** 1258-70.

COX, J. H., BENNINK, J. R. & YEWDELL, J. W. 1991. Retention of adenovirus E19 glycoprotein in the endoplasmic reticulum is essential to its ability to block antigen presentation. *J Exp Med,* 174**,** 1629-37.

CRAWFORD-MIKSZA, L. & SCHNURR, D. P. 1996. Analysis of 15 adenovirus hexon proteins reveals the location and structure of seven hypervariable regions containing serotype-specific residues. *J Virol,* 70**,** 1836-44.

DALES, S. & CHARDONNET, Y. 1973. Early events in the interaction of adenoviruses with HeLa cells. IV. Association with microtubules and the nuclear pore complex during vectorial movement of the inoculum. *Virology,* 56**,** 465-83.

DALLAIRE, F., BLANCHETTE, P., GROITL, P., DOBNER, T. & BRANTON, P. E. 2009. Identification of integrin alpha3 as a new substrate of the adenovirus E4orf6/E1B 55-kilodalton E3 ubiquitin ligase complex. *J Virol,* 83**,** 5329-38.

DANTHINNE, X. & IMPERIALE, M. J. 2000. Production of first generation adenovirus vectors: a review. *Gene Ther,* 7**,** 1707-14.

DAVISON, A. J., BENKO, M. & HARRACH, B. 2003. Genetic content and evolution of adenoviruses. *J Gen Virol,* 84**,** 2895-908.

DAVISON, E., DIAZ, R. M., HART, I. R., SANTIS, G. & MARSHALL, J. F. 1997. Integrin alpha5beta1-mediated adenovirus infection is enhanced by the integrin-activating antibody TS2/16. *J Virol,* 71**,** 6204-7.

DAVISON, E., KIRBY, I., ELLIOTT, T. & SANTIS, G. 1999. The human HLA-A*0201 allele, expressed in hamster cells, is not a high-affinity receptor for adenovirus type 5 fiber. *J Virol,* 73**,** 4513-7.

DAVISON, E., KIRBY, I., WHITEHOUSE, J., HART, I., MARSHALL, J. F. & SANTIS, G. 2001. Adenovirus type 5 uptake by lung adenocarcinoma cells in culture correlates with Ad5 fibre binding is mediated by alpha(v)beta1 integrin and can be modulated by changes in beta1 integrin function. *J Gene Med,* 3**,** 550-9.

DE BOER, I. H., RUE, T. C., HALL, Y. N., HEAGERTY, P. J., WEISS, N. S. & HIMMELFARB, J. 2011. Temporal trends in the prevalence of diabetic kidney disease in the United States. *JAMA,* 305**,** 2532-9.

DE GEEST, B., SNOEYS, J., VAN LINTHOUT, S., LIEVENS, J. & COLLEN, D. 2005. Elimination of innate immune responses and liver inflammation by PEGylation of adenoviral vectors and methylprednisolone. *Hum Gene Ther,* 16**,** 1439-51.

DE MEZERVILLE, M. H., TELLIER, R., RICHARDSON, S., HEBERT, D., DOYLE, J. & ALLEN, U. 2006. Adenoviral infections in pediatric transplant recipients: a hospital-based study. *Pediatr Infect Dis J,* 25**,** 815-8.

DEBBAS, M. & WHITE, E. 1993. Wild-type p53 mediates apoptosis by E1A, which is inhibited by E1B. *Genes Dev,* 7**,** 546-54.

DECHECCHI, M. C., MELOTTI, P., BONIZZATO, A., SANTACATTERINA, M., CHILOSI, M. & CABRINI, G. 2001. Heparan sulfate glycosaminoglycans are receptors sufficient to mediate the initial binding of adenovirus types 2 and 5. *J Virol,* 75**,** 8772-80.

DECHECCHI, M. C., TAMANINI, A., BONIZZATO, A. & CABRINI, G. 2000. Heparan sulfate glycosaminoglycans are involved in adenovirus type 5 and 2-host cell interactions. *Virology,* 268**,** 382-90.

DEDIEU, J. F., VIGNE, E., TORRENT, C., JULLIEN, C., MAHFOUZ, I., CAILLAUD, J. M., AUBAILLY, N., ORSINI, C., GUILLAUME, J. M., OPOLON, P., DELAERE, P., PERRICAUDET, M. & YEH, P. 1997. Long-term gene delivery into the livers of immunocompetent mice with E1/E4-defective adenoviruses. *J Virol,* 71**,** 4626-37.

DEFER, C., BELIN, M. T., CAILLET-BOUDIN, M. L. & BOULANGER, P. 1990. Human adenovirus-host cell interactions: comparative study with members of subgroups B and C. *J Virol,* 64**,** 3661-73.

DENBY, L., WORK, L. M., SEGGERN, D. J., WU, E., MCVEY, J. H., NICKLIN, S. A. & BAKER, A. H. 2007. Development of renal-targeted vectors through combined in vivo phage display and capsid engineering of adenoviral fibers from serotype 19p. *Mol Ther,* 15**,** 1647-54.

DEWS, I. C. & MACKENZIE, K. R. 2007. Transmembrane domains of the syndecan family of growth factor coreceptors display a hierarchy of homotypic and heterotypic interactions. *Proc Natl Acad Sci U S A,* 104**,** 20782-7.

DEYLE, D. R. & RUSSELL, D. W. 2009. Adeno-associated virus vector integration. *Curr Opin Mol Ther,* 11**,** 442-7.

DI, B., MAO, Q., ZHAO, J., LI, X., WANG, D. & XIA, H. 2012. A rapid generation of adenovirus vector with a genetic modification in hexon protein. *J Biotechnol,* 157**,** 373-8.

DI PAOLO, N. C., KALYUZHNIY, O. & SHAYAKHMETOV, D. M. 2007. Fiber shaft-chimeric adenovirus vectors lacking the KKTK motif efficiently infect liver cells in vivo. *J Virol,* 81**,** 12249-59.

DI PAOLO, N. C., MIAO, E. A., IWAKURA, Y., MURALI-KRISHNA, K., ADEREM, A., FLAVELL, R. A., PAPAYANNOPOULOU, T. & SHAYAKHMETOV, D. M. 2009a. Virus binding to a plasma membrane receptor triggers interleukin-1 alpha-mediated proinflammatory macrophage response in vivo. *Immunity,* 31**,** 110-21.

DI PAOLO, N. C., VAN ROOIJEN, N. & SHAYAKHMETOV, D. M. 2009b. Redundant and synergistic mechanisms control the sequestration of blood-born adenovirus in the liver. *Mol Ther,* 17**,** 675-84.

DIOURI, M., KEYVANI-AMINEH, H., GEOGHEGAN, K. F. & WEBER, J. M. 1996. Cleavage efficiency by adenovirus protease is site-dependent. *J Biol Chem,* 271**,** 32511-4.

DMITRIEV, I., KRASNYKH, V., MILLER, C. R., WANG, M., KASHENTSEVA, E., MIKHEEVA, G., BELOUSOVA, N. & CURIEL, D. T. 1998. An adenovirus vector with genetically modified fibers demonstrates expanded tropism via utilization of a coxsackievirus and adenovirus receptor-independent cell entry mechanism. *J Virol,* 72**,** 9706-13.

DMITRIEV, I. P., KASHENTSEVA, E. A. & CURIEL, D. T. 2002. Engineering of adenovirus vectors containing heterologous peptide sequences in the C terminus of capsid protein IX. *J Virol,* 76**,** 6893-9.

DORNER, A., XIONG, D., COUCH, K., YAJIMA, T. & KNOWLTON, K. U. 2004. Alternatively spliced soluble coxsackie-adenovirus receptors inhibit coxsackievirus infection. *J Biol Chem,* 279**,** 18497-503.

DORONIN, K., FLATT, J. W., DI PAOLO, N. C., KHARE, R., KALYUZHNIY, O., ACCHIONE, M., SUMIDA, J. P., OHTO, U., SHIMIZU, T., AKASHI-TAKAMURA, S., MIYAKE, K., MACDONALD, J. W., BAMMLER, T. K., BEYER, R. P., FARIN, F. M., STEWART, P. L. & SHAYAKHMETOV, D. M. 2012. Coagulation factor X activates innate immunity to human species C adenovirus. *Science,* 338**,** 795-8.

DOUCAS, V., ISHOV, A. M., ROMO, A., JUGUILON, H., WEITZMAN, M. D., EVANS, R. M. & MAUL, G. G. 1996. Adenovirus replication is coupled with the dynamic properties of the PML nuclear structure. *Genes Dev,* 10**,** 196-207.

DREYFUSS, J. L., REGATIERI, C. V., JARROUGE, T. R., CAVALHEIRO, R. P., SAMPAIO, L. O. & NADER, H. B. 2009. Heparan sulfate proteoglycans: structure, protein interactions and cell signaling. *An Acad Bras Cienc,* 81**,** 409-29.

DUAN, D., SHARMA, P., YANG, J., YUE, Y., DUDUS, L., ZHANG, Y., FISHER, K. J. & ENGELHARDT, J. F. 1998. Circular intermediates of recombinant adeno-associated virus have defined structural characteristics responsible for long-term episomal persistence in muscle tissue. *J Virol,* 72**,** 8568-77.

DUDLEY, R. W., LU, Y., GILBERT, R., MATECKI, S., NALBANTOGLU, J., PETROF, B. J. & KARPATI, G. 2004. Sustained improvement of muscle function one year after full-length dystrophin gene transfer into mdx mice by a gutted helper-dependent adenoviral vector. *Hum Gene Ther,* 15**,** 145-56.

DUFFY, M. R., BRADSHAW, A. C., PARKER, A. L., MCVEY, J. H. & BAKER, A. H. 2011. A cluster of basic amino acids in the factor X serine protease mediates surface attachment of adenovirus/FX complexes. *J Virol,* 85**,** 10914-9.

DUFFY, M. R., DOSZPOLY, A., TURNER, G., NICKLIN, S. A. & BAKER, A. H. 2016. The relevance of coagulation factor X protection of adenoviruses in human sera. *Gene Ther*.

DYSON, N., BUCHKOVICH, K., WHYTE, P. & HARLOW, E. 1989. Cellular proteins that are targetted by DNA tumor viruses for transformation. *Princess Takamatsu Symp,* 20**,** 191-8.

EBBINGHAUS, C., AL-JAIBAJI, A., OPERSCHALL, E., SCHOFFEL, A., PETER, I., GREBER, U. F. & HEMMI, S. 2001. Functional and selective targeting of adenovirus to high-affinity Fcgamma receptor I-positive cells by using a bispecific hybrid adapter. *J Virol,* 75**,** 480-9.

ECHAVARRIA, M. 2008. Adenoviruses in immunocompromised hosts. *Clin Microbiol Rev,* 21**,** 704-15.

ECKARDT, K. U., CORESH, J., DEVUYST, O., JOHNSON, R. J., KOTTGEN, A., LEVEY, A. S. & LEVIN, A. 2013. Evolving importance of kidney disease: from subspecialty to global health burden. *Lancet,* 382**,** 158-69.

EHRHARDT, A. & KAY, M. A. 2002. A new adenoviral helper-dependent vector results in long-term therapeutic levels of human coagulation factor IX at low doses in vivo. *Blood,* 99**,** 3923-30.

EINFELD, D. A., BROUGH, D. E., ROELVINK, P. W., KOVESDI, I. & WICKHAM, T. J. 1999. Construction of a pseudoreceptor that mediates transduction by adenoviruses expressing a ligand in fiber or penton base. *J Virol,* 73**,** 9130-6.

EINFELD, D. A., SCHROEDER, R., ROELVINK, P. W., LIZONOVA, A., KING, C. R., KOVESDI, I. & WICKHAM, T. J. 2001. Reducing the native tropism of adenovirus vectors requires removal of both CAR and integrin interactions. *J Virol,* 75**,** 11284-91.

EKKENS, M. J., SHEDLOCK, D. J., JUNG, E., TROY, A., PEARCE, E. L., SHEN, H. & PEARCE, E. J. 2007. Th1 and Th2 cells help CD8 T-cell responses. *Infect Immun,* 75**,** 2291-6.

ELSING, A. & BURGERT, H. G. 1998. The adenovirus E3/10.4K-14.5K proteins down-modulate the apoptosis receptor Fas/Apo-1 by inducing its internalization. *Proc Natl Acad Sci U S A,* 95**,** 10072-7.

ENDTER, C., HARTL, B., SPRUSS, T., HAUBER, J. & DOBNER, T. 2005. Blockage of CRM1-dependent nuclear export of the adenovirus type 5 early region 1B 55-kDa protein augments oncogenic transformation of primary rat cells. *Oncogene,* 24**,** 55-64.

ENDTER, C., KZHYSHKOWSKA, J., STAUBER, R. & DOBNER, T. 2001. SUMO-1 modification required for transformation by adenovirus type 5 early region 1B 55-kDa oncoprotein. *Proc Natl Acad Sci U S A,* 98**,** 11312-7.

ESKO, J. D. & LINDAHL, U. 2001. Molecular diversity of heparan sulfate. *J Clin Invest,* 108**,** 169-73.

ETO, Y., GAO, J. Q., SEKIGUCHI, F., KURACHI, S., KATAYAMA, K., MIZUGUCHI, H., HAYAKAWA, T., TSUTSUMI, Y., MAYUMI, T. & NAKAGAWA, S. 2004. Neutralizing antibody evasion ability of adenovirus vector induced by the bioconjugation of methoxypolyethylene glycol succinimidyl propionate (MPEG-SPA). *Biol Pharm Bull,* 27**,** 936-8.

ETO, Y., YOSHIOKA, Y., ISHIDA, T., YAO, X., MORISHIGE, T., NARIMATSU, S., MIZUGUCHI, H., MUKAI, Y., OKADA, N., KIWADA, H. & NAKAGAWA, S. 2010. Optimized PEGylated adenovirus vector reduces the anti-vector humoral immune response against adenovirus and induces a therapeutic effect against metastatic lung cancer. *Biol Pharm Bull,* 33**,** 1540-4.

EVANS, J. D. & HEARING, P. 2005. Relocalization of the Mre11-Rad50-Nbs1 complex by the adenovirus E4 ORF3 protein is required for viral replication. *J Virol,* 79**,** 6207-15.

EWING, S. G., BYRD, S. A., CHRISTENSEN, J. B., TYLER, R. E. & IMPERIALE, M. J. 2007. Ternary complex formation on the adenovirus packaging sequence by the IVa2 and L4 22-kilodalton proteins. *J Virol,* 81**,** 12450-7.

EXCOFFON, K. J., BOWERS, J. R. & SHARMA, P. 2014. 1. Alternative splicing of viral receptors: A review of the diverse morphologies and physiologies of adenoviral receptors. *Recent Res Dev Virol,* 9**,** 1-24.

EXCOFFON, K. J., GANSEMER, N. D., MOBILY, M. E., KARP, P. H., PAREKH, K. R. & ZABNER, J. 2010. Isoform-specific regulation and localization of the coxsackie and adenovirus receptor in human airway epithelia. *PLoS One,* 5**,** e9909.

EXCOFFON, K. J., TRAVER, G. L. & ZABNER, J. 2005. The role of the extracellular domain in the biology of the coxsackievirus and adenovirus receptor. *Am J Respir Cell Mol Biol,* 32**,** 498-503.

FABRY, C. M., ROSA-CALATRAVA, M., CONWAY, J. F., ZUBIETA, C., CUSACK, S., RUIGROK, R. W. & SCHOEHN, G. 2005. A quasi-atomic model of human adenovirus type 5 capsid. *EMBO J,* 24**,** 1645-54.

FABRY, C. M., ROSA-CALATRAVA, M., MORISCOT, C., RUIGROK, R. W., BOULANGER, P. & SCHOEHN, G. 2009. The C-terminal domains of adenovirus serotype 5 protein IX assemble into an antiparallel structure on the facets of the capsid. *J Virol,* 83**,** 1135-9.

FALGOUT, B. & KETNER, G. 1988. Characterization of adenovirus particles made by deletion mutants lacking the fiber gene. *J Virol,* 62**,** 622-5.

FALLAUX, F. J., BOUT, A., VAN DER VELDE, I., VAN DEN WOLLENBERG, D. J., HEHIR, K. M., KEEGAN, J., AUGER, C., CRAMER, S. J., VAN ORMONDT, H., VAN DER EB, A. J., VALERIO, D. & HOEBEN, R. C. 1998. New helper cells and matched early region 1-deleted adenovirus vectors prevent generation of replication-competent adenoviruses. *Hum Gene Ther,* 9**,** 1909-17.

FARLEY, D. C., BROWN, J. L. & LEPPARD, K. N. 2004. Activation of the early-late switch in adenovirus type 5 major late transcription unit expression by L4 gene products. *J Virol,* 78**,** 1782-91.

FARMER, C., MORTON, P. E., SNIPPE, M., SANTIS, G. & PARSONS, M. 2009. Coxsackie adenovirus receptor (CAR) regulates integrin function through activation of p44/42 MAPK. *Exp Cell Res,* 315**,** 2637-47.

FDA GENE THERAPY LETTER 2000. Gene Therapy Letter: Pre-clinical and Clinical Issues. Available at http://www.fda.gov/ohrms/dockets/ac/01/briefing/3739b1_05.pdf.

FEIL, S. C., ASCHER, D. B., KUIPER, M. J., TWETEN, R. K. & PARKER, M. W. 2014. Structural studies of Streptococcus pyogenes streptolysin O provide insights into the early steps of membrane penetration. *J Mol Biol,* 426**,** 785-92.

FENSTERL, V. & SEN, G. C. 2009. Interferons and viral infections. *Biofactors,* 35**,** 14-20.

FERRARI, R., PELLEGRINI, M., HORWITZ, G. A., XIE, W., BERK, A. J. & KURDISTANI, S. K. 2008. Epigenetic reprogramming by adenovirus e1a. *Science,* 321**,** 1086-8.

FESSLER, S. P. & YOUNG, C. S. 1999. The role of the L4 33K gene in adenovirus infection. *Virology,* 263**,** 507-16.

FISCHER, M. B., MA, M., GOERG, S., ZHOU, X., XIA, J., FINCO, O., HAN, S., KELSOE, G., HOWARD, R. G., ROTHSTEIN, T. L., KREMMER, E., ROSEN, F. S. & CARROLL, M. C. 1996. Regulation of the B cell response to T-dependent antigens by classical pathway complement. *J Immunol,* 157**,** 549-56.

FLANAGAN, S. P. 1966. 'Nude', a new hairless gene with pleiotropic effects in the mouse. *Genet Res,* 8**,** 295-309.

FLATT, J. W., KIM, R., SMITH, J. G., NEMEROW, G. R. & STEWART, P. L. 2013. An intrinsically disordered region of the adenovirus capsid is implicated in neutralization by human alpha defensin 5. *PLoS One,* 8**,** e61571.

FLINT, S. J. 1982. Organization and expression of viral genes in adenovirus-transformed cells. *Int Rev Cytol,* 76**,** 47-65.

FOLEY, R. N. & COLLINS, A. J. 2007. End-stage renal disease in the United States: an update from the United States Renal Data System. *J Am Soc Nephrol,* 18**,** 2644-8.

FONSECA, G. J., COHEN, M. J., NICHOLS, A. C., BARRETT, J. W. & MYMRYK, J. S. 2013. Viral retasking of hBre1/RNF20 to recruit hPaf1 for transcriptional activation. *PLoS Pathog,* 9**,** e1003411.

FONSECA, G. J., THILLAINADESAN, G., YOUSEF, A. F., ABLACK, J. N., MOSSMAN, K. L., TORCHIA, J. & MYMRYK, J. S. 2012. Adenovirus evasion of interferon-mediated innate immunity by direct antagonism of a cellular histone posttranslational modification. *Cell Host Microbe,* 11**,** 597-606.

FONTANA, L., NUZZO, M., URBANELLI, L. & MONACI, P. 2003. General strategy for broadening adenovirus tropism. *J Virol,* 77**,** 11094-104.

FOUQUE, D. & APARICIO, M. 2007. Eleven reasons to control the protein intake of patients with chronic kidney disease. *Nat Clin Pract Nephrol,* 3**,** 383-92.

FOWLKES, D. M., LORD, S. T., LINNE, T., PETTERSSON, U. & PHILIPSON, L. 1979. Interaction between the adenovirus DNA-binding protein and double-stranded DNA. *J Mol Biol,* 132**,** 163-80.

FOX, C. S., MATSUSHITA, K., WOODWARD, M., BILO, H. J., CHALMERS, J., HEERSPINK, H. J., LEE, B. J., PERKINS, R. M., ROSSING, P., SAIRENCHI, T., TONELLI, M., VASSALOTTI, J. A., YAMAGISHI, K., CORESH, J., DE JONG, P. E., WEN, C. P., NELSON, R. G. & CHRONIC KIDNEY DISEASE PROGNOSIS, C. 2012. Associations of kidney disease measures with mortality and end-stage renal disease in individuals with and without diabetes: a meta-analysis. *Lancet,* 380**,** 1662-73.

FRANCO, O. H., PEETERS, A., BONNEUX, L. & DE LAET, C. 2005. Blood pressure in adulthood and life expectancy with cardiovascular disease in men and women: life course analysis. *Hypertension,* 46**,** 280-6.

FRANCO, O. H., STEYERBERG, E. W., HU, F. B., MACKENBACH, J. & NUSSELDER, W. 2007. Associations of diabetes mellitus with total life expectancy and life expectancy with and without cardiovascular disease. *Arch Intern Med,* 167**,** 1145-51.

FREDMAN, J. N. & ENGLER, J. A. 1993. Adenovirus precursor to terminal protein interacts with the nuclear matrix in vivo and in vitro. *J Virol,* 67**,** 3384-95.

FREIMUTH, P., SPRINGER, K., BERARD, C., HAINFELD, J., BEWLEY, M. & FLANAGAN, J. 1999. Coxsackievirus and adenovirus receptor amino-terminal immunoglobulin V-related domain binds adenovirus type 2 and fiber knob from adenovirus type 12. *J Virol,* 73**,** 1392-8.

FRICKMANN, H., JUNGBLUT, S., HIRCHE, T. O., GROSS, U., KUHNS, M. & ZAUTNER, A. E. 2012. Spectrum of viral infections in patients with cystic fibrosis. *Eur J Microbiol Immunol (Bp),* 2**,** 161-75.

FUEYO, J., GOMEZ-MANZANO, C., ALEMANY, R., LEE, P. S., MCDONNELL, T. J., MITLIANGA, P., SHI, Y. X., LEVIN, V. A., YUNG, W. K. & KYRITSIS, A. P. 2000. A mutant oncolytic adenovirus targeting the Rb pathway produces anti-glioma effect in vivo. *Oncogene,* 19**,** 2-12.

FUJISHIRO, J., TAKEDA, S., TAKENO, Y., TAKEUCHI, K., OGATA, Y., TAKAHASHI, M., HAKAMATA, Y., KANEKO, T., MURAKAMI, T., OKADA, T., OZAWA, K., HASHIZUME, K. & KOBAYASHI, E. 2005. Gene transfer to the rat kidney in vivo and ex vivo using an adenovirus vector: factors influencing transgene expression. *Nephrol Dial Transplant,* 20**,** 1385-91.

FUKI, I. V., IOZZO, R. V. & WILLIAMS, K. J. 2000. Perlecan heparan sulfate proteoglycan: a novel receptor that mediates a distinct pathway for ligand catabolism. *J Biol Chem,* 275**,** 25742-50.

FUKI, I. V., KUHN, K. M., LOMAZOV, I. R., ROTHMAN, V. L., TUSZYNSKI, G. P., IOZZO, R. V., SWENSON, T. L., FISHER, E. A. & WILLIAMS, K. J. 1997. The syndecan family of proteoglycans. Novel receptors mediating internalization of atherogenic lipoproteins in vitro. *J Clin Invest,* 100**,** 1611-22.

FUKUHARA, H., INO, Y. & TODO, T. 2016. Oncolytic virus therapy: A new era of cancer treatment at dawn. *Cancer Sci*.

FURCINITTI, P. S., VAN OOSTRUM, J. & BURNETT, R. M. 1989. Adenovirus polypeptide IX revealed as capsid cement by difference images from electron microscopy and crystallography. *EMBO J,* 8**,** 3563-70.

FURIE, B. & FURIE, B. C. 1988. The molecular basis of blood coagulation. *Cell,* 53**,** 505-18.

GADEN, F., FRANQUEVILLE, L., MAGNUSSON, M. K., HONG, S. S., MERTEN, M. D., LINDHOLM, L. & BOULANGER, P. 2004. Gene transduction and cell entry pathway of fiber-modified adenovirus type 5 vectors carrying novel endocytic peptide ligands selected on human tracheal glandular cells. *J Virol,* 78**,** 7227-47.

GAGGAR, A., SHAYAKHMETOV, D. M., LISZEWSKI, M. K., ATKINSON, J. P. & LIEBER, A. 2005. Localization of regions in CD46 that interact with adenovirus. *J Virol,* 79**,** 7503-13.

GAHERY-SEGARD, H., FARACE, F., GODFRIN, D., GASTON, J., LENGAGNE, R., TURSZ, T., BOULANGER, P. & GUILLET, J. G. 1998. Immune response to recombinant capsid proteins of adenovirus in humans: antifiber and anti-penton base antibodies have a synergistic effect on neutralizing activity. *J Virol,* 72**,** 2388-97.

GALL, J., KASS-EISLER, A., LEINWAND, L. & FALCK-PEDERSEN, E. 1996. Adenovirus type 5 and 7 capsid chimera: fiber replacement alters receptor tropism without affecting primary immune neutralization epitopes. *J Virol,* 70**,** 2116-23.

GAMA-CARVALHO, M., CONDADO, I. & CARMO-FONSECA, M. 2003. Regulation of adenovirus alternative RNA splicing correlates with a reorganization of splicing factors in the nucleus. *Exp Cell Res,* 289**,** 77-85.

GANSEVOORT, R. T., CORREA-ROTTER, R., HEMMELGARN, B. R., JAFAR, T. H., HEERSPINK, H. J., MANN, J. F., MATSUSHITA, K. & WEN, C. P. 2013. Chronic kidney disease and cardiovascular risk: epidemiology, mechanisms, and prevention. *Lancet,* 382**,** 339-52.

GAO, W., ROBBINS, P. D. & GAMBOTTO, A. 2003. Human adenovirus type 35: nucleotide sequence and vector development. *Gene Ther,* 10**,** 1941-9.

GASTALDELLI, M., IMELLI, N., BOUCKE, K., AMSTUTZ, B., MEIER, O. & GREBER, U. F. 2008. Infectious adenovirus type 2 transport through early but not late endosomes. *Traffic,* 9**,** 2265-78.

GATTONI, A., PARLATO, A., VANGIERI, B., BRESCIANI, M. & DERNA, R. 2006. Interferon-gamma: biologic functions and HCV therapy (type I/II) (1 of 2 parts). *Clin Ter,* 157**,** 377-86.

GAUDET, D., DE WAL, J., TREMBLAY, K., DERY, S., VAN DEVENTER, S., FREIDIG, A., BRISSON, D. & METHOT, J. 2010. Review of the clinical development of alipogene tiparvovec gene therapy for lipoprotein lipase deficiency. *Atheroscler Suppl,* 11**,** 55-60.

GEORGE, S. J., WAN, S., HU, J., MACDONALD, R., JOHNSON, J. L. & BAKER, A. H. 2011. Sustained reduction of vein graft neointima formation by ex vivo TIMP-3 gene therapy. *Circulation,* 124**,** S135-42.

GERN, J. E., PAPPAS, T., VISNESS, C. M., JAFFEE, K. F., LEMANSKE, R. F., TOGIAS, A., BLOOMBERG, G. R., CRUIKSHANK, W. W., LAMM, C., TUZOVA, M., WOOD, R. A. & LEE, W. M. 2012. Comparison of the etiology of viral respiratory illnesses in inner-city and suburban infants. *J Infect Dis,* 206**,** 1342-9.

GIORDANO, A., MCCALL, C., WHYTE, P. & FRANZA, B. R., JR. 1991. Human cyclin A and the retinoblastoma protein interact with similar but distinguishable sequences in the adenovirus E1A gene product. *Oncogene,* 6**,** 481-5.

GO, A. S., CHERTOW, G. M., FAN, D., MCCULLOCH, C. E. & HSU, C. Y. 2004. Chronic kidney disease and the risks of death, cardiovascular events, and hospitalization. *N Engl J Med,* 351**,** 1296-305.

GOLDMAN, M. B., BANGALORE, S. & GOLDMAN, J. N. 1978. Functional and biochemical properties of the early classical complement system of mice. *J Immunol,* 120**,** 216-24.

GONZALEZ, R., VEREECQUE, R., WICKHAM, T. J., FACON, T., HETUIN, D., KOVESDI, I., BAUTERS, F., FENAUX, P. & QUESNEL, B. 1999. Transduction of bone marrow cells by the AdZ.F(pK7) modified adenovirus demonstrates preferential gene transfer in myeloma cells. *Hum Gene Ther,* 10**,** 2709-17.

GOODING, L. R., RANHEIM, T. S., TOLLEFSON, A. E., AQUINO, L., DUERKSEN-HUGHES, P., HORTON, T. M. & WOLD, W. S. 1991. The 10,400- and 14,500-dalton proteins encoded by region E3 of adenovirus function together to protect many but not all mouse cell lines against lysis by tumor necrosis factor. *J Virol,* 65**,** 4114-23.

GOOSNEY, D. L. & NEMEROW, G. R. 2003. Adenovirus infection: taking the back roads to viral entry. *Curr Biol,* 13**,** R99-R100.

GRAHAM, F. L., SMILEY, J., RUSSELL, W. C. & NAIRN, R. 1977. Characteristics of a human cell line transformed by DNA from human adenovirus type 5. *J Gen Virol,* 36**,** 59-74.

GRAWUNDER, U., ZIMMER, D., FUGMANN, S., SCHWARZ, K. & LIEBER, M. R. 1998. DNA ligase IV is essential for V(D)J recombination and DNA double-strand break repair in human precursor lymphocytes. *Mol Cell,* 2**,** 477-84.

GREBER, U. F., SUOMALAINEN, M., STIDWILL, R. P., BOUCKE, K., EBERSOLD, M. W. & HELENIUS, A. 1997. The role of the nuclear pore complex in adenovirus DNA entry. *EMBO J,* 16**,** 5998-6007.

GREBER, U. F., WEBSTER, P., WEBER, J. & HELENIUS, A. 1996. The role of the adenovirus protease on virus entry into cells. *EMBO J,* 15**,** 1766-77.

GREBER, U. F., WILLETTS, M., WEBSTER, P. & HELENIUS, A. 1993. Stepwise dismantling of adenovirus 2 during entry into cells. *Cell,* 75**,** 477-86.

GREEN, N. K., HERBERT, C. W., HALE, S. J., HALE, A. B., MAUTNER, V., HARKINS, R., HERMISTON, T., ULBRICH, K., FISHER, K. D. & SEYMOUR, L. W. 2004. Extended plasma circulation time and decreased toxicity of polymer-coated adenovirus. *Gene Ther,* 11**,** 1256-63.

GREIG, J. A., BUCKLEY, S. M., WADDINGTON, S. N., PARKER, A. L., BHELLA, D., PINK, R., RAHIM, A. A., MORITA, T., NICKLIN, S. A., MCVEY, J. H. & BAKER, A. H. 2009. Influence of coagulation factor x on in vitro and in vivo gene delivery by adenovirus (Ad) 5, Ad35, and chimeric Ad5/Ad35 vectors. *Mol Ther,* 17**,** 1683-91.

GRINES, C., RUBANYI, G. M., KLEIMAN, N. S., MARROTT, P. & WATKINS, M. W. 2003. Angiogenic gene therapy with adenovirus 5 fibroblast growth factor-4 (Ad5FGF-4): a new option for the treatment of coronary artery disease. *Am J Cardiol,* 92**,** 24N-31N.

GROLLEAU-JULIUS, A., GARG, M. R., MO, R., STOOLMAN, L. L. & YUNG, R. L. 2006. Effect of aging on bone marrow-derived murine CD11c+CD4-CD8alpha-dendritic cell function. *J Gerontol A Biol Sci Med Sci,* 61**,** 1039-47.

GROSCURTH, P. & KISTLER, G. 1975. [Histogenesis of the immune system of the "nude" mouse. Postnatal development of the thymus: a light microscopical study (author's transl)]. *Beitr Pathol,* 154**,** 109-24.

GROTZINGER, T., STERNSDORF, T., JENSEN, K. & WILL, H. 1996. Interferon-modulated expression of genes encoding the nuclear-dot-associated proteins Sp100 and promyelocytic leukemia protein (PML). *Eur J Biochem,* 238**,** 554-60.

GUGGENHEIMER, R. A., NAGATA, K., KENNY, M. & HURWITZ, J. 1984. Protein-primed replication of plasmids containing the terminus of the adenovirus genome. II. Purification and characterization of a host protein required for the replication of DNA templates devoid of the terminal protein. *J Biol Chem,* 259**,** 7815-25.

GUPTA, A., JHA, S., ENGEL, D. A., ORNELLES, D. A. & DUTTA, A. 2013. Tip60 degradation by adenovirus relieves transcriptional repression of viral transcriptional activator EIA. *Oncogene,* 32**,** 5017-25.

GUPTA, S., MANGEL, W. F., MCGRATH, W. J., PEREK, J. L., LEE, D. W., TAKAMOTO, K. & CHANCE, M. R. 2004. DNA binding provides a molecular strap activating the adenovirus proteinase. *Mol Cell Proteomics,* 3**,** 950-9.

GUSTIN, K. E. & IMPERIALE, M. J. 1998. Encapsidation of viral DNA requires the adenovirus L1 52/55-kilodalton protein. *J Virol,* 72**,** 7860-70.

GUTCH, M. J. & REICH, N. C. 1991. Repression of the interferon signal transduction pathway by the adenovirus E1A oncogene. *Proc Natl Acad Sci U S A,* 88**,** 7913-7.

GUYTON, A. C., COLEMAN, T. G., COWLEY, A. V., JR., SCHEEL, K. W., MANNING, R. D., JR. & NORMAN, R. A., JR. 1972. Arterial pressure regulation. Overriding dominance of the kidneys in long-term regulation and in hypertension. *Am J Med,* 52**,** 584-94.

HACEIN-BEY-ABINA, S., GARRIGUE, A., WANG, G. P., SOULIER, J., LIM, A., MORILLON, E., CLAPPIER, E., CACCAVELLI, L., DELABESSE, E., BELDJORD, K., ASNAFI, V., MACINTYRE, E., DAL CORTIVO, L., RADFORD, I., BROUSSE, N., SIGAUX, F., MOSHOUS, D., HAUER, J., BORKHARDT, A., BELOHRADSKY, B. H., WINTERGERST, U., VELEZ, M. C., LEIVA, L., SORENSEN, R., WULFFRAAT, N., BLANCHE, S., BUSHMAN, F. D., FISCHER, A. & CAVAZZANA-CALVO, M. 2008. Insertional oncogenesis in 4 patients after retrovirus-mediated gene therapy of SCID-X1. *J Clin Invest,* 118**,** 3132-42.

HACKER, U., NYBAKKEN, K. & PERRIMON, N. 2005. Heparan sulphate proteoglycans: the sweet side of development. *Nat Rev Mol Cell Biol,* 6**,** 530-41.

HAEGEL-KRONENBERGER, H., HAANSTRA, K., ZILLER-REMY, C., ORTIZ BUIJSSE, A. P., VERMEIREN, J., STOECKEL, F., VAN GOOL, S. W.,

CEUPPENS, J. L., MEHTALI, M., DE BOER, M., JONKER, M. & BOON, L. 2004. Inhibition of costimulation allows for repeated systemic administration of adenoviral vector in rhesus monkeys. *Gene Ther,* 11**,** 241-52.

HAISMA, H. J., KAMPS, J. A., KAMPS, G. K., PLANTINGA, J. A., ROTS, M. G. & BELLU, A. R. 2008. Polyinosinic acid enhances delivery of adenovirus vectors in vivo by preventing sequestration in liver macrophages. *J Gen Virol,* 89**,** 1097-105.

HALL, K., BLAIR ZAJDEL, M. E. & BLAIR, G. E. 2010. Unity and diversity in the human adenoviruses: exploiting alternative entry pathways for gene therapy. *Biochem J,* 431**,** 321-36.

HANNUM, L. G., HABERMAN, A. M., ANDERSON, S. M. & SHLOMCHIK, M. J. 2000. Germinal center initiation, variable gene region hypermutation, and mutant B cell selection without detectable immune complexes on follicular dendritic cells. *J Exp Med,* 192**,** 931-42.

HANSEN, T. H., KRASTEFF, T. N. & SHREFFLER, D. C. 1974. Quantitative variations in the expression of the mouse serum antigen Ss and its sex-limited allotype Slp. *Biochem Genet,* 12**,** 281-93.

HARADA, J. N., SHEVCHENKO, A., SHEVCHENKO, A., PALLAS, D. C. & BERK, A. J. 2002. Analysis of the adenovirus E1B-55K-anchored proteome reveals its link to ubiquitination machinery. *J Virol,* 76**,** 9194-206.

HARDONK, M. J., DIJKHUIS, F. W., HULSTAERT, C. E. & KOUDSTAAL, J. 1992. Heterogeneity of rat liver and spleen macrophages in gadolinium chloride-induced elimination and repopulation. *J Leukoc Biol,* 52**,** 296-302.

HARNETT, G. B., BUCENS, M. R., CLAY, S. J. & SAKER, B. M. 1982. Acute haemorrhagic cystitis caused by adenovirus type 11 in a recipient of a transplanted kidney. *Med J Aust,* 1**,** 565-7.

HARUI, A., SUZUKI, S., KOCHANEK, S. & MITANI, K. 1999. Frequency and stability of chromosomal integration of adenovirus vectors. *J Virol,* 73**,** 6141-6.

HARUKI, H., OKUWAKI, M., MIYAGISHI, M., TAIRA, K. & NAGATA, K. 2006. Involvement of template-activating factor I/SET in transcription of adenovirus early genes as a positive-acting factor. *J Virol,* 80**,** 794-801.

HARVEY, T. J., BURDON, D., STEELE, L., INGRAM, N., HALL, G. D., SELBY, P. J., VILE, R. G., COOPER, P. A., SHNYDER, S. D. & CHESTER, J. D. 2010. Retargeted adenoviral cancer gene therapy for tumour cells overexpressing epidermal growth factor receptor or urokinase-type plasminogen activator receptor. *Gene Ther,* 17**,** 1000-10.

HASSON, T. B., SOLOWAY, P. D., ORNELLES, D. A., DOERFLER, W. & SHENK, T. 1989. Adenovirus L1 52- and 55-kilodalton proteins are required for assembly of virions. *J Virol,* 63**,** 3612-21.

HAULER, F., MALLERY, D. L., MCEWAN, W. A., BIDGOOD, S. R. & JAMES, L. C. 2012. AAA ATPase p97/VCP is essential for TRIM21-mediated virus neutralization. *Proc Natl Acad Sci U S A,* 109**,** 19733-8.

HAVENGA, M. J., LEMCKERT, A. A., GRIMBERGEN, J. M., VOGELS, R., HUISMAN, L. G., VALERIO, D., BOUT, A. & QUAX, P. H. 2001. Improved adenovirus vectors for infection of cardiovascular tissues. *J Virol,* 75**,** 3335-42.

HAVIV, Y. S., BLACKWELL, J. L., KANERVA, A., NAGI, P., KRASNYKH, V., DMITRIEV, I., WANG, M., NAITO, S., LEI, X., HEMMINKI, A., CAREY, D. & CURIEL, D. T. 2002. Adenoviral gene therapy for renal cancer requires retargeting to alternative cellular receptors. *Cancer Res,* 62**,** 4273-81.

HAYES, B. W., TELLING, G. C., MYAT, M. M., WILLIAMS, J. F. & FLINT, S. J. 1990. The adenovirus L4 100-kilodalton protein is necessary for efficient translation of viral late mRNA species. *J Virol,* 64**,** 2732-42.

HE, J. Q., KATSCHKE, K. J., JR., GRIBLING, P., SUTO, E., LEE, W. P., DIEHL, L., EASTHAM-ANDERSON, J., PONAKALA, A., KOMUVES, L., EGEN, J. G. &

VAN LOOKEREN CAMPAGNE, M. 2013. CRIg mediates early Kupffer cell responses to adenovirus. *J Leukoc Biol,* 93**,** 301-6.

HEARING, P., SAMULSKI, R. J., WISHART, W. L. & SHENK, T. 1987. Identification of a repeated sequence element required for efficient encapsidation of the adenovirus type 5 chromosome. *J Virol,* 61**,** 2555-8.

HEHIR, K. M., ARMENTANO, D., CARDOZA, L. M., CHOQUETTE, T. L., BERTHELETTE, P. B., WHITE, G. A., COUTURE, L. A., EVERTON, M. B., KEEGAN, J., MARTIN, J. M., PRATT, D. A., SMITH, M. P., SMITH, A. E. & WADSWORTH, S. C. 1996. Molecular characterization of replication-competent variants of adenovirus vectors and genome modifications to prevent their occurrence. *J Virol,* 70**,** 8459-67.

HEIKKILA, P., PARPALA, T., LUKKARINEN, O., WEBER, M. & TRYGGVASON, K. 1996. Adenovirus-mediated gene transfer into kidney glomeruli using an ex vivo and in vivo kidney perfusion system - first steps towards gene therapy of Alport syndrome. *Gene Ther,* 3**,** 21-7.

HEIKKILA, P., TIBELL, A., MORITA, T., CHEN, Y., WU, G., SADO, Y., NINOMIYA, Y., PETTERSSON, E. & TRYGGVASON, K. 2001. Adenovirus-mediated transfer of type IV collagen alpha5 chain cDNA into swine kidney in vivo: deposition of the protein into the glomerular basement membrane. *Gene Ther,* 8**,** 882-90.

HILGENDORF, A., LINDBERG, J., RUZSICS, Z., HONING, S., ELSING, A., LOFQVIST, M., ENGELMANN, H. & BURGERT, H. G. 2003. Two distinct transport motifs in the adenovirus E3/10.4-14.5 proteins act in concert to down-modulate apoptosis receptors and the epidermal growth factor receptor. *J Biol Chem,* 278**,** 51872-84.

HINDLEY, C. E., LAWRENCE, F. J. & MATTHEWS, D. A. 2007. A role for transportin in the nuclear import of adenovirus core proteins and DNA. *Traffic,* 8**,** 1313-22.

HOFMANN, C., LÖSER, P., CICHON, G., ARNOLD, W., BOTH, G. W. & STRAUSS, M. 1999. Ovine adenovirus vectors overcome preexisting humoral immunity against human adenoviruses in vivo. *J Virol,* 73**,** 6930-6.

HOGGATT, J. 2016. Gene Therapy for "Bubble Boy" Disease. *Cell,* 166**,** 263.

HOLTERMAN, L., VOGELS, R., VAN DER VLUGT, R., SIEUWERTS, M., GRIMBERGEN, J., KASPERS, J., GEELEN, E., VAN DER HELM, E., LEMCKERT, A., GILLISSEN, G., VERHAAGH, S., CUSTERS, J., ZUIJDGEEST, D., BERKHOUT, B., BAKKER, M., QUAX, P., GOUDSMIT, J. & HAVENGA, M. 2004. Novel replication-incompetent vector derived from adenovirus type 11 (Ad11) for vaccination and gene therapy: low seroprevalence and non-cross-reactivity with Ad5. *J Virol,* 78**,** 13207-15.

HONG, S. S., HABIB, N. A., FRANQUEVILLE, L., JENSEN, S. & BOULANGER, P. A. 2003. Identification of adenovirus (ad) penton base neutralizing epitopes by use of sera from patients who had received conditionally replicative ad (addl1520) for treatment of liver tumors. *J Virol,* 77**,** 10366-75.

HONG, S. S., KARAYAN, L., TOURNIER, J., CURIEL, D. T. & BOULANGER, P. A. 1997. Adenovirus type 5 fiber knob binds to MHC class I alpha2 domain at the surface of human epithelial and B lymphoblastoid cells. *EMBO J,* 16**,** 2294-306.

HONG, S. S., SZOLAJSKA, E., SCHOEHN, G., FRANQUEVILLE, L., MYHRE, S., LINDHOLM, L., RUIGROK, R. W., BOULANGER, P. & CHROBOCZEK, J. 2005. The 100K-chaperone protein from adenovirus serotype 2 (Subgroup C) assists in trimerization and nuclear localization of hexons from subgroups C and B adenoviruses. *J Mol Biol,* 352**,** 125-38.

HONING, S., RICOTTA, D., KRAUSS, M., SPATE, K., SPOLAORE, B., MOTLEY, A., ROBINSON, M., ROBINSON, C., HAUCKE, V. & OWEN, D. J. 2005. Phosphatidylinositol-(4,5)-bisphosphate regulates sorting signal recognition by the clathrin-associated adaptor complex AP2. *Mol Cell,* 18**,** 519-31.

HOPPE, A., BEECH, S. J., DIMMOCK, J. & LEPPARD, K. N. 2006. Interaction of the adenovirus type 5 E4 Orf3 protein with promyelocytic leukemia protein isoform II is required for ND10 disruption. *J Virol,* 80**,** 3042-9.

HORTON, T. M., RANHEIM, T. S., AQUINO, L., KUSHER, D. I., SAHA, S. K., WARE, C. F., WOLD, W. S. & GOODING, L. R. 1991. Adenovirus E3 14.7K protein functions in the absence of other adenovirus proteins to protect transfected cells from tumor necrosis factor cytolysis. *J Virol,* 65**,** 2629-39.

HORWITZ, G. A., ZHANG, K., MCBRIAN, M. A., GRUNSTEIN, M., KURDISTANI, S. K. & BERK, A. J. 2008. Adenovirus small e1a alters global patterns of histone modification. *Science,* 321**,** 1084-5.

HORWITZ, J. P., CHUA, J., CURBY, R. J., TOMSON, A. J., DAROOGE, M. A., FISHER, B. E., MAURICIO, J. & KLUNDT, I. 1964. Substrates for Cytochemical Demonstration of Enzyme Activity. I. Some Substituted 3-Indolyl-Beta-D-Glycopyranosides. *J Med Chem,* 7**,** 574-5.

HOSOKAWA, M., NONAKA, M., OKADA, N., NONAKA, M. & OKADA, H. 1996. Molecular cloning of guinea pig membrane cofactor protein: preferential expression in testis. *J Immunol,* 157**,** 4946-52.

HOTZE, E. M. & TWETEN, R. K. 2012. Membrane assembly of the cholesterol-dependent cytolysin pore complex. *Biochim Biophys Acta,* 1818**,** 1028-38.

HOU, J. & GOODENOUGH, D. A. 2010. Claudin-16 and claudin-19 function in the thick ascending limb. *Curr Opin Nephrol Hypertens,* 19**,** 483-8.

HOZUMI, K., SUZUKI, N., NIELSEN, P. K., NOMIZU, M. & YAMADA, Y. 2006. Laminin alpha1 chain LG4 module promotes cell attachment through syndecans and cell spreading through integrin alpha2beta1. *J Biol Chem,* 281**,** 32929-40.

HUANG, S., KAMATA, T., TAKADA, Y., RUGGERI, Z. M. & NEMEROW, G. R. 1996. Adenovirus interaction with distinct integrins mediates separate events in cell entry and gene delivery to hematopoietic cells. *J Virol,* 70**,** 4502-8.

HUGO, F., REICHWEIN, J., ARVAND, M., KRAMER, S. & BHAKDI, S. 1986. Use of a monoclonal antibody to determine the mode of transmembrane pore formation by streptolysin O. *Infect Immun,* 54**,** 641-5.

IMELLI, N., RUZSICS, Z., PUNTENER, D., GASTALDELLI, M. & GREBER, U. F. 2009. Genetic reconstitution of the human adenovirus type 2 temperature-sensitive 1 mutant defective in endosomal escape. *Virol J,* 6**,** 174.

IRONS, E. E., FLATT, J. W., DORONIN, K., FOX, T. L., ACCHIONE, M., STEWART, P. L. & SHAYAKHMETOV, D. M. 2013. Coagulation factor binding orientation and dimerization may influence infectivity of adenovirus-coagulation factor complexes. *J Virol,* 87**,** 9610-9.

ITO, M., HIRAMATSU, H., KOBAYASHI, K., SUZUE, K., KAWAHATA, M., HIOKI, K., UEYAMA, Y., KOYANAGI, Y., SUGAMURA, K., TSUJI, K., HEIKE, T. & NAKAHATA, T. 2002. NOD/SCID/gamma(c)(null) mouse: an excellent recipient mouse model for engraftment of human cells. *Blood,* 100**,** 3175-82.

IZUMI, M., KAWAKAMI, Y., GLASGOW, J. N., BELOUSOVA, N., EVERTS, M., KIM-PARK, S., YAMAMOTO, S., WANG, M., LE, L. P., REYNOLDS, P. N. & CURIEL, D. T. 2005. In vivo analysis of a genetically modified adenoviral vector targeted to human CD40 using a novel transient transgenic model. *J Gene Med,* 7**,** 1517-25.

JACOBSON, S. G., CIDECIYAN, A. V., RATNAKARAM, R., HEON, E., SCHWARTZ, S. B., ROMAN, A. J., PEDEN, M. C., ALEMAN, T. S., BOYE, S. L., SUMAROKA, A., CONLON, T. J., CALCEDO, R., PANG, J. J., ERGER, K. E., OLIVARES, M. B., MULLINS, C. L., SWIDER, M., KAUSHAL, S., FEUER, W. J., IANNACCONE, A., FISHMAN, G. A., STONE, E. M., BYRNE, B. J. & HAUSWIRTH, W. W. 2012. Gene therapy for leber congenital amaurosis caused

by RPE65 mutations: safety and efficacy in 15 children and adults followed up to 3 years. *Arch Ophthalmol,* 130**,** 9-24.

JAKUBCZAK, J. L., ROLLENCE, M. L., STEWART, D. A., JAFARI, J. D., VON SEGGERN, D. J., NEMEROW, G. R., STEVENSON, S. C. & HALLENBECK, P. L. 2001. Adenovirus type 5 viral particles pseudotyped with mutagenized fiber proteins show diminished infectivity of coxsackie B-adenovirus receptor-bearing cells. *J Virol,* 75**,** 2972-81.

JAMES, N. J., HOWELL, G. J., WALKER, J. H. & BLAIR, G. E. 2010. The role of Cajal bodies in the expression of late phase adenovirus proteins. *Virology,* 399**,** 299-311.

JANKOVIC, D., LIU, Z. & GAUSE, W. C. 2001. Th1- and Th2-cell commitment during infectious disease: asymmetry in divergent pathways. *Trends Immunol,* 22**,** 450-7.

JEGGO, P. A., TACCIOLI, G. E. & JACKSON, S. P. 1995. Menage a trois: double strand break repair, V(D)J recombination and DNA-PK. *Bioessays,* 17**,** 949-57.

JHA, V., GARCIA-GARCIA, G., ISEKI, K., LI, Z., NAICKER, S., PLATTNER, B., SARAN, R., WANG, A. Y. & YANG, C. W. 2013. Chronic kidney disease: global dimension and perspectives. *Lancet,* 382**,** 260-72.

JIANG, H., WANG, Z., SERRA, D., FRANK, M. M. & AMALFITANO, A. 2004. Recombinant adenovirus vectors activate the alternative complement pathway, leading to the binding of human complement protein C3 independent of anti-ad antibodies. *Mol Ther,* 10**,** 1140-2.

JIMA, D. D., SHAH, R. N., ORCUTT, T. M., JOSHI, D., LAW, J. M., LITMAN, G. W., TREDE, N. S. & YODER, J. A. 2009. Enhanced transcription of complement and coagulation genes in the absence of adaptive immunity. *Mol Immunol,* 46**,** 1505-16.

JOHANSSON, C., JONSSON, M., MARTTILA, M., PERSSON, D., FAN, X. L., SKOG, J., FRANGSMYR, L., WADELL, G. & ARNBERG, N. 2007. Adenoviruses use lactoferrin as a bridge for CAR-independent binding to and infection of epithelial cells. *J Virol,* 81**,** 954-63.

JOHNSON, D. J., LANGDOWN, J. & HUNTINGTON, J. A. 2010. Molecular basis of factor IXa recognition by heparin-activated antithrombin revealed by a 1.7-A structure of the ternary complex. *Proc Natl Acad Sci U S A,* 107**,** 645-50.

JOHNSTONE, R. W., RUSSELL, S. M., LOVELAND, B. E. & MCKENZIE, I. F. 1993. Polymorphic expression of CD46 protein isoforms due to tissue-specific RNA splicing. *Mol Immunol,* 30**,** 1231-41.

JONES, K. A., KADONAGA, J. T., ROSENFELD, P. J., KELLY, T. J. & TJIAN, R. 1987. A cellular DNA-binding protein that activates eukaryotic transcription and DNA replication. *Cell,* 48**,** 79-89.

JONES, M. S., 2ND, HARRACH, B., GANAC, R. D., GOZUM, M. M., DELA CRUZ, W. P., RIEDEL, B., PAN, C., DELWART, E. L. & SCHNURR, D. P. 2007. New adenovirus species found in a patient presenting with gastroenteritis. *J Virol,* 81**,** 5978-84.

JONES, N. & SHENK, T. 1979. An adenovirus type 5 early gene function regulates expression of other early viral genes. *Proc Natl Acad Sci U S A,* 76**,** 3665-9.

JONSSON, M. I., LENMAN, A. E., FRANGSMYR, L., NYBERG, C., ABDULLAHI, M. & ARNBERG, N. 2009. Coagulation factors IX and X enhance binding and infection of adenovirus types 5 and 31 in human epithelial cells. *J Virol,* 83**,** 3816-25.

JOUNG, I., HARBER, G., GERECKE, K. M., CARROLL, S. L., COLLAWN, J. F. & ENGLER, J. A. 2005. Improved gene delivery into neuroglial cells using a fiber-modified adenovirus vector. *Biochem Biophys Res Commun,* 328**,** 1182-7.

KALIN, S., AMSTUTZ, B., GASTALDELLI, M., WOLFRUM, N., BOUCKE, K., HAVENGA, M., DIGENNARO, F., LISKA, N., HEMMI, S. & GREBER, U. F. 2010. Macropinocytotic uptake and infection of human epithelial cells with species B2 adenovirus type 35. *J Virol,* 84**,** 5336-50.

KALVAKOLANU, D. V., BANDYOPADHYAY, S. K., HARTER, M. L. & SEN, G. C. 1991. Inhibition of interferon-inducible gene expression by adenovirus E1A proteins: block in transcriptional complex formation. *Proc Natl Acad Sci U S A,* 88**,** 7459-63.

KALYUZHNIY, O., DI PAOLO, N. C., SILVESTRY, M., HOFHERR, S. E., BARRY, M. A., STEWART, P. L. & SHAYAKHMETOV, D. M. 2008. Adenovirus serotype 5 hexon is critical for virus infection of hepatocytes in vivo. *Proc Natl Acad Sci U S A,* 105**,** 5483-8.

KANAI, F., SHIRATORI, Y., YOSHIDA, Y., WAKIMOTO, H., HAMADA, H., KANEGAE, Y., SAITO, I., NAKABAYASHI, H., TAMAOKI, T., TANAKA, T., LAN, K. H., KATO, N., SHIINA, S. & OMATA, M. 1996. Gene therapy for alpha-fetoprotein-producing human hepatoma cells by adenovirus-mediated transfer of the herpes simplex virus thymidine kinase gene. *Hepatology,* 23**,** 1359-68.

KANERVA, A., MIKHEEVA, G. V., KRASNYKH, V., COOLIDGE, C. J., LAM, J. T., MAHASRESHTI, P. J., BARKER, S. D., STRAUGHN, M., BARNES, M. N., ALVAREZ, R. D., HEMMINKI, A. & CURIEL, D. T. 2002. Targeting adenovirus to the serotype 3 receptor increases gene transfer efficiency to ovarian cancer cells. *Clin Cancer Res,* 8**,** 275-80.

KANG, R., CHEN, R., ZHANG, Q., HOU, W., WU, S., CAO, L., HUANG, J., YU, Y., FAN, X. G., YAN, Z., SUN, X., WANG, H., WANG, Q., TSUNG, A., BILLIAR, T. R., ZEH, H. J., 3RD, LOTZE, M. T. & TANG, D. 2014. HMGB1 in health and disease. *Mol Aspects Med,* 40**,** 1-116.

KAO, C. C., YEW, P. R. & BERK, A. J. 1990. Domains required for in vitro association between the cellular p53 and the adenovirus 2 E1B 55K proteins. *Virology,* 179**,** 806-14.

KAREN, K. A. & HEARING, P. 2011. Adenovirus core protein VII protects the viral genome from a DNA damage response at early times after infection. *J Virol,* 85**,** 4135-42.

KATZE, M. G., HE, Y. & GALE, M. 2002. Viruses and interferon: a fight for supremacy. *Nat Rev Immunol,* 2**,** 675-87.

KAUFFMAN, R. S. & GINSBERG, H. S. 1976. Characterization of a temperature-sensitive, hexon transport mutant of type 5 adenovirus. *J Virol,* 19**,** 643-58.

KAWANO, R., ISHIZAKI, M., MAEDA, Y., UCHIDA, Y., KIMURA, E. & UCHINO, M. 2008. Transduction of full-length dystrophin to multiple skeletal muscles improves motor performance and life span in utrophin/dystrophin double knockout mice. *Mol Ther,* 16**,** 825-31.

KELKAR, S. A., PFISTER, K. K., CRYSTAL, R. G. & LEOPOLD, P. L. 2004. Cytoplasmic dynein mediates adenovirus binding to microtubules. *J Virol,* 78**,** 10122-32.

KHARE, R., HILLESTAD, M. L., XU, Z., BYRNES, A. P. & BARRY, M. A. 2013. Circulating antibodies and macrophages as modulators of adenovirus pharmacology. *J Virol,* 87**,** 3678-86.

KHARE, R., REDDY, V. S., NEMEROW, G. R. & BARRY, M. A. 2012. Identification of adenovirus serotype 5 hexon regions that interact with scavenger receptors. *J Virol,* 86**,** 2293-301.

KIANG, A., HARTMAN, Z. C., EVERETT, R. S., SERRA, D., JIANG, H., FRANK, M. M. & AMALFITANO, A. 2006. Multiple innate inflammatory responses induced after systemic adenovirus vector delivery depend on a functional complement system. *Mol Ther,* 14**,** 588-98.

KIDD, A. H., CHROBOCZEK, J., CUSACK, S. & RUIGROK, R. W. 1993. Adenovirus type 40 virions contain two distinct fibers. *Virology,* 192**,** 73-84.

KIM, I. H., JOZKOWICZ, A., PIEDRA, P. A., OKA, K. & CHAN, L. 2001. Lifetime correction of genetic deficiency in mice with a single injection of helper-dependent adenoviral vector. *Proc Natl Acad Sci U S A,* 98**,** 13282-7.

KING, A. J., TEERTSTRA, W. R. & VAN DER VLIET, P. C. 1997. Dissociation of the protein primer and DNA polymerase after initiation of adenovirus DNA replication. *J Biol Chem,* 272**,** 24617-23.

KING, A. J. & VAN DER VLIET, P. C. 1994. A precursor terminal protein-trinucleotide intermediate during initiation of adenovirus DNA replication: regeneration of molecular ends in vitro by a jumping back mechanism. *EMBO J,* 13**,** 5786-92.

KIRBY, A., GNIRKE, A., JAFFE, D. B., BARESOVA, V., POCHET, N., BLUMENSTIEL, B., YE, C., AIRD, D., STEVENS, C., ROBINSON, J. T., CABILI, M. N., GAT-VIKS, I., KELLIHER, E., DAZA, R., DEFELICE, M., HULKOVA, H., SOVOVA, J., VYLET'AL, P., ANTIGNAC, C., GUTTMAN, M., HANDSAKER, R. E., PERRIN, D., STEELMAN, S., SIGURDSSON, S., SCHEINMAN, S. J., SOUGNEZ, C., CIBULSKIS, K., PARKIN, M., GREEN, T., ROSSIN, E., ZODY, M. C., XAVIER, R. J., POLLAK, M. R., ALPER, S. L., LINDBLAD-TOH, K., GABRIEL, S., HART, P. S., REGEV, A., NUSBAUM, C., KMOCH, S., BLEYER, A. J., LANDER, E. S. & DALY, M. J. 2013. Mutations causing medullary cystic kidney disease type 1 lie in a large VNTR in MUC1 missed by massively parallel sequencing. *Nat Genet,* 45**,** 299-303.

KIRBY, I., DAVISON, E., BEAVIL, A. J., SOH, C. P., WICKHAM, T. J., ROELVINK, P. W., KOVESDI, I., SUTTON, B. J. & SANTIS, G. 2000. Identification of contact residues and definition of the CAR-binding site of adenovirus type 5 fiber protein. *J Virol,* 74**,** 2804-13.

KITAMURA, D., ROES, J., KUHN, R. & RAJEWSKY, K. 1991. A B cell-deficient mouse by targeted disruption of the membrane exon of the immunoglobulin mu chain gene. *Nature,* 350**,** 423-6.

KOCHANEK, S., CLEMENS, P. R., MITANI, K., CHEN, H. H., CHAN, S. & CASKEY, C. T. 1996. A new adenoviral vector: Replacement of all viral coding sequences with 28 kb of DNA independently expressing both full-length dystrophin and beta-galactosidase. *Proc Natl Acad Sci U S A,* 93**,** 5731-6.

KOIZUMI, N., MIZUGUCHI, H., SAKURAI, F., YAMAGUCHI, T., WATANABE, Y. & HAYAKAWA, T. 2003. Reduction of natural adenovirus tropism to mouse liver by fiber-shaft exchange in combination with both CAR- and alphav integrin-binding ablation. *J Virol,* 77**,** 13062-72.

KOKUBO, Y., NAKAMURA, S., OKAMURA, T., YOSHIMASA, Y., MAKINO, H., WATANABE, M., HIGASHIYAMA, A., KAMIDE, K., KAWANISHI, K., OKAYAMA, A. & KAWANO, Y. 2009. Relationship between blood pressure category and incidence of stroke and myocardial infarction in an urban Japanese population with and without chronic kidney disease: the Suita Study. *Stroke,* 40**,** 2674-9.

KOLONIN, M. G., SAHA, P. K., CHAN, L., PASQUALINI, R. & ARAP, W. 2004. Reversal of obesity by targeted ablation of adipose tissue. *Nat Med,* 10**,** 625-32.

KOROKHOV, N., MIKHEEVA, G., KRENDELSHCHIKOV, A., BELOUSOVA, N., SIMONENKO, V., KRENDELSHCHIKOVA, V., PEREBOEV, A., KOTOV, A., KOTOVA, O., TRIOZZI, P. L., ALDRICH, W. A., DOUGLAS, J. T., LO, K. M., BANERJEE, P. T., GILLIES, S. D., CURIEL, D. T. & KRASNYKH, V. 2003. Targeting of adenovirus via genetic modification of the viral capsid combined with a protein bridge. *J Virol,* 77**,** 12931-40.

KOSKI, A., KANGASNIEMI, L., ESCUTENAIRE, S., PESONEN, S., CERULLO, V., DIACONU, I., NOKISALMI, P., RAKI, M., RAJECKI, M., GUSE, K., RANKI, T., OKSANEN, M., HOLM, S. L., HAAVISTO, E., KARIOJA-KALLIO, A., LAASONEN, L., PARTANEN, K., UGOLINI, M., HELMINEN, A., KARLI, E.,

HANNUKSELA, P., PESONEN, S., JOENSUU, T., KANERVA, A. & HEMMINKI, A. 2010. Treatment of cancer patients with a serotype 5/3 chimeric oncolytic adenovirus expressing GMCSF. *Mol Ther,* 18**,** 1874-84.

KOTHA, P. L., SHARMA, P., KOLAWOLE, A. O., YAN, R., ALGHAMRI, M. S., BROCKMAN, T. L., GOMEZ-CAMBRONERO, J. & EXCOFFON, K. J. 2015. Adenovirus entry from the apical surface of polarized epithelia is facilitated by the host innate immune response. *PLoS Pathog,* 11**,** e1004696.

KOTTERMAN, M. A., CHALBERG, T. W. & SCHAFFER, D. V. 2015. Viral Vectors for Gene Therapy: Translational and Clinical Outlook. *Annu Rev Biomed Eng,* 17**,** 63-89.

KOTTGEN, A., RUSSELL, S. D., LOEHR, L. R., CRAINICEANU, C. M., ROSAMOND, W. D., CHANG, P. P., CHAMBLESS, L. E. & CORESH, J. 2007. Reduced kidney function as a risk factor for incident heart failure: the atherosclerosis risk in communities (ARIC) study. *J Am Soc Nephrol,* 18**,** 1307-15.

KRASNYKH, V., DMITRIEV, I., MIKHEEVA, G., MILLER, C. R., BELOUSOVA, N. & CURIEL, D. T. 1998. Characterization of an adenovirus vector containing a heterologous peptide epitope in the HI loop of the fiber knob. *J Virol,* 72**,** 1844-52.

KRITZ, A. B., NICOL, C. G., DISHART, K. L., NELSON, R., HOLBECK, S., VON SEGGERN, D. J., WORK, L. M., MCVEY, J. H., NICKLIN, S. A. & BAKER, A. H. 2007. Adenovirus 5 fibers mutated at the putative HSPG-binding site show restricted retargeting with targeting peptides in the HI loop. *Mol Ther,* 15**,** 741-9.

KRUTZKE, L., PRILL, J. M., ENGLER, T., SCHMIDT, C. Q., XU, Z., BYRNES, A. P., SIMMET, T. & KREPPEL, F. 2016. Substitution of blood coagulation factor X-binding to Ad5 by position-specific PEGylation: Preventing vector clearance and preserving infectivity. *J Control Release,* 235**,** 379-92.

KUBO, M., SATOH, T., TABATA, K. I., TSUMURA, H., IWAMURA, M., BABA, S., THOMPSON, T. C. & OBATA, F. 2015. Enhanced central memory cluster of differentiation 8+ and tumor antigen-specific T cells in prostate cancer patients receiving repeated in situ adenovirus-mediated suicide gene therapy. *Mol Clin Oncol,* 3**,** 515-521.

KUPGAN, G., HENTGES, D. C., MUSCHINSKE, N. J., PICKING, W. D., PICKING, W. L. & RAMSEY, J. D. 2014. The effect of fiber truncations on the stability of adenovirus type 5. *Mol Biotechnol,* 56**,** 979-91.

KURACHI, S., KOIZUMI, N., SAKURAI, F., KAWABATA, K., SAKURAI, H., NAKAGAWA, S., HAYAKAWA, T. & MIZUGUCHI, H. 2007a. Characterization of capsid-modified adenovirus vectors containing heterologous peptides in the fiber knob, protein IX, or hexon. *Gene Ther,* 14**,** 266-74.

KURACHI, S., TASHIRO, K., SAKURAI, F., SAKURAI, H., KAWABATA, K., YAYAMA, K., OKAMOTO, H., NAKAGAWA, S. & MIZUGUCHI, H. 2007b. Fiber-modified adenovirus vectors containing the TAT peptide derived from HIV-1 in the fiber knob have efficient gene transfer activity. *Gene Ther,* 14**,** 1160-5.

LACHMANN, P. J., GRENNAN, D., MARTIN, A. & DEMANT, P. 1975. Identification of Ss protein as murine C4. *Nature,* 258**,** 242-3.

LAEMMLI, U. K. 1970. Cleavage of structural proteins during the assembly of the head of bacteriophage T4. *Nature,* 227**,** 680-5.

LALLY, C., DORPER, T., GROGER, W., ANTOINE, G. & WINNACKER, E. L. 1984. A size analysis of the adenovirus replicon. *EMBO J,* 3**,** 333-7.

LAM, E., STEIN, S. & FALCK-PEDERSEN, E. 2014. Adenovirus detection by the cGAS/STING/TBK1 DNA sensing cascade. *J Virol,* 88**,** 974-81.

LANDER, E. S., LINTON, L. M., BIRREN, B., NUSBAUM, C., ZODY, M. C., BALDWIN, J., DEVON, K., DEWAR, K., DOYLE, M., FITZHUGH, W., FUNKE, R., GAGE, D., HARRIS, K., HEAFORD, A., HOWLAND, J., KANN, L., LEHOCZKY, J., LEVINE, R., MCEWAN, P., MCKERNAN, K., MELDRIM,

J., MESIROV, J. P., MIRANDA, C., MORRIS, W., NAYLOR, J., RAYMOND, C., ROSETTI, M., SANTOS, R., SHERIDAN, A., SOUGNEZ, C., STANGE-THOMANN, Y., STOJANOVIC, N., SUBRAMANIAN, A., WYMAN, D., ROGERS, J., SULSTON, J., AINSCOUGH, R., BECK, S., BENTLEY, D., BURTON, J., CLEE, C., CARTER, N., COULSON, A., DEADMAN, R., DELOUKAS, P., DUNHAM, A., DUNHAM, I., DURBIN, R., FRENCH, L., GRAFHAM, D., GREGORY, S., HUBBARD, T., HUMPHRAY, S., HUNT, A., JONES, M., LLOYD, C., MCMURRAY, A., MATTHEWS, L., MERCER, S., MILNE, S., MULLIKIN, J. C., MUNGALL, A., PLUMB, R., ROSS, M., SHOWNKEEN, R., SIMS, S., WATERSTON, R. H., WILSON, R. K., HILLIER, L. W., MCPHERSON, J. D., MARRA, M. A., MARDIS, E. R., FULTON, L. A., CHINWALLA, A. T., PEPIN, K. H., GISH, W. R., CHISSOE, S. L., WENDL, M. C., DELEHAUNTY, K. D., MINER, T. L., DELEHAUNTY, A., KRAMER, J. B., COOK, L. L., FULTON, R. S., JOHNSON, D. L., MINX, P. J., CLIFTON, S. W., HAWKINS, T., BRANSCOMB, E., PREDKI, P., RICHARDSON, P., WENNING, S., SLEZAK, T., DOGGETT, N., CHENG, J. F., OLSEN, A., LUCAS, S., ELKIN, C., UBERBACHER, E., FRAZIER, M., et al. 2001. Initial sequencing and analysis of the human genome. *Nature,* 409**,** 860-921.

LANDSEM, A., NIELSEN, E. W., FURE, H., CHRISTIANSEN, D., LUDVIKSEN, J. K., LAMBRIS, J. D., OSTERUD, B., MOLLNES, T. E. & BREKKE, O. L. 2013. C1-inhibitor efficiently inhibits Escherichia coli-induced tissue factor mRNA up-regulation, monocyte tissue factor expression and coagulation activation in human whole blood. *Clin Exp Immunol,* 173**,** 217-29.

LAU, A. A., ROZAKLIS, T., IBANES, S., LUCK, A. J., BEARD, H., HASSIOTIS, S., MAZOUNI, K., HOPWOOD, J. J., KREMER, E. J. & HEMSLEY, K. M. 2012. Helper-dependent canine adenovirus vector-mediated transgene expression in a neurodegenerative lysosomal storage disorder. *Gene,* 491**,** 53-7.

LAWRENCE, R., OLSON, S. K., STEELE, R. E., WANG, L., WARRIOR, R., CUMMINGS, R. D. & ESKO, J. D. 2008. Evolutionary differences in glycosaminoglycan fine structure detected by quantitative glycan reductive isotope labeling. *J Biol Chem,* 283**,** 33674-84.

LE, L. P., LE, H. N., NELSON, A. R., MATTHEWS, D. A., YAMAMOTO, M. & CURIEL, D. T. 2006. Core labeling of adenovirus with EGFP. *Virology,* 351**,** 291-302.

LEE, T. W., LAWRENCE, F. J., DAUKSAITE, V., AKUSJARVI, G., BLAIR, G. E. & MATTHEWS, D. A. 2004. Precursor of human adenovirus core polypeptide Mu targets the nucleolus and modulates the expression of E2 proteins. *J Gen Virol,* 85**,** 185-96.

LEEGWATER, P. A., VAN DRIEL, W. & VAN DER VLIET, P. C. 1985. Recognition site of nuclear factor I, a sequence-specific DNA-binding protein from HeLa cells that stimulates adenovirus DNA replication. *EMBO J,* 4**,** 1515-21.

LEEN, A. M., SILI, U., VANIN, E. F., JEWELL, A. M., XIE, W., VIGNALI, D., PIEDRA, P. A., BRENNER, M. K. & ROONEY, C. M. 2004. Conserved CTL epitopes on the adenovirus hexon protein expand subgroup cross-reactive and subgroup-specific CD8+ T cells. *Blood,* 104**,** 2432-40.

LEGRAND, V., SPEHNER, D., SCHLESINGER, Y., SETTELEN, N., PAVIRANI, A. & MEHTALI, M. 1999. Fiberless recombinant adenoviruses: virus maturation and infectivity in the absence of fiber. *J Virol,* 73**,** 907-19.

LEISSNER, P., LEGRAND, V., SCHLESINGER, Y., HADJI, D. A., VAN RAAIJ, M., CUSACK, S., PAVIRANI, A. & MEHTALI, M. 2001. Influence of adenoviral fiber mutations on viral encapsidation, infectivity and in vivo tropism. *Gene Ther,* 8**,** 49-57.

LEMCKERT, A. A., GRIMBERGEN, J., SMITS, S., HARTKOORN, E., HOLTERMAN, L., BERKHOUT, B., BAROUCH, D. H., VOGELS, R., QUAX, P., GOUDSMIT, J. & HAVENGA, M. J. 2006. Generation of a novel replication-incompetent adenoviral vector derived from human adenovirus type 49: manufacture on PER.C6 cells, tropism and immunogenicity. *J Gen Virol,* 87**,** 2891-9.

LENMAN, A., LIACI, A. M., LIU, Y., ARDAHL, C., RAJAN, A., NILSSON, E., BRADFORD, W., KAESHAMMER, L., JONES, M. S., FRANGSMYR, L., FEIZI, T., STEHLE, T. & ARNBERG, N. 2015. Human adenovirus 52 uses sialic acid-containing glycoproteins and the coxsackie and adenovirus receptor for binding to target cells. *PLoS Pathog,* 11**,** e1004657.

LENMAN, A., MULLER, S., NYGREN, M. I., FRANGSMYR, L., STEHLE, T. & ARNBERG, N. 2011. Coagulation factor IX mediates serotype-specific binding of species A adenoviruses to host cells. *J Virol,* 85**,** 13420-31.

LEOPOLD, P. L. & CRYSTAL, R. G. 2007. Intracellular trafficking of adenovirus: many means to many ends. *Adv Drug Deliv Rev,* 59**,** 810-21.

LEOPOLD, P. L., KREITZER, G., MIYAZAWA, N., REMPEL, S., PFISTER, K. K., RODRIGUEZ-BOULAN, E. & CRYSTAL, R. G. 2000. Dynein- and microtubule-mediated translocation of adenovirus serotype 5 occurs after endosomal lysis. *Hum Gene Ther,* 11**,** 151-65.

LEPPARD, K. N., EMMOTT, E., CORTESE, M. S. & RICH, T. 2009. Adenovirus type 5 E4 Orf3 protein targets promyelocytic leukaemia (PML) protein nuclear domains for disruption via a sequence in PML isoform II that is predicted as a protein interaction site by bioinformatic analysis. *J Gen Virol,* 90**,** 95-104.

LEVEY, A. S., ECKARDT, K. U., TSUKAMOTO, Y., LEVIN, A., CORESH, J., ROSSERT, J., DE ZEEUW, D., HOSTETTER, T. H., LAMEIRE, N. & EKNOYAN, G. 2005. Definition and classification of chronic kidney disease: a position statement from Kidney Disease: Improving Global Outcomes (KDIGO). *Kidney Int,* 67**,** 2089-100.

LEWITT, P. A., REZAI, A. R., LEEHEY, M. A., OJEMANN, S. G., FLAHERTY, A. W., ESKANDAR, E. N., KOSTYK, S. K., THOMAS, K., SARKAR, A., SIDDIQUI, M. S., TATTER, S. B., SCHWALB, J. M., POSTON, K. L., HENDERSON, J. M., KURLAN, R. M., RICHARD, I. H., VAN METER, L., SAPAN, C. V., DURING, M. J., KAPLITT, M. G. & FEIGIN, A. 2011. AAV2-GAD gene therapy for advanced Parkinson's disease: a double-blind, sham-surgery controlled, randomised trial. *Lancet Neurol,* 10**,** 309-19.

LI, E., BROWN, S. L., STUPACK, D. G., PUENTE, X. S., CHERESH, D. A. & NEMEROW, G. R. 2001. Integrin alpha(v)beta1 is an adenovirus coreceptor. *J Virol,* 75**,** 5405-9.

LI, E., STUPACK, D., BOKOCH, G. M. & NEMEROW, G. R. 1998a. Adenovirus endocytosis requires actin cytoskeleton reorganization mediated by Rho family GTPases. *J Virol,* 72**,** 8806-12.

LI, E., STUPACK, D., KLEMKE, R., CHERESH, D. A. & NEMEROW, G. R. 1998b. Adenovirus endocytosis via alpha(v) integrins requires phosphoinositide-3-OH kinase. *J Virol,* 72**,** 2055-61.

LI, H., RHEE, E. G., MASEK-HAMMERMAN, K., TEIGLER, J. E., ABBINK, P. & BAROUCH, D. H. 2012. Adenovirus serotype 26 utilizes CD46 as a primary cellular receptor and only transiently activates T lymphocytes following vaccination of rhesus monkeys. *J Virol,* 86**,** 10862-5.

LI, H. J., EVERTS, M., PEREBOEVA, L., KOMAROVA, S., IDAN, A., CURIEL, D. T. & HERSCHMAN, H. R. 2007. Adenovirus tumor targeting and hepatic untargeting by a coxsackie/adenovirus receptor ectodomain anti-carcinoembryonic antigen bispecific adapter. *Cancer Res,* 67**,** 5354-61.

LI, J., LAD, S., YANG, G., LUO, Y., IACOBELLI-MARTINEZ, M., PRIMUS, F. J., REISFELD, R. A. & LI, E. 2006. Adenovirus fiber shaft contains a trimerization element that supports peptide fusion for targeted gene delivery. *J Virol,* 80**,** 12324-31.

LICHTENSTEIN, D. L., TOTH, K., DORONIN, K., TOLLEFSON, A. E. & WOLD, W. S. 2004. Functions and mechanisms of action of the adenovirus E3 proteins. *Int Rev Immunol,* 23**,** 75-111.

LILES, W. C., CUSHING, H., HOLT, S., BRYAN, C. & HACKMAN, R. C. 1993. Severe adenoviral nephritis following bone marrow transplantation: successful treatment with intravenous ribavirin. *Bone Marrow Transplant,* 12**,** 409-12.

LIN, X. 2004. Functions of heparan sulfate proteoglycans in cell signaling during development. *Development,* 131**,** 6009-21.

LINDENBAUM, J. O., FIELD, J. & HURWITZ, J. 1986. The adenovirus DNA binding protein and adenovirus DNA polymerase interact to catalyze elongation of primed DNA templates. *J Biol Chem,* 261**,** 10218-27.

LINSTEDT, A. D. & HAURI, H. P. 1993. Giantin, a novel conserved Golgi membrane protein containing a cytoplasmic domain of at least 350 kDa. *Mol Biol Cell,* 4**,** 679-93.

LION, T. 2014. Adenovirus infections in immunocompetent and immunocompromised patients. *Clin Microbiol Rev,* 27**,** 441-62.

LION, T., BAUMGARTINGER, R., WATZINGER, F., MATTHES-MARTIN, S., SUDA, M., PREUNER, S., FUTTERKNECHT, B., LAWITSCHKA, A., PETERS, C., POTSCHGER, U. & GADNER, H. 2003. Molecular monitoring of adenovirus in peripheral blood after allogeneic bone marrow transplantation permits early diagnosis of disseminated disease. *Blood,* 102**,** 1114-20.

LISZEWSKI, M. K., POST, T. W. & ATKINSON, J. P. 1991. Membrane cofactor protein (MCP or CD46): newest member of the regulators of complement activation gene cluster. *Annu Rev Immunol,* 9**,** 431-55.

LIU, H., JIN, L., KOH, S. B., ATANASOV, I., SCHEIN, S., WU, L. & ZHOU, Z. H. 2010. Atomic structure of human adenovirus by cryo-EM reveals interactions among protein networks. *Science,* 329**,** 1038-43.

LIU, H., WU, L. & ZHOU, Z. H. 2011. Model of the trimeric fiber and its interactions with the pentameric penton base of human adenovirus by cryo-electron microscopy. *J Mol Biol,* 406**,** 764-74.

LIU, Q., WHITE, L. R., CLARK, S. A., HEFFNER, D. J., WINSTON, B. W., TIBBLES, L. A. & MURUVE, D. A. 2005. Akt/protein kinase B activation by adenovirus vectors contributes to NFkappaB-dependent CXCL10 expression. *J Virol,* 79**,** 14507-15.

LIVAK, K. J. & SCHMITTGEN, T. D. 2001. Analysis of relative gene expression data using real-time quantitative PCR and the 2(-Delta Delta C(T)) Method. *Methods,* 25**,** 402-8.

LOCHMULLER, H., JANI, A., HUARD, J., PRESCOTT, S., SIMONEAU, M., MASSIE, B., KARPATI, G. & ACSADI, G. 1994. Emergence of early region 1-containing replication-competent adenovirus in stocks of replication-defective adenovirus recombinants (delta E1 + delta E3) during multiple passages in 293 cells. *Hum Gene Ther,* 5**,** 1485-91.

LOGUNOV, D. Y., ILYINSKAYA, G. V., CHERENOVA, L. V., VERHOVSKAYA, L. V., SHMAROV, M. M., CHUMAKOV, P. M., KOPNIN, B. P. & NARODITSKY, B. S. 2004. Restoration of p53 tumor-suppressor activity in human tumor cells in vitro and in their xenografts in vivo by recombinant avian adenovirus CELO-p53. *Gene Ther,* 11**,** 79-84.

LOONSTRA, A., VOOIJS, M., BEVERLOO, H. B., ALLAK, B. A., VAN DRUNEN, E., KANAAR, R., BERNS, A. & JONKERS, J. 2001. Growth inhibition and DNA

damage induced by Cre recombinase in mammalian cells. *Proc Natl Acad Sci U S A,* 98**,** 9209-14.

LOPEZ-GORDO, E., DENBY, L., NICKLIN, S. A. & BAKER, A. H. 2014a. The importance of coagulation factors binding to adenovirus: historical perspectives and implications for gene delivery. *Expert Opin Drug Deliv,* 11**,** 1795-813.

LOPEZ-GORDO, E., PODGORSKI, II, DOWNES, N. & ALEMANY, R. 2014b. Circumventing antivector immunity: potential use of nonhuman adenoviral vectors. *Hum Gene Ther,* 25**,** 285-300.

LORTAT-JACOB, H., CHOUIN, E., CUSACK, S. & VAN RAAIJ, M. J. 2001. Kinetic analysis of adenovirus fiber binding to its receptor reveals an avidity mechanism for trimeric receptor-ligand interactions. *J Biol Chem,* 276**,** 9009-15.

LOTZE, M. T. & TRACEY, K. J. 2005. High-mobility group box 1 protein (HMGB1): nuclear weapon in the immune arsenal. *Nat Rev Immunol,* 5**,** 331-42.

LOUIS, N., EVELEGH, C. & GRAHAM, F. L. 1997. Cloning and sequencing of the cellular-viral junctions from the human adenovirus type 5 transformed 293 cell line. *Virology,* 233**,** 423-9.

LOUKINE, L., WATERS, C., CHOI, B. C. & ELLISON, J. 2011. Health-Adjusted Life Expectancy among Canadian Adults with and without Hypertension. *Cardiol Res Pract,* 2011**,** 612968.

LOWE, S. W. & RULEY, H. E. 1993. Stabilization of the p53 tumor suppressor is induced by adenovirus 5 E1A and accompanies apoptosis. *Genes Dev,* 7**,** 535-45.

LOWENSTEIN, P. R. 2008. With a little help from my f(X)riends!: the basis of Ad5-mediated transduction of the liver revealed. *Mol Ther,* 16**,** 1004-6.

LOZIER, J. N., CSAKO, G., MONDORO, T. H., KRIZEK, D. M., METZGER, M. E., COSTELLO, R., VOSTAL, J. G., RICK, M. E., DONAHUE, R. E. & MORGAN, R. A. 2002. Toxicity of a first-generation adenoviral vector in rhesus macaques. *Hum Gene Ther,* 13**,** 113-24.

LU, Y. 2004. Recombinant adeno-associated virus as delivery vector for gene therapy--a review. *Stem Cells Dev,* 13**,** 133-45.

LUDWIG, S. L., BRUNDAGE, J. F., KELLEY, P. W., NANG, R., TOWLE, C., SCHNURR, D. P., CRAWFORD-MIKSZA, L. & GAYDOS, J. C. 1998. Prevalence of antibodies to adenovirus serotypes 4 and 7 among unimmunized US Army trainees: results of a retrospective nationwide seroprevalence survey. *J Infect Dis,* 178**,** 1776-8.

LUKASHEV, A. N. & ZAMYATNIN, A. A., JR. 2016. Viral Vectors for Gene Therapy: Current State and Clinical Perspectives. *Biochemistry (Mosc),* 81**,** 700-8.

LUO, J., DENG, Z. L., LUO, X., TANG, N., SONG, W. X., CHEN, J., SHARFF, K. A., LUU, H. H., HAYDON, R. C., KINZLER, K. W., VOGELSTEIN, B. & HE, T. C. 2007. A protocol for rapid generation of recombinant adenoviruses using the AdEasy system. *Nat Protoc,* 2**,** 1236-47.

LUSKY, M. 2005. Good manufacturing practice production of adenoviral vectors for clinical trials. *Hum Gene Ther,* 16**,** 281-91.

LUTSCHG, V., BOUCKE, K., HEMMI, S. & GREBER, U. F. 2011. Chemotactic antiviral cytokines promote infectious apical entry of human adenovirus into polarized epithelial cells. *Nat Commun,* 2**,** 391.

LUTZ, P. & KEDINGER, C. 1996. Properties of the adenovirus IVa2 gene product, an effector of late-phase-dependent activation of the major late promoter. *J Virol,* 70**,** 1396-405.

MA, H. C. & HEARING, P. 2011. Adenovirus structural protein IIIa is involved in the serotype specificity of viral DNA packaging. *J Virol,* 85**,** 7849-55.

MA, J., DUFFY, M. R., DENG, L., DAKIN, R. S., UIL, T., CUSTERS, J., KELLY, S. M., MCVEY, J. H., NICKLIN, S. A. & BAKER, A. H. 2015. Manipulating adenovirus

hexon hypervariable loops dictates immune neutralisation and coagulation factor X-dependent cell interaction in vitro and in vivo. *PLoS Pathog,* 11**,** e1004673.

MABIT, H., NAKANO, M. Y., PRANK, U., SAAM, B., DOHNER, K., SODEIK, B. & GREBER, U. F. 2002. Intact microtubules support adenovirus and herpes simplex virus infections. *J Virol,* 76**,** 9962-71.

MAGNUSSON, M. K., HENNING, P., MYHRE, S., WIKMAN, M., UIL, T. G., FRIEDMAN, M., ANDERSSON, K. M., HONG, S. S., HOEBEN, R. C., HABIB, N. A., STAHL, S., BOULANGER, P. & LINDHOLM, L. 2007. Adenovirus 5 vector genetically re-targeted by an Affibody molecule with specificity for tumor antigen HER2/neu. *Cancer Gene Ther,* 14**,** 468-79.

MAGNUSSON, M. K., HONG, S. S., BOULANGER, P. & LINDHOLM, L. 2001. Genetic retargeting of adenovirus: novel strategy employing "deknobbing" of the fiber. *J Virol,* 75**,** 7280-9.

MAGUIRE, A. M., HIGH, K. A., AURICCHIO, A., WRIGHT, J. F., PIERCE, E. A., TESTA, F., MINGOZZI, F., BENNICELLI, J. L., YING, G. S., ROSSI, S., FULTON, A., MARSHALL, K. A., BANFI, S., CHUNG, D. C., MORGAN, J. I., HAUCK, B., ZELENAIA, O., ZHU, X., RAFFINI, L., COPPIETERS, F., DE BAERE, E., SHINDLER, K. S., VOLPE, N. J., SURACE, E. M., ACERRA, C., LYUBARSKY, A., REDMOND, T. M., STONE, E., SUN, J., MCDONNELL, J. W., LEROY, B. P., SIMONELLI, F. & BENNETT, J. 2009. Age-dependent effects of RPE65 gene therapy for Leber's congenital amaurosis: a phase 1 dose-escalation trial. *Lancet,* 374**,** 1597-605.

MAIER, O., GALAN, D. L., WODRICH, H. & WIETHOFF, C. M. 2010. An N-terminal domain of adenovirus protein VI fragments membranes by inducing positive membrane curvature. *Virology,* 402**,** 11-9.

MAIONE, D., DELLA ROCCA, C., GIANNETTI, P., D'ARRIGO, R., LIBERATOSCIOLI, L., FRANLIN, L. L., SANDIG, V., CILIBERTO, G., LA MONICA, N. & SAVINO, R. 2001. An improved helper-dependent adenoviral vector allows persistent gene expression after intramuscular delivery and overcomes preexisting immunity to adenovirus. *Proc Natl Acad Sci U S A,* 98**,** 5986-91.

MAJHEN, D., CALDERON, H., CHANDRA, N., FAJARDO, C. A., RAJAN, A., ALEMANY, R. & CUSTERS, J. 2014. Adenovirus-based vaccines for fighting infectious diseases and cancer: progress in the field. *Hum Gene Ther,* 25**,** 301-17.

MAJHEN, D., GABRILOVAC, J., ELOIT, M., RICHARDSON, J. & AMBRIOVIC-RISTOV, A. 2006. Disulfide bond formation in NGR fiber-modified adenovirus is essential for retargeting to aminopeptidase N. *Biochem Biophys Res Commun,* 348**,** 278-87.

MALLERY, D. L., MCEWAN, W. A., BIDGOOD, S. R., TOWERS, G. J., JOHNSON, C. M. & JAMES, L. C. 2010. Antibodies mediate intracellular immunity through tripartite motif-containing 21 (TRIM21). *Proc Natl Acad Sci U S A,* 107**,** 19985-90.

MANE, V. P., TOIETTA, G., MCCORMACK, W. M., CONDE, I., CLARKE, C., PALMER, D., FINEGOLD, M. J., PASTORE, L., NG, P., LOPEZ, J. & LEE, B. 2006. Modulation of TNFalpha, a determinant of acute toxicity associated with systemic delivery of first-generation and helper-dependent adenoviral vectors. *Gene Ther,* 13**,** 1272-80.

MANGEL, W. F., MCGRATH, W. J., TOLEDO, D. L. & ANDERSON, C. W. 1993. Viral DNA and a viral peptide can act as cofactors of adenovirus virion proteinase activity. *Nature,* 361**,** 274-5.

MANGEL, W. F. & SAN MARTIN, C. 2014. Structure, function and dynamics in adenovirus maturation. *Viruses,* 6**,** 4536-70.

MANICKAN, E., SMITH, J. S., TIAN, J., EGGERMAN, T. L., LOZIER, J. N., MULLER, J. & BYRNES, A. P. 2006. Rapid Kupffer cell death after intravenous injection of adenovirus vectors. *Mol Ther,* 13**,** 108-17.

MARSH, M. P., CAMPOS, S. K., BAKER, M. L., CHEN, C. Y., CHIU, W. & BARRY, M. A. 2006. Cryoelectron microscopy of protein IX-modified adenoviruses suggests a new position for the C terminus of protein IX. *J Virol,* 80**,** 11881-6.

MARTIN, K., BRIE, A., SAULNIER, P., PERRICAUDET, M., YEH, P. & VIGNE, E. 2003. Simultaneous CAR- and alpha V integrin-binding ablation fails to reduce Ad5 liver tropism. *Mol Ther,* 8**,** 485-94.

MARTIN, M. E. & BERK, A. J. 1998. Adenovirus E1B 55K represses p53 activation in vitro. *J Virol,* 72**,** 3146-54.

MARTIN, M. E. & BERK, A. J. 1999. Corepressor required for adenovirus E1B 55,000-molecular-weight protein repression of basal transcription. *Mol Cell Biol,* 19**,** 3403-14.

MARTINEZ-MARTINEZ, I., ORDONEZ, A., PEDERSEN, S., DE LA MORENA-BARRIO, M. E., NAVARRO-FERNANDEZ, J., KRISTENSEN, S. R., MINANO, A., PADILLA, J., VICENTE, V. & CORRAL, J. 2011. Heparin affinity of factor VIIa: implications on the physiological inhibition by antithrombin and clearance of recombinant factor VIIa. *Thromb Res,* 127**,** 154-60.

MARTTILA, M., PERSSON, D., GUSTAFSSON, D., LISZEWSKI, M. K., ATKINSON, J. P., WADELL, G. & ARNBERG, N. 2005. CD46 is a cellular receptor for all species B adenoviruses except types 3 and 7. *J Virol,* 79**,** 14429-36.

MARUMO, T., YAGI, S., KAWARAZAKI, W., NISHIMOTO, M., AYUZAWA, N., WATANABE, A., UEDA, K., HIRAHASHI, J., HISHIKAWA, K., SAKURAI, H., SHIOTA, K. & FUJITA, T. 2015. Diabetes Induces Aberrant DNA Methylation in the Proximal Tubules of the Kidney. *J Am Soc Nephrol,* 26**,** 2388-97.

MATHEWS, M. B. 1995. Structure, function, and evolution of adenovirus virus-associated RNAs. *Curr Top Microbiol Immunol,* 199 (Pt 2)**,** 173-87.

MATHEWS, M. B. & SHENK, T. 1991. Adenovirus virus-associated RNA and translation control. *J Virol,* 65**,** 5657-62.

MATHIAS, P., GALLENO, M. & NEMEROW, G. R. 1998. Interactions of soluble recombinant integrin alphav beta5 with human adenoviruses. *J Virol,* 72**,** 8669-75.

MATTHEWS, D. A. & RUSSELL, W. C. 1998. Adenovirus core protein V is delivered by the invading virus to the nucleus of the infected cell and later in infection is associated with nucleoli. *J Gen Virol,* 79 (Pt 7)**,** 1671-5.

MCCARTY, D. M., YOUNG, S. M., JR. & SAMULSKI, R. J. 2004. Integration of adeno-associated virus (AAV) and recombinant AAV vectors. *Annu Rev Genet,* 38**,** 819-45.

MCCORMICK, C., LEDUC, Y., MARTINDALE, D., MATTISON, K., ESFORD, L. E., DYER, A. P. & TUFARO, F. 1998. The putative tumour suppressor EXT1 alters the expression of cell-surface heparan sulfate. *Nat Genet,* 19**,** 158-61.

MCGRATH, W. J., BANIECKI, M. L., LI, C., MCWHIRTER, S. M., BROWN, M. T., TOLEDO, D. L. & MANGEL, W. F. 2001a. Human adenovirus proteinase: DNA binding and stimulation of proteinase activity by DNA. *Biochemistry,* 40**,** 13237-45.

MCGRATH, W. J., BANIECKI, M. L., PETERS, E., GREEN, D. T. & MANGEL, W. F. 2001b. Roles of two conserved cysteine residues in the activation of human adenovirus proteinase. *Biochemistry,* 40**,** 14468-74.

MCGRATH, W. J., DING, J., DIDWANIA, A., SWEET, R. M. & MANGEL, W. F. 2003. Crystallographic structure at 1.6-A resolution of the human adenovirus proteinase in a covalent complex with its 11-amino-acid peptide cofactor: insights on a new fold. *Biochim Biophys Acta,* 1648**,** 1-11.

MCNEES, A. L., GARNETT, C. T. & GOODING, L. R. 2002. The adenovirus E3 RID complex protects some cultured human T and B lymphocytes from Fas-induced apoptosis. *J Virol,* 76**,** 9716-23.

MCQUADE, K. J., BEAUVAIS, D. M., BURBACH, B. J. & RAPRAEGER, A. C. 2006. Syndecan-1 regulates alphavbeta5 integrin activity in B82L fibroblasts. *J Cell Sci,* 119**,** 2445-56.

MCSHARRY, B. P., BURGERT, H. G., OWEN, D. P., STANTON, R. J., PROD'HOMME, V., SESTER, M., KOEBERNICK, K., GROH, V., SPIES, T., COX, S., LITTLE, A. M., WANG, E. C., TOMASEC, P. & WILKINSON, G. W. 2008. Adenovirus E3/19K promotes evasion of NK cell recognition by intracellular sequestration of the NKG2D ligands major histocompatibility complex class I chain-related proteins A and B. *J Virol,* 82**,** 4585-94.

MCVEY, D., ZUBER, M., ETTYREDDY, D., REITER, C. D., BROUGH, D. E., NABEL, G. J., KING, C. R. & GALL, J. G. 2010. Characterization of human adenovirus 35 and derivation of complex vectors. *Virol J,* 7**,** 276.

MEIER, O., BOUCKE, K., HAMMER, S. V., KELLER, S., STIDWILL, R. P., HEMMI, S. & GREBER, U. F. 2002. Adenovirus triggers macropinocytosis and endosomal leakage together with its clathrin-mediated uptake. *J Cell Biol,* 158**,** 1119-31.

MESTAN, J., DIGEL, W., MITTNACHT, S., HILLEN, H., BLOHM, D., MOLLER, A., JACOBSEN, H. & KIRCHNER, H. 1986. Antiviral effects of recombinant tumour necrosis factor in vitro. *Nature,* 323**,** 816-9.

MILLER, A. D. 1992. Human gene therapy comes of age. *Nature,* 357**,** 455-60.

MILLER, C. R., BUCHSBAUM, D. J., REYNOLDS, P. N., DOUGLAS, J. T., GILLESPIE, G. Y., MAYO, M. S., RABEN, D. & CURIEL, D. T. 1998. Differential susceptibility of primary and established human glioma cells to adenovirus infection: targeting via the epidermal growth factor receptor achieves fiber receptor-independent gene transfer. *Cancer Res,* 58**,** 5738-48.

MILLER, D. L., RICKARDS, B., MASHIBA, M., HUANG, W. & FLINT, S. J. 2009. The adenoviral E1B 55-kilodalton protein controls expression of immune response genes but not p53-dependent transcription. *J Virol,* 83**,** 3591-603.

MINAMITANI, T., IWAKIRI, D. & TAKADA, K. 2011. Adenovirus virus-associated RNAs induce type I interferon expression through a RIG-I-mediated pathway. *J Virol,* 85**,** 4035-40.

MIWA, T., NONAKA, M., OKADA, N., WAKANA, S., SHIROISHI, T. & OKADA, H. 1998. Molecular cloning of rat and mouse membrane cofactor protein (MCP, CD46): preferential expression in testis and close linkage between the mouse Mcp and Cr2 genes on distal chromosome 1. *Immunogenetics,* 48**,** 363-71.

MIYAZAWA, N., CRYSTAL, R. G. & LEOPOLD, P. L. 2001. Adenovirus serotype 7 retention in a late endosomal compartment prior to cytosol escape is modulated by fiber protein. *J Virol,* 75**,** 1387-400.

MIYAZAWA, N., LEOPOLD, P. L., HACKETT, N. R., FERRIS, B., WORGALL, S., FALCK-PEDERSEN, E. & CRYSTAL, R. G. 1999. Fiber swap between adenovirus subgroups B and C alters intracellular trafficking of adenovirus gene transfer vectors. *J Virol,* 73**,** 6056-65.

MIZUGUCHI, H., KOIZUMI, N., HOSONO, T., ISHII-WATABE, A., UCHIDA, E., UTOGUCHI, N., WATANABE, Y. & HAYAKAWA, T. 2002. CAR- or alphav integrin-binding ablated adenovirus vectors, but not fiber-modified vectors containing RGD peptide, do not change the systemic gene transfer properties in mice. *Gene Ther,* 9**,** 769-76.

MIZUNO, H., FUJIMOTO, Z., ATODA, H. & MORITA, T. 2001. Crystal structure of an anticoagulant protein in complex with the Gla domain of factor X. *Proc Natl Acad Sci U S A,* 98**,** 7230-4.

MOK, H., PALMER, D. J., NG, P. & BARRY, M. A. 2005. Evaluation of polyethylene glycol modification of first-generation and helper-dependent adenoviral vectors to reduce innate immune responses. *Mol Ther,* 11**,** 66-79.

MOMBAERTS, P., IACOMINI, J., JOHNSON, R. S., HERRUP, K., TONEGAWA, S. & PAPAIOANNOU, V. E. 1992. RAG-1-deficient mice have no mature B and T lymphocytes. *Cell,* 68**,** 869-77.

MONTEIRO, R. Q., REZAIE, A. R., RIBEIRO, J. M. & FRANCISCHETTI, I. M. 2005. Ixolaris: a factor Xa heparin-binding exosite inhibitor. *Biochem J,* 387**,** 871-7.

MORRAL, N., O'NEAL, W. K., RICE, K., LELAND, M. M., PIEDRA, P. A., AGUILAR-CORDOVA, E., CAREY, K. D., BEAUDET, A. L. & LANGSTON, C. 2002. Lethal toxicity, severe endothelial injury, and a threshold effect with high doses of an adenoviral vector in baboons. *Hum Gene Ther,* 13**,** 143-54.

MORRIS, S. J. & LEPPARD, K. N. 2009. Adenovirus serotype 5 L4-22K and L4-33K proteins have distinct functions in regulating late gene expression. *J Virol,* 83**,** 3049-58.

MORRIS, S. J., SCOTT, G. E. & LEPPARD, K. N. 2010. Adenovirus late-phase infection is controlled by a novel L4 promoter. *J Virol,* 84**,** 7096-104.

MORRISON, J., BRIGGS, S. S., GREEN, N., FISHER, K., SUBR, V., ULBRICH, K., KEHOE, S. & SEYMOUR, L. W. 2008. Virotherapy of ovarian cancer with polymer-cloaked adenovirus retargeted to the epidermal growth factor receptor. *Mol Ther,* 16**,** 244-51.

MORRISON, J., BRIGGS, S. S., GREEN, N. K., THOMA, C., FISHER, K. D., KEHOE, S. & SEYMOUR, L. W. 2009. Cetuximab retargeting of adenovirus via the epidermal growth factor receptor for treatment of intraperitoneal ovarian cancer. *Hum Gene Ther,* 20**,** 239-51.

MOULLIER, P., FRIEDLANDER, G., CALISE, D., RONCO, P., PERRICAUDET, M. & FERRY, N. 1994. Adenoviral-mediated gene transfer to renal tubular cells in vivo. *Kidney Int,* 45**,** 1220-5.

MOYER, C. L., WIETHOFF, C. M., MAIER, O., SMITH, J. G. & NEMEROW, G. R. 2011. Functional genetic and biophysical analyses of membrane disruption by human adenovirus. *J Virol,* 85**,** 2631-41.

MUL, Y. M. & VAN DER VLIET, P. C. 1992. Nuclear factor I enhances adenovirus DNA replication by increasing the stability of a preinitiation complex. *EMBO J,* 11**,** 751-60.

MUL, Y. M. & VAN DER VLIET, P. C. 1993. The adenovirus DNA binding protein effects the kinetics of DNA replication by a mechanism distinct from NFI or Oct-1. *Nucleic Acids Res,* 21**,** 641-7.

MULLER, S. & DOBNER, T. 2008. The adenovirus E1B-55K oncoprotein induces SUMO modification of p53. *Cell Cycle,* 7**,** 754-8.

MUND, A., SCHUBERT, T., STAEGE, H., KINKLEY, S., REUMANN, K., KRIEGS, M., FRITSCH, L., BATTISTI, V., AIT-SI-ALI, S., HOFFBECK, A. S., SOUTOGLOU, E. & WILL, H. 2012. SPOC1 modulates DNA repair by regulating key determinants of chromatin compaction and DNA damage response. *Nucleic Acids Res,* 40**,** 11363-79.

MUNDEL, P. & SHANKLAND, S. J. 2002. Podocyte biology and response to injury. *J Am Soc Nephrol,* 13**,** 3005-15.

MURAKAMI, M. T., RIOS-STEINER, J., WEAVER, S. E., TULINSKY, A., GEIGER, J. H. & ARNI, R. K. 2007. Intermolecular interactions and characterization of the novel factor Xa exosite involved in macromolecular recognition and inhibition: crystal structure of human Gla-domainless factor Xa complexed with the anticoagulant protein NAPc2 from the hematophagous nematode Ancylostoma caninum. *J Mol Biol,* 366**,** 602-10.

MURAMATSU, S., FUJIMOTO, K., KATO, S., MIZUKAMI, H., ASARI, S., IKEGUCHI, K., KAWAKAMI, T., URABE, M., KUME, A., SATO, T., WATANABE, E., OZAWA, K. & NAKANO, I. 2010. A phase I study of aromatic L-amino acid decarboxylase gene therapy for Parkinson's disease. *Mol Ther,* 18**,** 1731-5.

MURPHY, G. F., WOOD, D. P., JR., MCROBERTS, J. W. & HENSLEE-DOWNEY, P. J. 1993. Adenovirus-associated hemorrhagic cystitis treated with intravenous ribavirin. *J Urol,* 149**,** 565-6.

MURUVE, D. A., PETRILLI, V., ZAISS, A. K., WHITE, L. R., CLARK, S. A., ROSS, P. J., PARKS, R. J. & TSCHOPP, J. 2008. The inflammasome recognizes cytosolic microbial and host DNA and triggers an innate immune response. *Nature,* 452**,** 103-7.

MYHRE, S., HENNING, P., FRIEDMAN, M., STAHL, S., LINDHOLM, L. & MAGNUSSON, M. K. 2009. Re-targeted adenovirus vectors with dual specificity; binding specificities conferred by two different Affibody molecules in the fiber. *Gene Ther,* 16**,** 252-61.

MYHRE, S., HENNING, P., GRANIO, O., TYLÖ, A. S., NYGREN, P. A., OLOFSSON, S., BOULANGER, P., LINDHOLM, L. & HONG, S. S. 2007. Decreased immune reactivity towards a knobless, affibody-targeted adenovirus type 5 vector. *Gene Ther,* 14**,** 376-81.

NAGATA, K., GUGGENHEIMER, R. A., ENOMOTO, T., LICHY, J. H. & HURWITZ, J. 1982. Adenovirus DNA replication in vitro: identification of a host factor that stimulates synthesis of the preterminal protein-dCMP complex. *Proc Natl Acad Sci U S A,* 79**,** 6438-42.

NAGATA, K., GUGGENHEIMER, R. A. & HURWITZ, J. 1983a. Adenovirus DNA replication in vitro: synthesis of full-length DNA with purified proteins. *Proc Natl Acad Sci U S A,* 80**,** 4266-70.

NAGATA, K., GUGGENHEIMER, R. A. & HURWITZ, J. 1983b. Specific binding of a cellular DNA replication protein to the origin of replication of adenovirus DNA. *Proc Natl Acad Sci U S A,* 80**,** 6177-81.

NAGATA, S. 1997. Apoptosis by death factor. *Cell,* 88**,** 355-65.

NAGEL, H., MAAG, S., TASSIS, A., NESTLE, F. O., GREBER, U. F. & HEMMI, S. 2003. The alphavbeta5 integrin of hematopoietic and nonhematopoietic cells is a transduction receptor of RGD-4C fiber-modified adenoviruses. *Gene Ther,* 10**,** 1643-53.

NAHMAN, N. S., SFERRA, T. J., KRONENBERGER, J., URBAN, K. E., TROIKE, A. E., JOHNSON, A., HOLYCROSS, B. J., NUOVO, G. J. & SEDMAK, D. D. 2000. Microsphere-adenoviral complexes target and transduce the glomerulus in vivo. *Kidney Int,* 58**,** 1500-10.

NAKAI, H., YANT, S. R., STORM, T. A., FUESS, S., MEUSE, L. & KAY, M. A. 2001. Extrachromosomal recombinant adeno-associated virus vector genomes are primarily responsible for stable liver transduction in vivo. *J Virol,* 75**,** 6969-76.

NAKANO, M. Y., BOUCKE, K., SUOMALAINEN, M., STIDWILL, R. P. & GREBER, U. F. 2000. The first step of adenovirus type 2 disassembly occurs at the cell surface, independently of endocytosis and escape to the cytosol. *J Virol,* 74**,** 7085-95.

NAN, X., PENG, B., HAHN, T. W., RICHARDSON, E., LIZONOVA, A., KOVESDI, I. & ROBERT-GUROFF, M. 2003. Development of an Ad7 cosmid system and generation of an Ad7deltaE1deltaE3HIV(MN) env/rev recombinant virus. *Gene Ther,* 10**,** 326-36.

NASS, K. & FRENKEL, G. D. 1980. Adenovirus-specific DNA-binding protein inhibits the hydrolysis of DNA by DNase in vitro. *J Virol,* 35**,** 314-9.

NATHWANI, A. C., TUDDENHAM, E. G., RANGARAJAN, S., ROSALES, C., MCINTOSH, J., LINCH, D. C., CHOWDARY, P., RIDDELL, A., PIE, A. J., HARRINGTON, C., O'BEIRNE, J., SMITH, K., PASI, J., GLADER, B., RUSTAGI, P., NG, C. Y., KAY, M. A., ZHOU, J., SPENCE, Y., MORTON, C. L., ALLAY, J., COLEMAN, J., SLEEP, S., CUNNINGHAM, J. M., SRIVASTAVA, D., BASNER-TSCHAKARJAN, E., MINGOZZI, F., HIGH, K. A., GRAY, J. T., REISS, U. M., NIENHUIS, A. W. & DAVIDOFF, A. M. 2011. Adenovirus-associated virus vector-mediated gene transfer in hemophilia B. *N Engl J Med,* 365**,** 2357-65.

NATIONAL KIDNEY, F. 2002. K/DOQI clinical practice guidelines for chronic kidney disease: evaluation, classification, and stratification. *Am J Kidney Dis,* 39**,** S1-266.

NEELS, J. G., VAN DEN BERG, B. M., MERTENS, K., TER MAAT, H., PANNEKOEK, H., VAN ZONNEVELD, A. J. & LENTING, P. J. 2000. Activation of factor IX zymogen results in exposure of a binding site for low-density lipoprotein receptor-related protein. *Blood,* 96**,** 3459-65.

NEMEROW, G. R., STEWART, P. L. & REDDY, V. S. 2012. Structure of human adenovirus. *Curr Opin Virol,* 2**,** 115-21.

NETTELBECK, D. M., MILLER, D. W., JEROME, V., ZUZARTE, M., WATKINS, S. J., HAWKINS, R. E., MULLER, R. & KONTERMANN, R. E. 2001. Targeting of adenovirus to endothelial cells by a bispecific single-chain diabody directed against the adenovirus fiber knob domain and human endoglin (CD105). *Mol Ther,* 3**,** 882-91.

NETTELBECK, D. M., RIVERA, A. A., KUPSCH, J., DIECKMANN, D., DOUGLAS, J. T., KONTERMANN, R. E., ALEMANY, R. & CURIEL, D. T. 2004. Retargeting of adenoviral infection to melanoma: combining genetic ablation of native tropism with a recombinant bispecific single-chain diabody (scDb) adapter that binds to fiber knob and HMWMAA. *Int J Cancer,* 108**,** 136-45.

NI, S., BERNT, K., GAGGAR, A., LI, Z. Y., KIEM, H. P. & LIEBER, A. 2005. Evaluation of biodistribution and safety of adenovirus vectors containing group B fibers after intravenous injection into baboons. *Hum Gene Ther,* 16**,** 664-77.

NICKLIN, S. A., VON SEGGERN, D. J., WORK, L. M., PEK, D. C., DOMINICZAK, A. F., NEMEROW, G. R. & BAKER, A. H. 2001. Ablating adenovirus type 5 fiber-CAR binding and HI loop insertion of the SIGYPLP peptide generate an endothelial cell-selective adenovirus. *Mol Ther,* 4**,** 534-42.

NICKLIN, S. A., WHITE, S. J., NICOL, C. G., VON SEGGERN, D. J. & BAKER, A. H. 2004. In vitro and in vivo characterisation of endothelial cell selective adenoviral vectors. *J Gene Med,* 6**,** 300-8.

NICOL, C. G., GRAHAM, D., MILLER, W. H., WHITE, S. J., SMITH, T. A., NICKLIN, S. A., STEVENSON, S. C. & BAKER, A. H. 2004. Effect of adenovirus serotype 5 fiber and penton modifications on in vivo tropism in rats. *Mol Ther,* 10**,** 344-54.

NIEDERMEYER, W. 1985. Interaction of streptolysin-O with biomembranes: kinetic and morphological studies on erythrocyte membranes. *Toxicon,* 23**,** 425-39.

NOCIARI, M., OCHERETINA, O., SCHOGGINS, J. W. & FALCK-PEDERSEN, E. 2007. Sensing infection by adenovirus: Toll-like receptor-independent viral DNA recognition signals activation of the interferon regulatory factor 3 master regulator. *J Virol,* 81**,** 4145-57.

NOKISALMI, P., PESONEN, S., ESCUTENAIRE, S., SARKIOJA, M., RAKI, M., CERULLO, V., LAASONEN, L., ALEMANY, R., ROJAS, J., CASCALLO, M., GUSE, K., RAJECKI, M., KANGASNIEMI, L., HAAVISTO, E., KARIOJA-KALLIO, A., HANNUKSELA, P., OKSANEN, M., KANERVA, A., JOENSUU, T., AHTIAINEN, L. & HEMMINKI, A. 2010. Oncolytic adenovirus ICOVIR-7 in patients with advanced and refractory solid tumors. *Clin Cancer Res,* 16**,** 3035-43.

NORD, K., GUNNERIUSSON, E., RINGDAHL, J., STAHL, S., UHLEN, M. & NYGREN, P. A. 1997. Binding proteins selected from combinatorial libraries of an alpha-helical bacterial receptor domain. *Nat Biotechnol,* 15**,** 772-7.

NORD, K., NILSSON, J., NILSSON, B., UHLEN, M. & NYGREN, P. A. 1995. A combinatorial library of an alpha-helical bacterial receptor domain. *Protein Eng,* 8**,** 601-8.

NOREN, K. A. & NOREN, C. J. 2001. Construction of high-complexity combinatorial phage display peptide libraries. *Methods,* 23**,** 169-78.

NORRBY, E. 1969. The structural and functional diversity of Adenovirus capsid components. *J Gen Virol,* 5**,** 221-36.

NWANEGBO, E., VARDAS, E., GAO, W., WHITTLE, H., SUN, H., ROWE, D., ROBBINS, P. D. & GAMBOTTO, A. 2004. Prevalence of neutralizing antibodies to adenoviral serotypes 5 and 35 in the adult populations of The Gambia, South Africa, and the United States. *Clin Diagn Lab Immunol,* 11**,** 351-7.

O'MALLEY, R. P., DUNCAN, R. F., HERSHEY, J. W. & MATHEWS, M. B. 1989. Modification of protein synthesis initiation factors and the shut-off of host protein synthesis in adenovirus-infected cells. *Virology,* 168**,** 112-8.

O'MALLEY, R. P., MARIANO, T. M., SIEKIERKA, J. & MATHEWS, M. B. 1986. A mechanism for the control of protein synthesis by adenovirus VA RNAI. *Cell,* 44**,** 391-400.

O'NEILL, E. A., FLETCHER, C., BURROW, C. R., HEINTZ, N., ROEDER, R. G. & KELLY, T. J. 1988. Transcription factor OTF-1 is functionally identical to the DNA replication factor NF-III. *Science,* 241**,** 1210-3.

OLIVE, M., EISENLOHR, L., FLOMENBERG, N., HSU, S. & FLOMENBERG, P. 2002. The adenovirus capsid protein hexon contains a highly conserved human CD4+ T-cell epitope. *Hum Gene Ther,* 13**,** 1167-78.

ONION, D., CROMPTON, L. J., MILLIGAN, D. W., MOSS, P. A., LEE, S. P. & MAUTNER, V. 2007. The CD4+ T-cell response to adenovirus is focused against conserved residues within the hexon protein. *J Gen Virol,* 88**,** 2417-25.

OOSTEROM-DRAGON, E. A. & GINSBERG, H. S. 1981. Characterization of two temperature-sensitive mutants of type 5 adenovirus with mutations in the 100,000-dalton protein gene. *J Virol,* 40**,** 491-500.

ORAZIO, N. I., NAEGER, C. M., KARLSEDER, J. & WEITZMAN, M. D. 2011. The adenovirus E1b55K/E4orf6 complex induces degradation of the Bloom helicase during infection. *J Virol,* 85**,** 1887-92.

ORD, E. N., SHIRLEY, R., MCCLURE, J. D., MCCABE, C., KREMER, E. J., MACRAE, I. M. & WORK, L. M. 2013. Combined antiapoptotic and antioxidant approach to acute neuroprotection for stroke in hypertensive rats. *J Cereb Blood Flow Metab,* 33**,** 1215-24.

OSTAPCHUK, P., ALMOND, M. & HEARING, P. 2011. Characterization of Empty adenovirus particles assembled in the absence of a functional adenovirus IVa2 protein. *J Virol,* 85**,** 5524-31.

OSTAPCHUK, P. & HEARING, P. 2001. Pseudopackaging of adenovirus type 5 genomes into capsids containing the hexon proteins of adenovirus serotypes B, D, or E. *J Virol,* 75**,** 45-51.

OSTAPCHUK, P. & HEARING, P. 2008. Adenovirus IVa2 protein binds ATP. *J Virol,* 82**,** 10290-4.

OSTAPCHUK, P., YANG, J., AUFFARTH, E. & HEARING, P. 2005. Functional interaction of the adenovirus IVa2 protein with adenovirus type 5 packaging sequences. *J Virol,* 79**,** 2831-8.

OTHMAN, M., LABELLE, A., MAZZETTI, I., ELBATARNY, H. S. & LILLICRAP, D. 2007. Adenovirus-induced thrombocytopenia: the role of von Willebrand factor and P-selectin in mediating accelerated platelet clearance. *Blood,* 109**,** 2832-9.

PAHL, J. H., VERHOEVEN, D. H., KWAPPENBERG, K. M., VELLINGA, J., LANKESTER, A. C., VAN TOL, M. J. & SCHILHAM, M. W. 2012. Adenovirus type 35, but not type 5, stimulates NK cell activation via plasmacytoid dendritic cells and TLR9 signaling. *Mol Immunol,* 51**,** 91-100.

PALMER, D. & NG, P. 2003. Improved system for helper-dependent adenoviral vector production. *Mol Ther,* 8**,** 846-52.

PALMER, M., HARRIS, R., FREYTAG, C., KEHOE, M., TRANUM-JENSEN, J. & BHAKDI, S. 1998. Assembly mechanism of the oligomeric streptolysin O pore: the early membrane lesion is lined by a free edge of the lipid membrane and is extended gradually during oligomerization. *EMBO J,* 17**,** 1598-605.

PANDE, J., SZEWCZYK, M. M. & GROVER, A. K. 2010. Phage display: concept, innovations, applications and future. *Biotechnol Adv,* 28**,** 849-58.

PANTELIC, R. S., LOCKETT, L. J., ROTHNAGEL, R., HANKAMER, B. & BOTH, G. W. 2008. Cryoelectron microscopy map of Atadenovirus reveals cross-genus structural differences from human adenovirus. *J Virol,* 82**,** 7346-56.

PARDO-MATEOS, A. & YOUNG, C. S. 2004. Adenovirus IVa2 protein plays an important role in transcription from the major late promoter in vivo. *Virology,* 327**,** 50-9.

PARKER, A. L., FISHER, K. D., OUPICKY, D., READ, M. L., NICKLIN, S. A., BAKER, A. H. & SEYMOUR, L. W. 2005. Enhanced gene transfer activity of peptide-targeted gene-delivery vectors. *J Drug Target,* 13**,** 39-51.

PARKER, A. L., WADDINGTON, S. N., BUCKLEY, S. M., CUSTERS, J., HAVENGA, M. J., VAN ROOIJEN, N., GOUDSMIT, J., MCVEY, J. H., NICKLIN, S. A. & BAKER, A. H. 2009. Effect of neutralizing sera on factor x-mediated adenovirus serotype 5 gene transfer. *J Virol,* 83**,** 479-83.

PARKER, A. L., WADDINGTON, S. N., NICOL, C. G., SHAYAKHMETOV, D. M., BUCKLEY, S. M., DENBY, L., KEMBALL-COOK, G., NI, S., LIEBER, A., MCVEY, J. H., NICKLIN, S. A. & BAKER, A. H. 2006. Multiple vitamin K-dependent coagulation zymogens promote adenovirus-mediated gene delivery to hepatocytes. *Blood,* 108**,** 2554-61.

PARKER, E. J., BOTTING, C. H., WEBSTER, A. & HAY, R. T. 1998. Adenovirus DNA polymerase: domain organisation and interaction with preterminal protein. *Nucleic Acids Res,* 26**,** 1240-7.

PARKS, R. J., BRAMSON, J. L., WAN, Y., ADDISON, C. L. & GRAHAM, F. L. 1999. Effects of stuffer DNA on transgene expression from helper-dependent adenovirus vectors. *J Virol,* 73**,** 8027-34.

PARKS, R. J. & GRAHAM, F. L. 1997. A helper-dependent system for adenovirus vector production helps define a lower limit for efficient DNA packaging. *J Virol,* 71**,** 3293-8.

PASQUALINI, R. & RUOSLAHTI, E. 1996. Organ targeting in vivo using phage display peptide libraries. *Nature,* 380**,** 364-6.

PATSTON, P. A., GETTINS, P., BEECHEM, J. & SCHAPIRA, M. 1991. Mechanism of serpin action: evidence that C1 inhibitor functions as a suicide substrate. *Biochemistry,* 30**,** 8876-82.

PATTERSON, S. & RUSSELL, W. C. 1983. Ultrastructural and immunofluorescence studies of early events in adenovirus-HeLa cell interactions. *J Gen Virol,* 64**,** 1091-9.

PATTHY, L. 1985. Evolution of the proteases of blood coagulation and fibrinolysis by assembly from modules. *Cell,* 41**,** 657-63.

PAYNE, C. K., JONES, S. A., CHEN, C. & ZHUANG, X. 2007. Internalization and trafficking of cell surface proteoglycans and proteoglycan-binding ligands. *Traffic,* 8**,** 389-401.

PAZGIER, M., HOOVER, D. M., YANG, D., LU, W. & LUBKOWSKI, J. 2006. Human beta-defensins. *Cell Mol Life Sci,* 63**,** 1294-313.

PEARSON, T., GREINER, D. L. & SHULTZ, L. D. 2008. Creation of "humanized" mice to study human immunity. *Curr Protoc Immunol,* Chapter 15**,** Unit 15 21.

PENG, Z. 2005. Current status of gendicine in China: recombinant human Ad-p53 agent for treatment of cancers. *Hum Gene Ther,* 16**,** 1016-27.

PENNELLA, M. A., LIU, Y., WOO, J. L., KIM, C. A. & BERK, A. J. 2010. Adenovirus E1B 55-kilodalton protein is a p53-SUMO1 E3 ligase that represses p53 and stimulates its nuclear export through interactions with promyelocytic leukemia nuclear bodies. *J Virol,* 84**,** 12210-25.

PEREIRA, L. F., DE SOUZA, A. P., BORGES, T. J. & BONORINO, C. 2011. Impaired in vivo CD4+ T cell expansion and differentiation in aged mice is not solely due to T cell defects: decreased stimulation by aged dendritic cells. *Mech Ageing Dev,* 132**,** 187-94.

PEREZ-BERNA, A. J., MANGEL, W. F., MCGRATH, W. J., GRAZIANO, V., FLINT, J. & SAN MARTIN, C. 2014. Processing of the l1 52/55k protein by the adenovirus protease: a new substrate and new insights into virion maturation. *J Virol,* 88**,** 1513-24.

PEREZ-BERNA, A. J., MARABINI, R., SCHERES, S. H., MENENDEZ-CONEJERO, R., DMITRIEV, I. P., CURIEL, D. T., MANGEL, W. F., FLINT, S. J. & SAN MARTIN, C. 2009. Structure and uncoating of immature adenovirus. *J Mol Biol,* 392**,** 547-57.

PEREZ-ROMERO, P., GUSTIN, K. E. & IMPERIALE, M. J. 2006. Dependence of the encapsidation function of the adenovirus L1 52/55-kilodalton protein on its ability to bind the packaging sequence. *J Virol,* 80**,** 1965-71.

PEREZ-ROMERO, P., TYLER, R. E., ABEND, J. R., DUS, M. & IMPERIALE, M. J. 2005. Analysis of the interaction of the adenovirus L1 52/55-kilodalton and IVa2 proteins with the packaging sequence in vivo and in vitro. *J Virol,* 79**,** 2366-74.

PERREAU, M., WELLES, H. C., PELLATON, C., GJOKSI, B., POTIN, L., MARTIN, R., HARARI, A., BETT, A., CASIMIRO, D., GALL, J., BAROUCH, D. H., KREMER, E. J. & PANTALEO, G. 2012. The number of Toll-like receptor 9-agonist motifs in the adenovirus genome correlates with induction of dendritic cell maturation by adenovirus immune complexes. *J Virol,* 86**,** 6279-85.

PERRIO, M. J., EWEN, D., TREVETHICK, M. A., SALMON, G. P. & SHUTE, J. K. 2007. Fibrin formation by wounded bronchial epithelial cell layers in vitro is essential for normal epithelial repair and independent of plasma proteins. *Clin Exp Allergy,* 37**,** 1688-700.

PERSSON, H., MATHISEN, B., PHILIPSON, L. & PETTERSSON, U. 1979. A maturation protein in adenovirus morphogenesis. *Virology,* 93**,** 198-208.

POLLER, W., SCHNEIDER-RASP, S., LIEBERT, U., MERKLEIN, F., THALHEIMER, P., HAACK, A., SCHWAAB, R., SCHMITT, C. & BRACKMANN, H. H. 1996. Stabilization of transgene expression by incorporation of E3 region genes into an adenoviral factor IX vector and by transient anti-CD4 treatment of the host. *Gene Ther,* 3**,** 521-30.

POMBO, A., FERREIRA, J., BRIDGE, E. & CARMO-FONSECA, M. 1994. Adenovirus replication and transcription sites are spatially separated in the nucleus of infected cells. *EMBO J,* 13**,** 5075-85.

POTASH, A. E., WALLEN, T. J., KARP, P. H., ERNST, S., MONINGER, T. O., GANSEMER, N. D., STOLTZ, D. A., ZABNER, J. & CHANG, E. H. 2013. Adenoviral gene transfer corrects the ion transport defect in the sinus epithelia of a porcine CF model. *Mol Ther,* 21**,** 947-53.

PRUIJN, G. J., VAN DRIEL, W. & VAN DER VLIET, P. C. 1986. Nuclear factor III, a novel sequence-specific DNA-binding protein from HeLa cells stimulating adenovirus DNA replication. *Nature,* 322**,** 656-9.

PUNTENER, D., ENGELKE, M. F., RUZSICS, Z., STRUNZE, S., WILHELM, C. & GREBER, U. F. 2011. Stepwise loss of fluorescent core protein V from human adenovirus during entry into cells. *J Virol,* 85**,** 481-96.

PUVION-DUTILLEUL, F. & PUVION, E. 1990. Replicating single-stranded adenovirus type 5 DNA molecules accumulate within well-delimited intranuclear areas of lytically infected HeLa cells. *Eur J Cell Biol,* 52**,** 379-88.

QIAGEN. 2016. *Available at* http://www.qiagen.com [Online]. [Accessed].

QUERIDO, E., BLANCHETTE, P., YAN, Q., KAMURA, T., MORRISON, M., BOIVIN, D., KAELIN, W. G., CONAWAY, R. C., CONAWAY, J. W. & BRANTON, P. E. 2001. Degradation of p53 by adenovirus E4orf6 and E1B55K proteins occurs via a novel mechanism involving a Cullin-containing complex. *Genes Dev,* 15**,** 3104-17.

QUINONEZ, R. & SUTTON, R. E. 2002. Lentiviral vectors for gene delivery into cells. *DNA Cell Biol,* 21**,** 937-51.

RAJOTTE, D., ARAP, W., HAGEDORN, M., KOIVUNEN, E., PASQUALINI, R. & RUOSLAHTI, E. 1998. Molecular heterogeneity of the vascular endothelium revealed by in vivo phage display. *J Clin Invest,* 102**,** 430-7.

RAKI, M., SÄRKIOJA, M., DESMOND, R. A., CHEN, D. T., BÜTZOW, R., HEMMINKI, A. & KANERVA, A. 2008. Oncolytic adenovirus Ad5/3-delta24 and chemotherapy for treatment of orthotopic ovarian cancer. *Gynecol Oncol,* 108**,** 166-72.

RANCOURT, C., KEYVANI-AMINEH, H., SIRCAR, S., LABRECQUE, P. & WEBER, J. M. 1995. Proline 137 is critical for adenovirus protease encapsidation and activation but not enzyme activity. *Virology,* 209**,** 167-73.

RANCOURT, C., TIHANYI, K., BOURBONNIERE, M. & WEBER, J. M. 1994. Identification of active-site residues of the adenovirus endopeptidase. *Proc Natl Acad Sci U S A,* 91**,** 844-7.

RANKI, T., KANERVA, A., RISTIMAKI, A., HAKKARAINEN, T., SARKIOJA, M., KANGASNIEMI, L., RAKI, M., LAAKKONEN, P., GOODISON, S. & HEMMINKI, A. 2007. A heparan sulfate-targeted conditionally replicative adenovirus, Ad5.pk7-Delta24, for the treatment of advanced breast cancer. *Gene Ther,* 14**,** 58-67.

RAPER, S. E., CHIRMULE, N., LEE, F. S., WIVEL, N. A., BAGG, A., GAO, G. P., WILSON, J. M. & BATSHAW, M. L. 2003. Fatal systemic inflammatory response syndrome in a ornithine transcarbamylase deficient patient following adenoviral gene transfer. *Mol Genet Metab,* 80**,** 148-58.

RAPER, S. E., YUDKOFF, M., CHIRMULE, N., GAO, G. P., NUNES, F., HASKAL, Z. J., FURTH, E. E., PROPERT, K. J., ROBINSON, M. B., MAGOSIN, S., SIMOES, H., SPEICHER, L., HUGHES, J., TAZELAAR, J., WIVEL, N. A., WILSON, J. M. & BATSHAW, M. L. 2002. A pilot study of in vivo liver-directed gene transfer with an adenoviral vector in partial ornithine transcarbamylase deficiency. *Hum Gene Ther,* 13**,** 163-75.

RAUMA, T., TUUKKANEN, J., BERGELSON, J. M., DENNING, G. & HAUTALA, T. 1999. rab5 GTPase regulates adenovirus endocytosis. *J Virol,* 73**,** 9664-8.

RAWLINS, D. R., ROSENFELD, P. J., WIDES, R. J., CHALLBERG, M. D. & KELLY, T. J., JR. 1984. Structure and function of the adenovirus origin of replication. *Cell,* 37**,** 309-19.

REBETZ, J., NA, M., SU, C., HOLMQVIST, B., EDQVIST, A., NYBERG, C., WIDEGREN, B., SALFORD, L. G., SJOGREN, H. O., ARNBERG, N., QIAN, Q. & FAN, X. 2009. Fiber mediated receptor masking in non-infected bystander cells

restricts adenovirus cell killing effect but promotes adenovirus host co-existence. *PLoS One,* 4**,** e8484.

REDDY, V. S., NATCHIAR, S. K., STEWART, P. L. & NEMEROW, G. R. 2010. Crystal structure of human adenovirus at 3.5 A resolution. *Science,* 329**,** 1071-5.

REDDY, V. S. & NEMEROW, G. R. 2014. Structures and organization of adenovirus cement proteins provide insights into the role of capsid maturation in virus entry and infection. *Proc Natl Acad Sci U S A,* 111**,** 11715-20.

REGAD, T. & CHELBI-ALIX, M. K. 2001. Role and fate of PML nuclear bodies in response to interferon and viral infections. *Oncogene,* 20**,** 7274-86.

REICHEL, R., KOVESDI, I. & NEVINS, J. R. 1987. Developmental control of a promoter-specific factor that is also regulated by the E1A gene product. *Cell,* 48**,** 501-6.

REICHEL, R., KOVESDI, I. & NEVINS, J. R. 1988. Activation of a preexisting cellular factor as a basis for adenovirus E1A-mediated transcription control. *Proc Natl Acad Sci U S A,* 85**,** 387-90.

REIN, D. T., BREIDENBACH, M., WU, H., HAN, T., HAVIV, Y. S., WANG, M., KIRBY, T. O., KAWAKAMI, Y., DALL, P., ALVAREZ, R. D. & CURIEL, D. T. 2004. Gene transfer to cervical cancer with fiber-modified adenoviruses. *Int J Cancer,* 111**,** 698-704.

REKOSH, D. M., RUSSELL, W. C., BELLET, A. J. & ROBINSON, A. J. 1977. Identification of a protein linked to the ends of adenovirus DNA. *Cell,* 11**,** 283-95.

REYNOLDS, P., DMITRIEV, I. & CURIEL, D. 1999. Insertion of an RGD motif into the HI loop of adenovirus fiber protein alters the distribution of transgene expression of the systemically administered vector. *Gene Ther,* 6**,** 1336-9.

REZAIE, A. R. 2000. Identification of basic residues in the heparin-binding exosite of factor Xa critical for heparin and factor Va binding. *J Biol Chem,* 275**,** 3320-7.

RISTOLA, M. & LEHTONEN, S. 2014. Functions of the podocyte proteins nephrin and Neph3 and the transcriptional regulation of their genes. *Clin Sci (Lond),* 126**,** 315-28.

RITTNER, K., SCHREIBER, V., ERBS, P. & LUSKY, M. 2007. Targeting of adenovirus vectors carrying a tumor cell-specific peptide: in vitro and in vivo studies. *Cancer Gene Ther,* 14**,** 509-18.

ROBERTS, D. M., NANDA, A., HAVENGA, M. J., ABBINK, P., LYNCH, D. M., EWALD, B. A., LIU, J., THORNER, A. R., SWANSON, P. E., GORGONE, D. A., LIFTON, M. A., LEMCKERT, A. A., HOLTERMAN, L., CHEN, B., DILRAJ, A., CARVILLE, A., MANSFIELD, K. G., GOUDSMIT, J. & BAROUCH, D. H. 2006. Hexon-chimaeric adenovirus serotype 5 vectors circumvent pre-existing anti-vector immunity. *Nature,* 441**,** 239-43.

ROBERTS, M. M., WHITE, J. L., GRUTTER, M. G. & BURNETT, R. M. 1986. Three-dimensional structure of the adenovirus major coat protein hexon. *Science,* 232**,** 1148-51.

ROBINSON, M., LI, B., GE, Y., KO, D., YENDLURI, S., HARDING, T., VANROEY, M., SPINDLER, K. R. & JOOSS, K. 2009. Novel immunocompetent murine tumor model for evaluation of conditionally replication-competent (oncolytic) murine adenoviral vectors. *J Virol,* 83**,** 3450-62.

ROBINSON, M. S. 2004. Adaptable adaptors for coated vesicles. *Trends Cell Biol,* 14**,** 167-74.

RODRIGUEZ, R., SCHUUR, E. R., LIM, H. Y., HENDERSON, G. A., SIMONS, J. W. & HENDERSON, D. R. 1997. Prostate attenuated replication competent adenovirus (ARCA) CN706: a selective cytotoxic for prostate-specific antigen-positive prostate cancer cells. *Cancer Res,* 57**,** 2559-63.

ROELVINK, P. W., LIZONOVA, A., LEE, J. G., LI, Y., BERGELSON, J. M., FINBERG, R. W., BROUGH, D. E., KOVESDI, I. & WICKHAM, T. J. 1998. The

coxsackievirus-adenovirus receptor protein can function as a cellular attachment protein for adenovirus serotypes from subgroups A, C, D, E, and F. *J Virol,* 72**,** 7909-15.

ROELVINK, P. W., MI LEE, G., EINFELD, D. A., KOVESDI, I. & WICKHAM, T. J. 1999. Identification of a conserved receptor-binding site on the fiber proteins of CAR-recognizing adenoviridae. *Science,* 286**,** 1568-71.

ROGOZHIN, V. N., LOGUNOV, D. Y., SHCHEBLIAKOV, D. V., SHMAROV, M. M., KHODUNOVA, E. E., GALTSEVA, I. V., BELOUSOVA, R. V., NARODITSKY, B. S. & GINTSBURG, A. L. 2011. An Efficient Method for the Delivery of the Interleukin-2 Gene to Human Hematopoietic Cells using the Fiber-Modified Recombinant Adenovirus. *Acta Naturae,* 3**,** 100-6.

ROJAS, L. A., MORENO, R., CALDERON, H. & ALEMANY, R. 2016. Adenovirus coxsackie adenovirus receptor-mediated binding to human erythrocytes does not preclude systemic transduction. *Cancer Gene Ther,* 23**,** 411-414.

ROMANCZUK, H., GALER, C. E., ZABNER, J., BARSOMIAN, G., WADSWORTH, S. C. & O'RIORDAN, C. R. 1999. Modification of an adenoviral vector with biologically selected peptides: a novel strategy for gene delivery to cells of choice. *Hum Gene Ther,* 10**,** 2615-26.

ROSENFELD, P. J., O'NEILL, E. A., WIDES, R. J. & KELLY, T. J. 1987. Sequence-specific interactions between cellular DNA-binding proteins and the adenovirus origin of DNA replication. *Mol Cell Biol,* 7**,** 875-86.

ROSEWELL SHAW, A. & SUZUKI, M. 2016. Recent advances in oncolytic adenovirus therapies for cancer. *Curr Opin Virol,* 21**,** 9-15.

ROSS, P. J., KENNEDY, M. A., CHRISTOU, C., RISCO QUIROZ, M., POULIN, K. L. & PARKS, R. J. 2011. Assembly of helper-dependent adenovirus DNA into chromatin promotes efficient gene expression. *J Virol,* 85**,** 3950-8.

ROSSI, V., BALLY, I., ANCELET, S., XU, Y., FREMEAUX-BACCHI, V., VIVES, R. R., SADIR, R., THIELENS, N. & ARLAUD, G. J. 2010. Functional characterization of the recombinant human C1 inhibitor serpin domain: insights into heparin binding. *J Immunol,* 184**,** 4982-9.

ROUTES, J. M., RYAN, S., MORRIS, K., TAKAKI, R., CERWENKA, A. & LANIER, L. L. 2005. Adenovirus serotype 5 E1A sensitizes tumor cells to NKG2D-dependent NK cell lysis and tumor rejection. *J Exp Med,* 202**,** 1477-82.

ROWE, W. P., HUEBNER, R. J., GILMORE, L. K., PARROTT, R. H. & WARD, T. G. 1953. Isolation of a cytopathogenic agent from human adenoids undergoing spontaneous degeneration in tissue culture. *Proc Soc Exp Biol Med,* 84**,** 570-3.

ROY, S., CLAWSON, D. S., CALCEDO, R., LEBHERZ, C., SANMIGUEL, J., WU, D. & WILSON, J. M. 2005. Use of chimeric adenoviral vectors to assess capsid neutralization determinants. *Virology,* 333**,** 207-14.

ROY, S., SHIRLEY, P. S., MCCLELLAND, A. & KALEKO, M. 1998. Circumvention of immunity to the adenovirus major coat protein hexon. *J Virol,* 72**,** 6875-9.

RUGGENENTI, P., PERTICUCCI, E., CRAVEDI, P., GAMBARA, V., COSTANTINI, M., SHARMA, S. K., PERNA, A. & REMUZZI, G. 2008. Role of remission clinics in the longitudinal treatment of CKD. *J Am Soc Nephrol,* 19**,** 1213-24.

RUIGROK, R. W., BARGE, A., ALBIGES-RIZO, C. & DAYAN, S. 1990. Structure of adenovirus fibre. II. Morphology of single fibres. *J Mol Biol,* 215**,** 589-96.

RUOTSALAINEN, V., LJUNGBERG, P., WARTIOVAARA, J., LENKKERI, U., KESTILA, M., JALANKO, H., HOLMBERG, C. & TRYGGVASON, K. 1999. Nephrin is specifically located at the slit diaphragm of glomerular podocytes. *Proc Natl Acad Sci U S A,* 96**,** 7962-7.

RUSSELL, W. C. 2009. Adenoviruses: update on structure and function. *J Gen Virol,* 90**,** 1-20.

RUTKOWSKI, B. 2000. Changing pattern of end-stage renal disease in central and eastern Europe. *Nephrol Dial Transplant,* 15**,** 156-60.

RUX, J. J. & BURNETT, R. M. 2000. Type-specific epitope locations revealed by X-ray crystallographic study of adenovirus type 5 hexon. *Mol Ther,* 1**,** 18-30.

RUZINDANA-UMUNYANA, A., IMBEAULT, L. & WEBER, J. M. 2002. Substrate specificity of adenovirus protease. *Virus Res,* 89**,** 41-52.

SABAN, S. D., SILVESTRY, M., NEMEROW, G. R. & STEWART, P. L. 2006. Visualization of alpha-helices in a 6-angstrom resolution cryoelectron microscopy structure of adenovirus allows refinement of capsid protein assignments. *J Virol,* 80**,** 12049-59.

SABBATINI, P., CHIOU, S. K., RAO, L. & WHITE, E. 1995. Modulation of p53-mediated transcriptional repression and apoptosis by the adenovirus E1B 19K protein. *Mol Cell Biol,* 15**,** 1060-70.

SAKURAI, F., MIZUGUCHI, H. & HAYAKAWA, T. 2003. Efficient gene transfer into human CD34+ cells by an adenovirus type 35 vector. *Gene Ther,* 10**,** 1041-8.

SALOMONI, P. & KHELIFI, A. F. 2006. Daxx: death or survival protein? *Trends Cell Biol,* 16**,** 97-104.

SALONE, B., MARTINA, Y., PIERSANTI, S., CUNDARI, E., CHERUBINI, G., FRANQUEVILLE, L., FAILLA, C. M., BOULANGER, P. & SAGGIO, I. 2003. Integrin alpha3beta1 is an alternative cellular receptor for adenovirus serotype 5. *J Virol,* 77**,** 13448-54.

SAN MARTIN, C. 2012. Latest insights on adenovirus structure and assembly. *Viruses,* 4**,** 847-77.

SAN MARTIN, C. & BURNETT, R. M. 2003. Structural studies on adenoviruses. *Curr Top Microbiol Immunol,* 272**,** 57-94.

SAN MARTIN, C., GLASGOW, J. N., BOROVJAGIN, A., BEATTY, M. S., KASHENTSEVA, E. A., CURIEL, D. T., MARABINI, R. & DMITRIEV, I. P. 2008. Localization of the N-terminus of minor coat protein IIIa in the adenovirus capsid. *J Mol Biol,* 383**,** 923-34.

SANDOVICI, M., DEELMAN, L. E., SMIT-VAN OOSTEN, A., VAN GOOR, H., ROTS, M. G., DE ZEEUW, D. & HENNING, R. H. 2006. Enhanced transduction of fibroblasts in transplanted kidney with an adenovirus having an RGD motif in the HI loop. *Kidney Int,* 69**,** 45-52.

SAONCELLA, S., ECHTERMEYER, F., DENHEZ, F., NOWLEN, J. K., MOSHER, D. F., ROBINSON, S. D., HYNES, R. O. & GOETINCK, P. F. 1999. Syndecan-4 signals cooperatively with integrins in a Rho-dependent manner in the assembly of focal adhesions and actin stress fibers. *Proc Natl Acad Sci U S A,* 96**,** 2805-10.

SAPHIRE, A. C., GUAN, T., SCHIRMER, E. C., NEMEROW, G. R. & GERACE, L. 2000. Nuclear import of adenovirus DNA in vitro involves the nuclear protein import pathway and hsc70. *J Biol Chem,* 275**,** 4298-304.

SARRAZIN, S., LAMANNA, W. C. & ESKO, J. D. 2011. Heparan sulfate proteoglycans. *Cold Spring Harb Perspect Biol,* 3.

SARRAZIN, S., WILSON, B., SLY, W. S., TOR, Y. & ESKO, J. D. 2010. Guanidinylated neomycin mediates heparan sulfate-dependent transport of active enzymes to lysosomes. *Mol Ther,* 18**,** 1268-74.

SCHALLER, M., HOGABOAM, C. M., LUKACS, N. & KUNKEL, S. L. 2006. Respiratory viral infections drive chemokine expression and exacerbate the asthmatic response. *J Allergy Clin Immunol,* 118**,** 295-302; quiz 303-4.

SCHMID, M., GONZALEZ, R. A. & DOBNER, T. 2012. CRM1-dependent transport supports cytoplasmic accumulation of adenoviral early transcripts. *J Virol,* 86**,** 2282-92.

SCHOEHN, G., EL BAKKOURI, M., FABRY, C. M., BILLET, O., ESTROZI, L. F., LE, L., CURIEL, D. T., KAJAVA, A. V., RUIGROK, R. W. & KREMER, E. J. 2008.

Three-dimensional structure of canine adenovirus serotype 2 capsid. *J Virol,* 82**,** 3192-203.

SCHREINER, S., KINKLEY, S., BURCK, C., MUND, A., WIMMER, P., SCHUBERT, T., GROITL, P., WILL, H. & DOBNER, T. 2013. SPOC1-mediated antiviral host cell response is antagonized early in human adenovirus type 5 infection. *PLoS Pathog,* 9**,** e1003775.

SCHREINER, S., MARTINEZ, R., GROITL, P., RAYNE, F., VAILLANT, R., WIMMER, P., BOSSIS, G., STERNSDORF, T., MARCINOWSKI, L., RUZSICS, Z., DOBNER, T. & WODRICH, H. 2012. Transcriptional activation of the adenoviral genome is mediated by capsid protein VI. *PLoS Pathog,* 8**,** e1002549.

SCHREINER, S., WIMMER, P., SIRMA, H., EVERETT, R. D., BLANCHETTE, P., GROITL, P. & DOBNER, T. 2010. Proteasome-dependent degradation of Daxx by the viral E1B-55K protein in human adenovirus-infected cells. *J Virol,* 84**,** 7029-38.

SCHULTE, M., SORKIN, M., AL-BENNA, S., STUPKA, J., HIRSCH, T., DAIGELER, A., KESTING, M. R., STEINAU, H. U., JACOBSEN, F. & STEINSTRAESSER, L. 2013. Innate immune response after adenoviral gene delivery into skin is mediated by AIM2, NALP3, DAI and mda5. *Springerplus,* 2**,** 234.

SCHUMACHER, L., RIBAS, A., DISSETTE, V. B., MCBRIDE, W. H., MUKHERJI, B., ECONOMOU, J. S. & BUTTERFIELD, L. H. 2004. Human dendritic cell maturation by adenovirus transduction enhances tumor antigen-specific T-cell responses. *J Immunother,* 27**,** 191-200.

SEGURA, M. M., ALBA, R., BOSCH, A. & CHILLON, M. 2008. Advances in helper-dependent adenoviral vector research. *Curr Gene Ther,* 8**,** 222-35.

SEIRADAKE, E., HENAFF, D., WODRICH, H., BILLET, O., PERREAU, M., HIPPERT, C., MENNECHET, F., SCHOEHN, G., LORTAT-JACOB, H., DREJA, H., IBANES, S., KALATZIS, V., WANG, J. P., FINBERG, R. W., CUSACK, S. & KREMER, E. J. 2009. The cell adhesion molecule "CAR" and sialic acid on human erythrocytes influence adenovirus in vivo biodistribution. *PLoS Pathog,* 5**,** e1000277.

SEKIYA, K., SATOH, R., DANBARA, H. & FUTAESAKU, Y. 1993. A ring-shaped structure with a crown formed by streptolysin O on the erythrocyte membrane. *J Bacteriol,* 175**,** 5953-61.

SELSTED, M. E. & OUELLETTE, A. J. 2005. Mammalian defensins in the antimicrobial immune response. *Nat Immunol,* 6**,** 551-7.

SESHIDHAR REDDY, P., GANESH, S., LIMBACH, M. P., BRANN, T., PINKSTAFF, A., KALOSS, M., KALEKO, M. & CONNELLY, S. 2003. Development of adenovirus serotype 35 as a gene transfer vector. *Virology,* 311**,** 384-93.

SHARMA, A., BANGARI, D. S., TANDON, M., PANDEY, A., HOGENESCH, H. & MITTAL, S. K. 2009a. Comparative analysis of vector biodistribution, persistence and gene expression following intravenous delivery of bovine, porcine and human adenoviral vectors in a mouse model. *Virology,* 386**,** 44-54.

SHARMA, A., LI, X., BANGARI, D. S. & MITTAL, S. K. 2009b. Adenovirus receptors and their implications in gene delivery. *Virus Res,* 143**,** 184-94.

SHASHKOVA, E. V., CHERENOVA, L. V., KAZANSKY, D. B. & DORONIN, K. 2005. Avian adenovirus vector CELO-TK displays anticancer activity in human cancer cells and suppresses established murine melanoma tumors. *Cancer Gene Ther,* 12**,** 617-26.

SHASHKOVA, E. V., MAY, S. M., DORONIN, K. & BARRY, M. A. 2009. Expanded anticancer therapeutic window of hexon-modified oncolytic adenovirus. *Mol Ther,* 17**,** 2121-30.

SHAW, C. A., HOLLAND, P. C., SINNREICH, M., ALLEN, C., SOLLERBRANT, K., KARPATI, G. & NALBANTOGLU, J. 2004. Isoform-specific expression of the

Coxsackie and adenovirus receptor (CAR) in neuromuscular junction and cardiac intercalated discs. *BMC Cell Biol,* 5**,** 42.

SHAYAKHMETOV, D. M., EBERLY, A. M., LI, Z. Y. & LIEBER, A. 2005a. Deletion of penton RGD motifs affects the efficiency of both the internalization and the endosome escape of viral particles containing adenovirus serotype 5 or 35 fiber knobs. *J Virol,* 79**,** 1053-61.

SHAYAKHMETOV, D. M., GAGGAR, A., NI, S., LI, Z. Y. & LIEBER, A. 2005b. Adenovirus binding to blood factors results in liver cell infection and hepatotoxicity. *J Virol,* 79**,** 7478-91.

SHAYAKHMETOV, D. M., LI, Z. Y., GAGGAR, A., GHARWAN, H., TERNOVOI, V., SANDIG, V. & LIEBER, A. 2004a. Genome size and structure determine efficiency of postinternalization steps and gene transfer of capsid-modified adenovirus vectors in a cell-type-specific manner. *J Virol,* 78**,** 10009-22.

SHAYAKHMETOV, D. M., LI, Z. Y., NI, S. & LIEBER, A. 2004b. Analysis of adenovirus sequestration in the liver, transduction of hepatic cells, and innate toxicity after injection of fiber-modified vectors. *J Virol,* 78**,** 5368-81.

SHAYAKHMETOV, D. M., LI, Z. Y., TERNOVOI, V., GAGGAR, A., GHARWAN, H. & LIEBER, A. 2003. The interaction between the fiber knob domain and the cellular attachment receptor determines the intracellular trafficking route of adenoviruses. *J Virol,* 77**,** 3712-23.

SHAYAKHMETOV, D. M., PAPAYANNOPOULOU, T., STAMATOYANNOPOULOS, G. & LIEBER, A. 2000. Efficient gene transfer into human CD34(+) cells by a retargeted adenovirus vector. *J Virol,* 74**,** 2567-83.

SHIELDS, A. F., HACKMAN, R. C., FIFE, K. H., COREY, L. & MEYERS, J. D. 1985. Adenovirus infections in patients undergoing bone-marrow transplantation. *N Engl J Med,* 312**,** 529-33.

SHIMIZU, T., ICHIHARA, M., YOSHIOKA, Y., ISHIDA, T., NAKAGAWA, S. & KIWADA, H. 2012. Intravenous administration of polyethylene glycol-coated (PEGylated) proteins and PEGylated adenovirus elicits an anti-PEG immunoglobulin M response. *Biol Pharm Bull,* 35**,** 1336-42.

SHINKAI, Y., RATHBUN, G., LAM, K. P., OLTZ, E. M., STEWART, V., MENDELSOHN, M., CHARRON, J., DATTA, M., YOUNG, F., STALL, A. M. & ET AL. 1992. RAG-2-deficient mice lack mature lymphocytes owing to inability to initiate V(D)J rearrangement. *Cell,* 68**,** 855-67.

SHIRATSUCHI, T., RAI, U., KRAUSE, A., WORGALL, S. & TSUJI, M. 2010. Replacing adenoviral vector HVR1 with a malaria B cell epitope improves immunogenicity and circumvents preexisting immunity to adenovirus in mice. *J Clin Invest,* 120**,** 3688-701.

SHULTZ, L. D., ISHIKAWA, F. & GREINER, D. L. 2007. Humanized mice in translational biomedical research. *Nat Rev Immunol,* 7**,** 118-30.

SHULTZ, L. D., LYONS, B. L., BURZENSKI, L. M., GOTT, B., CHEN, X., CHALEFF, S., KOTB, M., GILLIES, S. D., KING, M., MANGADA, J., GREINER, D. L. & HANDGRETINGER, R. 2005. Human lymphoid and myeloid cell development in NOD/LtSz-scid IL2R gamma null mice engrafted with mobilized human hemopoietic stem cells. *J Immunol,* 174**,** 6477-89.

SHULTZ, L. D., SCHWEITZER, P. A., CHRISTIANSON, S. W., GOTT, B., SCHWEITZER, I. B., TENNENT, B., MCKENNA, S., MOBRAATEN, L., RAJAN, T. V., GREINER, D. L. & ET AL. 1995. Multiple defects in innate and adaptive immunologic function in NOD/LtSz-scid mice. *J Immunol,* 154**,** 180-91.

SILVESTRY, M., LINDERT, S., SMITH, J. G., MAIER, O., WIETHOFF, C. M., NEMEROW, G. R. & STEWART, P. L. 2009. Cryo-electron microscopy structure of adenovirus type 2 temperature-sensitive mutant 1 reveals insight into the cell entry defect. *J Virol,* 83**,** 7375-83.

SIMONSEN, A., WURMSER, A. E., EMR, S. D. & STENMARK, H. 2001. The role of phosphoinositides in membrane transport. *Curr Opin Cell Biol,* 13**,** 485-92.

SMITH, A. C., POULIN, K. L. & PARKS, R. J. 2009. DNA genome size affects the stability of the adenovirus virion. *J Virol,* 83**,** 2025-8.

SMITH, J. G. & NEMEROW, G. R. 2008. Mechanism of adenovirus neutralization by Human alpha-defensins. *Cell Host Microbe,* 3**,** 11-9.

SMITH, J. G., SILVESTRY, M., LINDERT, S., LU, W., NEMEROW, G. R. & STEWART, P. L. 2010. Insight into the mechanisms of adenovirus capsid disassembly from studies of defensin neutralization. *PLoS Pathog,* 6**,** e1000959.

SMITH, J. S., XU, Z., TIAN, J., STEVENSON, S. C. & BYRNES, A. P. 2008. Interaction of systemically delivered adenovirus vectors with Kupffer cells in mouse liver. *Hum Gene Ther,* 19**,** 547-54.

SMITH, T., IDAMAKANTI, N., KYLEFJORD, H., ROLLENCE, M., KING, L., KALOSS, M., KALEKO, M. & STEVENSON, S. C. 2002. In vivo hepatic adenoviral gene delivery occurs independently of the coxsackievirus-adenovirus receptor. *Mol Ther,* 5**,** 770-9.

SMITH, T. A., IDAMAKANTI, N., MARSHALL-NEFF, J., ROLLENCE, M. L., WRIGHT, P., KALOSS, M., KING, L., MECH, C., DINGES, L., IVERSON, W. O., SHERER, A. D., MARKOVITS, J. E., LYONS, R. M., KALEKO, M. & STEVENSON, S. C. 2003a. Receptor interactions involved in adenoviral-mediated gene delivery after systemic administration in non-human primates. *Hum Gene Ther,* 14**,** 1595-604.

SMITH, T. A., IDAMAKANTI, N., ROLLENCE, M. L., MARSHALL-NEFF, J., KIM, J., MULGREW, K., NEMEROW, G. R., KALEKO, M. & STEVENSON, S. C. 2003b. Adenovirus serotype 5 fiber shaft influences in vivo gene transfer in mice. *Hum Gene Ther,* 14**,** 777-87.

SNIJDER, J., REDDY, V. S., MAY, E. R., ROOS, W. H., NEMEROW, G. R. & WUITE, G. J. 2013. Integrin and defensin modulate the mechanical properties of adenovirus. *J Virol,* 87**,** 2756-66.

SOHN, S. Y. & HEARING, P. 2012. Adenovirus regulates sumoylation of Mre11-Rad50-Nbs1 components through a paralog-specific mechanism. *J Virol,* 86**,** 9656-65.

SOMIA, N. & VERMA, I. M. 2000. Gene therapy: trials and tribulations. *Nat Rev Genet,* 1**,** 91-9.

SORIA, C., ESTERMANN, F. E., ESPANTMAN, K. C. & O'SHEA, C. C. 2010. Heterochromatin silencing of p53 target genes by a small viral protein. *Nature,* 466**,** 1076-81.

SPITKOVSKY, D., JANSEN-DURR, P., KARSENTI, E. & HOFFMAN, I. 1996. S-phase induction by adenovirus E1A requires activation of cdc25a tyrosine phosphatase. *Oncogene,* 12**,** 2549-54.

STABA, M. J., WICKHAM, T. J., KOVESDI, I. & HALLAHAN, D. E. 2000. Modifications of the fiber in adenovirus vectors increase tropism for malignant glioma models. *Cancer Gene Ther,* 7**,** 13-9.

STADLER, M., CHELBI-ALIX, M. K., KOKEN, M. H., VENTURINI, L., LEE, C., SAIB, A., QUIGNON, F., PELICANO, L., GUILLEMIN, M. C., SCHINDLER, C. & ET AL. 1995. Transcriptional induction of the PML growth suppressor gene by interferons is mediated through an ISRE and a GAS element. *Oncogene,* 11**,** 2565-73.

STEIN, S. C. & FALCK-PEDERSEN, E. 2012. Sensing adenovirus infection: activation of interferon regulatory factor 3 in RAW 264.7 cells. *J Virol,* 86**,** 4527-37.

STEINSTRAESSER, L., SORKIN, M., JACOBSEN, F., AL-BENNA, S., KESTING, M. R., NIEDERBICHLER, A. D., OTTE, J. M., HIRSCH, T., STUPKA, J., STEINAU, H. U. & SCHULTE, M. 2011. Evaluation of signal transduction pathways after transient cutaneous adenoviral gene delivery. *BMC Immunol,* 12**,** 8.

STEPHEN, S. L., MONTINI, E., SIVANANDAM, V. G., AL-DHALIMY, M., KESTLER, H. A., FINEGOLD, M., GROMPE, M. & KOCHANEK, S. 2010. Chromosomal integration of adenoviral vector DNA in vivo. *J Virol,* 84**,** 9987-94.

STEPHEN, S. L., SIVANANDAM, V. G. & KOCHANEK, S. 2008. Homologous and heterologous recombination between adenovirus vector DNA and chromosomal DNA. *J Gene Med,* 10**,** 1176-89.

STEVENSON, M., HALE, A. B., HALE, S. J., GREEN, N. K., BLACK, G., FISHER, K. D., ULBRICH, K., FABRA, A. & SEYMOUR, L. W. 2007. Incorporation of a laminin-derived peptide (SIKVAV) on polymer-modified adenovirus permits tumor-specific targeting via alpha6-integrins. *Cancer Gene Ther,* 14**,** 335-45.

STEWART, A. R., TOLLEFSON, A. E., KRAJCSI, P., YEI, S. P. & WOLD, W. S. 1995. The adenovirus E3 10.4K and 14.5K proteins, which function to prevent cytolysis by tumor necrosis factor and to down-regulate the epidermal growth factor receptor, are localized in the plasma membrane. *J Virol,* 69**,** 172-81.

STEWART, P. L., BURNETT, R. M., CYRKLAFF, M. & FULLER, S. D. 1991. Image reconstruction reveals the complex molecular organization of adenovirus. *Cell,* 67**,** 145-54.

STEWART, P. L., FULLER, S. D. & BURNETT, R. M. 1993. Difference imaging of adenovirus: bridging the resolution gap between X-ray crystallography and electron microscopy. *EMBO J,* 12**,** 2589-99.

STILLMAN, B. 1989. Initiation of eukaryotic DNA replication in vitro. *Annu Rev Cell Biol,* 5**,** 197-245.

STILWELL, J. L. & SAMULSKI, R. J. 2004. Role of viral vectors and virion shells in cellular gene expression. *Mol Ther,* 9**,** 337-46.

STONE, D., LIU, Y., SHAYAKHMETOV, D., LI, Z. Y., NI, S. & LIEBER, A. 2007. Adenovirus-platelet interaction in blood causes virus sequestration to the reticuloendothelial system of the liver. *J Virol,* 81**,** 4866-71.

STONE, D., NI, S., LI, Z. Y., GAGGAR, A., DIPAOLO, N., FENG, Q., SANDIG, V. & LIEBER, A. 2005. Development and assessment of human adenovirus type 11 as a gene transfer vector. *J Virol,* 79**,** 5090-104.

STRACKER, T. H., CARSON, C. T. & WEITZMAN, M. D. 2002. Adenovirus oncoproteins inactivate the Mre11-Rad50-NBS1 DNA repair complex. *Nature,* 418**,** 348-52.

STRACKER, T. H., LEE, D. V., CARSON, C. T., ARAUJO, F. D., ORNELLES, D. A. & WEITZMAN, M. D. 2005. Serotype-specific reorganization of the Mre11 complex by adenoviral E4orf3 proteins. *J Virol,* 79**,** 6664-73.

STRUNZE, S., ENGELKE, M. F., WANG, I. H., PUNTENER, D., BOUCKE, K., SCHLEICH, S., WAY, M., SCHOENENBERGER, P., BURCKHARDT, C. J. & GREBER, U. F. 2011. Kinesin-1-mediated capsid disassembly and disruption of the nuclear pore complex promote virus infection. *Cell Host Microbe,* 10**,** 210-23.

STRUNZE, S., TROTMAN, L. C., BOUCKE, K. & GREBER, U. F. 2005. Nuclear targeting of adenovirus type 2 requires CRM1-mediated nuclear export. *Mol Biol Cell,* 16**,** 2999-3009.

STUIVER, M. H. & VAN DER VLIET, P. C. 1990. Adenovirus DNA-binding protein forms a multimeric protein complex with double-stranded DNA and enhances binding of nuclear factor I. *J Virol,* 64**,** 379-86.

SUMIDA, S. M., TRUITT, D. M., LEMCKERT, A. A., VOGELS, R., CUSTERS, J. H., ADDO, M. M., LOCKMAN, S., PETER, T., PEYERL, F. W., KISHKO, M. G., JACKSON, S. S., GORGONE, D. A., LIFTON, M. A., ESSEX, M., WALKER, B. D., GOUDSMIT, J., HAVENGA, M. J. & BAROUCH, D. H. 2005. Neutralizing antibodies to adenovirus serotype 5 vaccine vectors are directed primarily against the adenovirus hexon protein. *J Immunol,* 174**,** 7179-85.

SUN, Y., JIANG, X., XU, Y., AYRAPETOV, M. K., MOREAU, L. A., WHETSTINE, J. R. & PRICE, B. D. 2009. Histone H3 methylation links DNA damage detection to activation of the tumour suppressor Tip60. *Nat Cell Biol,* 11**,** 1376-82.

SUNDARARAJAN, R. & WHITE, E. 2001. E1B 19K blocks Bax oligomerization and tumor necrosis factor alpha-mediated apoptosis. *J Virol,* 75**,** 7506-16.

SUNG, R. S., QIN, L. & BROMBERG, J. S. 2001. TNFalpha and IFNgamma induced by innate anti-adenoviral immune responses inhibit adenovirus-mediated transgene expression. *Mol Ther,* 3**,** 757-67.

SUOMALAINEN, M., LUISONI, S., BOUCKE, K., BIANCHI, S., ENGEL, D. A. & GREBER, U. F. 2013. A direct and versatile assay measuring membrane penetration of adenovirus in single cells. *J Virol,* 87**,** 12367-79.

SUOMALAINEN, M., NAKANO, M. Y., BOUCKE, K., KELLER, S. & GREBER, U. F. 2001. Adenovirus-activated PKA and p38/MAPK pathways boost microtubule-mediated nuclear targeting of virus. *EMBO J,* 20**,** 1310-9.

SUOMALAINEN, M., NAKANO, M. Y., KELLER, S., BOUCKE, K., STIDWILL, R. P. & GREBER, U. F. 1999. Microtubule-dependent plus- and minus end-directed motilities are competing processes for nuclear targeting of adenovirus. *J Cell Biol,* 144**,** 657-72.

SUZUKI, T., SAKURAI, F., NAKAMURA, S., KOUYAMA, E., KAWABATA, K., KONDOH, M., YAGI, K. & MIZUGUCHI, H. 2008. miR-122a-regulated expression of a suicide gene prevents hepatotoxicity without altering antitumor effects in suicide gene therapy. *Mol Ther,* 16**,** 1719-26.

TAMANINI, A., NICOLIS, E., BONIZZATO, A., BEZZERRI, V., MELOTTI, P., ASSAEL, B. M. & CABRINI, G. 2006. Interaction of adenovirus type 5 fiber with the coxsackievirus and adenovirus receptor activates inflammatory response in human respiratory cells. *J Virol,* 80**,** 11241-54.

TAMANOI, F. & STILLMAN, B. W. 1983. Initiation of adenovirus DNA replication in vitro requires a specific DNA sequence. *Proc Natl Acad Sci U S A,* 80**,** 6446-50.

TANDON, M., SHARMA, A., VEMULA, S. V., BANGARI, D. S. & MITTAL, S. K. 2012. Sequential administration of bovine and human adenovirus vectors to overcome vector immunity in an immunocompetent mouse model of breast cancer. *Virus Res,* 163**,** 202-11.

TANG, J., OLIVE, M., PULMANAUSAHAKUL, R., SCHNELL, M., FLOMENBERG, N., EISENLOHR, L. & FLOMENBERG, P. 2006. Human CD8+ cytotoxic T cell responses to adenovirus capsid proteins. *Virology,* 350**,** 312-22.

TAO, N., GAO, G. P., PARR, M., JOHNSTON, J., BARADET, T., WILSON, J. M., BARSOUM, J. & FAWELL, S. E. 2001. Sequestration of adenoviral vector by Kupffer cells leads to a nonlinear dose response of transduction in liver. *Mol Ther,* 3**,** 28-35.

TARASSISHIN, L., SZAWLOWSKI, P., KIDD, A. H. & RUSSELL, W. C. 2000. An epitope on the adenovirus fibre tail is common to all human subgroups. *Arch Virol,* 145**,** 805-11.

TAVALAI, N., PAPIOR, P., RECHTER, S. & STAMMINGER, T. 2008. Nuclear domain 10 components promyelocytic leukemia protein and hDaxx independently contribute to an intrinsic antiviral defense against human cytomegalovirus infection. *J Virol,* 82**,** 126-37.

TAYLOR, P. R., NASH, J. T., THEODORIDIS, E., BYGRAVE, A. E., WALPORT, M. J. & BOTTO, M. 1998. A targeted disruption of the murine complement factor B gene resulting in loss of expression of three genes in close proximity, factor B, C2, and D17H6S45. *J Biol Chem,* 273**,** 1699-704.

TEIGLER, J. E., KAGAN, J. C. & BAROUCH, D. H. 2014. Late endosomal trafficking of alternative serotype adenovirus vaccine vectors augments antiviral innate immunity. *J Virol,* 88**,** 10354-63.

TEODORO, J. G. & BRANTON, P. E. 1997. Regulation of p53-dependent apoptosis, transcriptional repression, and cell transformation by phosphorylation of the 55-kilodalton E1B protein of human adenovirus type 5. *J Virol,* 71**,** 3620-7.

THE JOURNAL OF GENE MEDICINE: CLINICAL TRIAL. 2016. *The Journal of Gene Medicine: Clinical Trial. Available at:* http://www.wiley.com//legacy/wileychi/genmed/clinical/ [Online]. [Accessed].

THOELEN, I., MAGNUSSON, C., TAGERUD, S., POLACEK, C., LINDBERG, M. & VAN RANST, M. 2001. Identification of alternative splice products encoded by the human coxsackie-adenovirus receptor gene. *Biochem Biophys Res Commun,* 287**,** 216-22.

THORNER, A. R., VOGELS, R., KASPERS, J., WEVERLING, G. J., HOLTERMAN, L., LEMCKERT, A. A., DILRAJ, A., MCNALLY, L. M., JEENA, P. M., JEPSEN, S., ABBINK, P., NANDA, A., SWANSON, P. E., BATES, A. T., O'BRIEN, K. L., HAVENGA, M. J., GOUDSMIT, J. & BAROUCH, D. H. 2006. Age dependence of adenovirus-specific neutralizing antibody titers in individuals from sub-Saharan Africa. *J Clin Microbiol,* 44**,** 3781-3.

TIAN, J., XU, Z., SMITH, J. S., HOFHERR, S. E., BARRY, M. A. & BYRNES, A. P. 2009. Adenovirus activates complement by distinctly different mechanisms in vitro and in vivo: indirect complement activation by virions in vivo. *J Virol,* 83**,** 5648-58.

TIBBETTS, C. 1977. Physical organization of subgroup B human adenovirus genomes. *J Virol,* 24**,** 564-79.

TIBBLES, L. A., SPURRELL, J. C., BOWEN, G. P., LIU, Q., LAM, M., ZAISS, A. K., ROBBINS, S. M., HOLLENBERG, M. D., WICKHAM, T. J. & MURUVE, D. A. 2002. Activation of p38 and ERK signaling during adenovirus vector cell entry lead to expression of the C-X-C chemokine IP-10. *J Virol,* 76**,** 1559-68.

TILLOU, X., POIRIER, N., LE BAS-BERNARDET, S., HERVOUET, J., MINAULT, D., RENAUDIN, K., VISTOLI, F., KARAM, G., DAHA, M., SOULILLOU, J. P. & BLANCHO, G. 2010. Recombinant human C1-inhibitor prevents acute antibody-mediated rejection in alloimmunized baboons. *Kidney Int,* 78**,** 152-9.

TKACHENKO, E., LUTGENS, E., STAN, R. V. & SIMONS, M. 2004. Fibroblast growth factor 2 endocytosis in endothelial cells proceed via syndecan-4-dependent activation of Rac1 and a Cdc42-dependent macropinocytic pathway. *J Cell Sci,* 117**,** 3189-99.

TOLLEFSON, A. E., HERMISTON, T. W., LICHTENSTEIN, D. L., COLLE, C. F., TRIPP, R. A., DIMITROV, T., TOTH, K., WELLS, C. E., DOHERTY, P. C. & WOLD, W. S. 1998. Forced degradation of Fas inhibits apoptosis in adenovirus-infected cells. *Nature,* 392**,** 726-30.

TOLLEFSON, A. E., RYERSE, J. S., SCARIA, A., HERMISTON, T. W. & WOLD, W. S. 1996a. The E3-11.6-kDa adenovirus death protein (ADP) is required for efficient cell death: characterization of cells infected with adp mutants. *Virology,* 220**,** 152-62.

TOLLEFSON, A. E., SCARIA, A., HERMISTON, T. W., RYERSE, J. S., WOLD, L. J. & WOLD, W. S. 1996b. The adenovirus death protein (E3-11.6K) is required at very late stages of infection for efficient cell lysis and release of adenovirus from infected cells. *J Virol,* 70**,** 2296-306.

TOLLEFSON, A. E., STEWART, A. R., YEI, S. P., SAHA, S. K. & WOLD, W. S. 1991. The 10,400- and 14,500-dalton proteins encoded by region E3 of adenovirus form a complex and function together to down-regulate the epidermal growth factor receptor. *J Virol,* 65**,** 3095-105.

TOLLEFSON, A. E., YING, B., DORONIN, K., SIDOR, P. D. & WOLD, W. S. 2007. Identification of a new human adenovirus protein encoded by a novel late l-strand transcription unit. *J Virol,* 81**,** 12918-26.

TOMASEC, P., WANG, E. C., GROH, V., SPIES, T., MCSHARRY, B. P., AICHELER, R. J., STANTON, R. J. & WILKINSON, G. W. 2007. Adenovirus vector delivery stimulates natural killer cell recognition. *J Gen Virol,* 88**,** 1103-8.

TOMKO, R. P., XU, R. & PHILIPSON, L. 1997. HCAR and MCAR: the human and mouse cellular receptors for subgroup C adenoviruses and group B coxsackieviruses. *Proc Natl Acad Sci U S A,* 94**,** 3352-6.

TOYOMURA, K., FUJIMURA, T., MURAKAMI, H., NATSUME, T., SHIGEHISA, T., INOUE, N., TAKEDA, J. & KINOSHITA, T. 1997. Molecular cloning of a pig homologue of membrane cofactor protein (CD46). *Int Immunol,* 9**,** 869-76.

TRADTRANTIP, L., ASAVAPANUMAS, N., PHUAN, P. W. & VERKMAN, A. S. 2014. Potential therapeutic benefit of C1-esterase inhibitor in neuromyelitis optica evaluated in vitro and in an experimental rat model. *PLoS One,* 9**,** e106824.

TRAN, L., OUISSE, L. H., RICHARD-FIARDO, P., FRANKEN, P. R., DARCOURT, J., CORNILLEAU, G., BENIHOUD, K. & VASSAUX, G. 2013. Adrenal gland infection by serotype 5 adenovirus requires coagulation factors. *PLoS One,* 8**,** e62191.

TREMBLAY, M. L., DERY, C. V., TALBOT, B. G. & WEBER, J. 1983. In vitro cleavage specificity of the adenovirus type 2 proteinase. *Biochim Biophys Acta,* 743**,** 239-45.

TRIBOULEY, C., LUTZ, P., STAUB, A. & KEDINGER, C. 1994. The product of the adenovirus intermediate gene IVa2 is a transcriptional activator of the major late promoter. *J Virol,* 68**,** 4450-7.

TRINH, H. V., LESAGE, G., CHENNAMPARAMPIL, V., VOLLENWEIDER, B., BURCKHARDT, C. J., SCHAUER, S., HAVENGA, M., GREBER, U. F. & HEMMI, S. 2012. Avidity binding of human adenovirus serotypes 3 and 7 to the membrane cofactor CD46 triggers infection. *J Virol,* 86**,** 1623-37.

TROTMAN, L. C., MOSBERGER, N., FORNEROD, M., STIDWILL, R. P. & GREBER, U. F. 2001. Import of adenovirus DNA involves the nuclear pore complex receptor CAN/Nup214 and histone H1. *Nat Cell Biol,* 3**,** 1092-100.

TSUJIMURA, A., SHIDA, K., KITAMURA, M., NOMURA, M., TAKEDA, J., TANAKA, H., MATSUMOTO, M., MATSUMIYA, K., OKUYAMA, A., NISHIMUNE, Y., OKABE, M. & SEYA, T. 1998. Molecular cloning of a murine homologue of membrane cofactor protein (CD46): preferential expression in testicular germ cells. *Biochem J,* 330 (Pt 1)**,** 163-8.

TUVE, S., WANG, H., JACOBS, J. D., YUMUL, R. C., SMITH, D. F. & LIEBER, A. 2008. Role of cellular heparan sulfate proteoglycans in infection of human adenovirus serotype 3 and 35. *PLoS Pathog,* 4**,** e1000189.

TUVE, S., WANG, H., WARE, C., LIU, Y., GAGGAR, A., BERNT, K., SHAYAKHMETOV, D., LI, Z., STRAUSS, R., STONE, D. & LIEBER, A. 2006. A new group B adenovirus receptor is expressed at high levels on human stem and tumor cells. *J Virol,* 80**,** 12109-20.

TWETEN, R. K. 2005. Cholesterol-dependent cytolysins, a family of versatile pore-forming toxins. *Infect Immun,* 73**,** 6199-209.

UGAI, H., DOBBINS, G. C., WANG, M., LE, L. P., MATTHEWS, D. A. & CURIEL, D. T. 2012. Adenoviral protein V promotes a process of viral assembly through nucleophosmin 1. *Virology,* 432**,** 283-95.

UHLEN, M., GUSS, B., NILSSON, B., GATENBECK, S., PHILIPSON, L. & LINDBERG, M. 1984. Complete sequence of the staphylococcal gene encoding protein A. A gene evolved through multiple duplications. *J Biol Chem,* 259**,** 1695-702.

UHRIG, S., COUTELLE, O., WIEHE, T., PERABO, L., HALLEK, M. & BUNING, H. 2012. Successful target cell transduction of capsid-engineered rAAV vectors requires clathrin-dependent endocytosis. *Gene Ther,* 19**,** 210-8.

ULASOV, I. V., RIVERA, A. A., HAN, Y., CURIEL, D. T., ZHU, Z. B. & LESNIAK, M. S. 2007. Targeting adenovirus to CD80 and CD86 receptors increases gene transfer efficiency to malignant glioma cells. *J Neurosurg,* 107**,** 617-27.

UUSI-KERTTULA, H., DAVIES, J., COUGHLAN, L., HULIN-CURTIS, S., JONES, R., HANNA, L., CHESTER, J. D. & PARKER, A. L. 2016. Pseudotyped alphavbeta6 integrin-targeted adenovirus vectors for ovarian cancer therapies. *Oncotarget*.

VAN DER VELDE, M., MATSUSHITA, K., CORESH, J., ASTOR, B. C., WOODWARD, M., LEVEY, A., DE JONG, P., GANSEVOORT, R. T., CHRONIC KIDNEY DISEASE PROGNOSIS, C., VAN DER VELDE, M., MATSUSHITA, K., CORESH, J., ASTOR, B. C., WOODWARD, M., LEVEY, A. S., DE JONG, P. E., GANSEVOORT, R. T., LEVEY, A., EL-NAHAS, M., ECKARDT, K. U., KASISKE, B. L., NINOMIYA, T., CHALMERS, J., MACMAHON, S., TONELLI, M., HEMMELGARN, B., SACKS, F., CURHAN, G., COLLINS, A. J., LI, S., CHEN, S. C., HAWAII COHORT, K. P., LEE, B. J., ISHANI, A., NEATON, J., SVENDSEN, K., MANN, J. F., YUSUF, S., TEO, K. K., GAO, P., NELSON, R. G., KNOWLER, W. C., BILO, H. J., JOOSTEN, H., KLEEFSTRA, N., GROENIER, K. H., AUGUSTE, P., VELDHUIS, K., WANG, Y., CAMARATA, L., THOMAS, B. & MANLEY, T. 2011. Lower estimated glomerular filtration rate and higher albuminuria are associated with all-cause and cardiovascular mortality. A collaborative meta-analysis of high-risk population cohorts. *Kidney Int,* 79**,** 1341-52.

VAN DER VLIET, P. C., KEEGSTRA, W. & JANSZ, H. S. 1978. Complex formation between the adenovirus type 5 DNA-binding protein and single-stranded DNA. *Eur J Biochem,* 86**,** 389-98.

VAN GEER, M. A., BAKKER, C. T., KOIZUMI, N., MIZUGUCHI, H., WESSELING, J. G., OUDE ELFERINK, R. P. & BOSMA, P. J. 2009. Ephrin A2 receptor targeting does not increase adenoviral pancreatic cancer transduction in vivo. *World J Gastroenterol,* 15**,** 2754-62.

VAN OOSTRUM, J. & BURNETT, R. M. 1985. Molecular composition of the adenovirus type 2 virion. *J Virol,* 56**,** 439-48.

VAN RAAIJ, M. J., MITRAKI, A., LAVIGNE, G. & CUSACK, S. 1999. A triple beta-spiral in the adenovirus fibre shaft reveals a new structural motif for a fibrous protein. *Nature,* 401**,** 935-8.

VAN ROOIJEN, N. & VAN KESTEREN-HENDRIKX, E. 2003. "In vivo" depletion of macrophages by liposome-mediated "suicide". *Methods Enzymol,* 373**,** 3-16.

VANDENDRIESSCHE, T., THORREZ, L., ACOSTA-SANCHEZ, A., PETRUS, I., WANG, L., MA, L., L, D. E. W., IWASAKI, Y., GILLIJNS, V., WILSON, J. M., COLLEN, D. & CHUAH, M. K. 2007. Efficacy and safety of adeno-associated viral vectors based on serotype 8 and 9 vs. lentiviral vectors for hemophilia B gene therapy. *J Thromb Haemost,* 5**,** 16-24.

VARNAVSKI, A. N., CALCEDO, R., BOVE, M., GAO, G. & WILSON, J. M. 2005. Evaluation of toxicity from high-dose systemic administration of recombinant adenovirus vector in vector-naive and pre-immunized mice. *Gene Ther,* 12**,** 427-36.

VELLINGA, J., RABELINK, M. J., CRAMER, S. J., VAN DEN WOLLENBERG, D. J., VAN DER MEULEN, H., LEPPARD, K. N., FALLAUX, F. J. & HOEBEN, R. C. 2004. Spacers increase the accessibility of peptide ligands linked to the carboxyl terminus of adenovirus minor capsid protein IX. *J Virol,* 78**,** 3470-9.

VELLINGA, J., SMITH, J. P., LIPIEC, A., MAJHEN, D., LEMCKERT, A., VAN OOIJ, M., IVES, P., YALLOP, C., CUSTERS, J. & HAVENGA, M. 2014. Challenges in manufacturing adenoviral vectors for global vaccine product deployment. *Hum Gene Ther,* 25**,** 318-27.

VELLINGA, J., VAN DER HEIJDT, S. & HOEBEN, R. C. 2005. The adenovirus capsid: major progress in minor proteins. *J Gen Virol,* 86**,** 1581-8.

VENKATESWARLU, D., PERERA, L., DARDEN, T. & PEDERSEN, L. G. 2002. Structure and dynamics of zymogen human blood coagulation factor X. *Biophys J,* 82**,** 1190-206.

VIGANT, F., DESCAMPS, D., JULLIENNE, B., ESSELIN, S., CONNAULT, E., OPOLON, P., TORDJMANN, T., VIGNE, E., PERRICAUDET, M. & BENIHOUD, K. 2008. Substitution of hexon hypervariable region 5 of adenovirus serotype 5 abrogates blood factor binding and limits gene transfer to liver. *Mol Ther,* 16**,** 1474-80.

VIGNE, E., MAHFOUZ, I., DEDIEU, J. F., BRIE, A., PERRICAUDET, M. & YEH, P. 1999. RGD inclusion in the hexon monomer provides adenovirus type 5-based vectors with a fiber knob-independent pathway for infection. *J Virol,* 73**,** 5156-61.

VOEKS, D., MARTINIELLO-WILKS, R., MADDEN, V., SMITH, K., BENNETTS, E., BOTH, G. W. & RUSSELL, P. J. 2002. Gene therapy for prostate cancer delivered by ovine adenovirus and mediated by purine nucleoside phosphorylase and fludarabine in mouse models. *Gene Ther,* 9**,** 759-68.

VOGELS, R., ZUIJDGEEST, D., VAN RIJNSOEVER, R., HARTKOORN, E., DAMEN, I., DE BÉTHUNE, M. P., KOSTENSE, S., PENDERS, G., HELMUS, N., KOUDSTAAL, W., CECCHINI, M., WETTERWALD, A., SPRANGERS, M., LEMCKERT, A., OPHORST, O., KOEL, B., VAN MEERENDONK, M., QUAX, P., PANITTI, L., GRIMBERGEN, J., BOUT, A., GOUDSMIT, J. & HAVENGA, M. 2003. Replication-deficient human adenovirus type 35 vectors for gene transfer and vaccination: efficient human cell infection and bypass of preexisting adenovirus immunity. *J Virol,* 77**,** 8263-71.

VOLK, A. L., RIVERA, A. A., KANERVA, A., BAUERSCHMITZ, G., DMITRIEV, I., NETTELBECK, D. M. & CURIEL, D. T. 2003. Enhanced adenovirus infection of melanoma cells by fiber-modification: incorporation of RGD peptide or Ad5/3 chimerism. *Cancer Biol Ther,* 2**,** 511-5.

VON SEGGERN, D. J., CHIU, C. Y., FLECK, S. K., STEWART, P. L. & NEMEROW, G. R. 1999. A helper-independent adenovirus vector with E1, E3, and fiber deleted: structure and infectivity of fiberless particles. *J Virol,* 73**,** 1601-8.

VONGCHAN, P., WARDA, M., TOYODA, H., TOIDA, T., MARKS, R. M. & LINHARDT, R. J. 2005. Structural characterization of human liver heparan sulfate. *Biochim Biophys Acta,* 1721**,** 1-8.

VUJANOVIC, L., WHITESIDE, T. L., POTTER, D. M., CHU, J., FERRONE, S. & BUTTERFIELD, L. H. 2009. Regulation of antigen presentation machinery in human dendritic cells by recombinant adenovirus. *Cancer Immunol Immunother,* 58**,** 121-33.

WADDINGTON, S. N., MCVEY, J. H., BHELLA, D., PARKER, A. L., BARKER, K., ATODA, H., PINK, R., BUCKLEY, S. M., GREIG, J. A., DENBY, L., CUSTERS, J., MORITA, T., FRANCISCHETTI, I. M., MONTEIRO, R. Q., BAROUCH, D. H., VAN ROOIJEN, N., NAPOLI, C., HAVENGA, M. J., NICKLIN, S. A. & BAKER, A. H. 2008. Adenovirus serotype 5 hexon mediates liver gene transfer. *Cell,* 132**,** 397-409.

WADEI, H. M. & TEXTOR, S. C. 2012. The role of the kidney in regulating arterial blood pressure. *Nat Rev Nephrol,* 8**,** 602-9.

WALTERS, R. W., FREIMUTH, P., MONINGER, T. O., GANSKE, I., ZABNER, J. & WELSH, M. J. 2002. Adenovirus fiber disrupts CAR-mediated intercellular adhesion allowing virus escape. *Cell,* 110**,** 789-99.

WALTERS, R. W., GRUNST, T., BERGELSON, J. M., FINBERG, R. W., WELSH, M. J. & ZABNER, J. 1999. Basolateral localization of fiber receptors limits adenovirus infection from the apical surface of airway epithelia. *J Biol Chem,* 274**,** 10219-26.

WANG, C. H., CHAN, L. W., JOHNSON, R. N., CHU, D. S., SHI, J., SCHELLINGER, J. G., LIEBER, A. & PUN, S. H. 2011a. The transduction of Coxsackie and

Adenovirus Receptor-negative cells and protection against neutralizing antibodies by HPMA-co-oligolysine copolymer-coated adenovirus. *Biomaterials,* 32**,** 9536-45.

WANG, D. Y., LIU, S. H., LI, X., ZHAO, J. L., CHEN, H., FENG, F. X., WANG, L. X. & XIA, H. B. 2011b. [Study on construction of chimeric adenovirus vector Ad5/11 carrying human eGFP and endostatin-K5 and its experimental investigation in vitro]. *Xi Bao Yu Fen Zi Mian Yi Xue Za Zhi,* 27**,** 143-5.

WANG, H., LI, Z. Y., LIU, Y., PERSSON, J., BEYER, I., MOLLER, T., KOYUNCU, D., DRESCHER, M. R., STRAUSS, R., ZHANG, X. B., WAHL, J. K., 3RD, URBAN, N., DRESCHER, C., HEMMINKI, A., FENDER, P. & LIEBER, A. 2011c. Desmoglein 2 is a receptor for adenovirus serotypes 3, 7, 11 and 14. *Nat Med,* 17**,** 96-104.

WANG, I. H., SUOMALAINEN, M., ANDRIASYAN, V., KILCHER, S., MERCER, J., NEEF, A., LUEDTKE, N. W. & GREBER, U. F. 2013. Tracking viral genomes in host cells at single-molecule resolution. *Cell Host Microbe,* 14**,** 468-80.

WANG, K., GUAN, T., CHERESH, D. A. & NEMEROW, G. R. 2000. Regulation of adenovirus membrane penetration by the cytoplasmic tail of integrin beta5. *J Virol,* 74**,** 2731-9.

WANG, K., HUANG, S., KAPOOR-MUNSHI, A. & NEMEROW, G. 1998. Adenovirus internalization and infection require dynamin. *J Virol,* 72**,** 3455-8.

WANG, Q. & FINER, M. H. 1996. Second-generation adenovirus vectors. *Nat Med,* 2**,** 714-6.

WANG, Q., GREENBURG, G., BUNCH, D., FARSON, D. & FINER, M. H. 1997. Persistent transgene expression in mouse liver following in vivo gene transfer with a delta E1/delta E4 adenovirus vector. *Gene Ther,* 4**,** 393-400.

WARREN, H. S. & SMYTH, M. J. 1999. NK cells and apoptosis. *Immunol Cell Biol,* 77**,** 64-75.

WATTANAKIT, K., FOLSOM, A. R., SELVIN, E., CORESH, J., HIRSCH, A. T. & WEATHERLEY, B. D. 2007. Kidney function and risk of peripheral arterial disease: results from the Atherosclerosis Risk in Communities (ARIC) Study. *J Am Soc Nephrol,* 18**,** 629-36.

WEBER, J. 1976. Genetic analysis of adenovirus type 2 III. Temperature sensitivity of processing viral proteins. *J Virol,* 17**,** 462-71.

WEIDEN, M. D. & GINSBERG, H. S. 1994. Deletion of the E4 region of the genome produces adenovirus DNA concatemers. *Proc Natl Acad Sci U S A,* 91**,** 153-7.

WESSELING, J. G., BOSMA, P. J., KRASNYKH, V., KASHENTSEVA, E. A., BLACKWELL, J. L., REYNOLDS, P. N., LI, H., PARAMESHWAR, M., VICKERS, S. M., JAFFEE, E. M., HUIBREGTSE, K., CURIEL, D. T. & DMITRIEV, I. 2001. Improved gene transfer efficiency to primary and established human pancreatic carcinoma target cells via epidermal growth factor receptor and integrin-targeted adenoviral vectors. *Gene Ther,* 8**,** 969-76.

WESSELS, M. R., BUTKO, P., MA, M., WARREN, H. B., LAGE, A. L. & CARROLL, M. C. 1995. Studies of group B streptococcal infection in mice deficient in complement component C3 or C4 demonstrate an essential role for complement in both innate and acquired immunity. *Proc Natl Acad Sci U S A,* 92**,** 11490-4.

WHITE, E., SABBATINI, P., DEBBAS, M., WOLD, W. S., KUSHER, D. I. & GOODING, L. R. 1992. The 19-kilodalton adenovirus E1B transforming protein inhibits programmed cell death and prevents cytolysis by tumor necrosis factor alpha. *Mol Cell Biol,* 12**,** 2570-80.

WHITE, K., NICKLIN, S. A. & BAKER, A. H. 2007. Novel vectors for in vivo gene delivery to vascular tissue. *Expert Opin Biol Ther,* 7**,** 809-21.

WICKHAM, T. J., FILARDO, E. J., CHERESH, D. A. & NEMEROW, G. R. 1994. Integrin alpha v beta 5 selectively promotes adenovirus mediated cell membrane permeabilization. *J Cell Biol,* 127**,** 257-64.

WICKHAM, T. J., MATHIAS, P., CHERESH, D. A. & NEMEROW, G. R. 1993. Integrins alpha v beta 3 and alpha v beta 5 promote adenovirus internalization but not virus attachment. *Cell,* 73**,** 309-19.

WICKHAM, T. J., SEGAL, D. M., ROELVINK, P. W., CARRION, M. E., LIZONOVA, A., LEE, G. M. & KOVESDI, I. 1996. Targeted adenovirus gene transfer to endothelial and smooth muscle cells by using bispecific antibodies. *J Virol,* 70**,** 6831-8.

WICKHAM, T. J., TZENG, E., SHEARS, L. L., 2ND, ROELVINK, P. W., LI, Y., LEE, G. M., BROUGH, D. E., LIZONOVA, A. & KOVESDI, I. 1997. Increased in vitro and in vivo gene transfer by adenovirus vectors containing chimeric fiber proteins. *J Virol,* 71**,** 8221-9.

WIDES, R. J., CHALLBERG, M. D., RAWLINS, D. R. & KELLY, T. J. 1987. Adenovirus origin of DNA replication: sequence requirements for replication in vitro. *Mol Cell Biol,* 7**,** 864-74.

WIETHOFF, C. M., WODRICH, H., GERACE, L. & NEMEROW, G. R. 2005. Adenovirus protein VI mediates membrane disruption following capsid disassembly. *J Virol,* 79**,** 1992-2000.

WIGGINS, K. J. & KELLY, D. J. 2009. Aliskiren: a novel renoprotective agent or simply an alternative to ACE inhibitors? *Kidney Int,* 76**,** 23-31.

WIGGINS, R. C. 2007. The spectrum of podocytopathies: a unifying view of glomerular diseases. *Kidney Int,* 71**,** 1205-14.

WIMMER, P., SCHREINER, S., EVERETT, R. D., SIRMA, H., GROITL, P. & DOBNER, T. 2010. SUMO modification of E1B-55K oncoprotein regulates isoform-specific binding to the tumour suppressor protein PML. *Oncogene,* 29**,** 5511-22.

WINDHEIM, M., SOUTHCOMBE, J. H., KREMMER, E., CHAPLIN, L., URLAUB, D., FALK, C. S., CLAUS, M., MIHM, J., BRAITHWAITE, M., DENNEHY, K., RENZ, H., SESTER, M., WATZL, C. & BURGERT, H. G. 2013. A unique secreted adenovirus E3 protein binds to the leukocyte common antigen CD45 and modulates leukocyte functions. *Proc Natl Acad Sci U S A,* 110**,** E4884-93.

WITTRUP, A., ZHANG, S. H., SVENSSON, K. J., KUCHARZEWSKA, P., JOHANSSON, M. C., MORGELIN, M. & BELTING, M. 2010. Magnetic nanoparticle-based isolation of endocytic vesicles reveals a role of the heat shock protein GRP75 in macromolecular delivery. *Proc Natl Acad Sci U S A,* 107**,** 13342-7.

WITTRUP, A., ZHANG, S. H., TEN DAM, G. B., VAN KUPPEVELT, T. H., BENGTSON, P., JOHANSSON, M., WELCH, J., MORGELIN, M. & BELTING, M. 2009. ScFv antibody-induced translocation of cell-surface heparan sulfate proteoglycan to endocytic vesicles: evidence for heparan sulfate epitope specificity and role of both syndecan and glypican. *J Biol Chem,* 284**,** 32959-67.

WODRICH, H., CASSANY, A., D'ANGELO, M. A., GUAN, T., NEMEROW, G. & GERACE, L. 2006. Adenovirus core protein pVII is translocated into the nucleus by multiple import receptor pathways. *J Virol,* 80**,** 9608-18.

WODRICH, H., GUAN, T., CINGOLANI, G., VON SEGGERN, D., NEMEROW, G. & GERACE, L. 2003. Switch from capsid protein import to adenovirus assembly by cleavage of nuclear transport signals. *EMBO J,* 22**,** 6245-55.

WODRICH, H., HENAFF, D., JAMMART, B., SEGURA-MORALES, C., SEELMEIR, S., COUX, O., RUZSICS, Z., WIETHOFF, C. M. & KREMER, E. J. 2010. A capsid-encoded PPxY-motif facilitates adenovirus entry. *PLoS Pathog,* 6**,** e1000808.

WOHLFART, C. 1988. Neutralization of adenoviruses: kinetics, stoichiometry, and mechanisms. *J Virol,* 62**,** 2321-8.

WOLFF, G., WORGALL, S., VAN ROOIJEN, N., SONG, W. R., HARVEY, B. G. & CRYSTAL, R. G. 1997. Enhancement of in vivo adenovirus-mediated gene transfer and expression by prior depletion of tissue macrophages in the target organ. *J Virol,* 71**,** 624-9.

WONG, C. & GOLDSTEIN, D. R. 2013. Impact of aging on antigen presentation cell function of dendritic cells. *Curr Opin Immunol,* 25**,** 535-41.

WONG, C. P., MAGNUSSON, K. R. & HO, E. 2010. Aging is associated with altered dendritic cells subset distribution and impaired proinflammatory cytokine production. *Exp Gerontol,* 45**,** 163-9.

WONG, G. H. & GOEDDEL, D. V. 1986. Tumour necrosis factors alpha and beta inhibit virus replication and synergize with interferons. *Nature,* 323**,** 819-22.

WONGANAN, P. & CROYLE, M. A. 2010. PEGylated Adenoviruses: From Mice to Monkeys. *Viruses,* 2**,** 468-502.

WOO, J. L. & BERK, A. J. 2007. Adenovirus ubiquitin-protein ligase stimulates viral late mRNA nuclear export. *J Virol,* 81**,** 575-87.

WOODS, A., LONGLEY, R. L., TUMOVA, S. & COUCHMAN, J. R. 2000. Syndecan-4 binding to the high affinity heparin-binding domain of fibronectin drives focal adhesion formation in fibroblasts. *Arch Biochem Biophys,* 374**,** 66-72.

WORK, L. M., NICKLIN, S. A., BRAIN, N. J., DISHART, K. L., VON SEGGERN, D. J., HALLEK, M., BUNING, H. & BAKER, A. H. 2004. Development of efficient viral vectors selective for vascular smooth muscle cells. *Mol Ther,* 9**,** 198-208.

WORLD WSM AND HORWITZ MS 2007. Adenoviruses. *In:* PM, K. D. A. H. (ed.) *Fields Virology.* 5th ed. (Lippincott Williams & Wilkins, Philadelphia).

WOUTERS, D. & ZEERLEDER, S. 2015. Complement inhibitors to treat IgM-mediated autoimmune hemolysis. *Haematologica,* 100**,** 1388-95.

WU, E., TRAUGER, S. A., PACHE, L., MULLEN, T. M., VON SEGGERN, D. J., SIUZDAK, G. & NEMEROW, G. R. 2004. Membrane cofactor protein is a receptor for adenoviruses associated with epidemic keratoconjunctivitis. *J Virol,* 78**,** 3897-905.

WU, H., DMITRIEV, I., KASHENTSEVA, E., SEKI, T., WANG, M. & CURIEL, D. T. 2002. Construction and characterization of adenovirus serotype 5 packaged by serotype 3 hexon. *J Virol,* 76**,** 12775-82.

WU, H., HAN, T., BELOUSOVA, N., KRASNYKH, V., KASHENTSEVA, E., DMITRIEV, I., KATARAM, M., MAHASRESHTI, P. J. & CURIEL, D. T. 2005. Identification of sites in adenovirus hexon for foreign peptide incorporation. *J Virol,* 79**,** 3382-90.

WU, K., GUIMET, D. & HEARING, P. 2013. The adenovirus L4-33K protein regulates both late gene expression patterns and viral DNA packaging. *J Virol,* 87**,** 6739-47.

WU, L., MATHERLY, J., SMALLWOOD, A., ADAMS, J. Y., BILLICK, E., BELLDEGRUN, A. & CAREY, M. 2001. Chimeric PSA enhancers exhibit augmented activity in prostate cancer gene therapy vectors. *Gene Ther,* 8**,** 1416-26.

WU, L., ROSSER, D. S., SCHMIDT, M. C. & BERK, A. 1987. A TATA box implicated in E1A transcriptional activation of a simple adenovirus 2 promoter. *Nature,* 326**,** 512-5.

WU, X., LI, Y., CRISE, B. & BURGESS, S. M. 2003. Transcription start regions in the human genome are favored targets for MLV integration. *Science,* 300**,** 1749-51.

XIA, D., HENRY, L. J., GERARD, R. D. & DEISENHOFER, J. 1994. Crystal structure of the receptor-binding domain of adenovirus type 5 fiber protein at 1.7 A resolution. *Structure,* 2**,** 1259-70.

XIA, H., ANDERSON, B., MAO, Q. & DAVIDSON, B. L. 2000. Recombinant human adenovirus: targeting to the human transferrin receptor improves gene transfer to brain microcapillary endothelium. *J Virol,* 74**,** 11359-66.

XU, Z., QIU, Q., TIAN, J., SMITH, J. S., CONENELLO, G. M., MORITA, T. & BYRNES, A. P. 2013. Coagulation factor X shields adenovirus type 5 from attack by natural antibodies and complement. *Nat Med,* 19**,** 452-7.

XU, Z., TIAN, J., SMITH, J. S. & BYRNES, A. P. 2008. Clearance of adenovirus by Kupffer cells is mediated by scavenger receptors, natural antibodies, and complement. *J Virol,* 82**,** 11705-13.

XUE, Y., JOHNSON, J. S., ORNELLES, D. A., LIEBERMAN, J. & ENGEL, D. A. 2005. Adenovirus protein VII functions throughout early phase and interacts with cellular proteins SET and pp32. *J Virol,* 79**,** 2474-83.

YAMAGUCHI, T., KAWABATA, K., KOIZUMI, N., SAKURAI, F., NAKASHIMA, K., SAKURAI, H., SASAKI, T., OKADA, N., YAMANISHI, K. & MIZUGUCHI, H. 2007. Role of MyD88 and TLR9 in the innate immune response elicited by serotype 5 adenoviral vectors. *Hum Gene Ther,* 18**,** 753-62.

YANG, L., MANITHODY, C. & REZAIE, A. R. 2002. Localization of the heparin binding exosite of factor IXa. *J Biol Chem,* 277**,** 50756-60.

YANG, T. C., DAYBALL, K., WAN, Y. H. & BRAMSON, J. 2003. Detailed analysis of the CD8+ T-cell response following adenovirus vaccination. *J Virol,* 77**,** 13407-11.

YANG, Y., NUNES, F. A., BERENCSI, K., FURTH, E. E., GONCZOL, E. & WILSON, J. M. 1994. Cellular immunity to viral antigens limits E1-deleted adenoviruses for gene therapy. *Proc Natl Acad Sci U S A,* 91**,** 4407-11.

YATHERAJAM, G., HUANG, W. & FLINT, S. J. 2011. Export of adenoviral late mRNA from the nucleus requires the Nxf1/Tap export receptor. *J Virol,* 85**,** 1429-38.

YAZDANBAKHSH, K., KANG, S., TAMASAUSKAS, D., SUNG, D. & SCARADAVOU, A. 2003. Complement receptor 1 inhibitors for prevention of immune-mediated red cell destruction: potential use in transfusion therapy. *Blood,* 101**,** 5046-52.

YAZDANBAKHSH, K. & SCARADAVOU, A. 2004. CR1-based inhibitors for prevention of complement-mediated immune hemolysis. *Drug News Perspect,* 17**,** 314-20.

YE, X., ROBINSON, M. B., PABIN, C., BATSHAW, M. L. & WILSON, J. M. 2000. Transient depletion of CD4 lymphocyte improves efficacy of repeated administration of recombinant adenovirus in the ornithine transcarbamylase deficient sparse fur mouse. *Gene Ther,* 7**,** 1761-7.

YEH, H. Y., PIENIAZEK, N., PIENIAZEK, D., GELDERBLOM, H. & LUFTIG, R. B. 1994. Human adenovirus type 41 contains two fibers. *Virus Res,* 33**,** 179-98.

YEW, P. R., LIU, X. & BERK, A. J. 1994. Adenovirus E1B oncoprotein tethers a transcriptional repression domain to p53. *Genes Dev,* 8**,** 190-202.

YING, B., TOLLEFSON, A. E. & WOLD, W. S. 2010. Identification of a previously unrecognized promoter that drives expression of the UXP transcription unit in the human adenovirus type 5 genome. *J Virol,* 84**,** 11470-8.

YING, B. & WOLD, W. S. 2003. Adenovirus ADP protein (E3-11.6K), which is required for efficient cell lysis and virus release, interacts with human MAD2B. *Virology,* 313**,** 224-34.

YONDOLA, M. A. & HEARING, P. 2007. The adenovirus E4 ORF3 protein binds and reorganizes the TRIM family member transcriptional intermediary factor 1 alpha. *J Virol,* 81**,** 4264-71.

YOUIL, R., TONER, T. J., SU, Q., CHEN, M., TANG, A., BETT, A. J. & CASIMIRO, D. 2002. Hexon gene switch strategy for the generation of chimeric recombinant adenovirus. *Hum Gene Ther,* 13**,** 311-20.

YU, B., DONG, J., WANG, C., ZHAN, Y., ZHANG, H., WU, J., KONG, W. & YU, X. 2013. Characteristics of neutralizing antibodies to adenovirus capsid proteins in human and animal sera. *Virology,* 437**,** 118-23.

ZACCA, E. R., CRESPO, M. I., ACLAND, R. P., ROSELLI, E., NUNEZ, N. G., MACCIONI, M., MALETTO, B. A., PISTORESI-PALENCIA, M. C. & MORON, G. 2015. Aging Impairs the Ability of Conventional Dendritic Cells to Cross-Prime CD8+ T Cells upon Stimulation with a TLR7 Ligand. *PLoS One,* 10**,** e0140672.

ZAISS, A. K., FOLEY, E. M., LAWRENCE, R., SCHNEIDER, L. S., HOVEIDA, H., SECREST, P., CATAPANG, A. B., YAMAGUCHI, Y., ALEMANY, R., SHAYAKHMETOV, D. M., ESKO, J. D. & HERSCHMAN, H. R. 2015. Hepatocyte Heparan Sulfate Is Required for Adeno-Associated Virus 2 but Dispensable for Adenovirus 5 Liver Transduction In Vivo. *J Virol,* 90**,** 412-20.

ZAISS, A. K., LAWRENCE, R., ELASHOFF, D., ESKO, J. D. & HERSCHMAN, H. R. 2011. Differential effects of murine and human factor X on adenovirus transduction via cell-surface heparan sulfate. *J Biol Chem,* 286**,** 24535-43.

ZAISS, A. K., VILAYSANE, A., COTTER, M. J., CLARK, S. A., MEIJNDERT, H. C., COLARUSSO, P., YATES, R. M., PETRILLI, V., TSCHOPP, J. & MURUVE, D. A. 2009. Antiviral antibodies target adenovirus to phagolysosomes and amplify the innate immune response. *J Immunol,* 182**,** 7058-68.

ZERIAL, M. & MCBRIDE, H. 2001. Rab proteins as membrane organizers. *Nat Rev Mol Cell Biol,* 2**,** 107-17.

ZHANG, B., YAN, Y., JIN, J., LIN, H., LI, Z., ZHANG, X., LIU, J., XI, C., LIEBER, A., FAN, X. & RAN, L. 2015. Two types of functionally distinct fiber containing structural protein complexes are produced during infection of adenovirus serotype 5. *PLoS One,* 10**,** e0117976.

ZHANG, W. & ARCOS, R. 2005. Interaction of the adenovirus major core protein precursor, pVII, with the viral DNA packaging machinery. *Virology,* 334**,** 194-202.

ZHANG, W. & IMPERIALE, M. J. 2000. Interaction of the adenovirus IVa2 protein with viral packaging sequences. *J Virol,* 74**,** 2687-93.

ZHANG, W. F., WU, F. L., SHAO, H. W., WANG, T., HUANG, X. T., LI, W. L., SHEN, H. & HUANG, S. L. 2013. Chimeric adenoviral vector Ad5F35L containing the Ad5 natural long-shaft exhibits efficient gene transfer into human T lymphocytes. *J Virol Methods,* 194**,** 52-9.

ZHANG, W. J., SUI, Y. X., BUDHA, A., ZHENG, J. B., SUN, X. J., HOU, Y. C., WANG, T. D. & LU, S. Y. 2012. Affinity peptide developed by phage display selection for targeting gastric cancer. *World J Gastroenterol,* 18**,** 2053-60.

ZHANG, Y. & BERGELSON, J. M. 2005. Adenovirus receptors. *J Virol,* 79**,** 12125-31.

ZHENG, X., RAO, X. M., GOMEZ-GUTIERREZ, J. G., HAO, H., MCMASTERS, K. M. & ZHOU, H. S. 2008. Adenovirus E1B55K region is required to enhance cyclin E expression for efficient viral DNA replication. *J Virol,* 82**,** 3415-27.

ZHOU, Q., FACCIPONTE, J., JIN, M., SHEN, Q. & LIN, Q. 2014. Humanized NOD-SCID IL2rg-/- mice as a preclinical model for cancer research and its potential use for individualized cancer therapies. *Cancer Lett,* 344**,** 13-9.

ZHOU, S., FATIMA, S., MA, Z., WANG, Y. D., LU, T., JANKE, L. J., DU, Y. & SORRENTINO, B. P. 2016. Evaluating the Safety of Retroviral Vectors Based on Insertional Oncogene Activation and Blocked Differentiation in Cultured Thymocytes. *Mol Ther,* 24**,** 1090-9.

ZHU, G., NICOLSON, A. G., COWLEY, B. D., ROSEN, S. & SUKHATME, V. P. 1996. In vivo adenovirus-mediated gene transfer into normal and cystic rat kidneys. *Gene Ther,* 3**,** 298-304.

ZHU, J., HUANG, X. & YANG, Y. 2007. Innate immune response to adenoviral vectors is mediated by both Toll-like receptor-dependent and -independent pathways. *J Virol,* 81**,** 3170-80.

ZHU, J., HUANG, X. & YANG, Y. 2008. A critical role for type I IFN-dependent NK cell activation in innate immune elimination of adenoviral vectors in vivo. *Mol Ther,* 16**,** 1300-7.

ZIMMERMANN, P., ZHANG, Z., DEGEEST, G., MORTIER, E., LEENAERTS, I., COOMANS, C., SCHULZ, J., N'KULI, F., COURTOY, P. J. & DAVID, G. 2005. Syndecan recycling [corrected] is controlled by syntenin-PIP2 interaction and Arf6. *Dev Cell,* 9**,** 377-88.

ZUBIETA, C., SCHOEHN, G., CHROBOCZEK, J. & CUSACK, S. 2005. The structure of the human adenovirus 2 penton. *Mol Cell,* 17**,** 121-35.

Appendix

Plasmid DNA genetic maps

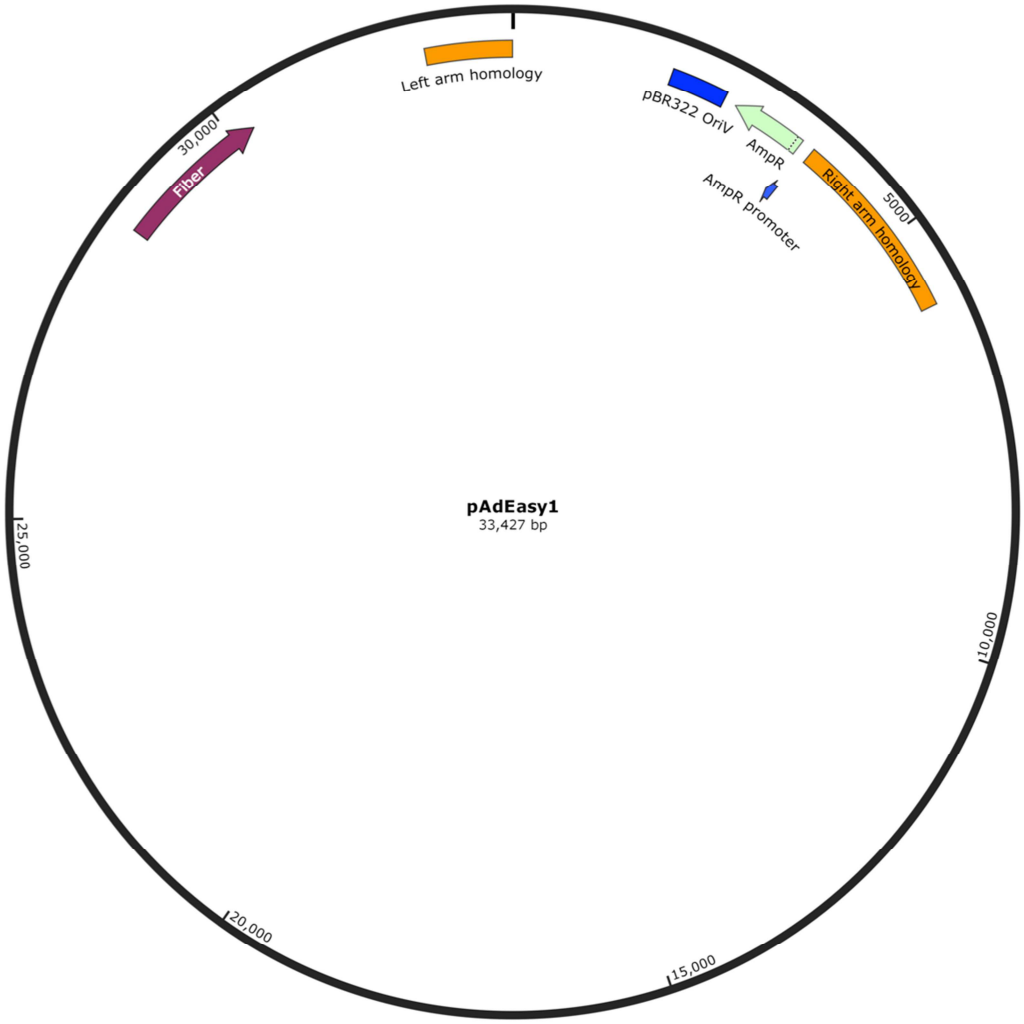

Figure A-1. pAdEasy1. Genetic elements are shown as coloured boxes or arrows. AmpR, ampicillin resistance gene. The genetic map was generated with SnapGene v2.8.3.

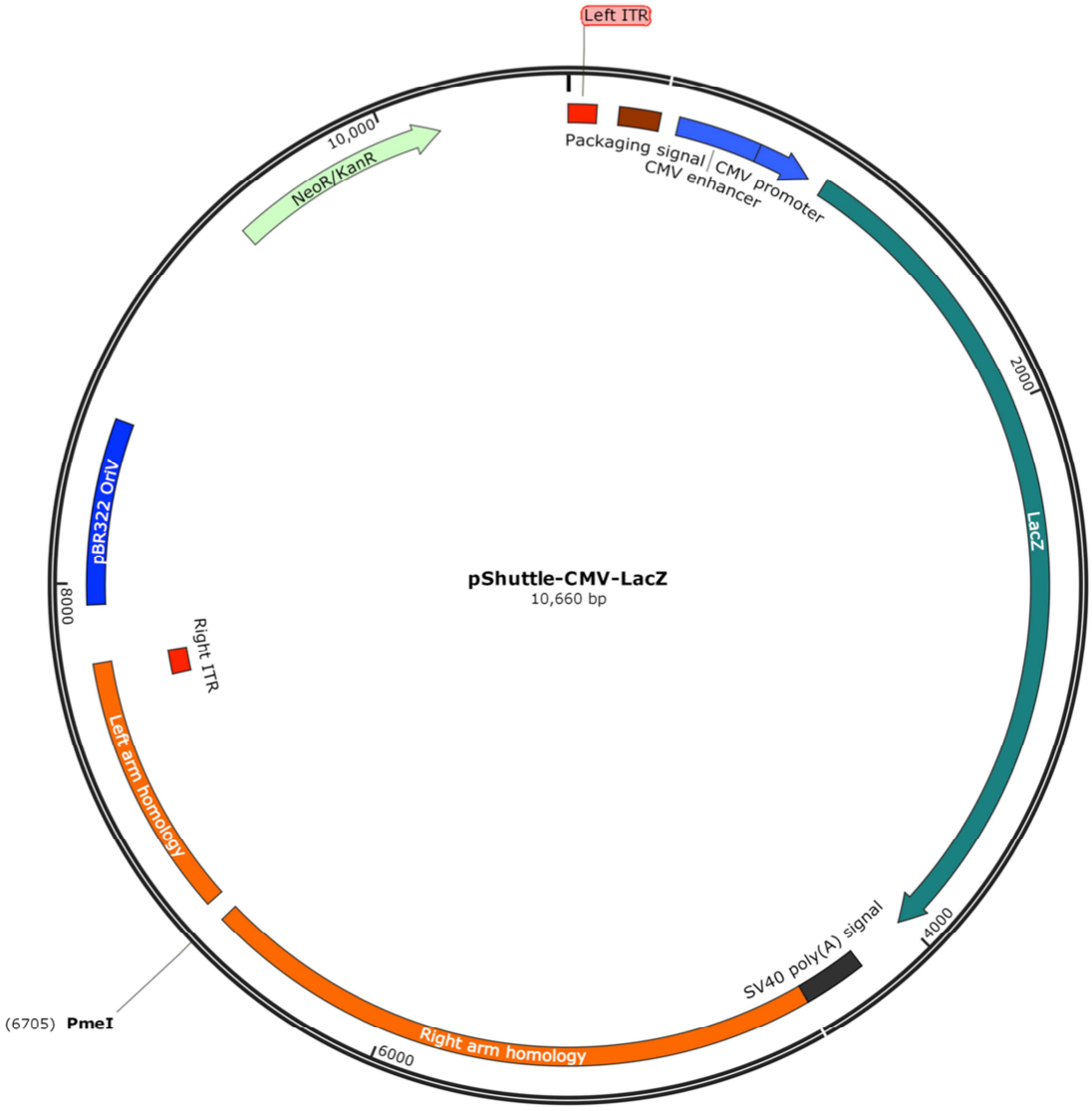

Figure A-2. pShuttle-CMV-*LacZ*. Genetic elements are shown as coloured boxes or arrows. Right and left homology arms represent homologous DNA sequences with pAdEasy1. Restriction enzyme used for cloning is indicated on the map. ITR; inverted terminal repeat, NeoR; neomycin resistance gene, KanR; kanamycin resistance gene. The genetic map was generated with SnapGene v2.8.3.

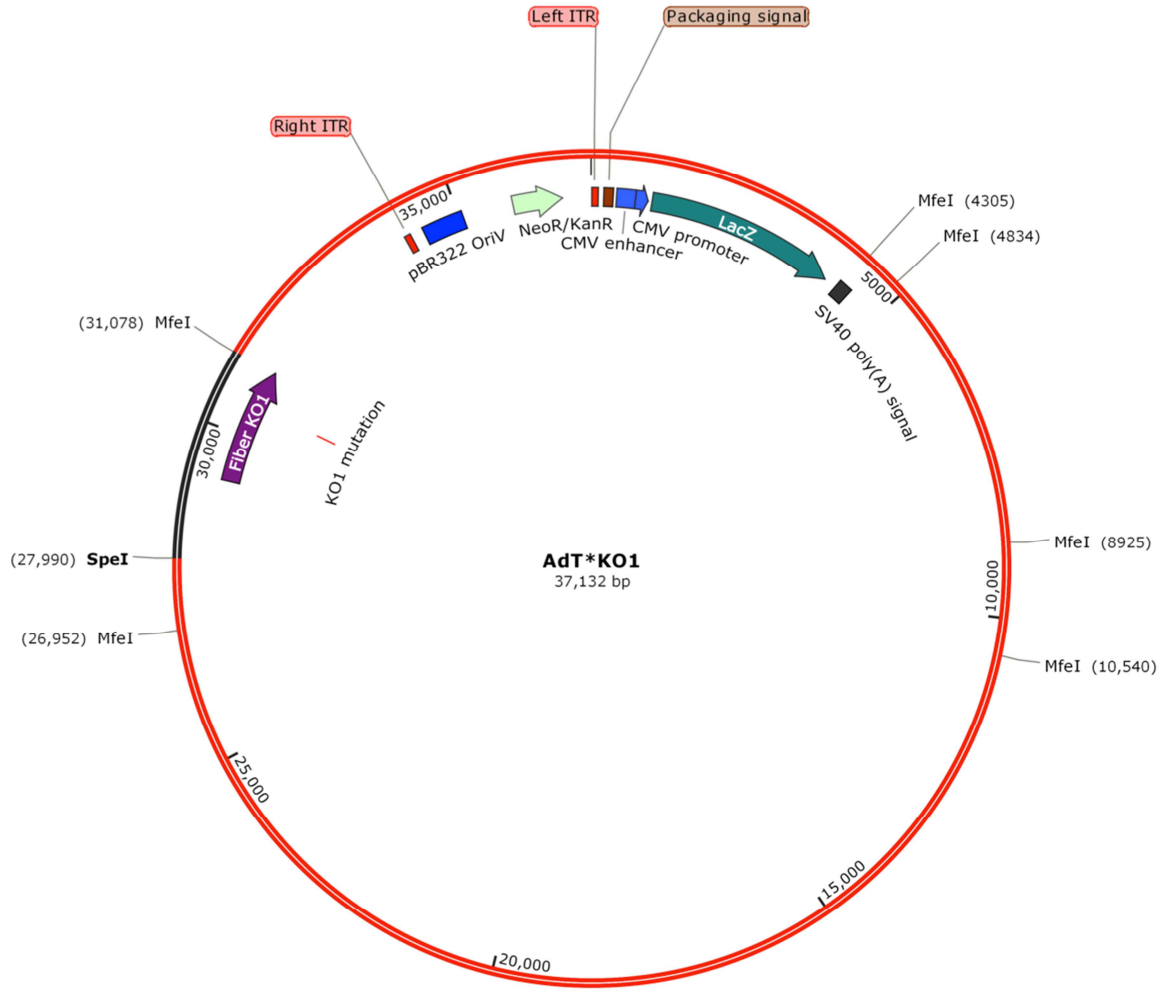

Figure A-3. pAdT*KO1. Genetic elements are shown as coloured boxes or arrows. DNA sequence in red represent the region removed from the plasmid for ligation with enzymatically digested pShuttle-KO1-AAA. Restriction enzymes used for cloning are indicated on the map. ITR; inverted terminal repeat, NeoR; neomycin resistance gene, KanR; kanamycin resistance gene. The genetic map was generated with SnapGene v2.8.3.

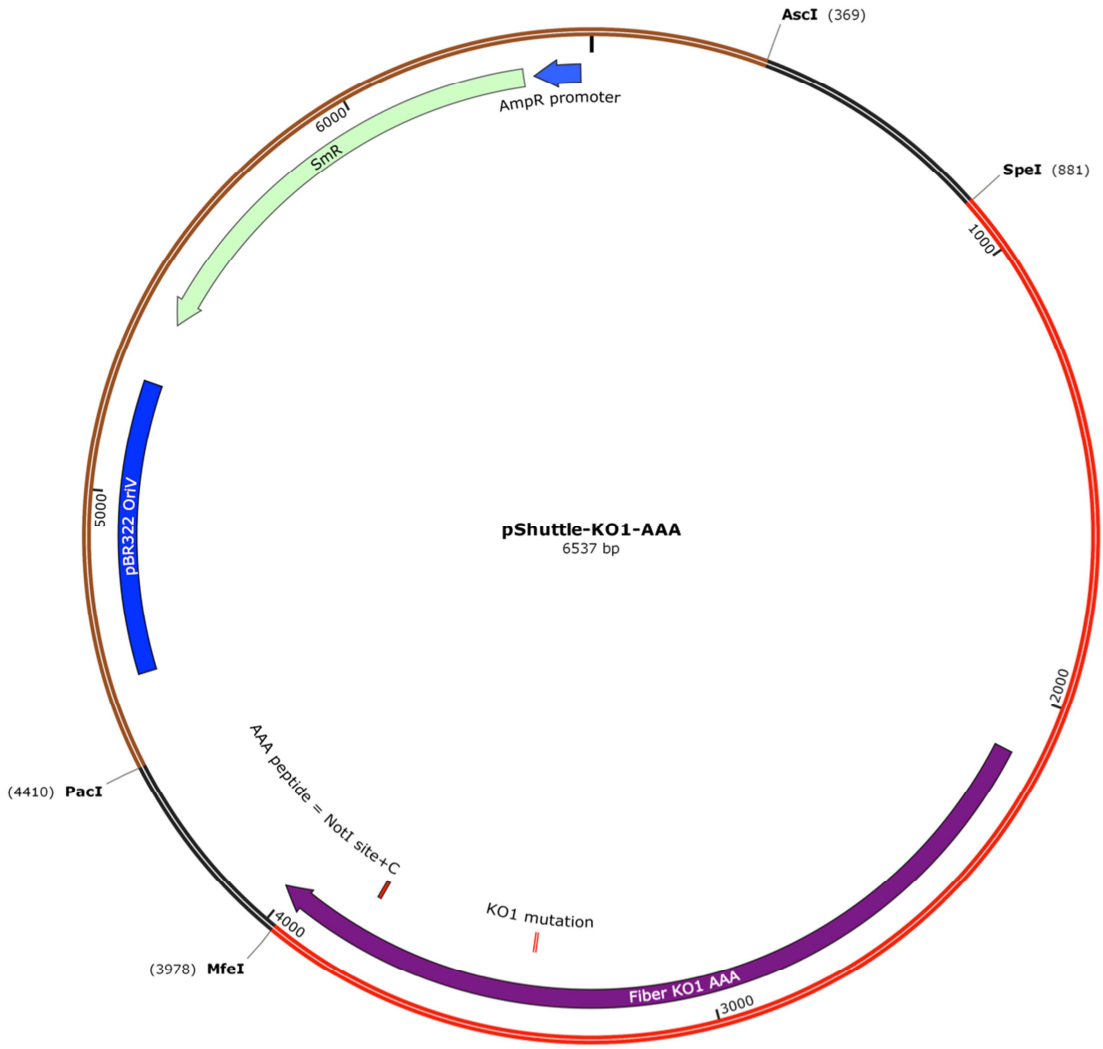

Figure A-4. pShuttle-KO1-AAA. Genetic elements are shown as coloured boxes or arrows. DNA sequence in red represent the region removed from the plasmid for ligation with enzymatically digested pAdT*KO1. DNA sequence in brown represent the region removed from the plasmid for homologous DNA recombination with pAdT*. Restriction enzymes used for cloning are indicated on the map. SmR; streptomycin resistance gene. The genetic map was generated with SnapGene v2.8.3.

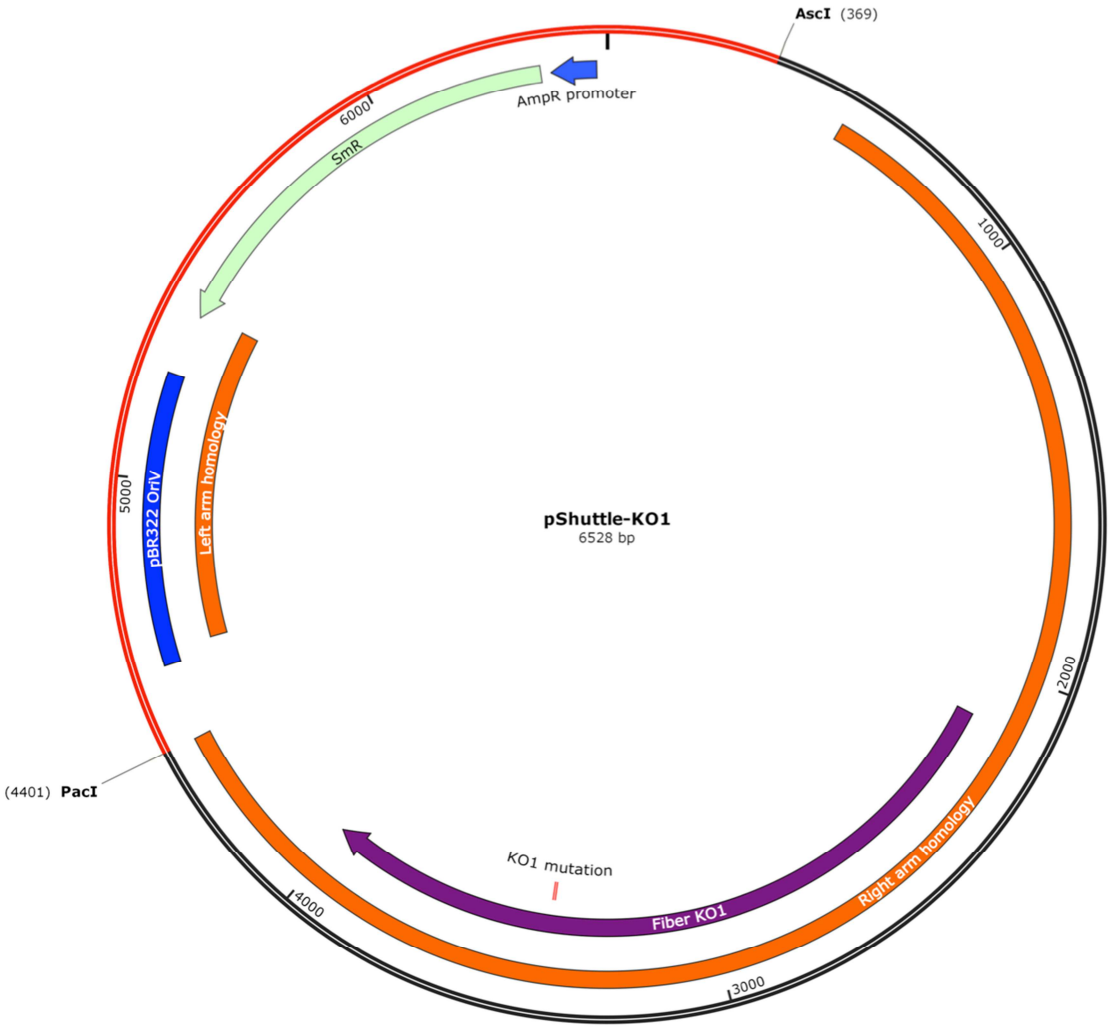

Figure A-5. pShuttle-KO1. Genetic elements are shown as coloured boxes or arrows. Right and left homology arms represent homologous DNA sequences with pAdEasy1-CMV-*LacZ*. DNA sequence in red represent the region removed from the plasmid for homologous DNA recombination with pAdEasy1-CMV-*LacZ*. Restriction enzymes used for cloning are indicated on the map. SmR; streptomycin resistance gene. The genetic map was generated with SnapGene v2.8.3.

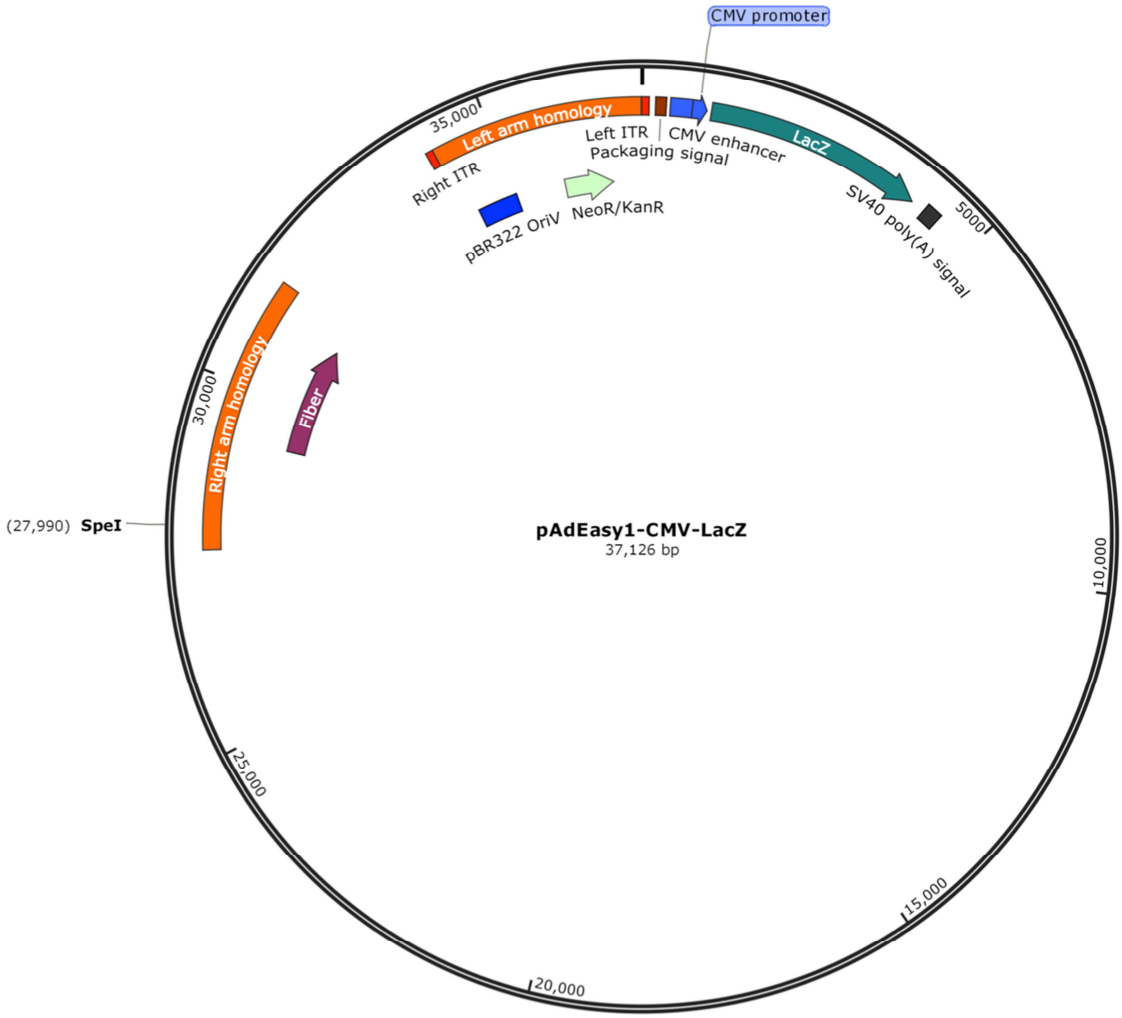

Figure A-6. pAdEasy1-CMV-*LacZ*. Genetic elements are shown as coloured boxes or arrows. Right and left homology arms represent homologous DNA sequences with pShuttle-KO1. Restriction enzyme used for cloning is indicated on the map. ITR; inverted terminal repeat, NeoR; neomycin resistance gene, KanR; kanamycin resistance gene. The genetic map was generated with SnapGene v2.8.3.

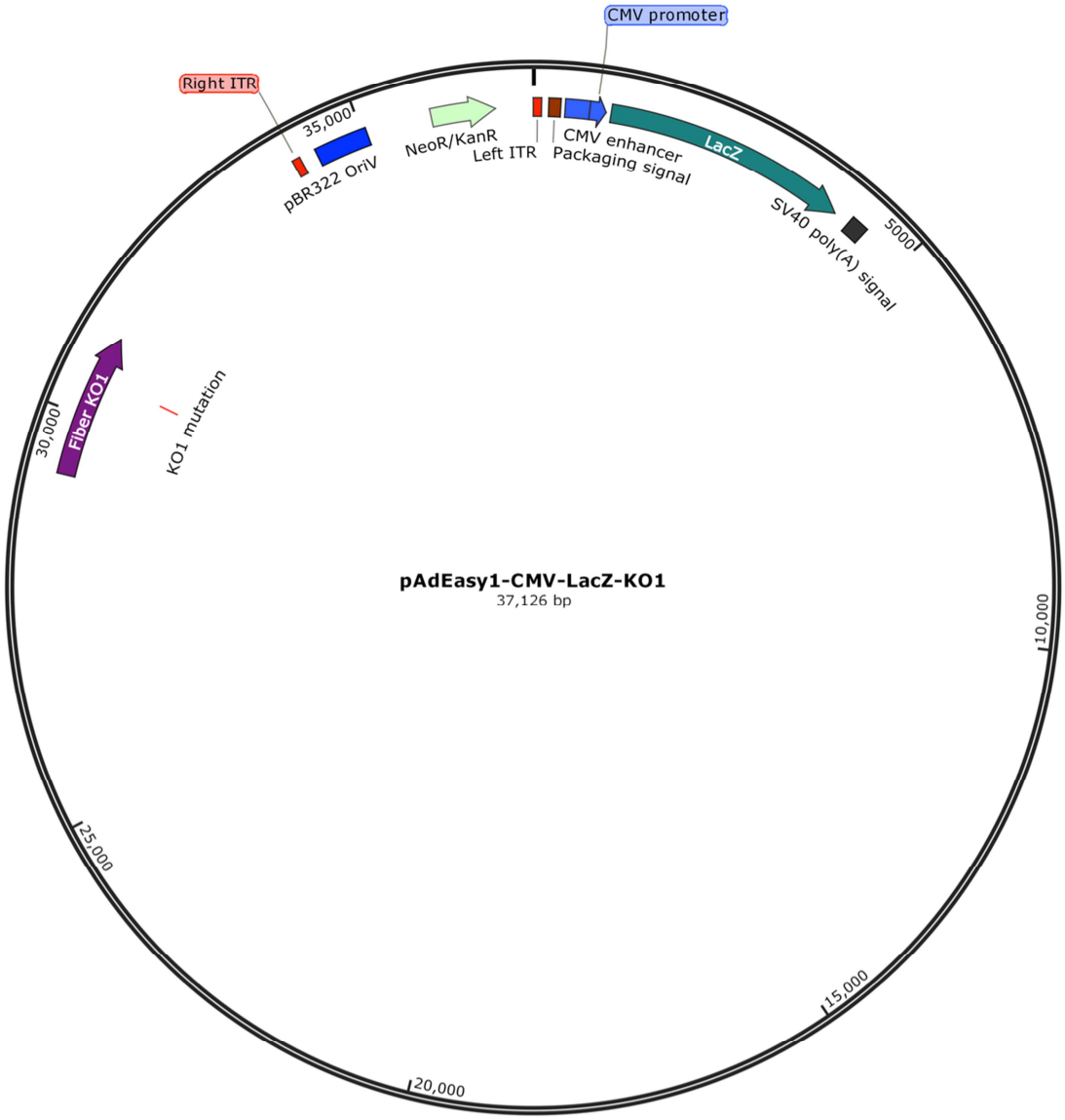

Figure A-7. pAdEasy1-CMV-*LacZ*-KO1. Genetic elements are shown as coloured boxes or arrows. ITR; inverted terminal repeat, NeoR; neomycin resistance gene, KanR; kanamycin resistance gene. The genetic map was generated with SnapGene v2.8.3.

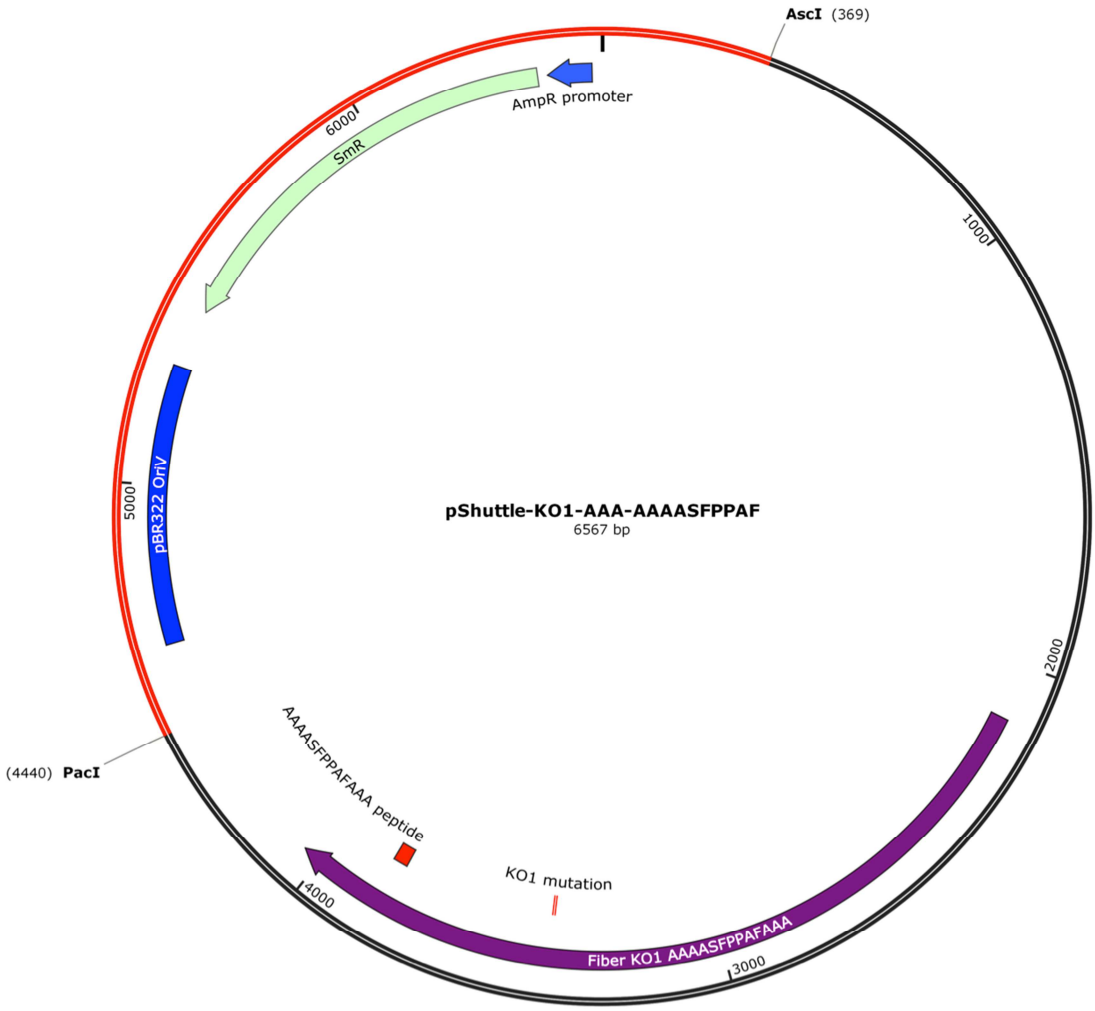

Figure A-8. pShuttle-KO1-AAA-AAAASFPPAF. Genetic elements are shown as coloured boxes or arrows. DNA sequence in red represent the region removed from the plasmid for homologous DNA recombination with pAdT*. Restriction enzymes used for cloning are indicated on the map. SmR; streptomycin resistance gene. The genetic map was generated with SnapGene v2.8.3.

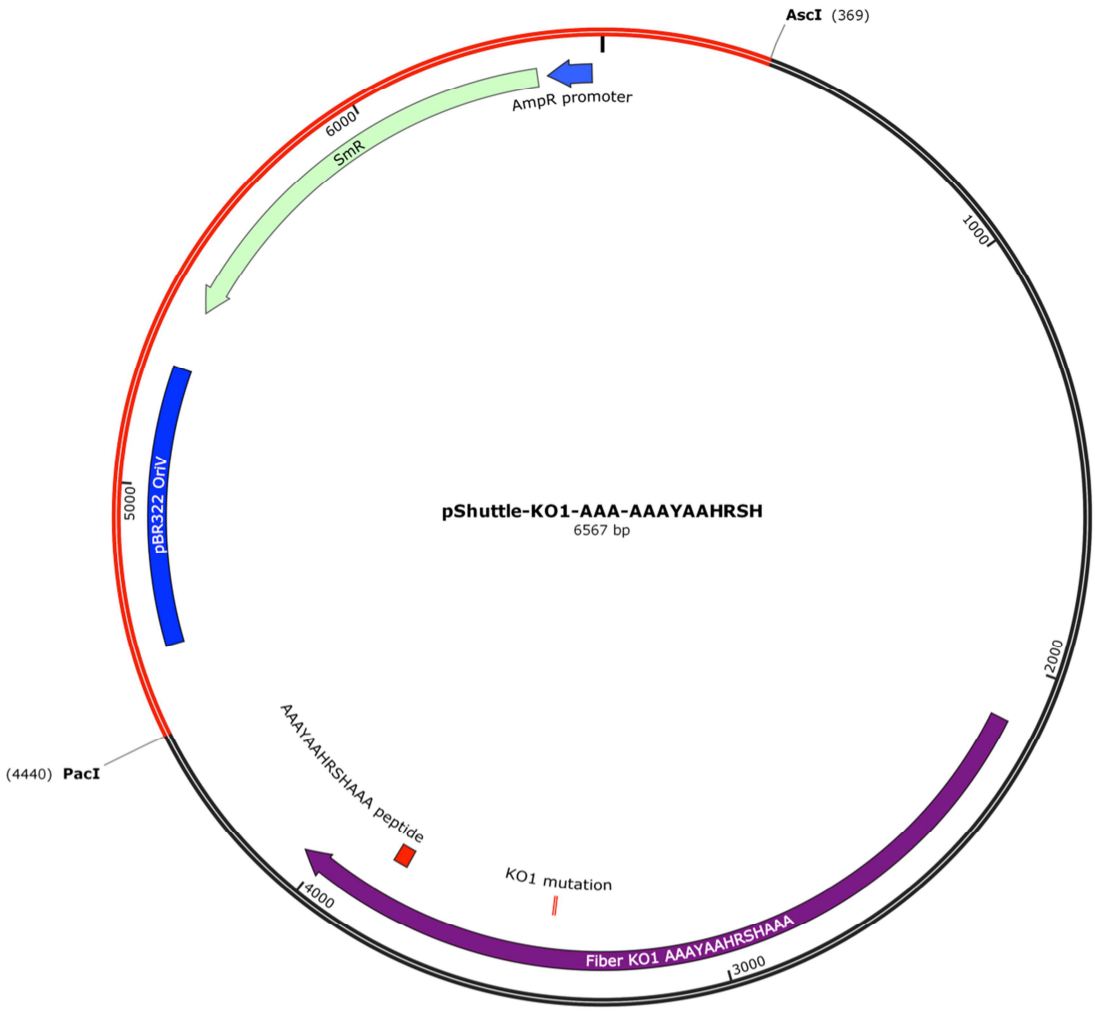

Figure A-9. pShuttle-KO1-AAA-AAAYAAHRSH. Genetic elements are shown as coloured boxes or arrows. DNA sequence in red represent the region removed from the plasmid for homologous DNA recombination with pAdT*. Restriction enzymes used for cloning are indicated on the map. SmR; streptomycin resistance gene. The genetic map was generated with SnapGene v2.8.3.

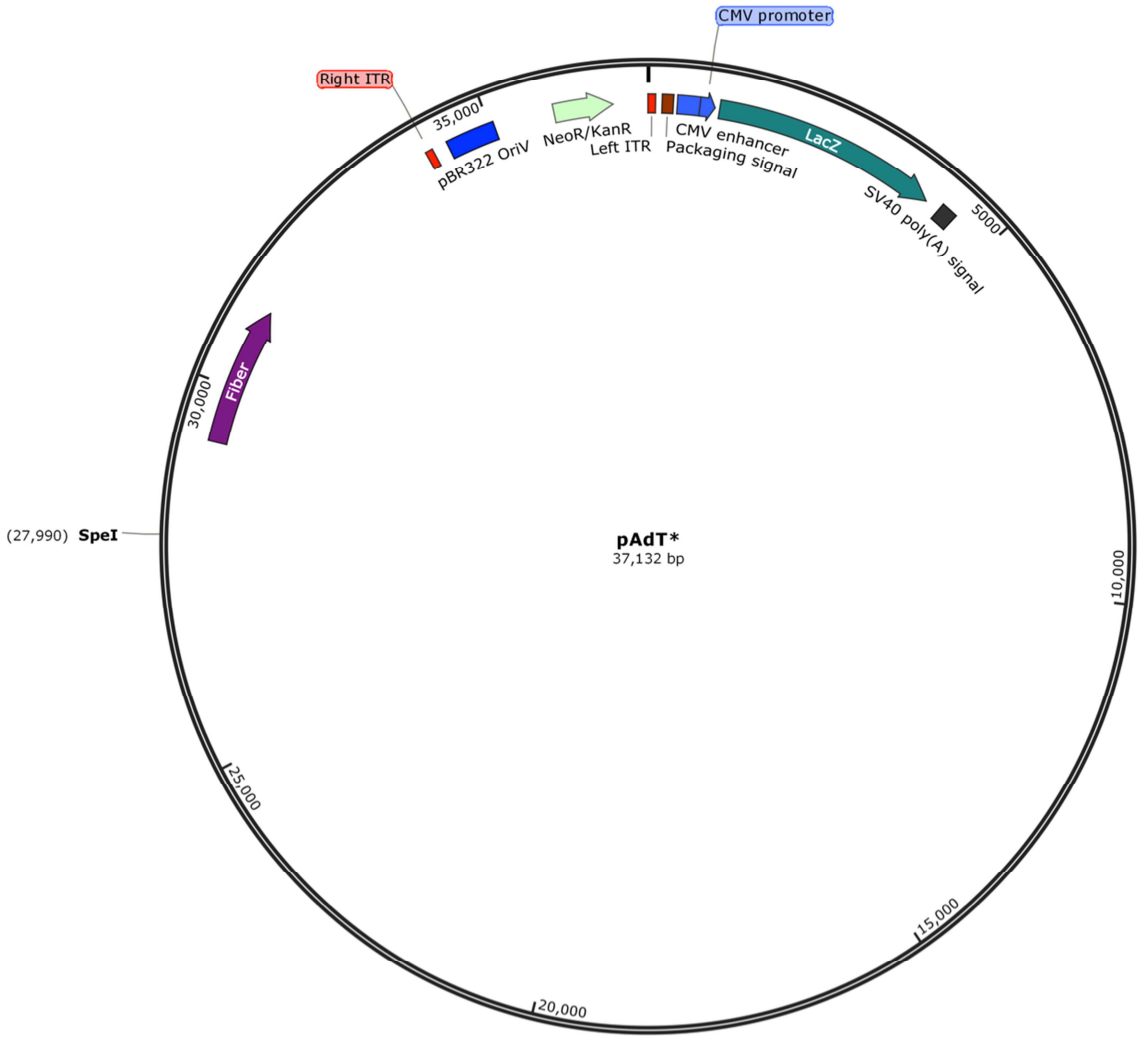

Figure A-10. pAdT*. Genetic elements are shown as coloured boxes or arrows. Restriction enzymes used for cloning are indicated on the map. ITR; inverted terminal repeat, NeoR; neomycin resistance gene, KanR; kanamycin resistance gene. The genetic map was generated with SnapGene v2.8.3.

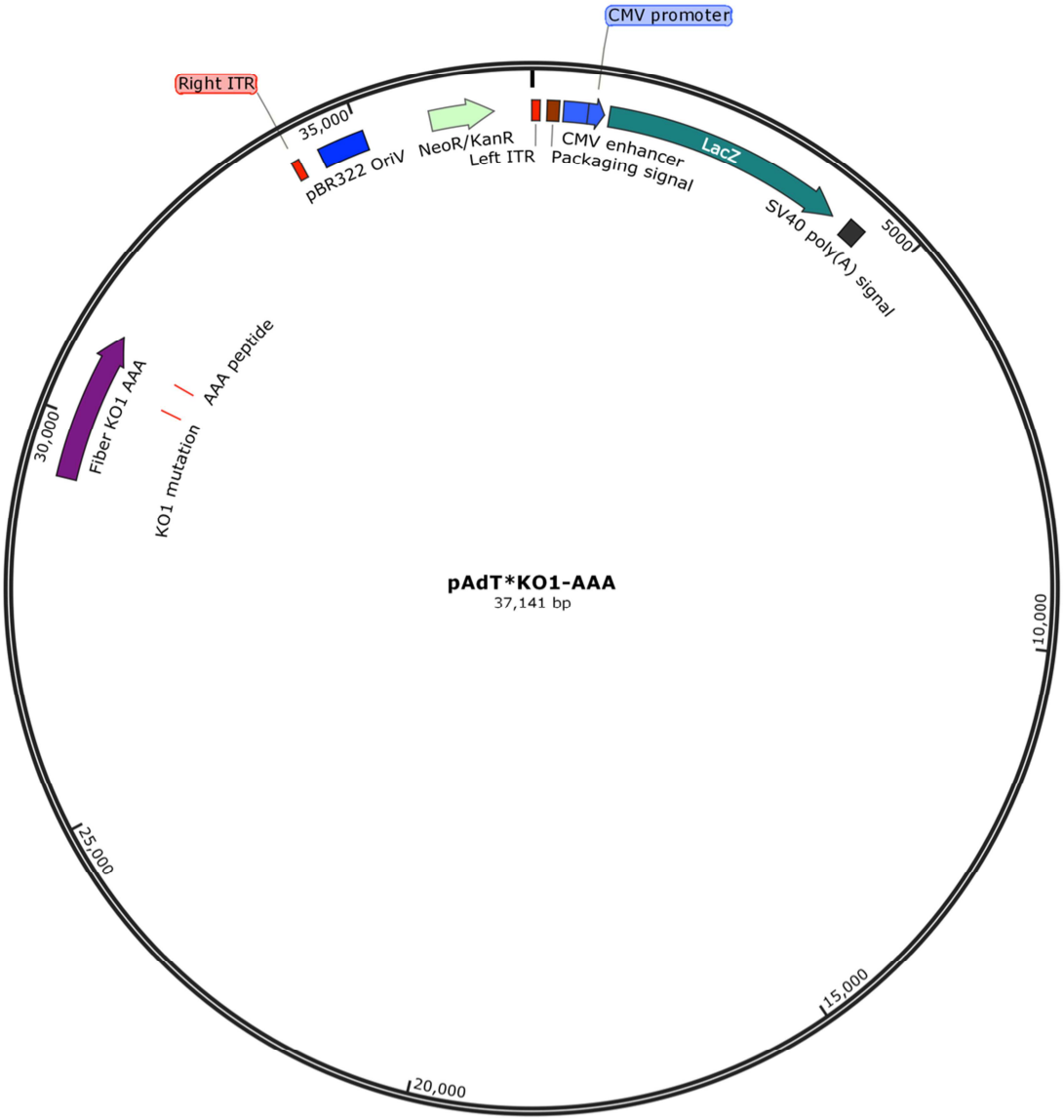

Figure A-11. pAdT*KO1-AAA. Genetic elements are shown as coloured boxes or arrows. ITR; inverted terminal repeat, NeoR; neomycin resistance gene, KanR; kanamycin resistance gene. The genetic map was generated with SnapGene v2.8.3.

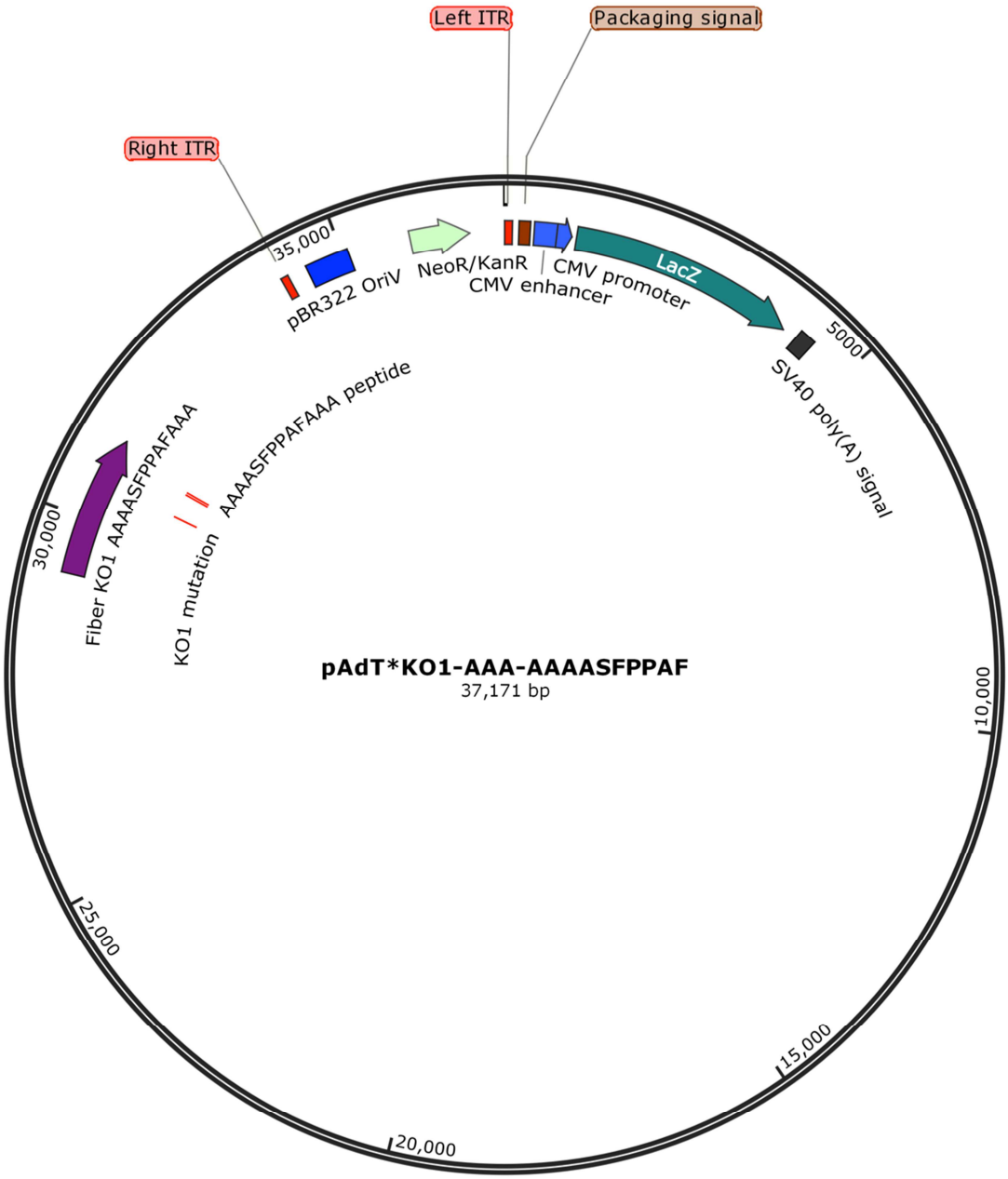

Figure A-12. pAdT*KO1-AAA-AAAASFPPAF. Genetic elements are shown as coloured boxes or arrows. ITR; inverted terminal repeat, NeoR; neomycin resistance gene, KanR; kanamycin resistance gene. The genetic map was generated with SnapGene v2.8.3.

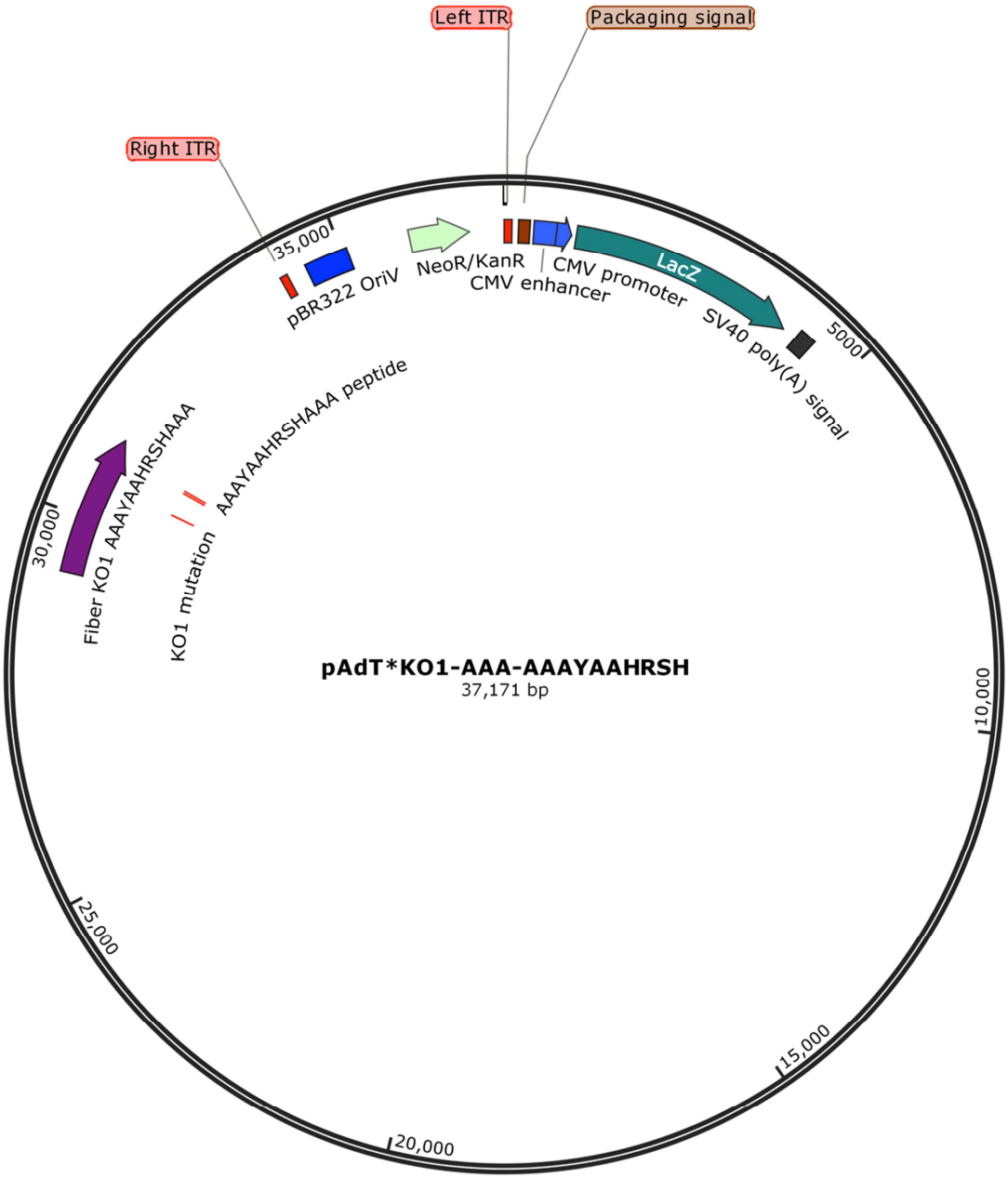

Figure A-13. pAdT*KO1-AAA-AAAYAAHRSH. Genetic elements are shown as coloured boxes or arrows. ITR; inverted terminal repeat, NeoR; neomycin resistance gene, KanR; kanamycin resistance gene. The genetic map was generated with SnapGene v2.8.3.